
Rationally designed aplyronine analogues for use in antibody–drug conjugates

*A dissertation submitted in partial fulfillment of the requirements for the degree
of Doctor of Philosophy at the University of Cambridge*

TALIA PETTIGREW
SEPTEMBER 2018

TRINITY COLLEGE

DEPARTMENT OF CHEMISTRY

Declaration

I hereby declare that this dissertation is the result of my own work and includes nothing which is the outcome of work done in collaboration except as declared in the Preface and specified in the text. It is not substantially the same as any that I have submitted, or, is being concurrently submitted for a degree or diploma or other qualification at the University of Cambridge or any other University or similar institution except as declared in the Preface and specified in the text. I further state that no substantial part of my dissertation has already been submitted, or, is being concurrently submitted for any such degree, diploma or other qualification at the University of Cambridge or any other University or similar institution except as declared in the Preface and specified in the text. In accordance with the Board of Graduate Studies guidelines, this document does not exceed 60,000 words.

Talia Rosemaree Pettigrew

August 2018

Acknowledgements

This dissertation is the result of many people's efforts, and I would like to take advantage of this chance to thank some of them.

Firstly, I thank Professor Ian Paterson for accepting me into his group and giving me the opportunity to take on a project in natural product synthesis. I quickly came to appreciate the opportunities to learn and work together in a friendly and stimulating environment. In particular, his help and advice while compiling this dissertation has been deeply appreciated.

Thanks also to Professor David Spring for welcoming me into his group, giving me the chance to expand my chemical knowledge and to collaborate with other researchers. Both of my supervisors have invested in building a positive working environment in their research groups, which has allowed me to develop a strong social support network for which I am grateful. I thank Professor Jonathan Goodman as well for his help and encouragement.

We have been fortunate in having excellent technical support from Nic Davies, Matt Pond and Naomi Hobbs. Members of the Paterson group have given many hours of their time to keep Lab 122 running smoothly. For running NMRs I thank Simon Williams, Callum MacGregor, Andrew Phillips, Leroy Han and Nelson Lam. Thanks as well to all the members of Team Aplyronine and Team ADC, most especially to Rachel Porter as my aplyrologue buddy and proofreader extraordinaire.

This project has been carried out with assistance from AstraZeneca. In particular I am indebted to Jeremy Parker for inviting me to carry out a placement at AstraZeneca's process chemistry facility in Macclesfield, UK. It was a valuable learning experience – one which I would not have had an opportunity to take up otherwise – and his support in both the scientific and practical aspects of sojourning in the North were much appreciated.

For supporting my early forays into chemistry and for encouraging me to apply to Cambridge, I am grateful to James de Voss, Joanne Blanchfield and Mary Garson. Thanks are due to Deborah Longbottom and Rachel MacDonald for helping me with any PhD issue large or small, and for fostering such a supportive community in the Department of Chemistry.

I am grateful to Trinity College for granting me an External Research Studentship, and to Cambridge Australia Scholarships. Thanks also to the University of Cambridge and to Ian Paterson for financial support.

Many thanks to Patersons and Springles past and present for being excellent colleagues and friends. I've looked forward to going to the lab every day because all my mates are there. I would also like to thank my dear friends Emma Durham and Bianca Provost for being a boundless source of kindness and advice, and Adam Yip and Bing Yuan Han for being my constant and trusty companions for the last four years.

Thank you to Mum and Dad for encouraging me always and especially for teaching me to keep chipping away at it. Finally, Mitch is the reason this dissertation has been completed, and if I were to thank him for everything, it would take another dissertation at least this size, and hopefully much more eloquent. I'm sure my words can hardly do them justice, but I treasure their support above all else.



Summary

The aplyronines are a family of antimitotic marine macrolides which show highly potent antiproliferative effects at picomolar concentrations in human cancer cell lines. Through a novel dual protein-targeting mechanism of action, their exquisite potency renders the aplyronines promising drug candidates.

However, the scarcity and structural complexity of the aplyronines brings challenges in supplying material to enable these studies, and calls into question their viability as commercial targets. Based on structure–activity relationship studies for the aplyronines and some related actin-binding macrolides, we have designed simplified analogues with the aim of reducing the synthetic effort, whilst retaining the extraordinary potency of the natural products. Our highly convergent route has led to a substantial reduction in the step count and improved scalability. Importantly, recent advances in cancer chemotherapy have led us to consider conjugating the aplyronines to monoclonal antibodies to produce improved antibody–drug conjugates to target specific tumour cells.

Chapter 1 places this project in the context of marine natural products research for applications in the clinic. Background is given on the extensive work previously undertaken on the aplyronines in our group and others. Based on this, the rational design of analogues is justified and a plan is laid out for their efficient synthesis. The field of targeted cancer therapy is introduced, with particular reference to the antibody–drug conjugate approach.

Chapter 2 discusses the methods used to construct key fragments for these designed aplyronine analogues. The southern fragment contains two of three key structural simplifications, while the side chain contains the final modification. Details are also given for the re-synthesis of the northern fragment, originally devised for the natural product, to supply this research.

Chapter 3 recounts how these fragments were combined and elaborated to a highly advanced intermediate. We examine the selection of an optimal protecting group strategy for the northern region from two options, leading to the scaled-up synthesis of a fully protected macrocyclic compound. Finally, attachment of the modified side chain provides the full carbon skeleton.

Chapter 4 culminates in endgame manipulations to furnish the desired analogues, and explores the potential of these compounds to be advanced to the clinic for cancer therapy. Strategies for conjugation to antibodies to develop a targeted therapy are considered, along with prospects for further streamlining of structure and methodology leading to a new generation of analogues.

Nomenclature

Metal enolate stereochemistry

According to the accepted IUPAC conventions, the two metal enolates **A** and **B** will be referred to as (*E*)- and (*Z*)-enolates, respectively (Figure 1). In all cases the metal–oxygen substituent will have higher priority than the R¹ substituent.

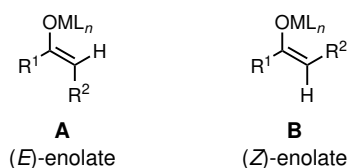


Figure 1: Naming convention for enolates

Syn- and *anti*-diastereomers

The convention devised by Masamune¹ for assigning the relative stereochemistry of vicinal stereocentres as *syn* and *anti* is used in this dissertation. A *syn*-relationship is defined by two substituents (R¹ and R²) pointing in the same direction relative to the plane represented by the main chain drawn in a zigzag conformation, as shown in Figure 2. An *anti*-relationship is defined by two substituents pointing in opposite directions relative to the plane. Hence, the two diastereomers **C** and **D** are referred to as *syn* and *anti*, respectively.

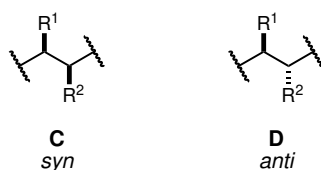


Figure 2: Naming convention for diastereoisomers

Aldol adduct stereochemistry

For aldol reactions where an α -chiral ketone directs the stereochemical outcome, the aldol adduct is referred to as shown in Figure 3. In these cases, the pre-existing ketone stereocentre is labelled as “1” for reference. This convention recognises the origin of the stereochemistry while also defining the relative stereochemistry between substituents.

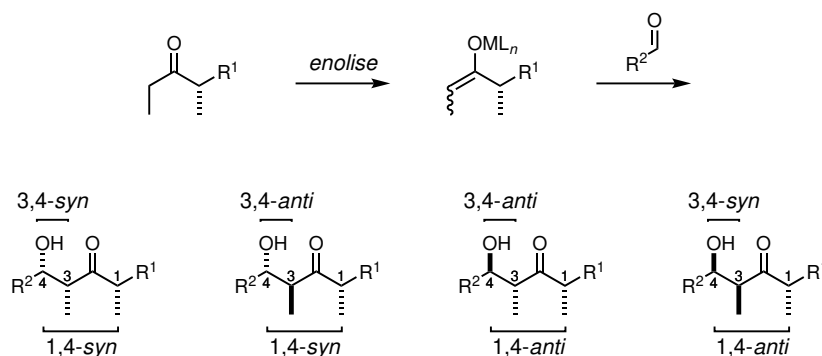
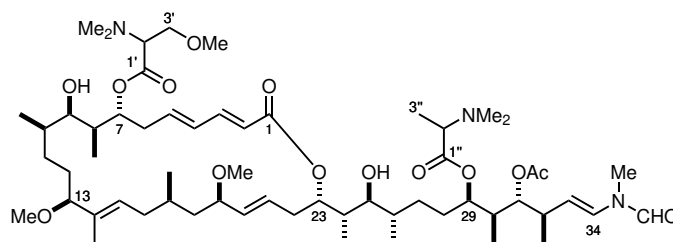


Figure 3: Naming convention for aldol adducts

Compound numbering

The naming and numbering of compounds follow priorities set out by IUPAC throughout this dissertation. The numbering system used for aplyronine intermediates and analogues follows that proposed by Yamada and co-workers in their original publication covering the isolation and characterisation of the aplyronines.² This system is shown in Figure 4.



Aplyronine A

Figure 4: Compound numbering for the aplyronines

Abbreviations

$[\alpha]_D$	specific rotation
Ac	acetyl
ADC	antibody–drug conjugate
ADP	adenosine diphosphate
Alloc	allyloxycarbonyl
ApA, ApB etc	aplyronine A, B etc
app	apparent
aq.	aqueous
Ar	aryl
ASAP	Atmospheric Solids Analysis Probe
ATP	adenosine triphosphate
BBN	9-borabicyclo[3.3.1]nonyl
Bn	benzyl
Boc	<i>tert</i> -butoxycarbonyl
bp	boiling point
br	broad
brsm	based on recovered starting material
Bu	butyl
Bz	benzoyl
<i>c</i>	concentration
calc.	calculated
cat.	catalytic
CBS	Corey–Bakshi–Shibata
cm^{-1}	wavenumber(s)
cod	cyclooctadiene
corr.	corrected
COSY	^1H – ^1H correlation spectroscopy

CSA	camphor-10-sulfonic acid
Cy	cyclohexyl
d	doublet
DAR	drug–antibody ratio
DBU	1,8-diazabicyclo[5.4.0]undec-7-ene
DCC	<i>N,N'</i> -dicyclohexylcarbodiimide
DDQ	2,3-dichloro-5,6-dicyano-1,4-benzoquinone
DEAD	diethyl azodicarboxylate
δ	chemical shift
DFT	density functional theory
DIAD	diisopropyl azodicarboxylate
DIBAL	diisobutylaluminium hydride
DMAIa	<i>N,N</i> -dimethylalanine
DMAP	4-(<i>N,N</i> -dimethylamino)pyridine
DME	1,2-dimethoxyethane
DMF	dimethylformamide
DMGly	<i>N,N</i> -dimethylglycine
DMP	Dess–Martin periodinane
DMSer	<i>N,O</i> -dimethylserine
DMSO	dimethylsulfoxide
<i>dr</i>	diastereomeric ratio
<i>ee</i>	enantiomeric excess
<i>ent</i>	enantiomer
<i>epi</i>	epimer
eq	equivalent(s)
EI	electron ionisation
ESI	electrospray ionisation
Et	ethyl
EtOAc	ethyl acetate
FDA	Food and Drug Administration (USA)
GC	gas chromatography
h	hour(s)
HMDS	hexamethyldisilazane
HeLa	human cervical adenocarcinoma cell line
HMBC	heteronuclear multiple-bond correlation spectroscopy

HMPA	hexamethylphosphoramide
HPLC	high-performance liquid chromatography
HRMS	high-resolution mass spectroscopy
HTS	high throughput screening
HWE	Horner–Wadsworth–Emmons
Hz	hertz
<i>i</i> -	<i>iso</i> -
i.p.	intraperitoneal
IC ₅₀	half maximal inhibitory concentration
IgG	human immunoglobulin G
imid.	imidazole
Ipc	<i>iso</i> -pinocampheyl
IR	infrared
<i>J</i>	coupling constant
K _d	dissociation constant
KHMDS	potassium hexamethyldisilazide
L	ligand
LDA	lithium diisopropylamide
LiHMDS	lithium hexamethyldisilazide
LLS	longest linear sequence
2,6-lut.	2,6-lutidine
M	molar
m	multiplet
<i>m</i> -CPBA	<i>meta</i> -chloroperoxybenzoic acid
mAb	monoclonal antibody
Me	methyl
min	minute(s)
MMAla	<i>N</i> -monomethylalanine
MNBA	2-methyl-6-nitrobenzoic acid
mol	mole(s)
MOM	methoxymethyl
mp	melting point
MS	mass spectrometry
Ms	methylsulfonyl (mesyl)
MTBE	methyl <i>tert</i> -butyl ether

MTPA	α -methoxy- α -(trifluoromethyl)phenylacetyl
m/z	mass-to-charge-ratio
<i>n</i> -	<i>normal</i> -
n.d.	not determined
NCI	National Cancer Institute
NCS	<i>N</i> -chlorosuccinimide
NHK	Nozaki–Hiyama–Kishi
NMO	<i>N</i> -methylmorpholine- <i>N</i> -oxide
NMR	nuclear magnetic resonance
nOe	nuclear Overhauser effect
Nu	nucleophile
obs	obsured
P	unspecified protecting group
PAB	<i>para</i> -aminobenzyl
PABQ	<i>para</i> -aminobenzyl quaternary ammonium
PE	petroleum ether, bp 40–60 °C
PEG	polyethyleneglycol
Ph	phenyl
Piv	pivaloyl
PMB	<i>para</i> -methoxybenzyl
PMP	<i>para</i> -methoxyphenyl
ppm	parts per million
PPTS	pyridinium <i>para</i> -toluenesulfonate
Pr	propyl
py	pyridine
q	quartet
quint	quintuplet
R	unspecified substituent
Red-Al	sodium <i>bis</i> (2-methoxyethoxy)aluminium hydride
R_f	retention factor
ROS	reactive oxygen species
rt	room temperature
s	singlet
SAR	structure–activity relationship
sat.	saturated

SD	subdomain
SET	single electron transfer
<i>t</i> -	<i>tertiary</i> -
t	triplet
TAMRA	tetramethylrhodamine
TBAF	tetrabutylammonium fluoride
TBAI	tetrabutylammonium iodide
TBDPS	<i>tert</i> -butyldiphenylsilyl
TBS	<i>tert</i> -butyldimethylsilyl
TCA	2,2,2-trichloroacetimidate
TCBC	2,4,6-trichlorobenzoyl chloride
TCNB	1,2,4,5-tetrachloro-3-nitrobenzene
TES	triethylsilyl
Tf	trifluoromethanesulfonyl (triflyl)
THF	tetrahydrofuran
TIPS	triisopropylsilyl
TLC	thin-layer chromatography
TMS	trimethylsilyl
TMSer	<i>N,N,O</i> -trimethylserine
Tr	triphenylmethyl (trityl)
TS	transition state
Ts	<i>para</i> -toluenesulfonyl (tosyl)
UV	ultraviolet

Contents

Declaration	i
Acknowledgements	ii
Summary	v
Nomenclature	vi
Abbreviations	viii
1 Introduction	1
1.1 Marine natural products	1
1.2 Targeted therapies	4
1.3 Antibody–drug conjugates	6
1.3.1 Antibody selection	8
1.3.2 Linker design	9
1.3.3 Natural products as cytotoxic payloads	10
1.3.4 Further considerations	12
1.4 The aplyronines	13
1.4.1 Isolation and structure elucidation	13
1.4.2 Biological activity	14
1.4.3 Structure–activity relationship studies	16
1.4.4 Related actin-binding natural products	19
1.4.5 Analogue development	20
1.5 Previous synthetic efforts	20
1.5.1 Yamada approach	22
1.5.2 Paterson approach and modifications for analogue synthesis	22
1.6 Aims	26
2 Synthesis of key fragments	29
2.1 Southern fragment analogue (C ₁₅ –C ₂₇)	29

2.1.1	Aldol coupling	29
2.1.2	1,3- <i>anti</i> reduction	37
2.1.3	Elaboration to the full C ₁₅ –C ₂₇ analogue fragment	38
2.2	Side chain analogue (C ₂₈ –C ₃₄)	40
2.2.1	Titanium aldol coupling	40
2.2.2	Diversification to natural and analogue side chain components	43
2.2.3	Preliminary investigations towards <i>N</i> -vinylformamide installation	44
2.2.4	Process scale synthesis of Roche ester ethyl ketone	46
2.3	Northern fragment (C ₁ –C ₁₄)	50
2.3.1	PMP-protected northern fragment synthesis	50
2.3.2	TES-protected northern fragment synthesis	53
2.4	Summary and conclusions	58
3	Fragment coupling to construct advanced macrolactone intermediates	63
3.1	Coupling of southern and northern fragments	63
3.1.1	Initial studies: comparing PMP and <i>bis</i> -TES protected fragments	63
3.1.2	Selective reduction and installation of the C ₁₃ methyl ether	66
3.1.3	Advancement towards the macrocycle	69
3.1.4	Macrolactonisation	74
3.1.5	Selection of protecting group strategy for the onward synthesis	76
3.1.6	Fully protected macrocycle scale-up	77
3.2	Macrocycle to side chain coupling and elaboration	79
3.2.1	Side chain attachment by aldol coupling and dehydration	79
3.2.2	Conjugate reduction to the C ₂₉ ketone	82
3.3	Summary	85
4	Completion of the synthesis and conclusions	87
4.1	Endgame	87
4.1.1	Completion of scytophycin-type hybrid analogues	87
4.1.2	Studies towards C ₂₉ -esterified analogues	88
4.2	Planned biological testing	92
4.3	Modifications to generate a second round of analogues	95
4.4	Potential to streamline the overall synthesis	97
4.5	ADC development	101
4.5.1	Development of a linker–payload species	101
4.5.2	Bioconjugation to form ADCs	104

4.6	Overall conclusions	106
5	Experimental	109
5.1	General comments	109
5.1.1	General experimental details	109
5.1.2	Analytical techniques	110
5.2	Preparation of reagents	111
5.3	Experimental procedures for Roche ester-derived ethyl ketones	116
5.4	Experimental procedures for Chapter 2	119
5.4.1	Southern fragment (C ₁₅ –C ₂₇)	119
5.4.2	Side chain fragment (C ₂₈ –C ₃₄)	133
5.4.3	PMP-protected northern fragment (C ₁ –C ₁₄)	142
5.4.4	<i>Bis</i> -TES-protected northern fragment (C ₁ –C ₁₄)	146
5.5	Experimental procedures for Chapter 3	150
5.5.1	PMP-protected macrocycle (C ₁ –C ₂₇)	150
5.5.2	<i>Bis</i> -TES-protected macrocycle (C ₁ –C ₂₇)	159
5.5.3	Full carbon skeleton (C ₁ –C ₃₄)	169
5.6	Experimental procedures for Chapter 4	175
	Appendix	193

Chapter 1

Introduction

1.1 Marine natural products

The oceanic environment is a source of fascination to the scientific community, representing a vast and even now largely unexplored resource. To date, only a small fraction of the estimated total number of marine species have been described. Regrettably, current threats to biodiversity due to climate change and habitat destruction mean that there is growing urgency to study these species. Underwater exploration has been pursued in earnest only in the last few decades, since the advent of modern snorkelling along with the introduction of scuba and submarine technology.

Though there is much yet to learn, we do know that marine organisms are masters of biosynthesis, producing all manner of structurally complex and biochemically surprising secondary metabolites. As such, they offer tantalising challenges to the synthetic chemist. Invertebrates such as sponges and molluscs quickly became a prized source of natural products, with over 11 000 novel structures discovered from these creatures between 1990 and 2014.³ A large number of these compounds, often secondary metabolites, are used by their hosts in a system of chemical defences against predators, competitors and microorganismal parasites. They therefore grant an evolutionary advantage to organisms, whether synthesised *de novo* or sequestered from prey species or symbionts.⁴ Indeed, many natural products originally isolated from filter feeders such as sponges may in fact be of bacterial or fungal origin.^{5–7} Microorganisms are prolific producers of all classes of secondary metabolites, which play an essential role in communication. Modes of social interaction including commensalism, amensalism, neutralism, cooperation, competition, and predation may all be modulated by the exchange of chemical information.⁸ The ability

to form consortia and other symbioses is a key characteristic for microbial survival, and hence chemical signalling is extremely important in all types of marine environments.^{9–11}

Great breakthroughs came with the recognition that marine natural products often show broad cross-phylum biological activity, and can act as extremely potent biochemical effectors in human systems. Studies on the mechanisms of action of biologically active natural products showed that they can bind efficiently to many cellular proteins and inhibit or enhance enzymatic activity for the treatment of disease. In a sense, this is not surprising, because at a fundamental level humans and all other known organisms have many common goals. In general we wish to avoid predators, deter parasites, benefit from symbioses, attract mates, and respond to changes in our environment and accordingly hasten or slow growth. Given the common evolutionary origin of all living species, and the resulting similarity in biochemical structures across taxa, it is understandable that natural products which have resulted from a selective process could have potent biological effects in other species, even distantly related ones. In the modern age, humans have controlled many of the external dangers to our survival, leaving internal threats (*i.e.* to health) as important determinants of the length and quality of our lives. For instance, cancer is now one of the most common causes of morbidity and mortality, accounting for 8.8 million deaths (1 in 6) annually worldwide.¹²

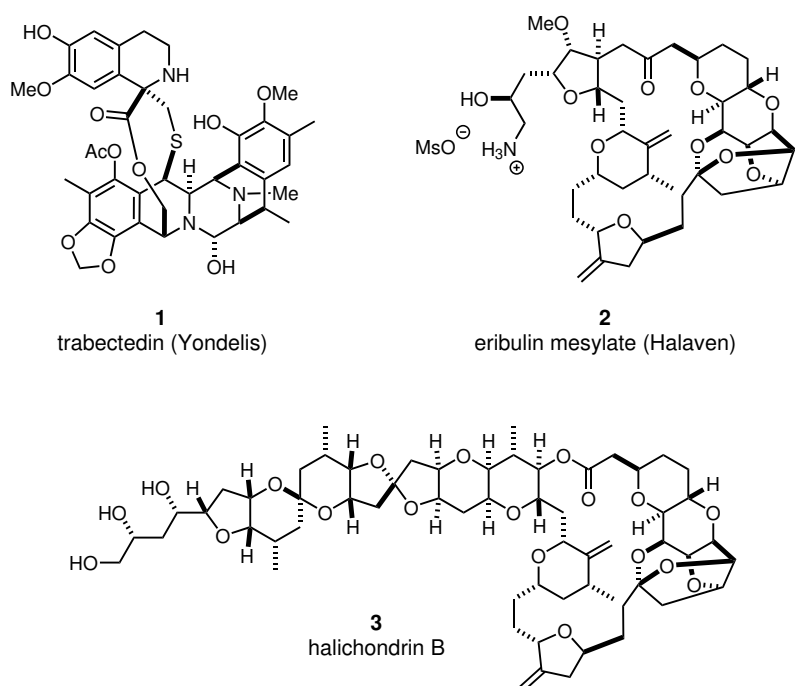


Figure 1.1: Marine natural products which have been developed as anticancer drugs

Marine natural products have made an impact in the field of cancer treatment, due to their cytotoxic effects *via* modes of action such as interruption of microtubule assembly or DNA damage.¹³ The first anticancer drug of marine origin was trabectedin (Yondelis, **1**), approved for treatment of soft tissue sarcoma in 2007 (Figure 1.1). In 2010, eribulin mesylate (Halaven, **2**), a synthetic analogue of marine natural product halichondrin B (**3**), was approved for metastatic breast cancer treatment. This example typified a successful function-oriented synthesis.¹⁴ Scarce supply of the compound from natural sources and the large investment of resources, time and cost in producing it by total synthesis meant that economies had to be found if the product were ever to reach the market for clinical use. Structure–activity relationship (SAR) studies of the analogues and intermediates generated during the total synthesis of halichondrin B by Kishi and co-workers¹⁵ were used to identify the parts of the molecule most necessary for bioactivity. This led to the development of an optimised synthetic route towards the structurally simpler analogue eribulin for production on an industrial scale.

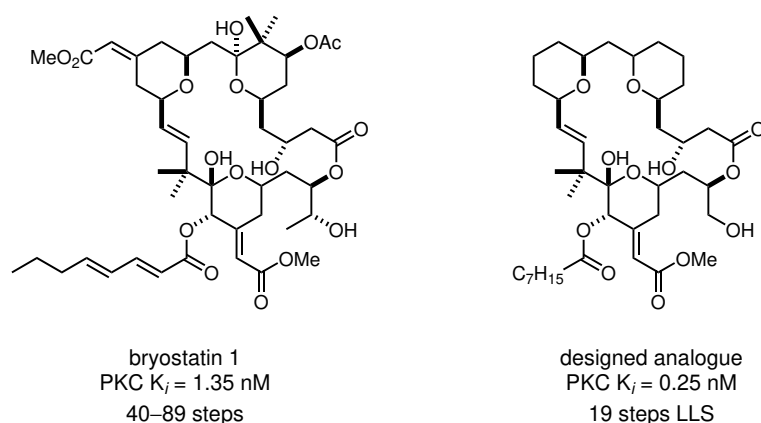


Figure 1.2: Function-oriented development of bryostatin analogues with similar or improved biological activity (PKC = protein kinase C)^{16,17}

The level of complexity inherent in many of the natural products in question means that, although they may be accessible in the laboratory by total synthesis, commercial-scale manufacture may seem to be beyond the limits of practicality.¹⁸ As a result these compounds may be questionable candidates even at the earliest stages of pharmaceutical development. Function-oriented synthesis is an extremely valuable approach by which chemists may achieve molecular function with synthetic economy, thus addressing the supply issue.^{19,20} A further example is the development of “bryologs”, analogues of the clinically relevant bryostatins, by Wender and co-workers. At a time when total syntheses of the natural products required over 70 steps, the researchers succeeded in generating their first simplified analogue with similarly potent growth inhibition activity in under 30 steps (Figure 1.2).¹⁷ Indeed, a recent publication from the Wender group

tissues to be affected. This results in suboptimal clinical outcomes and unpleasant or even dangerous side effects for the patient, for instance nausea, myeloid suppression, peripheral neuropathy, and organ toxicity.³⁰ It is desirable to achieve the maximum benefit with minimal exposure to a given anticancer agent. The lowest dosage that leads to a positive therapeutic outcome is known as the minimum effective dose. Exceptionally potent compounds are desired in order to lower the dose needed to achieve a clinical effect. Meanwhile, the maximum tolerated dose of a drug is dictated by the dose at which harm is caused to normal tissues. This places an upper limit on exposure (Figure 1.4). A complementary approach to widening the therapeutic window is increasing selectivity for neoplastic cells, minimising the risk to normal cells and allowing the agent to be better tolerated by the patient.³⁰

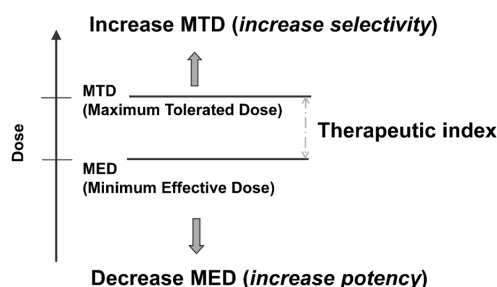


Figure 1.4: Approach to maximising the therapeutic index of drugs³⁰

As a result, recent approaches to cancer drug discovery have become focused on the development of targeted therapies, with the aim of selectively delivering potent anticancer agents to the tumour site. These can include certain tumour-targeted small molecules*, monoclonal antibody therapies, and importantly, conjugated species which contain a targeting portion linked to a cytotoxic effector.³³ These conjugates consist of a receptor-binding (bio)molecule such as an antibodies, peptide, small molecule or polymer, which is linked to anticancer therapeutic effectors such as small molecule drugs, radionuclides, or protein toxins.^{33,34}

The use of these targeting strategies will often rely on molecular profiling of a patient's specific disease subtype, allowing treatment to be tailored to individual characteristics (Figure 1.5). Targeted therapy therefore falls under the banner of personalised medicine, and has immense potential to improve treatment outcomes.³² This methodology is by no means limited to cancer therapy and could be applied more widely: for instance, to autoimmune conditions and infectious diseases.

*These are generally limited to cases where tumour enzymes have particular mutations not shared with healthy cells, thus the binding mode of the small molecule drug makes it necessarily selective for a tumour-specific target. Imatinib, an inhibitor of a mutant tyrosine kinase for treatment of chronic myeloid leukaemia, is an example.^{31,32}

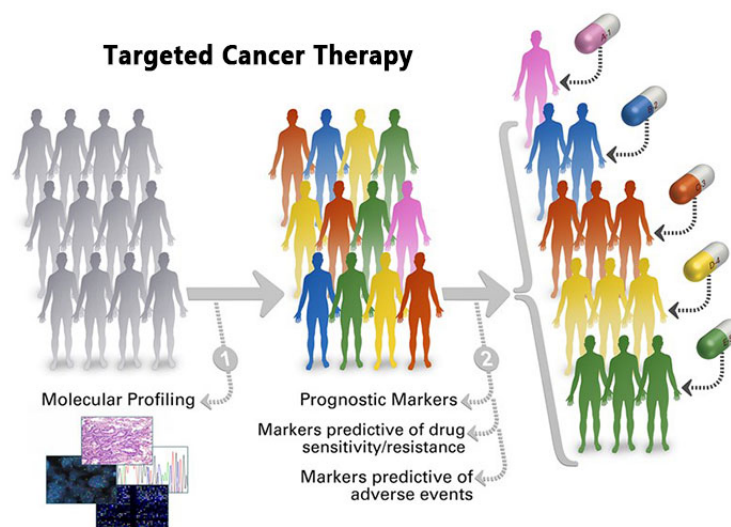


Figure 1.5: Targeted therapy relies on molecular profiling of disease and enables stratified or individualised medical treatment³⁵

1.3 Antibody–drug conjugates

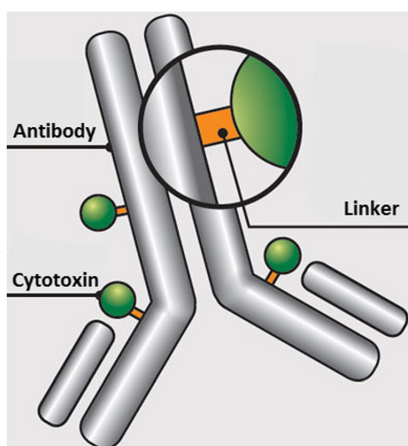


Figure 1.6: Structure of an antibody-drug conjugate³⁶

Antibody-drug conjugates (ADCs) have emerged as a highly promising avenue for targeted therapies. The field has grown rapidly over the past decade, with four ADCs currently available on the market and over 50 in clinical trials.³⁷ These entities consist of a monoclonal antibody attached to a cytotoxic small molecule payload *via* a chemical linker (Figure 1.6). Antibodies can be selected or genetically engineered to have high selectivity for receptors which are either overexpressed or, rarely, solely expressed on the cancer cell surface and not in healthy tissues, thereby delivering the payload to the site of interest.

The ADC is administered intravenously and is transported in the bloodstream to the tumour, where it undergoes antigen-specific binding and internalisation into the cell *via* receptor-mediated endocytosis (Figure 1.7). Depending on the antigen of interest, a number of pathways are then possible. Often, the conjugate is trafficked to the lysosome where the linker undergoes enzymatic or chemical cleavage. This releases the therapeutic agent into the cytosol, where it binds to its intracellular target and ultimately causes cell death.³⁶

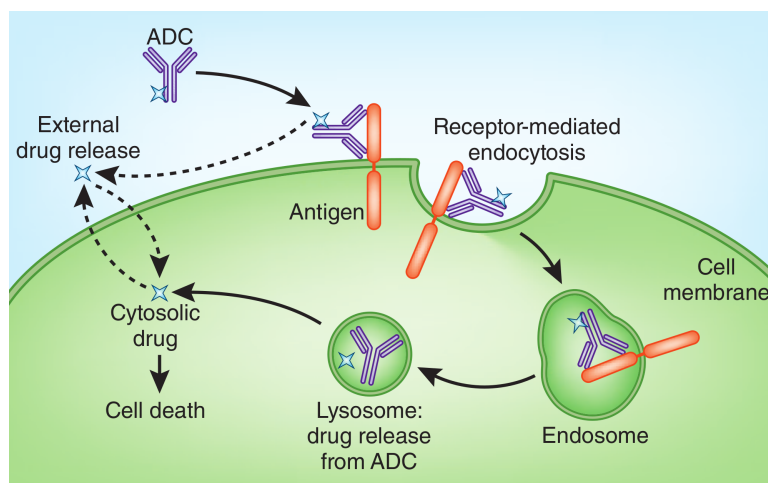


Figure 1.7: Mechanism of action of an ADC³⁸

The immunoconjugate approach brings a number of benefits as a form of targeted therapy. Firstly, due to the larger contact surface areas involved in protein-protein interactions, antibodies exhibit extremely high selectivity for their target receptors relative to small molecule and peptide drugs.³⁹ They also have long plasma half-lives, up to three weeks in circulation.³⁰ Antibodies alone can be used as clinical therapeutics, but in cancer indications these tend to have much more limited mechanisms of action and show lower clinical efficacy than ADCs, as they lack the attached cytotoxic payload. Payload wastage due to metabolism and excretion from the system is reduced relative to using the naked small molecules, which is of great benefit given the time and resource costs of producing these complex molecules.²²

Challenges in ADC design chiefly lie in identification of an appropriate target receptor, engineering of a suitable antibody, payload selection, and development of compatible linker chemistry. The three key components of an ADC, namely the antibody, linker and payload, will be discussed in the following sections.

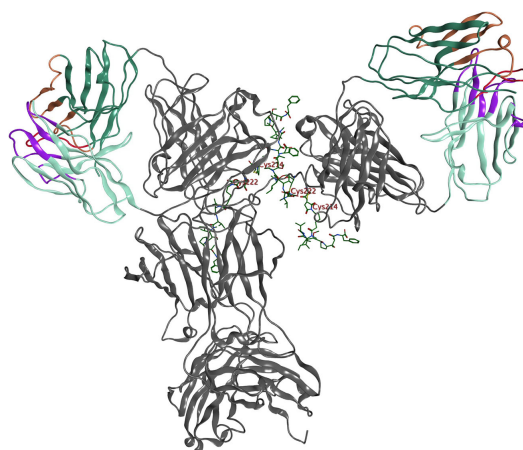


Figure 1.8: Structural model of an ADC with 4 auristatin drug molecules attached to a human IgG1 monoclonal antibody. The ribbon diagram represents the antibody, while the stick representations are given for the linker and payload. The antigen binding sites are shown in colour.⁴⁰

1.3.1 Antibody selection

The majority of the biomolecules used for conjugation are based on immunoglobulin G (IgG) scaffolds, which consist of two identical heavy chains and two identical light chains arranged in a characteristic Y-shape. Antigen binding sites are located at each end of the fork, and can be altered to maximise the affinity of the antibody for the chosen receptor (Figure 1.8). Advances in genetic engineering have led to the generation of fully human monoclonal antibodies. These bind target antigen with high specificity while minimising or even eliminating host immune response, which was a major drawback of previously used murine antibodies (Figure 1.9).^{30,33,41}

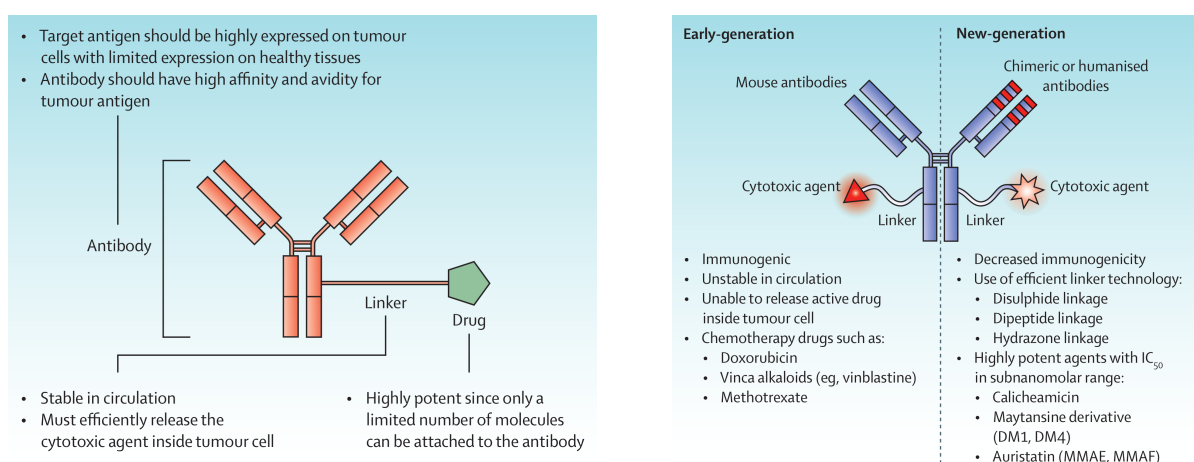


Figure 1.9: Desired properties of an ADC, and comparison of early and more recent ADC characteristics⁴¹

Much recent interest in the field has centred upon creating homogeneous immunoconjugates, in which a controlled number of drug molecules are attached at pre-determined sites on the antibody.⁴² The first generation of ADCs used native amino acids such as lysines and cysteines to attach the linker–payload unit at various points on the antibody, leading to stochastic mixtures in terms of drug position, proximity and number. These heterogeneous distributions of species generally showed drug-to-antibody ratios (DARs) ranging between 0 and 9 (Figure 1.10).⁴³ By contrast, more recent developments in site-specific conjugation involve antibody design to introduce discrete, chemically accessible cysteines or non-natural amino acids containing reactive functional groups for attachment of the drug in a controlled manner.^{36,44} Alternatively, methods using novel linker designs with native antibody sequences limit conjugation to sites compatible with the chosen chemistry.⁴³ Some typical examples, including cysteine alkylation and re-bridging, are shown in Figure 1.11.

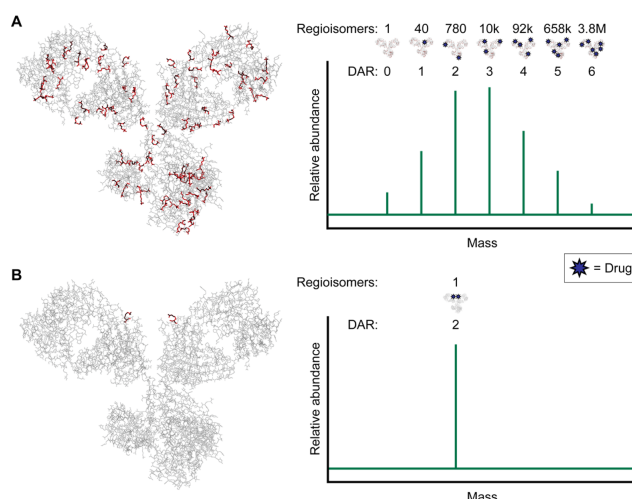


Figure 1.10: Theoretical distributions for native lysine and site-specifically conjugated antibodies. (A) Forty potential conjugation sites exist on the protein surface, leading to highly heterogeneous product distributions. (B) An engineered antibody with precisely two conjugation sites, leading to homogeneous products with a DAR of exactly 2.⁴²

1.3.2 Linker design

In most early cases, and in some current examples, ADCs have contained non-cleavable linkers. These can convey the advantage of extended plasma half-life, but rely upon enzymatic degradation of the full antibody to release their payload.³⁶ Much more common in modern ADC constructs is to use a cleavable linker strategy. There has been a proliferation of research around the development of linker chemistry which is completely serum-stable, but readily labile in the

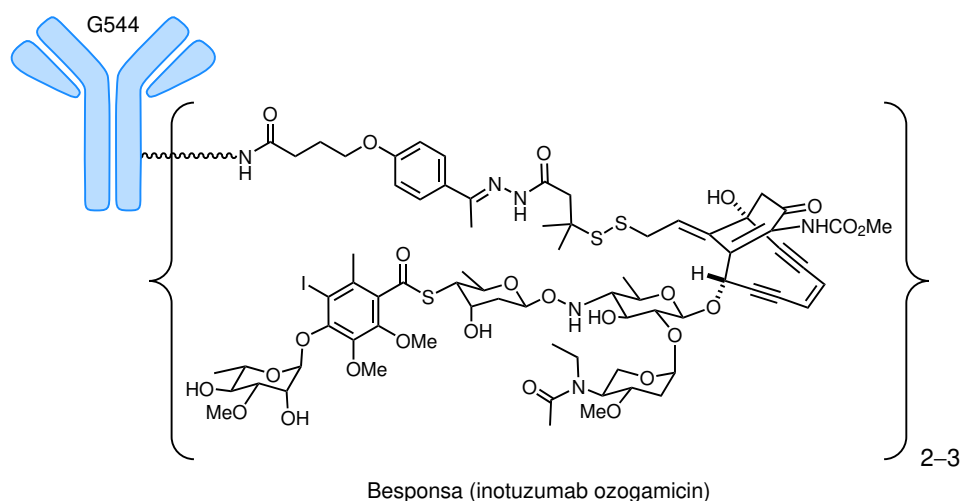
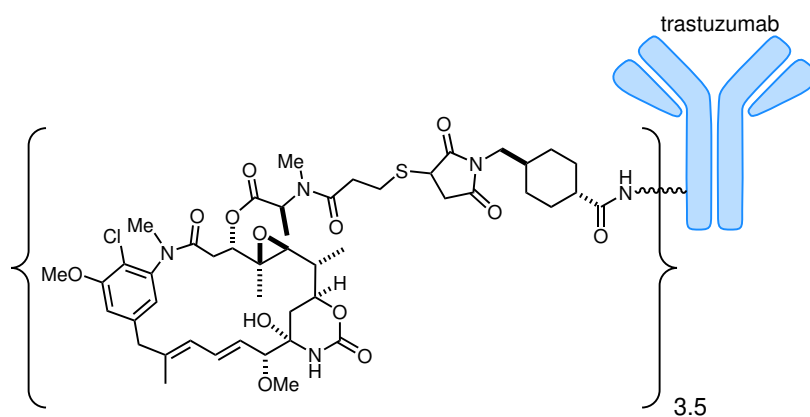
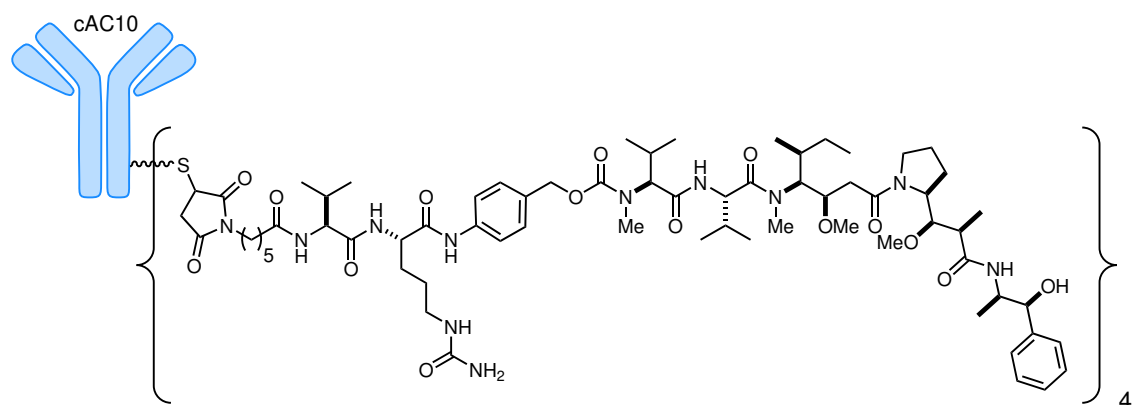


Figure 1.12: Current FDA-approved ADCs Adcetris, Kadcyca, and Besponsa. Mylotarg (not shown), like Besponsa, contains the calicheamicin-derived DNA damaging agent ozogamicin

used classes of cytotoxic warheads present in ADCs currently under development is the auristatins, synthetic derivatives of the marine pentapeptide dolastatin 10 which was isolated from the sea hare *Dolabella auricularia*.^{30,33,40} A member of this analogue family, monomethyl auristatin E, induces cytotoxicity by inhibition of microtubule dynamics and features in Adcetris (brentuximab vedotin, Figure 1.12), currently on the market for treatment of Hodgkin lymphoma.³⁰ The plant-derived maytansinoids operate by a similar mode of action and feature in a number of ADCs, including Kadcyla (ado-trastuzumab emtansine), recently approved for metastatic breast cancer.^{30,33,40} Also present in multiple ADCs are the calicheamicins, bacterial-derived antitumour antibiotics which cause double-strand DNA breakage leading to cell death.^{30,40} The analogue ozogamicin appears in Besponsa (inotuzumab ozogamicin), first released in 2017, and Mylotarg (gemtuzumab ozogamicin), which was re-introduced to the market in 2017 based on new evidence after having been excluded due to toxicity. All of these compound classes exhibit low picomolar antiproliferative activity and were considered unsuitable for use as single agent therapeutics due to potential off-target toxicities. However, owing to their exceptional potencies they were excellent candidates for development in immunoconjugates.

1.3.4 Further considerations

It has been shown that the antigen receptor need not be internalised into the tumour cell: instead, the warhead may be liberated in the extracellular space and diffuse into the surroundings, facilitating bystander killing.³⁴ Non-internalisation may be advantageous in eradicating heterogeneous tumours containing antigen-negative cells. This process may also allow the drug to penetrate deeper into neoplastic sites distant from blood vessels and to directly kill endothelial cells in the tumour neovasculature.^{30,50} However, issues of off-target toxicity to neighbouring healthy tissues may be more of a concern than with counterpart ADCs that deliver payloads into the cytoplasmic matrix.

Notably, ADCs can target malignant epithelial cells over healthy cells even where both express the target antigen. The loss of intercellular junctions in tumours leads to random distribution of normally apically-restricted receptors across the entire plasma membrane, granting access *via* the bloodstream to targeted drugs (Figure 1.13).⁴⁶

Although they have mainly been used in oncology to date, there are significant opportunities to expand ADCs to other fields of medicine, including autoimmune and infectious diseases. Recently, the first antibody–antibiotic conjugate was reported, with potentially huge significance in the current climate of concern over antibiotic resistance.^{51,52}

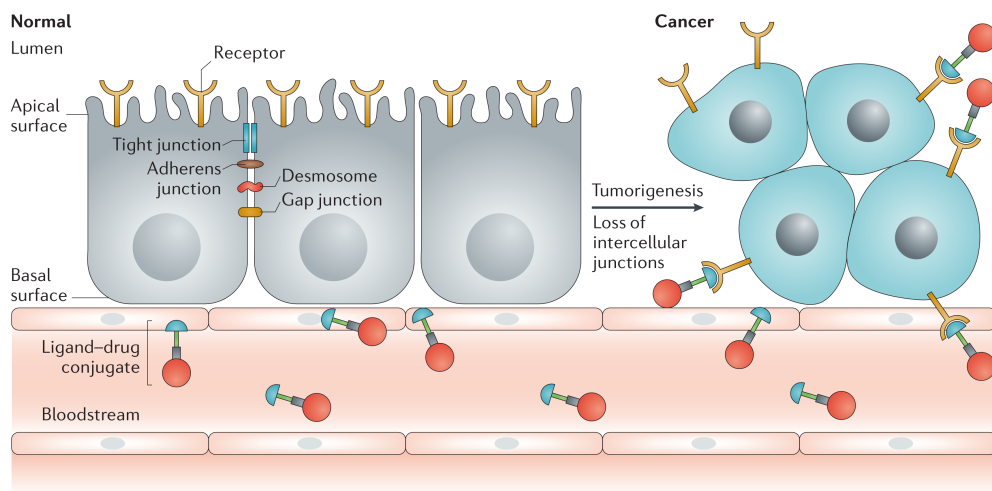


Figure 1.13: Normal cells can block ADC passage through intercellular junctions, while malignant cells lack this level of protection. This promotes selectivity with judicious choice of the target receptor.⁴⁶

The high cost of ADC therapy is a serious issue with important ethical implications. These will not be dealt with in this discussion, other than to note that this form of treatment is as yet in very exploratory stages of development. It is to be expected that as the technology matures, the costs of development and production should decrease significantly.

1.4 The aplyronines

In the ongoing search for effective cytotoxic ADC payloads, especially those with novel modes of action, the aplyronines have surfaced as a compelling candidate. This structurally interesting class of marine macrolides bears similarities to a number of known marine natural products, but exhibits a unique binding mode which gives rise to its highly potent antitumour activity.⁵³

1.4.1 Isolation and structure elucidation

The aplyronines were originally isolated from the sea hare *Aplysia kurodai* by Yamada and co-workers in 1993.² Specimens were collected off the Pacific coast of Mie Prefecture, Japan, and subjected to repeated partitioning and chromatographic separation steps, guided by *in vitro* cytotoxicity against the HeLa-S3 cell line. This led to the isolation of aplyronines A–C (**5–7**,

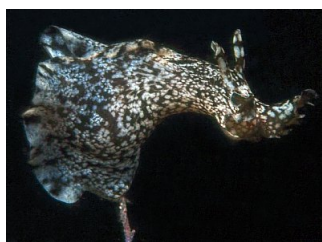


Figure 1.14: *Aplysia kurodai* swimming at 20 m, Jeju Island, South Korea⁵⁴

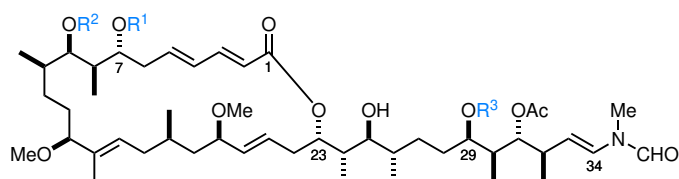
Table 1.1). In 2000, Yamada reported the isolation of five further congeners in very low abundance, aplyronines D–H (**8–12**).^{55,56}

Structurally, the family differs almost solely in the number and type of amino acid residues at C₇, C₉ and C₂₉. Each congener consists of a 24-membered macrolactone and a functionalised 11-carbon side chain, bearing a total of fifteen stereocentres. Analysis of IR, UV and 1D ¹H and ¹³C NMR data for **5** allowed the identification of key structural features, including an $\alpha,\beta,\gamma,\delta$ -unsaturated ester with (*E,E*)-geometry, two additional (*E*)-olefins, an acetate ester, two additional esters, two hydroxyl groups, three methoxy groups, two dimethylamino groups, and a terminal *N*-methyl-*N*-vinylformamide. Rotamers at the *N*-methyl-*N*-vinylformamide terminus as well as scalemic mixtures of the C₇ and C₂₉ amino acids cause the NMR spectra of **5** to appear as a complex mixture of four diastereomers. Detailed 2D NMR spectral analysis, including ¹H–¹H COSY and HMBC experiments, as well as degradation studies assisted in the elucidation of the overall structure. The full relative and absolute stereochemical assignments were confirmed *via* enantioselective synthesis of the degradative fragments by Yamada and co-workers, culminating in the first total synthesis of aplyronine A, **5**.^{58–62} The structures of congeners B and C (**6** and **7**) were also confirmed by Yamada's total synthesis,⁶³ and aplyronines D–H (**8–12**) were assigned by analogy to the known aplyronine A.⁵⁶

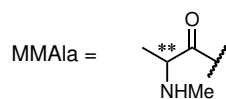
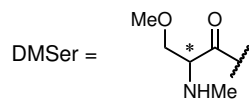
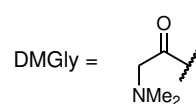
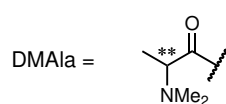
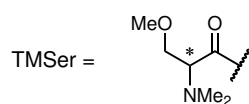
1.4.2 Biological activity

From their earliest discovery, the aplyronines were noted to show potent *in vitro* activity against the HeLa-S3 cell line (see Table 1.1).^{2,57} It is notable that small differences in the amino acid profile of each of the aplyronines have a significant effect on their biological activities. For instance, aplyronines A (**5**) and C (**7**) differ only in the presence of the trimethylserine moiety at C₇, yet the former shows almost 50-fold greater cytotoxicity against HeLa-S3 cells. Similarly, aplyronine D (**8**) differs from its congener aplyronine A only by one methyl group on the C₂₉ amino acid, but is six-fold more toxic.

Table 1.1: Structures, abundance and cytotoxicity of aplyronines A–H (**5–12**)⁵⁷



Congener	R ¹	R ²	R ³	Isolation yield (mg / 297 kg sea hare)	IC ₅₀ (nM, HeLa-S3)
A (5)	TMSer	H	DMAla	75	0.45
B (6)	H	TMSer	DMAla	4.3	2.9
C (7)	H	H	DMAla	0.9	22
D (8)	TMSer	H	DMGly	2.6	0.071
E (9)	= 22-methylaplyronine A			4.0	0.18
F (10)	TMSer	H	MMAla	0.7	0.18
G (11)	DMSer	H	DMAla	1.6	0.12
H (12)	H	DMSer	DMAla	0.6	9.8



* 1.3–1.1 : 1 *S/R*
 ** 2.5–4.0 : 1 *S/R*

Due to the low natural abundance of the other congeners, further biological testing has to date been restricted to aplyronine A. Promising results emerged from *in vivo* testing in mouse xenografts of five tumour types (Table 1.2).⁶⁴ Potent dose-dependent growth inhibitory activity was shown, especially in P388 leukaemia, Lewis lung carcinoma and Ehrlich carcinoma, and in the former two, particularly high survival rates were observed. This remarkable antitumour activity has led aplyronine A to be considered a promising preclinical candidate.⁶⁵

Table 1.2: Antitumour activity of aplyronine A (**5**) in mouse xenograft studies⁶⁴

Tumour	Route ^a	Dose (mg kg ⁻¹ day ⁻¹)	Survival time		No. survivors after 60 days
			Median time (days)	Test/control (%)	
P388 leukaemia	i.p.	0.08	59.9	545	4/6
	Control	—	11.0		0/7
Colon C26 carcinoma	i.p.	0.08	40.0	255	0/6
	Control	—	15.7		0/10
Lewis lung carcinoma	i.p.	0.04	60.1	556	6/6
	Control	—	10.8		0/8
B16 melanoma	i.p.	0.04	46.8	201	0/6
	Control	—	23.3		1/9
Ehrlich carcinoma	i.p.	0.04	59.7	398	2/6
	Control	—	15.0		0/8

^a Schedule: intraperitoneal (i.p.) days 1–5. Aplyronine A (**5**) was dissolved in DMSO (0.08 mg mL⁻¹) and then diluted with a physiological solution of NaCl.

1.4.3 Structure–activity relationship studies

Fluorescence experiments by Karaki and co-workers in 1996 identified that aplyronine A binds to actin, the most abundant eukaryotic cellular protein.^{66,67} These findings have since been supported by various studies, including one resulting in the publication of an X-ray structure of the actin–aplyronine complex (Figure 1.16).^{68–71} Two forms of actin are found in eukaryotic cells: monomeric globular actin (G-actin) and polymeric filamentous actin (F-actin). The dynamic equilibrium between the two is regulated by interactions with various other cellular proteins to maintain the vital cellular functions of the actin cytoskeleton.⁷² Interconversion is modulated by ATP in a concentration-dependent process known as “treadmilling”, which allows directional growth of filaments (Figure 1.15).⁷³ Takata and co-workers found that aplyronine A intercalates its side chain into a hydrophobic cleft between G-actin subdomains 1 and 3, sequestering the monomers and inhibiting polymerisation to F-actin. It also causes rapid depolymerisation of F-

actin by capping and severing existing filaments.⁶⁸ Disruption of the complex actin modulation pathway interferes with cell motility and cytokinesis, and can ultimately lead to apoptosis.^{74,75}

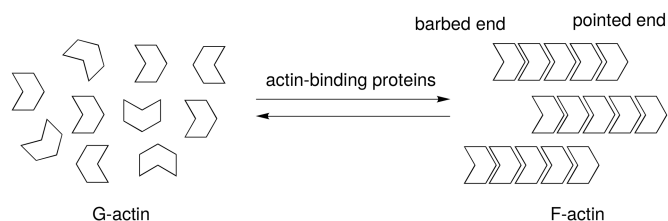


Figure 1.15: Schematic of the dynamic equilibrium between monomeric and filamentous actin⁷²

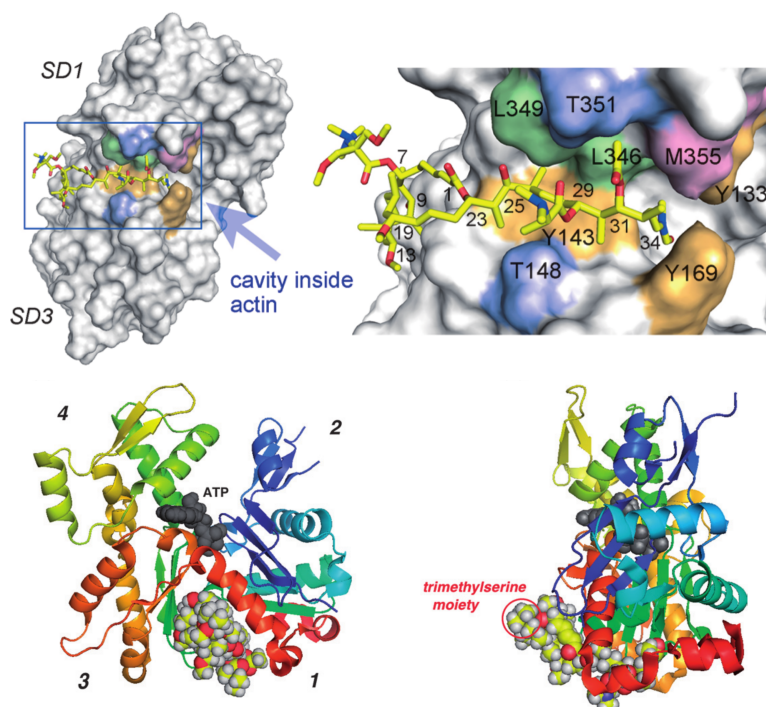


Figure 1.16: X-ray structure of the actin-aplyronine A complex^{57,68,76}

Structure–activity relationship (SAR) studies on the aplyronines were undertaken by Yamada and co-workers, largely based on intermediates and analogues generated during their fragment and total syntheses. This enabled an analysis of the aplyronine pharmacophore, identifying structural features which are necessary for both actin depolymerising activity and cytotoxicity. These results are summarised in Figure 1.17.^{64,77–82}

Perplexingly, it appeared from these SAR studies that for potent cytotoxicity, actin binding is a necessary but insufficient condition. This mystery deepened further when Kigoshi and co-workers synthesised a hybrid compound (**13**) in which the macrolactone of aplyronine A was

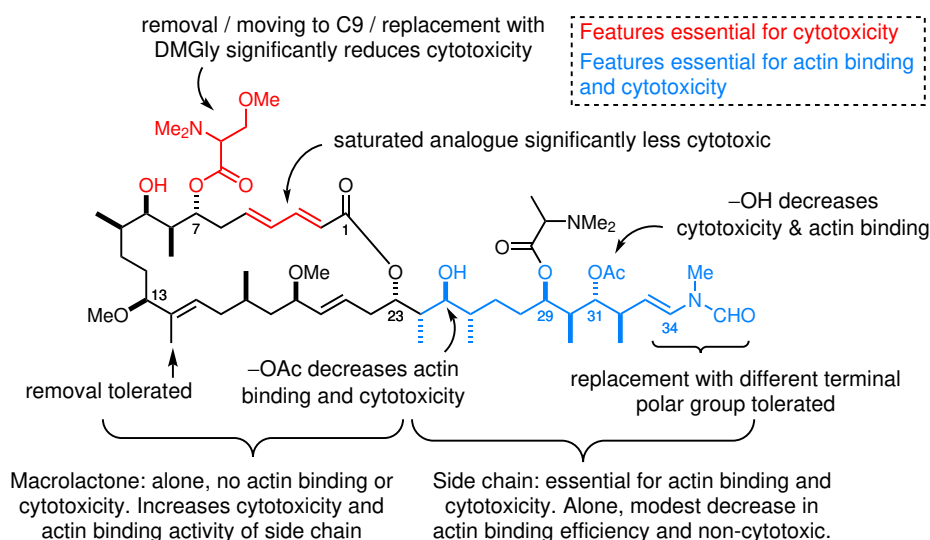


Figure 1.17: Summary of SAR studies on aplyronine A^{64,77–82}

fused with the side chain of mycalolide B (Figure 1.18).^{82–84} The researchers had hoped to achieve more potent actin-depolymerising activity and thus an improved cytotoxicity profile compared to aplyronine A. Instead they found no direct correlation between these two effects: although the hybrid showed somewhat more potent actin-depolymerising activity than aplyronine A, its cytotoxicity against HeLa-S3 cells was around 1000-fold lower.

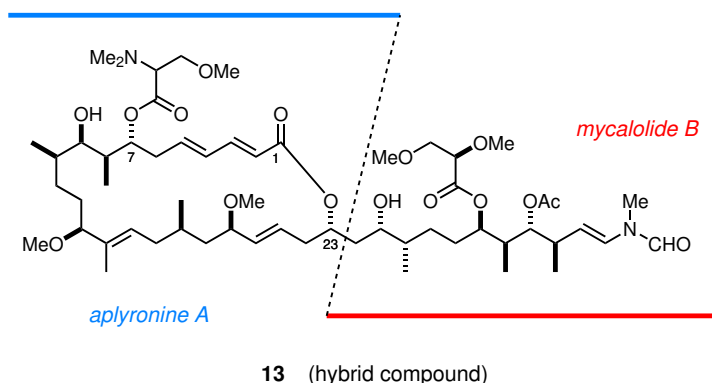


Figure 1.18: Kigoshi's aplyronine A–mycalolide B hybrid^{82,83}

In 2013, Kigoshi and co-workers made a breakthrough when they reported that aplyronine A forms an unprecedented 1:1:1 heterotrimeric complex with actin and tubulin, another abundant cell protein with vital functions as part of the cytoskeleton (Figure 1.19).⁵³ They suggest that after actin binding occurs, the trimethylserine moiety protruding into bulk solvent may generate a new tubulin binding site on the actin–aplyronine complex. Inhibition of tubulin dynamics, perhaps by capping microtubules or copolymerisation into the microtubule lattice, further destabilises cytoskeletal processes and eventually results in cell death (Figure 1.19).⁸⁵ Side chain ana-

logues designed to strongly bind actin may not necessarily produce the conformational changes required for this protein–protein interaction (PPI), which would account for the previously unpredictable relationship between actin binding efficiency and cytotoxicity. Its unique mode of action as a PPI inducer gives aplyronine A all the more potential as an anticancer therapeutic, as it could be applied to new disease indications and could help overcome known drug resistance mechanisms. Further studies will provide insight into the formation of this complex and the optimal functionalities needed to exploit the cytoskeletal depolymerising effect.

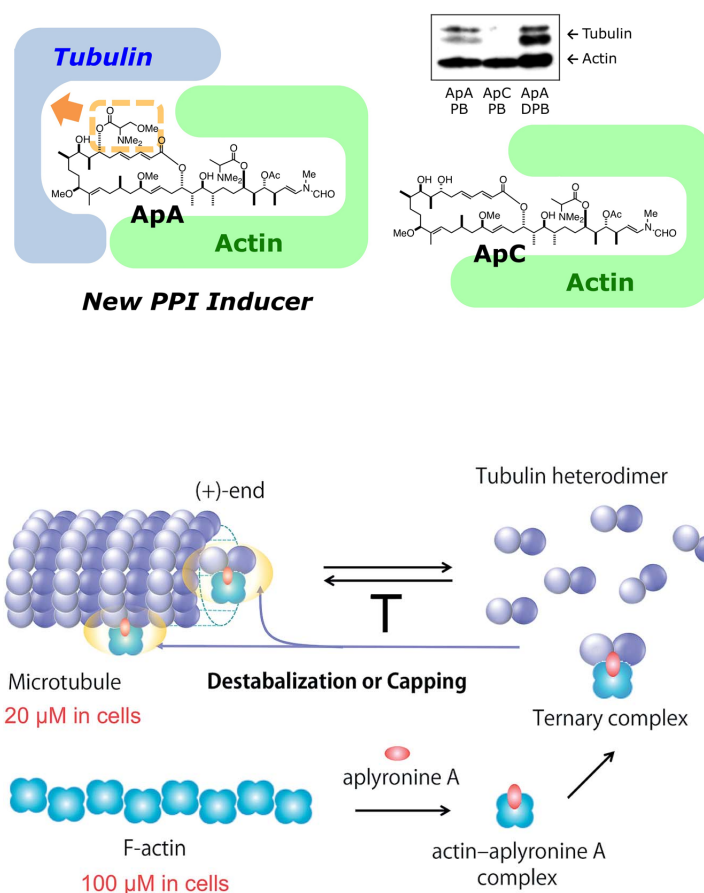


Figure 1.19: Heterotrimeric complex between aplyronine A, actin and tubulin,⁵³ and the proposed mechanism of microtubule assembly inhibition⁸⁵

1.4.4 Related actin-binding natural products

The aplyronine side chain bears a significant resemblance to those of a number of other potent actin-binding marine macrolides, notably reidispongioidide A (**14**), mycalolide B (**15**), and scytophycin C (**16**, Figure 1.20).^{72,86–88} These compounds all feature a complex macrolactone core

with a highly conserved 11-carbon hydrophobic side chain terminating in a polar *N*-methyl-*N*-vinylformamide group, with only minor differences in side chain functionality and stereochemistry. They bind actin at the same site, and exhibit a similar mode of action to aplyronine A (*vide supra*, Section 1.4.3).^{72,89,90} However, to date none of these natural products has been shown to induce formation of a ternary complex such as the aplyronine–actin–tubulin trimer described above.⁵³ This makes aplyronine A exceptional in its mechanism of action and a clear candidate for development towards new anticancer treatments.

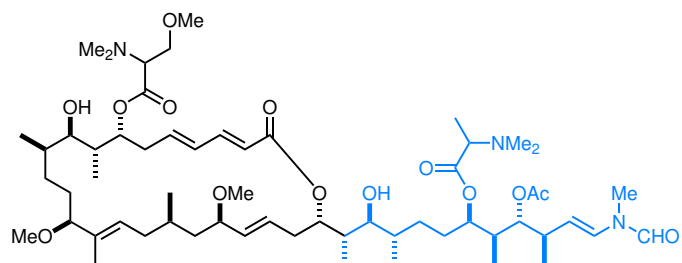
1.4.5 Analogue development

In order to further probe the biological activity and therapeutic potential of the aplyronines, it is proposed that novel analogues be developed. Ideally these “aplyrologues” would be structurally simpler than natural aplyronine A, whilst retaining or even improving its potent biological activity. This calls for a function-oriented synthetic approach (see Section 1.1). Simpler targets and more streamlined syntheses are of course preferable, especially if large-scale production is to ensue, due to the associated economies of time, effort, resources and environmental impact.¹⁷ Creating simplified analogues presents an opportunity to further increase the efficiency of the synthetic route developed in the Paterson group.

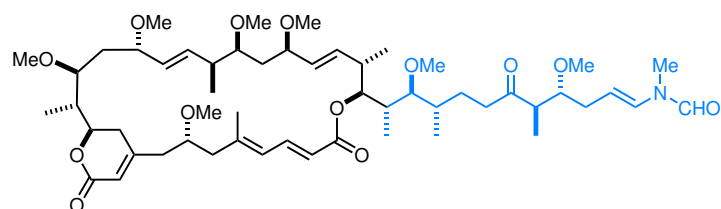
Discovery of one or more suitable analogues, in particular those which can be prepared easily and on large scale, will aid in the consideration of this family of natural products for development as ADC payloads. This process would also need to include consideration of the appropriate linker chemistry, which will require analysis of various analogues for their potency and stability. It is to be hoped that this process will produce an even better ADC payload candidate than aplyronine A.

1.5 Previous synthetic efforts

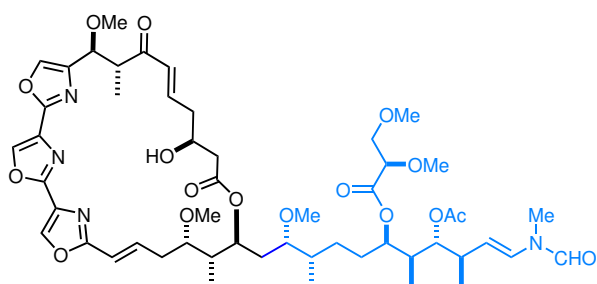
The first total synthesis of aplyronine A (**5**) was successfully brought to completion by Yamada and co-workers in 1994.^{2,58,61,62} This was swiftly followed by syntheses of congeners B and C from an advanced common intermediate, and provided confirmation of the structural and stereochemical assignments of all three natural products.^{63,77} In addition to delivering further material for biological testing, which was in short supply given the extremely low isolation yields, the synthesis also gave access to various analogues for use in SAR studies.^{78,79}



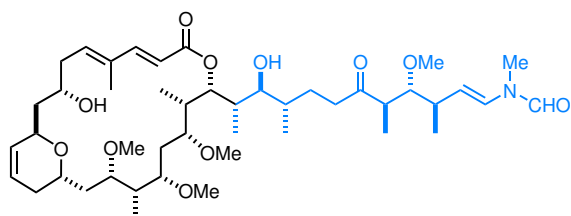
Aplyronine A **5**



Reidispongiolide A **14**



Mycalolide B **15**



Scytophycin C **16**

Figure 1.20: Selected actin-binding natural products with a characteristic side chain^{57,90}

Paterson and co-workers published the total synthesis of aplyronine C in 2013.⁹¹ The completion of aplyronines A and D followed.⁹² Marshall,^{93,94} Calter^{95–100} and Fuchs^{101–106} have carried out partial syntheses of aplyronine fragments, generally following the major disconnections of the Yamada and Paterson strategies. Recently, Kigoshi has also completed a revised total synthesis of aplyronine A, building upon the earlier mycalolide B hybrid synthesis (see Section 1.4.3).¹⁰⁷

1.5.1 Yamada approach

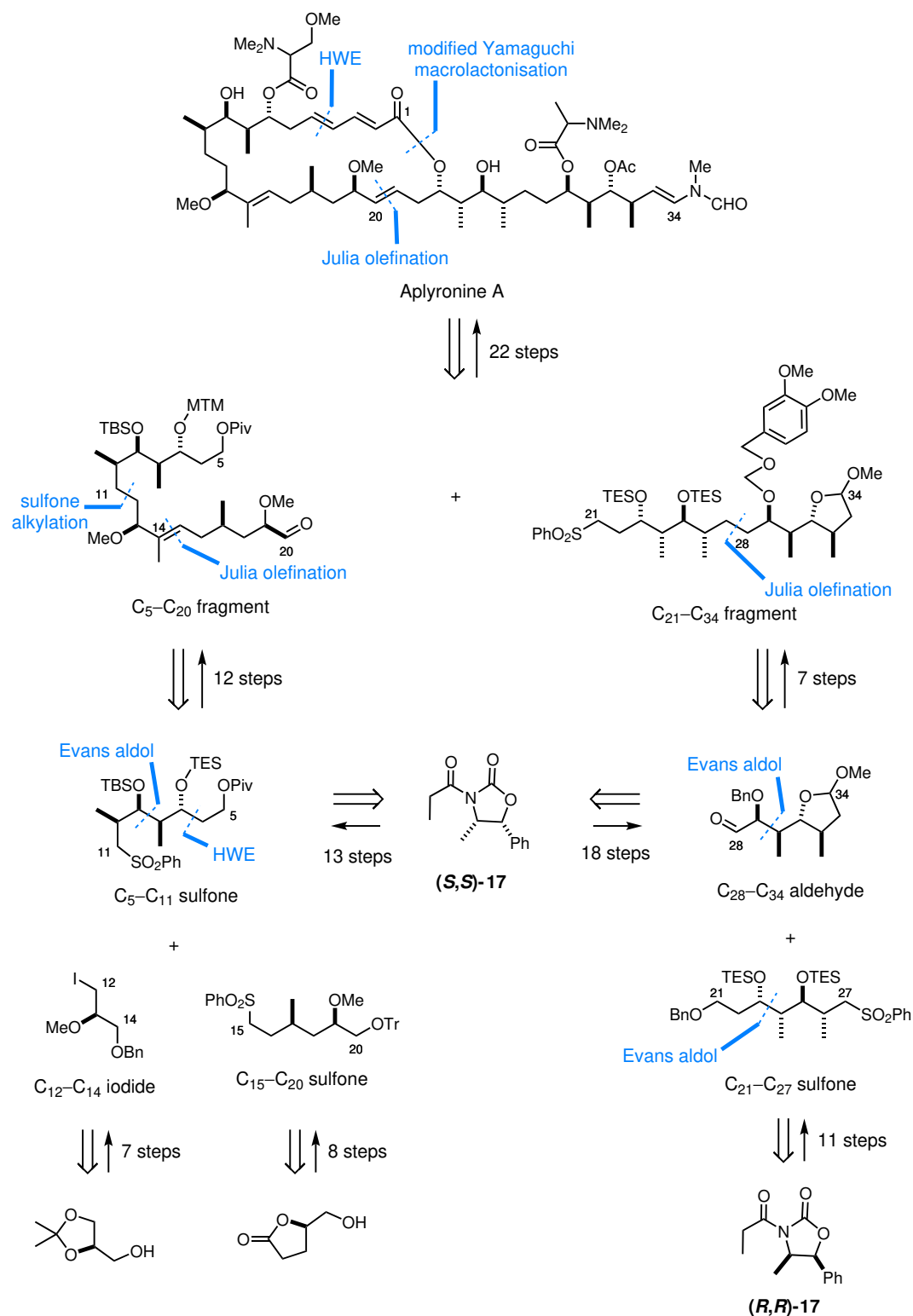
Yamada's synthetic approach relied upon a late-stage Horner–Wadsworth–Emmons reaction to install the (*E,E*)-dienoate, followed by a modified Yamaguchi macrolactonisation (Scheme 1.1). Other disconnections included sulfone alkylation and multiple uses of the Julia olefination to join the key fragments. The three stereotetrads were constructed using a common eight-step sequence involving Evans aldol methodology, starting from the appropriate enantiomer of oxazolidinone **17**, as well as the Sharpless asymmetric epoxidation.

Ultimately, the synthesis of aplyronine A required a total of 98 steps (47 steps LLS) and gave an overall yield of 0.39% from Evans imide (*S,S*)-**17**. The level of convergence in the route is to be commended, and its length justified by the need to be highly flexible in order to allow for any necessary modifications to the stereochemistry, which at the time remained unconfirmed. With the configuration confidently assigned, there remained much scope for improvement upon this first total synthesis of the aplyronines.

1.5.2 Paterson approach and modifications for analogue synthesis

Studies towards the total synthesis of the aplyronines in the Paterson group began in 1995, and are ongoing today. A key moment in this long-term project was the publication of the total synthesis of aplyronine C in 2013.⁹¹ Since that work, aplyronines A and D have also been completed as part of a scalable second-generation route, featuring a revised protecting group strategy.^{92,108} Specific details of the forward synthesis will be given in the text where relevant, but for context, a brief retrosynthetic overview is given here (Scheme 1.2).

An initial disconnection was to be a Keck esterification to attach the C₂₉ amino acid residue, revealing advanced fragment **18** that could be diversified to form different aplyronine congeners.



Scheme 1.1: Total synthesis of aplyronine A by Yamada and co-workers^{61,62}

The final esterification step would ambitiously rely on the greater reactivity of the less hindered C₇ hydroxyl over that at C₉.

In the early approach to aplyronine C,¹⁰⁹ it was envisaged that the C₂₇–C₂₈ bond would be accessible *via* HWE coupling of macrocyclic aldehyde **19** and β-ketophosphonate **22**. However, later work showed an aldol disconnection to be more appropriate, and in the successful synthetic route the coupling was achieved *via* the boron-mediated aldol reaction of **19** and ketone **23**. Important disconnections within the C₁–C₂₇ macrocycle **19** were a Yamaguchi macrolactonisation and HWE coupling to selectively install the (*E*)-trisubstituted olefin. This revealed the C₁–C₁₄ phosphonate **20** and C₁₅–C₂₇ aldehyde **21** as key fragments, in addition to the C₂₈–C₃₄ side chain fragment **23**.

Each of these three key fragments (**20**, **21** and **23**) contained a set of three or four contiguous stereocentres, which were efficiently constructed through a combination of substrate-controlled aldol reactions and 1,3-*anti* diastereoselective reductions. Of particular note was the use of all-*syn* tin(II) aldol methodology to set the C₂₃–C₂₆ and C₂₉–C₃₂ stereoclusters.¹¹⁰ Common starting materials were used to construct the three stereotetrads, with the required enantiomer of appropriately protected Roche ester derived ethyl ketone **24** or **26** inducing the desired absolute configuration (Figure 1.21). The remaining stereocentres were either sourced from the chiral pool (C₁₇) or installed by reagent-controlled reduction (C₁₃, C₁₉ and C₂₉).

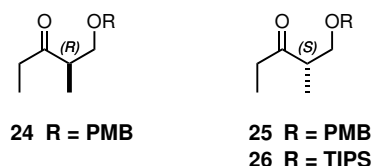
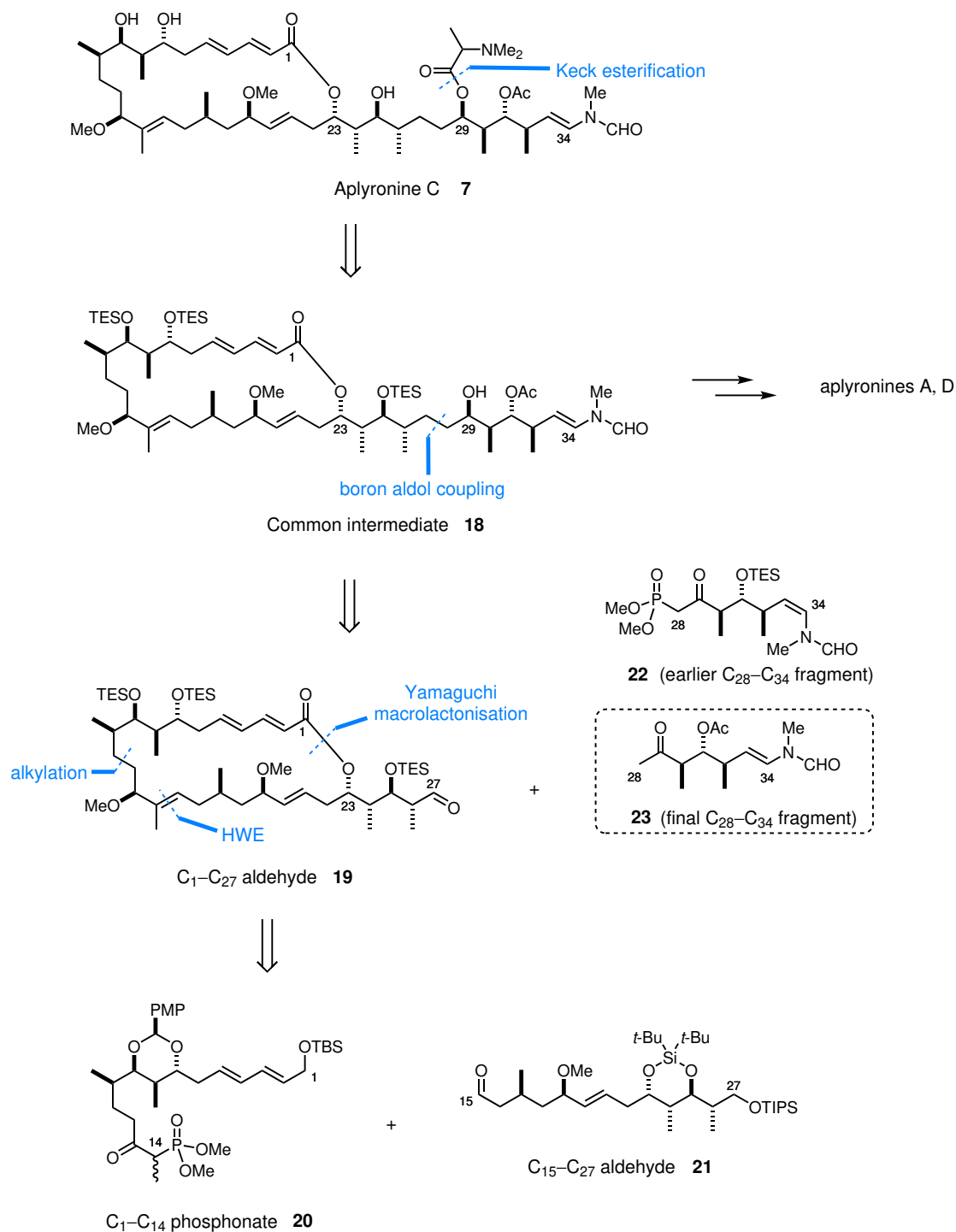


Figure 1.21: Roche ester-derived starting materials for construction of stereotetrads

This route gave access to aplyronine C (**7**) in 29 steps LLS and 3.6% overall yield from ketone **24**.¹¹¹ This compares favourably with the Yamada aplyronine A synthesis (47 steps LLS, 0.39% overall yield) which, as discussed, was necessarily lengthy. The group synthesis has since been improved during diversification and scale-up studies with a focus on streamlining the protecting group strategy. Although this led to a lower recorded overall yield of 2.7%, that figure represents a more realistic output on scales amenable to providing gram quantities of the aplyronines.^{92,108,112} As described in Section 1.4.5, further synthetic efficiencies were then anticipated through simplification of the scaffold in the development of analogues. The structural modifications we proposed are described below.

On the basis of SAR studies, the southern region of the aplyronine macrocycle does not appear



Scheme 1.2: Paterson approach to the total synthesis of the aplyronines

to make essential protein contacts in the actin or tubulin binding sites (see Figure 1.16, Section 1.4.3).^{53,64,71,78–82} It was therefore anticipated that simplifying this region of the molecule should have little effect on binding efficiency, whilst conferring a number of synthetic advantages. Altering the C₁₇–C₂₁ backbone to a plain hydrocarbon chain eliminates two stereocentres and an olefin from the original structure. This would remove the need to use a chiral starting material to supply the stereocentre at C₁₇ in the southern fragment, and avoid several synthetic steps.¹¹³

A challenging step in the Paterson aplyronine synthesis was the formation of the 24-membered macrolactone. Upon submission of the C₂₃/C₂₅ diol substrate to macrolactonisation (Scheme 1.2), the C₂₅ hydroxyl group was found to be the preferred reaction site, leading to an undesired 26-membered ring as the predominant product.¹¹⁴ Substituting this hydroxyl group for a methyl ether would block the site towards macrolactonisation, promoting reaction at the desired C₂₃ alcohol instead. This would improve synthetic efficiency by avoiding the need for an isomerisation step to form the desired 24-membered ring. Although the side chain region is key for actin binding affinity, it is reasonable to expect that this modification should not have a detrimental effect. In the related natural products reidispongiolide A and mycalolide B, a methoxy group replaces the equivalent C₂₅ hydroxyl group in the aplyronines (Figure 1.20, Section 1.4.4); these two natural products interact with actin with comparable binding efficiency,⁷² which suggests that this substitution should be well tolerated.

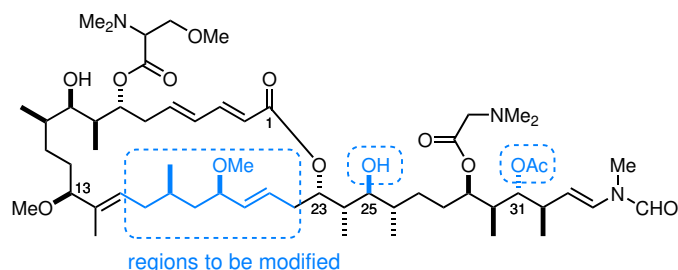
Similarly, reidispongiolide A and scytophycin C both feature a methoxy group in place of the aplyronines' C₃₁ acetoxy group. This was the source of many difficulties in the natural product synthesis, in most cases stemming from facile acetate elimination. Installation of a methoxy group in aplyronine analogues could help protect the site from undesired reactivity, as well as reducing the need to manipulate protecting groups.

1.6 Aims

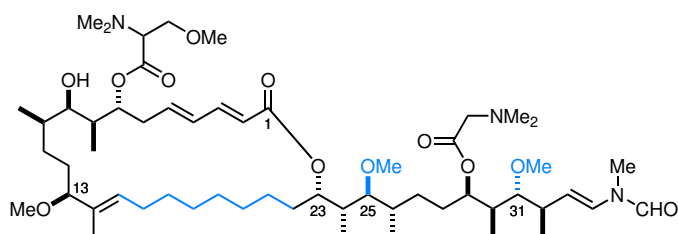
The key objective of this project was to devise and synthesise analogues of the aplyronines that retain the highly potent biological activity of the natural products while simplifying the scaffold and allowing for a more streamlined synthesis, enabling their use as novel payloads for ADCs. Three main modifications to the aplyronine structure were proposed (Figure 1.22):

- (1) simplification of the C₁₇–C₂₁ region to an unfunctionalised carbon chain, eliminating two stereocentres and an olefin;

- (2) replacing the C₂₅ hydroxyl group with a methyl ether; and
- (3) replacing the C₃₁ acetoxy group with a methyl ether.



Aplyronine D **8**



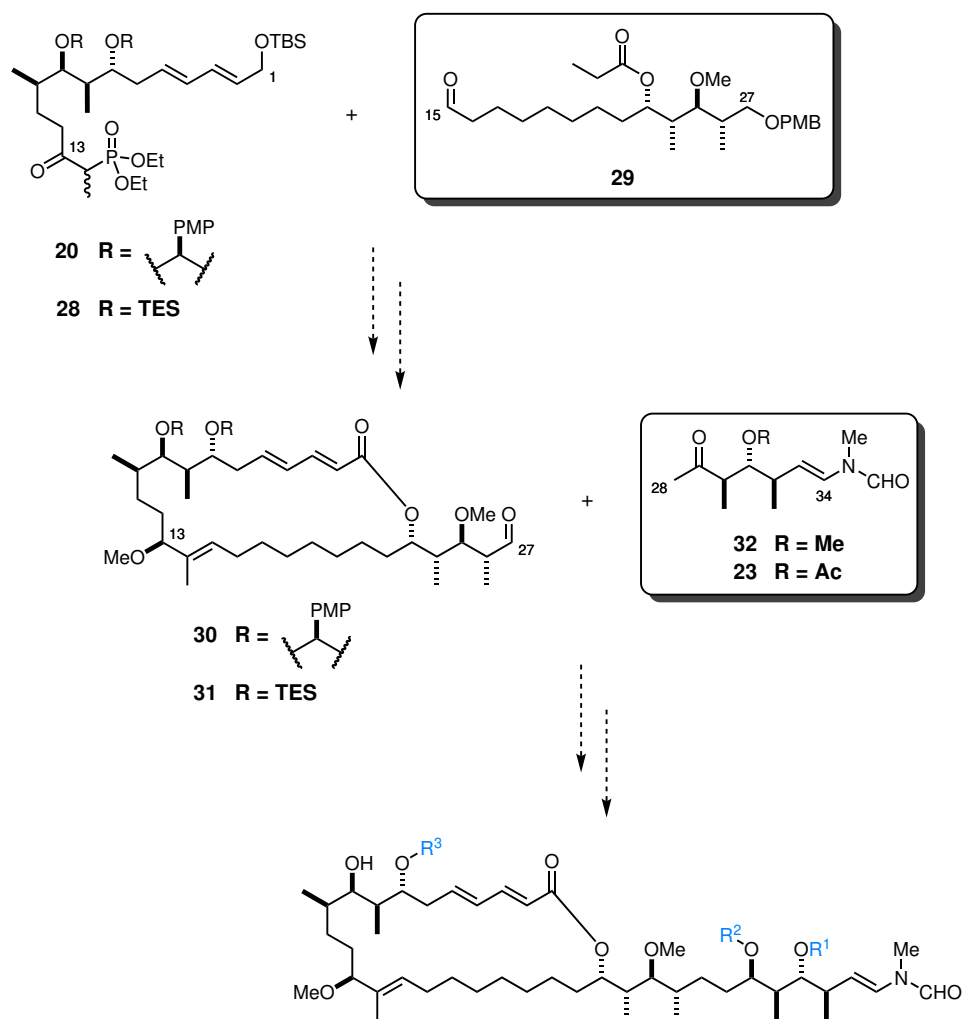
Target analogue **27**

Figure 1.22: Modifications to the aplyronine scaffold for analogue development

The proposed C₁₅–C₂₇ (**29**) and C₂₈–C₃₄ (**32**) analogue fragments were to be incorporated into the established Paterson aplyronine synthesis. HWE coupling of **29** to the C₁–C₁₄ fragment **20** or alternative target **28**⁹² and macrolactonisation steps to give the macrocycle (**30** or **31**) would be followed by aldol coupling with **32** and endgame modifications to give analogues (Scheme 1.3). The potential for late-stage diversification allows for the synthesis of a number of different analogues, particularly by varying the amino acids at C₇ and C₂₉. Furthermore, the side chain fragment could be varied, for instance by substituting natural product fragment **23** for analogue fragment **32** to give an analogue that retains the C₃₁ acetoxy group found in the natural product. Other modified fragments could be included with appropriate functionalisation for ADC linkage.

With a library of analogues in hand, we would need to carry out cytotoxicity assays to determine whether our synthesis-informed design had been successful in retaining biological function.

This thesis will discuss efforts towards these goals and the results achieved to date.



Scheme 1.3: Target fragments **20** (or **28**), **29** and **32** for assembly into a variety of analogues

Chapter 2

Synthesis of key fragments

2.1 Southern fragment analogue (C₁₅–C₂₇)

Two of the three modifications to the aplyronine structure **8** discussed in Section 1.6 are found in the C₁₅–C₂₇ region (Figure 2.1). The first goal of this work was therefore to efficiently synthesise the simplified fragment **29** on gram scale to provide enough material for further investigations and for elaboration to the full analogue. The key disconnections from the Paterson aplyronine synthesis were applied to take advantage of previously optimised chemistry. This would entail the use of a 1,4-*syn*-3,4-*syn* selective aldol reaction to install the correct stereochemistry at C₂₃ and C₂₄, followed by a substrate-controlled 1,3-*anti* reduction of the resulting β -hydroxy ketone. The C₁₅ aldehyde function would ultimately be necessary in the key fragment **29** for the planned coupling to the northern C₁–C₁₄ phosphonate in a HWE olefination.

2.1.1 Aldol coupling

The chiral ketone **33** required for the diastereoselective aldol reaction was accessed from commercially available (*S*)-Roche ester **34** in 3 steps (Scheme 2.1). The primary alcohol was protected as the benzyl ether (BnTCA, TfOH, 96%) and converted to Weinreb amide **36** (*N,O*-dimethylhydroxylamine hydrochloride, *i*-PrMgCl, 69%). The desired ketone **33** was then accessed *via mono*-addition of an ethyl Grignard reagent (EtMgBr, 75%).

The long-chain aliphatic aldehyde **39** was obtained in two steps (Scheme 2.2) by *mono*-protection of 1,9-nonanediol (**37**) as the PMB ether (PMBCl, NaH, TBAI, 72%)¹¹⁵ followed by Swern oxi-

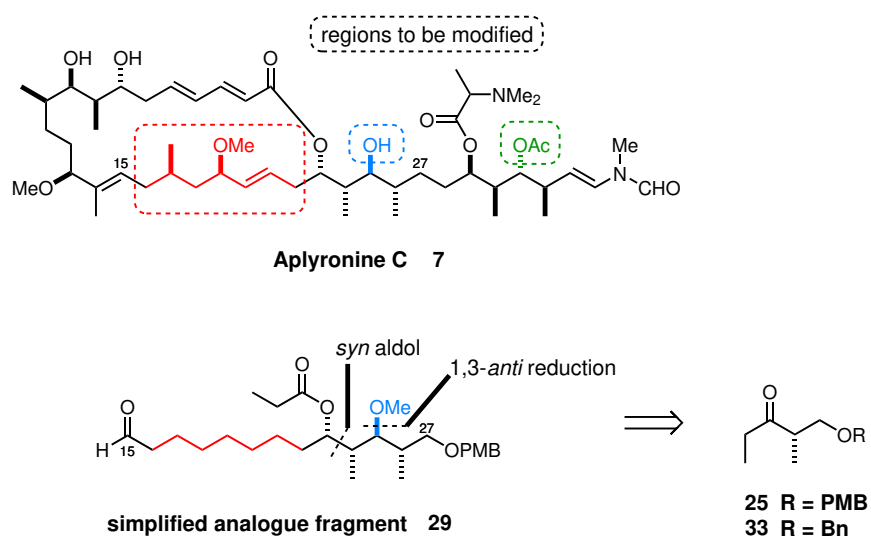
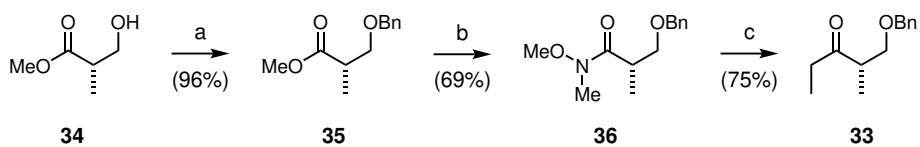


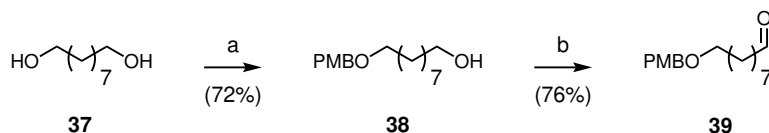
Figure 2.1: Comparison of aplyronine C (**7**) with analogue fragment **29**



(a) BnTCA, TfOH, Et₂O, 0 °C → rt, 2 h; (b) MeO(Me)NH·HCl, *i*-PrMgCl, THF, −15 °C, 16 h; (c) EtMgBr, Et₂O, 0 °C, 16 h

Scheme 2.1: Synthesis of ethyl ketone **33** from (*S*)-Roche ester **34**

dation (DMSO, COCl_2 , Et_3N , 76%).¹¹⁶ PMBCl was used as the limiting reagent in the presence of three equivalents of diol in dilute solution to favour *mono*-protection of the diol and minimise formation of a *bis*-PMB protected byproduct (*ca.* 6% observed). Conveniently, the excess starting material **37** was easily recovered by flash chromatography.



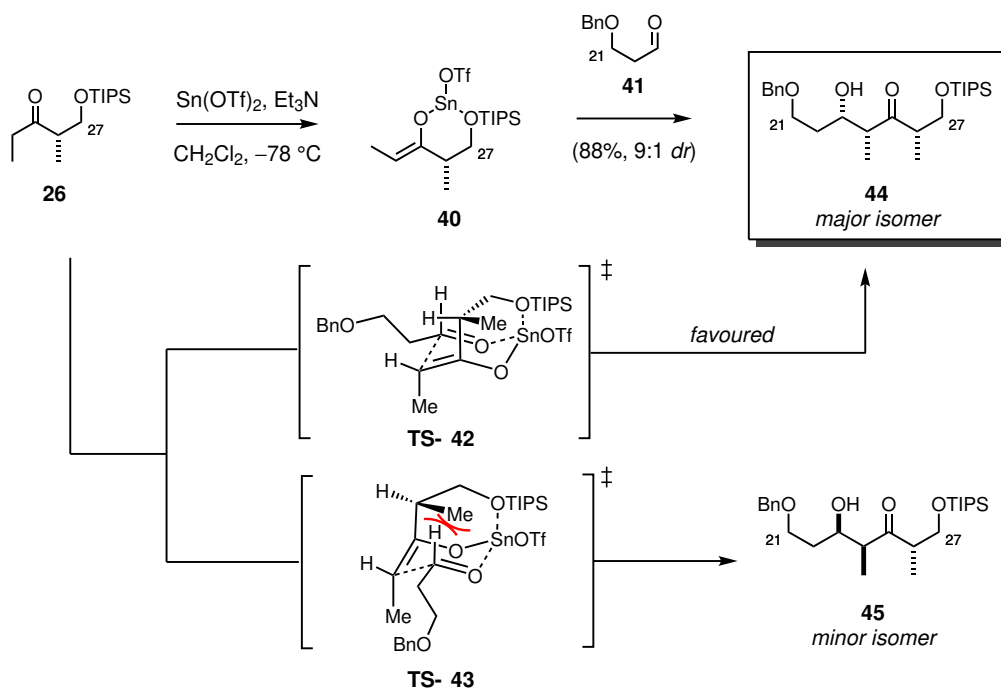
(a) PMBCl, NaH, TBAI, THF/DMSO (2:1), 0 °C → rt, 72 h; (b) DMSO, $(\text{COCl})_2$, Et_3N , CH_2Cl_2 , -78 °C → rt, 4 h

Scheme 2.2: Synthesis of aldehyde **39** from 1,9-nonanediol (**37**)

Attention then turned to the aldol coupling of ketone **33** and aldehyde **39**. In the Paterson aplyronine C synthesis, the C_{23} – C_{26} stereotetrad had been constructed using a $\text{Sn}(\text{OTf})_2$ mediated *syn* aldol reaction of chiral ketone **26** with aldehyde **41** to give adduct **44** in excellent yield (88%) and diastereoselectivity (9:1 *dr*).¹¹³ Selective formation of the (*Z*)-enolate **40** means that only two diastereomeric products are possible (Scheme 2.3). The Zimmerman–Traxler transition states¹¹⁷ **TS-42** and **TS-43** clearly show that the all-*syn* isomer **44** is the product of the less sterically congested **TS-42**. The high levels of stereoselectivity could be attributed to the conformationally restricted transition state, as the silyl ether oxygen is understood to be internally chelated to the Lewis-acidic tin centre.^{111,118}

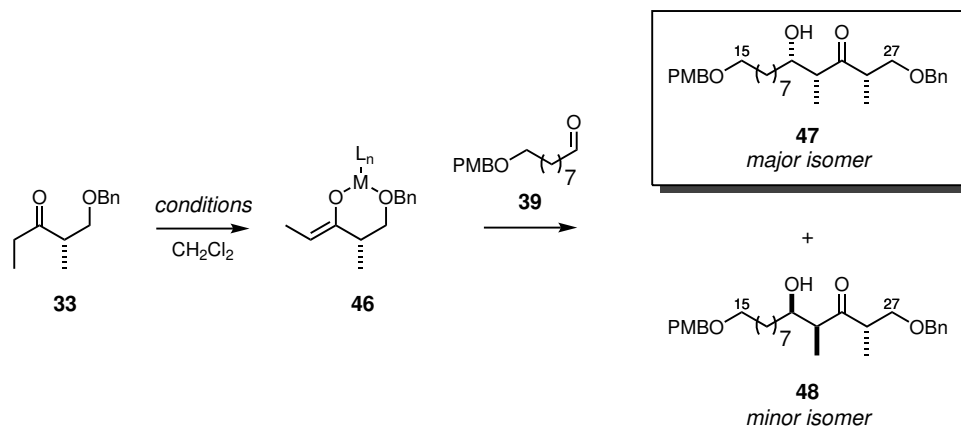
Despite this earlier success, however, a number of drawbacks are associated with the use of $\text{Sn}(\text{OTf})_2$. Asymmetric aldol reactions mediated by this Lewis acid appear to be highly dependent on reagent quality. The procedure followed to prepare the reagent is lengthy, typically taking 6–8 days, and involves hazardous reagents. Working with $\text{Sn}(\text{OTf})_2$ also brings disadvantages such as the formation of problematic emulsions upon aqueous workup and consequent generation of large volumes of toxic tin(II) waste. In this case, efforts to prepare the $\text{Sn}(\text{OTf})_2$ reagent were met with poor reagent quality, with attendant low yields and diastereoselectivity. These difficulties led us to reconsider the methodology for this aldol reaction. Results of initial testing with alternative Lewis acids are shown in Table 2.1.

A chiral boron reagent was considered based on earlier work in the Paterson group using ketone substrate **33**.¹¹⁹ For the boron aldol reaction, (+)- Ipc_2BOTf was selected as the Lewis acid in order to give the 1,4-*syn*, 3,4-*syn* aldol product **47** based on the literature precedent. The opposite enantiomer of the boron Lewis acid is expected to give the 1,4-*anti*-3,4-*syn* product **48** in aldol reactions with ketone **33**. It transpired that the product was difficult to separate chromatographically from IpcOH , a product of the reaction workup, which made accurate determination of the



Scheme 2.3: Tin(II)-mediated aldol coupling in the Paterson aplyronine C synthesis¹¹³

Table 2.1: Optimisation studies for aldol coupling of ethyl ketone **33** to aldehyde **39**



Entry	Conditions	Isolated <i>dr</i> (47:48) ^a	Yield ^b (%)
1	$\text{Sn}(\text{OTf})_2$, Et_3N , -78°C	—	nr
2	(+)- Ipc_2BOTf , $i\text{-Pr}_2\text{NEt}$, 0°C	3:1	79
3	$\text{Ti}(i\text{-PrO})\text{Cl}_3$, $i\text{-Pr}_2\text{NEt}$, -78°C	5:1	78
4	TiCl_4 , $i\text{-Pr}_2\text{NEt}$, -78°C	1:1	53

^a Based on ^1H NMR analysis of isolated material. ^b Overall yield of the diastereomeric mixture.

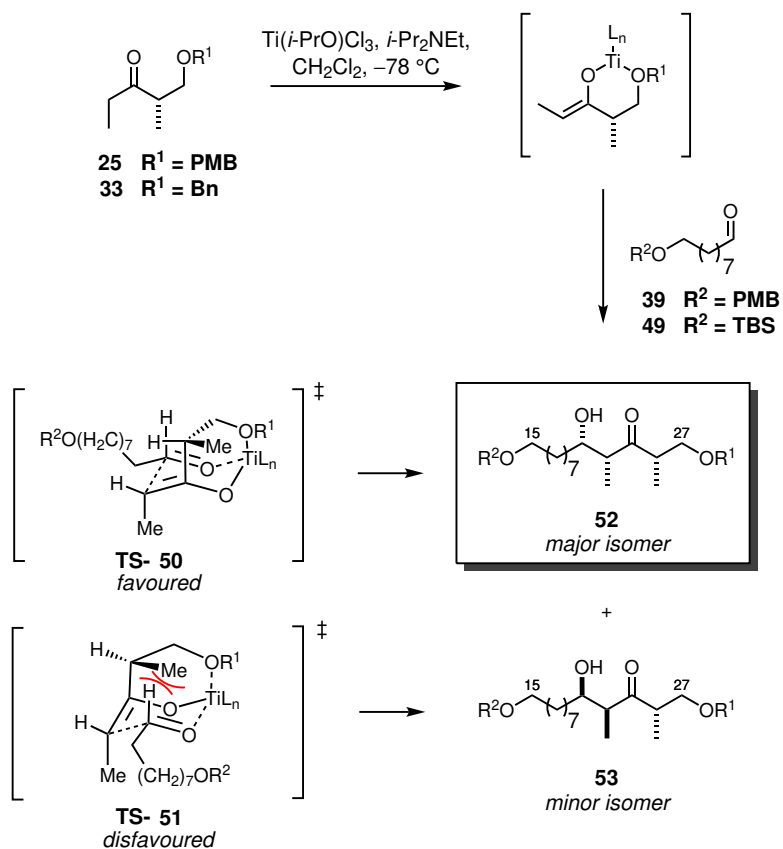
reaction yield difficult. Although this method may have shown better potential under further optimisation, this was deferred for the time being in order to investigate the prospect of using a titanium Lewis acid to effect the transformation.

Results in our group following a publication by Urpí, Romea and co-workers showed that titanium(IV) reagents offer a desirable alternative to tin(II) reagents to establish the 1,3,4-*syn* stereochemistry of the required product.¹²⁰ Urpí and Romea reported that titanium Lewis acids such as TiCl₄ and Ti(*i*-PrO)Cl₃ can be used to generate (*Z*)-enolates from ketones such as **33** at low temperature (Table 2.1). Upon reaction with an aldehyde, these will diastereoselectively give the 1,3,4-*syn* polypropionate motif.¹²⁰ These Lewis acids were tested, using *i*-Pr₂N₂Et as a base in CH₂Cl₂ at -78 °C (Table 2.1, entries 3 and 4). Consistent with Urpí's findings, Ti(*i*-PrO)Cl₃ showed promising results, giving a good yield (78%) and a diastereomeric ratio of 5:1. The more powerful Lewis acid TiCl₄ was found to give a non-synthetically useful ratio of diastereomers (1:1 **47/48**), along with a lower yield of aldol addition product. The softer Lewis acid was therefore settled upon as the best avenue for further investigation, based on its relative operational ease of use, reproducibility and the accessibility of the reagent. The respectable 5:1 *dr* was expected to be improved upon in the optimisation process.

The reaction is understood to proceed *via* a chelated transition state similar to that which has been described for Sn(OTf)₂ aldol reactions (see Scheme 2.3), enhancing the selectivity for the major isomer **52** *via* the favoured transition state **TS-50**.¹¹⁰ Formation of the minor isomer **53** is disfavoured due to its more sterically congested transition state **TS-51** (Table 2.2). Based on Lee's work on this reaction,¹¹⁸ it was hypothesised that the diastereoselectivity might be further improved by using a more electron-rich protecting group at the chelating β-hydroxy site, such as a PMB ether in place of the benzyl ether in **33**. This did not appear to be borne out by the results of this aldol coupling, however: a similar *dr* was achieved in each case (Table 2.2, entries 1–3). The main reason to reconsider the protecting group strategy arose from concurrent studies in the group suggesting that the benzyl ether at this position might later prove difficult to remove while leaving other functionality in the elaborated fragment intact.¹¹² Use of a PMB ether, which would be selectively cleavable in the presence of DDQ, therefore seemed preferable. This would necessitate a change in protecting group for aldehyde **39** for differentiation purposes. An orthogonal TBS ether was selected for this purpose due to its favourable properties with regards to ease and efficiency of protection and deprotection in the current system as well as stability under the required conditions. The required aldehyde **49** was synthesised in 2 steps (TBSCl, imidazole, 83%, then DMSO, (COCl)₂, Et₃N, 91%).

The selectivity of the Ti(*i*-PrO)Cl₃-mediated aldol (≥10:1 *dr*, 67% yield, Table 2.2) was akin

Table 2.2: Optimisation of titanium mediated aldol reaction to set C₂₃–C₂₆ stereochemistry



Entry	R ₁	R ₂	Scale (mg ketone)	Isolated <i>dr</i> (52:53) ^a	Yield (%) ^b
1	Bn	PMB	100	5:1	78
2	Bn	TBS	100	10:1	70
3	PMB	TBS	100	10:1	63
4	PMB	TBS	500	12:1	63
5	PMB	TBS	1600	10:1	67
6	PMB	TBS	3700	18:1	85

^a Based on ¹H NMR analysis of isolated material. ^b Overall yield of the diastereomeric mixture.

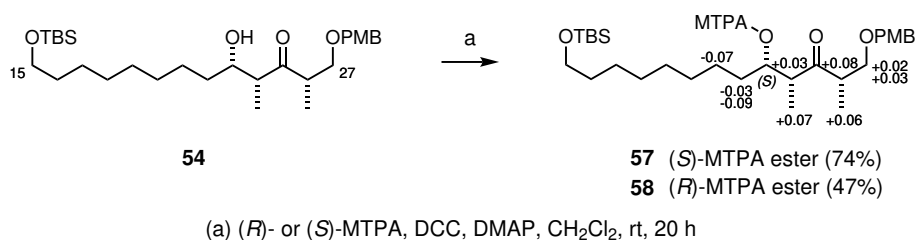
to that of the $\text{Sn}(\text{OTf})_2$ -mediated aldol reaction (9:1 *dr*, 88% yield) in the Paterson aplyronine C synthesis.¹¹³ The relative ease of carrying out this reaction made it vastly preferable to the tin(II) methodology, and much more amenable to scale-up. Interestingly, the yield and diastereoselectivity of the reaction with PMB ketone **25** were comparable to those of the benzyl ketone **33** with TBS-protected aldehyde **49** (Table 2.2, entry 2 *vs* entry 5). Nevertheless, the predicted difficulties in selectively removing the benzyl protecting group influenced us to proceed with a PMB protecting group strategy.

The moderate yields of the desired aldol adduct **54** could be partially explained by deprotection of either the PMB or TBS groups during the aldol reaction, giving small amounts of byproducts **55** and **56** (Scheme 2.4). This was not entirely unexpected, given the chance that the chelated titanium could promote cleavage of the electron-rich PMB ether. Similarly, titanium chelating to the C₁₅ oxygen could cause the silyl ether linkage to be cleaved. Fortunately, the resulting primary alcohols could be re-protected without difficulty to give the desired product **54** in 99% and 64% yield respectively. This amounted to an effective yield of 91% in initial studies. During later scale-up efforts, improved yields of the desired product **54** were recorded without the need for re-protection steps. The conditions were optimised by minimising the time of exposure of the substrates **25** and **49** to $\text{Ti}(i\text{-PrO})\text{Cl}_3$ (1.5 h), while keeping the other reaction conditions constant (*i*-Pr₂NEt, CH₂Cl₂, -78 °C, Scheme 2.4). In this way, a 3.5 g batch yielded 85% of **54** in 18:1 *dr* in a single manipulation (Table 2.2, entry 6; also Scheme 2.4).

The advanced Mosher method was used to rigorously confirm the configuration of the newly formed C₂₃-hydroxyl stereocentre. This method was first described by Mosher and co-workers^{121,122} and later extended to the use of high-field NMR systems by Kakisawa and colleagues.^{123–125} A chiral carbinol is derivatised with each enantiomer of α -methoxy- α -trifluoromethylphenylacetic acid (MTPA-OH) to form diastereomers, which differ by ¹H NMR spectroscopy. The relevant conformation is one in which the trifluoromethyl group, the ester carbonyl and the carbinol methine proton are *syn*-coplanar, such that the phenyl ring of the Mosher ester exerts a magnetic shielding effect on any protons on the same side of the plane (Scheme 2.5). In the (*S*)-MTPA ester, protons in substructure R¹ will be relatively more shielded than their equivalents in the (*R*)-MTPA ester, resulting in an upfield shift; the opposite is true for protons in substructure R². This difference in shift for the two diastereomers can be expressed as $\Delta\delta^{SR}$ ($\delta_S - \delta_R$). When calculated for as many protons on each side of the chiral alcohol as possible, the sign of this value is diagnostic for the position of each R-group relative to the MTPA plane.

Accordingly, the (*S*)- and (*R*)- Mosher esters **57** and **58** were prepared under Steglich conditions (DCC, DMAP)¹²⁷ according to the standard procedure (Scheme 2.6).¹²⁶ The signs for the

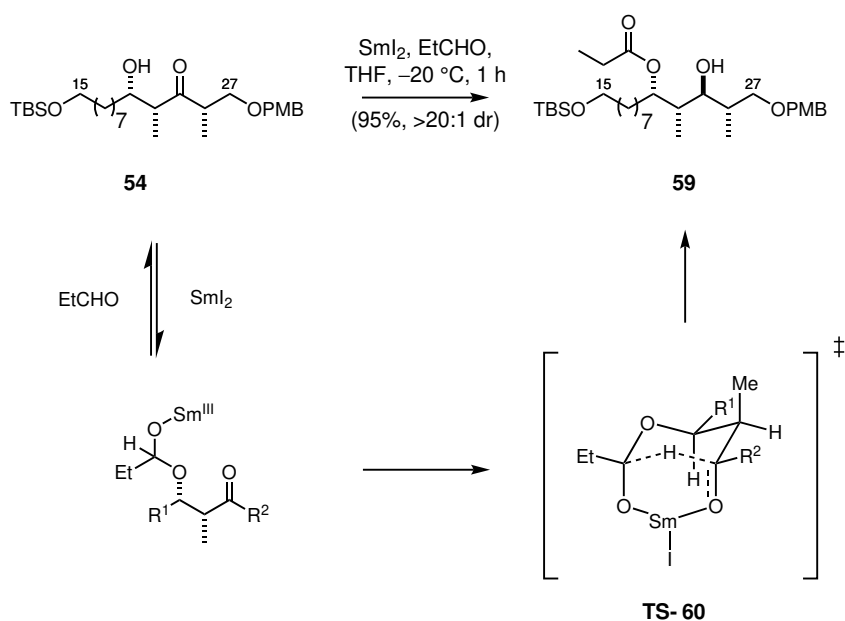
determined $\Delta\delta^{SR}$ values were consistent with the anticipated (*S*)-configuration at C₂₃.



Scheme 2.6: Determination of C₂₃ stereochemistry by formation of Mosher esters¹²⁶

2.1.2 1,3-*anti* reduction

With aldol adduct **54** in hand, a directed reduction of the C₂₅ ketone was carried out to set the configuration of the full C₂₃–C₂₆ stereotetrad. A number of selective 1,3-*anti* reduction approaches are available for β-hydroxy ketones, one such being the samarium-mediated Evans–Tishchenko reduction.¹²⁸ This protocol is renowned due to its ability to differentiate between the two resulting alcohols, in this case giving the C₂₃ propionate ester **59**. This would be required in order to selectively introduce the C₂₅ methyl ether modification for the proposed aplyronine analogues at the next step.



Scheme 2.7: Evans–Tishchenko reduction mechanism for β-hydroxy ketone **54**¹²⁸

The mechanism for the Evans–Tishchenko reduction is thought to involve intramolecular hydride transfer in a 6,6-chair-type hemiacetal transition state **TS-60** (Scheme 2.7).¹²⁸ Initially, SmI₂ is

oxidised to a Sm(III) species, evidenced by a change from the blue-green colour of Sm(II) to the yellow Sm(III) upon addition to propionaldehyde. Coordination of the aldehyde and hydroxy ketone to the metal centre and hemiacetal formation set the scene for the intramolecular hydride transfer from the hemiacetal to the carbonyl group *via* **TS-60**. Dissociation of the complex delivers the 1,3-*anti* diol with the directing hydroxyl protected as the propionate ester **59**.

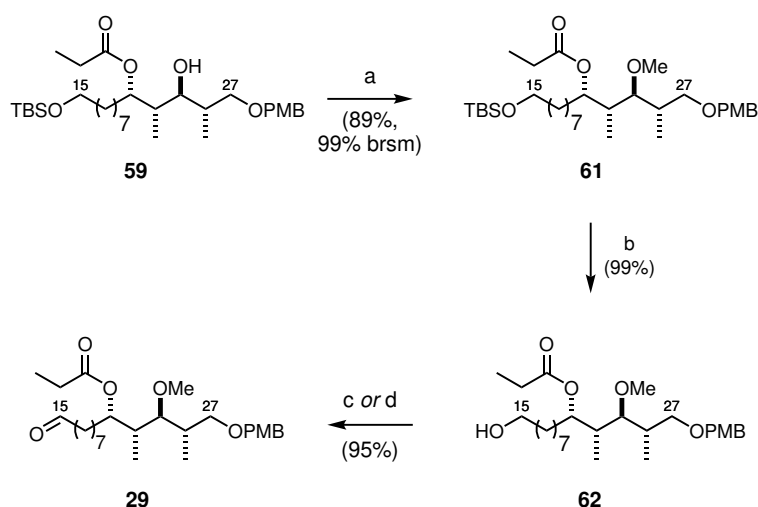
The reaction typically proceeds with very high stereochemical control due to the coordination of the oxophilic samarium to both the hemiacetal and ketone carbonyl oxygens. Even in the presence of α -methyl groups of either *syn* or *anti* configuration, the level of asymmetric induction from the β -hydroxy stereocentre dominates to reliably give the 1,3-*anti* product in high diastereomeric excess.

As anticipated, the selective reduction of ketone **54** using SmI₂ (10 mol%) and EtCHO on multi-gram scale proceeded to give **59** in excellent yield (95%) and diastereoselectivity (>20:1 *dr*). Although some past examples have shown migration of the propionate ester from the directing hydroxyl to the newly formed hydroxyl, such difficulties were fortunately not observed in this case.¹¹² Conveniently, the minor 1,4-*anti* diastereomer carried through from the aldol reaction was found to be more readily separable from the desired 1,4-*syn* product by flash chromatography after reduction to the corresponding diol monoester. With the full C₂₃–C₂₆ stereotetrad in place in **59**, further manipulation was now required to complete the desired C₁₅–C₂₇ fragment **29**.

2.1.3 Elaboration to the full C₁₅–C₂₇ analogue fragment

For the southern fragment analogue, a methyl ether was desired at C₂₅ in place of the hydroxyl group present in the natural aplyronines. Upon observing that the C₂₃ propionate ester moiety did not undergo undesired migration to the C₂₅ hydroxyl, the decision was taken to carry this through as the C₂₃ protecting group.

Methylation of C₂₅ alcohol **59** was carried out using Meerwein salt and Proton Sponge (Scheme 2.8). This reaction initially proceeded to give methyl ether **61** in very good yield on small scale (86% from 50 mg of **59**; 91% brsm). Some issues were encountered upon scale-up, with a drop in yield to 55% from 1 g of **59**. In addition, the reaction was reluctant to go to completion: after extending the reaction time to 16 h, starting material was still present by TLC analysis. These problems were ameliorated when the reaction time was reduced back to 4 h, as for the small-scale reaction. Under these conditions, the methylated product **61** could easily be



(a) Me₃O·BF₄, Proton Sponge, CH₂Cl₂, rt, 3 h; (b) THF/H₂O/3M HCl (5:2:1), rt, 1 h;
 (c) DMP, NaHCO₃, CH₂Cl₂, rt, 1 h; (d) DMSO, (COCl)₂, Et₃N, -78 °C → rt, CH₂Cl₂, 2.5 h

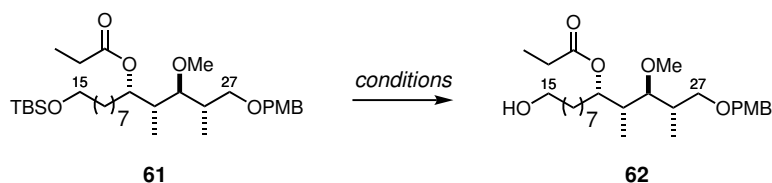
Scheme 2.8: Synthesis of the C₁₅-C₂₇ southern fragment analogue **29**

separated in very good yield from any remaining starting material, even on larger scale: a yield of 89% (99% brsm) of **61** was achieved on a batch of over 8 g.

The fully protected substrate **61** had been deliberately designed to allow selective deprotection at either the C₁₅ or C₂₇ ends in order to elaborate the fragment for coupling to the C₁-C₁₄ fragment in a HWE reaction or to the C₂₈-C₃₄ side chain *via* a boron-mediated aldol condensation. The HWE coupling was pursued first, as this approach had good precedent in previous aplyronine studies.¹¹⁴ The southern fragment-side chain coupling would subsequently be investigated by Rachel Porter.¹²⁹

A screen of conditions to selectively cleave the C₁₅ silyl ether protecting group in **61** was undertaken (Table 2.3). Despite concerns about the stability of the potentially acid-labile C₂₃ propionate ester, all methods were found to give the C₁₅ alcohol **62** in excellent yield without extraneous deprotection being observed. Simple THF/aqueous acidic conditions (Table 2.3, entry 3) were considered the most preferable due to the fast reaction time and operational ease, giving 93% yield of **62** on 32 mg scale and, eventually, 99% yield on 2 g scale. The final step was to oxidise the revealed primary alcohol in **62** to the C₁₅ aldehyde in fragment **29**. This was easily achieved under Dess-Martin (DMP, NaHCO₃) or Swern (DMSO, (COCl)₂, Et₃N) conditions to give **29** in almost quantitative yield (Scheme 2.8).

With fragment **29** in hand, two of the three modifications to the aplyronine skeleton discussed in Section 1.6 were set in place, ready for incorporation into the full analogues. Before this could

Table 2.3: Screen of conditions for deprotection of C₁₅ silyl ether **61**

Entry	Conditions ^a	Scale (mg)	Reaction time ^b	Yield (%)
1	cat. PPTS, MeOH	18	26 h	>99
2	TBAF (1.1 eq), THF	16	26 h	>99
3	THF/H ₂ O/3M HCl (5:2:1)	32	30 min	93
4	THF/H ₂ O/3M HCl (5:2:1)	2000	1 h	99

^a All reactions carried out at rt. ^b Time to completion by TLC analysis.

be constructed, however, stocks of the C₁–C₁₄ northern phosphonate **20** and C₂₈–C₃₄ side chain fragment **32** (see Scheme 1.3, p. 28) were required. Dr Mike Housden was preparing the required phosphonate for HWE coupling, for shared use between the analogue and natural product studies concurrently in progress in the group. Therefore, attention now turned to preparation of the side chain fragment **32** in a divergent synthetic approach that would allow for inclusion of a third modification to the native aplyronines, which could be incorporated into analogues.

2.2 Side chain analogue (C₂₈–C₃₄)

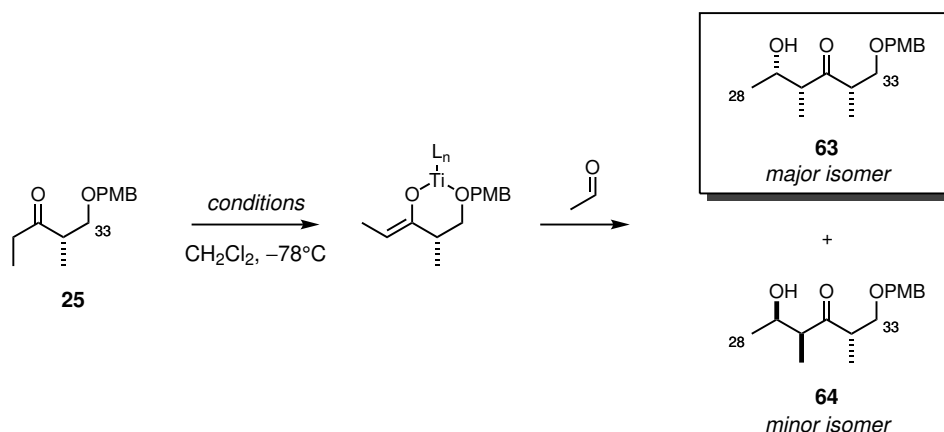
Since the completion of the Paterson aplyronine C synthesis, stocks of the C₂₈–C₃₄ fragment **23** had been depleted during further investigations. In order to provide sufficient material to advance this project and other aplyronine work concurrently being undertaken in the group, it was therefore necessary to re-synthesise this fragment on multi-gram scale. This brought opportunities to investigate the parallel titanium aldol chemistry in place of the previously used tin aldol reaction, and to explore the route towards a side chain analogue with methyl ether functionality at C₃₁.

2.2.1 Titanium aldol coupling

As discussed in Section 2.1.1, ongoing issues with Sn(OTf)₂ made an alternative method for the aldol coupling an alluring prospect. Given the success achieved with Ti(*i*-PrO)Cl₃ as the Lewis acid in the 1,3,4-*syn* selective aldol reaction in the southern fragment, employing a similar

protocol was expected to deliver pleasing results. With plentiful stocks of the (*S*)-ethyl ketone **25** in hand at the time, preliminary studies of the titanium aldol reaction with acetaldehyde were carried out on the enantiomeric substrate to establish the feasibility of this approach. The reaction was performed on various scales to probe reproducibility and scalability (Table 2.4) before progressing to the desired (*R*)-enantiomer of the Roche ester-derived ketone **24**.

Table 2.4: Titanium-mediated aldol coupling of ketone (*S*)-**25** with acetaldehyde



Entry	Conditions	Scale (ketone 25)	Isolated <i>dr</i> (63 : 64) ^a	Yield (%) ^b
1	Sn(OTf) ₂ , Et ₃ N	2.18 g	15:1	97 ^c
2	Sn(OTf) ₂ , Et ₃ N	200 mg	3.5:1	30
3	Ti(<i>i</i> -PrO)Cl ₃ , <i>i</i> -Pr ₂ NEt	200 mg	14:1	77
4	Ti(<i>i</i> -PrO)Cl ₃ , <i>i</i> -Pr ₂ NEt	560 mg	15:1	82
5	Ti(<i>i</i> -PrO)Cl ₃ , <i>i</i> -Pr ₂ NEt	2.00 g	12:1	>80 ^d

^a Based on ¹H NMR analysis of isolated material. ^b Overall yield of the diastereomeric mixture.

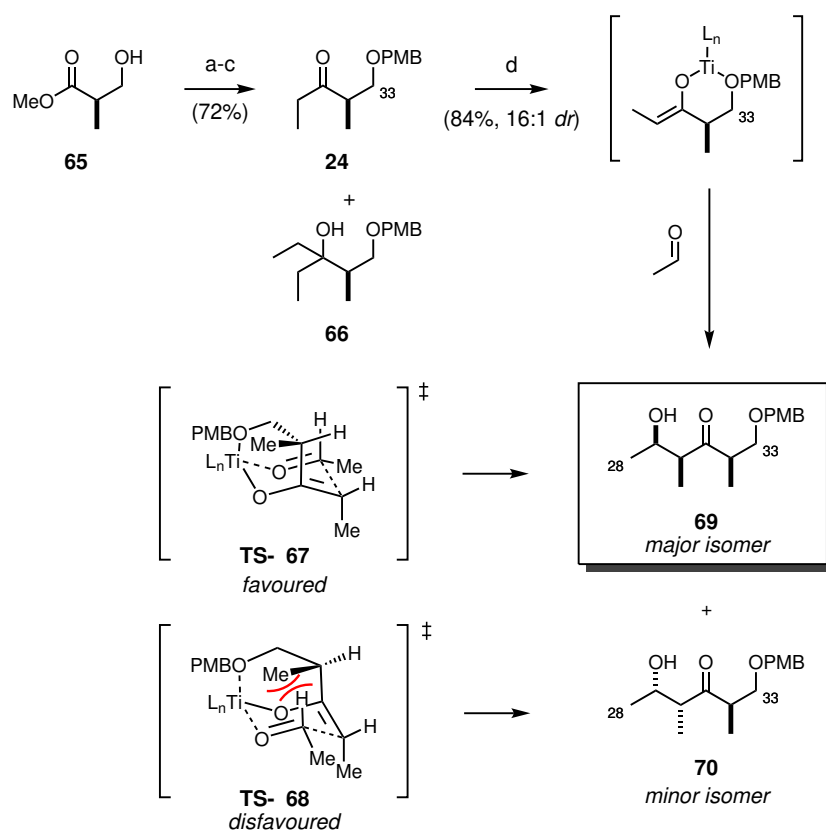
^c Results reported by Fink.¹¹¹ ^d Some product lost after purification.

Fink had previously noted that the diastereoselectivity of the reaction was dependent on the quality of tin(II) triflate (Table 2.4, entry 1), and this finding was indeed borne out in these studies. Difficulties in procuring good quality reagent meant that the author was unable to replicate the previous covetable result (entry 2).

Gratifyingly, the titanium methodology gave a very good yield and selectivity for the formation of adduct **63** on multi-gram scale. The diastereoselectivity of this reaction (12–15:1 *dr*) was comparable to that previously achieved with tin(II) (15:1 *dr*).⁹¹ Yields for this reaction appeared to improve somewhat upon scale-up (Table 2.4, entries 3–5).

Thus, the correct enantiomer of aldol adduct **69** was subsequently prepared as shown in Scheme 2.9. PMB protection of (*R*)-Roche ester **65** with PMBTCA and PPTS (88%; 95% brsm) was followed by conversion to the Weinreb amide (94%) and addition of the Grignard reagent

to give the ethyl ketone **24** (87%). A small amount of inseparable byproduct **66** (16:1 **24/66**) was generated during the Grignard addition, perhaps due to the large scale and attendant difficulty in maintaining constant low internal temperature for the exothermic reaction. However, this byproduct could be carried through the aldol step without deleterious effect and afterwards was readily removed by flash chromatography.



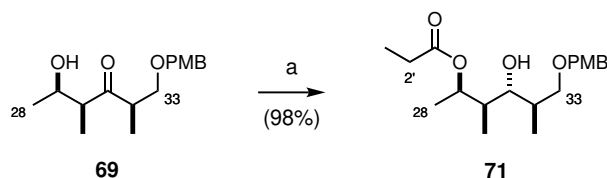
(a) PMBTCA, PPTS, CH_2Cl_2 , $0\text{ }^\circ\text{C} \rightarrow \text{rt}$, 16 h; (b) $\text{MeO}(\text{Me})\text{NH}\cdot\text{HCl}$, $i\text{-PrMgCl}$, THF, $-15\text{ }^\circ\text{C}$, 2.5 h; (c) EtMgBr , Et_2O , $0\text{ }^\circ\text{C}$, 3 h; (d) $\text{Ti}(i\text{-PrO})\text{Cl}_3$, $i\text{-Pr}_2\text{NEt}$, CH_2Cl_2 , $-78\text{ }^\circ\text{C}$, 1 h

Scheme 2.9: Preparation of ketone **24**, and titanium aldol reaction with acetaldehyde in the correct enantiomeric series

The proposed transition states **TS-67** and **TS-68** are analogous to those described earlier for titanium(IV) in Table 2.2 and tin(II) in Scheme 2.3. As discussed previously, the less congested transition state **TS-67** is favoured, resulting in isolation of the all-syn aldol product **69** in 84% yield and 16:1 *dr* on multi-gram scale (Scheme 2.9). The identity of the major isomer **69** was confirmed by comparison of NMR and optical rotation data to the previously made tin(II) aldol product.^{91,111}

An Evans–Tishchenko reduction of the aldol adduct **63** was also tested in order to establish conditions for the more valuable substrate **69**. The results were pleasing, giving product *ent*-**71**

in 84% yield and very high selectivity for the 1,3-*anti* diol monoester (>20:1). These conditions (SmI₂, EtCHO) were therefore applied in the desired enantiomeric series (Scheme 2.10), and even showed an improvement to 98% yield on scale. This provided over 7 g of intermediate **71** with the full stereotetrad in place to supply further studies.



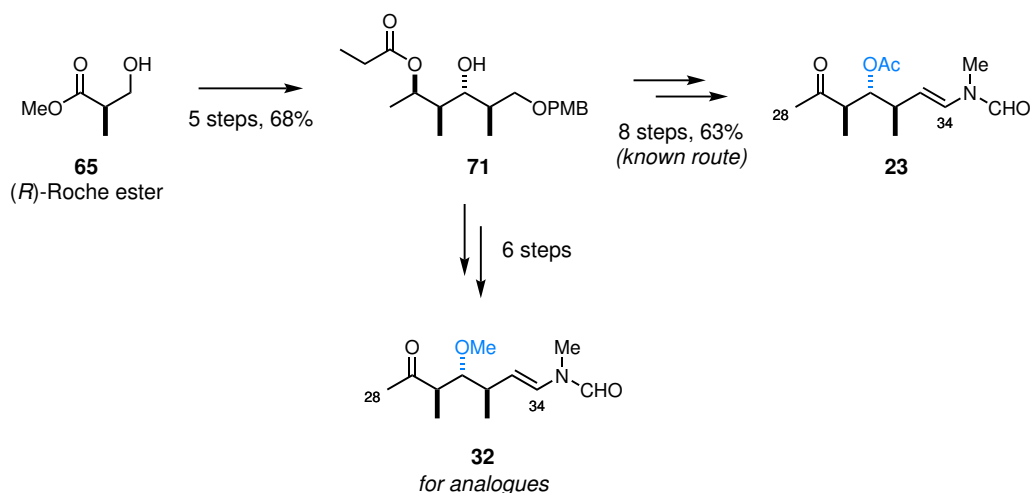
(a) SmI₂, EtCHO, THF, -20 °C, 1.5 h

Scheme 2.10: Evans–Tishchenko reduction of C₂₈–C₃₃ aldol adduct

2.2.2 Diversification to natural and analogue side chain components

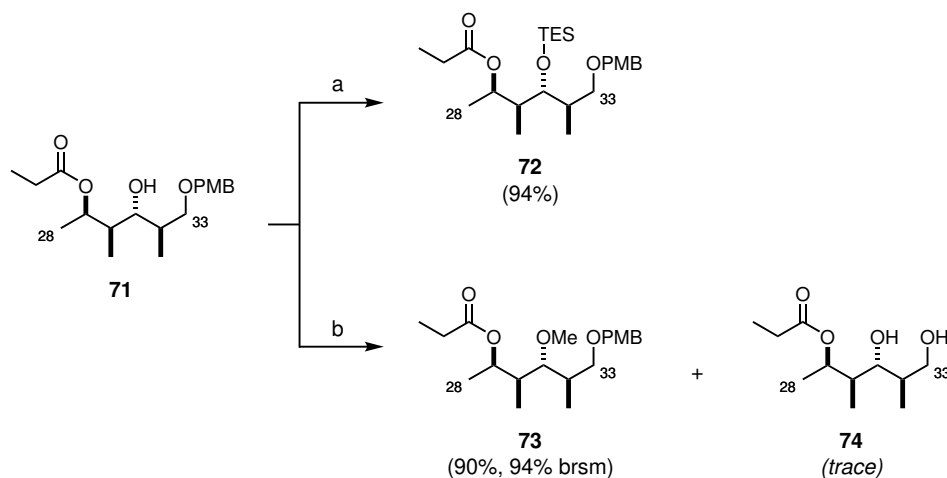
The C₃₁ alcohol **71** represented a key branching point in our plan for synthesising the differentially functionalised natural and analogue fragments. From this point, we could either carry on to the C₃₁ acetate fragment **23** *via* the known route in 8 steps,⁹¹ or to the methyl ether-containing fragment **32** in a proposed 6 steps (Scheme 2.11). The shorter route is, of course, more attractive from a step economy point of view. Two steps could be saved by avoiding a protecting group manipulation that was found to be necessary for the elimination-sensitive acetate ester. A more robust methyl ether group was expected to survive the required conditions without further protection. This would therefore lead to a saving of the time and cost of resources for these protection steps. As detailed in Section 1.5.2, the methyl ether was expected to be equivalent to the acetate ester in terms of actin binding efficiency, as evidenced by its presence in the similar actin-binding natural product reidispogiolide A.

For the present work, therefore, the analogue fragment **32** was to be prepared. Nevertheless, ongoing studies in the group towards the natural products would eventually require access to fragment **23**. Thus, the material was split equally across the two routes. Half of the material was protected as the triethylsilyl ether **72** under standard conditions (TESOTf, 2,6-lutidine, 94%, Scheme 2.12) and set aside for use elsewhere.^{92,112} The remainder was converted to the C₃₁ methyl ether **73** using Meerwein salt and Proton Sponge (90%, 94% brsm). This reaction proceeded smoothly and the product could readily be stored at -20 °C for many months without significant degradation, allowing its direct use in subsequent steps without further purification. On some occasions, diol **74** was isolated as a minor byproduct, possibly resulting from a Lewis



Scheme 2.11: Diversification from common intermediate **71** to fragment **23** via the known route⁹¹ or analogue fragment **32**

acid-type PMB cleavage during the workup procedure.¹³⁰ However, the byproduct was present in very low quantities (0–2%), and was easily removed by flash chromatography.

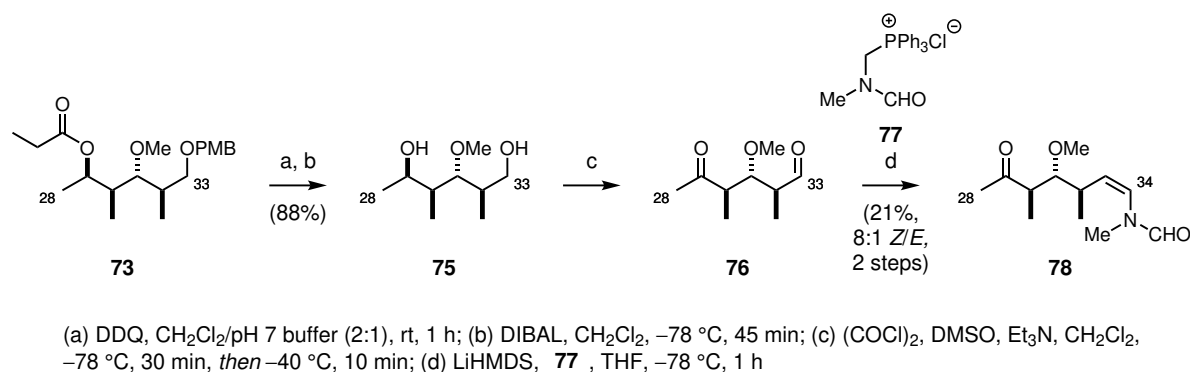


(a) TESOTf, 2,6-lutidine, CH₂Cl₂, -78 °C, 1.5 h; (b) Me₃O-BF₄, Proton Sponge, CH₂Cl₂, rt, 4 h

Scheme 2.12: Division of material towards silyl ether **72** for natural product fragments and methyl ether **73** for analogues

2.2.3 Preliminary investigations towards *N*-vinylformamide installation

From this point, it was necessary to install the *N*-methyl-*N*-vinylformamide moiety at the C₃₃ end, and a ketone functionality at the C₂₉ position for later fragment coupling. Dr Sarah Fink



Scheme 2.13: Introduction of *N*-methyl-*N*-vinylformamide moiety in compound **78**

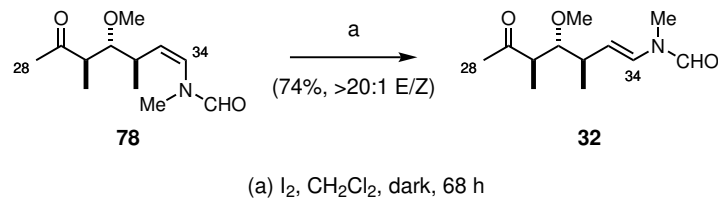
had found that the most efficient way of doing so was by using a double Swern oxidation, which would concurrently oxidise a C₂₉ alcohol to a ketone and a C₃₃ alcohol to an aldehyde, without risking formation of a cyclic hemiacetal *via* any reactive intermediates.^{111,116} Thus, the protecting groups were cleaved from each end of the substrate (DDQ, then DIBAL, Scheme 2.13) to give diol **75** in 88% yield over 2 steps. The Swern oxidation was then carried out under standard conditions (DMSO, (COCl)₂, Et₃N), taking care during the workup to wash away any triethylamine hydrochloride salt from the product which could quench the ylid in the subsequent Wittig reaction. The crude material was then used immediately to minimise the risk of epimerisation of either of the two α -chiral carbonyls.

After trialling a number of conditions to append the challenging *N*-methyl-*N*-vinylformamide unit, Fink had achieved the best results by using phosphonium salt **77** to form the ylid for a Wittig reaction.¹¹¹ This generated the required alkene, but as expected favoured the (*Z*)-substituted product (8:1 *Z/E*), and hence required isomerisation to the thermodynamically favoured *E*-product. Fortunately, conditions were found to effect this isomerisation in quantitative yield.

This transformation had proven to be impossible with the C₃₁ acetate in place, necessitating the use of a TES ether. However, we were hopeful that the methyl ether would prove resistant to elimination and reproduce the success of Fink's synthesis (63% over 8 steps from intermediate **71**) while saving two steps.

Thus, aldehyde **76** was reacted with the ylid from **77** at low temperature to obtain alkene **78** (21% over two steps from diol **75**, 8:1 *Z/E*). This mixture of double bond isomers was then stirred with catalytic iodine in the dark for 68 h (Scheme 2.14), at which point ¹H NMR analysis showed full conversion to the (*E*)-enamide **32** (74% isolated yield). At this stage, the low yields of these two steps were attributed to the small scale and exploratory intent of the reactions, and were confidently expected to improve upon further investigation. However, it soon transpired

that the Swern-Wittig transformation brought challenges that had been foreshadowed by Fink's previously arduous efforts.



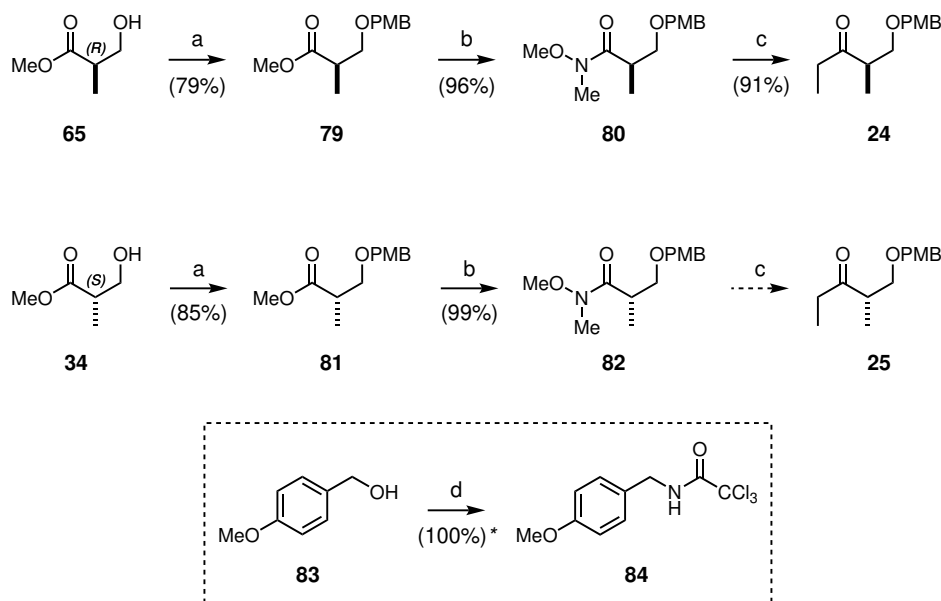
Scheme 2.14: Isomerisation of (*Z*)-*N*-vinylformamide **78** to the desired (*E*)-*N*-vinylformamide **32**

It was at this point that Rachel Porter joined the project, and expanded upon these very preliminary results in much more detail.¹²⁹ The full particulars of her work on this challenging fragment and its further applications in the synthesis of aplyronine analogues will be discussed in an upcoming publication.¹³¹ Ultimately, Porter was able to complete the efficient synthesis of side chain fragment **32** in 5 steps and 57% yield from fully protected intermediate **73**. This provided a reliable route to multi-gram stocks of the fragment which could be returned to on a number of occasions when further material was needed.

2.2.4 Process scale synthesis of Roche ester ethyl ketone

During the course of this project, an opportunity arose to undertake the large-scale synthesis of intermediates using the process chemistry facilities at AstraZeneca's Macclesfield campus. We decided to target the two enantiomers of PMB-protected Roche ester ethyl ketone, **24** and **25**. These chiral starting materials provide the basis for the diastereoselective synthesis of the three polyketide stereotetrads in our aplyronine analogues. They are also common intermediates in a number of total syntheses under investigation in our group. Having a stockpile of these precursors would allow us to access complex intermediates more directly, bypassing the need to carry out the three-step synthesis every time. A batch of 100 g of each enantiomer of Roche ester was generously provided for the purpose of constructing these two key intermediates *via* the three-step route outlined in Scheme 2.15.

To accomplish this, it would be necessary to make a number of modifications to the procedure generally used in our research laboratory. The typical workflow for this process would involve four chromatographic purification steps, comprising an alumina-based flash column to isolate the reagent *p*-methoxybenzyl trichloroacetimidate (PMBTCA, **84**), and a silica column after



(a) **84**, PPTS (25 mol%), CH_2Cl_2 , 20 °C, 4 h; (b) *i*-PrMgCl, $\text{MeO}(\text{Me})\text{NH}\cdot\text{HCl}$, 2-MeTHF, -10 °C, 5 h;
 (c) EtMgBr, 2-MeTHF, -10 °C, 18 h; (d) Cl_3CCN , DBU (1 mol%), CH_2Cl_2 , 20 °C, 1 h
 * Conversion determined by GC analysis

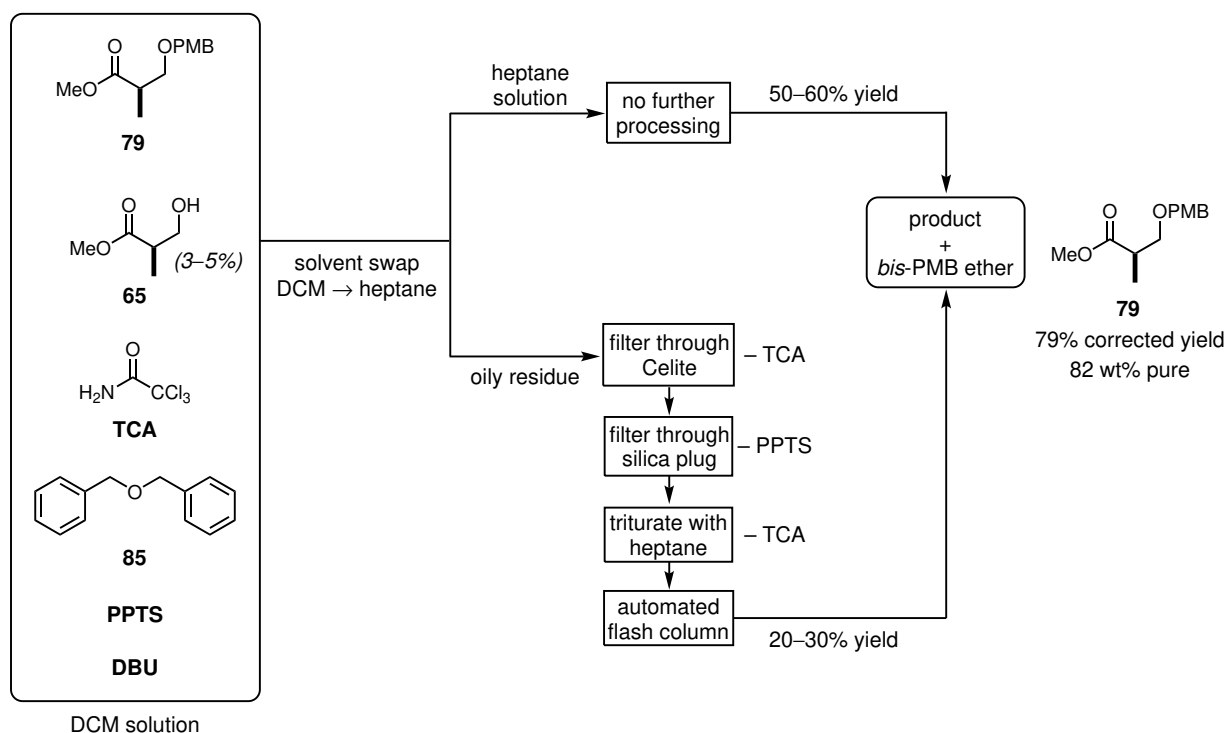
Scheme 2.15: Large-scale synthetic route to access the key fragments **24** and **25**

each reactive step. The goal of this process-scale synthesis was to accomplish the transformation without any chromatography steps. In many cases this might be achieved simply and practically by crystallisation methods, but not so here: all of the intermediates exist as oils under standard laboratory conditions. The challenge, therefore, would be to devise a method which would cleanly provide each intermediate in the synthesis, with full conversion of starting materials, and allow its separation from any other components of the reaction mixture that could cause problems at the next step. As part of this method development, we planned to make use of more process-friendly solvents: for instance, substituting the diethyl ether commonly used on small scale for the non-peroxidisable solvent methyl *tert*-butyl ether (MTBE). The process efficiency of the route was to be improved by using high reaction concentrations, minimising the use of solvents as far as possible.

The first step, it transpired, was to be the most challenging with regards to the aims laid out above. It was necessary to protect the Roche ester hydroxyl as a PMB ether before exposing the substrate to Grignard reagents, but the PMBTCA reagent can be readily hydrolysed, returning the *p*-methoxybenzyl alcohol (PMBOH, **83**) starting material. A new method was needed to telescope the reagent directly into the protection step, ideally without carrying through any PMBOH, which would be undesirable in the later Grignard steps. Most of the methods attempted did not

achieve full conversion of PMBOH. Despite conscientious efforts, we were unable to replicate the conditions used by Novartis researchers in their 70 kg synthesis of **81** as an intermediate for discodermolide (PMBOH, NaH, Cl_3CCN , MTBE).²⁴ After trialling various conditions, it was found that using catalytic DBU (PMBOH, DBU, Cl_3CCN , CH_2Cl_2)¹³² gave full conversion of PMBOH to PMBTCA in under 1 h, monitored by GC analysis. The DBU loading could be dropped as low as 1 mol% without any decrease in conversion or reaction rate.

The Roche ester starting material **65** (or **34**) could then be added directly to the reaction mixture, and acidification with the mild acid pyridinium *p*-toluenesulfonate (PPTS) catalysed the conversion to **79** or **81**. A number of acid catalysts (PPTS, camphorsulfonic acid, *p*-toluenesulfonic acid) were screened, and portionwise addition of 25 mol% PPTS over 2–6 h was found to give the best conversion of the Roche ester starting material. Nevertheless, full conversion was evasive as there was always a risk of self-attack of the PMB reagent to form *bis*-PMB ether **85**, and the reactions generally stalled with 3–5% Roche ester remaining. Thus, the reaction vessel at this point contained a mixed solution of product **79**, starting material **65**, byproduct **85**, DBU, PPTS, and trichloroacetamide ($\text{Cl}_3\text{CCONH}_2$) in dichloromethane (Scheme 2.16).



Scheme 2.16: Workup procedure for the PMB protection of Roche ester **65**

The workup for this step was challenging, and was eventually divided into a number of steps. First, a batch solvent swap distillation replaced the CH_2Cl_2 solvent with *n*-heptane. This re-

sulted in a heptane fraction which contained approximately 50–60% yield of the product **79** as well as some *bis*-PMB ether **85**. This could be concentrated and used directly in the next step, as the byproduct is unreactive and can readily be removed at a later stage. The remainder formed an oily residue which could be separated and purified by filtration and trituration to remove the trichloroacetamide (TCA), followed by a simple gradient flash column to isolate a further 20–30% of the desired product and recover the remaining starting material **65**. Thus, our objective to complete this synthesis without any form of chromatographic purification was not met in the end. Nevertheless, the gradient column method could be automated to ultimately obtain the product with a minimal investment of further practical effort. The overall corrected yield for this reaction, determined by quantitative NMR analysis, was 79–85%.

From this point, the next two steps were carried out with relative ease. To form the Weinreb amide **80**, *i*-Pr-MgCl (2.0 M in THF) was used as a base to deprotonate Weinreb salt MeO(Me)NH·HCl in the presence of PMB-protected Roche ester **79** in 2-MeTHF. The temperature was controlled to –10 °C or below *via* active cooling through a jacketed vessel. Upon completion, as determined by GC analysis, the reaction was quenched with aqueous NH₄Cl, and a simple extraction allowed the isolation of product **80** in 96–99% corrected yield.

Difficulties with reagent supply hampered the completion of the final step to provide ethyl ketone **24** on the full batch of material. However, it was possible to carry out this step on a 30 g batch to demonstrate the feasibility of this approach. Thus, EtMgBr (3.4 M in 2-MeTHF) was added slowly to **80**, controlling the internal temperature to below –10 °C to ensure mono-addition of the Grignard reagent. Again, an aqueous quench and biphasic extraction were all that was needed to obtain the desired ethyl ketone as a viscous oil (78.7 wt% **24**) in 91% corrected yield. The mass balance of the resulting oil was comprised of the *bis*-PMB ether **85** carried through from the first step and residual solvent (2-MeTHF). This material was later submitted directly to aldol reactions in our research laboratory, giving yields comparable to those obtained with column-purified starting materials.¹³¹ The highly non-polar contaminant **85** could be removed by silica chromatography after the aldol reaction. The same was true of the Weinreb amide material, which could also be diverted to other useful intermediates, such as forming the methyl variant in place of the ethyl ketone.^{133,134}

By this route, a stockpile of useful intermediates for our aplyronine synthesis and other projects in our group were generated in high yields and large quantities (Table 2.5). These materials have been stored at –20 °C for over 1 year to date without significant degradation. This has provided a convenient reserve which has been drawn upon as needed to further our research goals.

Table 2.5: Stocks resulting from large-scale synthesis efforts

Material	Compound	Quantity
(<i>R</i>)-Roche ester (recovered)	65	3.5 g
(<i>S</i>)-Roche ester (recovered)	34	3.5 g
(<i>R</i>)-Weinreb amide	80	200 g
(<i>S</i>)-Weinreb amide	82	190 g
(<i>R</i>)-ethyl ketone	24	26 g

2.3 Northern fragment (C₁–C₁₄)

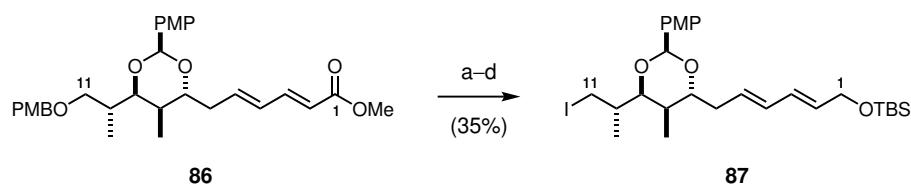
The third and final fragment which would be needed to construct our aplyronine analogues was to be the northern fragment. The northern region of the molecule is understood to play a key role in promoting the interaction of the actin–aplyronine complex with tubulin. Indeed, SAR studies on aplyronine A had shown that modifications to the C₇ amino acid or saturation of the dienoate have deleterious effects on the activity of the compounds.⁷⁸ We therefore planned to retain this region intact from the existing Paterson synthesis of the natural products.

Nevertheless, this left two feasible options open, resulting from the extensive studies that had previously been undertaken in the group. At the time this work commenced, an earlier synthetic route utilising a *para*-methoxyphenyl (PMP) group to protect the C₇ and C₉ alcohols was in use in the group, concurrently with a more recently developed strategy involving *bis*-TES protection of the same diol. These were both being investigated for studies towards a more efficient total synthesis of the natural products. Fortunately, this meant that intermediates for each were available to allow access to the required coupling partners in relatively short order. Since it was unclear at this early stage which of the two would be the better for an analogue synthesis, we set about testing both fragments to determine the best way forward.

2.3.1 PMP-protected northern fragment synthesis

For initial testing, phosphonate **20** was prepared from intermediate **86** (Scheme 2.17), which was generously provided by Rachel Porter. The synthesis of this fragment was carried out according to the established protocol¹¹³ and was analogous to that of the *bis*-TES fragment, which will be summarised below (Section 2.3.2).

The conversion into the required phosphonate was achieved in 5 steps (Scheme 2.17 and Scheme 2.20). Firstly, a primary iodide was needed at the the C₁₁ position to act as a leav-

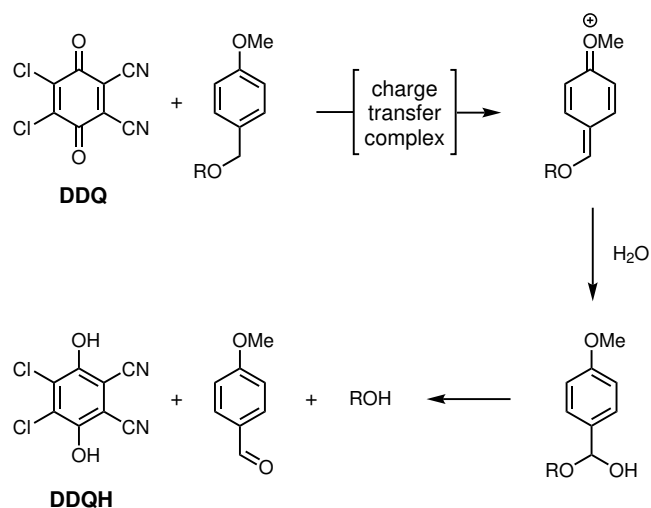


(a) DDQ, CH₂Cl₂/pH 9.2 buffer, rt, 30 min (65%); (b) PPh₃, imidazole, I₂, Et₂O/MeCN (1:1), 0 °C → rt, 2h (82%); (c) DIBAL, CH₂Cl₂, -78 °C, 1.5 h (72%); (d) TBSOTf, 2,6-lutidine, CH₂Cl₂, -78 °C, 1 h (92%)

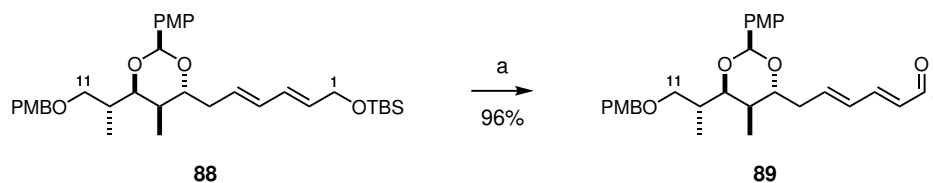
Scheme 2.17: Synthesis of iodide **87** in 4 steps *via* the established route

ing group in the later alkylation step. This was achieved by oxidative cleavage of the primary PMB ether (DDQ, CH₂Cl₂/pH 9.2 buffer (4:1), 65%) followed by an Appel-type substitution (PPh₃, I₂, imidazole, 82%) to install the iodide.¹³⁵ In the PMB deprotection step, pH 9.2 buffer was needed in place of the standard pH 7 solution to inhibit migration of the PMP acetal to the terminal C₉/C₁₁ diol promoted by weakly acidic DDQH (Scheme 2.18).^{118,136} The methyl ester at the C₁ end was then fully reduced to the primary alcohol (DIBAL, -78 °C, 72%) and protected as the TBS ether under standard conditions (TBSOTf, 2,6-lutidine, 92%). It was necessary to carry out the procedure in this order, as opposed to forming the potentially more sensitive iodide last. Formation of the allylic TBS ether before exposing the substrate to DDQ to remove the PMB group would have risked competitive deprotection and oxidation of the silyl ether, giving rise to the kinetically favoured dienal **89** (Scheme 2.19). Indeed, this serendipitous discovery by Dr Michael Woodrow in the course of the aplyronines project was to be capitalised upon later in the synthesis to give access to the seco-acid needed to close the macrolactone.¹³⁷ At this stage, however, such a transformation was not desired, and as such the fragment was prepared in the order shown. The iodide could successfully be carried through the two synthetic steps, but was indeed found to degrade upon storage in the freezer for more than a few weeks. Thus, it was best to store material at earlier or later stages as was needed at any given time.

From the protected iodide **87**, it was then possible to install the requisite β-ketophosphate moiety *via* a substitutive alkylation with linker piece **90**, according to the conditions of Grieco.¹³⁸ This had proven to be a challenging step in previous aplyronine studies, particularly for Dr Lydia Lee,¹¹⁸ who found that the product tended to form as a mixture of regioisomers (**20** and **91**, Scheme 2.20). This was contrary to the expectation of much greater reactivity at the less sterically hindered (and less acidic) terminal position, based on Grieco's findings. After extensive optimisation studies, the best result for this transformation as reported by Lee was 88% yield with a 4:1 ratio of **20** and undesired regiomer **91**. This reaction was regularly performed on batches of 200–400 mg of iodide **87**. Fortunately, the method turned out to be reproducible, reliably giving a synthetically useful yield (effectively 70%) of the desired phosphonate **20**. It also ensued that



Scheme 2.18: Mechanism for the deprotection of electron-rich PMB ethers with DDQ¹³⁶

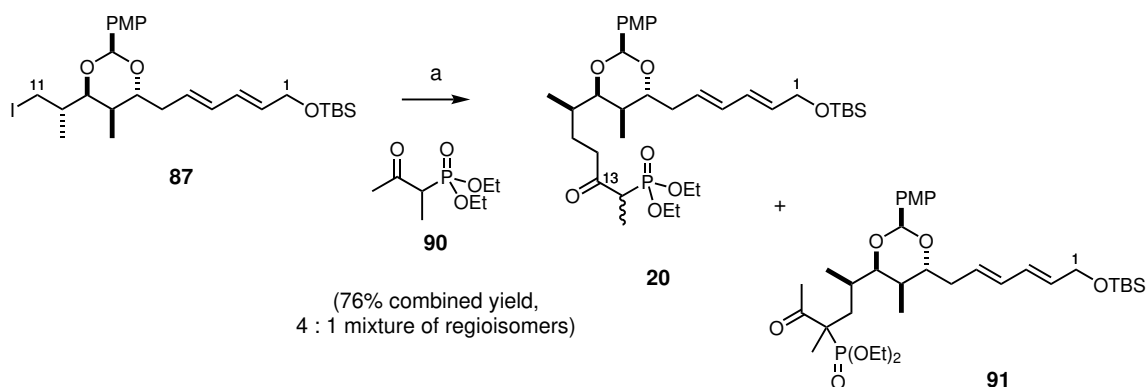


(a) DDQ (1.0 eq), CH₂Cl₂/pH 7 buffer, 0 °C → rt, 30 min

Scheme 2.19: Woodrow's discovery of the kinetically favoured deprotection and oxidation of electron-rich silyl ether **88**¹³⁷

the unwanted minor regioisomer was unreactive in the immediately subsequent HWE coupling step, and could readily be separated from the coupled product afterward. This outcome was therefore considered workable for the ongoing synthesis.

Thus, the reaction was carried out under the conditions established by Lee.¹¹⁸ The dianion was formed from **90** using NaH followed by *n*-BuLi at 0 °C, and was then added to the iodide **87** at –78 °C in the presence of HMPA. The reaction was encouraged to go to completion by warming gradually to –10 °C. This enabled the isolation of product **20** and the undesired regioisomer **91** in 76% combined yield as a 4:1 mixture that was inseparable by column chromatography. This was comparable with Lee's results, providing sufficient quantities of phosphonate **20** to continue investigations, and thus attempts to optimise this protocol were left to a later stage (*vide infra*, Section 2.3.2).



(a) **90** , NaH, THF, 0 °C, 30 min, then *n*-BuLi, 0 °C, 30 min, then **87** , HMPA, THF, –78 → –10 °C, 3h

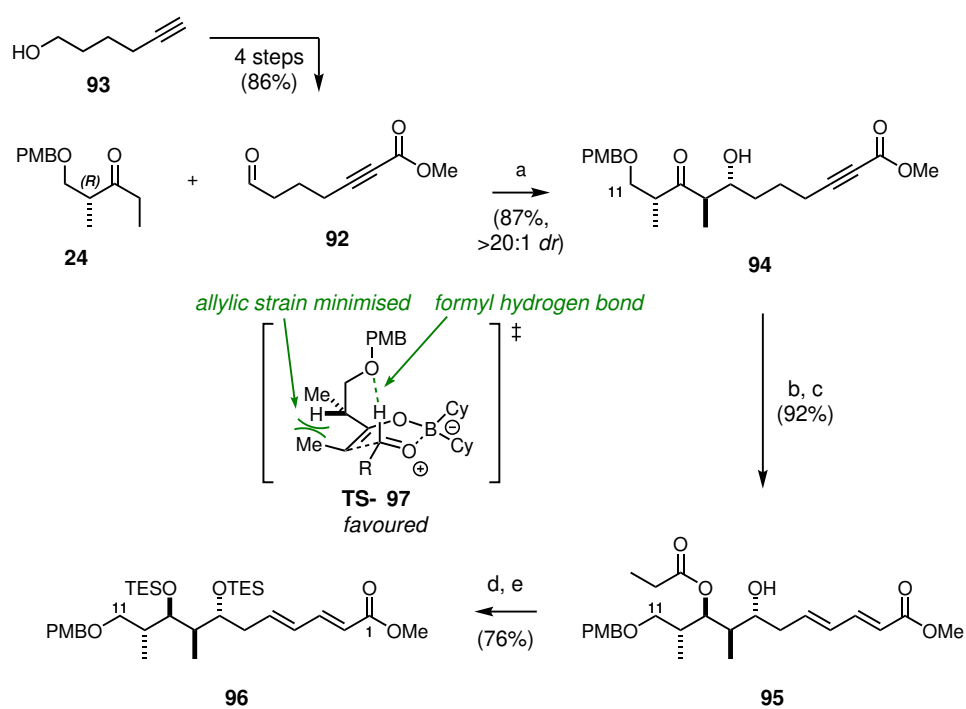
Scheme 2.20: Alkylation of iodide **87** to form phosphonate **20**

The PMP-protected northern fragment **20** was thus attained in 5 steps and 21% yield from intermediate **86**. This was then to be compared with the equivalent *bis*-TES fragment **28** as we progressed towards forming the advanced macrocyclic intermediate.

2.3.2 TES-protected northern fragment synthesis

Thanks to the efforts of Dr Mike Housden, a generous stock of the intermediate **96** with the full C₇–C₁₀ stereotetrad in place was available for aplyronine studies. A summary of Housden's synthesis of this fragment is shown in Scheme 2.21.

The first key step in the synthesis requires the coupling of (*R*)-Roche ester derived ethyl ketone **24** and aldehyde **92**, directing the formation of two new stereocentres. The ketone was synthesised



(a) Cy_2BCl , Et_3N , Et_2O , 0°C , 1 h, then **92**, $-78 \rightarrow -20^\circ\text{C}$, 12 h; (b) Sml_2 , EtCHO , THF , 0°C , 2 h;
 (c) PPh_3 , PhOH , C_6H_6 , rt, 14 h; (d) K_2CO_3 , MeOH , rt, 2 h; (e) TESOTf , 2,6-lutidine, CH_2Cl_2 , -78°C , 1 h

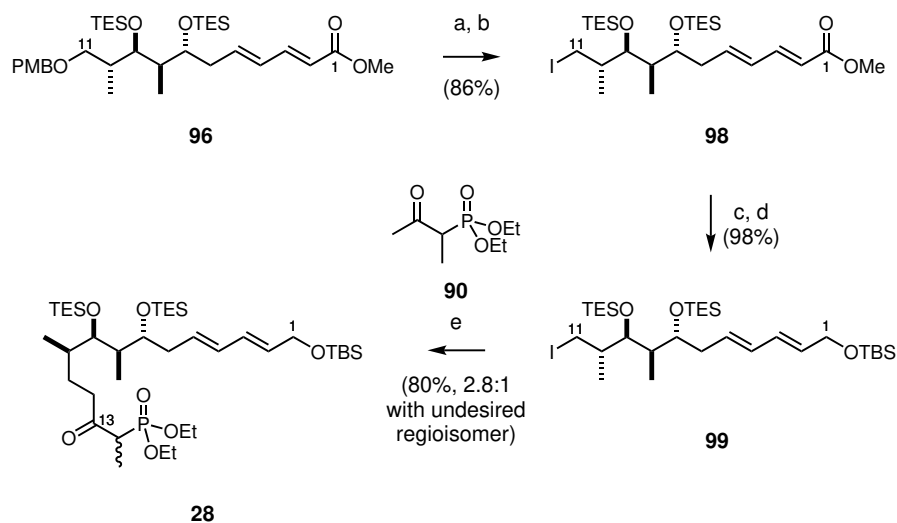
Scheme 2.21: Housden's synthesis of intermediate **96** according to the established protocol¹¹³

as described above (Section 2.2), and the aldehyde could be accessed in 4 steps and 86% yield from 5-hexyn-1-ol (**93**). To couple these two fragments, the high levels of diastereoselectivity attainable through boron aldol chemistry were used to advantage. Enolisation of ketone **24** with dicyclohexylboron chloride (Cy₂BCl) and triethylamine (Et₃N) gives the (*E*)-enolate, which can react with aldehydes such as **92** through a boat-like transition state **TS-97** to give the 1,4-*syn*-3,4-*anti* product **94**. This model for the high levels of stereoinduction observed in reactions of this type was developed by Paton and Goodman with the aid of density functional theory (DFT) calculations.^{139–141} Their work showed that a stabilising hydrogen bond between the formyl proton and the β-alkoxy group can influence the facial preference of enolate attack, such that 1,3-allylic strain is minimised. Thus, the aldol adduct **94** was accessed in 87% yield and >20:1 *dr*. The northern stereotetrad was completed using an Evans–Tishchenko reduction to establish the *anti*-configuration of the C₇/C₉ diol (98%, >20:1 *dr*).¹²⁸

The conjugated alkyne was then isomerised to the corresponding dienolate **95** by Rychnovsky's protocol (PPh₃, PhOH, 94%),¹⁴² followed by hydrolysis of the propionate ester and installation of the desired triethylsilyl protecting groups (76%, 2 steps). This translated to an overall yield of 61% over the 5 steps to **96** achieved by Housden.⁹²

One advantage of this protecting group strategy was the early installation of the TES ethers that would be needed in the endgame. The rigid PMP ether protecting group had been selected by Woodrow in an attempt to bias the substrate towards macrolactonisation at the intended site.¹⁴³ After this step, it had been necessary to insert two manipulations in order to switch to the silyl ethers which would be readily cleaved in the final stages of the synthesis. These considerations were no longer essential in the new synthetic route, as only one site would be available for macrolactonisation, and the more flexible substrate was expected to react as intended. It would thus be advantageous to avoid the protecting group swap that would otherwise be required at a much further advanced stage. Nevertheless, the chemistry of the PMP-protected substrate had been comprehensively tested in previous work, and so it remained a valid contender for the northern substrate that would be taken forward to more complex intermediates.

Housden's helpful stockpile material could then be converted as needed into the phosphonate **28**, which would form the coupling partner for the southern aldehyde **29**. This transformation was carried out in 5 steps, in much the same way as for the PMP-containing fragment (Section 2.3.1). Thus, the PMB protecting group was cleaved (DDQ, 97%) and the resulting hydroxyl substituted for an iodide (PPh₃, I₂, imidazole, 89%). The methyl ester was reduced (DIBAL, –78 °C, quant.) and protected as the TBS ether **99** (TBSOTf, 2,6-lutidine, 98%).



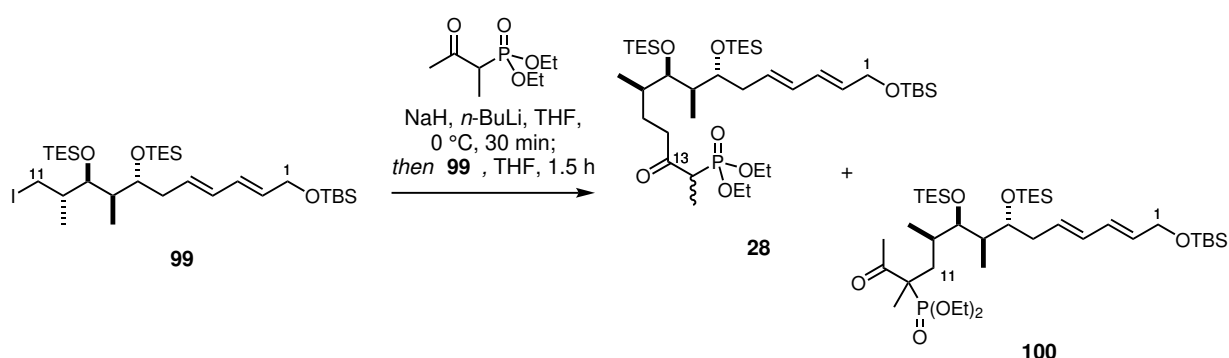
- (a) DDQ, $\text{CH}_2\text{Cl}_2/\text{pH } 7 \text{ buffer}$, rt, 40 min; (b) PPh_3 , imidazole, I_2 , $\text{Et}_2\text{O}/\text{MeCN}$ (1:1), $0^\circ\text{C} \rightarrow \text{rt}$, 2 h;
 (c) DIBAL, CH_2Cl_2 , -78°C , 1.5 h; (d) TBSOTf, 2,6-lutidine, CH_2Cl_2 , -78°C , 1 h;
 (e) **90**, NaH, THF, 0°C , 30 min, then *n*-BuLi, 0°C , 30 min, then **99**, HMPA, THF, 0°C , 1.5 h

Scheme 2.22: Synthesis of phosphonate **28** from intermediate **96**

This material then stood in readiness for the alkylation step, and at this stage it seemed appropriate to attempt optimising conditions for this reaction. It would be advantageous to stretch the stock material as far as possible if improved conditions could be found. Furthermore, this newer substrate, although functionally equivalent to the PMP-protected fragment, had appeared to show somewhat different reactivity in the alkylation step in the hands of other researchers due to the greater steric bulk of the silyl protecting groups.^{112,144} For instance, the reaction was sluggish at -78°C , and generally had to be run at much higher temperatures to promote reactivity. A range of conditions was trialled in an attempt to improve upon the results achieved to date, and these are summarised in Table 2.6.

The influence of HMPA as a cation solvating agent was considered. Due to the carcinogenicity of HMPA and its potential to cause difficulties on scale-up, we preferred to avoid its use if at all possible. To our surprise, it was found that the selectivity of the reaction was unaffected when HMPA was not used, while the yield even appeared to be improved (Table 2.6, entries 1 and 2). Meanwhile, the iodide concentration was posited to have an effect; in this study, higher concentration appeared to have a mildly positive effect on conversion (entry 3). Raising the temperature from -20°C to 0°C also seemed to assist with conversion (entry 4). However, puzzlingly, the effective yield of **28** under these conditions was equivalent to that at lower temperature and without HMPA (entry 2). It was hoped that in combination, the factors of higher concentration and temperature would have an additive effect (entry 5); but the increased yields could not be

Table 2.6: Conditions for optimisation of the alkylation reaction with iodide **99**



Entry	Variation from standard conditions	Scale	28 : 100 ^a	Combined yield, % (yield of 28 , %) ^b
1	HMPA (2 eq), 0.09 M, -20 °C	50 mg	2.2 : 1	68 (47)
2	0.09 M, -20 °C	50 mg	2.2 : 1	84 (58)
3	HMPA (2 eq), 0.35 M, -20 °C	50 mg	2.4 : 1	79 (56)
4	HMPA (2 eq), 0.09 M, 0 °C	65 mg	2.8 : 1	80 (59)
5	HMPA (2 eq), 0.2 M, 0 °C	150 mg	3.8 : 1	65 (51)
6	0.2 M, 0 °C	1.16 g	2.5 : 1	69 (49)
7	0.2 M, 0 °C	2.20 g	3.0 : 1	60 (45)

^a Determined by integration of ¹H NMR signals in the purified mixture. ^b Isolated yields.

replicated, although the selectivity saw a sudden improvement to 3.8:1, the best achieved in these studies. Finally, in hopes that the selectivity seen in entry 5 would be met by higher yields with economies of scale, these conditions were applied to larger quantities of iodide **99** (entries 6 and 7). This was carried out without the addition of HMPA, as it had been seen to have little effect on the selectivity. Unfortunately, a return to the more typical levels of regioselectivity and, disappointingly, lower yields were obtained in these larger-scale reactions.

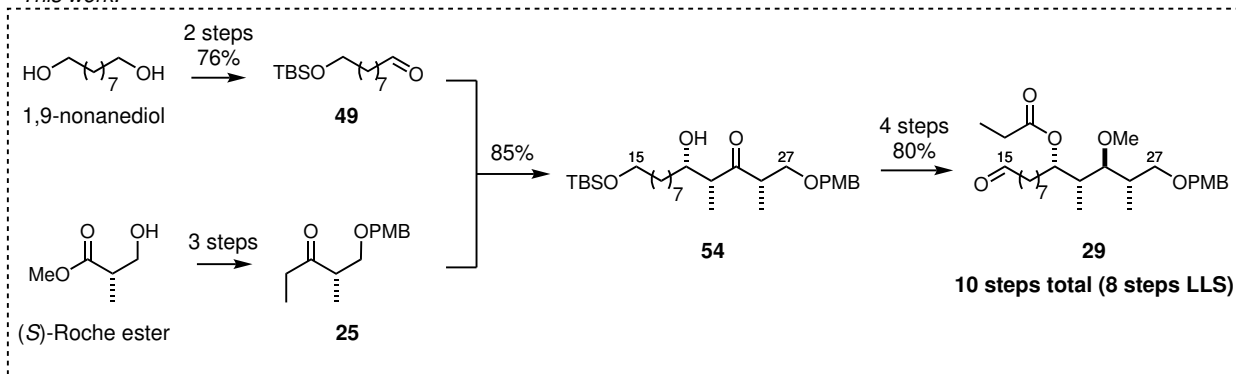
Ultimately, the reaction appeared to be capricious, and results could not be definitively tied to any one particular aspect of the reaction conditions. Dr Nika Anžiček had also tried to find improved conditions to access the phosphonate fragment, but to no avail.¹¹² It was necessary at this point to accept a moderate yield for this step so that we could press on toward more advanced stages of the analogue synthesis. This leaves open the opportunity in future studies to further optimise this step, or to consider alternative disconnections to introduce the desired phosphonate to carry forward for HWE coupling.

The successful acquisition of the northern fragment **28** (and PMP version **20**) signalled the completion of the three fragments needed for coupling and advancement towards the full aplyronine analogues. Indeed, the phosphonate-containing fragments proved unsuitable for long-term storage in the freezer due to gradual degradation, so we were motivated to press on to the planned HWE coupling with the southern aldehyde **29** and further. This fragment coupling and the development of advanced intermediates for the synthesis of aplyronine analogues will be discussed in the next chapter.

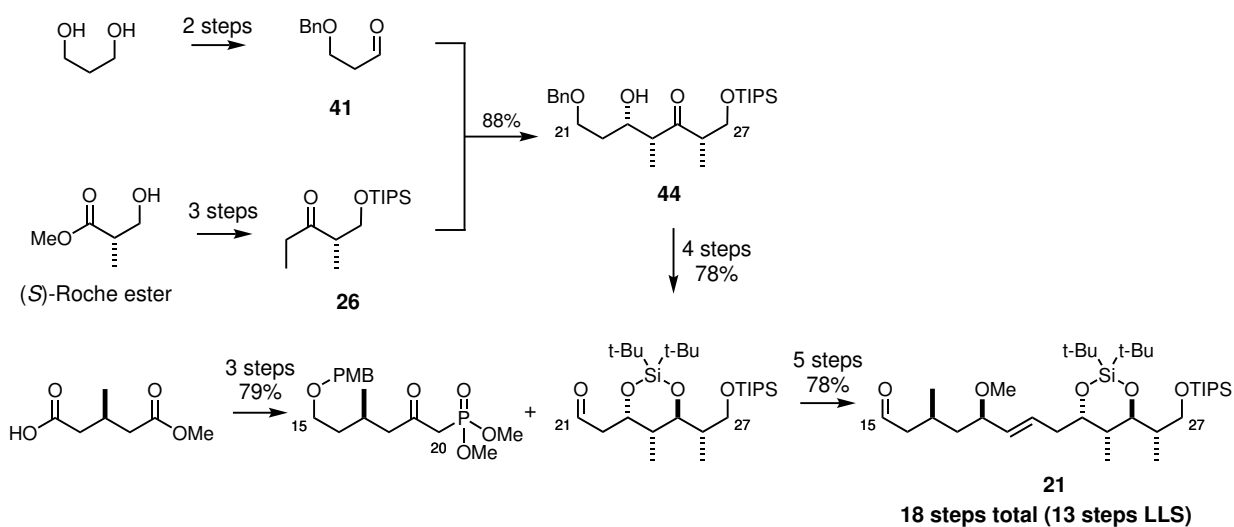
2.4 Summary and conclusions

The highly stereocontrolled preparation of aldehyde **29** was achieved in 5 steps and 68% yield from ethyl ketone **25** (Scheme 2.23). It is estimated that to make 1 g of fragment **29** *via* this route would require 8 days, which amounts to half the time required to access equivalent fragment **21** for the Paterson aplyronine C synthesis,¹¹³ approximately 16 days. This work extended upon previous efforts towards constructing the aplyronine C₂₃–C₂₆ stereotetrad using tin(II)^{113,118} and titanium(IV)⁹² aldol methodologies. The titanium aldol approach was found to be the more favourable and provided aldol adduct **54** in good yield and pleasing diastereoselectivity on multi-gram scale. Further elaboration to aldehyde **29** provided a new C₁₅–C₂₇ southern fragment analogue for insertion into the previously established Paterson aplyronine synthetic route (Scheme 2.23).

This work:

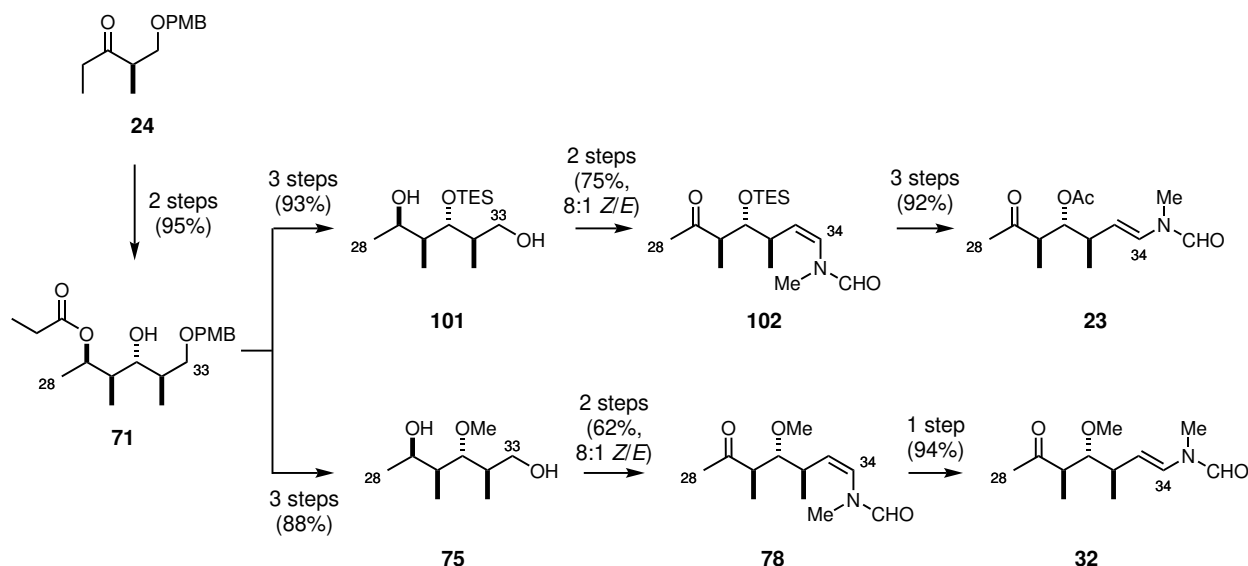


Paterson aplyronine C synthesis:



Scheme 2.23: Summary of southern fragment syntheses¹¹³

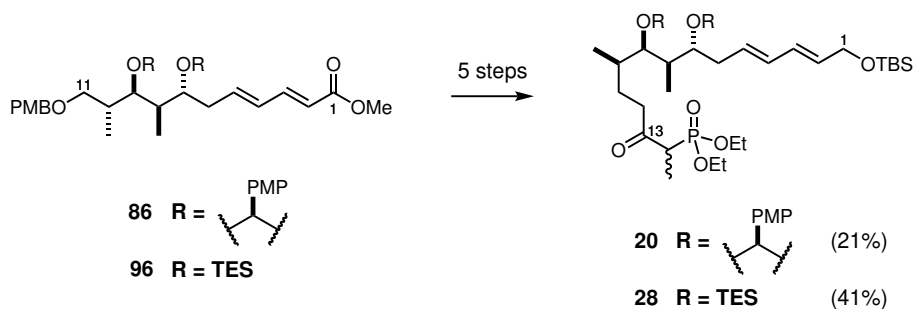
Methodology to construct the C₂₉–C₃₂ stereotetrad using a titanium(IV) Lewis acid provided similarly high diastereoselectivity when compared to the previously used tin(II)-mediated aldol reaction.^{91,111} The newly adopted protocol represents an operationally simpler procedure, and furnished **69** in multi-gram quantity. This allowed for elaboration to either the third-generation C₂₈–C₃₄ side chain fragment **23** *via* the established route or to structurally altered fragments for aplyronine analogue synthesis. Fink previously completed the synthesis of **23** as shown in Scheme 2.24 *via* a 10-step route in 61% yield. In all, this synthesis would take approximately 9 working days.¹¹¹ For this dissertation, the fragment **32**, which contains a C₃₁-methyl ether equivalent to that found in the natural product scytophycin C, was synthesised in 8 steps from ketone **24**. This approach shortened the route by two steps by circumventing the need to install the acetoxy group after the Wittig reaction. On the basis of these studies, it was also expected that the methyl ether would be less fragile than the acetate in later steps with advanced intermediates, being less prone to elimination under various conditions. This proof-of-concept synthesis was later refined by Rachel Porter, who was able eventually to generate a batch of 1 g of ketone **32** for fragment coupling in 42% overall yield and in only 6.5 days (Scheme 2.24). To date, approximately 7 g of side chain fragment **32** have been prepared *via* this reliable route. Given its low molecular weight relative to the macrocycle-containing fragment, this quantity is sufficient to match with 25 g of macrocycle. The material is sufficiently stable to be stored in the freezer for at least 1 year without significant degradation, such that it could be used as needed in fragment coupling studies.



Scheme 2.24: Previous synthesis of fragment **23** by Fink⁹¹ and route to analogue fragment **32** discussed in this work, subsequently completed by Porter¹²⁹

The two alternative northern fragments **20** and **28** were also re-synthesised in 21% and 41%

yield respectively in 5 steps from the equivalent intermediates **86** and **96** (Scheme 2.25). This was consistent with the findings of earlier studies, and would enable us to identify which would be the better of the two for the current purposes. This comparison will be discussed in detail in Chapter 3.



Scheme 2.25: Summary of the re-synthesis of northern fragments **20** and **28** for this work

The aim of this project as a whole was to synthesise function-oriented analogues of the aplyronines that simplify the scaffold and overall synthetic route. Of the three key structural modifications laid out at the beginning of this work, two have been included in the C₁₅–C₂₇ fragment analogue **29**, and the third was incorporated into the C₂₈–C₃₄ side chain analogue **32**. The northern fragment was also synthesised in two versions (**20** and **28**) containing different protecting groups, for comparison in fragment coupling studies to determine the better route to take forward. With these three fragments in hand, the scene was set to push forward towards advanced intermediates that would eventually grant us access to our desired aplyronine analogues.

Chapter 3

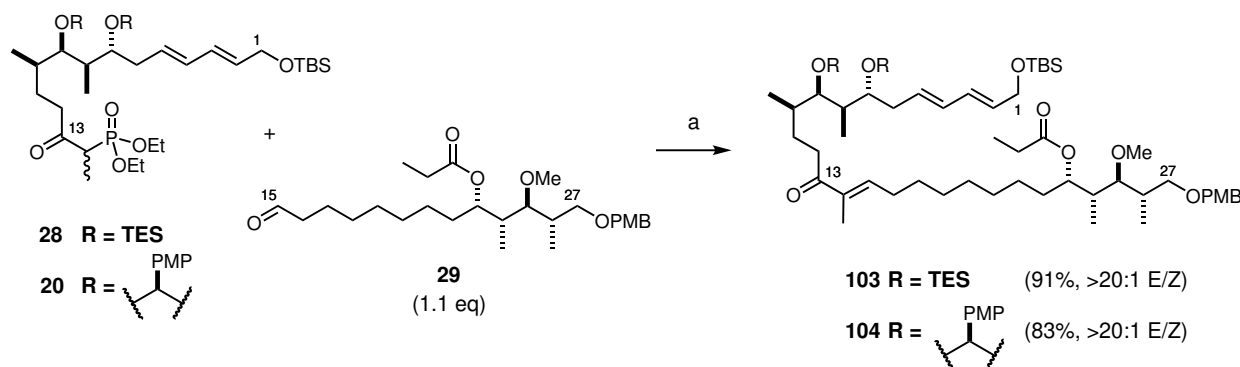
Fragment coupling to construct advanced macrolactone intermediates

3.1 Coupling of southern and northern fragments

The three key fragments for our envisioned “aplyrologues” were in hand, and to move the project forward, the southern and northern pieces would need to be combined and advanced to form the macrolactone. At the time this work was begun, two possible northern fragments (**20** and **28**, Scheme 3.1) were available for inclusion in a route that would more closely resemble either the first- or second-generation aplyronine synthetic strategies.^{91,92} An initial consideration, therefore, was which fragment to carry forward in working towards constructing our desired analogues, and we embarked upon an exploration of this chemistry.

3.1.1 Initial studies: comparing PMP and *bis*-TES protected fragments

The strategy from this point was to use a Horner–Wadsworth–Emmons (HWE) reaction to couple the southern aldehyde **29** with β -ketophosphonate **28** or **20** to form the enones **103** and **104** (Scheme 3.1). The HWE olefination reaction gives high selectivity for (*E*)-enones *via* the mechanism shown in Scheme 3.2.¹⁴⁵ Deprotonation of the acidic β -ketophosphonate **105** gives a stabilised enolate-type carbanion **106**. Addition of this species to the electrophilic carbon of an aldehyde leads to the formation of an oxaphosphetane, which collapses to give predominantly the (*E*)-enone product **107**. Loss of a phosphate ester provides the driving force for the reaction.



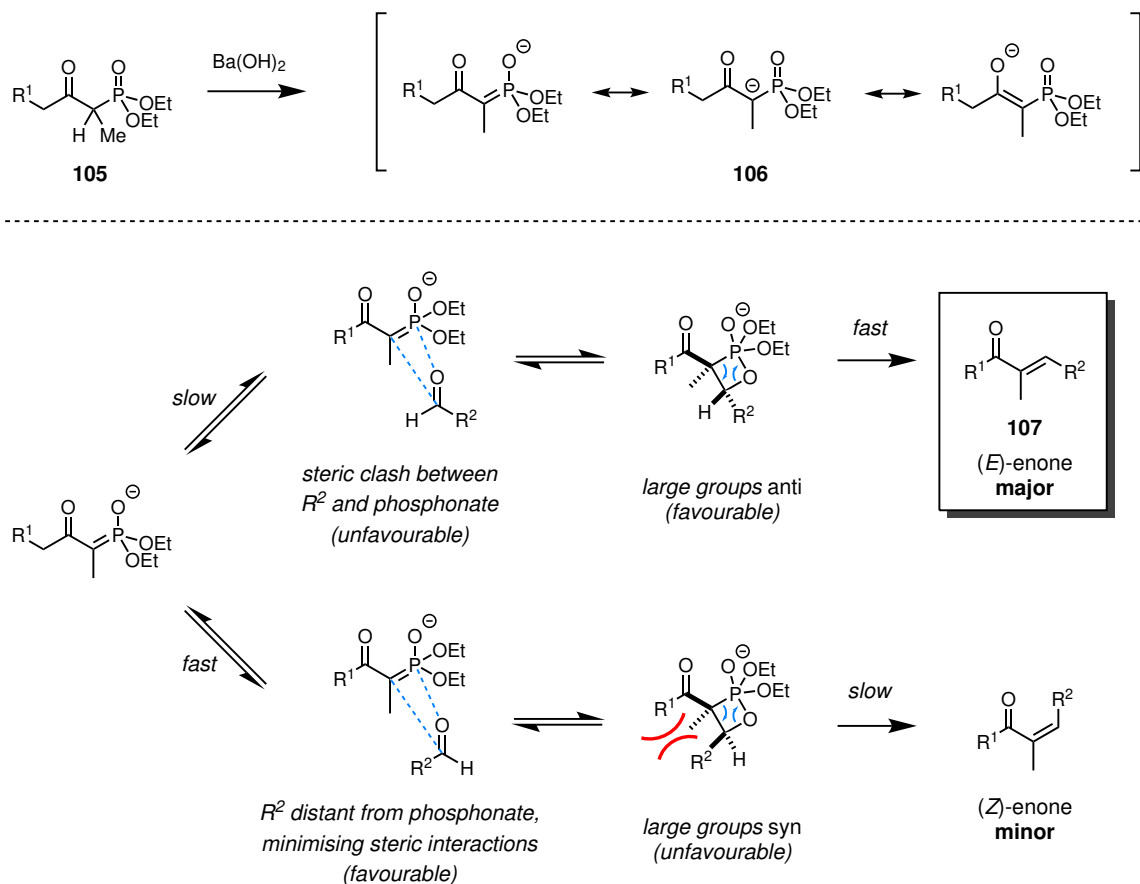
(a) Ba(OH)₂, THF, rt, 2 h, then **29**, THF/H₂O (40:1), 72 h

Scheme 3.1: Horner–Wadsworth–Emmons reaction to form enones **103** and **104**

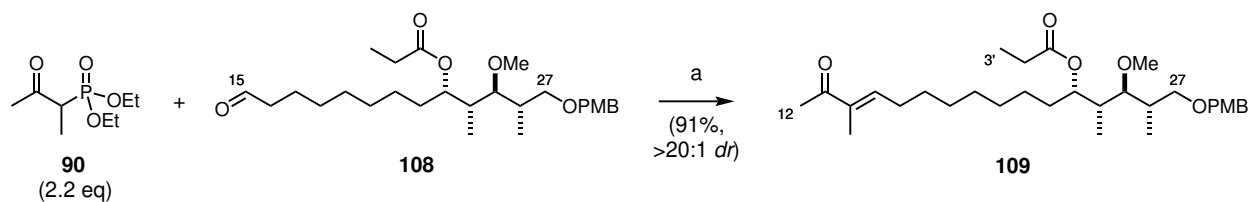
The current understanding of the stereoselectivity of the HWE reaction is that the relatively high stability of the phosphonate carbanion makes the initial rate-determining step reversible, allowing the reaction to proceed along the two diastereomeric pathways under thermodynamic control. Minimisation of steric interactions between the bulky phosphoranyl group and the aldehydic proton is favoured, but leads to an oxaphosphetane intermediate in which the aldehyde R group eclipses the β-carbonyl. Conversion of this intermediate into the (*Z*)-enone is sluggish. By contrast, approach of the aldehyde as per the top pathway is less favoured, but results in an intermediate in which steric clash between the large substituents is avoided, and allows fast conversion into the (*E*)-enone **107** in the stereospecific step. Equilibration of intermediates therefore drives the reaction towards this product almost exclusively.

The HWE reaction is classically carried out using an alkoxide, sodium hydride or a lithium base, but milder conditions have been developed to accommodate sensitive substrates for complex natural product synthesis. Our group has found that barium hydroxide is effective under very mild conditions (wet THF, rt), giving high (*E*)-selectivity for disubstituted olefins.^{146,147} Our Ba(OH)₂ methodology is compatible with highly functionalised substrates,^{148–150} and has been used to construct even the more challenging trisubstituted olefins.¹⁴⁶ The successful application of this HWE variant in the aplyronine natural product synthesis (96% yield, >20:1 *E/Z*) led us to expect similar success for these closely related reactants.⁹² A test reaction of aldehyde **29** with the simple phosphonate **90** lent support to this prediction, giving the (*E*)-enone **109** in 91% yield as a single diastereomer (Scheme 3.3).

Each of the β-ketophosphonates **28** and **20** was therefore deprotonated with Ba(OH)₂ in anhydrous THF for 1–2 h, before addition of the southern aldehyde **29** in wet THF (THF/H₂O 40:1) at room temperature. The respective phosphonates were used as mixtures with their inseparable



Scheme 3.2: Horner–Wadsworth–Emmons reaction mechanism



Scheme 3.3: Test reaction to establish conditions for the HWE olefination

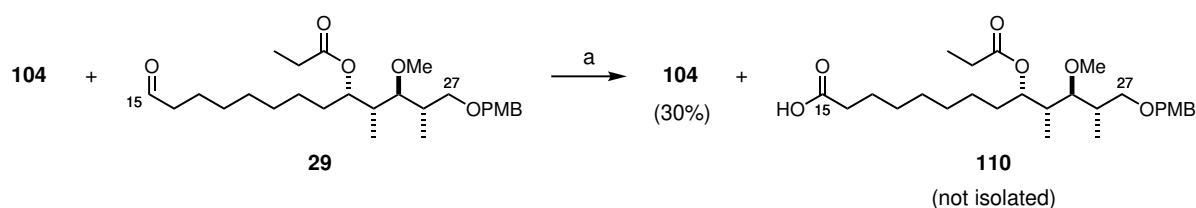
regioisomers **91** and **100** (see Section 2.3), which were unreactive under the reaction conditions. Molar ratios in the crude product mixture were determined by integration of characteristic signals in the ^1H NMR spectra, and in each case the unreactive isomer was recovered quantitatively after workup and column chromatography. As the aldehyde component **29** was the more readily accessible (in 5 steps from Roche ester ethyl ketone **25**, as opposed to 10 steps for the phosphonates **20** and **28**), it was used in slight excess (1.1 eq). Extended reaction times (48–72 h) were used mainly for convenience, as it was found that under these mild conditions, the reactants could be left to stir over the weekend without detrimental effect. The results were pleasing, with the *bis*-TES product **103** being isolated in 91% and the PMP version **104** in 83% yield. The (*Z*)-enone was not detectable by spectroscopic methods in either case, thus displaying excellent diastereoselectivity (>20:1 *E/Z*).

However, a key difference did arise during the comparison of the two substrates. The PMP-containing enone **104** proved difficult to separate from any unreacted aldehyde **29**, and repeated careful chromatographic separations were needed to isolate this product in useful amounts. Keeping the stoichiometry of the reaction as close as possible to 1:1 did not appear to offer a remedy, as in these cases the starting materials would not be fully consumed. Attempts were made to differentiate the two compounds by submitting the troublesome mixture to a Pinnick oxidation in order to mildly and selectively oxidise the aldehyde to lower its retention factor. Yet these efforts were met with low yields of coupled product (30%) and extensive degradation to unidentified side products (Scheme 3.4). The best option was merely to subject the mixed material to somewhat laborious sequential chromatography steps. This difficulty had not been encountered previously in the course of the aplyronines project; presumably, the substitution of the hydrophobic alkyl chain in the southern fragment analogue rendered these two compounds very similar in retention factor.

By contrast, the lower polarity of the multiple silyl ether-containing enone product **103** allowed its easy separation from both starting materials. This was a strike against the PMP option, but investigations were continued to fully consider the implications of each route.

3.1.2 Selective reduction and installation of the C₁₃ methyl ether

With the two fragments coupled, the next step in the sequence was a selective reduction of the C₁₃ ketone to the (*S*)-alcohol. The lack of existing stereodirecting substitution in this region of the molecule led us away from considering a substrate-controlled approach, and instead towards the well-established chemistry of the Corey–Bakshi–Shibata asymmetric reduc-



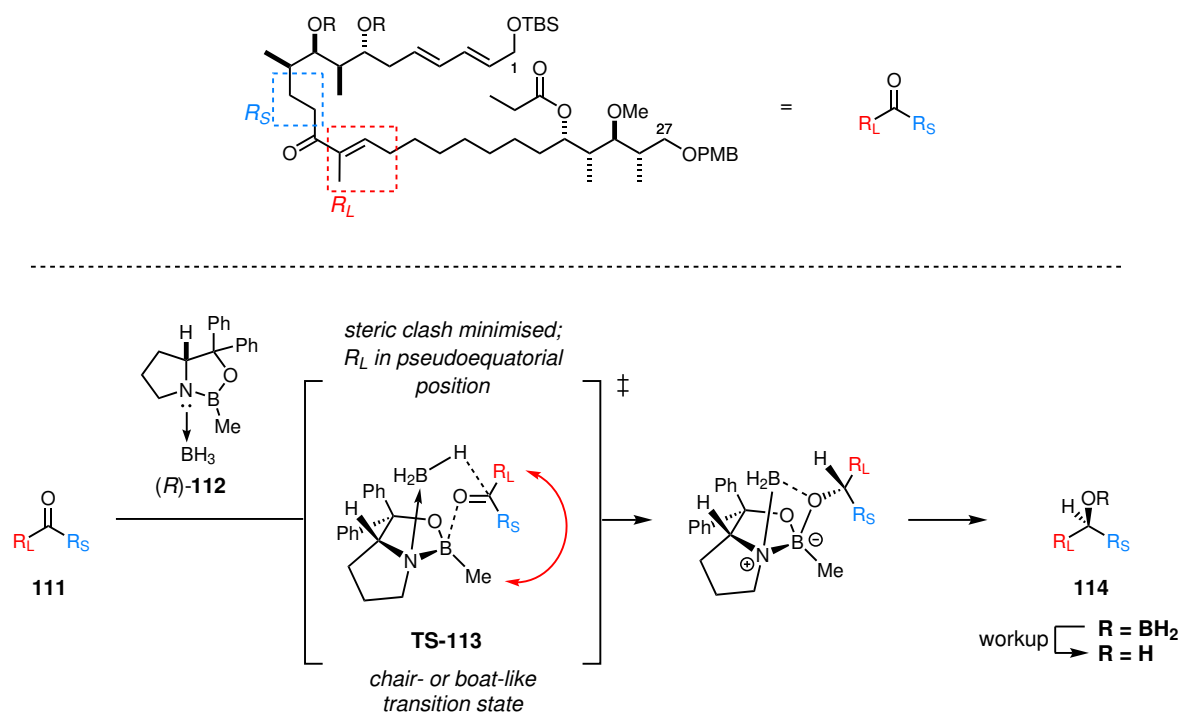
(a) NaClO_2 , $\text{NaH}_2\text{PO}_4 \cdot 2\text{H}_2\text{O}$, 2-methyl-2-butene, *t*-BuOH/ H_2O (1:1)

Scheme 3.4: Attempt to isolate enone **104** from starting material **29** by a Pinnick oxidation

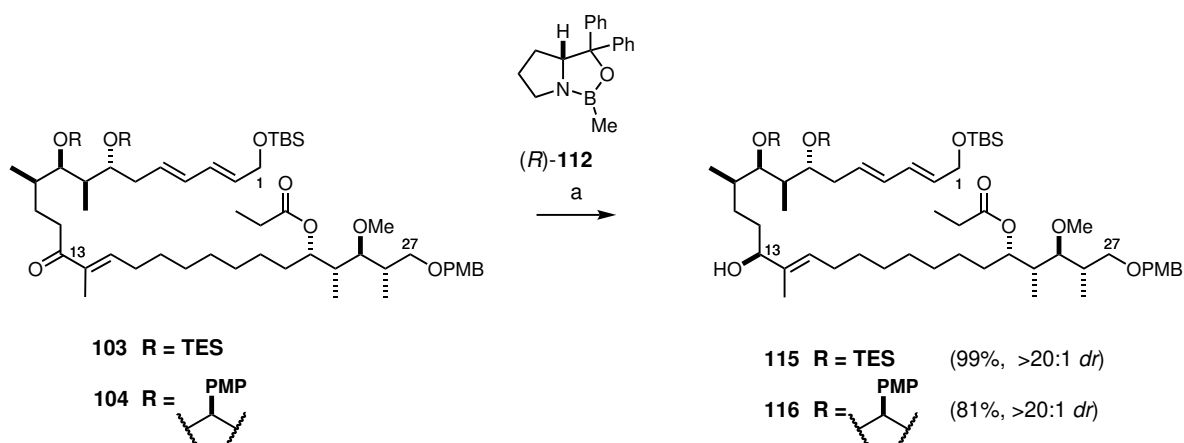
tion (Scheme 3.5).^{151–153} In this reaction, high levels of enantioselectivity are achieved in ketones with a clear size difference between their two substituents. In enones such as **103** and **104**, the trisubstituted olefin constitutes the large substituent (R_L), while the alkyl chain represents the small (R_S).

In this reaction, the chiral oxazaborolidine catalyst **112** supplants the Lewis basic ligand in $\text{BH}_3 \cdot \text{SMe}_2$ or $\text{BH}_3 \cdot \text{THF}$ to form a nitrogen–borane adduct (Scheme 3.5). The effects of this coordination are threefold: (1) the borane reagent is activated as a hydride donor relative to the starting complex, (2) the Lewis acidity of the endocyclic boron is increased, promoting coordination of a ketone substrate, and (3) the borane is positioned in a chiral environment close to the coordinated ketone. Face-selective hydride transfer proceeds through a 6-membered cyclic transition state **TS-113**, which may take either a chair- or boat-like conformation.¹⁵⁴ The selectivity stems from the preferential coordination of the ketone **111** such that the large group is distant from the oxazaborolidine methyl group (or other boron substituent), where it can adopt a pseudoequatorial position and thus minimise steric interactions. The catalyst is regenerated upon liberation of an alkoxyborane, which is converted to the alcohol **114** via a simple methanolic workup with release of volatile trimethoxyborane.

In our system, use of the (*R*)-MeCBS catalyst **112** with $\text{BH}_3 \cdot \text{SMe}_2$ in THF at -10°C gave high yields of the alcohols **115** (99%) and **116** (81%), with only a single diastereomer observed in each case (Scheme 3.6). This was assigned at this stage as the 13*S*-alcohol by analogy to very similar aplyronine substrates studied by Lee and Anžiček, leaving more detailed configurational analysis until a later stage (*vide infra*, Section 3.1.6).^{112,118} Although this reaction is catalytic in nature with respect to the oxazaborolidine, the decision was taken at this stage to use the CBS “catalyst” in stoichiometric quantities to ensure high reaction rate and selectivity. Under these conditions, the reactions quickly went to completion, with reaction times of under 1 h. There remains scope to improve the atom economy of this step by lowering the catalyst loading by as much as possible in future studies.



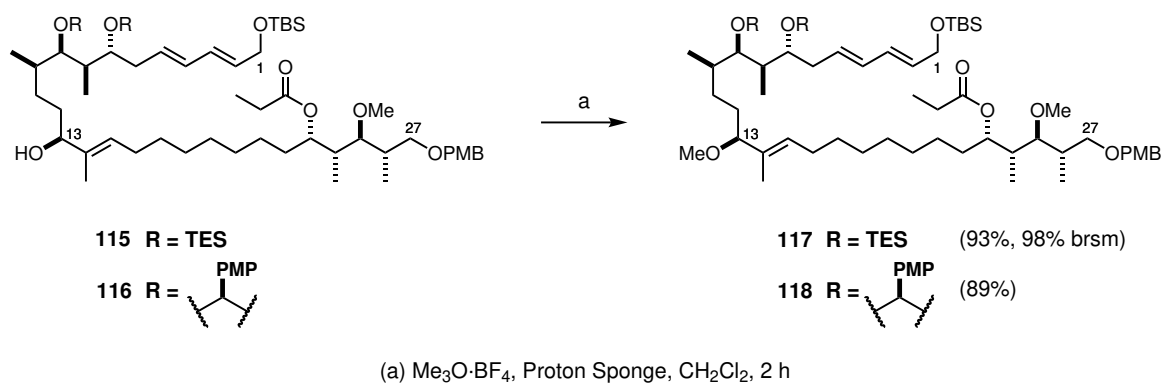
Scheme 3.5: Mechanism for the Corey–Bakshi–Shibata reduction¹⁵⁴



(a) (R) -112 (1.2 eq), $BH_3 \cdot SMe_2$, THF, $-10\text{ }^\circ\text{C}$, 45 min

Scheme 3.6: CBS reduction of enones **103** and **104**

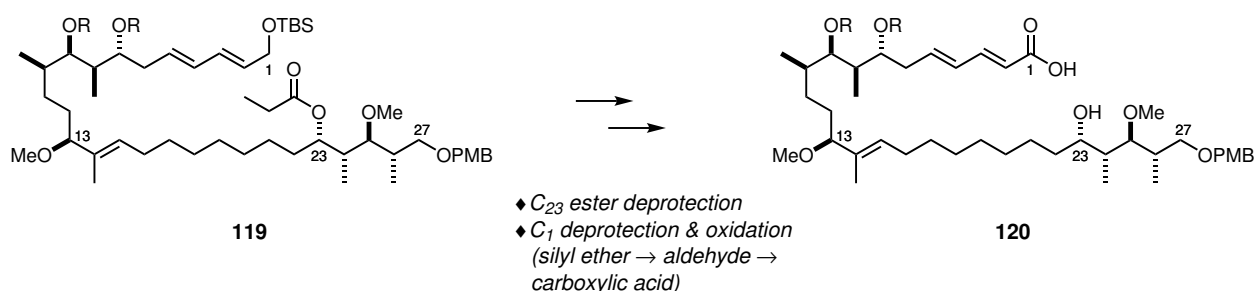
From the C₁₃ alcohol **115** or **116**, a straightforward conversion using the methylating reagent Meerwein salt (Me₃O · BF₄) and Proton Sponge furnished the desired methyl ethers **117** and **118** in 93% and 89% yield respectively.



Scheme 3.7: Installation of C₁₃ methyl ether

3.1.3 Advancement towards the macrocycle

With the necessary functionality having been incorporated in the carbon skeleton, it was now time to work towards closing the 24-membered macrocyclic ring by a macrolactonisation procedure. To achieve this, it would be necessary to unmask the C₂₃ alcohol and reveal a carboxylic acid at C₁. A three-step conversion to the seco-acid **120** was planned: deprotection of the C₂₃ ester, tandem silyl ether deprotection and oxidation of the allylic TBS ether, and oxidation of the resultant aldehyde (Scheme 3.8). This stepwise approach would allow the use of mild conditions compatible with the various functional groups already present in the intermediate. However, the precise order of steps was yet to be decided.



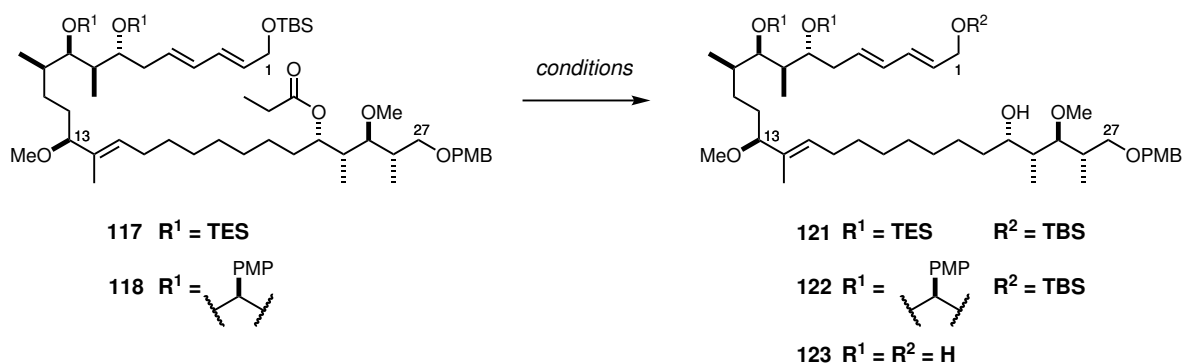
Scheme 3.8: Plan for synthesis of the seco-acid in three steps

We therefore set out to investigate removing the propionate ester from the *bis*-TES substrate **117**. Since the installation of the propionate ester in the southern fragment, we had been encouraged

by its stability under a variety of reaction conditions. Previous work had suggested that such a protecting group might be labile when exposed to acids or bases, and at each stage we had been prepared to see loss or migration of the ester as a side reaction. However, this was not observed: it had been possible to carry through the ester directly to this point without any need for a switch in hydroxyl protection. It was convenient indeed that this moiety was already orthogonal to the methyl, silyl and aryl ethers present elsewhere in the molecule. We therefore reasoned that we could simply hydrolyse the ester **117** to alcohol **121** at this point (Table 3.1).

In this expectation we were deceived. Attempts at hydrolysis under increasingly harsh conditions (entries 1-3, Table 3.1) were unsuccessful, and invariably, starting material was returned. In an effort to push the substrate to react at all, exposure to a high concentration of KOH did indeed result in ester hydrolysis – but not before the loss of all three silyl ethers, giving tetrol **123** (entry 3). All signs suggested that continuing in this vein would be futile, and so we decided to switch tack to a metal hydride reduction approach. Fortunately, reduction with DIBAL did give the desired products **121** in 75% yield (entry 4) and **122** in 99% yield (entry 5). In anticipation that a milder hydride source might give an even better result, the reaction was attempted with lithium borohydride on the equivalent PMP-containing substrate, but regrettably slow conversion and a wider range of side products were observed, with accordingly lower yield (59%, entry 6).

Table 3.1: Studies for deprotection of propionate esters **117** and **118**

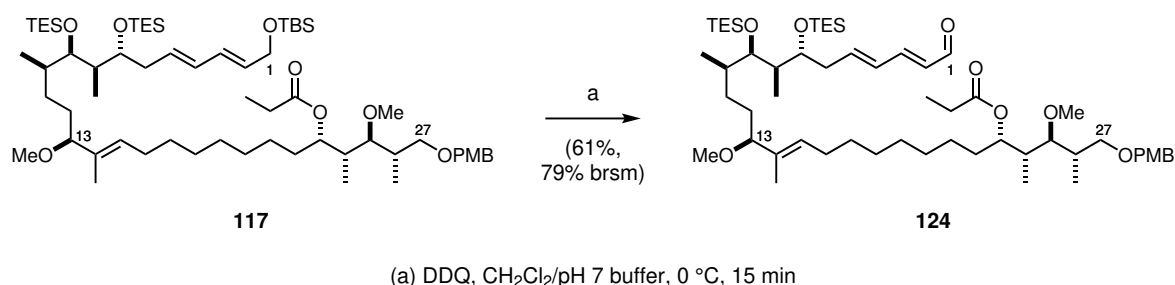


Entry	Substrate	Conditions	Product	Yield (%)
1	117	K_2CO_3 , MeOH, rt, 20 h	–	nr
2	117	LiOH, THF/ H_2O (2:1), rt, 6 d	–	nr
3	117	KOH, MeOH, rt, 72 h	123	92
4	117	DIBAL, CH_2Cl_2 , -78°C , 1 h	121	75 ^a
5	118	DIBAL, CH_2Cl_2 , -78°C , 1 h	122	99 ^a
6	118	LiBH_4 , Et_2O , $0^\circ\text{C} \rightarrow \text{rt}$, 24 h	122	59
7	117	DIBAL, CH_2Cl_2 , -78°C , 1 h	121	98 ^b

^a Test reaction, 10–15 mg scale ^b Preparative reaction, 1.36 g scale

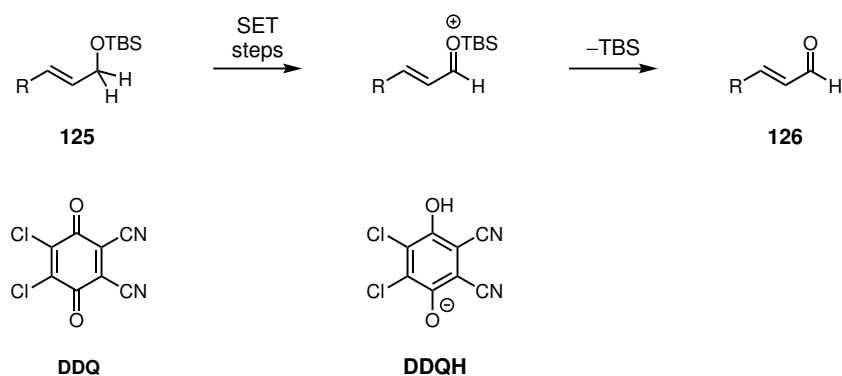
Thus, we surmised that the DIBAL reduction strategy would be the best way to forge ahead with the synthesis. This would fortunately be a fast and simple step, and on larger scale the yield of **121** was almost quantitative (entry 7, Table 3.1). This also resolved the question of which order to carry out the three steps towards the seco-acid, as the use of DIBAL would be incompatible with any functionality needed beyond the C₁-TBS ether.

We had meanwhile begun to investigate the viability of the silyl ether to aldehyde conversion by oxidation of the *bis*-TES substrate **117** with DDQ (Scheme 3.9).¹³⁷ Initial results were promising, with 61% yield (79% brsm) of the enal **124** achieved on small scale. These conditions were then applied to the C₂₃ alcohol **121**.



Scheme 3.9: Concomitant deprotection and allylic oxidation of substrate **117**

The reactivity of the allylic silyl ether on exposure to DDQ was a serendipitous discovery by Dr Michael Woodrow as part of the aplyronines project.¹⁴³ The proposed mechanism is as shown in Scheme 3.10, and involves single-electron transfer steps to translocate a hydride from the activated methylene of **125** to DDQ. Loss of the silyl group then reveals the aldehyde **126**. Previous studies had shown that the conversion is fast, generally going to completion in 15 min or less. We therefore anticipated that aldehyde **127**, with the PMB ether intact, would be the kinetic product, as observed by Woodrow.¹³⁷



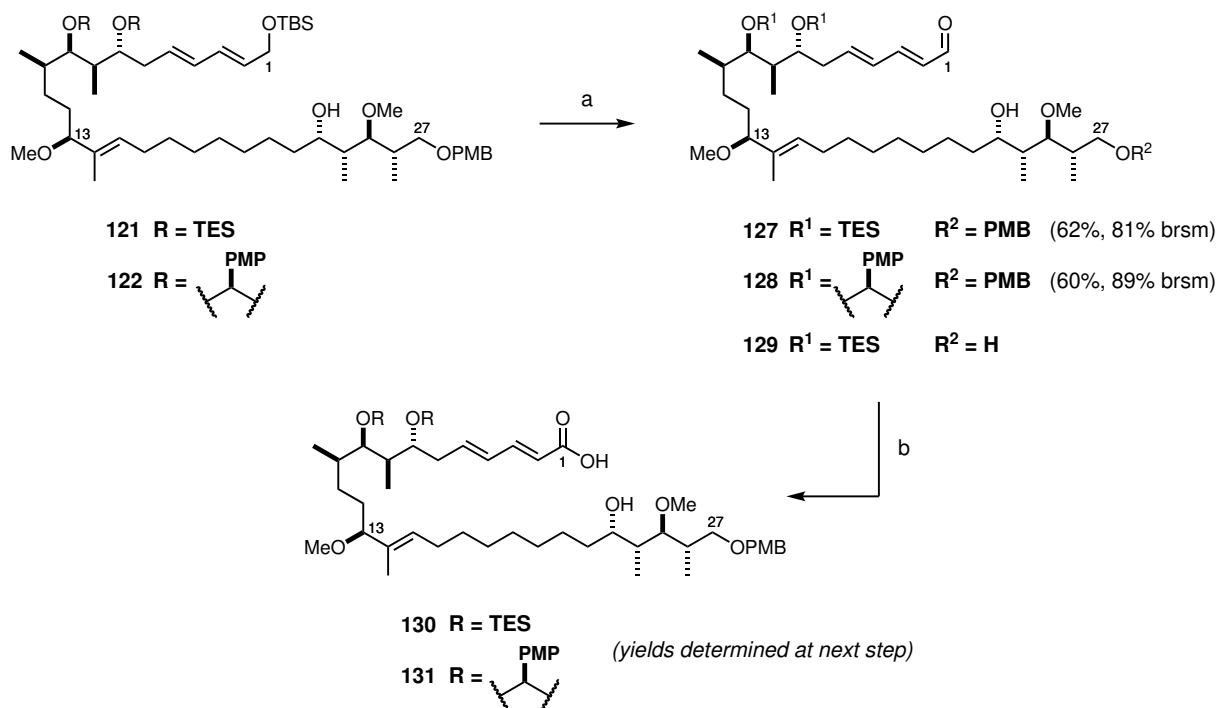
Scheme 3.10: Proposed mechanism for oxidation of allylic silyl ethers with DDQ¹³⁷

The reaction is operationally simple. Solid DDQ is added to the silyl ether and stirred in biphasic CH₂Cl₂ and aqueous buffer solution under ambient air at 0 °C. As the desired reaction was expected to be kinetically favoured, with competing PMB cleavage proceeding more slowly, the mixture was usually left to stir for only 10–15 min, and never more than 30 min. Workup and column chromatography were generally straightforward.

Despite this practical simplicity, controlling the desired chemoselectivity of the reaction proved something of a challenge, and some efforts were needed to optimise the conditions to a satisfactory level. In early studies, yields ranging from 58–73% were obtained in the *bis*-TES series (**127**), and 59% in the PMP series (**128**). After a short time the reactions appeared to stall. Although starting material was still observed by TLC analysis, any efforts to push the reaction to completion would result in appearance of a lower R_f spot, surmised to be **129**, the product of pentadienylic oxidation followed by PMB deprotection. It was deemed more judicious to recover and recycle the starting material than to push it towards overreaction and risk wasting material, so the reactions were generally quenched after a set time of 15 min. This resulted in the recovery of 10–20% starting material by mass (equating to 82–84% yield brsm).

However, concern was raised when attempts to recycle the recovered material resulted in significantly lower yields, or the reactions failed entirely. Initially this was put down to the small scale of the reactions, and left for later optimisation. As the work progressed to a larger scale, it became apparent that the recovered material had suffered some off-target reactivity to give a byproduct or mixture of byproducts that was spectroscopically similar to the original substrate. Inspection of the ¹H NMR spectra suggested that under the reaction conditions, the silyl groups may have migrated to give byproducts that were similar in retention factor to the starting material, but not synthetically useful at this stage. Based on this reasoning, the reaction conditions were reconsidered. It was not possible to lower the temperature to suppress unwanted reactivity, as the aqueous medium would freeze at lower temperatures. We therefore decided to revisit Lee's work,¹¹⁸ in which she had managed to suppress unwanted protecting group migration during a DDQ reaction by using pH 9.2 buffer instead of the usual pH 7 solution. Lee reasoned that the migration might be promoted by the weakly acidic DDQH generated during the reaction (Scheme 3.10). Testing these conditions in our system gave reassuring results. While the yields remained similar to those already observed, the recovered material was spectroscopically identical to starting material, and could be successfully recycled to increase the overall throughput. In the end, a 62% yield (81% brsm) was achieved on a scale of 1 g of **121**, with starting material being recycled to achieve an effective yield of 75%. This was satisfactory for the advancement of the project and the matter was considered closed at this point. However, it ought to be noted

that even these optimised conditions did not lead to full mass recovery, whether in the form of starting material, desired product or as-yet-identifiable byproducts. The source of this material loss remains unexplained and presents an opportunity for improvement in future iterations of this synthesis.

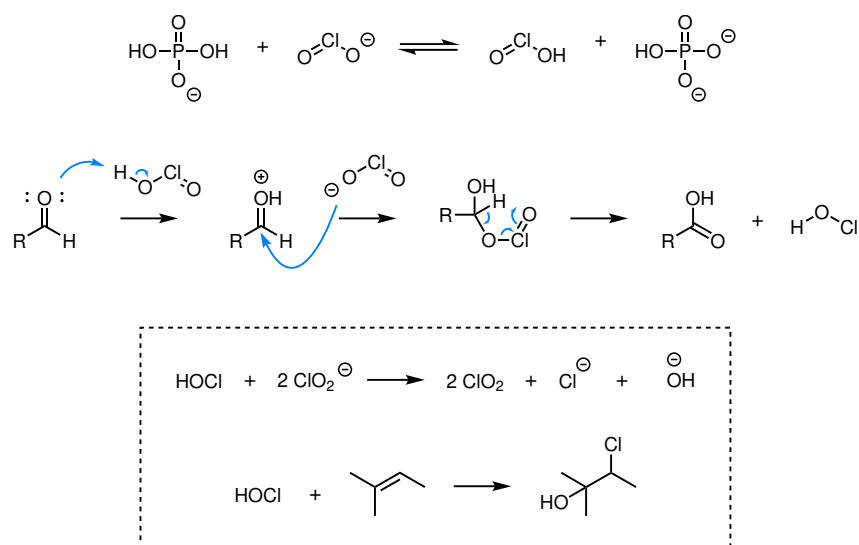


Scheme 3.11: Two-step conversion of TBS ethers **121** and **122** to carboxylic acids **130** and **131**

After this point, our goal was to obtain the seco-acids **130** and **131** as substrates for macro-lactonisation. The Pinnick oxidation was ideal for this purpose, given its mild conditions and chemoselectivity for aldehydes in the presence of many other potentially sensitive functional groups.

Oxidation of aldehydes using sodium chlorite was first described by Lindgren and Nilsson.¹⁵⁵ The procedure was generalised by Pinnick, who found that these mild oxidation conditions could be applied to complex aldehydes with a high level of chemoselectivity, without damaging other sensitive functional groups.¹⁵⁶ In particular, he described its application to α,β -unsaturated aldehydes without affecting the *E/Z* configuration of the olefin. The mechanism as it is currently understood is shown in Scheme 3.12.

Under mildly acidic conditions, sodium chlorite (NaClO₂) exists at equilibrium with chlorous acid (ClO₂H). This species can carry out a nucleophilic attack on an aldehyde to form an



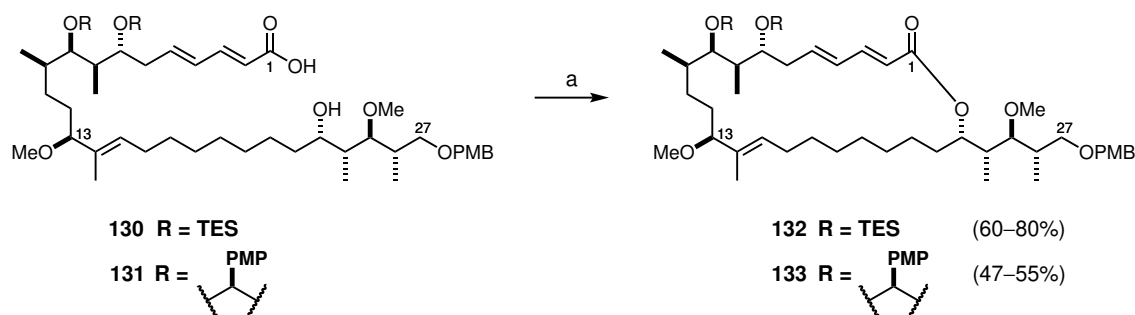
Scheme 3.12: Mechanism of the Pinnick oxidation of aldehydes to carboxylic acids¹⁵⁶

adduct, which then undergoes a pericyclic transformation to form the carboxylic acid, with loss of hypochlorous acid (HOCl). This byproduct can participate in a number of unwanted side reactions, including inactivating the sodium chlorite reagent by oxidation to chlorine dioxide (ClO_2), and halooxygenation of any olefins in the starting material to generally unwanted halohydrins (Scheme 3.12, see box). For this reason, sacrificial additives such as 2-methyl-2-butene are usually added to the reaction mixture as scavengers for the hypochlorous acid generated.^{157,158}

In this case, the Pinnick oxidation reactions of **127** and **128** proceeded smoothly when left to stir overnight at room temperature. Large excesses of each reagent were used, and on some occasions further reagent had to be added to ensure full conversion. Care was taken to also add further 2-methyl-2-butene in excess. Upon completion, a simple aqueous workup allowed isolation of the products **130** and **131** in apparently quantitative yield. The acids could be purified by column chromatography with acetic acid as a minor additive to avoid streaking. However, typically the crude product was sufficiently clean to submit directly to the next reaction, avoiding an unnecessary chromatographic step. With the seco-acids **130** and **131** in hand, it was now possible to explore the macrocyclisation of this advanced intermediate.

3.1.4 Macrolactonisation

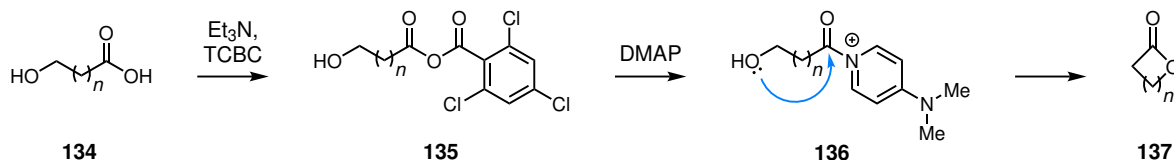
The final step in the current reaction sequence was to close the macrolactone to obtain the fully protected macrocyclic compounds **132** and **133** (Scheme 3.13). Previously, Yamaguchi's esterification conditions (2,4,6-trichlorobenzoyl chloride, Et_3N , DMAP) had been used to great effect



(a) 2,4,6-trichlorobenzoyl chloride, Et₃N, THF, then DMAP, toluene, rt, 16 h

Scheme 3.13: Formation of the fully protected macrocyclic intermediates **132** and **133**

in the aplyronine natural product synthesis, and were therefore applied once again here. By this protocol, the carboxylic acid **134** is activated towards nucleophilic attack by conversion to a mixed anhydride species **135** (Scheme 3.14).¹⁵⁹ Adding the substrate to a solution of DMAP promotes the intramolecular reaction (**136** → **137**), with the high dilution factor and slow addition rate minimising the risk of oligomerisation. The Yonemitsu variant of this reaction enables esterification as a one-pot procedure, bypassing isolation of the mixed anhydride.¹⁶⁰ A more recent publication showed that the regioselectivity of nucleophilic attack by the alcohol may in fact stem from the formation of a symmetrical aliphatic anhydride as a reactive intermediate.^{161,162}

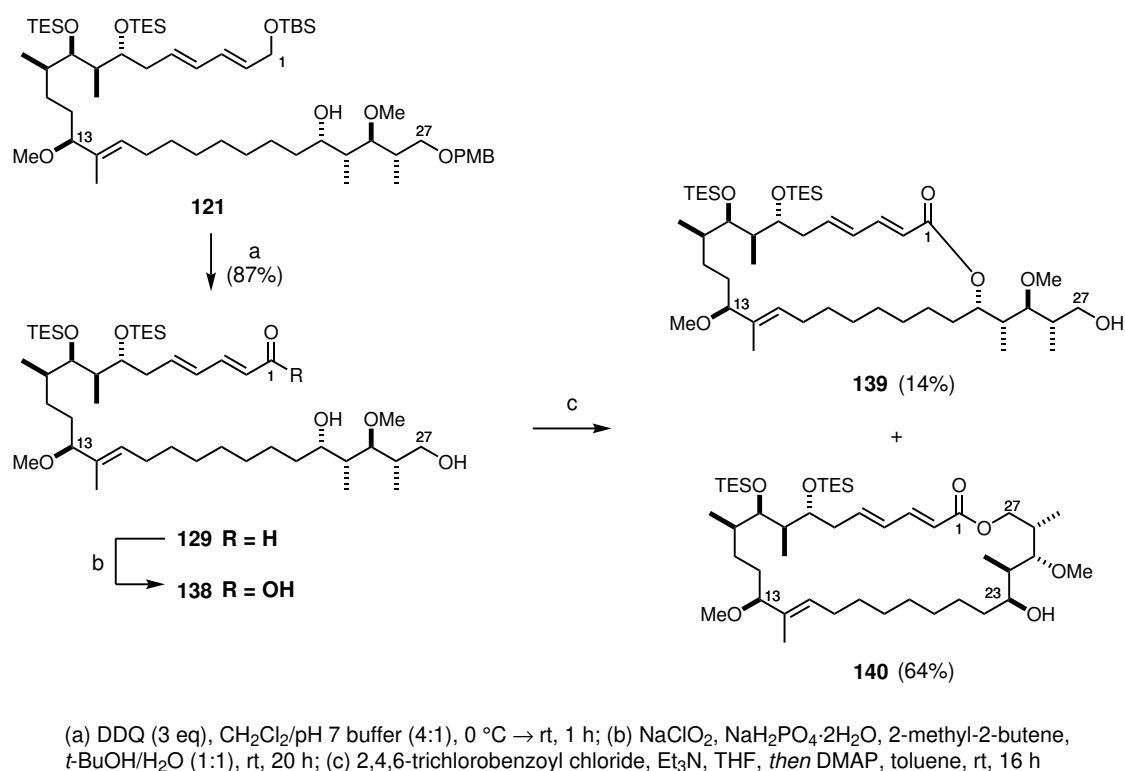


Scheme 3.14: Mechanism of the Yamaguchi macrolactonisation

In our systems **130** and **131**, this translated to addition of the mixed anhydride to a large excess of DMAP over 3–12 h *via* syringe pump. This resulted in yields ranging from 60–80% for the *bis*-TES product **132**, and 47–55% for the PMP product **133**, each calculated over 2 steps from the corresponding aldehyde. It is unclear at this point why the isolated yields were higher in the TES series, but nevertheless, this served to further bolster the case for its use over that of the PMP-protected material.

An adventurous attempt was made at improving the efficiency of this sequence by subjecting the C₂₃/C₂₇ diol **138** to the macrolactonisation conditions (Scheme 3.15). We maintained a slim hope that the substrate might show a conformational preference for forming the 24-membered ring found in the aplyronines, as opposed to the 28-membered ring resulting from cyclisation at the C₂₇ hydroxyl. If successful, this could have simplified the DDQ oxidation step by dispelling

the need to halt the reaction before PMB ether cleavage could occur, and would circumvent the later PMB deprotection step. Thus, the diol **129** was formed in a pleasing 87% yield by exposing alcohol **121** to excess DDQ, and oxidised under Pinnick conditions to the seco acid **138** (Scheme 3.15). The results of Yamaguchi macrolactonisation were, however, disappointing: the desired product **139** was isolated in only 14% yield, while an alternative esterified product, deduced to be the 28-membered macrolactone **140**, was obtained in 64% yield (a 4.4:1 ratio in favour of the undesired product). This result was easily explained on the basis that the primary C₂₇ hydroxyl is the more readily accessible of the two alcohols. Thus, our hopes for this shortcut were in vain, and the route described above was established as the best course of action.



Scheme 3.15: Attempt to form alcohol **139** by Yamaguchi macrolactonisation of the diol **138**

3.1.5 Selection of protecting group strategy for the onward synthesis

It was clear that we would need to select one or the other of the *bis*-TES and PMP protecting group strategies to simplify further work. Continuing to carry through two different but functionally equivalent intermediates would double the amount of effort in terms of experimental time and resources, as well as characterisation analysis. The PMP-protected northern segment **20**, despite being somewhat more easily accessible than the *bis*-TES version *via* the alkylation

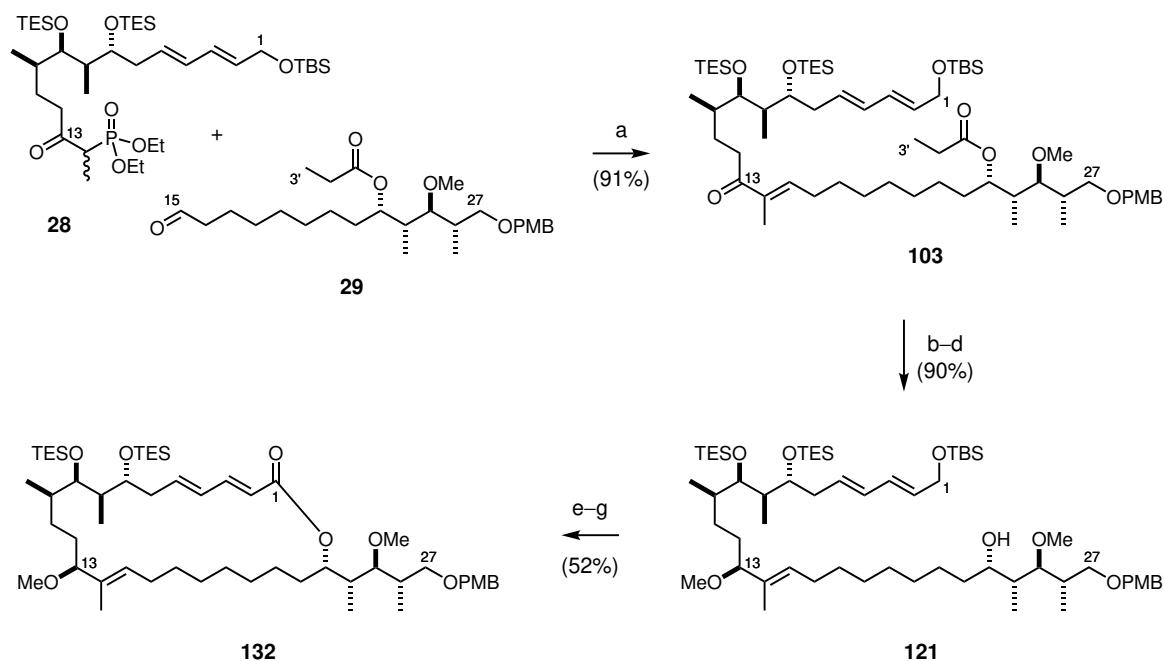
route (Sections 2.3.2 vs 2.3.1), had turned out to be much more troublesome at the HWE coupling stage. This was due to the difficulties in pushing the reaction to completion and separating leftover starting material from the coupled product.

Furthermore, although at the beginning of these investigations, this fragment **20** was in use in the natural product synthesis and therefore available in relative abundance, colleagues working on the next-generation synthesis had gradually moved more towards favouring the *bis*-TES material **28**. This was in part because its use forestalls a later protecting group switch after the forging of the macrolactone. This would therefore lead to an overall reduction by two synthetic steps which, although simple and high-yielding, nonetheless involve apparently unnecessary manipulations. With these thoughts in mind, it was concluded that the *bis*-TES-protected northern fragment **28** was the better choice for continued work towards the full analogues. As such, the synthesis of macrocycle **132** was now carried out on a larger scale to supply material to push towards the desired analogues.

3.1.6 Fully protected macrocycle scale-up

A campaign to scale up the macrocycle **132** synthesis was now embarked upon, following the route that has been described above. An overview of the results is presented in Scheme 3.16. Each step was carried out with cautious increases in the mass of substrate and minor changes to conditions to probe the reproducibility of this route. In most cases, reactions were carried out in 50–200 mg batches, then increased two- to five-fold in each repeat. Ultimately, the final three steps to form the macrolactone **132** were carried out on over 1 g of TBS ether **121** in a single batch. Almost all of the steps showed equal or improved yields on larger scale, with one exception being the alkylation to form northern phosphonate **28** (see Section 2.3.2), which remained variable and will be a focus for improvement in future studies.

In brief, the HWE olefination of the northern and southern fragments **28** and **29** gave enone **103** in 91% yield (Scheme 3.16). This was followed by CBS reduction of the enone at C₁₃ to give allylic alcohol **115** in 99% yield. At this stage, it was deemed prudent to unambiguously determine the configuration of the C₁₃ alcohol before carrying on further with the synthesis. This was achieved by Mosher ester analysis, as discussed in Section 2.1.1. Hence, the (*S*)- and (*R*)-MTPA esters **141** and **142** were formed from the corresponding enantiomers of Mosher's acid (Scheme 3.17). The sign of $\Delta\delta^{SR}$ for protons on each side of the derivatised alcohol was consistent with its assignment as the expected (*S*)-diastereomer, as shown in Scheme 3.17. Methylation of the C₁₃



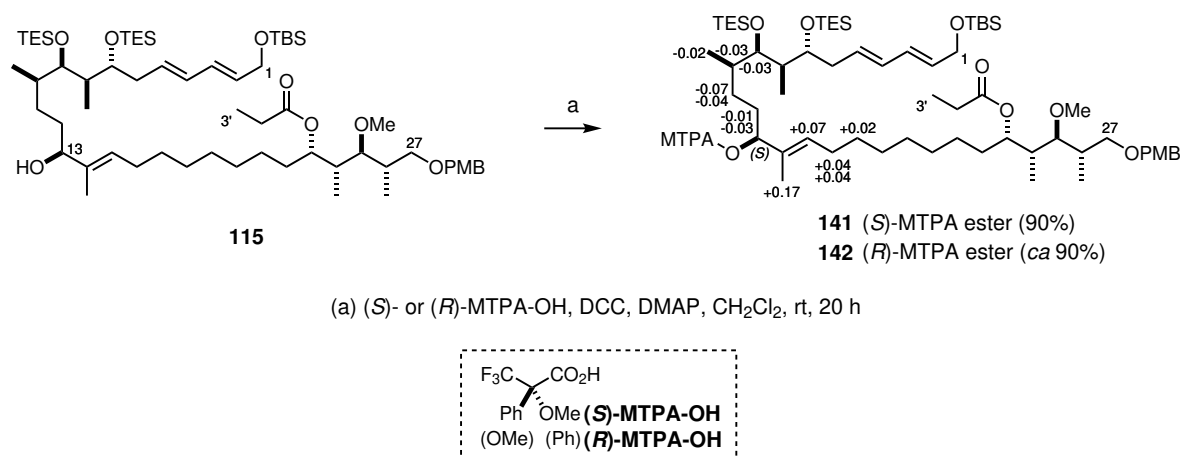
(a) $\text{Ba}(\text{OH})_2$, THF, rt, 2 h, then **29**, THF/ H_2O (40:1), rt, 24–72 h; (b) (*R*)-MeCBS oxazaborolidine, $\text{BH}_3\text{-SMe}_2$, THF, -10°C , 45 min; (c) $\text{Me}_3\text{O-BF}_4$, Proton Sponge, CH_2Cl_2 , rt, 2 h; (d) DIBAL, CH_2Cl_2 , -78°C , 1 h; (e) DDQ, $\text{CH}_2\text{Cl}_2/\text{pH } 9.2 \text{ buffer}$ (4:1), 0°C , 10 min; (f) NaClO_2 , $\text{NaH}_2\text{PO}_4\cdot 2\text{H}_2\text{O}$, 2-methyl-2-butene, $t\text{-BuOH}/\text{H}_2\text{O}$ (1:1), rt, 16 h; (g) TCBC, Et_3N , THF, rt, 1 h, then DMAP, toluene, rt, 12–24 h

Scheme 3.16: Overview of the synthesis of advanced intermediate **132** on gram scale

alcohol **115** and reduction of the C_{23} propionate ester **117** then gave intermediate **121** in 90% yield over the 3 steps.

Finally, a three-step sequence involving allylic TBS ether deprotection and oxidation with DDQ, Pinnick oxidation to obtain the seco-acid, and Yamaguchi macrolactonisation gave the macrocyclic intermediate **132** in 52% yield.

Thus, the fully protected macrocycle **132** was obtained in 7 steps and a respectable 43% yield from northern phosphonate **28** and southern aldehyde **29**. This represented an average yield of 89% per step. A total of 800 mg of macrocycle was generated in this way, with approximately 500 mg resulting from a single batch. The material could readily be stored at this stage until needed for further investigations.

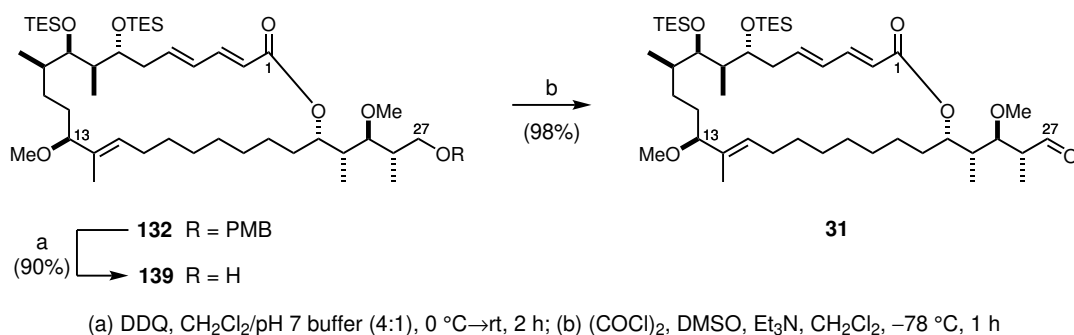


Scheme 3.17: Determination of absolute configuration at C₁₃ by Mosher's ester analysis

3.2 Macrocycle to side chain coupling and elaboration

3.2.1 Side chain attachment by aldol coupling and dehydration

With a sizeable amount (*ca* 800 mg) of fully protected macrolactone **132** in hand, it was now possible to investigate in detail the coupling to the side chain piece **32**. The planned analogues were to branch from a late-stage common intermediate. We would now advance the synthesis to this highly advanced compound. To this end, the macrocycle **132** was deprotected at the C₂₇ position (DDQ, CH₂Cl₂/pH 7 buffer, 0 °C, 90%) and oxidised under Swern conditions (DMSO, (COCl)₂, Et₃N) to the aldehyde **31** in 93–98% crude yield (Scheme 3.18). This aldehyde had to be handled with caution, as the C₂₆ stereocentre was observed to epimerise readily on exposure to both silica and Florisil. It was therefore carried through in crude form into the aldol coupling step.

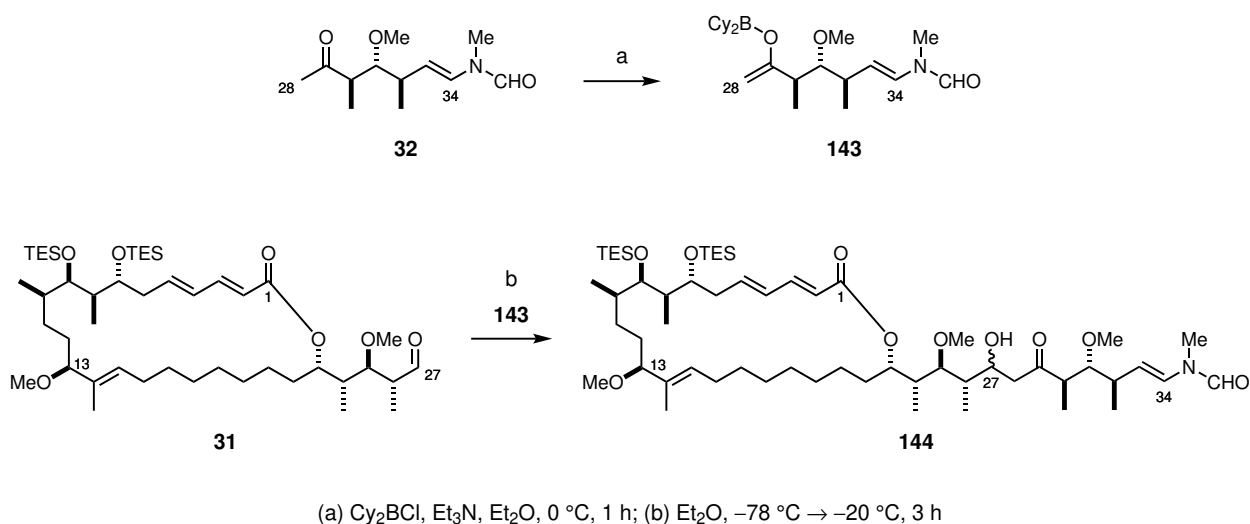


Scheme 3.18: Synthesis of aldehyde **31** from fully protected macrocycle **132**

The analogue fragment **32** (Section 2.2) was to be the ketone coupling partner for this reaction,

giving rise to hybrid-type analogues with side chains resembling that of scytophycin C (see Sections 1.5.2 and 4.1.1). A possible coupling with the C₃₁-acetate fragment as seen in the natural aplyronines was deferred to a later stage, to be investigated further pending the bioactivity results for the hybrid analogues.

The two fragments **31** and **32** were to be coupled *via* a boron-mediated aldol reaction. It was necessary for this reaction to proceed in a chemoselective fashion, given the range of potentially sensitive functionalities already present in each substrate. However, the diastereoselectivity was of little importance, as the new stereocentre introduced at the C₂₇ position would soon be reduced to a methylene unit. Based on the extensive previous efforts to forge this linkage under such challenging constraints, boron aldol chemistry had proven to reliably give high yields of the desired coupled product, as a result of its broad functional group tolerance which allows a highly site-selective reaction between the enolate and aldehyde.^{108,111}



Scheme 3.19: Boron aldol coupling of the macrocycle **31** and side chain **32** to forge the C₂₇ – C₂₈ bond

The reaction proceeds through formation of boron enolate **143**, and its subsequent reaction with aldehyde **31** to form β-hydroxy ketone **144** upon workup of the boron aldolate (Scheme 3.19). Typically, an oxidative workup is used;¹⁶³ however, we had concerns about the stability of the delicate functionality in our system under these conditions. In late-stage boron aldol coupling reactions during previous syntheses of related natural products in our group, both standard oxidative (MeOH, pH 7 buffer, H₂O₂, 94%, rhizopodin)¹⁶⁴ and non-oxidative (MeOH, pH 7 buffer, 70%, reidispongiolide A)⁸⁶ workup conditions had been used. During synthetic work on the aplyronines, the precedent had been to use a non-oxidative workup.^{108,111} Porter's investigations towards coupling the side chain and southern fragment before macrocycle closure sup-

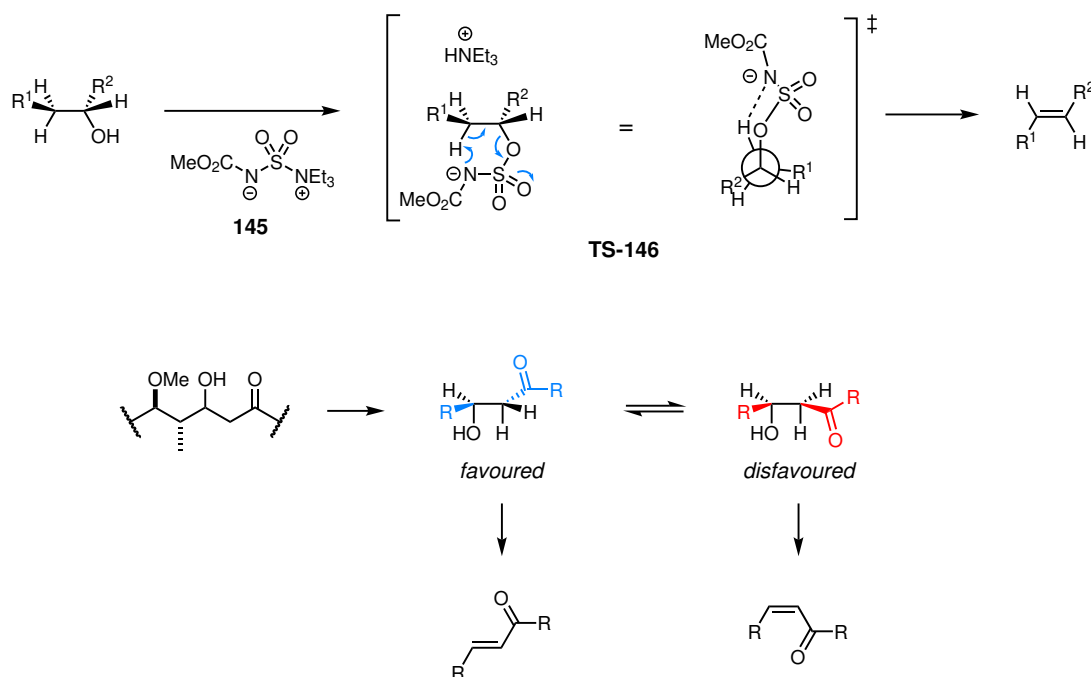
ported that this degree of caution was prudent, and further showed that stirring with silica and exposure to air could mildly reveal the desired β -hydroxy ketone without compromising the *N*-vinylformamide.^{129,165}

The macrocyclic aldehyde **31** was by far the more precious of the two coupling partners, being accessible in 18 linear steps as opposed to only 8 steps for ketone **32**. It was therefore chosen as the limiting substrate for the reaction. During early testing on small scale, a large enough excess of the ketone **32** (2–6 eq) was used to ensure full conversion of the valuable aldehyde **31**, but it was eventually found that only slightly superstoichiometric quantities (1.2 eq) were sufficient to push the reaction to completion. In either case, any excess enolate would regenerate the starting ketone **32** upon quenching, such that the material could be recovered for re-use later on.

In the event, ketone **32** was enolised with Cy_2BCl and Et_3N at 0 °C, then added to aldehyde **31** at –78 °C. The mixture was stirred at this temperature for 1 h, then slowly allowed to warm up to –20 °C, with monitoring of reaction progress by TLC analysis. This resulted in full consumption of the aldehyde after 2–3 h. When complete, the reaction was subjected to a very mild, non-oxidative workup by addition of silica and stirring under ambient air for 1 h, following the conditions which had been developed by Porter.¹²⁹ The aldol adduct **144** was obtained after column chromatography as an inconsequential mixture of diastereomers at the C_{27} position (*ca* 3:1 *dr*). A large increase in polarity due to the introduction of the terminal *N*-methyl-*N*-vinylformamide moiety made the product **144** difficult to separate chromatographically from the excess ketone **32**. This was of little consequence, however, as the ketone was unreactive in the next step, and so the material could be carried through as a mixture and then separated at that stage.

With this in mind, a Burgess dehydration was undertaken on **144** to form (*E*)-enone **147**, the product of a stereospecific *syn*-elimination of the newly formed C_{27} -hydroxyl group. This reaction makes use of the internal salt **145** (Scheme 3.20) to give olefins from secondary or tertiary alcohols, forming the conjugated product if adjacent to a carbonyl.^{166,167} The mechanism begins with formation of a sulfamate ester, with Et_3NH^+ as a counterion. An intramolecular *syn*-elimination of the β -hydrogen atom occurs *via* a 6-membered cyclic transition state, **TS-146**. The (*E*)-selectivity stems from the preference for the large R groups to eclipse hydrogens in the E_i transition state.

As the reaction does not require acidic conditions, it is compatible with a wide range of acid-sensitive functional groups, including the ester, amide and several methyl ether moieties present in our substrate. The intermediates are generally reactive enough to undergo dehydration at room



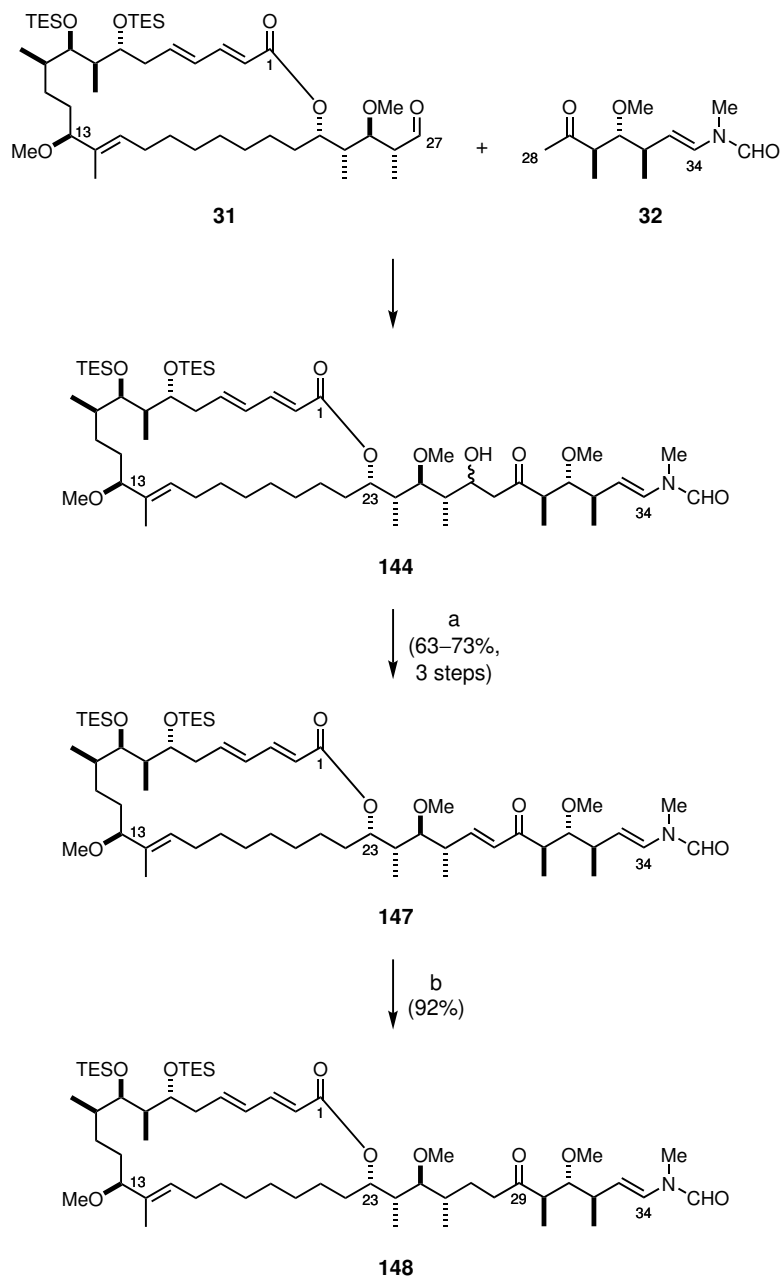
Scheme 3.20: Mechanism of the Burgess elimination reaction¹⁶⁶

temperature, minimising the risk of substrate degradation. This made the Burgess elimination ideal for our desired conversion.

Consequently, the mixture of aldol adduct **144** and remaining ketone **32** was stirred with Burgess salt in THF at rt, leading to moderate conversion tempered by slow reaction rate and eventual stalling (Scheme 3.21). By this method, a yield of 43% was calculated over 2 steps from aldehyde **31**. To improve the yield, the reaction mixture was warmed gently to 30 °C, leading to improved reaction progress without observation of new byproducts. However, stalling was still an issue, and when it occurred the best course of action was to halt the reaction and resubmit the crude mixture after a simple workup. In this way, yields of 63–73% (over 3 steps) in total after 1 recycle were achieved on scales of up to 65 mg based on alcohol precursor **139**.

3.2.2 Conjugate reduction to the C₂₉ ketone

To complete the aplyronine analogue backbone, a conjugate hydride addition to reduce the enone **147** to C₂₉ ketone **148** would be required. This would need to be done cautiously, as any conditions that would achieve this conversion could potentially also set the pentadienoate or the sensitive vinylformamide at risk. Fortunately, earlier studies on both the aplyronines and the related natural product reidispongiolide A had found that Stryker's reagent (triphenylphosphine copper

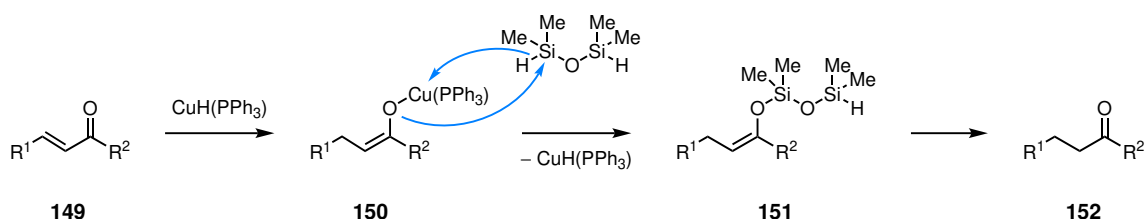


(a) Burgess salt, THF, 30 °C, 20 h; (b) $[\text{CuH}(\text{PPh}_3)]_6$, toluene, rt, 2 h

Scheme 3.21: Synthesis of advanced intermediate **148**, with the full carbon skeleton in place

hydride hexamer, $[\text{CuH}(\text{PPh}_3)]_6$ ^{168–170} was capable of carrying out this challenging transformation chemoselectively.

Mechanistically, the copper complex supplies a soft hydride nucleophile to the β -carbon of the enone **149** (Scheme 3.22). The resulting copper enolate **150** reacts with excess tetramethyldisiloxane (TMDS) to regenerate the active catalyst, stabilising the reactive intermediate as the silyl enol ether **151** which protects against overreduction.¹⁷¹ This species is then protonated to generate the ketone product **152**.



Scheme 3.22: Mechanism of conjugate reduction with Stryker's reagent¹⁶⁸

As a complementary approach to its isolation as an air-sensitive pure solid,¹⁷² Stryker's reagent and related copper hydride sources can be formed *in situ* using organosilanes, such that the reactions can be made catalytic in copper.^{171,173–175} For this work, the reagent was prepared as a solution in toluene *via* the method described by Yun.¹⁷⁶ According to this protocol, tetramethyldisiloxane (TMDS) is added to $\text{Cu}(\text{OAc})_2 \cdot \text{H}_2\text{O}$ and PPh_3 in toluene solution. A colour change is observed from the aqua-blue copper(II) acetate to a brick red colour characteristic of the copper(I) complex, indicating that the active reagent has been formed. The presence of excess TMDS in the solution provides a stoichiometric hydride source, allowing the copper species to be used in catalytic quantities and regenerated *in situ* during the reaction. For the purposes of this project it was found that the solution could be used fresh or stored at $-20\text{ }^\circ\text{C}$ for approximately 1 month, and that the colour of the solution was indicative of its quality. Indeed, it was clear that the quality of the Stryker's solution was important, as on one occasion when an older batch of starting materials was used to form the reagent, degradation of the *N*-vinylformamide moiety was observed. In a few cases, the integration of signals for $\text{H}_2\text{--H}_5$ in the ^1H NMR spectrum appeared to diminish, while signals in the upfield region increased. This seemed perhaps to indicate attack on the dienophile, but the high polarity of these compounds and their tendency to exist as stable rotamers made it difficult to visualise or separate different components by chromatographic methods. For this reason the reaction of **147** was carried out first on test scale to ensure success with the particular reagent batch, before carrying on to more preparative scale reactions.

In practice, aliquots of Stryker's solution equating to 20 mol% Cu(I) were added to the enone

147 at rt, and the conversion was monitored by TLC analysis (Scheme 3.21). Where necessary, further aliquots of reagent could be added. No special precautions were taken to de-gas the reaction solvent, as this method was not observed to be particularly air sensitive. The reaction was generally complete within 2–3 h and the mixture could be loaded directly onto a silica column without the need for aqueous workup. In this way the complex fragment **148** was obtained in excellent yield (80–92%).

3.3 Summary

With this objective achieved, the full skeleton of our desired unnatural aplyronine congeners had been established. Only modifications to the functional appendages of the highly advanced intermediate **148** would be needed to complete our planned analogues using a late-stage diversification strategy. We were poised to finish the first of our much-anticipated library of aplyronine analogues to submit to biological testing in comparison with the natural products.

From this point, the synthesis would split into various branches, together representing a divergent family of analogues. The endgame strategy and the the branches of inquiry that follow will be the focus of Chapter 4. We shall discuss the outcomes of studies to finalise the first round of aplyrologues, and consider the outlook for those yet to be pursued.

Chapter 4

Completion of the synthesis and conclusions

4.1 Endgame

Having set the correct connectivities and stereochemistry for the full carbon chain, our aplyronine analogues were at last within reach. As was set forth in Section 1.6, the library of analogues that were targeted in this work would be differentiated at this late stage by the chemistry of the side chain, as well as the pendant amino acids at C₇ and C₂₉. We decided in the first instance to target scytophycin-type hybrid analogues with the C₂₉ ketone intact, followed by aplyronine A/D analogues with esterification through the 29*R*-hydroxyl group. These efforts will now be described.

4.1.1 Completion of scytophycin-type hybrid analogues

From ketone **148**, the product of the conjugate reduction with Stryker's reagent (see Section 3.2.2), two steps would be required to form the epimeric analogues **154** and **155**, with a ketone at C₂₉ and an (*S*)- or (*R*)-*N,N,O*-trimethylserine (TMSer) ester at C₇ (Scheme 4.1). The first step would require cleavage of the two silyl protecting groups at C₇ and C₉ to form diol **153** for our library of analogues. This was achieved on treatment of **148** with HF·py in 82% yield. This compound bears two free hydroxyl groups in the northern region, as does aplyronine C, and therefore represents the first of our desired aplyrologues for biological testing.

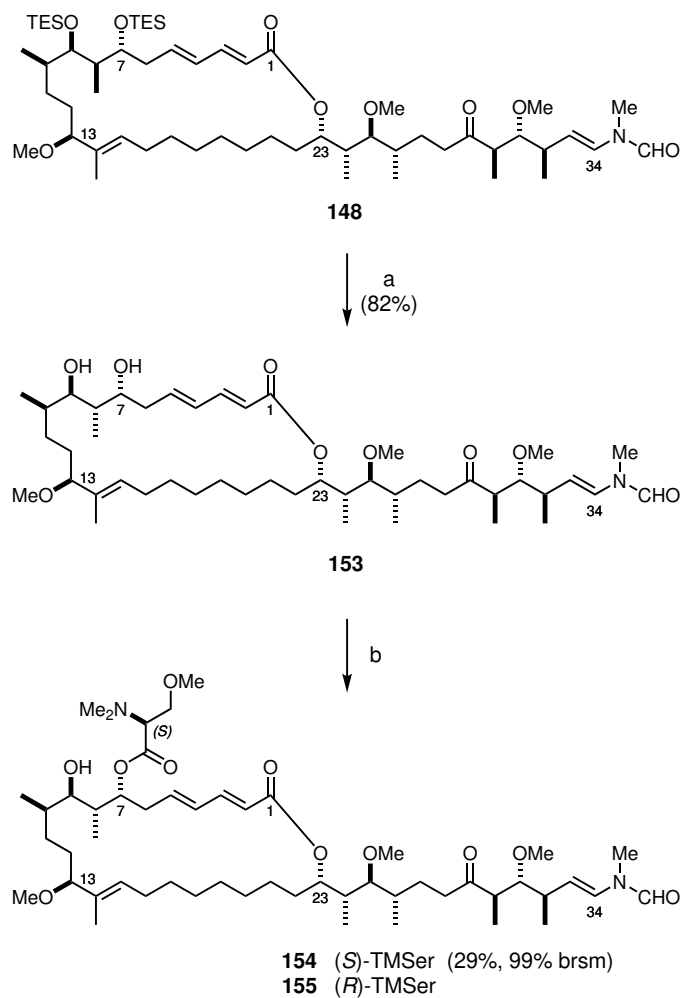
Due to the significantly higher levels of cytotoxicity observed in the natural congeners containing a C₇-TMSer moiety (aplyronines A and D), we were keen to incorporate this functionality next. Each enantiomer of TMSer had been prepared by Dr Simon Williams in this laboratory, and a small stock of these useful intermediates was available for the studies reported here. Williams had found that, with careful monitoring, acylation could be achieved site-selectively at the C₇ alcohol, as it is less hindered than that at the C₉ position.¹⁰⁸ This could be done under either Keck (DCC, DMAP, DMAP·HCl)¹⁷⁷ or Yonemitsu (DMAP, TCBC, Et₃N)¹⁶⁰ esterification conditions, with the latter proving more reliable.

Thus, the (*S*)-TMSer was installed in **154** according to Yonemitsu's protocol. These conditions are a variant of those developed by Yamaguchi: instead of pre-forming the mixed anhydride with TCBC followed by exposure to nucleophilic DMAP, in this case all of the components are combined simultaneously. Higher concentrations are also generally used. In this way, the (*S*)-epimer **154** was formed in 29% yield (99% brsm) without any by-product formation (Scheme 4.1). The configuration of the amino acid chiral centre was retained under the reaction conditions, as had been observed by Williams.^{92,108} The low conversion at this stage can be attributed to the small scale of the reaction and the desire to proceed cautiously in light of the highly advanced nature of the material. It is likely that this result can be improved upon in future studies: Williams was able to achieve 50–80% conversion with almost quantitative starting material recovery in the synthesis of aplyronines A and D. This initial attempt generated a sufficient sample for full characterisation and preliminary biological testing.

It still remains unclear whether the scalemic mixture of amino acid epimers observed in the aplyronines is a true reflection of the natural composition of these compounds, or an artefact of the isolation process. As we desired to investigate these effects further in our testing library, the naturally occurring (*S*)-(+)-enantiomer of TMSer was pursued first. The (*R*)-epimer **155** is expected to be formed shortly *via* the same procedure.

4.1.2 Studies towards C₂₉-esterified analogues

Meanwhile, investigations into synthesising analogues extending from a C₂₉-(*R*) hydroxyl group were begun. Inspection of the crystal structure of actin-bound aplyronine A suggests that the configuration of this stereocentre allows the pendant amino acid to point into bulk solvent. This suggests that inversion of the configuration could result in a significant change in the binding conformation and possible loss of activity. Thus, although each epimer could ideally be tested to



(a) HF-py, THF, 0 °C → rt, 16 h; (b) (*S*)- or (*R*)-TMSer, DMAP, TCBC, Et₃N, CH₂Cl₂/benzene, 0 °C → rt, 1.5 h

Scheme 4.1: Synthesis of analogues **153**, **154** and **155** with C₂₉ ketone moiety

provide further SAR information, our first priority was to form the (*R*)-alcohol to create mimics that would not differ too greatly from the natural aplyronine congeners.

Dr Sarah Fink had performed this reduction in a stereoselective manner by using zinc borohydride to carry out a substrate-directed hydride transfer.¹⁷⁸ Fink had reasoned that high stereoselectivity for the formation of either C₂₉ epimer would be acceptable, as the desired amino acids could then be introduced either through standard esterification procedures, or by a Mitsunobu reaction.^{179,180} In the event, reduction with Zn(BH₄)₂ gave the desired (*R*)-alcohol in 90% yield and 10:1 *dr* on small scale. However, studies by Williams on both the real system and side chain models, and by Rachel Porter on analogue side chain–southern fragments, found this reaction to be highly capricious.^{108,129} Results varied between 40–90% yield and 1:1 → 10:1 *dr*, and appeared to depend heavily on the quality of the reagent, which was impossible to determine other than by testing directly on the limited quantities of precious substrates. Thus, this step was expected to present further challenges in the ongoing synthesis. Propitiously, an outcome of Porter’s work was that the epimers **156** and **157** (Figure 4.1) were separable by column chromatography, allowing the minor (*S*)-epimer **157** to be recycled by oxidation and resubmission to the reaction conditions.

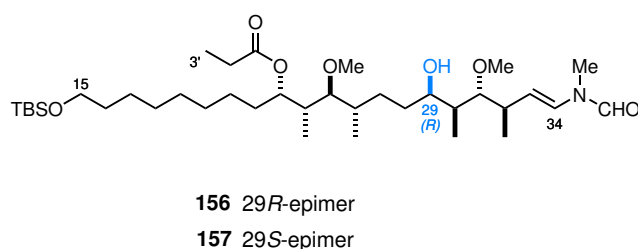
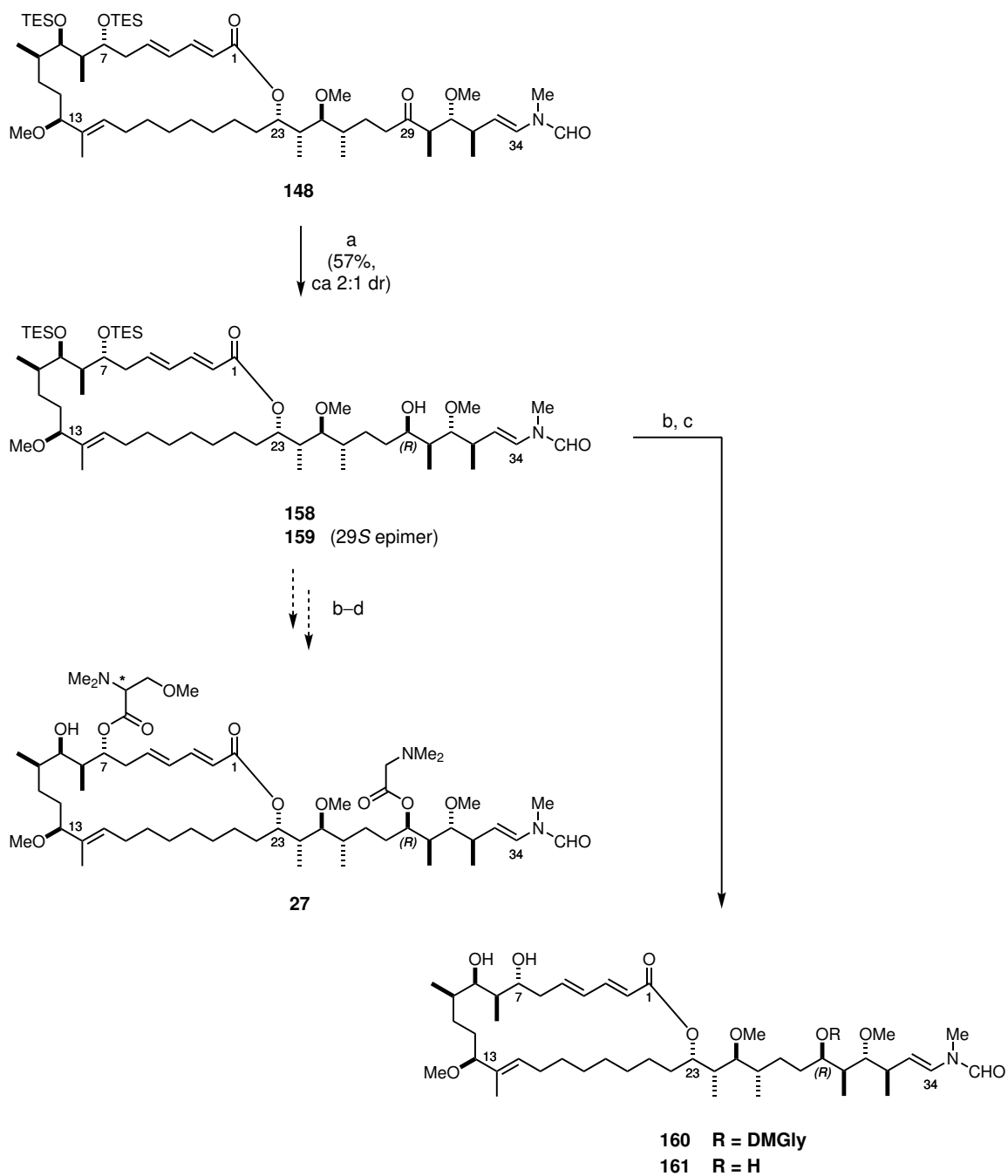


Figure 4.1: Chromatographically separable side chain analogues synthesised by Porter¹²⁹

Initial testing of the zinc borohydride reduction in our analogue system **148** was afflicted by similar limitations to those experienced by Williams and Porter. Test reactions achieved yields of 76% (1.1:1 *dr*) and 57% (*ca* 2:1 *dr*, Scheme 4.2) of alcohol **158**. The two diastereomers did appear to be separable by careful silica chromatography, but this was a non-trivial process. The compounds are difficult to visualise by TLC analysis due to their high polarity and tendency to streak or to appear as two spots, presumably because they exist as two stable rotamers at the *N*-vinylformamide terminus. Analysis by ¹H NMR does show a clear difference between the two isomers, with H₂₉ and H₃₁ appearing at significantly different chemical shifts.

A preliminary attempt was also made to form the diester **27** in three steps (Scheme 4.2). A small sample of the putative alcohol **158** was subjected to the Yonemitsu esterification conditions described in Section 4.1.1 with *N,N*-dimethylglycine (DMGly), then the crude was sub-



(a) $\text{Zn}(\text{BH}_4)_2$, Et_2O , 0 °C, 3 h; (b) DMGly, DMAP, TCBC, Et_3N , THF/toluene, rt, 2.5 h; (c) HF-py, THF, 0 °C \rightarrow rt, 16 h;
(d) (*S*)- or (*R*)-TMSer, DMAP, TCBC, Et_3N , CH_2Cl_2 /benzene, 0 °C \rightarrow rt, 1.5 h

Scheme 4.2: Studies towards the synthesis of diester **27**

mitted directly to HF · py in anticipation of forming the diol monoester **160**. However, no signal that would correspond to H₂₉ in the esterified product was observed by ¹H NMR. Inspection of the spectra along with the high polarity of the compound indicated that the esterification step may have failed, giving triol **161** as the likely product. This compound was not fully characterised for the purposes of this project, but could be included in future testing libraries if deemed appropriate.

The difficulty in obtaining clean samples of each C₂₉-epimer (**158** and **159**) for analysis has hampered the continuation of this work. These investigations will now be taken up by Rachel Porter, whose work towards synthesising further unnatural aplyrologues and the results of their testing in biological assays will be detailed in an upcoming publication.¹³¹

4.2 Planned biological testing

The next stage of this work will be to test the synthetic analogues in cytotoxicity assays. In the first instance, testing will be carried out in the HeLa-S3 cell line, to allow for direct comparison with the natural products. Extending upon this, we will submit the compounds to AstraZeneca's CLIMB panel for testing against a wide range of cell lines. These cell lines represent many different families of cancers and would give an early indication of any particular diseases of interest for further development. Previous results for the aplyronines in both this panel and the NCI-60 cell line panel have demonstrated their broad-spectrum cytotoxic activity in human tumour models. As a result we expect that, if comparably active in the HeLa-S3 line, the current analogues would show a similarly broad range of potential disease applications.

Figure 4.2 shows the library of analogues either currently in hand (**153** and **154**) or expected to be completed in the near future for submission to bioactivity testing. The (*R*)-TMSer epimer **155** will shortly be completed and fully characterised following the procedure for compound **154**. These constitute our “scytophycin hybrid”-type analogues, with C₃₁ methyl ether and C₂₉ ketone functionalities. In addition, the analogues with pendant amino acids at C₂₉ as in the aplyronines will be prepared *via* the methods discussed in Section 4.1.2. The first of these will be the aplyronine D-like analogues, with DMGly at C₂₉ and the free alcohol or TMSer at C₇ (**162**, **163** and **164**). These may be accompanied by the aplyronine A-like variants containing DMAla at C₂₉ (**165–170**). The DMGly-containing analogues will be prioritised because of the apparently greater cytotoxicity of aplyronine D in earlier assays, with the corollary benefit that the lack of a chiral centre in the amino acid somewhat deconvolutes the process of synthesising

and characterising the products.

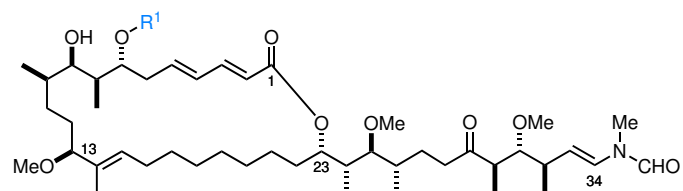
Our analogues have been rationally designed to be more synthetically accessible without affecting the pharmacophore. If this hypothesis is indeed borne out, we expect to see that their antiproliferative activity will be similar to that of the natural products, which show picomolar IC₅₀ values in the HeLa-S3 cell line. There is only a small likelihood of an improvement in activity, although the inherent complexity of predicting ligand binding in biological systems means that such an improvement could arise unexpectedly. If, contrary to our intentions, we have indeed modified the aplyronine pharmacophore in such a way as activity is lowered, this would be reflected in a significant increase in IC₅₀. If this is the case, there could be a number of causes:

- (1) essential actin or tubulin binding contacts may have been removed or transformed,
- (2) the overall shape of the molecule may have changed, such that its preferred conformation is not compatible with actin binding,
- (3) the molecule may still bind to actin, but in an altered binding mode so that interaction with tubulin is no longer possible, or
- (4) cell permeability has been reduced.

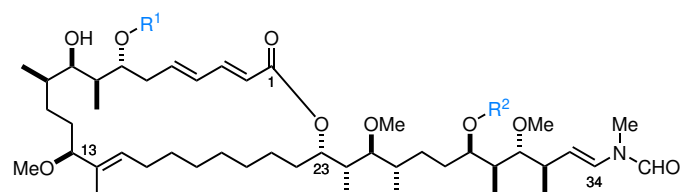
Depending on the results of biological testing, we may need to look further into these possible impediments. Deeper considerations would be assisted by additional data from actin binding studies of the sort which have previously been carried out on aplyronine tail analogues in collaboration with Prof. Gerard Marriott.¹⁸¹ We also anticipate that a crystal structure of the actin–aplyronine–tubulin ternary complex will soon be available, and understand that work towards this challenging target is ongoing.^{108,182} On the basis of this information, we shall generate new hypotheses relating to structure–activity relationships for the aplyronines, and thus design a second round of analogues which would overcome any obstacles that become evident.

If, on the other hand, the biological activity of our analogues is as we hope, we will nonetheless have recourse to design further analogues – in this case to further simplify the synthesis and perhaps generate even more potent analogues. Our goal would be to test the limits of structural abridgement, finding the optimal balance between process simplicity and cytotoxic activity.

In either case, we expect that these results will lead to the suggestion of new analogues based on function-oriented design principles. Some preliminary ideas regarding the form of these second-generation analogues are presented here.



	R ¹
153	H
154	(<i>S</i>)-TMSer
155	(<i>R</i>)-TMSer



	R ¹	R ²
162	H	DMGly
163	(<i>S</i>)-TMSer	
164	(<i>R</i>)-TMSer	
165	H	(S)-DMAla
166	(<i>S</i>)-TMSer	
167	(<i>R</i>)-TMSer	
168	H	(R)-DMAla
169	(<i>S</i>)-TMSer	
170	(<i>R</i>)-TMSer	

Figure 4.2: Library of analogues, both in-hand and planned, for imminent submission to biological testing

4.3 Modifications to generate a second round of analogues

In terms of designing a second round of analogues for further structure–activity testing, late-stage diversification will be the preferred strategy to capitalise on the work already achieved while investigating the effects of modifications. Since we wish to probe the relationship between structure and function in an already potent interaction, the modifications at this stage are not intended to be too drastic: rather, to be relatively minor changes that could induce small but potentially significant changes in protein binding interactions.

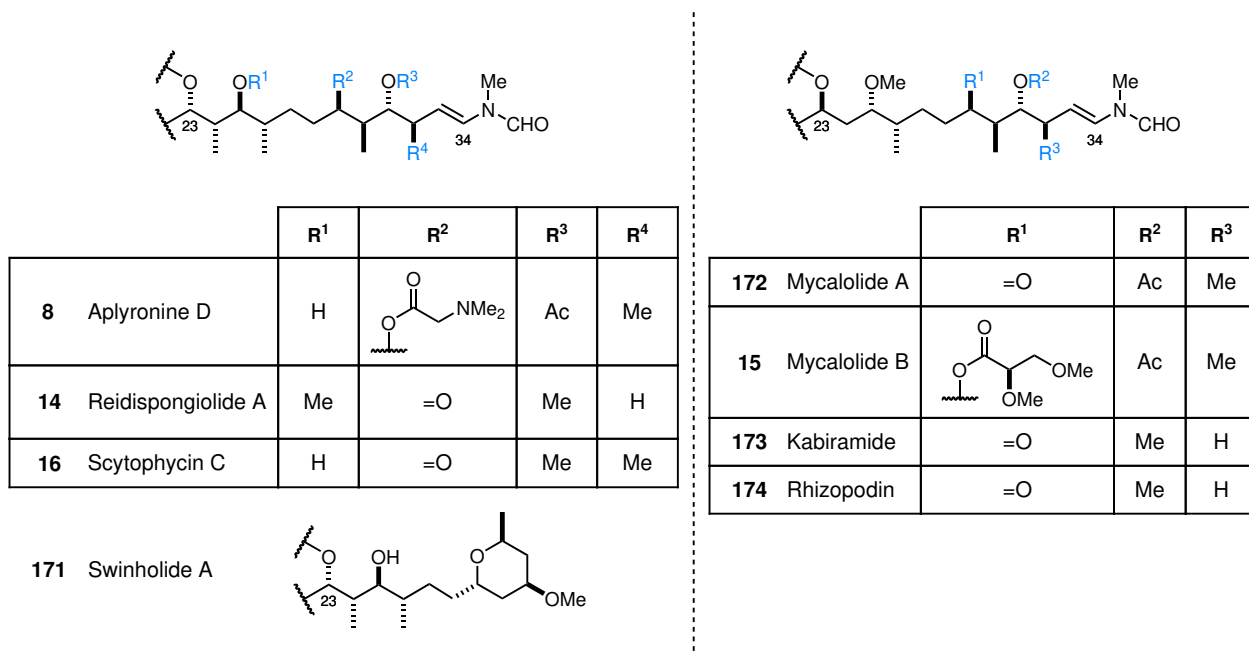


Figure 4.3: Side chain segments of related actin-binding natural products (numbering based on the aplyronines). Left: stereochemistry in C₂₃–C₂₅ region equivalent to the aplyronines. Right: altered stereochemistry in the C₂₃–C₂₅ region.

To this end, we could consider altering properties of the side chain region at a late stage by incorporation of revised fragments at the aldol coupling stage. For this we could seek inspiration from actin-binding natural products with similar side chains terminating in the *N*-methyl-*N*-vinylformamide moiety (Figure 4.3; see also Section 1.4.4). Compounds to the left of the dashed line are those which have equivalent stereochemistry in the C₂₃–C₂₅ region to that of the aplyronines; compounds to the right have altered configuration in this region. An elegant publication by Kigoshi and co-workers recently demonstrated that this stereochemistry has a strong effect on the binding mode of these compounds, resulting in the macrocycle portion being oriented in two different directions when in complex with actin.¹⁸³ This difference explains why the group's

earlier aplyronine A–mycalolide B hybrid showed strong actin depolymerising ability, but significantly decreased cytotoxicity relative to aplyronine A (see Figure 1.18, p. 18). Based on these findings, the researchers synthesised a new hybrid containing the macrocycle part of aplyronine A and the side chain of swinholide A as a structurally simpler substitute that occupies the same binding mode (Figure 4.4). This new hybrid retained picomolar cytotoxicity to HeLa-S3, although the actin depolymerising activity was less potent, presumably due to the introduction of the swinholide portion. These results lend support to the principle that simplified structures based on the aplyronines may be synthetically more accessible while retaining high levels of cytotoxic activity.

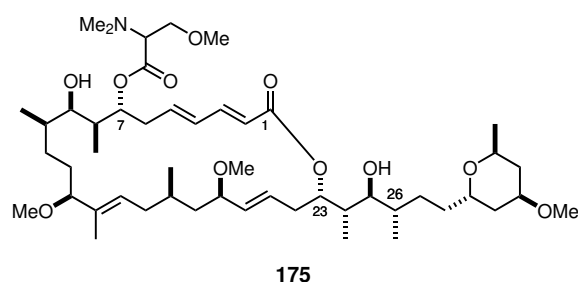
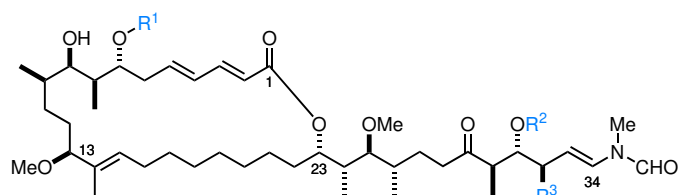


Figure 4.4: Kigoshi and co-workers' aplyronine/swinholide hybrid¹⁸³

Future modifications should follow this lead by adopting the simplified-hybrid model. For example, we could consider similarly combining our simplified macrocycle with the swinholide side chain, although this would involve developing some new chemistry to introduce the side chain portion in our route. More straightforwardly, we could generate variants that more closely resemble the side chain of reidispongioidide A by using the equivalent aldol–dehydration–reduction sequence from the total synthesis of this natural product.⁸⁶ These would have the form of compounds **176** and **177** (Figure 4.5). Although it would be preferable not to return to the C₃₁ acetate-containing fragment from the aplyronine total synthesis due to its tendency to undergo elimination under various conditions,^{91,92} if desired we could readily carry this out to produce compounds **178** and **179** (Figure 4.5).

Additionally, a variety of changes could be made to the pendant amino acids at C₇ and C₂₉. In the northern region, all evidence to date suggests that the trimethylserine moiety is very important in promoting binding of tubulin to the actin–aplyronine complex; nevertheless, it may be that some modifications are tolerated or even improve activity. Thus, a range of methylated serine variants could be appended to any of the analogues already described (Figure 4.6). More so, however, the range of modifications at C₂₉ are of interest given our current investigations towards extending this region for antibody conjugation. For this purpose it would be informative to test whether the presence of a C_{2'} methyl group (DMGly vs DMAla) and the degree of *N*-methylation



	R ¹	R ²	R ³
176	(S)-TMSer	Me	H
177	(R)-TMSer		
178	(S)-TMSer	Ac	Me
179	(R)-TMSer		

Figure 4.5: Proposed second generation of analogues with altered side chains based on reidispongiolide A and the aplyronines

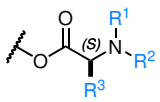
is significant (Figure 4.6). The importance of the basic nitrogen at this position would also be enlightening; this could be analysed by comparing a DMGly-functionalised substrate with equivalents containing a non-basic nitrogen (e.g. from *N*-acetyl-*N*-methylglycine) or no nitrogen (e.g. from isovaleric acid) at the same position.

4.4 Potential to streamline the overall synthesis

Much discussion in this dissertation has centred on “efficient” and “scalable” routes and reactions, and mention has even been made of the developing steps for early process-scale synthesis. Nevertheless, the synthesis of small quantities of analogues for exploratory biological testing and the manufacture of commercial targets are two quite different concepts. To excerpt from Allred, Manoni and Harran’s recent review on the manufacture of complex natural product-based drug candidates by *de novo* synthesis,

the laboratory synthesis of complex natural products and the manufacture of small-molecule drugs are chemistry compatriots that seldom meet. The former is typically an academic pursuit in which emerging methods are tested and assembly tactics are explored, whereas the latter are beautifully engineered exercises in brevity, efficiency, and scale. The two operate on common principles, of course, but thereafter, they focus on different goals with markedly different criteria for success.¹⁸

At this stage of the current project, our focus has been to develop an efficient synthesis to produce



	R ¹	R ²	R ³
DMGly	Me	Me	H
MMGly	Me	H	H
Gly	H	H	H
DMAla	Me	Me	Me
MMAla	Me	H	Me
Ala	H	H	Me
TMSer	Me	Me	CH ₂ OMe
DMSer	Me	Me	CH ₂ OH
	Me	H	CH ₂ OMe
MMSer	Me	H	CH ₂ OH
	H	H	CH ₂ OMe
Ser	H	H	CH ₂ OH

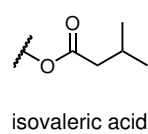
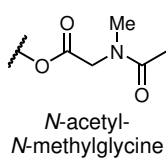
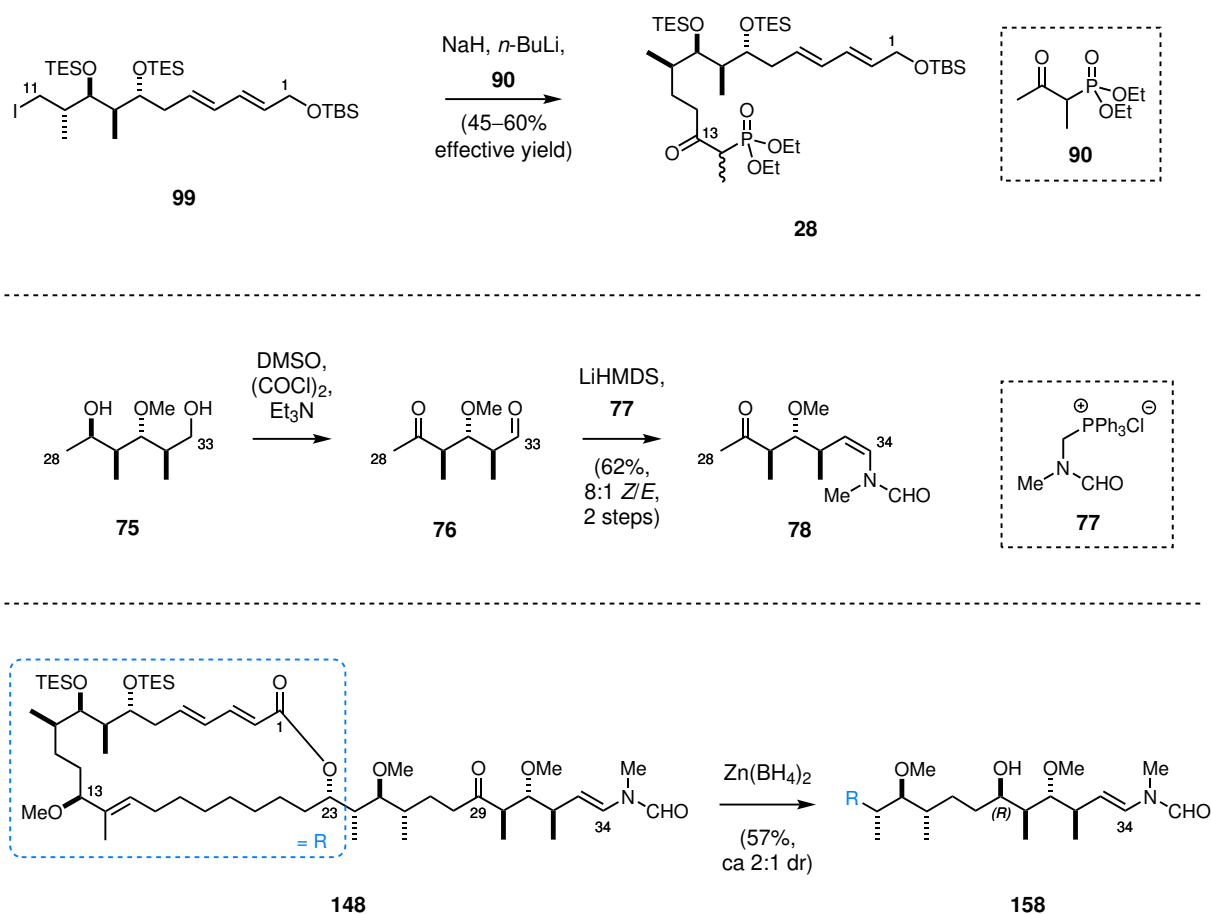


Figure 4.6: Natural and modified amino acids for potential late-stage functionalisation of aplyronine analogues

aplyronine analogues on small scales for biological testing, on the order of milligrams. Beyond this, however, we have set our sights on generating structurally simplified candidates with the potential for highly efficient manufacture in the future. Any manufacturing routes that might eventuate are likely to contain some significant departures from our laboratory synthesis, and it is left to those with relevant expertise to identify and enact these efficiencies. However, a priority during this work has been to find reliable, highly stereoselective chemistry that would allow late-stage modifications to produce a variety of analogues. Our synthesis has been highly effective in this regard. Nevertheless, there remain a number of steps which could greatly improve the efficiency of our route if they could be optimised for the current purposes. These have mainly been discussed in the text where relevant, but three key examples are presented here.



Scheme 4.3: Challenging synthetic steps which could benefit from further optimisation

Firstly, the alkylation step to introduce a phosphonate moiety into the northern fragment for HWE coupling has continued to cause difficulties. The best results reported here represented 45–60% effective yield of the desired product **28** (Scheme 4.3, top), with lower yields attained on larger scales. In future studies, it may be possible to redesign this disconnection. It is worth

noting that SAR studies have indicated that removal of the C₁₄ methyl group can be tolerated, suggesting that future analogues could incorporate a simpler disubstituted olefin. This could open up new opportunities for improving this sequence.^{78,79}

Secondly, the Swern/Wittig protocol that installs the terminal *N*-methyl-*N*-vinylformamide into the side chain fragment has been carried out in an optimised yield of 62% to date for the analogue fragment discussed in this dissertation (Scheme 4.3, middle). This had been a challenging transformation for Fink¹¹¹ and the results achieved here did overcome the difficulties that still remained. For instance, the need for constant vigilance in case of acetate elimination in subsequent steps was almost completely suppressed when using the methyl ether variant. However, it would be advantageous to improve the overall yield and reliability of this step. The simplest ways of achieving this might be to look for further inspiration in actin-binding macrolides with conserved features, such as reidispongiolide A, which has the same structure bar the C₃₂ methyl group. A synthesis for the side chain fragment of reidispongiolide A has been reported,⁸⁶ and could be put to use in the design of new analogues (*vide supra*, Section 4.3). More adventurously, we could consider substituting the *N*-vinylformamide for a different polar group entirely, such as an alcohol, oxime or hydrazone, all of which were found to be tolerated in Kigoshi's SAR studies.^{70,76,78,79} Although this moiety is found in many actin-binding natural products, its level of complexity may be somewhat incidental if what is needed is merely a hydrophilic group. If an alternative can indeed be found without decreasing actin binding ability or overall cytotoxicity, it could be a boon to the development of a much further simplified analogue, with the additional benefit of making the NMR characterisation of intermediates more straightforward.

Thirdly, setting the desired stereochemistry at the C₂₉ position presented a challenge which slowed work at the final stages of the synthesis (Scheme 4.3, bottom). A lack of time and reluctance to deplete valuable late-stage material meant that the best result achieved in this work was only moderate in both yield (57%) and *dr* (2:1). Recommendations for immediate future work are to investigate more reliable sources of the zinc borohydride reagent, if they can be found. If not, less diastereoselective methods such as reduction with sodium borohydride could be considered if the overall yield is higher. Provided the two epimers **158** and **159** can be separated, as early results suggest, the undesired compound could either be oxidised and recycled as has previously been demonstrated in model studies,¹²⁹ or Mitsunobu esterification could be attempted.¹¹¹ Reagent-controlled methods could also be investigated, although previous work has ruled out the CBS reduction as a feasible option.^{111,131}

If these challenging transformations can be accomplished more efficiently, either by re-evaluating the methodology or the intended products, we will be able to realise even greater improvements

to achieve a more practical aplyronine synthesis than those which have been described in this work.

4.5 ADC development

Towards our ultimate goal of developing the aplyronine family of natural product-derived compounds as novel cytotoxic payloads for antibody–drug conjugates, significant further work will be needed to develop suitable linker species and reliable chemical methods for conjugation.

ADC linkers have been the subject of a rapidly growing chemical and biological literature. In essence, we can consider linkers to have three main components: (1) part(s) for linkage to the drug, (2) a spacer region which may affect the chemical and pharmacological properties of the ADC, and (3) part(s) for linkage to natural or engineered conjugation sites on the antibody (Figure 4.7). In the following sections, the conjugation chemistry at either end of the linker species will be discussed.

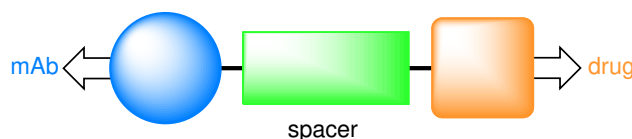


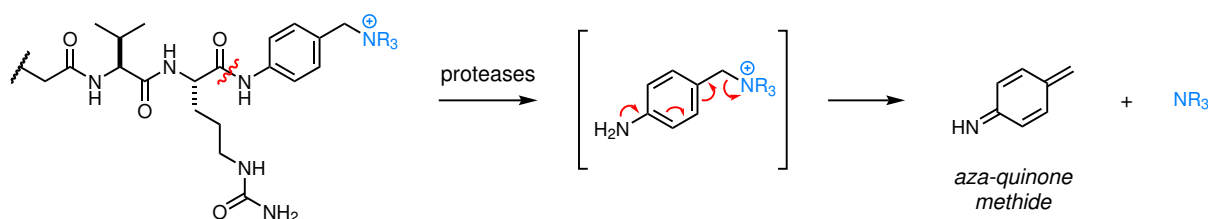
Figure 4.7: Generalised schematic of the structure of an ADC linker

4.5.1 Development of a linker–payload species

In tandem with our investigations to improve the properties of aplyronine analogues for use as ADC payloads, methods of linking these payloads to antibodies through functional handles on the aplyronine scaffold are being explored. It will be necessary to identify optimal linker attachment points, and to develop a method for linker conjugation that does not interfere with the range of sensitive functionalities in the chosen analogue. The aplyronine–linker unit must also be capable of undergoing conjugation to antibodies under bioorthogonal conditions.

Recently many interesting conjugation strategies for complex natural products accessible by total synthesis have been proposed in the literature.^{30,47,184,185} For our objectives, a late-stage functionalisation was desired in order to avoid the need for further structure–activity studies and

(Scheme 4.4).^{*} Porter's recent efforts to apply this strategy to the aplyronines have been centred around the Genentech system, using a protease-cleavable valine-citrulline (Val–Cit) dipeptide to set off the self-immolation of the PABQ unit.^{51,188,196} By this methodology, it should be possible to introduce the linker molecule during an esterification step in the final stages of the analogue synthesis. Importantly, physiological cleavage of this type of linker would lead to the release of tertiary amine-containing aplyronine congeners exactly as proposed above (e.g. Scheme 4.2, analogue **27**).



Scheme 4.4: Structure of the planned Val–Cit–PABQ linker and mechanism of intracellular cleavage

In principle, as this strategy would cleanly release the desired drug entity, there is no fundamental reason that the conjugation should be carried out at the C₂₉ position in preference to C₇. Further studies will demonstrate whether one or the other is more viable. The advantages of linkage at C₂₉ include reacting at the less sterically hindered site and less need for monitoring of possible overreaction in comparison with the C₇/C₉ diol. On the other hand, successful linkage at C₇ would mean installing the linker at the very last step in the synthesis, and opens up the possibility of conjugating species containing a C₂₉-ketone moiety, such as **153** (Scheme 4.1).

The quaternary amine strategy will be the starting point for our investigations into antibody conjugation; for completeness, two other possibilities are presented here.

Another possibility we considered was to use the oxygenated C₁₃ position as a conjugation site. However, this strategy has a number of drawbacks. Foremost, it has been proposed that together with the C₉ hydroxyl and C₁₀ methyl groups, the C₁₃ methyl ether forms an important anchoring interaction with actin that positions the TMSer moiety to interact with tubulin. Substitution might have been tolerated if a well-defined entity with no residual linker debris could be cleaved in the cytosol; however, our route to reveal a C₁₃ alcohol at a late stage proved problematic and work has been discontinued at present. Full details of these investigations will be presented by Porter.¹³¹

^{*}More research may be needed in the near future to fully assess the properties and safety profile of the aza-quinone methide side product^{191,192} given its similarity to quinone methides, which are known pan-assay interference compounds (PAINs).^{193–195}

Alternatively, the *N*-vinylformamide terminus may provide an appropriate conjugation site, as SAR studies showed that modification of this moiety to other polar functional groups did not give rise to significant decreases in actin-binding activity. Attachment could occur *via* a C₃₄-terminal oxime linkage, as was used by Kigoshi and co-workers to introduce various groups containing both hydrophobic and hydrophilic portions as biological probes without appreciable loss of actin binding activity (e.g. **181**, Figure 4.9).^{53,70,76,197} However, a limitation of this approach is that oximes can be labile under physiological conditions, leading to spillage of the valuable cytotoxic drug in circulation and consequently less clinical benefit and greater risk of off-target toxicity. Accordingly, depending on the outcomes of investigations into second-generation analogues (see Section 4.3), we could investigate more stable, enzyme-cleavable linkages through polar groups at this terminal position.

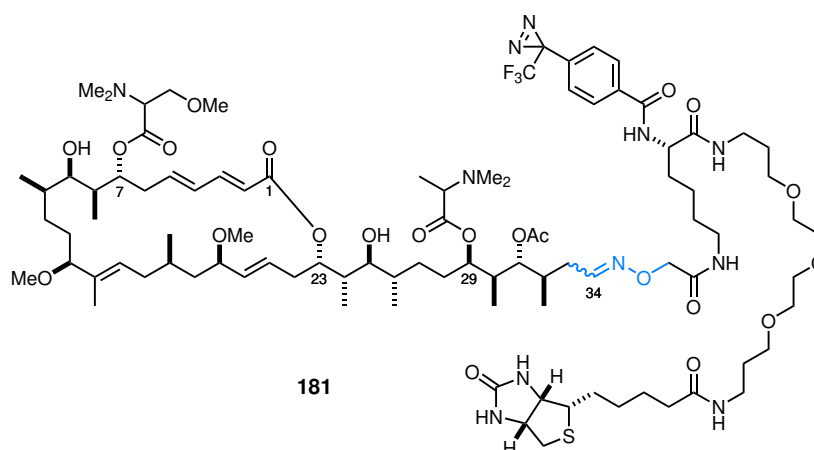


Figure 4.9: Photoaffinity-tagged aplyronine derivative synthesised by Kigoshi and co-workers *via* a terminal oxime linkage^{53,197}

4.5.2 Bioconjugation to form ADCs

Alongside developing a good understanding of the chemistry required to adjoin our analogues to linkers, we will need to develop compatible bioconjugation chemistry for attachment to antibodies. In addition, any information that can be gleaned about the pharmacological properties of the resulting ADCs, such as solubility and potential to aggregate, must be taken into account.¹⁹⁸ These considerations comprise the spacer and antibody-linkage parts of the linker unit.

As discussed in Chapter 1, maleimides have been extensively used to conjugate through native cysteine residues accessible on the antibody surface. However, they are known to undergo retro-Michael addition in circulation, leading to premature loss of the cytotoxic payload and associ-

ated off-target toxicity. Attempts have been made to stabilise maleimide linkages by promoting hydrolysis of the succinimide resulting from conjugation.^{199–201} Nevertheless, heterogeneous ADCs with highly variable drug–antibody ratio (DAR) are generally obtained *via* these traditional methods. Recently, a variety of approaches have surfaced in attempts to overcome these two key problems of plasma instability and heterogeneity. Antibody engineering can be used to incorporate non-native amino acids at accessible sites for reaction under specified conditions.²⁰² Alternatively, reduction of the four key interchain disulfides in an IgG generates precisely eight free thiols which can act as nucleophiles in conjugation reactions, leading to more homogeneous ADCs with more precise DAR and drug–linkers located at predictable sites. Spacer units are also becoming more sophisticated, with options to include hydrophilic moieties for improved solubility, or to use branched spacers.^{198,203} These can allow for multiple attachment either at the drug or antibody end, for example for site-specific or bridging linkage strategies.

We intend to develop ADC constructs of the general form illustrated in Figure 4.10. These will comprise payload–linker chemistry as discussed in Section 4.5.1 (*vide supra*), joined by a hydrophilic spacer to the antibody-linkage site. The bioconjugation will be carried out site-specifically to give ADCs with predictable DAR.

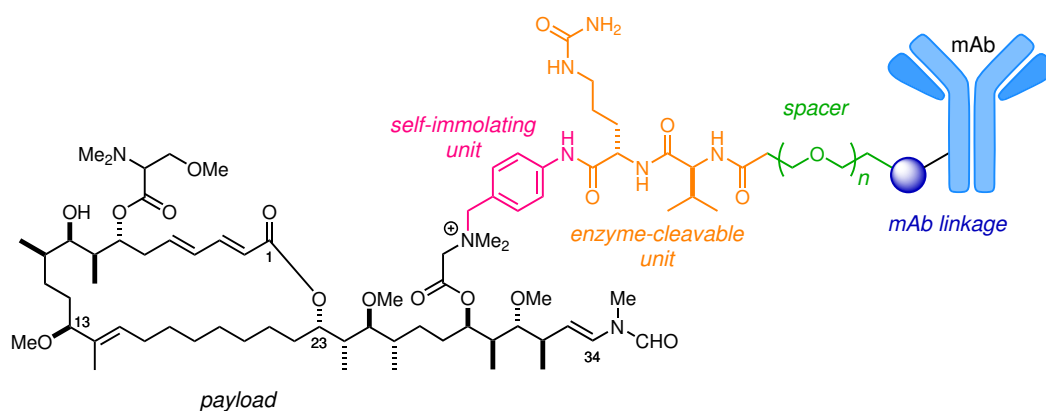


Figure 4.10: General form of our intended ADCs

In collaboration with colleagues from Prof. David Spring’s research group, suitable techniques for biomolecule conjugation that will be compatible with aplyronine payloads are currently in development. These methods include interchain cysteine rebridging using divinylpyrimidines,^{204–206} sequence-dependent bioconjugation,²⁰⁷ and novel enzymatically-cleavable linker methodologies.²⁰⁸ This will enable us to synthesise highly homogeneous, plasma-stable ADCs with finely tuned pharmacokinetic properties. These constructs will be used to deliver cytotoxic aplyronine payloads to target cells, realising our ultimate goal of crafting an efficient, targeted cancer therapy.

4.6 Overall conclusions

In Chapter 1, the vastly underexploited potential of marine natural products for medicinal applications was introduced. Species that thrive in the challenging oceanic environment have evolved extremely bioactive small molecules to aid their survival, and many of these compounds can be repurposed to aid in overcoming human diseases and medical conditions.

Meanwhile, despite great advances in modern medicine throughout the past century, our approach remains limited by the need to apply general treatments to specific diseases. This is true both on the level of individual patients and heterogeneous cell populations within individuals.²⁰⁹

This thesis has formed part of a body of research that will help propel us towards better patient outcomes through the development of targeted therapies.

It has been demonstrated herein that the aplyronines, a family of marine natural products which were previously excluded from the search for medicinal treatments due to their extreme toxicity, can re-surface not only as a viable but as a highly attractive candidate when that toxicity can be harnessed effectively.

In this work, a function-oriented total synthesis of simplified analogues of the aplyronines has been developed. The aim was to craft modified structures which would retain the exquisite bioactivity of the natural products, but would represent more realistic commercial targets due to their greater accessibility by means of synthesis.

In Chapter 2, the synthesis of three key fragments that would enable the construction of the full molecules was discussed. Chapter 3 presented the coupling of these fragments and their advancement towards the intended analogues.

This final chapter has described the completion of the first two members of this analogue library, and plans for their imminent submission to biological testing. The outcomes thereof will serve to confirm or disprove the validity of our SAR-informed simplifications. This will enable the design of a new generation of aplyronine analogues, working towards optimised payloads for delivery as part of a targeted therapeutic in the form of an antibody–drug conjugate.

The synthesis of analogue **153** was carried out in 6.5% yield and 23 steps LLS (38 steps total) from Roche ester ethyl ketone **24**. In terms of feasibility for a synthetic campaign on the larger scale that would be needed in advance of clinical trials, this compares very favourably with the Paterson second-generation total synthesis of aplyronine C, which required 29 steps LLS

and was accomplished in 2.7% yield.⁹² This ultimately reflects the sheer level of complexity of these delicate natural products, given the extensive efforts that were exerted to make the natural product synthesis efficient and scalable, and the improvements that were made relative to previous work. The industrial manufacture of marine natural product-inspired drug Halaven (eribulin mesylate) by Eisai requires 30 steps LLS and 62 steps in total.¹⁸ Placed in this context, our analogue synthesis could be eminently achievable. This seems particularly promising when we consider that global supply for such a highly potent drug compound, anchored to an antibody for targeted delivery, would be very low in comparison with a less biologically active equivalent. With approximately 800 mg of macrocyclic intermediate **132** currently in hand, it should be possible to generate a wide range of analogues in quantities amenable to the desired biological testing (>1 mg).

Targeted therapies will form part of the wider field of personalised medicine, and will help shape the future of clinical science. By causing drug treatments to act at the intended site within the body, better overall patient outcomes and less resource wastage are among the many benefits that can be achieved. This research has been a small part of a great movement towards improving the standard of medical treatment available to the public, while reducing the resources required to provide that treatment. Synthetic chemistry certainly has a role as an integral part of the technologies which will shape a more compassionate and sustainable world.

Chapter 5

Experimental

5.1 General comments

5.1.1 General experimental details

All experiments were performed under anhydrous conditions and under an inert atmosphere of argon, except where stated or when water or aqueous solutions were used, using oven-dried apparatus and employing standard techniques for handling air-sensitive materials.

Purification of reagents and solvents was carried out according to standard procedures.²¹⁰ Acetonitrile (MeCN), benzene (C₆H₆), dichloromethane (CH₂Cl₂), and dimethyl sulfoxide (DMSO) were distilled from calcium hydride (CaH₂) and stored under an argon atmosphere. Tetrahydrofuran (THF) and diethyl ether (Et₂O) were distilled from benzophenone ketyl radical and sodium or potassium wire, respectively, under an argon atmosphere. Solvents used in workup, extraction, recrystallisation and column chromatography were distilled prior to use.

Triethylamine (Et₃N), pyridine (py), diethyl ethylphosphonate and hexamethyldisilazane (HMDS) were distilled from and stored over CaH₂. 2,6-lutidine was distilled from CaH₂ and stored neat under argon. Diisopropylethylamine (*i*-Pr₂NEt) was first distilled from ninhydrin, then distilled from and stored over CaH₂. Titanium tetrachloride (TiCl₄), titanium tetraisopropoxide (Ti(O*i*-Pr)₄) and oxalyl chloride ((COCl)₂) were distilled and stored at –20 °C under an argon atmosphere. Acetaldehyde and propionaldehyde were distilled from calcium chloride (CaCl₂) immediately prior to use. Proton Sponge was recrystallised from methanol. DDQ was recrystallised from chloroform. Barium hydroxide (Ba(OH)₂) was dried under high vacuum at 130 °C

and stored under argon. All other chemicals were used as received, except where noted otherwise.

Sodium bicarbonate (NaHCO_3), ammonium chloride (NH_4Cl), sodium/potassium (Na^+/K^+) tartrate, brine (NaCl) and sodium thiosulfate ($\text{Na}_2\text{S}_2\text{O}_3$) were used as saturated aqueous solutions, unless otherwise stated in the text. Buffer solutions were prepared as directed from stock tablets with deionised water.

Flash column chromatography was carried out on Merck Kieselgel 60 (230–400 mesh) silica gel under a positive pressure of regulated compressed air. Merck Kieselgel F254 plates were used for preparative thin layer chromatography. All solvent mixtures are reported as volume ratios. Solvents were subsequently evaporated *in vacuo*.

Process-scale reactions were carried out in jacketed vessels under nitrogen atmosphere with external temperature control and internal temperature monitoring.

5.1.2 Analytical techniques

^1H nuclear magnetic resonance (NMR) spectra were recorded using an internal deuterium lock at ambient probe temperature (298 K) on the following instruments: Bruker Avance BB or Bruker Avance TCI (500 MHz); and Bruker DPX400 (400 MHz). An internal reference of $\delta_{\text{H}} = 7.26$ ppm was used for residual solvent protons in CDCl_3 . All ^1H NMR data are represented as: chemical shift (in ppm on the δ scale relative to $\delta_{\text{TMS}} = 0$ ppm), integration, multiplicity (s = singlet, d = doublet, t = triplet, q = quartet, quint = quintet, m = multiplet, br = broad, obs = obscured, app = apparent), coupling constant (J in Hz), and assignment. Coupling constants were taken directly from the spectra and are uncorrected. Assignments were determined either on the basis of unambiguous chemical shift or coupling pattern; ^1H – ^1H COSY, HSQC, and HMBC experiments; or by analogy to fully interpreted data for related compounds. Product strengths on large-scale reactions were determined by quantitative ^1H NMR analysis with 1,2,4,5-tetrachloro-3-nitrobenzene as an internal standard.

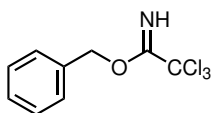
Proton-decoupled ^{13}C NMR spectra were recorded using an internal deuterium lock at ambient probe temperature (298 K) on the following instruments: Bruker Avance BB or Bruker Avance TCI (125 MHz); and Bruker DPX400 (100 MHz). An internal reference of $\delta_{\text{C}} = 77.0$ ppm was used for carbons in CDCl_3 . All chemical shift values are reported in ppm on the δ scale relative to $\delta_{\text{TMS}} = 0$ ppm.

Infrared spectra were recorded on a Perkin–Elmer Spectrum One FT-IR spectrometer. Absorbance frequencies (ν) are reported in cm^{-1} . Optical rotations were measured on an Anton Paar MCP100 polarimeter or on a Perkin-Elmer 343 polarimeter at 589 nm and are reported as follows: $[\alpha]_{\text{D}}^{20}$ at 20 °C, concentration (c in g dL^{-1}), and solvent. High resolution mass spectra (HRMS) were recorded at the EPSRC Mass Spectrometry Service (Swansea, UK) or at the departmental mass spectrometry service (University Chemical Laboratories, Cambridge) using electron impact (EI), electrospray ionisation (ESI) or atmospheric solids analysis probe (ASAP) techniques. The parent ion is quoted with the indicated cation: $[\text{M}+\text{H}]^+$, $[\text{M}+\text{Na}]^+$ or $[\text{M}+\text{NH}_4]^+$.

Analytical thin layer chromatography (TLC) was performed on Merck Kieselgel 60 F₂₅₄ plates coated with a 0.25 mm thickness of silica gel. Visualisation was accomplished by ultraviolet light (254 nm) and potassium permanganate or phosphomolybic acid/cerium(IV) sulphate stains.

5.2 Preparation of reagents

Benzyl-2,2,2-trichloroacetimidate (BnTCA)

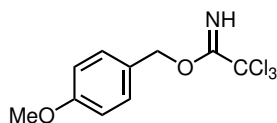


To a solution of benzyl alcohol (2.01 g, 18.6 mmol) in CH_2Cl_2 (22 mL) at $-10\text{ }^\circ\text{C}$ was added tetrabutylammonium hydrogensulfate (69 mg, 0.203 mmol) followed by KOH (22 mL, 50% w/v aq.) portionwise. Trichloroacetonitrile (2.10 mL, 20.9 mmol) was added dropwise over 30 min to the rapidly stirring biphasic mixture. The pale yellow reaction mixture was warmed to rt and stirred overnight (16 h). The phases were separated and the aqueous layer extracted with Et_2O ($3 \times 20\text{ mL}$). The combined organics were dried over Na_2SO_4 and concentrated *in vacuo*. Crude product was purified by flash chromatography on alumina (1:10 EtOAc/PE) to yield benzyl-2,2,2-trichloroacetimidate as a colourless oil (3.75 g, 80%).

R_f 0.79 (1:5 EtOAc/PE); **¹H NMR** (500 MHz, CDCl_3) δ_{H} 8.39 (1H, br s, NH), 7.45–7.34 (5H, m, ArH), 5.35 (2H, s, ArCH_2O).

These data are in agreement with those previously reported.²¹¹

4-Methoxybenzyl-2,2,2-trichloroacetimidate (PMBTCA, **84**)

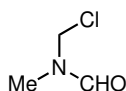


To a solution of KOH (78 mL, 50% w/v aq.) at $-10\text{ }^{\circ}\text{C}$ was added a solution of 4-methoxybenzyl alcohol (9.19 g, 66.5 mmol) and tetrabutylammonium hydrogensulfate (229 mg, 0.674 mmol) in CH_2Cl_2 (78 mL) dropwise *via* pipette. Trichloroacetonitrile (7.75 mL, 77.3 mmol) was added dropwise over 10 min to the rapidly stirring biphasic mixture, ensuring the temperature remained below $-10\text{ }^{\circ}\text{C}$. The pale yellow reaction mixture was warmed to rt over 1 h, and stirred for a further 1.5 h. The phases were separated and the aqueous layer extracted with Et_2O ($3 \times 80\text{ mL}$). The combined organics were dried over MgSO_4 and concentrated *in vacuo*. Purification by flash chromatography on alumina (1:19 EtOAc/PE) gave 4-methoxybenzyl-2,2,2-trichloroacetimidate **84** as a colourless oil (15.3 g, 81%).

R_f 0.50 (1:9 EtOAc/PE); **¹H NMR** (500 MHz, CDCl_3) δ_{H} 8.36 (1H, br s, NH), 7.38 (2H, d, $J = 8.7\text{ Hz}$, ArH), 6.91 (2H, d, $J = 8.7\text{ Hz}$, ArH), 5.28 (2H, s, ArCH_2O), 3.82 (3H, s, ArOMe).

These data are in agreement with those previously reported.²¹²

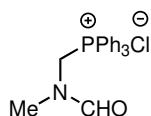
N-(chloromethyl)-*N*-methylformamide (**182**)



To a stirred solution of paraformaldehyde (1.67 g, 55.6 mmol) in CHCl_3 (150 mL) was added *N*-methylformamide (2.95 mL, 50.5 mmol) and TMSCl (19.0 mL, 150 mmol). The mixture was heated to reflux for 2 h then cooled to rt, filtered through Celite and concentrated *in vacuo* to give crude **182** as a pale yellow oil. The crude material was used directly in the next reaction.

¹H NMR (400 MHz, CDCl_3) δ_{H} 8.27 (0.67H, s, NCHO), [8.04] (0.33H, s, NCHO*), 5.24 (1.33H, s, CH_2Cl), [5.22] (0.67H, s, CH_2Cl^*), [3.05] (1H, s, NMe^*), 2.95 (2H, s, NMe). Distinguishable resonances of the minor rotamer (2:1 ratio) are given in brackets and assignments denoted with an asterisk.

((*N*-methylformamido)methyl)triphenylphosphonium chloride (77**)**

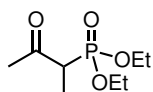


Crude *N*-chloromethyl-*N*-methylformamide (**182**) was added to a stirred solution of triphenylphosphine (14.3 g, 54.3 mmol) in Et₂O (100 mL) and stirred at rt for 24 h. The resulting slurry was filtered and washed with anhydrous Et₂O (3 × 15 mL), then dried under high vacuum to give a free-flowing yellow solid. The crude was recrystallised from CHCl₃/Et₂O to give **77** as white crystals (8.94 g, 48% over 2 steps).

¹H NMR (500 MHz, CDCl₃) δ_H 8.17–7.64 (16H, m, NCHO, NCHO*, ArH), [6.60] (0.40H, d, *J* = 2.4 Hz, NCH₂P*), 6.22 (1.60H, d, *J* = 4.1 Hz, NCH₂P), 3.18 (2.40H, s, NMe), [2.77] (0.60H, s, NMe*); **HRMS** calc. for C₂₁H₂₁NOP [M–Cl]⁺ 334.1355, found 334.1355. Distinguishable resonances of the minor rotamer (4:1 ratio) are given in brackets and assignments denoted with an asterisk.

These data are in agreement with those previously reported.^{213–215}

Diethyl (3-oxobutan-2-yl)phosphonate (90**)**



To a solution of diethyl ethylphosphonate (5.01 g, 30.2 mmol) in THF (40 mL) at –78 °C was added *n*-BuLi (21 mL, 1.6 M in hexane, 33.6 mmol). The mixture was allowed to stir for 1 h, then EtOAc (3.00 mL, 30.7 mmol, freshly distilled from CaH₂) was added dropwise. After 2 h stirring at –78 °C, the reaction was quenched with NH₄Cl (70 mL) and warmed to rt. The layers were separated and the aqueous extracted with EtOAc (5 × 50 mL). The combined organics were dried over MgSO₄ and concentrated *in vacuo*. Distillation under reduced pressure (0.4 Torr, 85–86 °C) gave phosphonate **90** as a colourless oil (3.03 g, 48%).

R_f 0.09 (1:1 EtOAc/PE); **¹H NMR** (500 MHz, CDCl₃) δ_H 4.17–4.09 (4H, m, P(OCH₂CH₃)₂), 3.20 (1H, dq, *J* = 25.6, 7.1 Hz, H₁₂), 2.33 (3H, s, H₁₄ × 3), 1.35 (3H, dd, *J* = 21.3, 7.1 Hz, Me₁₄), 1.35–1.30 (6H, m, P(OCH₂CH₃)₂).

These data are in agreement with those previously reported.²¹⁶

Tin(II) triflate ($\text{Sn}(\text{OTf})_2$)¹¹¹

Tin granules (2.63 g, 22.2 mmol) were stirred under vacuum for 24 h, with occasional heating to melt. The reaction flask was purged with argon, and TfOH (10.0 g, 66.6 mmol) was added into the reaction flask *via* cannula. The reaction was stirred at 85 °C for 48 h. The resulting white slurry was washed with Et₂O without exposure to air until the supernatant appeared colourless, and dried under vacuum with vigorous stirring for 16 h to give Sn(OTf)₂ (3.79 g, 41%) as a very pale grey powder, which was stored under an argon atmosphere.

Samarium diiodide (SmI_2)

Method A:²¹⁷ To samarium metal (23 mg, 150 μmol) and 1,2-diiodoethane (23 mg, 82 μmol) was added THF (0.75 mL) and the suspension sonicated for 20 min at rt. The resulting dark blue-green solution of SmI₂ (*ca.* 0.1 M) was used immediately.

Method B:²¹⁸ Iodine (407 mg, 1.60 mmol) was dissolved in THF (16 mL) and added to samarium (267 mg, 1.78 mmol) *via* syringe. The mixture was allowed to stir at rt overnight (20 h), resulting in a dark blue-green solution of SmI₂ (*ca.* 0.1 M).

Isopropylmagnesium chloride (*i*-PrMgCl)

To magnesium turnings (3.79 g, 156 mmol) in THF (70 mL) was added a portion of *i*-PrCl (1.30 mL, 14.2 mmol) and one bead of iodine (*ca.* 10 mg). The dark yellow reaction mixture quickly turned colourless as the reaction initiated. The temperature was carefully controlled with an ice bath as the remaining *i*-PrCl (11.5 mL, 126 mmol) was added dropwise over 1 h. The dark grey solution of *i*-PrMgCl (*ca.* 2.0 M) was cooled to rt and used immediately.

Ethylmagnesium bromide (EtMgBr)

A portion of EtBr (1.00 mL, 13.4 mmol) was cautiously added to magnesium turnings (3.62 g, 149 mmol) in Et₂O (45 mL). Within 1 min the reaction was seen to initiate, and turned pale grey in colour. The remaining EtBr (9.00 mL, 121 mmol) was carefully added dropwise over 30 min. The dark grey solution of EtMgBr (*ca.* 3.0 M) was cooled to rt and used immediately.

Lithium hexamethyldisilazide (LiHMDS)

To a solution of HMDS (0.14 mL, 0.67 mmol) in THF (0.22 mL) at 0 °C was added *n*-BuLi (0.38 mL, 1.6 M in hexane, 0.61 mmol). The mixture was stirred for 30 min at 0 °C, then used immediately.

Cyclohexylboron chloride (Cy₂BCl)

Cyclohexene (40 mL, 395 mmol, freshly distilled from CaH₂) was dissolved in Et₂O (250 mL) and cooled to −10 °C. Monochloroborane methyl sulfide complex (ClBH₂ · SMe₂, 20.6 mL, 198 mmol) was added dropwise over 15 min, and the solution was stirred at 0 °C for 1 h, then at rt for 1 h. The solvent was removed by distillation at ambient pressure (35 °C) under argon. Distillation under reduced pressure (0.7 Torr, 92–94 °C) then gave Cy₂BCl as a colourless liquid, which was stored under argon at −20 °C.

Stryker's reagent([CuH(PPh₃)]₆)¹⁷⁶

To a solution of Cu(OAc)₂ · H₂O (25.0 mg, 0.125 mmol) and PPh₃ (65.0 mg, 0.248 mmol) in toluene (4.66 mL) was added tetramethyldisiloxane (0.33 mL, 1.87 mmol). The mixture underwent a colour change from aqua blue to brick red while stirring at rt for 16 h. The resulting solution (0.025 M in copper, 0.37 M in hydride) was used directly in conjugate reduction reactions or stored at −20 °C for up to 1 month.

Zinc borohydride (Zn(BH₄)₂)

Zinc(II) chloride (3.68 g, 27.0 mmol) was dried under high vacuum at 150 °C for 2 h then suspended in Et₂O (125 mL) and refluxed for 2 h. The solution was cooled and added to a suspension of sodium borohydride (2.04 g, 54.0 mmol) in Et₂O (30 mL). The reaction was stirred at rt for 16 h, then the supernatant was decanted and stored under argon at −20 °C.

5.3 Experimental procedures for Roche ester-derived ethyl ketones

Methyl (*R*)-3-((4-methoxybenzyl)oxy)-2-methylpropanoate (**79**)

and

Methyl (*S*)-3-((4-methoxybenzyl)oxy)-2-methylpropanoate (**81**)



Method A (Small scale):

PMBTCA (13.40 g, 47.4 mmol) was dissolved in CH₂Cl₂ (21 mL) and added to methyl (*R*)-3-hydroxy-2-methylpropanoate (4.59 g, 38.8 mmol) in CH₂Cl₂ (34 mL) at 0 °C, followed by PPTS (0.98 g, 3.9 mmol) in a single portion. The mixture was warmed to rt and allowed to stir for 16 h. The mixture was cooled in an ice bath and quenched slowly with NaHCO₃ (60 mL). The layers were separated and the aqueous phase extracted with CH₂Cl₂ (3 × 30 mL). The organic phases were combined, dried over MgSO₄ and concentrated *in vacuo*. The resulting white slurry was triturated with ice-cold PE and filtered through Celite. The filtrate was concentrated *in vacuo* and purified by flash chromatography (1:10 → 1:8 EtOAc/PE) to give PMB ether **79** as a colourless oil (8.15 g, 88%).

Method B (Large scale):

A solution of *p*-methoxybenzyl alcohol (140 g, 1.01 mol) in CH₂Cl₂ (1400 mL) was charged to a 2 L jacketed vessel under N₂ atmosphere. DBU (1.52 mL) was added in one portion, followed by addition of trichloroacetonitrile (112 mL) over 30 min with internal temperature controlled to 20 °C. The mixture was stirred for 30 min, during which a dark yellow colour developed. GC analysis indicated full conversion to PMBTCA (**84**).

(*R*)-Roche ester **65** (103.6 g, 0.877 mol) was added as a solution in CH₂Cl₂ (200 mL), followed by PPTS (21.2 g, 0.0843 mol), and stirring continued at 20 °C. Further portions of PPTS (3 × 10.6 g, 0.0421 mol) were added hourly until the reaction was judged to be complete by ¹H NMR analysis after 4 h. Solvent swap distillation replaced the CH₂Cl₂ solvent with *n*-heptane (800 mL), which upon cooling to rt formed a clear solution along with an oily brown residue.

The clear heptane fraction was concentrated *in vacuo* to a colourless oil (160.2 g, 80.0% w/w **79**). The residue was dissolved in CH₂Cl₂ (200 mL) and filtered through Celite, then through a plug of silica, and concentrated *in vacuo*. The resulting crude material was triturated with heptane to remove the trichloroacetamide, then subjected to automated gradient column chromatography (7–60% EtOAc/heptane). The resultant product was combined with the heptane fraction to give a colourless oil (202.5 g, 81.6% w/w, equivalent to 165.3 g **79**), containing the desired PMB ether in 79% corrected yield.

By the same procedure, starting from (*S*)-Roche ester **34** (50.6 g, 0.428 mol), the opposite enantiomer (102.7 g, 84.2% w/w, equivalent to 86.5 g **81**) was obtained as a colourless oil in 85% corrected yield.

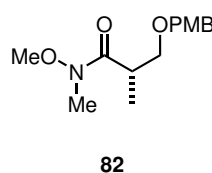
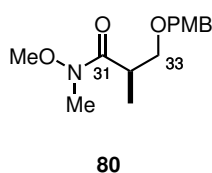
R_f 0.59 (1:3 EtOAc/PE); **¹H NMR** (500 MHz, CDCl₃) δ_H 7.23 (2H, d, *J* = 8.7 Hz, ArH), 6.87 (2H, d, *J* = 8.7 Hz, ArH), 4.47 (1H, d, *J* = 11.8 Hz, ArCH_aH_bO), 4.44 (1H, d, *J* = 11.8 Hz, ArCH_aH_bO), 3.80 (3H, s, ArOMe), 3.69 (3H, s, COOMe), 3.63 (1H, dd, *J* = 9.2, 7.3 Hz, H_{33a}), 3.46 (1H, dd, *J* = 9.2, 6.0 Hz, H_{33b}), 2.77 (1H, dqd, *J* = 7.1, 7.1, 6.1 Hz, H₃₂), 1.17 (3H, d, *J* = 7.1 Hz, Me₃₂).

These data are in agreement with those previously reported.²¹⁹

(*R*)-*N*-methoxy-3-((4-methoxybenzyl)oxy)-*N*,2-dimethylpropanamide (80**)**

and

(*S*)-*N*-methoxy-3-((4-methoxybenzyl)oxy)-*N*,2-dimethylpropanamide (82**)**



Method A (Small scale):

A solution of PMB ether **79** (8.06 g, 33.8 mmol) in THF (60 mL) was added to vacuum-dried *N,O*-dimethylhydroxylamine hydrochloride (5.02 g, 51.4 mmol) and cooled to –30 °C. *i*-PrMgCl (61 mL, 2.0 M in THF, 122 mmol) was added dropwise over 1 h, while keeping the internal temperature below –20 °C. The reaction mixture was stirred at –15 °C for 1.5 h, then carefully quenched with NH₄Cl (120 mL), controlling the temperature with an ice bath. The mixture was diluted with H₂O (80 mL) and partitioned with Et₂O (3 × 100 mL). The combined organic layers

were dried over MgSO₄, concentrated *in vacuo*, and purified by flash chromatography (1:2 → 1.5:1 EtOAc/PE) to give Weinreb amide **80** as a pale yellow oil (8.53 g, 94%).

Method B (Large scale):

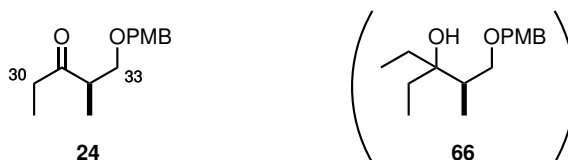
Vacuum-dried *N,O*-dimethylhydroxylamine hydrochloride (101.5 g, 1.04 mol) was charged to a 3 L jacketed vessel under N₂ atmosphere, and PMB ether **79** (165.3 g corr., 0.694 mol) in 2-MeTHF (990 mL) was added. The solution was pre-cooled to –10 °C and *i*-PrMgCl (1040 mL, 2.0 M in THF, 2.08 mol) was added over 4 h, controlling the internal temperature to –10 °C or below. After the addition was complete, the solution was stirred for 30 min, then quenched slowly with NH₄Cl (900 mL, 15% w/w aq). The layers were separated; the organics were washed with brine (900 mL, 20% w/w aq) and the aqueous extracted with 2-MeTHF (300 mL). The solvent was removed *in vacuo*, giving (*R*)-Weinreb amide **80** as a yellow oil (216.4 g, 82.4% w/w, equivalent to 178.3 g) in 96% corrected yield.

The equivalent procedure in the opposite enantiomeric series starting from compound **81** (86.5 g corr., 0.363 mol) gave the (*S*)-Weinreb amide **82** as a yellow oil (111.3 g, 86.1% w/w, equivalent to 95.9 g) in 99% corrected yield.

R_f 0.11 (1:3 EtOAc/PE); **¹H NMR** (400 MHz, CDCl₃) δ_H 7.23 (2H, d, *J* = 8.4 Hz, ArH), 6.86 (2H, d, *J* = 8.4 Hz, ArH), 4.48 (1H, d, *J* = 11.6 Hz, ArCH_aH_bO), 4.40 (1H, d, *J* = 11.6 Hz, ArCH_aH_bO), 3.80 (3H, s, ArOMe), 3.70–3.66 (4H, m, N(OMe), H_{33a}), 3.39 (1H, dd, *J* = 8.8, 5.9 Hz, H_{33b}), 3.30–3.20 (1H, m, H₃₂), 3.20 (3H, s, NMe), 1.10 (3H, d, *J* = 6.9 Hz, Me₃₂).

These data are in agreement with those previously reported.²²⁰

(*R*)-1-((4-methoxybenzyl)oxy)-2-methylpentan-3-one (**24**)



Method A (Small scale):

To a vigorously stirred solution of (*R*)-Weinreb amide **80** (8.48 g, 31.7 mmol) in Et₂O (80 mL) at –5 °C was added EtMgBr (40 mL, 3.0 M in Et₂O, 120 mmol) dropwise over 75 min, keeping the internal temperature below 5 °C. The mixture was stirred at 0 °C for 1.5 h, then quenched very

cautiously with NH₄Cl (110 mL) and diluted with H₂O (30 mL). The phases were separated, the aqueous layer extracted with Et₂O (2 × 80 mL) and the combined organics dried over MgSO₄ and concentrated *in vacuo*. Flash chromatography (1:8 EtOAc/PE) gave a pale yellow oil, an inseparable mixture of ketone **24** and byproduct **66** (6.96 g, 16:1 by ¹H NMR, 87% calculated yield of desired product).

Method B: Large scale

To a solution of (*R*)-Weinreb amide **80** (30.9 g corr., 0.116 mol) in 2-MeTHF (90 mL) in a 250 mL jacketed vessel under N₂ atmosphere was added EtMgBr (102 mL, 3.4 M in 2-MeTHF, 0.347 mol) over 2 h, controlling the internal temperature of the reaction to –10 °C or lower. The reaction was left to stir for 16 h, then quenched slowly with NH₄Cl (90 mL, 15% w/w aq) and gradually raised to rt. The aqueous layer was separated and the organics washed with brine (90 mL, 20% w/w aq) and concentrated *in vacuo*. The resulting brown oil contained (*R*)-ethyl ketone **24** (31.6 g, 78.7% w/w, equivalent to 24.9 g) in 91% corrected yield.

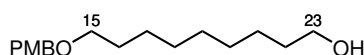
R_f 0.59 (1:3 EtOAc/PE); **¹H NMR** (500 MHz, CDCl₃) δ_H 7.20 (2H, d, *J* = 8.7 Hz, ArH), 6.86 (2H, d, *J* = 8.7 Hz, ArH), 4.41 (1H, d, *J* = 11.6 Hz, ArCH_aH_bO), 4.38 (1H, d, *J* = 11.7 Hz, ArCH_aH_bO), 3.78 (3H, s, ArOMe), 3.58 (1H, dd, *J* = 9.1, 7.8 Hz, H_{33a}), 3.42 (1H, dd, *J* = 9.1, 5.5 Hz, H_{33b}), 2.85 (1H, dqd, *J* = 7.4, 7.4, 5.6 Hz, H₃₂), 2.49 (2H, q, *J* = 7.3 Hz, H₃₀ × 2), 1.05 (3H, d, *J* = 7.2 Hz, Me₃₂), 1.03 (3H, t, *J* = 7.3 Hz, Me₃₀); [α]_D²⁰ –22.2 (*c* 1.02, CHCl₃), lit. –22.5 (*c* 1.12, CHCl₃).

These data are in agreement with those previously reported.^{221,222}

5.4 Experimental procedures for Chapter 2

5.4.1 Southern fragment (C₁₅–C₂₇)

9-((4-methoxybenzyl)oxy)nonan-1-ol (**38**)



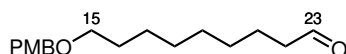
Sodium hydride (60% in mineral oil, 0.46 g, 11.4 mmol) was added portionwise to a solution of 1,9-nonanediol (5.00 g, 31.2 mmol) in THF/DMSO (2:1, 93 mL) at 0 °C and stirred for 1 h.

To the yellow solution was added TBAI (0.36 g, 0.97 mmol) followed by PMBCl (1.45 mL, 10.7 mmol) dropwise over 30 min. The mixture was warmed to rt and stirred for 70 h, then quenched by addition of NH₄Cl (90 mL). The phases were separated and the aqueous layer extracted with EtOAc (3 × 50 mL). The combined organics were dried over Na₂SO₄ and concentrated *in vacuo*. Purification by flash chromatography (1:5 → 1:3 EtOAc/PE) gave alcohol **38** as an orange oil (2.17 g, 72% based on PMBCl).

R_f 0.28 (1:3 EtOAc/PE); **¹H NMR** (400 MHz, CDCl₃) δ_H 7.26 (2H, d, *J* = 8.5 Hz, ArH), 6.88 (2H, d, *J* = 8.6 Hz, ArH), 4.43 (2H, s, ArCH₂O), 3.80 (3H, s, ArOMe), 3.63 (2H, t, *J* = 6.6 Hz, H₂₃), 3.43 (2H, t, *J* = 6.6 Hz, H₁₅), 1.65–1.48 (4H, m, H₁₆, H₂₂), 1.40–1.23 (11H, m, H_{17–21}, C₂₃OH).

These data are in agreement with those previously reported.¹¹⁵

9-((4-methoxybenzyl)oxy)nonanal (**39**)

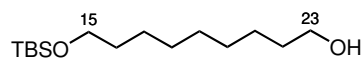


To a solution of oxalyl chloride (0.98 mL, 11.6 mmol) in CH₂Cl₂ (15 mL) at –78 °C was added DMSO (1.10 mL, 15.5 mmol). The mixture was stirred for 1 h. A solution of alcohol **38** (2.16 g, 7.70 mmol) in CH₂Cl₂ (15 mL) was then added *via* cannula and the reaction mixture stirred for a further 30 min. After addition of Et₃N (3.2 mL, 23.1 mmol), the mixture was warmed to rt and stirred for 3 h. Upon completion, the reaction was quenched with NH₄Cl (18 mL). The phases were separated and the aqueous layer extracted with CH₂Cl₂ (3 × 15 mL). The combined organics were washed with NaHCO₃ (30 mL), dried over MgSO₄ and concentrated *in vacuo*. Crude product was purified by flash chromatography (1:15 → 1:10 EtOAc/PE) to give aldehyde **39** as a pale yellow oil (1.62 g, 76%).

R_f 0.27 (1:8 EtOAc/PE); **¹H NMR** (400 MHz, CDCl₃) δ_H 9.76 (1H, t, *J* = 1.8 Hz, H₂₃), 7.26 (2H, d, *J* = 8.6 Hz, ArH), 6.88 (2H, d, *J* = 8.6 Hz, ArH), 4.43 (2H, s, ArCH₂O), 3.80 (3H, s, ArOMe), 3.43 (2H, t, *J* = 6.6 Hz, H₁₅), 2.41 (2H, td, *J* = 7.4, 1.8 Hz, H₂₂), 1.67–1.52 (4H, m, H₁₆, H₂₁), 1.39–1.24 (8H, m, H_{17–20}); **HRMS** calc. for C₁₇H₃₀NO₃ [M+NH₄]⁺ 296.2222, found 296.2220.

These data are in agreement with those previously reported.¹¹⁵

9-((*tert*-butyldimethylsilyl)oxy)nonan-1-ol (**183**)

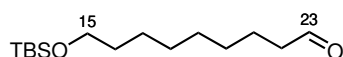


To a solution of 1,9-nonanediol (12.0 g, 74.9 mmol) and imidazole (2.04 g, 68.1 mmol) in THF (80 mL) at 0 °C was added a solution of TBSCl (3.77 g, 25.0 mmol) in THF (70 mL) dropwise over 40 min. The mixture was slowly warmed to rt and allowed to stir for 65 h, then quenched by addition of H₂O. The phases were separated and the aqueous layer extracted with EtOAc (3 × 100 mL). The combined organics were washed with H₂O (50 mL), dried over Na₂SO₄ and concentrated *in vacuo*. Purification by flash chromatography (1:3 → 1:2 EtOAc/PE) gave alcohol **183** as a colourless oil (5.69 g, 83%).

R_f 0.27 (1:6 EtOAc/PE); **¹H NMR** (400 MHz, CDCl₃) δ_H 3.64 (2H, t, *J* = 6.6 Hz, H₂₃), 3.59 (2H, t, *J* = 6.6 Hz, H₁₅), 1.61–1.45 (4H, m, H₁₆, H₂₂), 1.39–1.24 (10H, m, H_{17–21}), 0.89 (9H, s, SiC(CH₃)₃), 0.04 (6H, s, Si(CH₃)₂); **¹³C NMR** (125 MHz, CDCl₃) δ_C 63.3, 63.0, 32.8, 32.8, 29.6, 29.3, 29.3, 26.0, 25.8, 25.7, 18.4, –5.3; **HRMS** calc. for C₁₅H₃₅O₂Si [M+H]⁺ 275.2401, found 275.2402.

These data are in agreement with those previously reported.²²³

9-((*tert*-butyldimethylsilyl)oxy)nonanal (**49**)



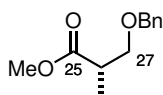
To a solution of oxalyl chloride (2.39 mL, 28.2 mmol) in CH₂Cl₂ (50 mL) at –78 °C was added DMSO (2.67 mL, 37.6 mmol). The mixture was stirred for 30 min, then a solution of alcohol **183** (5.16 g, 18.8 mmol) in CH₂Cl₂ (25 mL) was added *via* cannula and stirred for a further 1 h. Addition of Et₃N (7.86 mL, 56.4 mmol) dropwise at –78 °C caused the reaction mixture to seize. After warming to rt with stirring and addition of CH₂Cl₂ (20 mL), the resulting yellow solution was allowed to stir for 16 h. The reaction was quenched carefully with NH₄Cl (40 mL). The phases were separated and the aqueous layer extracted with CH₂Cl₂ (2 × 80 mL). The combined organics were washed with NaHCO₃ (50 mL), dried over MgSO₄ and concentrated *in vacuo*. The crude product was purified by flash chromatography (1:15 EtOAc/PE) to give aldehyde **49** as a colourless oil (4.68 g, 91%).

R_f 0.50 (1:8 EtOAc/PE); **¹H NMR** (400 MHz, CDCl₃) δ_H 9.76 (1H, t, *J* = 1.9 Hz, H₂₃), 3.59 (2H, t, *J* = 6.6 Hz, H₁₅), 2.41 (2H, td, *J* = 7.4, 1.9 Hz, H₂₂), 1.68–1.57 (2H, m, H₁₆), 1.55–

1.43 (2H, m, H₂₁), 1.37–1.24 (8H, m, H_{17–20}), 0.89 (9H, s, SiC(CH₃)₃), 0.04 (6H, s, Si(CH₃)₂); **HRMS** calc. for C₁₅H₃₃O₂Si [M+H]⁺ 273.2244, found 273.2248.

These data are in agreement with those previously reported.²²⁴

Methyl (*S*)-3-(benzyloxy)-2-methylpropanoate (**35**)

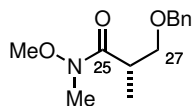


To a solution of methyl (*S*)-3-hydroxy-2-methylpropanoate (1.19 g, 10.1 mmol) in Et₂O (18 mL) at 0 °C was added BnTCA (2.60 mL, 14.0 mmol) and TfOH (0.20 mL, 2.3 mmol). The mixture was stirred at 0 °C for 20 min, then warmed to rt and stirred for a further 2 h. Upon completion the yellow reaction mixture was cooled in an ice bath and NaHCO₃ (36 mL) was carefully added. The mixture was extracted with Et₂O (3 × 20 mL) and the combined organics dried over MgSO₄ and concentrated *in vacuo* to a yellow oil containing a large amount of white precipitate. The crude mixture was triturated with ice-cold hexane and filtered through Celite. The filtrate was concentrated *in vacuo* and purified by flash chromatography (1:50 → 1:20 EtOAc/PE) to give benzyl ether **35** as a pale yellow oil (2.01 g, 96%).

R_f 0.44 (1:8 EtOAc/PE); **¹H NMR** (400 MHz, CDCl₃) δ_H 7.40–7.27 (5H, m, PhH), 4.52 (2H, s, PhCH₂O), 3.70 (3H, s, COOMe), 3.66 (1H, dd, *J* = 8.9, 7.3 Hz, H_{27a}), 3.50 (1H, dd, *J* = 9.1, 5.9 Hz, H_{27b}), 2.79 (1H, m, H₂₆), 1.18 (3H, d, *J* = 7.1 Hz, Me₂₆).

These data are in agreement with those previously reported.²²⁵

(*S*)-3-(benzyloxy)-*N*-methoxy-*N*,2-dimethylpropanamide (**36**)



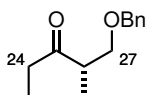
A solution of benzyl ether **35** (2.01 g, 9.7 mmol) in THF (19 mL) was added to vacuum-dried *N,O*-dimethylhydroxylamine hydrochloride (1.51 g, 15.5 mmol) and cooled to –30 °C. *i*-PrMgCl (14.5 mL, 2.0 M in THF, 29 mmol) was added dropwise over 15 min, keeping the internal temperature below –25 °C. The reaction mixture was allowed to warm to –15 °C and stirred for 30 min. A further aliquot of *i*-PrMgCl (4.8 mL, 9.6 mmol) was added over 20 min, before

leaving the reaction to stir for 16 h at $-10\text{ }^{\circ}\text{C}$. Once complete, the reaction was quenched by careful addition of NH_4Cl (30 mL), controlling the temperature with an ice bath. The mixture was diluted with H_2O (30 mL) and partitioned with Et_2O ($3 \times 40\text{ mL}$). The combined organic layers were dried over MgSO_4 , concentrated *in vacuo*, and purified by flash chromatography (1:5 \rightarrow 1:3 EtOAc/PE) to give Weinreb amide **36** as a pale yellow oil (1.58 g, 69%).

R_f 0.65 (1:1 EtOAc/PE); **¹H NMR** (400 MHz, CDCl_3) δ_{H} 7.39–7.27 (5H, m, PhH), 4.56 (1H, d, $J = 12.1\text{ Hz}$, $\text{PhCH}_a\text{H}_b\text{O}$), 4.48 (1H, d, $J = 12.1\text{ Hz}$, $\text{PhCH}_a\text{H}_b\text{O}$), 3.72 (1H, m, H_{27a}), 3.70 (3H, s, N(OMe)), 3.43 (1H, dd, $J = 8.9, 5.9\text{ Hz}$, H_{27b}), 3.34–3.23 (1H, m, H_{26}), 3.21 (3H, s, NMe), 1.12 (3H, d, $J = 6.9\text{ Hz}$, Me_{26}).

These data are in agreement with those previously reported.²²⁵

(S)-1-(benzyloxy)-2-methylpentan-3-one (**33**)

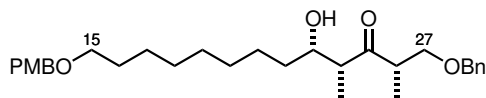


To a vigorously stirred solution of Weinreb amide **36** (5.00 g, 21.1 mmol) in Et_2O (53 mL) at $0\text{ }^{\circ}\text{C}$ was added EtMgBr (21.5 mL, 3.0 M in Et_2O , 64.5 mmol) dropwise over 75 min. The mixture was stirred at $0\text{ }^{\circ}\text{C}$ for 16 h, then quenched very carefully with NH_4Cl (70 mL). The mixture was diluted with H_2O (20 mL), partitioned with Et_2O ($3 \times 70\text{ mL}$) and the combined organics dried over MgSO_4 and concentrated *in vacuo*. Purification by flash chromatography (1:20 EtOAc/PE) afforded ketone **33** as a pale yellow oil (3.24 g, 75%).

R_f 0.68 (1:3 EtOAc/PE); **¹H NMR** (400 MHz, CDCl_3) δ_{H} 7.38–7.27 (5H, m, PhH), 4.50 (1H, d, $J = 12.0\text{ Hz}$, $\text{PhCH}_a\text{H}_b\text{O}$), 4.46 (1H, d, $J = 12.2\text{ Hz}$, $\text{PhCH}_a\text{H}_b\text{O}$), 3.63 (1H, app t, $J = 8.4\text{ Hz}$, H_{27a}), 3.46 (1H, dd, $J = 9.1, 5.5\text{ Hz}$, H_{27b}), 2.93–2.84 (1H, m, H_{26}), 2.51 (2H, q, $J = 7.2\text{ Hz}$, $\text{H}_{24} \times 2$), 1.08 (3H, d, $J = 7.2\text{ Hz}$, Me_{26}), 1.03 (3H, t, $J = 7.2\text{ Hz}$, Me_{24}); $[\alpha]_{\text{D}}^{20} +22.7$ ($c\ 1.00$, CHCl_3); **IR** (thin film) ν_{max} (cm^{-1}) 2968, 2933, 2853, 2353, 1713, 1455, 1374, 1360, 1092, 1072, 1027, 975, 953, 735, 698; **HRMS** calc. for $\text{C}_{13}\text{H}_{19}\text{O}_2$ $[\text{M}+\text{H}]^+$ 207.1380, found 207.1379.

These data are in agreement with those previously reported.²²⁵

(2*S*,4*R*,5*S*)-1-(benzyloxy)-5-hydroxy-13-((4-methoxybenzyl)oxy)-2,4-dimethyltridecan-3-one
(47)



Method A: Titanium aldol

To a solution of TiCl_4 (45 μL , 0.41 mmol) in CH_2Cl_2 (1 mL) at 0 $^\circ\text{C}$ was added $\text{Ti}(\text{O}i\text{-Pr})_4$ (40 μL , 0.14 mmol). The mixture was stirred at 0 $^\circ\text{C}$ for 10 min, then at rt for 20 min. The resulting colourless solution was added to a solution of ketone **33** (99.0 mg, 0.480 mmol, dried azeotropically from C_6H_6 and stirred over CaH_2 immediately prior to use) in CH_2Cl_2 (2.5 mL) at -78°C . Upon dropwise addition of $i\text{-Pr}_2\text{NEt}$ (95 μL , 0.55 mmol), the yellow solution underwent a gradual colour change to bright red. The reaction mixture was allowed to enolise at -78°C for 45 min, before addition of aldehyde **39** (201 mg, 0.722 mmol, dried azeotropically from C_6H_6 and stirred over CaH_2 immediately prior to use) in CH_2Cl_2 (2.5 mL) *via* cannula. The mixture was stirred at -78°C for a further 2.5 h, then quenched with MeOH (1 mL), causing a colour change back to yellow. After warming to rt, Na^+/K^+ tartrate (2 mL) was added and the biphasic mixture was stirred rapidly overnight (16 h). The reaction mixture was diluted with CH_2Cl_2 (10 mL) and the organic phase washed sequentially with H_2O (10 mL) then brine (5 mL). The combined aqueous washings were then extracted with CH_2Cl_2 (20 mL). The combined organics were dried over Na_2SO_4 , concentrated *in vacuo* and purified by flash chromatography (1:6 \rightarrow 1:3 EtOAc/PE) to give aldol adduct **47** as a colourless oil (183 mg, 78%, 5:1 *dr*).

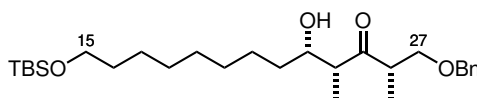
Method B: Boron aldol

To a suspension of (+)- Ipc_2BH (0.763 g, 2.67 mmol) in hexane (1.35 mL) at 0 $^\circ\text{C}$ was added TfOH (0.235 mL, 2.65 mmol). The mixture was warmed to rt and stirred gently. Upon completion, the colourless upper layer (0.61 mL, *ca.* 1.2 M) was removed by syringe, diluted with CH_2Cl_2 (0.3 mL) and cooled to -78°C . $i\text{-Pr}_2\text{NEt}$ (250 μL , 1.44 mmol) was added, followed by ketone **33** (103 mg, 0.499 mmol, dried azeotropically from C_6H_6 and stirred over CaH_2 immediately prior to use) in CH_2Cl_2 (0.6 mL). The mixture was allowed to enolise at -78°C for 15 min, then at 0 $^\circ\text{C}$ for 2 h. It was then re-cooled to -78°C and aldehyde **39** (402 mg, 1.44 mmol, dried azeotropically from C_6H_6 and stirred over CaH_2 immediately prior to use) in CH_2Cl_2 (0.6 mL) was added. The reaction mixture was stirred at -60°C for 2 h, then at -20°C for 14 h, after which it was quenched by addition of MeOH (2 mL), pH 7 buffer (2 mL) and dropwise H_2O_2 (1 mL, 30% w/w aqueous) at 0 $^\circ\text{C}$. After warming to rt, the mixture was stirred for 1 h, then ex-

tracted with CH₂Cl₂ (3 × 8 mL). The combined organics were dried over Na₂SO₄, concentrated *in vacuo*, and purified by flash chromatography (1:4 → 1:3 EtOAc/PE) to give aldol adduct **47** as a pale yellow oil (191 mg, 79%, 3:1 *dr*).

R_f 0.34 (1:3 EtOAc/PE); **¹H NMR** (500 MHz, CDCl₃) δ_H 7.36–7.24 (7H, m, ArH, PhH), 6.88 (2H, d, *J* = 8.7 Hz, ArH), 4.47 (1H, d, *J* = 11.7 Hz, PhCH_aH_bO), 4.46–4.42 (3H, m, PhCH_aH_bO, ArCH₂O), 4.01–3.96 (1H, m, H₂₃), 3.80 (3H, s, ArOMe), 3.64 (1H, app t, *J* = 9.0 Hz, H_{27a}), 3.46 (1H, dd, *J* = 8.7, 4.8 Hz, H_{27b}), 3.43 (2H, t, *J* = 6.7 Hz, H₁₅ × 2), 3.17 (1H, dqd, *J* = 9.3, 7.0, 4.9 Hz, H₂₆), 2.84 (1H, v br s, C₂₃OH), 2.74 (1H, qd, *J* = 7.1, 2.7 Hz, H₂₄), 1.59 (2H, app quint, *J* = 7.0 Hz, H₁₆ × 2), 1.49–1.42 (1H, m, H_{22a}), 1.40–1.19 (11H, m, H_{17–21}, H_{22b}), 1.07 (3H, d, *J* = 7.1 Hz, Me₂₄), 1.02 (3H, d, *J* = 6.9 Hz, Me₂₆); **¹³C NMR** (125 MHz, CDCl₃) δ_C 218.0, 159.0, 137.5, 130.7, 129.1, 128.3, 127.7, 127.6, 113.6, 73.4, 73.1, 72.4, 70.6, 70.1, 55.1, 50.8, 44.8, 33.6, 29.7, 29.5, 29.5, 29.3, 26.1, 26.1, 13.5, 8.8; [α]_D²⁰ +3.0 (*c* 1.01, CHCl₃); **IR** (thin film) ν_{max} (cm^{–1}) 3480, 2933, 2853, 1705, 1611, 1586, 1510, 1455, 1364, 1302, 1247, 1207, 1173, 1034, 991, 820, 735, 700; **HRMS** calc. for C₃₀H₄₅O₅ [M+H]⁺ 485.3262, found 485.3256.

(2*S*,4*R*,5*S*)-1-(benzyloxy)-13-((*tert*-butyldimethylsilyl)oxy)-5-hydroxy-2,4-dimethyltridecan-3-one (184)

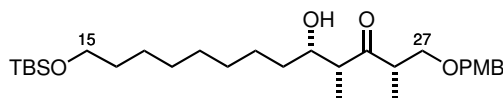


To a solution of TiCl₄ (45 μL, 0.41 mmol) in CH₂Cl₂ (1 mL) at 0 °C was added Ti(*Oi*-Pr)₄ (40 μL, 0.14 mmol). The mixture was stirred at 0 °C for 10 min, then at rt for 20 min. The resulting colourless solution was added to a solution of ketone **33** (100 mg, 0.485 mmol, dried azeotropically from C₆H₆ and stirred over CaH₂ immediately prior to use) in CH₂Cl₂ (2.5 mL) at –78 °C. Upon dropwise addition of *i*-Pr₂NEt (95 μL, 0.55 mmol), the yellow solution changed colour to bright red. The reaction mixture was stirred at –78 °C for 35 min to allow to enolise, before addition of aldehyde **49** (200 mg, 0.734 mmol, dried azeotropically from C₆H₆ and stirred over CaH₂ immediately prior to use) in CH₂Cl₂ (2.5 mL) slowly *via* cannula. The mixture was stirred at –78 °C for a further 1.5 h, then quenched with MeOH (1 mL), causing a colour change back to yellow. After warming to rt, Na⁺/K⁺ tartrate (2 mL) was added and the biphasic mixture was stirred rapidly for 30 min. The reaction mixture was diluted with CH₂Cl₂ (10 mL) and H₂O (10 mL) and the organic phase was washed with H₂O (10 mL). The combined aqueous fractions were then extracted with CH₂Cl₂ (3 × 10 mL). The combined organic phases were dried over

Na₂SO₄, concentrated *in vacuo* and purified by flash chromatography (1:10 → 1:6 EtOAc/PE) to give aldol adduct **184** as a colourless oil (161 mg, 70%, 5:1 *dr*).

R_f 0.48 (1:4 EtOAc/PE); **¹H NMR** (400 MHz, CDCl₃) δ_H 7.37–7.24 (5H, m, PhH), 4.48 (1H, d, *J* = 11.7 Hz, PhCH_aH_bO), 4.44 (1H, d, *J* = 11.7 Hz, PhCH_aH_bO), 4.03–3.95 (1H, m, H₂₃), 3.64 (1H, app t, *J* = 8.9 Hz, H_{27a}), 3.59 (2H, t, *J* = 6.6 Hz, H₁₅ × 2), 3.46 (1H, dd, *J* = 8.6, 4.8 Hz, H_{27b}), 3.17 (1H, dqd, *J* = 8.8, 7.2, 4.9 Hz, H₂₆), 2.84 (1H, br s, C₂₃OH), 2.74 (1H, qd, *J* = 7.0, 2.6 Hz, H₂₄), 1.59–1.40 (4H, m, H₁₆ × 2, H₂₂ × 2), ArH 1.36–1.19 (10H, m, H_{17–21}), 1.07 (3H, d, *J* = 7.1 Hz, Me₂₆), 1.02 (3H, d, *J* = 6.9 Hz, Me₂₄), 0.89 (9H, s, SiC(CH₃)₃), 0.05 (6H, s, Si(CH₃)₂); **¹³C NMR** (125 MHz, CDCl₃) δ_C 218.2, 137.5, 128.4, 127.8, 127.7, 73.5, 73.2, 70.6, 63.3, 50.8, 44.9, 33.6, 32.9, 29.6, 29.5, 29.4, 26.1, 26.0, 25.8, 18.4, 13.6, 8.8, –5.3; [α]_D²⁰ –3.2 (*c* 0.99, CHCl₃); **IR** (thin film) ν_{max} (cm^{–1}) 3484, 2929, 2853, 1703, 1457, 1385, 1372, 1362, 1253, 1096, 1029, 1005, 989, 834, 815, 777, 733, 700, 664; **HRMS** calc. for C₂₈H₅₁O₄Si [M+H]⁺ 479.3551, found 479.3539.

(2*S*,4*R*,5*S*)-13-((*tert*-butyldimethylsilyl)oxy)-5-hydroxy-1-((4-methoxybenzyl)oxy)-2,4-dimethyltridecan-3-one (54)

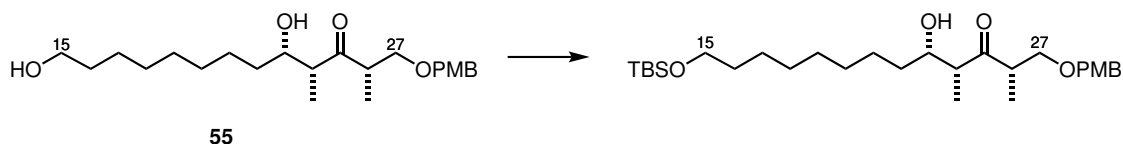


To a solution of TiCl₄ (1.37 mL, 12.5 mmol) in CH₂Cl₂ (50 mL) at 0 °C was added Ti(O*i*-Pr)₄ (1.23 mL, 4.17 mmol). The mixture was stirred at 0 °C for 10 min, then at rt for 30 min. The resulting colourless solution was added dropwise to a solution of ketone **25** (3.52 g, 14.9 mmol, stirred over CaH₂ immediately before use) in CH₂Cl₂ (150 mL) at –78 °C, during which the solution gradually turned through yellow to light orange. Dropwise addition of *i*-Pr₂NEt (2.85 mL, 16.4 mmol) caused a further colour change to dark red. The reaction mixture was stirred at –78 °C for 30 min to allow full enolisation. Aldehyde **49** (4.46 g, 16.4 mmol, stirred over CaH₂ immediately before use) in CH₂Cl₂ (100 mL) was then added *via* cannula down the side of the reaction flask over 10 min. Shortly thereafter the solution was observed to return to a light orange colour. The mixture was stirred at –78 °C for a further 40 min. Upon completion the reaction was quenched with NaHCO₃/Na⁺/K⁺ tartrate (1:1, 90 mL) and warmed to rt. The biphasic mixture was stirred vigorously for 2 h and then left to stand overnight. The layers were separated and the organic phase washed with brine (100 mL). The combined aqueous fractions were then extracted with EtOAc (2 × 100 mL). The organics were dried over Na₂SO₄ and concentrated *in*

vacuo. Purification by flash chromatography (1:10 → 1:5 EtOAc/PE) afforded aldol adduct **54** as a colourless oil (6.42 g, 85%, 18:1 *dr*).

R_f 0.26 (1:5 EtOAc/PE); **¹H NMR** (500 MHz, CDCl₃) δ_H 7.18 (2H, d, *J* = 8.7 Hz, ArH), 6.85 (2H, d, *J* = 8.7 Hz, ArH), 4.39 (1H, d, *J* = 11.4 Hz, ArCH_aH_bO), 4.36 (1H, d, *J* = 11.5 Hz, ArCH_aH_bO), 4.00–3.95 (1H, m, H₂₃), 3.79 (3H, s, ArOMe), 3.61 (1H, app t, *J* = 8.7 Hz, H_{27a}), 3.59 (2H, t, *J* = 6.7 Hz, H₁₅ × 2), 3.42 (1H, dd, *J* = 8.7, 4.7 Hz, H_{27b}), 3.15 (1H, dqd, *J* = 9.3, 6.9, 4.9 Hz, H₂₆), 2.88 (1H, d, *J* = 3.9 Hz, C₂₃OH), 2.72 (1H, qd, *J* = 7.1, 2.7 Hz, H₂₄), 1.50 (2H, app quint, *J* = 6.8 Hz, H₁₆ × 2), 1.47–1.34 (2H, m, H₂₂ × 2), 1.34–1.18 (10H, m, H_{17–21}), 1.05 (3H, d, *J* = 7.1 Hz, Me₂₄), 1.00 (3H, d, *J* = 6.9 Hz, Me₂₆), 0.89 (9H, s, SiC(CH₃)₃), 0.04 (6H, s, Si(CH₃)₂); **¹³C NMR** (125 MHz, CDCl₃) δ_C 218.1, 159.3, 129.6, 129.3, 113.8, 73.1, 72.9, 70.6, 63.3, 55.2, 50.9, 44.8, 33.6, 32.9, 29.6, 29.6, 29.4, 26.2, 25.9, 25.8, 18.3, 13.6, 8.8, –5.3; [α]_D²⁰ –2.0 (*c* 0.10, CHCl₃); **IR** (thin film) ν_{max} (cm^{–1}) 3500, 2929, 2853, 1709, 1615, 1514, 1461, 1360, 1302, 1249, 1173, 1037, 1005, 991, 834, 777; **HRMS** calc. for C₂₉H₅₆NO₅Si [M+NH₄]⁺ 526.3922, found 526.3909.

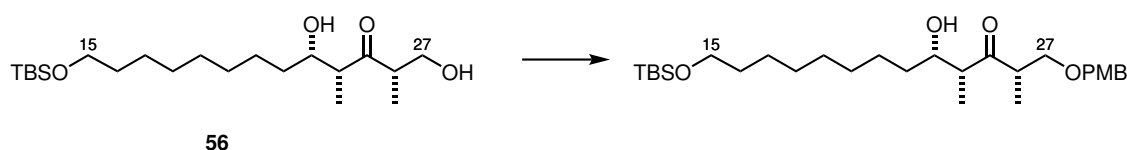
Re-protection 1:



Alcohol **55** (19 mg, 48 μmol) was dissolved in THF (1 mL) and cooled to 0 °C. Imidazole (4 mg, 58 μmol) and TBSCl (11 mg, 72 μmol) were added, and the mixture was stirred at rt for 16 h. The reaction was quenched with H₂O (2 mL), diluted with Et₂O, and the aqueous layer extracted with Et₂O (3 × 2 mL). The combined organics were washed with H₂O (4 mL), dried over MgSO₄, and concentrated *in vacuo*. Purification by flash chromatography (1:5 EtOAc/PE) yielded TBS ether **54** as a colourless oil (24 mg, 98%).

All characterisation data matched those given above for **54**.

Re-protection 2:



To alcohol **56** (202 mg, 520 μmol) in CH_2Cl_2 (5 mL) at 0 °C was added PMBTCA (120 μL , 578 μmol) and PPTS (14 mg, 56 μmol). The mixture was warmed to rt and stirred for 21 h. Upon completion, the reaction was quenched by addition of NaHCO_3 (5 mL). The layers were separated and the aqueous extracted with CH_2Cl_2 (3×5 mL). The combined organics were dried over Na_2SO_4 and concentrated *in vacuo*, then purified by flash chromatography (1:3 EtOAc/PE) to give PMB ether **54** as a colourless oil (169 mg, 64%).

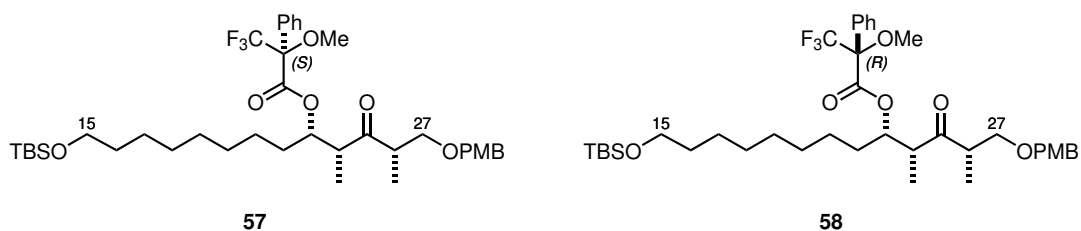
All characterisation data matched those given above for **54**.

Mosher esters of alcohol **54**

(2*S*,4*R*,5*S*)-13-((*tert*-butyldimethylsilyl)oxy)-1-((4-methoxybenzyl)oxy)-2,4-dimethyl-3-oxotridecan-5-yl (*S*)-3,3,3-trifluoro-2-methoxy-2-phenylpropanoate (**57**)

and

(2*S*,4*R*,5*S*)-13-((*tert*-butyldimethylsilyl)oxy)-1-((4-methoxybenzyl)oxy)-2,4-dimethyl-3-oxotridecan-5-yl (*R*)-3,3,3-trifluoro-2-methoxy-2-phenylpropanoate (**58**)



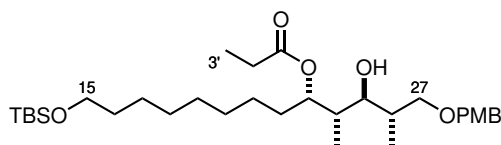
To a solution of alcohol **54** (10.1 mg, 19.8 μmol) and (*S*)- α -methoxy- α -trifluoromethylphenylacetic acid (13.9 mg, 59.4 μmol) in CH_2Cl_2 (1 mL) was added DCC (60 μL , 1.0 M in CH_2Cl_2 , 60.0 μmol) followed by DMAP (8.4 mg, 68.8 μmol). The reaction was stirred at rt for 19 h, then filtered and concentrated. Flash chromatography (1:30 \rightarrow 1:20 EtOAc/PE) gave the (*S*)-MTPA ester **57** as a colourless oil (10.6 mg, 74%).

R_f 0.65 (1:4 EtOAc/PE); **¹H NMR** (500 MHz, CDCl_3) δ_{H} 7.58–7.53 (2H, m, PhH), 7.40–7.36 (3H, m, PhH), 7.19 (2H, d, $J = 8.6$ Hz, PMB ArH), 6.85 (2H, d, $J = 8.7$ Hz, PMB ArH), 5.44 (1H, app dt, $J = 7.6, 5.2$ Hz, H₂₃), 4.39 (1H, d, $J = 11.6$ Hz, ArCH_aH_bO), 4.33 (1H, d, $J = 11.6$ Hz, ArCH_aH_bO), 3.79 (3H, s, ArOMe), 3.59 (2H, t, $J = 6.7$ Hz, H₁₅ \times 2), 3.56 (1H, dd, $J = 8.9, 8.2$ Hz, H_{27a}), 3.52 (3H, s, OMe), 3.39 (1H, dd, $J = 9.0, 5.4$ Hz, H_{27b}), 3.08–2.99 (1H, m, H₂₆), 2.93 (1H, dq, $J = 7.1, 6.7$ Hz, H₂₄), 1.60–1.53 (1H, m, H_{22a}), 1.53–1.43 (3H, m, H₁₆ \times 2, H_{22b}), 1.31–1.10 (10H, m, H_{17–21}), 1.09 (3H, d, $J = 7.2$ Hz, Me₂₄), 1.03 (3H, d, $J = 7.0$ Hz, Me₂₆), 0.89 (9H, s, SiC(CH₃)₃), 0.05 (6H, s, Si(CH₃)₂).

The analogous procedure gave the (*R*)-MTPA ester **58** in 47% yield.

R_f 0.65 (1:4 EtOAc/PE); **¹H NMR** (500 MHz, CDCl₃) δ_H 7.59–7.52 (2H, m, PhH), 7.41–7.35 (3H, m, PhH), 7.19 (2H, d, *J* = 8.7 Hz, PMB ArH), 6.85 (2H, d, *J* = 8.7 Hz, PMB ArH), 5.42 (1H, app q, *J* = 6.1 Hz, H₂₃), 4.38 (1H, d, *J* = 11.5 Hz, ArCH_aH_bO), 4.34 (1H, d, *J* = 11.6 Hz, ArCH_aH_bO), 3.79 (3H, s, ArOMe), 3.58 (2H, t, *J* = 6.7 Hz, H₁₅ × 2), 3.56–3.51 (4H, m, OMe, H_{27a}), 3.36 (1H, dd, *J* = 9.0, 5.4 Hz, H_{27b}), 3.00–2.92 (1H, m, H₂₆), 2.90 (1H, dq, *J* = 7.3, 6.9 Hz, H₂₄), 1.62–1.52 (2H, m, H₂₂ × 2), 1.48 (2H, app quint, *J* = 7.1 Hz, H₁₆ × 2), 1.31–1.12 (10H, m, H_{17–21}), 1.02 (3H, d, *J* = 7.2 Hz, Me₂₄), 0.97 (3H, d, *J* = 7.0 Hz, Me₂₆), 0.89 (9H, s, SiC(CH₃)₃), 0.04 (6H, s, Si(CH₃)₂).

(2*S*,3*S*,4*S*,5*S*)-13-((*tert*-butyldimethylsilyl)oxy)-3-hydroxy-1-((4-methoxybenzyl)oxy)-2,4-dimethyltridecan-5-yl propionate (59**)**

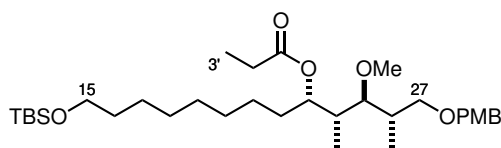


Freshly prepared SmI₂ (18.7 mL, *ca.* 0.1 M in THF, 1.87 mmol) was added dropwise to a solution of propionaldehyde (8.1 mL, 112 mmol, distilled from CaCl₂ immediately prior to use) in THF (120 mL) at 0 °C. The blue-green colour of SmI₂ faded upon addition to give a golden yellow solution, which was stirred at 0 °C for 15 min then cooled to –20 °C. Ketone **54** (9.34 g, 18.3 mmol) was dissolved in THF (70 mL) and added to the reaction mixture *via* cannula. The reaction was kept at –20 °C for 1 h, then quenched with NaHCO₃ (100 mL) and warmed to rt. The aqueous fraction was extracted with Et₂O (3 × 100 mL). The combined organics were dried over Na₂SO₄, concentrated *in vacuo*, and purified by flash chromatography (1:15 EtOAc/PE) to give alcohol **59** as a pale yellow oil (9.91 g, 95%, >20:1 *dr*).

R_f 0.48 (1:5 EtOAc/PE); **¹H NMR** (500 MHz, CDCl₃) δ_H 7.23 (2H, d, *J* = 8.6 Hz, ArH), 6.87 (2H, d, *J* = 8.6 Hz, ArH), 5.27 (1H, ddd, *J* = 8.7, 5.0, 1.5 Hz, H₂₃), 4.43 (1H, d, *J* = 11.6 Hz, ArCH_aH_bO), 4.39 (1H, d, *J* = 11.6 Hz, ArCH_aH_bO), 3.80 (3H, s, ArOMe), 3.59 (2H, t, *J* = 6.6 Hz, H₁₅ × 2), 3.55 (1H, dd, *J* = 9.2, 5.1 Hz, H_{27a}), 3.43 (1H, dd, *J* = 9.2, 5.8 Hz, H_{27b}), 3.35 (1H, d, *J* = 5.7 Hz, C₂₅OH), 3.10 (1H, ddd, *J* = 8.9, 5.7, 3.5 Hz, H₂₅), 2.33 (2H, q, *J* = 7.6 Hz, H₂' × 2), 2.05–1.98 (1H, m, H₂₆), 1.76 (1H, dqd, *J* = 8.5, 6.9, 1.3 Hz, H₂₄), 1.72–1.63 (1H, m, H_{22a}), 1.50 (2H, app quint, *J* = 6.9 Hz, H₁₆ × 2), 1.45–1.36 (1H, m, H_{22b}), 1.34–1.20 (10H, m, H_{17–21}), 1.14 (3H, t, *J* = 7.6 Hz, H₃' × 3), 1.06 (3H, d, *J* = 7.0 Hz, Me₂₆), 0.89 (9H, s, SiC(CH₃)₃), 0.87 (3H,

d, $J = 6.9$ Hz, Me₂₄), 0.04 (6H, s, Si(CH₃)₂); ¹³C NMR (125 MHz, CDCl₃) δ_C 175.3, 159.1, 130.4, 129.1, 113.7, 76.3, 73.7, 72.9, 71.7, 63.3, 55.2, 40.2, 34.7, 32.8, 32.6, 29.5, 29.4, 29.3, 27.8, 26.0, 26.0, 25.7, 18.3, 16.3, 10.1, 9.3, −5.3; [α]_D²⁰ −3.5 (*c* 1.00, CHCl₃); IR (thin film) ν_{max} (cm^{−1}) 3504, 2929, 2849, 1728, 1711, 1617, 1514, 1463, 1364, 1247, 1203, 1096, 1039, 1001, 832, 777; HRMS calc. for C₃₂H₆₂NO₆Si [M+NH₄]⁺ 584.4341, found 584.4325.

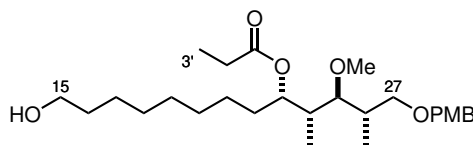
(2*S*,3*S*,4*R*,5*S*)-13-((*tert*-butyldimethylsilyl)oxy)-3-methoxy-1-((4-methoxybenzyl)oxy)-2,4-dimethyltridecan-5-yl propionate (61)



Proton Sponge (9.30 g, 43.4 mmol) and Me₃O · BF₄ (4.28 g, 28.9 mmol) were charged to a flask in an argon-filled glove box, then a solution of alcohol **59** (8.17 g, 14.4 mmol) in CH₂Cl₂ (300 mL) was added at rt. The reaction was stirred for 3 h, during which time it gradually turned yellow, then bright orange. The mixture was then quenched by addition of NH₄Cl (150 mL) and stirred overnight. The aqueous layer was extracted with CH₂Cl₂ (3 × 100 mL), then the combined organics were washed with citric acid (2 × 200 mL, 10% w/v aq.), dried over MgSO₄, and concentrated *in vacuo*. Purification by flash chromatography (1:20 EtOAc/PE) provided the methyl ether **61** as a colourless oil (7.42 g, 89%, 99% brsm).

R_f 0.48 (1:8 EtOAc/PE); ¹H NMR (500 MHz, CDCl₃) δ_H 7.24 (2H, d, $J = 8.7$ Hz, ArH), 6.86 (2H, d, $J = 8.7$ Hz, ArH), 5.18 (1H, app td, $J = 7.4, 2.0$ Hz, H₂₃), 4.43 (1H, d, $J = 11.5$ Hz, ArCH_aH_bO), 4.39 (1H, d, $J = 11.6$ Hz, ArCH_aH_bO), 3.80 (3H, s, ArOMe), 3.59 (2H, t, $J = 6.7$ Hz, H₁₅ × 2), 3.53 (1H, dd, $J = 9.2, 4.9$ Hz, H_{27a}), 3.38 (3H, s, C₂₅OMe), 3.32 (1H, dd, $J = 9.1, 7.3$ Hz, H_{27b}), 2.87 (1H, dd, $J = 8.5, 3.6$ Hz, H₂₅), 2.31 (2H, q, $J = 7.6$ Hz, H₂ × 2), 2.12–2.04 (1H, m, H₂₆), 1.78 (1H, dqd, $J = 8.9, 7.0, 2.0$ Hz, H₂₄), 1.66–1.58 (1H, m, H_{22a}), 1.49 (2H, app quint, $J = 7.0$ Hz, H₁₆ × 2), 1.46–1.39 (1H, m, H_{22b}), 1.33–1.19 (10H, m, H_{17–21}), 1.14 (3H, t, $J = 7.6$ Hz, H₃ × 3), 1.06 (3H, d, $J = 7.1$ Hz, Me₂₆), 0.92–0.88 (12H, m, Me₂₄, SiC(CH₃)₃), 0.04 (6H, s, Si(CH₃)₂); ¹³C NMR (125 MHz, CDCl₃) δ_C 174.1, 159.0, 130.8, 129.0, 113.7, 85.9, 73.2, 72.7, 71.6, 63.3, 61.3, 55.2, 38.8, 35.9, 32.9, 32.7, 29.5, 29.5, 29.4, 28.0, 26.0, 25.8, 25.7, 18.4, 16.3, 10.6, 9.4, −5.3; [α]_D²⁰ −4.4 (*c* 0.79, CHCl₃); IR (thin film) ν_{max} (cm^{−1}) 2932, 2858, 1732, 1614, 1513, 1463, 1247, 1193, 1090, 1038, 834, 776; HRMS calc. for C₃₃H₆₄NO₆Si [M+NH₄]⁺ 598.4497, found 598.4482.

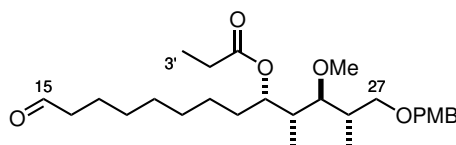
(2*S*,3*S*,4*R*,5*S*)-13-hydroxy-3-methoxy-1-((4-methoxybenzyl)oxy)-2,4-dimethyltridecan-5-yl propionate (62)



TBS ether **61** (2.03 g, 3.49 mmol) was dissolved in THF (50 mL) and cooled to 0 °C. HCl (30 mL, 1.0 M aq.) was added, then the reaction was stirred at rt. After 1 h the reaction was quenched by careful addition of NaHCO₃ (80 mL) with cooling in an ice bath. The resulting mixture was then diluted with H₂O (100 mL) and Et₂O (50 mL) and extracted with Et₂O (3 × 100 mL). The combined organics were dried over Na₂SO₄, concentrated *in vacuo*, and purified by flash chromatography (1:3 EtOAc/PE) to give alcohol **62** as a colourless oil (1.62 g, 99%).

R_f 0.15 (1:3 EtOAc/PE); **¹H NMR** (500 MHz, CDCl₃) δ_H 7.24 (2H, d, *J* = 8.5 Hz, ArH), 6.86 (2H, d, *J* = 8.5 Hz, ArH), 5.18 (1H, app td, *J* = 7.0, 1.6 Hz, H₂₃), 4.42 (1H, d, *J* = 11.6 Hz, ArCH_aH_bO), 4.39 (1H, d, *J* = 11.5 Hz, ArCH_aH_bO), 3.80 (3H, s, ArOMe), 3.62 (2H, t, *J* = 6.6 Hz, H₁₅ × 2), 3.53 (1H, dd, *J* = 9.2, 4.8 Hz, H_{27a}), 3.37 (3H, s, C₂₅OMe), 3.32 (1H, dd, *J* = 9.0, 7.4 Hz, H_{27b}), 2.86 (1H, dd, *J* = 8.5, 3.5 Hz, H₂₅), 2.31 (2H, q, *J* = 7.6 Hz, H₂' × 2), 2.12–2.04 (1H, m, H₂₆), 1.78 (1H, dqd, *J* = 8.6, 7.1, 1.6 Hz, H₂₄), 1.69–1.59 (1H, m, H_{22a}), 1.55 (2H, app quint, *J* = 6.9 Hz, H₁₆ × 2), 1.47–1.39 (1H, m, H_{22b}), 1.39–1.19 (10H, m, H_{17–21}), 1.14 (3H, t, *J* = 7.6 Hz, H₃' × 3), 1.05 (3H, d, *J* = 7.0 Hz, Me₂₆), 0.90 (3H, d, *J* = 7.0 Hz, Me₂₄); **¹³C NMR** (125 MHz, CDCl₃) δ_C 174.1, 159.0, 130.8, 129.0, 113.7, 85.9, 73.1, 72.7, 71.6, 63.0, 61.4, 55.2, 38.8, 35.9, 32.7, 32.7, 29.4, 29.3, 29.2, 28.0, 25.6, 25.6, 16.3, 10.6, 9.4; [α]_D²⁰ –8.0 (*c* 0.10, CHCl₃); **IR** (thin film) ν_{max} (cm^{–1}) 3452, 2972, 2933, 2857, 1730, 1613, 1588, 1514, 1463, 1423, 1364, 1300, 1247, 1195, 1086, 1037, 1003, 820; **HRMS** calc. for C₂₇H₄₇O₆ [M+H]⁺ 467.3367, found 467.3359.

(2*S*,3*S*,4*R*,5*S*)-3-methoxy-1-((4-methoxybenzyl)oxy)-2,4-dimethyl-13-oxotridecan-5-yl propionate (29)



Dess–Martin method:

To a solution of alcohol **62** (38.5 mg, 82.5 μmol) in CH_2Cl_2 (1.5 mL) was added NaHCO_3 (47.5 mg, 565 μmol). The mixture was cooled in an ice bath, and DMP (71.4 mg, 168 μmol) was added in one portion. The reaction was stirred at room temperature for 1 h, then quenched with NaHCO_3 (0.3 mL) and NaS_2O_3 (0.8 mL) and stirred for 1 h. The layers were separated and the aqueous extracted with CH_2Cl_2 (3×1 mL). The combined organics were dried over MgSO_4 and concentrated *in vacuo*, then purified by flash chromatography (1:5 \rightarrow 1:4 EtOAc/PE) to give aldehyde **29** as a colourless oil (38.5 mg, 100%).

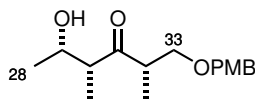
Swern method:

Oxalyl chloride (381 μL , 4.50 mmol) and CH_2Cl_2 (40 mL) were charged to a flask and cooled to -78°C . DMSO (426 μL , 6.00 mmol) was added dropwise, and the mixture was stirred for 30 min. A solution of alcohol **62** (1.41 g, 3.03 mmol) in CH_2Cl_2 (20 mL) was added and stirring continued for 20 min. After addition of Et_3N (1.25 mL, 9.00 mmol), the reaction was warmed to rt and stirred for 1.5 h. Addition of NH_4Cl (60 mL) to quench was followed by extraction with Et_2O (3×50 mL). The combined organics were washed with HCl (100 mL, 0.5 M aq.), brine (100 mL), and NaHCO_3 (100 mL), then dried over MgSO_4 and concentrated *in vacuo*. The product could be used crude or purified by flash chromatography (1:8 EtOAc/PE) to yield the aldehyde **29** as a colourless oil (1.32 g, 94%).

R_f 0.45 (1:3 EtOAc/PE); **¹H NMR** (500 MHz, CDCl_3) δ_{H} 9.75 (1H, t, $J = 1.8$ Hz, H_{15}), 7.24 (2H, d, $J = 8.6$ Hz, ArH), 6.86 (2H, d, $J = 8.7$ Hz, ArH), 5.17 (1H, app td, $J = 7.0, 1.9$ Hz, H_{23}), 4.43 (1H, d, $J = 11.5$ Hz, $\text{ArCH}_a\text{H}_b\text{O}$), 4.39 (1H, d, $J = 11.6$ Hz, $\text{ArCH}_a\text{H}_b\text{O}$), 3.80 (3H, s, ArOMe), 3.53 (1H, dd, $J = 9.2, 4.9$ Hz, H_{27a}), 3.38 (3H, s, C_{25}OMe), 3.32 (1H, dd, $J = 9.1, 7.4$ Hz, H_{27b}), 2.86 (1H, dd, $J = 8.5, 3.5$ Hz, H_{25}), 2.40 (2H, td, $J = 7.4, 1.8$ Hz, $\text{H}_{16} \times 2$), 2.31 (2H, q, $J = 7.6$ Hz, $\text{H}_{2'} \times 2$), 2.12–2.04 (1H, m, H_{26}), 1.78 (1H, dqd, $J = 8.9, 7.0, 1.9$ Hz, H_{24}), 1.66–1.58 (3H, m, $\text{H}_{17} \times 2$, H_{22a}), 1.47–1.38 (1H, m, H_{22b}), 1.33–1.20 (8H, m, H_{18-21}), 1.14 (3H, t, $J = 7.6$ Hz, $\text{H}_{3'} \times 3$), 1.05 (3H, d, $J = 7.0$ Hz, Me_{26}), 0.90 (3H, d, $J = 7.0$ Hz, Me_{24}); **¹³C NMR** (125 MHz, CDCl_3) δ_{C} 202.9, 174.1, 159.0, 130.8, 129.0, 113.7, 85.9, 73.1, 72.7, 71.6, 61.4, 55.3, 43.9, 38.8, 35.9, 32.7, 29.3, 29.2, 29.0, 28.0, 25.6, 22.0, 16.3, 10.6, 9.4; $[\alpha]_{\text{D}}^{20} -5.6$ (c 0.65, CHCl_3); **IR** (thin film) ν_{max} (cm^{-1}) 2936, 2858, 1726, 1614, 1511, 1461, 1364, 1247, 1195, 1088, 1038, 822; **HRMS** calc. for $\text{C}_{27}\text{H}_{48}\text{O}_6\text{N}$ $[\text{M}+\text{NH}_4]^+$ 482.3476, found 482.3471.

5.4.2 Side chain fragment (C₂₈–C₃₄)

(2*S*,4*R*,5*S*)-5-hydroxy-1-((4-methoxybenzyl)oxy)-2,4-dimethylhexan-3-one (**63**)



Method A: Tin aldol

Sn(OTf)₂ (459 mg, 1.10 mmol) was washed with Et₂O (3 × 3 mL), then dried under vacuum and dissolved in CH₂Cl₂ (1 mL) and cooled to –78 °C. Et₃N (165 μL, 1.18 mmol) was added, followed by a pre-cooled solution of ketone **25** (203 mg, 0.859 mmol, dried azeotropically from C₆H₆ and stirred over CaH₂ immediately prior to use) in CH₂Cl₂ (1.25 mL) at –78 °C. The reaction mixture was allowed to enolise at –78 °C for 3 h. Acetaldehyde (140 μL, 2.49 mmol, distilled from CaCl₂ immediately prior to use) was dissolved in CH₂Cl₂ (1 mL) and added to the reaction mixture. After stirring for 3.5 h at –78 °C, the reaction was quenched by addition of pH 7 buffer (3 mL) and warmed to rt. Na⁺/K⁺ tartrate (3 mL) was added, and the biphasic mixture was stirred vigorously overnight. It was then filtered through Celite and diluted with CH₂Cl₂. The aqueous layer was extracted with CH₂Cl₂ (3 × 5 mL), and the combined organics were washed with brine (15 mL), dried over Na₂SO₄, and concentrated *in vacuo*. Purification by flash chromatography (1:2 EtOAc/PE) gave aldol adduct **63** as a colourless oil (71 mg, 30%, 3.5:1 *dr*).

Method B: Titanium aldol

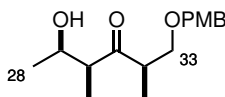
To a solution of TiCl₄ (218 μL, 1.99 mmol) in CH₂Cl₂ (5.6 mL) at 0 °C was added Ti(O*i*-Pr)₄ (196 μL, 0.66 mmol). The mixture was stirred at 0 °C for 10 min, then at rt for 20 min. The resulting colourless solution was added to a solution of **25** (562 mg, 2.38 mmol, dried azeotropically from C₆H₆ and stirred over CaH₂ immediately prior to use) in CH₂Cl₂ (13 mL) at –78 °C. Upon dropwise addition of *i*-Pr₂NEt (450 μL, 2.58 mmol), the yellow solution changed colour to dark red. The reaction mixture was allowed to enolise at –78 °C for 30 min. Acetaldehyde (1.00 mL, 17.8 mmol, distilled from CaCl₂ immediately prior to use) was dissolved in CH₂Cl₂ (10 mL) and added to the reaction mixture slowly *via* syringe, causing a colour change to light orange. The mixture was stirred at –78 °C for a further 45 min, then quenched with MeOH (8 mL). After warming to rt, Na⁺/K⁺ tartrate (20 mL) was added and the biphasic mixture was stirred rapidly for 30 min and left to stand overnight. The layers were separated and the organic phase washed with H₂O (25 mL). The aqueous fractions were then extracted with CH₂Cl₂ (2 ×

25 mL). The combined organics were dried over Na₂SO₄, concentrated *in vacuo* and purified by flash chromatography (1:2 EtOAc/PE) to give aldol adduct **63** as a colourless oil (545 mg, 82%, 14:1 *dr*).

R_f 0.18 (1:3 EtOAc/PE); **¹H NMR** (500 MHz, CDCl₃) δ_H 7.19 (2H, d, *J* = 8.7 Hz, ArH), 6.87 (2H, d, *J* = 8.7 Hz, ArH), 4.41 (1H, d, *J* = 11.6 Hz, ArCH_aH_bO), 4.36 (1H, d, *J* = 11.5 Hz, ArCH_aH_bO), 4.18 (1H, qdd, *J* = 6.5, 4.2, 3.2 Hz, H₂₉), 3.80 (3H, s, ArOMe), 3.61 (1H, app t, *J* = 9.0 Hz, H_{33a}), 3.42 (1H, dd, *J* = 8.7, 4.8 Hz, H_{33b}), 3.15 (1H, dqd, *J* = 9.2, 6.9, 4.8 Hz, H₃₂), 2.93 (1H, d, *J* = 4.2 Hz, C₂₉OH), 2.73 (1H, qd, *J* = 7.1, 3.1 Hz, H₃₀), 1.12 (3H, d, *J* = 6.5 Hz, H₂₈ × 3), 1.08 (3H, d, *J* = 7.2 Hz, Me₃₀), 1.00 (3H, d, *J* = 7.0 Hz, Me₃₂); [α]_D²⁰ +14.0 (*c* 0.10, CHCl₃); **IR** (thin film) ν_{max} (cm⁻¹) 3460, 2972, 2937, 1707, 1611, 1586, 1512, 1459, 1372, 1300, 1247, 1173, 1092, 1033, 997, 910, 820; **HRMS** calc. for C₁₆H₂₈NO₄ [M+NH₄]⁺ 298.2013, found 298.2015.

These data are consistent with those previously reported for the opposite enantiomer.⁹¹

(2*R*,4*S*,5*R*)-5-hydroxy-1-((4-methoxybenzyl)oxy)-2,4-dimethylhexan-3-one (69)

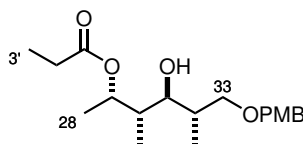


To a solution of TiCl₄ (1.19 mL, 10.9 mmol) in CH₂Cl₂ (30 mL) at 0 °C was added Ti(O*i*-Pr)₄ (1.07 mL, 3.63 mmol). The mixture was stirred at 0 °C for 10 min, then at rt for 20 min. The resulting colourless solution was added dropwise over 20 min to a solution of ketone **24** (2.86 g, 12.1 mmol, dried azeotropically from C₆H₆ and stirred over CaH₂ immediately prior to use) in CH₂Cl₂ (65 mL) at -78 °C. To the yellow solution was added *i*-Pr₂NEt (2.48 mL, 14.2 mmol) dropwise over 15 min, and the reaction mixture was allowed to enolise at -78 °C for 30 min. Acetaldehyde (6.20 mL, 110 mmol, distilled from CaCl₂ immediately prior to use) was dissolved in CH₂Cl₂ (70 mL) and added to the reaction mixture *via* syringe over 20 min, causing the deep red solution to gradually turn pale orange. The mixture was stirred at -78 °C for a further 15 min, then quenched with MeOH (30 mL). After warming to rt, Na⁺/K⁺ tartrate (110 mL) was added and the biphasic mixture was stirred vigorously overnight. The layers were separated and aqueous phase extracted with CH₂Cl₂ (3 × 70 mL). The combined organics were dried over Na₂SO₄, concentrated *in vacuo* and purified by flash chromatography (1:2 EtOAc/PE) to give aldol adduct **69** as a colourless oil (2.85 g, 84%, 16:1 *dr*).

R_f 0.24 (1:3 EtOAc/PE); **¹H NMR** (500 MHz, CDCl₃) δ_H 7.19 (2H, d, *J* = 8.7 Hz, ArH), 6.87 (2H, d, *J* = 8.7 Hz, ArH), 4.41 (1H, d, *J* = 11.6 Hz, ArCH_aH_bO), 4.36 (1H, d, *J* = 11.5 Hz, ArCH_aH_bO), 4.18 (1H, qdd, *J* = 6.5, 4.2, 3.2 Hz, H₂₉), 3.80 (3H, s, ArOMe), 3.61 (1H, app t, *J* = 9.0 Hz, H_{33a}), 3.42 (1H, dd, *J* = 8.7, 4.8 Hz, H_{33b}), 3.15 (1H, dqd, *J* = 9.2, 6.9, 4.8 Hz, H₃₂), 2.93 (1H, d, *J* = 4.2 Hz, C₂₉OH), 2.73 (1H, qd, *J* = 7.1, 3.1 Hz, H₃₀), 1.12 (3H, d, *J* = 6.5 Hz, H₂₈ × 3), 1.08 (3H, d, *J* = 7.2 Hz, Me₃₀), 1.00 (3H, d, *J* = 7.0 Hz, Me₃₂); [α]_D²⁰ −12.6 (*c* 1.02, CHCl₃).

These data are consistent with those previously reported.⁹¹

(2*S*,3*S*,4*S*,5*S*)-4-hydroxy-6-((4-methoxybenzyl)oxy)-3,5-dimethylhexan-2-yl propionate (ent-71)

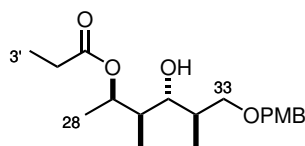


Freshly prepared SmI₂ (1.02 mL, *ca.* 0.1 M in THF, 0.102 mmol) was added dropwise to a solution of propionaldehyde (0.22 mL, 3.06 mmol, distilled from CaCl₂ immediately prior to use) in THF (1.5 mL) at 0 °C. The blue-green colour of SmI₂ faded upon addition to give a murky yellow solution, which was stirred at 0 °C for 10 min then cooled to −20 °C. Ketone **63** (143 mg, 0.510 mmol, 14:1 *dr*) was dissolved in THF (2.5 mL) and added to the reaction mixture *via* cannula, causing a colour change to bright yellow. The reaction was stirred at −20 °C for 1 h 15 min, then quenched with NaHCO₃ (5 mL) and warmed to rt. The aqueous layer was extracted with EtOAc (2 × 5 mL), and the combined organics were washed with brine (10 mL), dried over Na₂SO₄, and concentrated *in vacuo*. Purification by flash chromatography (1:5 EtOAc/PE) gave alcohol **ent-71** as a pale yellow oil (146 mg, 84%, 14:1 *dr*).

R_f 0.43 (1:3 EtOAc/PE); **¹H NMR** (500 MHz, CDCl₃) δ_H 7.23 (2H, d, *J* = 8.6 Hz, ArH), 6.87 (2H, d, *J* = 8.6 Hz, ArH), 5.40 (1H, qd, *J* = 6.6, 2.0 Hz, H₂₉), 4.43 (1H, d, *J* = 11.7 Hz, ArCH_aH_bO), 4.39 (1H, d, *J* = 11.6 Hz, ArCH_aH_bO), 3.80 (3H, s, ArOMe), 3.52 (1H, dd, *J* = 9.3, 4.8 Hz, H_{33a}), 3.49 (1H, dd, *J* = 9.3, 5.1 Hz, H_{33b}), 3.21–3.15 (2H, m, H₃₁, C₃₁OH), 2.30 (2H, q, *J* = 7.6 Hz, H₂' × 2), 2.02–1.94 (1H, m, H₃₂), 1.69–1.61 (1H, m, H₃₀), 1.23 (3H, d, *J* = 6.6 Hz, H₂₈ × 3), 1.12 (3H, t, *J* = 7.6 Hz, H₃' × 3), 1.08 (3H, d, *J* = 7.1 Hz, Me₃₂), 0.89 (3H, d, *J* = 7.0 Hz, Me₃₀); [α]_D²⁰ −1.9 (*c* 1.00, CHCl₃).

These data are consistent with those previously reported for the opposite enantiomer.⁹¹

(2*R*,3*R*,4*R*,5*R*)-4-hydroxy-6-((4-methoxybenzyl)oxy)-3,5-dimethylhexan-2-yl propionate (71)

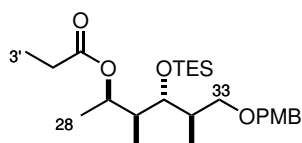


To a solution of propionaldehyde (4.50 mL, 62.1 mmol, freshly distilled from CaCl_2 immediately before use) in THF (60 mL) at 0 °C was added freshly prepared SmI_2 (10.3 mL, *ca.* 0.1 M in THF, 1.03 mmol) dropwise over 15 min. The resulting golden yellow solution was cooled to –20 °C and ketone **69** (2.88 g, 10.3 mmol) was added dropwise in THF (30 mL). After 1 h the reaction was quenched by addition of NaHCO_3 (80 mL). The layers were separated and the aqueous was extracted with Et_2O (3×70 mL). The combined organics were washed with brine (50 mL), dried over Na_2SO_4 , and concentrated *in vacuo*. Flash chromatography (1:5 EtOAc/PE) yielded alcohol **71** (3.40 g, 98%) as a pale yellow oil.

R_f 0.39 (1:3 EtOAc/PE); **¹H NMR** (500 MHz, CDCl_3) δ_{H} 7.23 (2H, d, $J = 8.7$ Hz, ArH), 6.87 (2H, d, $J = 8.7$ Hz, ArH), 5.40 (1H, qd, $J = 6.5, 2.0$ Hz, H_{29}), 4.43 (1H, d, $J = 11.6$ Hz, ArCH_aH_bO), 4.39 (1H, d, $J = 11.7$ Hz, ArCH_aH_bO), 3.80 (3H, s, ArOMe), 3.52 (1H, dd, $J = 9.3, 4.8$ Hz, H_{33a}), 3.49 (1H, dd, $J = 9.3, 5.1$ Hz, H_{33b}), 3.21–3.15 (2H, m, $\text{H}_{31}, \text{C}_{31}\text{OH}$), 2.30 (2H, q, $J = 7.4$ Hz, $\text{H}_{2'} \times 2$), 2.02–1.94 (1H, m, H_{32}), 1.70–1.60 (1H, m, H_{30}), 1.22 (3H, d, $J = 6.6$ Hz, $\text{H}_{28} \times 3$), 1.12 (3H, t, $J = 7.6$ Hz, $\text{H}_{3'} \times 3$), 1.08 (3H, d, $J = 7.1$ Hz, Me_{32}), 0.89 (3H, d, $J = 6.9$ Hz, Me_{30}); **¹³C NMR** (125 MHz, CDCl_3) δ_{C} 174.6, 159.2, 130.3, 129.2, 113.8, 76.6, 73.0, 71.8, 70.0, 55.3, 41.6, 34.7, 27.9, 18.2, 16.2, 10.2, 9.2; $[\alpha]_{\text{D}}^{20} +2.6$ (*c* 1.81, CHCl_3); **IR** (thin film) ν_{max} (cm^{-1}) 3508, 2976, 2937, 2905, 2878, 1730, 1613, 1512, 1463, 1370, 1300, 1276, 1249, 1203, 1174, 1082, 1035, 1007, 983, 819; **HRMS** calc. for $\text{C}_{19}\text{H}_{30}\text{O}_5\text{Na}$ $[\text{M}+\text{Na}]^+$ 361.1985, found 361.1987.

These data are in agreement with those previously reported.⁹¹

(2*R*,3*S*,4*R*,5*R*)-6-((4-methoxybenzyl)oxy)-3,5-dimethyl-4-((triethylsilyl)oxy)hexan-2-yl propionate (72)

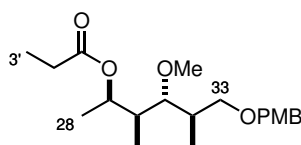


To alcohol **71** (3.77 g, 11.1 mmol) in CH₂Cl₂ (110 mL) at –78 °C were added dropwise sequentially 2,6-lutidine (3.90 mL, 33.5 mmol) and TESOTf (3.80 mL, 16.8 mmol). After stirring for 1.5 h at –78 °C, the reaction was quenched with NH₄Cl (90 mL) and allowed to warm to rt. The aqueous layer was extracted with EtOAc (3 × 70 mL), dried over MgSO₄, and concentrated *in vacuo*. Purification by flash chromatography (1:20 EtOAc/PE) gave silyl ether **72** as a colourless oil (4.73 g, 94%).

R_f 0.53 (1:8 EtOAc/PE); **¹H NMR** (500 MHz, CDCl₃) δ_H 7.25 (2H, d, *J* = 8.7 Hz, ArH), 6.87 (2H, d, *J* = 8.7 Hz, ArH), 5.06 (1H, qd, *J* = 6.3, 3.3 Hz, H₂₉), 4.41 (2H, s, OCH₂Ar), 3.56 (1H, dd, *J* = 9.5, 4.9 Hz, H_{33a}), 3.54 (1H, dd, *J* = 7.6, 3.2 Hz, H₃₁), 3.25 (1H, dd, *J* = 9.1, 8.0 Hz, H_{33b}), 2.28 (2H, q, *J* = 7.6 Hz, H_{2'} × 2), 2.07–1.99 (1H, m, H₃₂), 1.67 (1H, dqd, *J* = 7.1, 7.1, 3.3 Hz, H₃₀), 1.21 (3H, d, *J* = 6.5 Hz, H₂₈ × 3), 1.12 (3H, t, *J* = 7.6 Hz, H_{3'} × 3), 1.01 (3H, d, *J* = 7.0 Hz, Me₃₂), 0.93 (9H, obs t, *J* = 8.0 Hz, Si(CH₂CH₃)₃), 0.92 (3H, obs d, *J* = 8.3 Hz, Me₃₀), 0.59 (6H, q, *J* = 8.0 Hz, Si(CH₂CH₃)₃); **¹³C NMR** (125 MHz, CDCl₃) δ_C 173.9, 159.0, 130.8, 129.0, 113.6, 76.8, 72.6, 71.6, 70.6, 55.2, 42.7, 36.6, 28.0, 18.7, 16.0, 10.7, 9.1, 7.0, 5.3; [α]_D²⁰ +2.60 (*c* 1.00, CHCl₃); **IR** (thin film) ν_{max} (cm^{–1}) 2955, 2913, 2877, 1733, 1613, 1587, 1513, 1462, 1423, 1373, 1302, 1247, 1194, 1171, 1094, 1040, 1010, 821, 738; **HRMS** calc. for C₂₅H₄₅O₅Si [M+H]⁺ 453.3031, found 453.3024.

These data are in agreement with those previously reported.⁹¹

(2*R*,3*S*,4*R*,5*R*)-4-methoxy-6-((4-methoxybenzyl)oxy)-3,5-dimethylhexan-2-yl propionate (73)

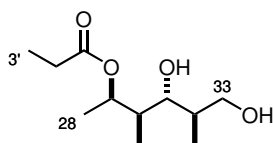


To a flask containing Me₃O · BF₄ (4.80 g, 32.5 mmol) and Proton Sponge (6.97 g, 32.5 mmol) was added a solution of alcohol **71** (2.20 g, 6.5 mmol) in CH₂Cl₂ (110 mL). The reaction was stirred at rt for 4 h, then quenched with NH₄Cl (90 mL) and stirred for a further 30 min. The biphasic mixture was filtered through Celite, then the layers were separated and the aqueous extracted with EtOAc (3 × 70 mL). The organics were dried over MgSO₄ and concentrated *in vacuo*. Flash chromatography (1:12 EtOAc/PE) gave the methyl ether **73** as a pale yellow oil (2.06 g, 90%, 94% brsm). The byproduct **74** was also isolated as a bright pink oil (33 mg, 2.3%).

R_f 0.59 (1:3 EtOAc/PE); **¹H NMR** (500 MHz, CDCl₃) δ_H 7.23 (2H, d, *J* = 8.8 Hz, ArH), 6.85 (2H, d, *J* = 8.8 Hz, ArH), 5.22 (1H, qd, *J* = 6.5, 2.4 Hz, H₂₉), 4.41 (1H, d, *J* = 11.2 Hz,

ArCH_aH_bO), 4.38 (1H, d, $J = 11.8$ Hz, ArCH_aH_bO), 3.78 (3H, s, ArOMe), 3.53 (1H, dd, $J = 9.2, 5.0$ Hz, H_{33a}), 3.35 (3H, s, C₃₁OMe), 3.29 (1H, dd, $J = 9.2, 7.6$ Hz, H_{33b}), 2.88 (1H, dd, $J = 8.9, 3.3$ Hz, H₃₁), 2.29 (2H, q, $J = 7.6$ Hz, H_{2'} × 2), 2.11–2.03 (1H, m, H₃₂), 1.69 (1H, dqd, $J = 9.3, 7.0, 2.3$ Hz, H₃₀), 1.20 (3H, d, $J = 6.6$ Hz, H₂₈ × 3), 1.13 (3H, t, $J = 7.6$ Hz, H_{3'} × 3), 1.06 (3H, d, $J = 7.1$ Hz, Me₃₂), 0.92 (3H, d, $J = 7.1$ Hz, Me₃₀); ¹³C NMR (125 MHz, CDCl₃) δ_C 173.8, 158.9, 130.7, 128.9, 113.6, 85.9, 72.6, 71.3, 69.6, 61.3, 55.1, 40.8, 35.8, 27.9, 18.2, 16.2, 10.3, 9.2; [α]_D²⁰ +2.3 (*c* 0.98, CHCl₃); IR (thin film) ν_{max} (cm⁻¹) 2974, 2937, 1731, 1613, 1513, 1462, 1367, 1302, 1246, 1195, 1172, 1083, 1036, 1011, 819; HRMS calc. for C₂₀H₃₆O₅N [M+NH₄]⁺ 370.2588, found 370.2589.

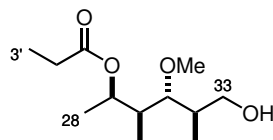
(2R,3R,4R,5R)-4,6-dihydroxy-3,5-dimethylhexan-2-yl propionate (74)



Diol **74** was isolated as a byproduct from the methylation of **71** (*vide supra*).

R_f 0.23 (1:1 EtOAc/PE); ¹H NMR (500 MHz, CDCl₃) δ_H 5.38 (1H, qd, $J = 6.6, 1.8$ Hz, H₂₉), 3.83 (1H, ddd, $J = 11.0, 2.8, 2.8$ Hz, H_{33a}), 3.71 (1H, d, $J = 5.2$ Hz, C₃₁OH), 3.56 (1H, ddd, $J = 11.1, 6.4, 4.8$ Hz, H_{33b}), 3.19 (1H, ddd, $J = 8.9, 4.8, 4.0$ Hz, H₃₁), 3.05 (1H, br s, C₃₃OH), 2.32 (2H, q, $J = 7.6$ Hz, H_{2'} × 2), 1.84–1.73 (2H, m, H₃₀, H₃₂), 1.25 (3H, d, $J = 6.5$ Hz, H₂₈ × 3), 1.12 (3H, t, $J = 7.6$ Hz, H_{3'} × 3), 1.09 (3H, d, $J = 7.1$ Hz, Me₃₂), 0.88 (3H, d, $J = 7.1$ Hz, Me₃₀); ¹³C NMR (125 MHz, CDCl₃) δ_C 175.2, 77.9, 70.1, 64.7, 41.6, 35.4, 27.8, 18.2, 15.6, 9.9, 9.2; [α]_D²⁰ +3.0 (*c* 1.02, CHCl₃); IR (thin film) ν_{max} (cm⁻¹) 3388, 2976, 2941, 2881, 1712, 1462, 1426, 1377, 1346, 1325, 1280, 1208, 1161, 1076, 1029, 1012, 976; HRMS calc. for C₁₁H₂₂O₄Na [M+Na]⁺ 241.1416, found 241.1405.

(2R,3S,4R,5R)-6-hydroxy-4-methoxy-3,5-dimethylhexan-2-yl propionate (185)

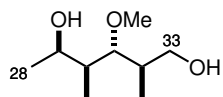


To a biphasic mixture containing PMB ether **73** (1.00 g, 2.84 mmol) in CH₂Cl₂ (30 mL) and pH 7 buffer (15 mL) at 0 °C was added DDQ (1.29 g, 5.68 mmol) in one portion. The reaction

was warmed to rt and stirred rapidly for 1 h, during which time a colour change from dark green to bright red was observed. NaHCO₃ (20 mL) and H₂O (20 mL) were added to quench the reaction, and the quenching mixture was stirred vigorously for 30 min. The layers were separated and the organic layer was washed with brine (30 mL). The combined aqueous fractions were then extracted with EtOAc (2 × 100 mL). The organics were dried over Na₂SO₄ and concentrated *in vacuo*. Flash chromatography (1:2 EtOAc/PE) allowed the isolation of alcohol **185** as a yellow oil (611 mg, 93%).

R_f 0.32 (1:2 EtOAc/PE); **¹H NMR** (500 MHz, CDCl₃) δ_H 5.22 (1H, qd, *J* = 6.4, 2.5 Hz, H₂₉), 3.78 (1H, dd, *J* = 11.1, 3.7 Hz, H_{33a}), 3.53 (1H, dd, *J* = 11.1, 4.5 Hz, H_{33b}), 3.40 (3H, s, C₃₁OMe), 2.96 (1H, dd, *J* = 8.9, 3.3 Hz, H₃₁), 2.67 (1H, br s, C₃₃OH), 2.30 (2H, q, *J* = 7.6 Hz, H_{2'} × 2), 1.91–1.83 (1H, m, H₃₂), 1.76 (1H, dqd, *J* = 9.5, 7.0, 2.6 Hz, H₃₀), 1.22 (3H, d, *J* = 6.5 Hz, H₂₈ × 3), 1.13 (3H, d, *J* = 7.2 Hz, Me₃₂), 1.12 (3H, t, *J* = 7.7 Hz, H_{3'} × 3), 0.90 (3H, d, *J* = 7.1 Hz, Me₃₀); **¹³C NMR** (125 MHz, CDCl₃) δ_C 173.9, 88.6, 69.6, 64.5, 61.7, 41.3, 36.0, 28.0, 18.3, 16.0, 10.3, 9.2; [α]_D²⁰ –8.8 (*c* 1.00, CHCl₃); **IR** (thin film) ν_{max} (cm^{–1}) 3425, 2977, 2938, 2881, 2829, 1731, 1462, 1376, 1276, 1194, 1158, 1123, 1083, 1032, 966, 936, 870, 807; **HRMS** calc. for C₁₂H₂₅O₄ [M+H]⁺ 233.1747, found 233.1749.

(2R,3R,4S,5R)-3-methoxy-2,4-dimethylhexane-1,5-diol (75)

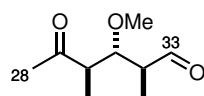


Ester **185** (600 mg, 2.58 mmol) was dissolved in CH₂Cl₂ (26 mL) and cooled to –78 °C. DIBAL (10.5 mL, 10.5 mmol, 1.0 M in hexane) was added cautiously, and the reaction was stirred at –78 °C for 45 min. The mixture was quenched with Na⁺/K⁺ tartrate (20 mL) and H₂O (20 mL) and stirred at rt for 2 h. The aqueous layer was then extracted with CH₂Cl₂ (4 × 40 mL), and the combined organics dried over Na₂SO₄ and concentrated *in vacuo*. Purification by flash chromatography (1:1 EtOAc/PE) gave diol **75** as a colourless oil (431 mg, 95%).

R_f 0.20 (1:1 EtOAc/PE); **¹H NMR** (500 MHz, CDCl₃) δ_H 4.16 (1H, qd, *J* = 6.5, 1.6 Hz, H₂₉), 3.68 (1H, dd, *J* = 10.8, 4.4 Hz, H_{33a}), 3.64 (1H, dd, *J* = 10.8, 4.9 Hz, H_{33b}), 3.52 (3H, s, C₃₁OMe), 3.16 (1H, dd, *J* = 7.6, 4.3 Hz, H₃₁), 3.07 (1H, br s, C₂₉OH), 2.54 (1H, br s, C₃₃OH), 1.99–1.91 (1H, m, H₃₂), 1.65 (1H, dqd, *J* = 7.1, 4.3, 1.7 Hz, H₃₀), 1.13 (3H, d, *J* = 6.5 Hz, H₂₈ × 3), 1.00 (3H, d, *J* = 7.3 Hz, Me₃₀), 0.94 (3H, d, *J* = 7.1 Hz, Me₃₂); **¹³C NMR** (125 MHz, CDCl₃) δ_C 90.7, 66.5, 65.3, 61.9, 39.7, 37.6, 20.7, 14.9, 11.0; [α]_D²⁰ +8.3 (*c* 1.00, CHCl₃); **IR**

(thin film) ν_{\max} (cm⁻¹) 3392, 2968, 2932, 2833, 1456, 1413, 1371, 1193, 1157, 1076, 1032, 1010, 998, 963, 937, 903, 887; **HRMS** calc. for C₉H₂₁O₃ [M+H]⁺ 177.1485, found 177.1483.

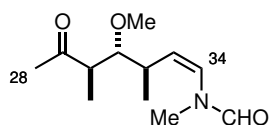
(2S,3R,4R)-3-methoxy-2,4-dimethyl-5-oxohexanal (76)



Oxalyl chloride (52 μ L, 0.615 mmol) was charged to a flask with CH₂Cl₂ (2.6 mL) and cooled to -78 °C. DMSO (90 μ L, 1.23 mmol) was added, and the solution was stirred for 15 min. A solution of diol **75** (33.2 mg, 0.188 mmol) in CH₂Cl₂ (1.4 mL) was added dropwise. After a further 15 min, Et₃N (340 μ L, 2.43 mmol) was added, and stirring was continued at -78 °C for 30 min, then at -40 °C for 10 min. The reaction mixture was then quenched with NH₄Cl (3 mL), warmed to rt, and extracted with CH₂Cl₂ (3 \times 3 mL). The combined organics were washed sequentially with HCl (5 mL, 0.5 M), H₂O (5 mL), NaHCO₃ (5 mL), and brine (5 mL), and then dried over MgSO₄ and concentrated *in vacuo* to afford **76** as a pale yellow oil. The crude material was carried through directly to the next step without further purification.

R_f 0.42 (1:2 EtOAc/PE); **¹H NMR** (500 MHz, CDCl₃) δ_{H} 9.76 (1H, d, *J* = 1.6 Hz, H₃₃), 3.74 (1H, dd, *J* = 8.6, 3.5 Hz, H₃₁), 3.36 (3H, s, C₃₁OMe), 2.89 (1H, dq, *J* = 7.7, 7.2 Hz, H₃₀), 2.69–2.60 (1H, m, H₃₂), 2.21 (3H, s, Me₂₈), 1.18 (3H, d, *J* = 7.0 Hz, Me₃₂), 0.98 (3H, d, *J* = 7.1 Hz, Me₃₀).

N-((3R,4R,5R,Z)-4-methoxy-3,5-dimethyl-6-oxohept-1-en-1-yl)-N-methylformamide (78)



To a solution of HMDS (0.14 mL, 0.67 mmol) in THF (0.22 mL) was added *n*-BuLi (0.38 mL, 0.38 mmol, 1.6 M in hexane) dropwise at 0 °C. This mixture was stirred for 30 min to form a 1.0 M solution of LiHMDS. Meanwhile, phosphonium salt **77** (115 mg, 0.311 mmol) was suspended in THF (2 mL) and cooled to -78 °C. The LiHMDS solution (0.29 mL, 0.29 mmol) was added, then the mixture was warmed to 0 °C, stirred for 30 min, and re-cooled to -78 °C.

Aldehyde **76** (*ca* 32 mg, crude material, \leq 0.188 mmol) was stirred over CaH₂ in THF (3 mL) for 45 min, then was added *via* cannula to the ylid solution. The mixture was stirred at -78 °C

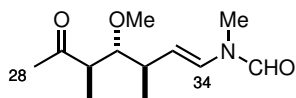
for 1 h, then quenched with NH₄Cl (3 mL) and warmed to rt. The aqueous layer was extracted with Et₂O (3 × 5 mL) and the combined organics dried over MgSO₄ and concentrated *in vacuo*. Purification by flash chromatography (1:1 EtOAc/PE) gave the *N*-methyl-*N*-vinylformamide **78** as a colourless oil (9.2 mg, 21% from **75**, 8:1 *Z/E*).

R_f 0.24 (1:1 EtOAc/PE); **¹H NMR** (500 MHz, CDCl₃) δ_H 8.16 (0.87H, s, NCHO), [8.05] (0.13H, s, NCHO*), [6.24] (0.13H, d, *J* = 9.4 Hz, H₃₄*), 5.97 (0.87H, d, *J* = 8.7 Hz, H₃₄), 5.32 (0.87H, dd, *J* = 10.8, 8.7 Hz, H₃₃), [5.27] (0.13H, dd, *J* = 10.3, 9.5 Hz, H₃₃*), 3.37 (3H, s, C₃₁OMe), 3.26 (1H, dd, *J* = 9.1, 3.0 Hz, H₃₁), [3.15] (0.39H, s, NMe*), 3.00 (2.61H, s, NMe), 2.79–2.62 (2H, m, H₃₀, H₃₂), 2.19 (3H, s, Me₂₈), 1.15 (3H, d, *J* = 6.9 Hz, Me₃₂), [0.93] (0.39H, d, *J* = 7.0 Hz, Me₃₀*), 0.90 (2.61H, d, *J* = 7.1 Hz, Me₃₀).

Distinguishable resonances of the minor rotamer (*ca* 2:1 ratio) are given in brackets and marked with an asterisk.

These data are in agreement with those previously reported.¹²⁹

N-((3*R*,4*R*,5*R*,*E*)-4-methoxy-3,5-dimethyl-6-oxohept-1-en-1-yl)-*N*-methylformamide (**32**)



A crystal of I₂ (3.3 mg, 0.013 mmol) was dissolved in CH₂Cl₂ (0.5 mL) under argon and added to a solution of enamide **78** (9.0 mg, 0.039 mmol, 8:1 *Z/E*) in CH₂Cl₂ (2 mL) at rt. The reaction was stirred in the dark for 68 h, then quenched by addition of Na₂S₂O₃ (2.5 mL) and stirred for 30 min. The mixture was extracted with CH₂Cl₂ (3 × 3 mL), dried over MgSO₄ and concentrated *in vacuo*. Flash chromatography (1:1 EtOAc/PE) gave the isomeric enamide **32** as a colourless oil (6.7 mg, 74%, >20:1 *E/Z*).

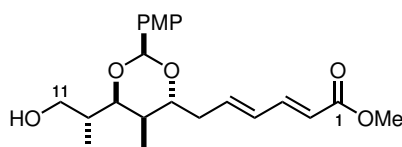
R_f 0.17 (1:1 EtOAc/PE); **¹H NMR** (500 MHz, CDCl₃) δ_H 8.29 (0.67H, s, NCHO), [8.07] (0.33H, s, NCHO*), [7.13] (0.33H, d, *J* = 14.7 Hz, H₃₄*), 6.46 (0.67H, d, *J* = 14.2 Hz, H₃₄), [5.13] (0.33H, dd, *J* = 14.6, 9.3 Hz, H₃₃*), 5.11 (0.67H, dd, *J* = 14.1, 9.1 Hz, H₃₃), 3.38 (3H, s, C₃₁OMe), 3.29 (1H, dd, *J* = 9.2, 2.5 Hz, H₃₁), [3.07] (1H, s, NMe*), 3.04 (2H, s, NMe), 2.76–2.65 (1H, m, H₃₀), [2.44] (0.33H, dqd, *J* = 9.3, 6.9, 2.4 Hz, H₃₂*), 2.39 (0.67H, dqd, *J* = 9.3, 6.9, 2.5 Hz, H₃₂), 2.20 (2H, s, Me₂₈), [2.18] (1H, s, Me₂₈*), 1.16 (3H, d, *J* = 7.0 Hz, Me₃₂), 0.96 (2H, d, *J* = 6.9 Hz, Me₃₀), [0.94] (1H, d, *J* = 6.7 Hz, Me₃₀*).

Distinguishable resonances of the minor rotamer (*ca* 2:1 ratio) are given in brackets and marked with an asterisk.

These data are in agreement with those previously reported.¹²⁹

5.4.3 PMP-protected northern fragment (C₁–C₁₄)

Methyl (2*E*,4*E*)-6-((2*S*,4*R*,5*R*,6*R*)-6-((*R*)-1-hydroxypropan-2-yl)-2-(4-methoxyphenyl)-5-methyl-1,3-dioxan-4-yl)hexa-2,4-dienoate (186)

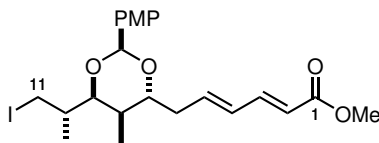


PMB ether **86** (75.8 mg, 0.148 mmol) was dissolved in CH₂Cl₂ (2 mL) and pH 9.2 buffer (0.5 mL) and stirred vigorously at 0 °C. After addition of DDQ (43.7 mg, 0.192 mmol), the mixture was warmed to rt, stirred for 30 min, then quenched with NaHCO₃ (2.5 mL) and H₂O (2 mL). The aqueous layer was extracted with CH₂Cl₂ (4 × 10 mL), and the combined organics washed with brine (40 mL), dried over Na₂SO₄, and concentrated *in vacuo*. Purification by flash chromatography (1:2 EtOAc/PE) gave alcohol **186** as a colourless oil (37.8 mg, 65%).

R_f 0.48 (1:1 EtOAc/PE); **¹H NMR** (400 MHz, CDCl₃) δ_H 7.35 (2H, d, *J* = 8.7 Hz, ArH), 7.26 (1H, dd, *J* = 15.4, 10.8 Hz, H₃), 6.88 (2H, d, *J* = 8.7 Hz, ArH), 6.29 (1H, dd, *J* = 15.2, 10.9 Hz, H₄), 6.13 (1H, dt, *J* = 14.7, 7.3 Hz, H₅), 5.83 (1H, d, *J* = 15.4 Hz, H₂), 5.74 (1H, s, ArCH₂O₂), 4.02 (1H, dd, *J* = 8.4, 6.8 Hz, H₇), 3.96 (1H, dd, *J* = 10.0, 2.3 Hz, H₉), 3.80 (3H, s, ArOMe), 3.74 (3H, s, CO₂Me), 3.73–3.60 (2H, m, H₁₁ × 2), 3.02 (1H, dd, *J* = 15.3, 7.6 Hz, H_{6a}), 2.63–2.53 (2H, m, H_{6b}, C₁₁OH), 2.07–2.00 (1H, m, H₁₀), 1.61–1.52 (1H, m, H₈), 1.26 (3H, d, *J* = 7.0 Hz, Me₁₀), 0.82 (3H, d, *J* = 7.0 Hz, Me₈).

These data are in agreement with those previously reported.²²⁶

Methyl (2*E*,4*E*)-6-((2*S*,4*R*,5*R*,6*S*)-6-((*S*)-1-iodopropan-2-yl)-2-(4-methoxyphenyl)-5-methyl-1,3-dioxan-4-yl)hexa-2,4-dienoate (187**)**

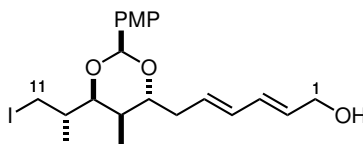


To a solution of alcohol **186** (37.8 mg, 0.0968 mmol) in Et₂O/MeCN (1:1, 3 mL) at 0 °C were added PPh₃ (100 mg, 0.383 mmol), imidazole (32.0 mg, 0.468 mmol), and iodine (99.7 mg, 0.392 mmol, portionwise). The reaction was stirred at 0 °C for 30 min, then at rt for 1.5 h, whereupon it was quenched with NaHCO₃ (3 mL). The layers were separated and the aqueous extracted with Et₂O (3 × 5 mL). The organics were then washed with brine (10 mL), dried over MgSO₄, and concentrated *in vacuo*. The crude was purified by flash chromatography (1:4 EtOAc/PE) to yield iodide **187** as a colourless oil (39.5 mg, 82%).

R_f 0.69 (1:2 EtOAc/PE); **¹H NMR** (400 MHz, CDCl₃) δ_H 7.39 (2H, d, *J* = 8.7 Hz, ArH), 7.27 (1H, dd, *J* = 15.4, 10.8 Hz, H₃), 6.89 (2H, d, *J* = 8.8 Hz, ArH), 6.30 (1H, dd, *J* = 15.2, 11.0 Hz, H₄), 6.15 (1H, dt, *J* = 14.7, 7.3 Hz, H₅), 5.84 (1H, d, *J* = 15.4 Hz, H₂), 5.71 (1H, s, ArCH(O₂)), 4.01 (1H, dd, *J* = 8.5, 6.7 Hz, H₇), 3.80 (3H, s, ArOMe), 3.77 (1H, dd, *J* = 9.7, 2.2 Hz, H₉), 3.74 (3H, s, CO₂Me), 3.55 (1H, dd, *J* = 9.5, 5.1 Hz, H_{11a}), 3.38 (1H, dd, *J* = 9.4, 2.5 Hz, H_{11b}), 3.02 (1H, ddd, *J* = 15.4, 7.7, 7.7 Hz, H_{6a}), 2.58 (1H, ddd, *J* = 14.4, 7.2, 7.2 Hz, H_{6b}), 1.62–1.54 (1H, m, H₈), 1.48–1.40 (1H, m, H₁₀), 1.23 (3H, d, *J* = 6.9 Hz, Me₁₀), 0.90 (3H, d, *J* = 6.6 Hz, Me₈).

These data are in agreement with those previously reported.²²⁶

(2*E*,4*E*)-6-((2*S*,4*R*,5*R*,6*S*)-6-((*S*)-1-iodopropan-2-yl)-2-(4-methoxyphenyl)-5-methyl-1,3-dioxan-4-yl)hexa-2,4-dien-1-ol (188**)**



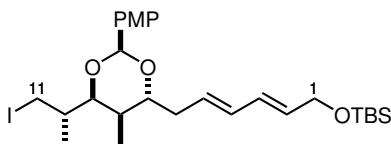
To methyl ester **187** (39.5 mg, 0.0789 mmol) in CH₂Cl₂ (2 mL) at –78 °C was added DIBAL (0.64 mL, 0.64 mmol, 1.0 M in hexane). After stirring for 1.5 h, the reaction was quenched with Na⁺/K⁺ tartrate (2.5 mL) and stirred vigorously while warming to rt. The mixture was diluted with H₂O (5 mL) and Et₂O (5 mL) and stirred for a further 1 h. The aqueous layer was extracted

with Et₂O (3 × 8 mL). The combined organics were dried over Na₂SO₄, concentrated *in vacuo*, and purified by flash chromatography (1:2 EtOAc/PE) giving product **188** as a pale yellow oil (26.7 mg, 72%).

R_f 0.25 (1:2 EtOAc/PE); **¹H NMR** (500 MHz, CDCl₃) δ_H 7.40 (2H, d, *J* = 8.6 Hz, ArH), 6.89 (2H, d, *J* = 8.8 Hz, ArH), 6.24 (1H, dd, *J* = 15.0, 10.5 Hz, H₃), 6.17 (1H, dd, *J* = 14.8, 10.5 Hz, H₄), 5.78 (1H, dt, *J* = 14.9, 5.9 Hz, H₂), 5.72 (1H, dt, *J* = 14.8, 7.1 Hz, H₅), 5.72 (1H, s, ArCHO₂), 4.18 (2H, dd, *J* = 5.6, 5.6 Hz, H₁ × 2), 3.95 (1H, dd, *J* = 7.7, 7.7 Hz, H₇), 3.80 (3H, s, ArOMe), 3.77 (1H, dd, *J* = 9.6, 2.2 Hz, H₉), 3.54 (1H, dd, *J* = 9.4, 5.1 Hz, H_{11a}), 3.38 (1H, dd, *J* = 9.5, 2.6 Hz, H_{11b}), 2.89 (1H, ddd, *J* = 14.7, 7.4, 7.4 Hz, H_{6a}), 2.56 (1H, ddd, *J* = 14.8, 7.4, 7.4 Hz, H_{6b}), 1.60 (1H, qd, *J* = 7.0, 1.3 Hz, H₈), 1.48–1.42 (1H, m, H₁₀), 1.29 (1H, t, *J* = 5.9 Hz, C₁OH), 1.22 (3H, d, *J* = 7.0 Hz, Me₁₀), 0.90 (3H, d, *J* = 6.6 Hz, Me₈).

These data are in agreement with those previously reported.²²⁶

tert-Butyl(((2*E*,4*E*)-6-((2*S*,4*R*,5*R*,6*S*)-6-((*S*)-1-iodopropan-2-yl)-2-(4-methoxyphenyl)-5-methyl-1,3-dioxan-4-yl)hexa-2,4-dien-1-yl)oxy)dimethylsilane (87**)**

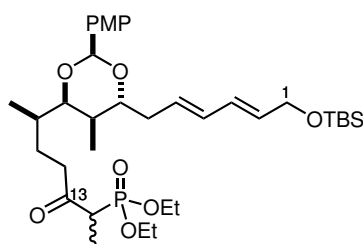


Alcohol **188** (26.7 mg, 0.0565 mmol) was dissolved in CH₂Cl₂ (2 mL) and cooled to –78 °C. To the solution were added 2,6-lutidine (20 μL, 0.085 mmol) and TBSOTf (20 μL, 0.17 mmol). After 1 h, the reaction was quenched with NH₄Cl (2 mL) and allowed to warm to rt while stirring briskly. The aqueous layer was extracted with CH₂Cl₂ (3 × 2 mL), dried over MgSO₄ and concentrated *in vacuo*. Flash chromatography (1:20 EtOAc/PE) yielded a colourless oil, TBS ether **87** (30.4 mg, 92%).

R_f 0.70 (1:5 EtOAc/PE); **¹H NMR** (500 MHz, CDCl₃) δ_H 7.41 (2H, d, *J* = 8.7 Hz, ArH), 6.89 (2H, d, *J* = 8.8 Hz, ArH), 6.25–6.12 (2H, m, H₄, H₅), 5.72 (1H, s, ArCHO₂), 5.72–5.63 (2H, m, H₂, H₃), 4.21 (2H, d, *J* = 5.6 Hz, H₁ × 2), 3.95 (1H, dd, *J* = 7.7, 7.7 Hz, H₇), 3.80 (3H, s, ArOMe), 3.77 (1H, dd, *J* = 9.7, 2.2 Hz, H₉), 3.54 (1H, dd, *J* = 9.5, 5.1 Hz, H_{11a}), 3.39 (1H, dd, *J* = 9.5, 2.6 Hz, H_{11b}), 2.86 (1H, ddd, *J* = 14.5, 7.3, 7.3 Hz, H_{6a}), 2.57 (1H, ddd, *J* = 14.9, 7.5, 7.5 Hz, H_{6b}), 1.61 (1H, qd, *J* = 6.9, 1.4 Hz, H₈), 1.49–1.41 (1H, m, H₁₀), 1.22 (3H, d, *J* = 7.0 Hz, Me₁₀), 0.92 (9H, s, SiC(CH₃)₃), 0.90 (3H, d, *J* = 6.6 Hz, Me₈), 0.08 (6H, s, Si(CH₃)₂).

These data are in agreement with those previously reported.²²⁶

Diethyl ((6*R*)-6-((2*S*,4*R*,5*R*,6*R*)-6-((2*E*,4*E*)-6-((*tert*-butyldimethylsilyl)oxy)hexa-2,4-dien-1-yl)-2-(4-methoxyphenyl)-5-methyl-1,3-dioxan-4-yl)-3-oxoheptan-2-yl)phosphonate (20**)**



Sodium hydride (271 mg, 60% dispersion in mineral oil, 6.78 mmol) was suspended in THF (8 mL) and cooled to 0 °C. A solution of phosphonate **90** (1.03 g, 4.95 mmol) in THF (4 mL) was added dropwise and stirred for 40 min, forming a white slurry. Maintaining the reaction at 0 °C, *n*-BuLi (3.61 mL, 1.6 M in hexane, 5.78 mmol) was added dropwise, giving rise to a cloudy yellow solution which was allowed to stir for 30 min then cooled to –78 °C.

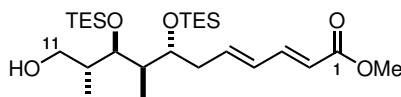
The dianion solution was added slowly *via* cannula to a solution of iodide **87** (565 mg, 0.963 mmol) and HMPA (0.50 mL, 2.9 mmol) in THF (3 mL) at –78 °C. The reaction was stirred at this temperature for 2 h, then warmed to –30 °C and allowed to gradually warm to –10 °C over 1 h. The dark yellow reaction mixture was then quenched with NH₄Cl (10 mL), warmed to rt, and extracted with Et₂O (3 × 10 mL). The organic extracts were combined and dried over MgSO₄, concentrated *in vacuo*, and purified by flash chromatography (1:2 EtOAc/PE) to give a 4:1 inseparable mixture of phosphonate **20** and the undesired regioisomer **91** (488 mg, 76%) as a pale yellow oil.

R_f 0.25 (1:1 EtOAc/PE); **¹H NMR** (500 MHz, CDCl₃) δ_H 7.39 (2H, d, *J* = 8.5 Hz, ArH), 6.86 (2H, d, *J* = 8.5 Hz, ArH), 6.24–6.09 (2H, m, H₃, H₄), 5.73–5.61 (3H, m, H₂, H₅, ArCH=O), 4.20 (2H, d, *J* = 5.0 Hz, H₁ × 2), 4.14–4.01 (4H, m, P(OCH₂CH₃)₂), 3.92 (1H, dd, *J* = 7.5, 7.5 Hz, H₇), 3.79 (3H, s, ArOMe), 3.65 (1H, dd, *J* = 10.0, 1.9 Hz, H₉), 3.18 (1H, dq, *J* = 24.8, 7.2 Hz, H₁₄), 2.94–2.79 (2H, m, H_{6a}, H_{12a}), 2.78–2.65 (1H, m, H_{12b}), 2.59–2.48 (1H, m, H_{6b}), 2.11–2.00 (1H, m, H_{11a}), 1.71–1.63 (1H, m, H₈), 1.63–1.56 (1H, m, H₁₀), 1.34–1.23 (10H, m, H_{11b}, Me₁₄, P(OCH₂CH₃)₂), 1.17 (3H, d, *J* = 6.9 Hz, Me₁₀), 0.91 (9H, s, Si(CH₃)₃), 0.81 (3H, dd, *J* = 6.7, 1.7 Hz, Me₈), 0.07 (6H, s, Si(CH₃)₂).

These data are in agreement with those previously reported.¹¹⁸

5.4.4 Bis-TES-protected northern fragment (C₁–C₁₄)

Methyl (2*E*,4*E*,7*R*,8*R*,9*R*,10*R*)-11-hydroxy-8,10-dimethyl-7,9-bis((triethylsilyl)oxy)undeca-2,4-dienoate (**189**)

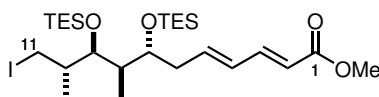


To a rapidly stirred solution of PMB ether **96** (1.07 g, 1.73 mmol) in CH₂Cl₂ (20 mL) and pH 7 buffer (10 mL) at 0 °C was added DDQ (650 mg, 2.86 mmol). The mixture was allowed to warm to rt, and a colour change from dark green to red was observed over 1 h. NaHCO₃ (20 mL) was added to quench the reaction, and the solution was diluted with H₂O (30 mL) and CH₂Cl₂ (20 mL) and stirred for a further 30 min. The aqueous layer was then extracted with EtOAc (3 × 20 mL), dried over Na₂SO₄, and concentrated *in vacuo*. Purification by flash chromatography (1:8 EtOAc/PE) gave the alcohol **189** as a pale yellow oil (839 mg, 97%).

R_f 0.52 (1:4 EtOAc/PE); **¹H NMR** (500 MHz, CDCl₃) δ_H 7.26 (1H, obs dd, H₃), 6.21 (1H, dd, *J* = 15.3, 10.1 Hz, H₄), 6.15 (1H, ddd, *J* = 15.2, 7.0, 6.9 Hz, H₅), 5.80 (1H, d, *J* = 15.4 Hz, H₂), 3.80–3.74 (2H, m, H₉, H_{11a}), 3.75 (3H, s, COOMe), 3.71 (1H, ddd, *J* = 6.3, 6.3, 3.9 Hz, H₇), 3.56 (1H, ddd, *J* = 12.0, 6.2, 6.2 Hz, H_{11b}), 2.60 (1H, dd, *J* = 6.4, 5.2 Hz, C₁₁OH), 2.37–2.22 (2H, m, H₆ × 2), 1.87–1.79 (1H, m, H₈), 1.79–1.71 (1H, m, H₁₀), 1.00 (3H, d, *J* = 7.7 Hz, Me₁₀), 0.98 (9H, t, *J* = 8.0 Hz, Si(CH₂CH₃)₃), 0.95 (9H, t, *J* = 8.0 Hz, Si(CH₂CH₃)₃), 0.89 (3H, d, *J* = 7.0 Hz, Me₈), 0.65 (6H, q, *J* = 8.1 Hz, Si(CH₂CH₃)₃), 0.60 (6H, q, *J* = 8.0 Hz, Si(CH₂CH₃)₃).

These data are in agreement with those previously reported.⁹²

Methyl (2*E*,4*E*,7*R*,8*R*,9*S*,10*S*)-11-iodo-8,10-dimethyl-7,9-bis((triethylsilyl)oxy)undeca-2,4-dienoate (**98**)



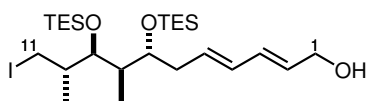
To a solution of alcohol **189** (839 mg, 1.68 mmol) in MeCN/Et₂O (1:1, 30 mL) at 0 °C was added PPh₃ (791 mg, 3.02 mmol), imidazole (229 mg, 3.36 mmol) and, in small portions, iodine (765 mg, 3.02 mmol). After stirring for 30 min at this temperature, the reaction was warmed to rt for 2 h, then quenched with NaHCO₃ (30 mL). The layers were separated and the aqueous extracted with Et₂O (3 × 20 mL). The combined organics were dried over MgSO₄, concentrated *in*

vacuo, and purified *via* flash chromatography (1:15 EtOAc/PE) to yield iodide **98** as a colourless oil (906 mg, 89%).

R_f 0.76 (1:4 EtOAc/PE); **¹H NMR** (500 MHz, CDCl₃) δ_H 7.27 (1H, dd, *J* = 15.4, 10.2 Hz, H₃), 6.22 (1H, dd, *J* = 15.3, 10.1 Hz, H₄), 6.16 (1H, ddd, *J* = 15.2, 6.8, 6.2 Hz, H₅), 5.81 (1H, d, *J* = 15.4 Hz, H₂), 3.75 (3H, s, COOMe), 3.70 (1H, ddd, *J* = 6.1, 5.9, 4.5 Hz, H₇), 3.66 (1H, app t, *J* = 4.4 Hz, H₉), 3.29 (1H, dd, *J* = 9.9, 4.3 Hz, H_{11a}), 3.00 (1H, dd, *J* = 9.8, 8.8 Hz, H_{11b}), 2.32–2.27 (2H, m, H₆ × 2), 1.88–1.79 (1H, m, H₁₀), 1.73–1.65 (1H, m, H₈), 1.05 (3H, d, *J* = 6.8 Hz, Me₁₀), 0.97 (9H, t, *J* = 7.9 Hz, Si(CH₂CH₃)₃), 0.96 (9H, t, *J* = 7.9 Hz, Si(CH₂CH₃)₃), 0.85 (3H, d, *J* = 7.0 Hz, Me₈), 0.63 (6H, q, *J* = 8.0 Hz, Si(CH₂CH₃)₃), 0.60 (6H, q, *J* = 8.1 Hz, Si(CH₂CH₃)₃).

These data are in agreement with those previously reported.⁹²

(2*E*,4*E*,7*R*,8*R*,9*S*,10*S*)-11-iodo-8,10-dimethyl-7,9-bis((triethylsilyl)oxy)undeca-2,4-dien-1-ol (190)

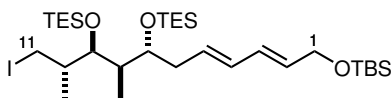


Ester **98** (906 mg, 1.48 mmol) was dissolved in CH₂Cl₂ (30 mL) and cooled to –78 °C. After dropwise addition of DIBAL (4.45 mL, 1.0 M in hexane, 4.45 mmol), the reaction was stirred for 1.5 h, then quenched with Na⁺/K⁺ tartrate (30 mL) and stirred vigorously for 30 min. The quenching mixture was diluted with H₂O (50 mL) and CH₂Cl₂ (50 mL), and the aqueous layer extracted with CH₂Cl₂ (3 × 60 mL). The combined organic fractions were dried over Na₂SO₄ and concentrated *in vacuo*. The crude was subjected to flash chromatography (1:10 EtOAc/PE), giving alcohol **190** as a colourless oil (833 mg, 96%).

R_f 0.33 (1:4 EtOAc/PE); **¹H NMR** (500 MHz, CDCl₃) δ_H 6.23 (1H, dd, *J* = 15.2, 10.4 Hz, H₃), 6.08 (1H, dd, *J* = 15.1, 10.4 Hz, H₄), 5.79–5.69 (2H, m, H₂, H₅), 4.18 (2H, app t, *J* = 5.9 Hz, H₁ × 2), 3.69–3.63 (2H, m, H₇, H₉), 3.32 (1H, dd, *J* = 9.9, 4.0 Hz, H_{11a}), 2.99 (1H, app t, *J* = 9.4 Hz, H_{11b}), 2.21 (2H, br t, *J* = 6.1 Hz, H₆ × 2), 1.88–1.79 (1H, m, H₁₀), 1.73–1.64 (1H, m, H₈), 1.27 (1H, t, *J* = 5.9 Hz, C₁OH), 1.05 (3H, d, *J* = 6.8 Hz, Me₁₀), 0.97 (9H, t, *J* = 7.9 Hz, Si(CH₂CH₃)₃), 0.96 (9H, t, *J* = 8.0 Hz, Si(CH₂CH₃)₃), 0.85 (3H, d, *J* = 7.0 Hz, Me₈), 0.63 (6H, q, *J* = 7.4 Hz, Si(CH₂CH₃)₃), 0.60 (6H, q, *J* = 7.5 Hz, Si(CH₂CH₃)₃).

These data are in agreement with those previously reported.⁹²

(6*E*,8*E*,11*R*,12*R*,13*S*)-15,15-diethyl-13-((*S*)-1-iodopropan-2-yl)-2,2,3,3,12-pentamethyl-11-((triethylsilyl)oxy)-4,14-dioxo-3,15-disilaheptadeca-6,8-diene (99)

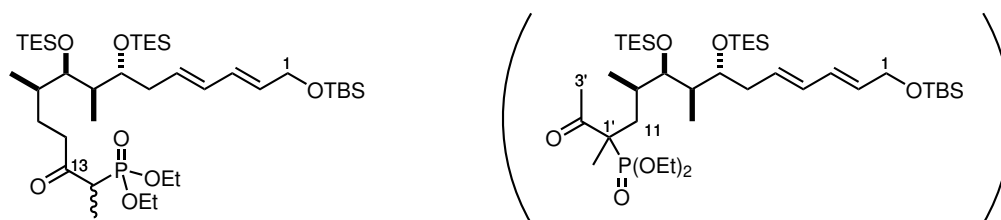


Imidazole (139 mg, 2.04 mmol) and TBSCl (359 mg, 2.38 mmol) were added sequentially to a stirred solution of alcohol **190** (992 mg, 1.70 mmol) in CH₂Cl₂ (35 mL) at rt. The mixture was stirred for 5 h, then quenched by addition of NH₄Cl (30 mL). The aqueous layer was extracted with CH₂Cl₂ (3 × 20 mL), and the combined organics were dried over MgSO₄ and concentrated *in vacuo*. Flash chromatography (1:30 EtOAc/PE) gave TBS ether **99** as a colourless oil (1.16 g, 98%).

R_f 0.51 (1:20 EtOAc/PE); **¹H NMR** (500 MHz, CDCl₃) δ_H 6.19 (1H, dd, *J* = 15.1, 10.6 Hz, H₃), 6.06 (1H, dd, *J* = 15.1, 10.6 Hz, H₄), 5.70–5.62 (2H, m, H₂, H₅), 4.21 (2H, d, *J* = 5.0 Hz, H₁ × 2), 3.68–3.63 (2H, m, H₇, H₉), 3.33 (1H, dd, *J* = 9.8, 3.9 Hz, H_{11a}), 2.98 (1H, app t, *J* = 9.5 Hz, H_{11b}), 2.19 (2H, br t, *J* = 6.2 Hz, H₆ × 2), 1.89–1.79 (1H, m, H₁₀), 1.73–1.65 (1H, m, H₈), 1.05 (3H, d, *J* = 6.7 Hz, Me₁₀), 0.97 (9H, t, *J* = 8.0 Hz, Si(CH₂CH₃)₃), 0.96 (9H, t, *J* = 8.0 Hz, Si(CH₂CH₃)₃), 0.91 (9H, s, Si(CH₃)₃), 0.85 (3H, d, *J* = 7.0 Hz, Me₈), 0.63 (6H, q, *J* = 7.7 Hz, Si(CH₂CH₃)₃), 0.60 (6H, q, *J* = 7.7 Hz, Si(CH₂CH₃)₃), 0.07 (6H, s, Si(CH₃)₂).

These data are in agreement with those previously reported.⁹²

Diethyl ((6*R*,7*R*,8*R*,9*R*,11*E*,13*E*)-15-((*tert*-butyldimethylsilyl)oxy)-6,8-dimethyl-3-oxo-7,9-bis((triethylsilyl)oxy)pentadeca-11,13-dien-2-yl)phosphonate (28)



Sodium hydride (60 mg, 60% in mineral oil, 1.50 mmol) was dissolved in THF (1 mL) and cooled to 0 °C. Phosphonate linker **90** (269 mg, 1.29 mmol) was added dropwise as a solution in THF (1 mL). H₂ evolution was initially observed as the grey slurry was stirred for 45 min at 0 °C, then the mixture seized and was re-suspended in THF (0.5 mL). To the monoanion suspension

was then added *n*-BuLi (0.82 mL, 1.58 M in hexane, 1.29 mmol) dropwise, and the resulting bright yellow solution was stirred for a further 45 min at 0 °C.

Iodide **99** (130 mg, 0.186 mmol) was dried azeotropically with C₆H₆ then dissolved in THF (1 mL) and HMPA (80 µL, 0.460 mmol). This solution was cooled to 0 °C, and the pre-cooled dianion solution was added dropwise over 5 min. After stirring for 1.5 h at 0 °C, the reaction was quenched with NH₄Cl (5 mL). The layers were separated and the aqueous extracted with Et₂O (3 × 5 mL). The combined organic fractions were dried over MgSO₄ and concentrated *in vacuo*. Flash chromatography (1:2 EtOAc/PE) gave a colourless oil containing the desired phosphonate **28** as an inconsequential mixture of diastereomers at the C₁₄ position, along with the inseparable branched regioisomer **100** (93.5 mg, 65% combined yield, 3.8:1 **28/100**).

R_f 0.67 (1:1 EtOAc/PE); **¹H NMR** (500 MHz, CDCl₃) δ_H 6.18 (1H, dd, *J* = 15.1, 10.5 Hz, H₃), 6.04 (1H, dd, *J* = 14.9, 10.6 Hz, H₄), 5.72–5.60 (2H, m, H₂, H₅), 4.20 (2H, d, *J* = 5.2 Hz, H₁ × 2), 4.16–4.07 (4H, m, P(OCH₂CH₃)₂), 3.67–3.56 (1H, m, H₇), 3.56–3.50 (1H, m, H₉), 3.22 (0.4H, dq, *J* = 21.4, 7.1 Hz, H₁₄), 3.21 (0.4H, dq, *J* = 21.4, 7.1 Hz, H₁₄[†]), 2.87 (0.4H, ddd, *J* = 17.5, 9.9, 5.1 Hz, H_{12a}[†]), 2.77–2.59 (0.8H, m, H_{12a}, H_{12b}), 2.46 (0.4H, ddd, *J* = 17.5, 9.7, 6.0 Hz, H_{12b}[†]), [2.35] (0.6H, s, Me_{3'}^{*}), 2.23–2.10 (2H, m, H₆ × 2), [1.88–1.81] (0.2H, m, H_{11a}^{*}), 1.79–1.61 (2H, m, H₈, H_{11a}, H_{11b}^{*}), 1.57–1.47 (1H, m, H₁₀), 1.42–1.30 (9.2H, m, Me₁₄, H_{11b}, P(OCH₂CH₃)₂), 0.99–0.90 (18.6H, m, Si(CH₂CH₃)₃ × 2, Me_{1'}^{*}), 0.91 (9H, s, SiC(CH₃)₃), 0.88 (3H, d, *J* = 7.0 Hz, Me₁₀), 0.86 (2.4H, d, *J* = 6.6 Hz, Me₈), [0.72] (0.6H, d, *J* = 7.0 Hz, Me₈^{*}), 0.65–0.54 (12H, m, Si(CH₂CH₃)₃ × 2), 0.07 (6H, s, Si(CH₃)₂).

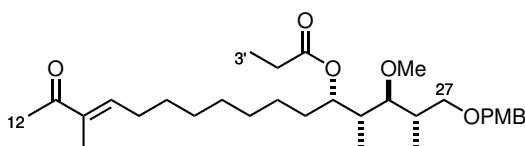
Distinguishable resonances of the minor regioisomer are given in brackets and marked with an asterisk (*). The diastereomeric ratio of the product at C₁₄ is approximately 1:1, and distinguishable resonances of the two diastereomers are noted with a dagger (†).

These data are in agreement with those previously reported.⁹²

5.5 Experimental procedures for Chapter 3

5.5.1 PMP-protected macrocycle (C₁–C₂₇)

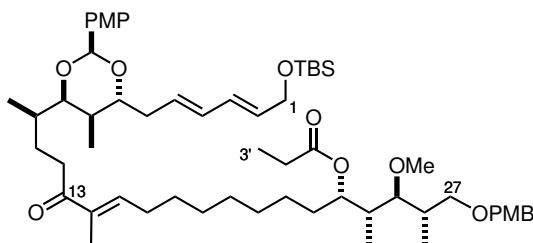
(2*S*,3*S*,4*R*,5*S*,*E*)-3-methoxy-1-((4-methoxybenzyl)oxy)-2,4,14-trimethyl-15-oxohexadec-13-en-5-yl propionate (**109**)



To a slurry of anhydrous Ba(OH)₂ (16.1 mg, 0.0940 mmol) in THF (0.5 mL) was added phosphonate **90** (10.0 mg, 0.0480 mmol) in THF (1 mL). After stirring for 1 h at rt, a solution of aldehyde **29** (10.3 mg, 0.0222 mmol) in THF/H₂O (40:1, 1 mL) was added and stirring was continued for 6.5 h. The reaction was quenched with NH₄Cl (2.5 mL), extracted with Et₂O (3 × 3 mL) and dried over MgSO₄. After concentrating *in vacuo*, the crude was purified by flash chromatography (1:10 EtOAc/PE) to give the coupled product **109** as a colourless oil (10.5 mg, 91%).

R_f 0.46 (1:4 EtOAc/PE); **¹H NMR** (500 MHz, CDCl₃) δ_H 7.24 (2H, d, *J* = 8.6 Hz, ArH), 6.86 (2H, d, *J* = 8.7 Hz, ArH), 6.62 (1H, td, *J* = 7.3, 1.1 Hz, H₁₅), 5.18 (1H, td, *J* = 7.0, 1.9 Hz, H₂₃), 4.43 (1H, d, *J* = 11.5 Hz, ArCH_aH_bO), 4.39 (1H, d, *J* = 11.6 Hz, ArCH_aH_bO), 3.80 (3H, s, ArOMe) 3.53 (1H, dd, *J* = 9.2, 4.9 Hz, H_{27a}), 3.38 (3H, s, C₂₅OMe) 3.32 (1H, dd, *J* = 9.1, 7.4 Hz, H_{27b}), 2.86 (1H, dd, *J* = 8.5, 3.5 Hz, H₂₅), 2.31 (2H, q, *J* = 7.6 Hz, H₂' × 2), 2.30 (3H, s, Me₁₂), 2.22 (2H, app q, *J* = 7.4 Hz, H₁₆ × 2), 2.11–2.05 (1H, m, H₂₆), 1.78 (1H, dqd, *J* = 7.2, 7.2, 1.8 Hz, H₂₄), 1.76 (3H, s, Me₁₄), 1.69–1.58 (1H, m, H_{22a}), 1.49–1.39 (3H, m, H_{22b}, H₁₇ × 2), 1.35–1.20 (8H, m, H_{18–21}), 1.14 (3H, t, *J* = 7.6 Hz, H₃' × 3), 1.05 (3H, d, *J* = 7.0 Hz, Me₂₆), 0.90 (3H, d, *J* = 7.1 Hz, Me₂₄); **¹³C NMR** (125 MHz, CDCl₃) δ_C 199.9, 174.1, 159.0, 143.9, 137.6, 130.8, 129.0, 113.7, 85.9, 73.1, 72.7, 71.6, 61.4, 55.2, 38.8, 35.9, 32.7, 29.4, 29.3, 29.3, 29.1, 28.6, 28.0, 25.7, 25.4, 16.3, 11.1, 10.6, 9.4; [α]_D²⁰ –6.4 (*c* 0.659, CHCl₃); **IR** (thin film) ν_{max} (cm^{–1}) 2927, 2855, 1730, 1668, 1614, 1514, 1462, 1366, 1302, 1276, 1247, 1193, 1087, 1037, 819; **HRMS** calc. for C₃₁H₅₄O₆N [M+NH₄]⁺ 536.3946, found 536.3953.

(2*S*,3*S*,4*R*,5*S*,18*R*,*E*)-18-((2*S*,4*R*,5*R*,6*R*)-6-((2*E*,4*E*)-6-((*tert*-butyldimethylsilyl)oxy)hexa-2,4-dien-1-yl)-2-(4-methoxyphenyl)-5-methyl-1,3-dioxan-4-yl)-3-methoxy-1-((4-methoxybenzyl)-oxy)-2,4,14-trimethyl-15-oxononadec-13-en-5-yl propionate (104)

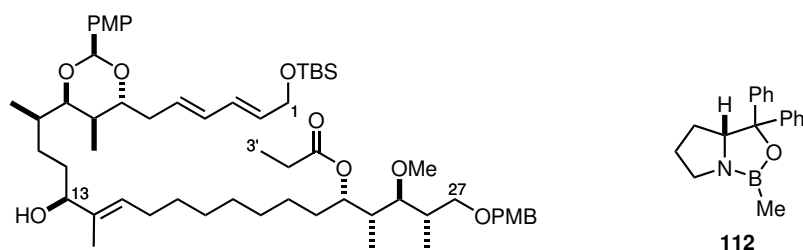


A solution of phosphonate **20** (471 mg, 4:1 ratio of regioisomers, 0.565 mmol) in THF (6 mL) was charged to a flask containing barium hydroxide (145 mg, 0.846 mmol) and stirred at rt for 2 h. Aldehyde **29** (297 mg, 0.639 mmol) was added as a solution in THF/H₂O (4 mL, 40:1). The reaction was left to stir for 68 h, then was quenched with NH₄Cl (10 mL). The aqueous fraction was extracted with Et₂O (3 × 8 mL) and the combined organics were washed with brine (20 mL), dried over MgSO₄, and concentrated *in vacuo*. The crude was purified by careful flash chromatography (1:15 → 1:8 EtOAc/PE) to yield enone **104** as a colourless oil (460 mg, 83%, >20:1 *E/Z*).

R_f 0.57 (1:3 EtOAc/PE); **¹H NMR** (500 MHz, CDCl₃) δ_H 7.38 (2H, d, *J* = 8.7 Hz, PMP ArH), 7.24 (2H, d, *J* = 8.7 Hz, PMB ArH), 6.86 (2H, d, *J* = 8.7 Hz, PMP ArH), 6.85 (2H, d, *J* = 8.8 Hz, PMB ArH), 6.54 (1H, td, *J* = 7.3, 1.0 Hz, H₁₅), 6.21 (1H, dd, *J* = 14.8, 10.5 Hz, H₃), 6.14 (1H, dd, *J* = 14.8, 10.6 Hz, H₄), 5.69 (1H, s, ArCH=O), 5.68 (1H, dt, *J* = 14.8, 5.2 Hz, H₂), 5.66 (1H, obs dt, H₅), 5.18 (1H, td, *J* = 7.9, 1.9 Hz, H₂₃), 4.43 (1H, d, *J* = 11.5 Hz, ArCH_aH_bO), 4.39 (1H, d, *J* = 11.6 Hz, ArCH_aH_bO), 4.20 (2H, d, *J* = 5.1 Hz, H₁ × 2), 3.92 (1H, dd, *J* = 7.7, 7.7 Hz, H₇), 3.80 (3H, s, ArOMe), 3.78 (3H, s, ArOMe), 3.67 (1H, dd, *J* = 9.9, 1.9 Hz, H₉), 3.52 (1H, dd, *J* = 9.2, 4.9 Hz, H_{27a}), 3.38 (3H, s, C₂₅OMe), 3.32 (1H, dd, *J* = 9.1, 7.4 Hz, H_{27b}), 2.87 (1H, dd, *J* = 8.4, 3.5 Hz, H₂₅), 2.84 (1H, ddd, *J* = 14.5, 7.2, 7.2 Hz, H_{6a}), 2.69 (2H, t, *J* = 8.0 Hz, H₁₂ × 2), 2.54 (1H, ddd, *J* = 14.8, 7.5, 7.5 Hz, H_{6b}), 2.31 (2H, q, *J* = 7.6 Hz, H_{2'} × 2), 2.14 (2H, app q, *J* = 7.3 Hz, H₁₆ × 2), 2.11–2.05 (1H, m, H₂₆), 2.05–1.98 (1H, m, H_{11a}), 1.78 (1H, dqd, *J* = 8.9, 7.1, 1.8 Hz, H₂₄), 1.73 (3H, s, Me₁₄), 1.73–1.65 (1H, m, H₁₀), 1.65–1.57 (2H, m, H₈, H_{22a}), 1.53–1.39 (2H, m, H_{11b}, H_{22b}), 1.39–1.32 (2H, m, H₁₇ × 2), 1.32–1.20 (8H, m, H_{18–21}), 1.18 (3H, d, *J* = 6.9 Hz, Me₈), 1.14 (3H, t, *J* = 7.6 Hz, H_{3'} × 3), 1.06 (3H, d, *J* = 7.0 Hz, Me₂₆), 0.91 (9H, s, Si(CH₃)₃), 0.90 (3H, obs d, Me₂₄), 0.83 (3H, d, *J* = 6.9 Hz, Me₁₀), 0.07 (6H, s, Si(CH₃)₂); **¹³C NMR** (125 MHz, CDCl₃) δ_C 202.5, 174.1, 159.8, 159.0, 142.5, 136.9, 132.2, 131.8, 131.3, 130.9, 129.8, 129.5, 129.0, 127.3, 113.7, 113.5, 94.9, 85.9, 79.8, 79.2, 73.1, 72.8,

71.6, 63.5, 61.4, 55.3, 55.3, 38.9, 35.9, 35.3, 34.0, 33.9, 32.7, 31.4, 29.5, 29.4, 29.3, 29.1, 29.0, 28.6, 28.1, 26.0, 25.7, 18.4, 16.3, 14.6, 13.0, 11.4, 10.7, 9.4, -5.2; $[\alpha]_D^{20} +2.4$ (c 1.01, CHCl_3); **IR** (thin film) ν_{max} (cm^{-1}) 2928, 2856, 1730, 1666, 1615, 1515, 1462, 1380, 1302, 1248, 1194, 1171, 1088, 1038, 993, 835, 777; **HRMS** calc. for $\text{C}_{58}\text{H}_{96}\text{O}_{10}\text{SiN}$ $[\text{M}+\text{NH}_4]^+$ 994.6798, found 994.6794.

(2*S*,3*S*,4*R*,5*S*,15*S*,18*R*,*E*)-18-((2*S*,4*R*,5*R*,6*R*)-6-((2*E*,4*E*)-6-((*tert*-butyldimethylsilyl)oxy)hexa-2,4-dien-1-yl)-2-(4-methoxyphenyl)-5-methyl-1,3-dioxan-4-yl)-15-hydroxy-3-methoxy-1-((4-methoxybenzyl)oxy)-2,4,14-trimethylnonadec-13-en-5-yl propionate (116)

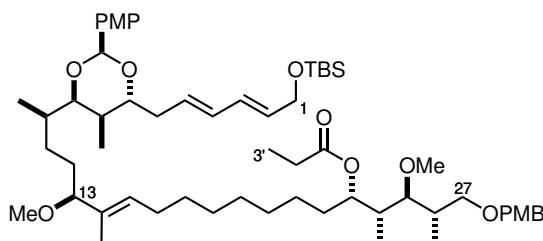


To a solution of enone **104** (34.8 mg, 0.0356 mmol) in THF (2.5 mL) at $-5\text{ }^{\circ}\text{C}$ was added Me-CBS catalyst (*R*)-**112** (47 μL , 1.0 M in toluene, 0.047 mmol) and borane dimethylsulfide (4 μL , 0.042 mmol). The mixture was stirred at this temperature for 40 min, then quenched by dropwise addition of MeOH (1 mL). Stirring continued for a further 20 min as the solution warmed to rt, then the solvent was then removed *in vacuo*. The crude material was re-dissolved in MeOH (1 mL) and concentrated *in vacuo* three times, then was purified by flash chromatography (1:3 EtOAc/PE) to give alcohol **116** as a colourless oil (28.4 mg, 81%, >20:1 *dr*).

R_f 0.30 (1:3 EtOAc/PE); **¹H NMR** (500 MHz, CDCl_3) δ_{H} 7.38 (2H, d, $J = 8.8$ Hz, PMP ArH), 7.24 (2H, d, $J = 8.6$ Hz, PMB ArH), 6.87 (2H, d, $J = 8.7$ Hz, PMP ArH), 6.86 (2H, d, $J = 8.6$ Hz, PMB ArH), 6.21 (1H, dd, $J = 14.9, 10.5$ Hz, H_3), 6.13 (1H, dd, $J = 14.9, 10.6$ Hz, H_4), 5.72–5.62 (2H, m, H_2, H_5), 5.68 (1H, s, ArCH O_2), 5.33 (1H, t, $J = 6.8$ Hz, H_{15}), 5.18 (1H, td, $J = 7.0, 1.9$ Hz, H_{23}), 4.43 (1H, d, $J = 11.6$ Hz, ArCH $\text{H}_a\text{H}_b\text{O}$), 4.39 (1H, d, $J = 11.6$ Hz, ArCH $\text{H}_a\text{H}_b\text{O}$), 4.20 (2H, d, $J = 5.1$ Hz, $\text{H}_1 \times 2$), 3.96–3.92 (1H, m, H_{13}), 3.92 (1H, dd, $J = 7.7, 7.7$ Hz, H_7), 3.80 (3H, s, ArOMe), 3.79 (3H, s, ArOMe), 3.64 (1H, dd, $J = 10.3, 1.9$ Hz, H_9), 3.53 (1H, dd, $J = 9.2, 4.9$ Hz, H_{27a}), 3.38 (3H, s, C_{25}OMe), 3.32 (1H, dd, $J = 9.2, 7.4$ Hz, H_{27b}), 2.86 (1H, dd, $J = 8.5, 3.6$ Hz, H_{25}), 2.83 (1H, ddd, $J = 14.7, 7.3, 7.3$ Hz, H_{6a}), 2.53 (1H, ddd, $J = 14.7, 7.4, 7.4$ Hz, H_{6b}), 2.31 (2H, q, $J = 7.6$ Hz, $\text{H}_{2'} \times 2$), 2.12–2.04 (1H, m, H_{26}), 2.03–1.89 (2H, m, $\text{H}_{16} \times 2$), 1.78 (1H, dqd, $J = 8.9, 7.2, 2.0$ Hz, H_{24}), 1.75–1.67 (2H, m, $\text{H}_{10}, \text{H}_{11a}$), 1.66–1.56 (3H, m, $\text{H}_8, \text{H}_{12a}, \text{H}_{22a}$), 1.55 (3H, s, Me_{14}), 1.53–1.48 (1H, m, H_{12b}), 1.48–1.39 (2H, m, $\text{H}_{22b}, \text{C}_{13}\text{OH}$), 1.35–1.20 (10H,

m, H₁₇₋₂₁), 1.17 (3H, d, J = 7.0 Hz, Me₈), 1.14 (3H, t, J = 7.6 Hz, H_{3'} × 3), 1.06 (3H, d, J = 7.1 Hz, Me₂₆), 1.06–1.00 (1H, m, H_{11b}), 0.91 (9H, s, SiC(CH₃)₃), 0.90 (3H, obs d, Me₂₄), 0.82 (3H, d, J = 6.8 Hz, Me₁₀), 0.07 (6H, s, Si(CH₃)₂); ¹³C NMR (125 MHz, CDCl₃) δ_C 174.1, 159.7, 159.0, 136.6, 132.1, 131.8, 131.2, 130.8, 129.8, 129.6, 129.0, 127.4, 127.3, 113.7, 113.5, 94.8, 85.9, 79.8, 78.6, 78.5, 73.1, 72.7, 71.6, 63.5, 61.4, 55.3, 55.2, 38.8, 35.9, 33.9, 33.7, 32.7, 31.3, 31.2, 29.5, 29.4, 29.3, 29.3, 28.8, 28.0, 27.5, 25.9, 25.7, 18.4, 16.3, 14.2, 13.0, 10.8, 10.6, 9.4, −5.2; [α]_D²⁰ +8.0 (*c* 1.01, CHCl₃); IR (thin film) ν_{max} (cm^{−1}) 3403, 2929, 2855, 1731, 1615, 1515, 1463, 1379, 1364, 1302, 1248, 1194, 1171, 1096, 1037, 991, 969, 835, 777; HRMS calc. for C₅₈H₉₈O₁₀SiN [M+NH₄]⁺ 996.6955, found 996.6953.

(2*S*,3*S*,4*R*,5*S*,15*S*,18*R*,*E*)-18-((2*S*,4*R*,5*R*,6*R*)-6-((2*E*,4*E*)-6-((*tert*-butyldimethylsilyl)oxy)hexa-2,4-dien-1-yl)-2-(4-methoxyphenyl)-5-methyl-1,3-dioxan-4-yl)-3,15-dimethoxy-1-((4-methoxybenzyl)oxy)-2,4,14-trimethylnonadec-13-en-5-yl propionate (118)

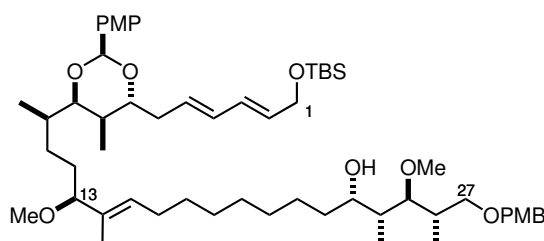


To a flask containing proton sponge (27.0 mg, 0.126 mmol) and Meerwein salt (15.5 mg, 0.105 mmol) was added a solution of alcohol **116** (20.4 mg, 0.0208 mmol) in CH₂Cl₂ (2 mL). The reaction mixture gradually turned yellow while stirring at rt. After 1.5 h no further reaction progress was observed, and the reaction was quenched with NH₄Cl (3 mL) and stirred until the mixture returned to colourless. The reaction mixture was then extracted with CH₂Cl₂ (2 × 3 mL), washed with citric acid (5 mL, 10% w/v), and dried over MgSO₄. After concentrating *in vacuo*, the crude was purified by flash chromatography (1:8 EtOAc/PE) to give methyl ether **118** as a colourless, viscous oil (18.5 mg, 89%).

R_f 0.35 (1:5 EtOAc/PE); ¹H NMR (500 MHz, CDCl₃) δ_H 7.38 (2H, d, J = 8.7 Hz, PMP ArH), 7.24 (2H, d, J = 8.7 Hz, PMB ArH), 6.86 (4H, d, J = 8.2 Hz, ArH), 6.21 (1H, dd, J = 14.9, 10.5 Hz, H₃), 6.12 (1H, dd, J = 14.7, 10.6 Hz, H₄), 5.68 (1H, dt, J = 14.9, 5.2 Hz, H₂), 5.67 (1H, s, ArCHO₂), 5.66 (1H, obs dt, H₅), 5.29 (1H, t, J = 7.1 Hz, H₁₅), 5.19 (1H, td, J = 7.0, 1.8 Hz, H₂₃), 4.43 (1H, d, J = 11.6 Hz, ArCH_aH_bO), 4.39 (1H, d, J = 11.6 Hz, ArCH_aH_bO), 4.20 (2H, d, J = 5.3 Hz, H₁ × 2), 3.91 (1H, dd, J = 7.6, 7.6 Hz, H₇), 3.80 (3H, s, ArOMe), 3.79 (3H, s, ArOMe), 3.63 (1H, dd, J = 10.0, 1.9 Hz, H₉), 3.53 (1H, dd, J = 9.2, 4.8 Hz, H_{27a}), 3.38 (3H,

s, C₂₅OMe), 3.36 (1H, t, $J = 7.0$ Hz, H₁₃), 3.32 (1H, dd, $J = 9.1, 7.5$ Hz, H_{27b}), 3.14 (3H, s, C₁₃OMe), 2.87 (1H, dd, $J = 8.5, 3.5$ Hz, H₂₅), 2.82 (1H, ddd, $J = 14.6, 7.3, 7.3$ Hz, H_{6a}), 2.52 (1H, ddd, $J = 14.7, 7.4, 7.4$ Hz, H_{6b}), 2.31 (2H, q, $J = 7.6$ Hz, H_{2'} × 2), 2.12–2.06 (1H, m, H₂₆), 2.06–1.98 (1H, m, H_{16a}), 1.98–1.90 (1H, m, H_{16b}), 1.78 (1H, dqd, $J = 8.8, 7.0, 1.8$ Hz, H₂₄), 1.74–1.66 (1H, m, H₁₀), 1.66–1.60 (2H, m, H_{11a}, H_{22a}), 1.60–1.51 (3H, m, H₈, H₁₂ × 2), 1.45 (3H, s, Me₁₄), 1.45–1.39 (1H, m, H_{22b}), 1.36–1.29 (2H, m, H₁₇ × 2), 1.29–1.20 (8H, m, H_{18–21}), 1.16 (3H, d, $J = 7.1$ Hz, Me₈), 1.14 (3H, t, $J = 7.6$ Hz, H_{3'} × 3), 1.06 (3H, d, $J = 7.0$ Hz, Me₂₆), 1.06–0.99 (1H, m, H_{11b}), 0.91 (9H, s, SiC(CH₃)₃), 0.90 (3H, obs d, Me₂₄), 0.80 (3H, d, $J = 6.8$ Hz, Me₁₀), 0.07 (6H, s, Si(CH₃)₂); ¹³C NMR (125 MHz, CDCl₃) δ_C 174.1, 159.7, 159.0, 133.5, 132.1, 131.9, 131.2, 130.8, 129.8, 129.8, 129.6, 129.0, 127.3, 113.7, 113.5, 94.8, 88.1, 85.9, 79.8, 78.3, 73.1, 72.7, 71.6, 63.5, 61.4, 55.5, 55.3, 55.2, 38.8, 35.9, 33.9, 33.6, 32.7, 31.3, 29.6, 29.6, 29.5, 29.4, 29.3, 28.6, 28.0, 27.5, 26.0, 25.8, 18.4, 16.3, 14.1, 13.0, 10.6, 10.0, 9.4, –5.2; [α]_D²⁰ +5.6 (c 0.804, CHCl₃); IR (thin film) ν_{max} (cm^{–1}) 2928, 2855, 1732, 1615, 1515, 1463, 1379, 1364, 1302, 1247, 1193, 1171, 1092, 1036, 991, 967, 834, 777; HRMS calc. for C₅₉H₁₀₀O₁₀SiN [M+NH₄]⁺ 1010.7111, found 1010.7110.

(2*S*,3*S*,4*R*,5*S*,15*S*,18*R*,*E*)-18-((2*S*,4*R*,5*R*,6*R*)-6-((2*E*,4*E*)-6-((*tert*-butyldimethylsilyl)oxy)hexa-2,4-dien-1-yl)-2-(4-methoxyphenyl)-5-methyl-1,3-dioxan-4-yl)-3,15-dimethoxy-1-((4-methoxybenzyl)oxy)-2,4,14-trimethylnonadec-13-en-5-ol (122)

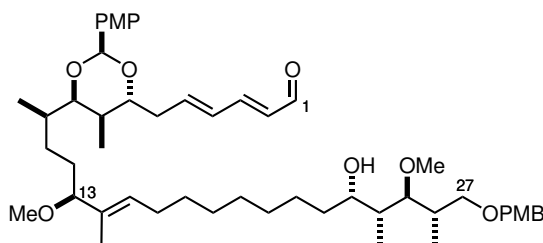


Ester **118** (15.7 mg, 0.0158 mmol) was dissolved in CH₂Cl₂ (1 mL) and cooled to –78 °C. DIBAL (70 μL, 0.070 mmol, 1.0 M in hexane) was added and the reaction was stirred for 1.5 h, then was quenched by addition of Na⁺/K⁺ tartrate (1 mL), warmed to rt and stirred for 30 min. The mixture was extracted with CH₂Cl₂ (3 × 1 mL), dried over Na₂SO₄, and concentrated *in vacuo*. Flash chromatography (1:5 EtOAc/PE) gave alcohol **122** as a colourless oil (14.6 mg, 99%).

R_f 0.43 (1:3 EtOAc/PE); ¹H NMR (500 MHz, CDCl₃) δ_H 7.38 (2H, d, $J = 8.7$ Hz, PMP ArH), 7.26 (2H, d, $J = 8.6$ Hz, PMB ArH), 6.88 (2H, d, $J = 8.7$ Hz, PMP ArH), 6.87 (2H, d, $J = 8.7$ Hz, PMB ArH), 6.21 (1H, dd, $J = 14.9, 10.5$ Hz, H₃), 6.12 (1H, dd, $J = 14.8, 10.6$ Hz, H₄),

5.72–5.62 (2H, m, H₂, H₅), 5.67 (1H, s, ArCH₂O₂), 5.29 (1H, t, *J* = 6.8 Hz, H₁₅), 4.44 (2H, s, ArCH₂O), 4.20 (2H, d, *J* = 5.2 Hz, H₁ × 2), 3.91 (1H, dd, *J* = 7.9, 7.9 Hz, H₇), 3.90 (1H, dd, *J* = 7.3, 7.3 Hz, H₂₃), 3.81 (3H, s, ArOMe), 3.80 (3H, s, ArOMe), 3.63 (1H, dd, *J* = 9.9, 1.8 Hz, H₉), 3.52 (1H, dd, *J* = 8.8, 5.3 Hz, H_{27a}), 3.49–3.45 (2H, m, H_{27b}, C₂₃OH), 3.44 (3H, s, C₂₅OMe), 3.36 (1H, t, *J* = 7.2 Hz, H₁₃), 3.18 (1H, dd, *J* = 8.9, 2.9 Hz, H₂₅), 3.14 (3H, s, C₁₃OMe), 2.82 (1H, ddd, *J* = 14.5, 7.2, 7.2 Hz, H_{6a}), 2.52 (1H, ddd, *J* = 14.7, 7.3, 7.3 Hz, H_{6b}), 2.10–2.00 (2H, m, H_{16a}, H₂₆), 2.00–1.90 (1H, m, H_{16b}), 1.76–1.61 (3H, m, H₁₀, H_{11a}, H₂₄), 1.61–1.47 (4H, m, H₈, H₁₂ × 2, H_{22a}), 1.45 (3H, s, Me₁₄), 1.41–1.20 (11H, m, H_{17–21}, H_{22b}), 1.16 (3H, d, *J* = 6.9 Hz, Me₈), 1.07–0.99 (1H, m, H_{11b}), 1.03 (3H, d, *J* = 7.1 Hz, Me₂₄), 0.94 (3H, d, *J* = 7.0 Hz, Me₂₆), 0.91 (9H, s, SiC(CH₃)₃), 0.80 (3H, d, *J* = 6.8 Hz, Me₁₀), 0.07 (6H, s, Si(CH₃)₂); ¹³C NMR (125 MHz, CDCl₃) δ_C 159.7, 159.1, 133.4, 132.1, 131.9, 131.2, 130.7, 129.9, 129.8, 129.6, 129.2, 127.3, 113.7, 113.5, 94.8, 89.1, 88.1, 79.8, 78.3, 72.8, 72.0, 70.6, 63.5, 61.7, 55.5, 55.3, 55.3, 37.1, 36.7, 34.7, 33.9, 33.6, 31.3, 29.8, 29.6, 29.5, 29.4, 29.3, 28.6, 27.5, 26.2, 26.0, 18.4, 15.0, 14.1, 13.0, 11.4, 10.0, –5.2; [α]_D²⁰ +4.7 (*c* 0.47, CHCl₃); IR (thin film) ν_{max} (cm^{–1}) 3674, 2957, 2928, 2856, 1615, 1516, 1463, 1380, 1303, 1249, 1172, 1097, 1038, 991, 836, 778; HRMS calc. for C₅₆H₉₂O₉NaSi [M+Na]⁺ 959.6408, found 959.6400.

(2*E*,4*E*)-6-((2*S*,4*R*,5*R*,6*R*)-6-((2*R*,5*S*,15*S*,16*R*,17*S*,18*S*,*E*)-15-hydroxy-5,17-dimethoxy-19-((4-methoxybenzyl)oxy)-6,16,18-trimethylnonadec-6-en-2-yl)-2-(4-methoxyphenyl)-5-methyl-1,3-dioxan-4-yl)hexa-2,4-dienal (128)

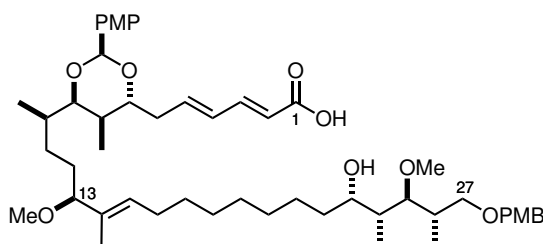


To a rapidly stirred biphasic solution of silyl ether **122** (40.8 mg, 0.0435 mmol) in CH₂Cl₂ (2 mL) and aqueous pH 9.2 buffer (0.5 mL) at 0 °C was added DDQ (12.0 mg, 0.0529 mmol). After 20 min, the reaction was quenched with NaHCO₃ (2.5 mL) and warmed to rt. After extraction with CH₂Cl₂ (3 × 5 mL) and washing with brine/H₂O (1:3, 20 mL), the organics were dried over MgSO₄ and concentrated *in vacuo*. The crude was purified by flash chromatography (1:4 → 1:2 EtOAc/hexane) to give the aldehyde **128** as a pale yellow oil (21.3 mg, 60%, 89% brsm).

R_f 0.24 (1:2 EtOAc/PE); ¹H NMR (500 MHz, CDCl₃) δ_H 9.54 (1H, d, *J* = 8.0 Hz, H₁), 7.36 (2H, d, *J* = 8.7 Hz, PMP ArH), 7.25 (2H, d, *J* = 8.6 Hz, PMB ArH), 7.09 (1H, dd, *J* = 15.3,

10.7 Hz, H₃), 6.88 (2H, d, *J* = 8.7 Hz, PMP ArH), 6.87 (2H, d, *J* = 8.8 Hz, PMB ArH), 6.42 (1H, dd, *J* = 15.1, 10.7 Hz, H₄), 6.30 (1H, dt, *J* = 15.2, 7.1 Hz, H₅), 6.10 (1H, dd, *J* = 15.3, 8.0 Hz, H₂), 5.67 (1H, s, ArCH₂O₂), 5.29 (1H, t, *J* = 7.1 Hz, H₁₅), 4.43 (2H, s, ArCH₂O), 4.02 (1H, dd, *J* = 9.3, 6.0 Hz, H₇), 3.90 (1H, dd, *J* = 6.3, 6.3 Hz, H₂₃), 3.80 (3H, s, ArOMe), 3.79 (3H, s, ArOMe), 3.63 (1H, dd, *J* = 9.9, 2.0 Hz, H₉), 3.51 (1H, dd, *J* = 8.9, 5.3 Hz, H_{27a}), 3.49 (1H, br s, C₂₃OH), 3.47 (1H, dd, *J* = 8.9, 3.6 Hz, H_{27b}), 3.44 (3H, s, C₂₅OMe), 3.36 (1H, t, *J* = 7.0 Hz, H₁₃), 3.18 (1H, dd, *J* = 8.9, 2.9 Hz, H₂₅), 3.14 (3H, s, C₁₃OMe), 3.07 (1H, dt, *J* = 15.7, 7.8 Hz, H_{6a}), 2.53 (1H, dt, *J* = 14.2, 7.1 Hz, H_{6b}), 2.09–2.00 (2H, m, H_{16a}, H₂₆), 2.00–1.90 (1H, m, H_{16b}), 1.77–1.60 (3H, m, H₁₀, H_{11a}, H₂₄), 1.59–1.47 (4H, m, H₈, H₁₂ × 2, H_{22a}), 1.45 (3H, s, Me₁₄), 1.42–1.22 (11H, m, H_{17–21}, H_{22b}), 1.19 (3H, d, *J* = 7.0 Hz, Me₈), 1.07–0.99 (1H, m, H_{11b}), 1.03 (3H, d, *J* = 7.2 Hz, Me₂₄), 0.94 (3H, d, *J* = 7.0 Hz, Me₂₆), 0.80 (3H, d, *J* = 6.8 Hz, Me₁₀); ¹³C NMR (125 MHz, CDCl₃) δ_C 193.8 (C₁), 159.8 (Ar C), 159.1 (Ar C), 152.0 (C₃), 142.3 (C₅), 133.4 (C₁₄), 131.5 (Ar C), 130.7 (C₂), 130.6 (C₄), 130.6 (Ar C), 129.9 (C₁₅), 129.2 (Ar C), 127.2 (Ar C), 113.7 (Ar C), 113.5 (Ar C), 94.9 (ArCHO₂), 89.0 (C₂₅), 88.1 (C₁₃), 79.1 (C₇), 78.4 (C₉), 72.7 (ArCH₂O), 72.0 (C₂₇), 70.6 (C₂₃), 61.7 (OMe₂₅), 55.5 (OMe₁₃), 55.3 (ArOMe), 55.2 (ArOMe), 37.0 (C₂₄), 36.7 (C₂₆), 34.7 (C₂₂), 34.4 (C₆), 33.5 (C₁₀), 32.0 (C₈), 29.8, 29.5, 29.5, 29.4, 29.3 (C₁₂, C_{17–20}), 28.6 (C₁₁), 27.5 (C₁₆), 26.2 (C₂₁), 14.9 (Me₂₆), 14.1 (Me₁₀), 13.0 (Me₈), 11.4 (Me₂₄), 10.0 (Me₁₄); [α]_D²⁰ +11.0 (*c* 0.97, CHCl₃); IR (thin film) ν_{max} (cm⁻¹) 3513, 2961, 2931, 2858, 1683, 1642, 1615, 1516, 1462, 1303, 1249, 1172, 1114, 1092, 1037, 1011, 989, 827; HRMS calc. for C₅₀H₇₇O₉ [M+H]⁺ 821.5568, found 821.5562.

(2*E*,4*E*)-6-((2*S*,4*R*,5*R*,6*R*)-6-((2*R*,5*S*,15*S*,16*R*,17*S*,18*S*,*E*)-15-hydroxy-5,17-dimethoxy-19-((4-methoxybenzyl)oxy)-6,16,18-trimethylnonadec-6-en-2-yl)-2-(4-methoxyphenyl)-5-methyl-1,3-dioxan-4-yl)hexa-2,4-dienoic acid (131)

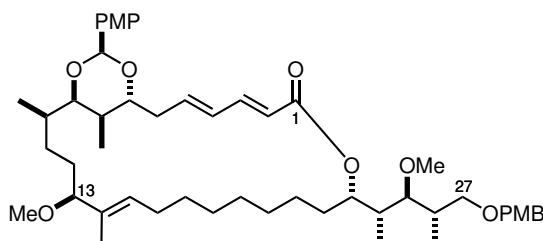


Aldehyde **128** (21.3 mg, 0.0259 mmol) was dissolved in *t*-BuOH (1 mL) and 2-methyl-2-butene (0.5 mL). A solution of NaH₂PO₄ · 2 H₂O (175 mg, 1.12 mmol) and NaClO₂ (91 mg, 80% technical grade, 0.80 mmol) in H₂O (1 mL) was added, and the mixture was stirred rapidly at rt for 20 h. After dilution with brine (3 mL) and extraction with EtOAc (3 × 3 mL), the organics were

dried over Na₂SO₄ and concentrated *in vacuo*. The crude was purified by flash chromatography (50:1 EtOAc/AcOH) to yield the seco-acid **131** as a pale yellow oil (21.5 mg, 99%).

R_f 0.41 (50:50:1 EtOAc/PE/AcOH); **¹H NMR** (500 MHz, CDCl₃) δ_H 7.36 (2H, d, *J* = 8.7 Hz, PMP ArH), 7.33 (1H, dd, *J* = 15.3, 10.9 Hz, H₃), 7.25 (2H, d, *J* = 8.6 Hz, PMB ArH), 6.88 (2H, d, *J* = 8.7 Hz, PMP ArH), 6.87 (2H, d, *J* = 8.9 Hz, PMB ArH), 6.30 (1H, dd, *J* = 15.1, 11.0 Hz, H₄), 6.19 (1H, dt, *J* = 14.6, 7.3 Hz, H₅), 5.81 (1H, d, *J* = 15.3 Hz, H₂), 5.66 (1H, s, ArCHO₂), 5.29 (1H, t, *J* = 6.9 Hz, H₁₅), 4.43 (2H, s, ArCH₂O), 3.99 (1H, dd, *J* = 8.2, 6.8 Hz, H₇), 3.91 (1H, dd, *J* = 6.2, 6.2 Hz, H₂₃), 3.80 (3H, s, ArOMe), 3.79 (3H, s, ArOMe), 3.62 (1H, dd, *J* = 10.0, 1.4 Hz, H₉), 3.52 (1H, dd, *J* = 8.8, 5.3 Hz, H_{27a}), 3.47 (1H, dd, *J* = 8.8, 3.6 Hz, H_{27b}), 3.44 (3H, s, C₂₅OMe), 3.36 (1H, t, *J* = 7.1 Hz, H₁₃), 3.18 (1H, dd, *J* = 8.9, 2.7 Hz, H₂₅), 3.13 (3H, s, C₁₃OMe), 3.00 (1H, ddd, *J* = 15.2, 7.6, 7.6 Hz, H_{6a}), 2.54 (1H, ddd, *J* = 14.2, 7.1, 7.1 Hz, H_{6b}), 2.10–2.00 (2H, m, H_{16a}, H₂₆), 2.00–1.90 (1H, m, H_{16b}), 1.76–1.59 (3H, m, H₁₀, H_{11a}, H₂₄), 1.59–1.47 (4H, m, H₈, H₁₂ × 2, H_{22a}), 1.45 (3H, s, Me₁₄), 1.40–1.22 (11H, m, H_{17–21}, H_{22b}), 1.18 (3H, d, *J* = 6.9 Hz, Me₈), 1.07–1.00 (1H, m, H_{11b}), 1.03 (3H, d, *J* = 7.1 Hz, Me₂₄), 0.94 (3H, d, *J* = 7.0 Hz, Me₂₆), 0.80 (3H, d, *J* = 6.8 Hz, Me₁₀); **¹³C NMR** (125 MHz, CDCl₃) δ_C 171.6 (C₁), 159.7 (Ar C), 159.1 (Ar C), 146.5 (C₃), 141.0 (C₅), 133.4 (C₁₄), 131.5 (Ar C), 130.6 (Ar C), 130.3 (C₄), 129.9 (C₁₅), 129.2 (Ar C), 127.2 (Ar C), 119.3 (C₂), 113.7 (Ar C), 113.5 (Ar C), 94.8 (ArCHO₂), 89.0 (C₂₅), 88.1 (C₁₃), 79.1 (C₇), 78.4 (C₉), 72.7 (ArCH₂O), 72.0 (C₂₇), 70.7 (C₂₃), 61.7 (OMe₂₅), 55.4 (OMe₁₃), 55.3 (ArOMe), 55.2 (ArOMe), 37.0 (C₂₄), 36.6 (C₂₆), 34.6 (C₂₂), 34.3 (C₆), 33.6 (C₁₀), 31.8 (C₈), 29.8, 29.5, 29.5, 29.4, 29.3 (C₁₂, C_{18–21}), 28.6 (C₁₁), 27.5 (C₁₆), 26.2 (C₁₇), 14.9 (Me₂₆), 14.1 (Me₁₀), 13.0 (Me₈), 11.4 (Me₂₄), 10.0 (Me₁₄); [α]_D²⁰ +10.5 (*c* 1.00, CHCl₃); **IR** (thin film) ν_{max} (cm⁻¹) 3481, 2965, 2932, 2854, 1709, 1644, 1615, 1516, 1462, 1381, 1302, 1248, 1172, 1089, 1035, 1001, 828; **HRMS** calc. for C₅₀H₇₆O₁₀Na [M+Na]⁺ 859.5336, found 859.5331.

(1*R*,3*E*,5*E*,9*S*,17*E*,19*S*,22*R*,23*R*,25*S*,27*R*)-19-methoxy-9-((2*R*,3*S*,4*S*)-3-methoxy-5-((4-methoxybenzyl)oxy)-4-methylpentan-2-yl)-25-(4-methoxyphenyl)-18,22,27-trimethyl-8,24,26-trioxabicyclo[21.3.1]heptacos-3,5,17-trien-7-one (133)

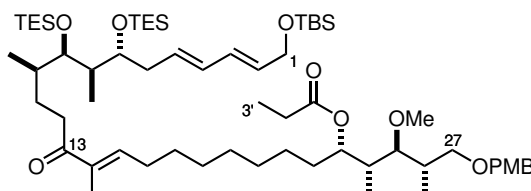


Seco-acid **131** (21.5 mg, 0.0257 mmol) was dried azeotropically with C₆H₆ and dried under high vacuum for 16 h, then was dissolved in THF (2.5 mL) at rt. Et₃N (40 µL, 0.287 mmol) and 2,4,6-trichlorobenzoyl chloride (30 µL, 0.192 mmol) were added, and the solution was stirred for 1 h 15 min, during which time a pale orange colour developed and a white precipitate formed. The mixture was then diluted with toluene (4 mL). A solution of DMAP (42 mg, 0.344 mmol) was made up in toluene (6 mL), and to this was added the mixed anhydride solution *via* syringe pump over 4.5 h. After the addition was complete, stirring continued at rt for a further 12 h. The reaction mixture was then filtered through a plug of silica and concentrated *in vacuo*. Flash chromatography (1:4 EtOAc/hexane) afforded the macrolactone **133** as a colourless oil (9.9 mg, 47%).

R_f 0.29 (1:4 EtOAc/PE); **¹H NMR** (500 MHz, CDCl₃) δ_H 7.42 (2H, d, *J* = 8.7 Hz, PMP ArH), 7.30 (1H, dd, *J* = 15.2, 10.8 Hz, H₃), 7.24 (2H, d, *J* = 8.6 Hz, PMB ArH), 6.89 (2H, d, *J* = 8.8 Hz, PMP ArH), 6.87 (2H, d, *J* = 8.6 Hz, PMB ArH), 6.31 (1H, dd, *J* = 14.7, 11.3 Hz, H₄), 6.13 (1H, ddd, *J* = 15.0, 9.6, 5.5 Hz, H₅), 5.87 (1H, d, *J* = 15.3 Hz, H₂), 5.81 (1H, s, ArCHO₂), 5.32 (1H, app dt, *J* = 10.2, 2.8 Hz, H₂₃), 5.29 (1H, t, *J* = 6.8 Hz, H₁₅), 4.43 (1H, d, *J* = 11.6 Hz, ArCH_aH_bO), 4.39 (1H, d, *J* = 11.6 Hz, ArCH_aH_bO), 4.01 (1H, dd, *J* = 8.4, 5.4 Hz, H₇), 3.80 (3H, s, ArOMe), 3.80 (3H, s, ArOMe), 3.71 (1H, dd, *J* = 8.4, 1.9 Hz, H₉), 3.53 (1H, dd, *J* = 9.1, 4.6 Hz, H_{27a}), 3.44 (3H, s, C₂₅OMe), 3.35–3.30 (2H, m, H₁₃, H_{27b}), 3.14 (3H, s, C₁₃OMe), 3.02 (1H, app dt, *J* = 14.4, 9.3 Hz, H_{6a}), 2.92 (1H, dd, *J* = 8.0, 3.8 Hz, H₂₅), 2.64 (1H, app dt, *J* = 14.6, 4.8 Hz, H_{6b}), 2.14–2.06 (1H, m, H₂₆), 2.06–1.97 (2H, m, H₁₆ × 2), 1.83–1.75 (1H, m, H₂₄), 1.75–1.61 (3H, m, H₈, H₁₀, H_{22a}), 1.56–1.52 (2H, m, H₁₂ × 2), 1.50 (3H, s, Me₁₄), 1.47–1.40 (1H, m, H_{22b}), 1.39–1.22 (11H, m, H_{11a}, H_{17–21}), 1.20 (3H, d, *J* = 6.9 Hz, Me₈), 1.06 (3H, d, *J* = 7.0 Hz, Me₂₆), 0.92 (3H, d, *J* = 7.1 Hz, Me₂₄), 0.90–0.82 (1H, m, H_{11b}), 0.82 (3H, d, *J* = 6.9 Hz, Me₁₀); **¹³C NMR** (125 MHz, CDCl₃) δ_C 167.0, 159.9, 159.0, 144.1, 139.2, 133.5, 131.7, 131.0, 130.8, 129.8, 129.1, 127.4, 120.8, 113.7, 113.6, 96.3, 88.0, 85.7, 78.9, 77.7, 73.9, 72.7, 71.6, 61.1, 55.6, 55.3, 55.2, 40.4, 36.3, 36.0, 35.1, 33.4, 30.7, 30.6, 29.0, 28.7, 28.6, 28.4, 27.9, 27.2, 25.1, 16.2, 14.5, 14.3, 11.3, 10.4; [α]_D²⁰ –58.4 (*c* 0.45, CHCl₃); **IR** (thin film) ν_{max} (cm^{–1}) 2929, 2854, 1709, 1641, 1614, 1514, 1457, 1302, 1247, 1171, 1137, 1111, 1094, 1035, 999, 825, 755; **HRMS** calc. for C₅₀H₇₅O₉ [M+H]⁺ 819.5411, found 819.5397.

5.5.2 Bis-TES-protected macrocycle (C₁–C₂₇)

(2*S*,3*S*,4*R*,5*S*,13*E*,18*R*,19*R*,20*R*,21*R*,23*E*,25*E*)-27-((*tert*-butyldimethylsilyl)oxy)-3-methoxy-1-((4-methoxybenzyl)oxy)-2,4,14,18,20-pentamethyl-15-oxo-19,21-bis((triethylsilyl)oxy)heptacos-13,23,25-trien-5-yl propionate (**103**)

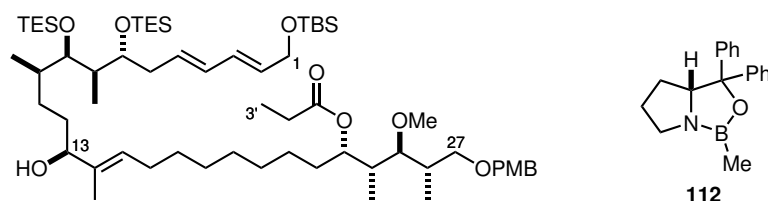


A solution of phosphonate **28** (1.48 g, 3:1 mixture with regioisomer **100**, 1.43 mmol) in THF (38 mL) was added to Ba(OH)₂ (392 mg, 2.29 mmol) at rt and stirred for 1.5 h. Aldehyde **29** (750 mg, 1.61 mmol) was added as a solution in THF/H₂O (40:1, 12 mL), and the reaction was left to stir under argon. After 68 h, NH₄Cl (30 mL) was added. The aqueous layer was extracted with Et₂O (3 × 30 mL), dried over MgSO₄, and concentrated *in vacuo*. Flash chromatography gave enone **103** as a colourless oil (1.42 g, 91%).

R_f 0.80 (1:3 EtOAc/PE); **¹H NMR** (500 MHz, CDCl₃) δ_H 7.24 (2H, d, *J* = 8.6 Hz, ArH), 6.86 (2H, d, *J* = 8.7 Hz, ArH), 6.59 (1H, td, *J* = 7.3, 1.0 Hz, H₁₅), 6.18 (1H, dd, *J* = 15.1, 10.5 Hz, H₃), 6.04 (1H, dd, *J* = 15.1, 10.5 Hz, H₄), 5.68 (1H, dt, *J* = 15.1, 7.2 Hz, H₅), 5.64 (1H, dt, *J* = 15.1, 5.4 Hz, H₂), 5.18 (1H, td, *J* = 7.0, 1.8 Hz, H₂₃), 4.43 (1H, d, *J* = 11.6 Hz, OCH_aH_bAr), 4.39 (1H, d, *J* = 11.6 Hz, OCH_aH_bAr), 4.20 (2H, d, *J* = 5.2 Hz, H₁ × 2), 3.80 (3H, s, ArOMe), 3.63 (1H, app q, *J* = 5.4 Hz, H₇), 3.56–3.51 (2H, m, H₉, H_{27a}), 3.38 (3H, s, C₂₅OMe), 3.32 (1H, dd, *J* = 9.1, 7.4 Hz, H_{27b}), 2.87 (1H, dd, *J* = 8.5, 3.5 Hz, H₂₅), 2.73 (1H, ddd, *J* = 15.7, 10.2, 5.4 Hz, H_{12a}), 2.56 (1H, ddd, *J* = 15.9, 9.8, 6.1 Hz, H_{12b}), 2.31 (2H, q, *J* = 7.6 Hz, H_{2'} × 2), 2.21 (2H, app q, *J* = 7.4 Hz, H₁₆ × 2), 2.18–2.13 (2H, m, H₆ × 2), 2.12–2.04 (1H, m, H₂₆), 1.82–1.68 (3H, m, H₈, H_{11a}, H₂₄), 1.76 (3H, s, Me₁₄), 1.67–1.59 (1H, m, H_{22a}), 1.58–1.50 (1H, m, H₁₀), 1.48–1.36 (4H, m, H_{11b}, H₁₇ × 2, H_{22b}), 1.35–1.20 (8H, m, H_{18–21}), 1.14 (3H, t, *J* = 7.6 Hz, H_{3'} × 3), 1.06 (3H, d, *J* = 7.0 Hz, Me₂₆), 0.96 (9H, t, *J* = 8.0 Hz, Si(CH₂CH₃)₃), 0.93 (9H, t, *J* = 8.0 Hz, Si(CH₂CH₃)₃), 0.91 (9H, s, Si(CH₃)₃), 0.91 (3H, obs d, Me₁₀), 0.90 (3H, obs d, Me₂₄), 0.86 (3H, d, *J* = 7.0 Hz, Me₈), 0.60 (6H, q, *J* = 8.1 Hz, Si(CH₂CH₃)₃), 0.57 (6H, q, *J* = 8.1 Hz, Si(CH₂CH₃)₃), 0.07 (6H, s, Si(CH₃)₂); **¹³C NMR** (125 MHz, CDCl₃) δ_C 202.1, 174.1, 159.0, 142.1, 137.1, 131.5, 131.4, 130.9, 130.3, 130.3, 129.0, 113.7, 85.9, 77.5, 74.5, 73.1, 72.8, 71.6, 63.7, 61.4, 55.2, 41.8, 38.9, 38.2, 36.0, 35.9, 35.4, 32.8, 29.5, 29.5, 29.4, 29.1, 28.7, 28.0, 26.9, 26.0, 25.8, 18.4, 16.3, 16.3, 11.4, 10.6, 10.5, 9.4, 7.2, 7.0, 5.6, 5.3, –5.2; [α]_D²⁰ –2.6 (*c* 1.01,

CHCl₃); **IR** (thin film) ν_{\max} (cm⁻¹) 2952, 2931, 2876, 2857, 1732, 1670, 1614, 1513, 1461, 1378, 1247, 1192, 1083, 1040, 1005, 990, 835, 775, 738, 725; **HRMS** calc. for C₆₂H₁₁₈O₉Si₃N [M+NH₄]⁺ 1104.8109, found 1104.8091.

(2*S*,3*S*,4*R*,5*S*,13*E*,15*S*,18*R*,19*R*,20*R*,21*R*,23*E*,25*E*)-27-((*tert*-butyldimethylsilyl)oxy)-15-hydroxy-3-methoxy-1-((4-methoxybenzyl)oxy)-2,4,14,18,20-pentamethyl-19,21-bis((triethylsilyl)oxy)-heptacos-13,23,25-trien-5-yl propionate (115**)**



To a solution of enone **103** (1.49 g, 1.37 mmol) in THF (27 mL) at -10 °C was added Me-CBS catalyst (*R*)-**112** (1.65 mL, 1.65 mmol, 1.0 M in toluene), followed by BH₃ · SMe₂ (144 μ L, 1.52 mmol). After 45 min, the reaction was quenched by addition of MeOH (20 mL). Bubbles of gas evolved as the mixture was stirred and warmed to rt. The volatiles were evaporated *in vacuo*. The crude material was re-suspended in MeOH (20 mL) and concentrated again *in vacuo*. This process was repeated twice further. The resulting crude was purified by flash chromatography (1:9 EtOAc/PE), yielding alcohol **115** as a colourless oil (1.47 g, 99%, >20:1 *dr*).

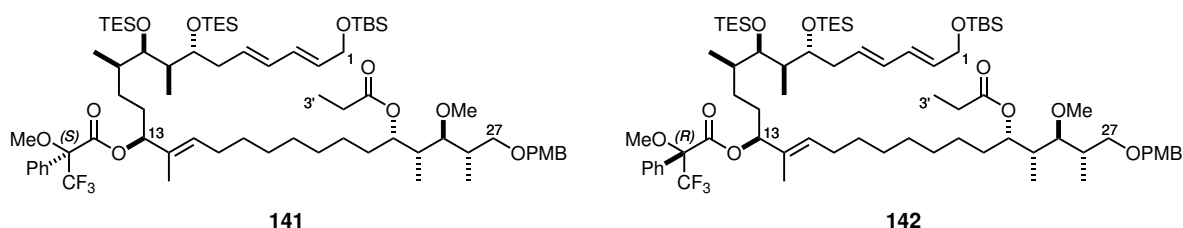
R_f 0.46 (1:5 EtOAc/PE); **¹H NMR** (500 MHz, CDCl₃) δ_{H} 7.24 (2H, d, *J* = 8.8 Hz, ArH), 6.86 (2H, d, *J* = 8.7 Hz, ArH), 6.18 (1H, ddt, *J* = 15.1, 10.6, 1.4 Hz, H₃), 6.04 (1H, dd, *J* = 15.0, 10.4 Hz, H₄), 5.68 (1H, dt, *J* = 15.0, 7.5 Hz, H₅), 5.64 (1H, dt, *J* = 15.2, 5.3 Hz, H₂), 5.36 (1H, t, *J* = 7.1 Hz, H₁₅), 5.18 (1H, td, *J* = 7.0, 2.0 Hz, H₂₃), 4.43 (1H, d, *J* = 11.5 Hz, ArCH_aH_bO), 4.39 (1H, d, *J* = 11.5 Hz, ArCH_aH_bO), 4.20 (2H, dd, *J* = 5.4, 1.1 Hz, H₁ × 2), 3.94 (1H, td, *J* = 6.8, 3.0 Hz, H₁₃), 3.80 (3H, s, ArOMe), 3.60 (1H, ddd, *J* = 7.0, 5.0, 4.2 Hz, H₇), 3.53 (1H, dd, *J* = 9.2, 4.8 Hz, H_{27a}), 3.50 (1H, dd, *J* = 5.1, 3.5 Hz, H₉), 3.38 (3H, s, C₂₅OMe), 3.32 (1H, dd, *J* = 9.1, 7.4 Hz, H_{27b}), 2.86 (1H, dd, *J* = 8.5, 3.6 Hz, H₂₅), 2.31 (2H, q, *J* = 7.6 Hz, H_{2'} × 2), 2.20–2.12 (2H, m, H₆ × 2), 2.12–2.05 (1H, m, H₂₆), 2.05–1.93 (2H, m, H₁₆ × 2), 1.78 (1H, dqd, *J* = 8.5, 7.1, 2.0 Hz, H₂₄), 1.73 (1H, dqd, *J* = 6.7, 5.2, 5.2 Hz, H₈), 1.67–1.59 (2H, m, H_{12a}, H_{22a}), 1.58 (3H, br s, Me₁₄), 1.55–1.48 (1H, m, H₁₀), 1.47–1.37 (4H, m, H_{12b}, H_{22b}, H₁₁ × 2), 1.35–1.30 (2H, m, H₁₇ × 2), 1.30–1.20 (8H, m, H_{18–21}), 1.14 (3H, t, *J* = 7.6 Hz, H_{3'} × 3), 1.06 (3H, d, *J* = 7.0 Hz, Me₂₆), 0.95 (9H, t, *J* = 8.0 Hz, Si(CH₂CH₃)₃), 0.94 (9H, t, *J* = 8.0 Hz, Si(CH₂CH₃)₃), 0.91 (9H, s, SiC(CH₃)₃), 0.90 (3H, d, *J* = 7.0 Hz, Me₂₄), 0.89 (3H, d, *J* = 5.9 Hz, Me₁₀), 0.85 (3H, d, *J* = 7.0 Hz, Me₈), 0.60 (6H, q, *J* = 7.9 Hz, Si(CH₂CH₃)₃), 0.57 (6H, q, *J* = 8.0 Hz,

Si(CH₂CH₃)₃), 0.07 (6H, s, Si(CH₃)₂); ¹³C NMR (125 MHz, CDCl₃) δ_C 174.1, 159.0, 136.7, 131.6, 131.4, 130.8, 130.3, 130.3, 129.0, 127.5, 113.7, 85.9, 78.7, 77.6, 74.6, 73.1, 72.7, 71.6, 63.7, 61.3, 55.2, 41.7, 38.8, 38.5, 35.9, 35.9, 33.0, 32.7, 29.5, 29.5, 29.4, 29.3, 28.0, 27.8, 27.5, 25.9, 25.7, 18.4, 16.3, 16.2, 10.8, 10.6, 10.3, 9.4, 7.1, 7.0, 5.6, 5.2, -5.2; [α]_D²⁰ +1.9 (c 1.01, CHCl₃); IR (thin film) ν_{max} (cm⁻¹) 2952, 2930, 2876, 2856, 1733, 1614, 1514, 1462, 1378, 1362, 1248, 1193, 1084, 1041, 1005, 990, 835, 776, 737, 725; HRMS calc. for C₆₂H₁₂₀O₉Si₃N [M+NH₄]⁺ 1106.8265, found 1106.8257.

Mosher esters of alcohol **115**

(2*E*,4*E*,7*R*,8*R*,9*R*,10*R*,13*S*,14*E*,23*S*,24*R*,25*S*,26*S*)-1-((*tert*-butyldimethylsilyl)oxy)-25-methoxy-27-((4-methoxybenzyl)oxy)-8,10,14,24,26-pentamethyl-23-(propionyloxy)-7,9-bis((triethylsilyl)oxy)heptacos-2,4,14-trien-13-yl (*S*)-3,3,3-trifluoro-2-methoxy-2-phenylpropanoate (**141**) and

(2*E*,4*E*,7*R*,8*R*,9*R*,10*R*,13*S*,14*E*,23*S*,24*R*,25*S*,26*S*)-1-((*tert*-butyldimethylsilyl)oxy)-25-methoxy-27-((4-methoxybenzyl)oxy)-8,10,14,24,26-pentamethyl-23-(propionyloxy)-7,9-bis((triethylsilyl)oxy)heptacos-2,4,14-trien-13-yl (*R*)-3,3,3-trifluoro-2-methoxy-2-phenylpropanoate (**142**)



To a solution of alcohol **115** (3.9 mg, 3.58 μmol) and (*S*)-α-methoxy-α-trifluoromethylphenylacetic acid (4.6 mg, 19.6 μmol) in CH₂Cl₂ (0.2 mL) was added DCC (8.0 mg, 38.8 μmol) followed by DMAP (6.5 mg, 53.2 μmol). The reaction was stirred at rt for 24 h, then filtered and concentrated. The crude was re-suspended in Et₂O (1 mL), filtered, and concentrated. Flash chromatography (1:20 EtOAc/PE) gave the (*S*)-MTPA ester **141** as a colourless oil (4.2 mg, 90%).

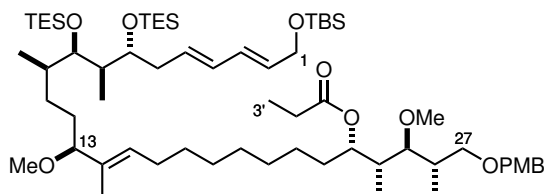
R_f 0.53 (1:5 EtOAc/PE); ¹H NMR (500 MHz, CDCl₃) δ_H 7.51–7.46 (2H, m, PhH), 7.41–7.33 (3H, m, PhH), 7.24 (2H, d, *J* = 8.7 Hz, PMB ArH), 6.86 (2H, d, *J* = 8.7 Hz, PMB ArH), 6.18 (1H, dd, *J* = 14.9, 10.4 Hz, H₃), 6.04 (1H, dd, *J* = 15.1, 10.5 Hz, H₄), 5.71–5.61 (2H, m, H₂, H₅), 5.57 (1H, t, *J* = 6.7 Hz, H₁₅), 5.36 (1H, t, *J* = 7.3 Hz, H₂₃), 5.18 (1H, br t, *J* = 7.0 Hz, H₁₃), 4.43 (1H, d, *J* = 11.5 Hz, ArCH_aH_bO), 4.39 (1H, d, *J* = 11.5 Hz, ArCH_aH_bO), 4.20 (2H, d, *J* = 5.1 Hz, H₁ × 2), 3.80 (3H, s, ArOMe), 3.59–3.55 (1H, m, H₇), 3.53 (1H, dd, *J* = 9.2, 4.8 Hz, H_{27a}), 3.52 (3H, s, OMe), 3.46 (1H, dd, *J* = 5.1, 3.4 Hz, H₉), 3.38 (3H, s, C₂₅OMe), 3.32 (1H,

dd, $J = 9.1, 7.5$ Hz, H_{27b}), 2.87 (1H, dd, $J = 8.6, 3.7$ Hz, H_{25}), 2.31 (2H, q, $J = 7.6$ Hz, $H_{2'} \times 2$), 2.20–2.11 (2H, m, $H_6 \times 2$), 2.11–2.05 (1H, m, H_{26}), 2.05–2.01 (1H, m, H_{16a}), 2.01–1.97 (1H, m, H_{16b}), 1.81–1.74 (1H, m, H_{24}), 1.74–1.68 (1H, m, H_{22a}), 1.68–1.60 (2H, m, H_8, H_{12a}), 1.58 (3H, s, Me_{14}), 1.57–1.51 (1H, m, H_{22b}), 1.51–1.43 (1H, m, H_{10}), 1.43–1.38 (1H, m, H_{12b}), 1.36–1.28 (3H, m, $H_{11a}, H_{17} \times 2$), 1.28–1.18 (8H, m, H_{18-21}), 1.14 (3H, t, $J = 7.6$ Hz, $H_{3'} \times 3$), 1.06 (3H, d, $J = 7.0$ Hz, Me_{26}), 0.95–0.91 (1H, obs m, H_{11b}), 0.94 (9H, t, $J = 7.9$ Hz, $Si(CH_2CH_3)_3$), 0.94 (9H, t, $J = 8.0$ Hz, $Si(CH_2CH_3)_3$), 0.91 (9H, s, $Si(CH_3)_3$), 0.90 (3H, obs d, Me_{24}), 0.86 (3H, d, $J = 6.6$ Hz, Me_{10}), 0.83 (3H, d, $J = 7.0$ Hz, Me_8), 0.58 (6H, q, $J = 7.9$ Hz, $Si(CH_2CH_3)_3$), 0.56 (6H, q, $J = 8.0$ Hz, $Si(CH_2CH_3)_3$), 0.07 (6H, s, $Si(CH_3)_2$).

The analogous procedure gave the (*R*)-MTPA ester **142** in *ca* 90% yield.

R_f 0.53 (1:5 EtOAc/PE); **¹H NMR** (500 MHz, $CDCl_3$) δ_H 7.51–7.46 (2H, m, PhH), 7.41–7.33 (3H, m, PhH), 7.24 (2H, d, $J = 8.8$ Hz, $PMB\ ArH$), 6.86 (2H, d, $J = 8.7$ Hz, $PMB\ ArH$), 6.18 (1H, dd, $J = 15.1, 10.5$ Hz, H_3), 6.04 (1H, dd, $J = 15.2, 10.6$ Hz, H_4), 5.70–5.61 (2H, m, H_2, H_5), 5.50 (1H, t, $J = 6.8$ Hz, H_{15}), 5.30 (1H, t, $J = 7.3$ Hz, H_{23}), 5.18 (1H, br t, $J = 7.0$ Hz, H_{13}), 4.43 (1H, d, $J = 11.6$ Hz, $ArCH_aH_bO$), 4.39 (1H, d, $J = 11.5$ Hz, $ArCH_aH_bO$), 4.20 (2H, d, $J = 5.3$ Hz, $H_1 \times 2$), 3.80 (3H, s, $ArOMe$), 3.60–3.55 (1H, m, H_7), 3.55 (3H, s, OMe), 3.53 (1H, dd, $J = 9.2, 4.8$ Hz, H_{27a}), 3.49 (1H, dd, $J = 4.9, 3.5$ Hz, H_9), 3.38 (3H, s, $C_{25}OMe$), 3.32 (1H, dd, $J = 9.1, 7.5$ Hz, H_{27b}), 2.87 (1H, dd, $J = 8.5, 3.6$ Hz, H_{25}), 2.31 (2H, q, $J = 7.6$ Hz, $H_{2'} \times 2$), 2.20–2.12 (2H, m, $H_6 \times 2$), 2.11–2.04 (1H, m, H_{26}), 2.03–1.95 (1H, m, H_{16a}), 1.98–1.90 (1H, m, H_{16b}), 1.82–1.72 (1H, m, H_{24}), 1.72–1.65 (1H, m, H_8), 1.65–1.56 (2H, m, H_{12a}, H_{22a}), 1.53–1.47 (1H, m, H_{10}), 1.41 (3H, s, Me_{14}), 1.47–1.42 (1H, m, H_{12b}), 1.42–1.35 (2H, m, H_{11a}, H_{22b}), 1.33–1.27 (2H, m, $H_{17} \times 2$), 1.28–1.19 (8H, m, H_{18-21}), 1.14 (3H, t, $J = 7.6$ Hz, $H_{3'} \times 3$), 1.06 (3H, d, $J = 7.0$ Hz, Me_{26}), 1.00–0.94 (1H, obs m, H_{11b}), 0.94 (18H, t, $J = 8.4$ Hz, $Si(CH_2CH_3)_3 \times 2$), 0.91 (9H, s, $Si(CH_3)_3$), 0.90 (3H, obs d, Me_{24}), 0.88 (3H, d, $J = 6.5$ Hz, Me_{10}), 0.84 (3H, d, $J = 7.0$ Hz, Me_8), 0.59 (6H, q, $J = 8.2$ Hz, $Si(CH_2CH_3)_3$), 0.55 (6H, q, $J = 8.1$ Hz, $Si(CH_2CH_3)_3$), 0.07 (6H, s, $Si(CH_3)_2$).

(2*S*,3*S*,4*R*,5*S*,13*E*,15*S*,18*R*,19*R*,20*R*,21*R*,23*E*,25*E*)-27-((*tert*-butyldimethylsilyl)oxy)-3,15-dimethoxy-1-((4-methoxybenzyl)oxy)-2,4,14,18,20-pentamethyl-19,21-bis((triethylsilyl)oxy)heptacos-13,23,25-trien-5-yl propionate (117)

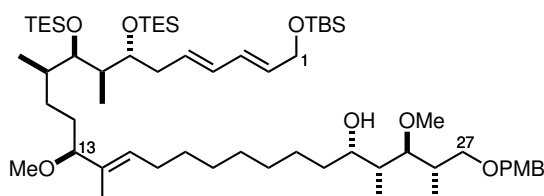


In an argon-filled glove box, $\text{Me}_3\text{O} \cdot \text{BF}_4$ (601 mg, 4.07 mmol) and Proton Sponge (1.16 g, 5.41 mmol) were weighed into a flask. A solution of alcohol **115** (1.45 g, 1.33 mmol) in CH_2Cl_2 (68 mL) was added *via* cannula at rt. The mixture turned from colourless to bright yellow while stirring at rt for 2 h. After quenching with NH_4Cl (68 mL), the yellow colour gradually faded during a further 1.5 h stirring. The layers were separated and the aqueous extracted with CH_2Cl_2 (3×30 mL). The combined organics were washed with citric acid (80 mL, 10% w/v aq.), dried over MgSO_4 , and concentrated *in vacuo*. Flash chromatography (1:15 EtOAc/PE) gave product **117** as a pale yellow oil (1.37 g, 93%, 98% brsm).

R_f 0.59 (1:5 EtOAc/PE); **¹H NMR** (500 MHz, CDCl_3) δ_{H} 7.24 (2H, d, $J = 8.6$ Hz, ArH), 6.86 (2H, d, $J = 8.7$ Hz, ArH), 6.18 (1H, dd, $J = 15.1, 10.5$ Hz, H₃), 6.03 (1H, dd, $J = 15.1, 10.5$ Hz, H₄), 5.68 (1H, dt, $J = 14.8, 7.4$ Hz, H₅), 5.64 (1H, dt, $J = 14.9, 5.2$ Hz, H₂), 5.31 (1H, t, $J = 6.5$ Hz, H₁₅), 5.18 (1H, td, $J = 7.0, 1.8$ Hz, H₂₃), 4.43 (1H, d, $J = 11.5$ Hz, ArCH_aH_bO), 4.39 (1H, d, $J = 11.6$ Hz, ArCH_aH_bO), 4.20 (2H, d, $J = 5.1$ Hz, H₁), 3.80 (3H, s, ArOMe), 3.59 (1H, dt, $J = 6.9, 4.7$ Hz, H₇), 3.53 (1H, dd, $J = 9.2, 4.8$ Hz, H_{27a}), 3.48 (1H, dd, $J = 4.6, 3.7$ Hz, H₉), 3.38 (3H, s, C₂₅OMe), 3.34 (1H, t, $J = 7.4$ Hz, H₁₃), 3.32 (1H, dd, $J = 9.3, 7.4$ Hz, H_{27b}), 3.14 (3H, s, C₁₃OMe), 2.87 (1H, dd, $J = 8.5, 3.6$ Hz, H₂₅), 2.31 (2H, q, $J = 7.6$ Hz, H_{2'} $\times 2$), 2.20–2.12 (2H, m, H₆ $\times 2$), 2.12–2.03 (2H, m, H_{16a}, H₂₆), 2.03–1.94 (1H, m, H_{16b}), 1.78 (1H, dqd, $J = 8.5, 7.0, 2.0$ Hz, H₂₄), 1.73 (1H, app sex, $J = 6.0$ Hz, H₈), 1.67–1.57 (1H, m, H_{22a}), 1.54–1.39 (4H, m, H₁₀, H₁₂ $\times 2$, H_{22b}), 1.49 (3H, s, Me₁₄), 1.39–1.31 (3H, m, H_{11a}, H₁₇ $\times 2$), 1.31–1.19 (8H, m, H_{18–21}), 1.14 (3H, t, $J = 7.6$ Hz, H_{3'} $\times 3$), 1.06 (3H, d, $J = 7.0$ Hz, Me₂₆), 0.96–0.90 (1H, m, H_{11b}), 0.95 (9H, t, $J = 8.0$ Hz, Si(CH₂CH₃)₃), 0.94 (9H, t, $J = 7.9$ Hz, Si(CH₂CH₃)₃), 0.91 (9H, s, Si(CH₃)₃), 0.90 (3H, obs d, Me₂₄), 0.87 (3H, d, $J = 6.9$ Hz, Me₁₀), 0.85 (3H, d, $J = 7.2$ Hz, Me₈), 0.59 (6H, q, $J = 8.2$ Hz, Si(CH₂CH₃)₃), 0.58 (6H, q, $J = 8.3$ Hz, Si(CH₂CH₃)₃), 0.07 (6H, s, Si(CH₃)₂); **¹³C NMR** (125 MHz, CDCl_3) δ_{C} 174.1 (C_{1'}), 159.0 (Ar C), 133.8 (C₁₄), 131.7 (C₅), 131.3 (C₄), 130.9 (Ar C), 130.3 (C₃), 130.3 (C₂), 129.6 (C₁₅), 129.0 (Ar C), 113.7 (Ar C), 88.3 (C₁₃), 85.9 (C₂₅), 77.6 (C₉), 74.7 (C₇), 73.1 (C₂₃), 72.8 (ArCH₂O), 71.6 (C₂₇), 63.7 (C₁),

61.4 (OMe₂₅), 55.5 (OMe₁₃), 55.2 (ArOMe), 41.7 (C₈), 38.9 (C₂₄), 38.6 (C₁₀), 35.9 (C₂₆), 35.8 (C₆), 32.8 (C₂₂), 31.8 (C₁₂), 29.6, 29.6, 29.5, 29.4 (C_{17–20}), 28.0 (C₁₁), 27.9 (C_{2'}), 27.6 (C₁₆), 26.0 (TBS), 25.8 (C₂₁), 18.4 (TBS), 16.3 (Me₂₆), 16.1 (Me₁₀), 10.6 (Me₂₄), 10.3 (Me₈), 10.1 (Me₁₄), 9.4 (C_{3'}), 7.2, 7.0, 5.6, 5.2 (TES × 4), –5.2 (TBS); [α]_D²⁰ +1.5 (*c* 0.89, CHCl₃); **IR** (thin film) ν_{\max} (cm^{–1}) 2952, 2926, 2876, 2855, 1734, 1615, 1514, 1462, 1378, 1362, 1248, 1192, 1171, 1093, 1043, 1006, 990, 836, 776, 739, 725; **HRMS** calc. for C₆₃H₁₂₂O₉Si₃N [M+NH₄]⁺ 1120.8422, found 1120.8420.

(2*S*,3*S*,4*R*,5*S*,13*E*,15*S*,18*R*,19*R*,20*R*,21*R*,23*E*,25*E*)-27-((*tert*-butyldimethylsilyl)oxy)-3,15-dimethoxy-1-((4-methoxybenzyl)oxy)-2,4,14,18,20-pentamethyl-19,21-bis((triethylsilyl)oxy)heptacos-13,23,25-trien-5-ol (121)

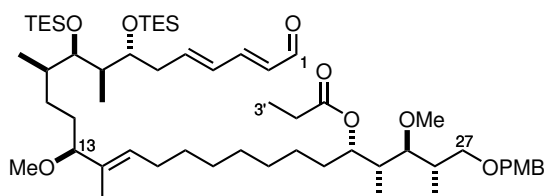


To a solution of propionate ester **117** (1.36 g, 1.23 mmol) in CH₂Cl₂ (25 mL) at –78 °C was added DIBAL (2.48 mL, 2.48 mmol, 1.0 M in hexane) dropwise. After stirring for 1 h, the reaction was quenched with Na⁺/K⁺ tartrate/H₂O (1:1, 25 mL) and stirred for 2 h at rt. The mixture was diluted with CH₂Cl₂ (25 mL) and H₂O (25 mL), then extracted with CH₂Cl₂ (3 × 25 mL). The combined organics were dried over Na₂SO₄, concentrated *in vacuo*, and purified by flash chromatography (1:14 EtOAc/PE) to give alcohol **121** as a colourless oil (1.26 g, 98%).

R_f 0.40 (1:5 EtOAc/PE); **¹H NMR** (500 MHz, CDCl₃) δ_{H} 7.26 (2H, d, *J* = 8.7 Hz, ArH), 6.87 (2H, d, *J* = 8.7 Hz, ArH), 6.18 (1H, dd, *J* = 15.1, 10.5 Hz, H₃), 6.03 (1H, dd, *J* = 15.1, 10.5 Hz, H₄), 5.68 (1H, dt, *J* = 15.1, 7.2 Hz, H₅), 5.63 (1H, dt, *J* = 15.1, 5.3 Hz, H₂), 5.31 (1H, t, *J* = 7.1 Hz, H₁₅), 4.43 (2H, s, ArCH₂O), 4.20 (2H, d, *J* = 5.3 Hz, H₁ × 2), 3.90 (1H, app t, *J* = 6.3 Hz, H₂₃), 3.80 (3H, s, ArOMe), 3.59 (1H, dt, *J* = 6.6, 4.7 Hz, H₇), 3.52 (1H, dd, *J* = 8.8, 5.3 Hz, H_{27a}), 3.50–3.45 (3H, m, H₉, H_{27b}, C₂₃OH), 3.44 (3H, s, C₂₅OMe), 3.34 (1H, t, *J* = 6.8 Hz, H₁₃), 3.18 (1H, dd, *J* = 8.9, 2.8 Hz, H₂₅), 3.14 (3H, s, C₁₃OMe), 2.20–2.10 (2H, m, H₆ × 2), 2.10–1.95 (3H, m, H₁₆ × 2, H₂₆), 1.78–1.65 (2H, m, H₈, H₂₄), 1.58–1.43 (4H, m, H₁₀, H₁₂ × 2, H_{22a}), 1.49 (3H, s, Me₁₄), 1.42–1.33 (3H, m, H_{11a}, H₁₇ × 2), 1.33–1.20 (9H, m, H_{18–21}, H_{22b}), 1.03 (3H, d, *J* = 7.2 Hz, Me₂₄), 0.95–0.92 (4H, obs m, H_{11b}, Me₂₆), 0.95 (9H, t, *J* = 7.9 Hz, Si(CH₂CH₃)₃), 0.94 (9H, t, *J* = 8.0 Hz, Si(CH₂CH₃)₃), 0.91 (9H, s, SiC(CH₃)₃), 0.87 (3H, d, *J* = 7.6 Hz, Me₁₀), 0.85 (3H, d, *J* = 7.1 Hz, Me₈), 0.59 (6H, q, *J* = 8.2 Hz, Si(CH₂CH₃)₃),

0.58 (6H, q, $J = 8.4$ Hz, $\text{Si}(\text{CH}_2\text{CH}_3)_3$), 0.07 (6H, s, $\text{Si}(\text{CH}_3)_2$); ^{13}C NMR (125 MHz, CDCl_3) δ_{C} 159.1, 133.7, 131.7, 131.3, 130.6, 130.3, 130.2, 129.6, 129.1, 113.7, 89.0, 88.2, 77.6, 74.7, 72.7, 72.0, 70.6, 63.7, 61.7, 55.5, 55.2, 41.6, 38.6, 37.1, 36.7, 35.8, 34.7, 31.7, 29.8, 29.6, 29.5, 29.4, 27.9, 28.5, 26.2, 25.9, 18.4, 16.0, 14.9, 11.4, 10.2, 10.0, 7.1, 7.0, 5.6, 5.2, -5.2 ; $[\alpha]_{\text{D}}^{20} -1.8$ (c 1.01, CHCl_3); IR (thin film) ν_{max} (cm^{-1}) 3507, 2952, 2928, 2876, 2853, 1613, 1514, 1460, 1413, 1377, 1359, 1300, 1246, 1169, 1084, 1042, 1006, 990, 965, 834, 776, 739, 725, 675; HRMS calc. for $\text{C}_{60}\text{H}_{118}\text{O}_8\text{Si}_3\text{N}$ $[\text{M}+\text{NH}_4]^+$ 1064.8160, found 1064.8128.

(2S,3S,4R,5S,13E,15S,18R,19R,20R,21R,23E,25E)-3,15-dimethoxy-1-((4-methoxybenzyl)oxy)-2,4,14,18,20-pentamethyl-27-oxo-19,21-bis((triethylsilyl)oxy)heptacos-13,23,25-trien-5-yl propionate (124)

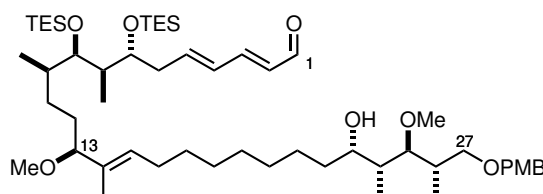


Silyl ether **117** (9.0 mg, 8.2 μmol) was dissolved in CH_2Cl_2 (0.6 mL) and pH 7 buffer (0.2 mL) and cooled to 0 $^\circ\text{C}$. The mixture was stirred rapidly as a solution of DDQ (2.0 mg, 8.8 μmol) in CH_2Cl_2 (0.2 mL) was added dropwise. After 20 min, the reaction was quenched with NaHCO_3 (1 mL), allowed to warm to rt, and extracted with CH_2Cl_2 (3×3 mL). The organics were dried over MgSO_4 and concentrated *in vacuo*. Purification by flash chromatography (1:8 EtOAc/PE) gave aldehyde **124** as a colourless oil (4.9 mg, 61%, 79% brsm).

R_f 0.42 (1:5 EtOAc/PE); ^1H NMR (500 MHz, CDCl_3) δ_{H} 9.55 (1H, d, $J = 8.0$ Hz, H_1), 7.24 (2H, d, $J = 8.7$ Hz, ArH), 7.08 (1H, dd, $J = 15.3, 10.0$ Hz, H_3), 6.86 (2H, d, $J = 8.7$ Hz, ArH), 6.37–6.27 (2H, m, H_4, H_5), 6.08 (1H, dd, $J = 15.3, 8.0$ Hz, H_2), 5.31 (1H, t, $J = 6.8$ Hz, H_{15}), 5.18 (1H, td, $J = 7.0, 1.8$ Hz, H_{23}), 4.43 (1H, d, $J = 11.5$ Hz, $\text{ArCH}_a\text{H}_b\text{O}$), 4.39 (1H, d, $J = 11.6$ Hz, $\text{ArCH}_a\text{H}_b\text{O}$), 3.80 (3H, s, ArOMe), 3.67 (1H, ddd, $J = 7.4, 4.9, 3.9$ Hz, H_7), 3.53 (1H, dd, $J = 9.2, 4.8$ Hz, H_{27a}), 3.50 (1H, app t, $J = 4.0$ Hz, H_9), 3.38 (3H, s, C_{25}OMe), 3.36–3.20 (2H, m, $\text{H}_{13}, \text{H}_{27b}$), 3.14 (3H, s, C_{13}OMe), 2.87 (1H, dd, $J = 8.5, 3.5$ Hz, H_{25}), 2.36–2.25 (2H, m, $\text{H}_6 \times 2$), 2.31 (2H, q, $J = 7.6$ Hz, $\text{H}_{2'} \times 2$), 2.12–2.02 (2H, m, $\text{H}_{16a}, \text{H}_{26}$), 1.99 (1H, dddd, $J = 14.4, 14.4, 7.1, 7.1$ Hz, H_{16b}), 1.81–1.72 (2H, m, $\text{H}_8, \text{H}_{24}$), 1.66–1.56 (1H, m, H_{22a}), 1.56–1.48 (2H, m, $\text{H}_{10}, \text{H}_{12a}$), 1.50 (3H, s, Me_{14}), 1.48–1.38 (2H, m, $\text{H}_{12b}, \text{H}_{22b}$), 1.38–1.31 (3H, m, $\text{H}_{11a}, \text{H}_{17} \times 2$), 1.31–1.20 (8H, m, H_{18-21}), 1.14 (3H, t, $J = 7.6$ Hz, $\text{H}_{3'} \times 3$), 1.06 (3H, d, $J = 7.0$ Hz, Me_{26}), 0.97–0.93 (1H, obs m, H_{11b}), 0.96 (9H, t, $J = 7.9$ Hz, $\text{Si}(\text{CH}_2\text{CH}_3)_3$), 0.95 (9H,

t, $J = 7.9$ Hz, Si(CH₂CH₃)₃), 0.90 (3H, d, $J = 7.1$ Hz, Me₂₄), 0.88 (3H, d, $J = 6.5$ Hz, Me₁₀), 0.87 (3H, d, $J = 6.8$ Hz, Me₈), 0.60 (6H, q, $J = 8.1$ Hz, Si(CH₂CH₃)₃), 0.58 (6H, q, $J = 8.1$ Hz, Si(CH₂CH₃)₃); ¹³C NMR (125 MHz, CDCl₃) δ_C 194.0 (C₁), 174.1 (C_{1'}), 159.0 (Ar C), 152.5 (C₃), 144.8 (C₅), 133.8 (C₁₄), 130.9 (Ar C), 130.3 (C₄), 130.2 (C₂), 129.6 (C₁₅), 129.0 (Ar C), 113.7 (Ar C), 88.2 (C₁₃), 85.9 (C₂₅), 77.4 (C₉), 74.4 (C₇), 73.1 (C₂₃), 72.8 (ArCH₂O), 71.6 (C₂₇), 61.4 (OMe₂₅), 55.5 (OMe₁₃), 55.3 (ArOMe), 41.6 (C₈), 38.9 (C₁₀), 38.8 (C₂₄), 36.4 (C₆), 35.9 (C₂₆), 32.8 (C₂₂), 31.9 (C₁₂), 29.7, 29.6, 29.4, 29.4 (C_{17–20}), 28.3 (C₁₁), 28.0 (C_{2'}), 27.6 (C₁₆), 25.8 (C₂₁), 16.3 (Me₂₆), 15.9 (Me₁₀), 10.6 (Me₂₄), 10.1 (Me₁₄), 10.0 (Me₈), 9.4 (C_{3'}), 7.2, 7.0, 5.6, 5.2 (TES × 4); [α]_D²⁰ –28.7 (c 0.017, CHCl₃); IR (thin film) ν_{max} (cm^{–1}) 2952, 2921, 2853, 2873, 1730, 1687, 1639, 1514, 1461, 1376, 1263, 1193, 1157, 1090, 1013, 803, 737, 706; HRMS calc. for C₅₇H₁₀₆O₉Si₂N [M+NH₄]⁺ 1004.7401, found 1004.7403.

(2E,4E,7R,8R,9R,10R,13S,14E,23S,24R,25S,26S)-23-hydroxy-13,25-dimethoxy-27-((4-methoxybenzyl)oxy)-8,10,14,24,26-pentamethyl-7,9-bis((triethylsilyl)oxy)heptacos-2,4,14-trienal (127)

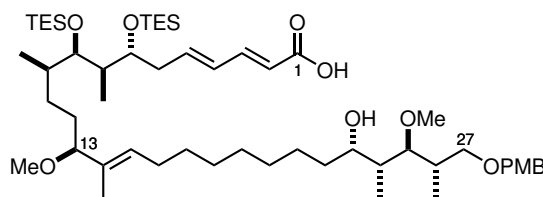


Dienyl silyl ether **121** (1.08 g, 1.03 mmol) was dissolved in CH₂Cl₂ (56 mL) and pH 9.2 buffer (14 mL) and cooled to 0 °C. DDQ (256 mg, 1.13 mmol) was added in one portion. The reaction was stirred for 10 min, then immediately quenched with NaHCO₃ (70 mL) and stirred vigorously while warming to rt. The mixture was extracted with CH₂Cl₂ (3 × 40 mL), dried over Na₂SO₄ and concentrated *in vacuo*. Product isolation by flash chromatography (1:6 EtOAc/PE) gave the aldehyde **127** as a colourless oil (589 mg, 62%, 81% brsm).

R_f 0.23 (1:5 EtOAc/PE); ¹H NMR (500 MHz, CDCl₃) δ_H 9.54 (1H, d, $J = 8.0$ Hz, H₁), 7.25 (2H, d, $J = 8.2$ Hz, ArH), 7.07 (1H, dd, $J = 15.3, 10.0$ Hz, H₃), 6.87 (2H, d, $J = 8.7$ Hz, ArH), 6.37–6.26 (2H, m, H₄, H₅), 6.08 (1H, dd, $J = 15.3, 8.0$ Hz, H₂), 5.31 (1H, t, $J = 6.8$ Hz, H₁₅), 4.43 (2H, s, ArCH₂O), 3.89 (1H, app t, $J = 6.4$ Hz, H₂₃), 3.80 (3H, s, ArOMe), 3.66 (1H, dt, $J = 7.4, 4.3$ Hz, H₇), 3.51 (1H, dd, $J = 8.9, 5.4$ Hz, H_{27a}), 3.50–3.45 (3H, m, H₉, H_{27b}, C₂₃OH), 3.44 (3H, s, C₂₅OMe), 3.33 (1H, t, $J = 7.0$ Hz, H₁₃), 3.18 (1H, dd, $J = 8.9, 2.9$ Hz, H₂₅), 3.14 (3H, s, C₁₃OMe), 2.36–2.24 (2H, m, H₆ × 2), 2.11–2.01 (2H, m, H_{16a}, H₂₆), 2.01–1.94 (1H, m, H_{16b}), 1.75 (1H, dqd, $J = 6.9, 6.9, 4.9$ Hz, H₈), 1.69 (1H, br q, $J = 7.0$ Hz, H₂₄), 1.58–1.42 (4H, m, H₁₀, H₁₂ × 2, H_{22a}), 1.49 (3H, s, Me₁₄), 1.42–1.18 (12H, m, H_{11a}, H_{17–21}, H_{22b}), 1.03 (3H, d,

$J = 7.2$ Hz, Me₂₄), 0.97–0.92 (4H, obs m, H_{11b}, Me₂₆), 0.95 (9H, t, $J = 8.0$ Hz, Si(CH₂CH₃)₃), 0.94 (9H, t, $J = 7.9$ Hz, Si(CH₂CH₃)₃), 0.88 (3H, d, $J = 6.8$ Hz, Me₁₀), 0.87 (3H, d, $J = 6.8$ Hz, Me₈), 0.59 (6H, q, $J = 8.1$ Hz, Si(CH₂CH₃)₃), 0.58 (6H, q, $J = 8.2$ Hz, Si(CH₂CH₃)₃); ¹³C NMR (125 MHz, CDCl₃) δ_C 193.9, 159.1, 152.5, 144.8, 133.7, 130.6, 130.3, 130.2, 129.6, 129.2, 113.7, 89.0, 88.2, 77.4, 74.3, 72.7, 72.0, 70.6, 61.7, 55.5, 55.2, 41.5, 38.9, 37.1, 36.7, 36.4, 34.7, 31.8, 29.8, 29.6, 29.5, 29.4, 28.3, 27.5, 26.2, 15.9, 14.9, 11.4, 10.1, 10.0, 7.1, 6.9, 5.6, 5.1; [α]_D²⁰ –2.4 (*c* 1.01, CHCl₃); IR (thin film) ν_{max} (cm^{–1}) 3486, 2952, 2931, 2876, 2853, 1685, 1640, 1613, 1514, 1459, 1416, 1378, 1367, 1302, 1247, 1171, 1159, 1087, 1038, 1009, 988, 820, 739, 725; HRMS calc. for C₅₄H₁₀₂O₈Si₂N [M+NH₄]⁺ 948.7138, found 948.7138.

(2*E*,4*E*,7*R*,8*R*,9*R*,10*R*,13*S*,14*E*,23*S*,24*R*,25*S*,26*S*)-23-hydroxy-13,25-dimethoxy-27-((4-methoxybenzyl)oxy)-8,10,14,24,26-pentamethyl-7,9-bis((triethylsilyl)oxy)heptacos-2,4,14-trienoic acid (130)

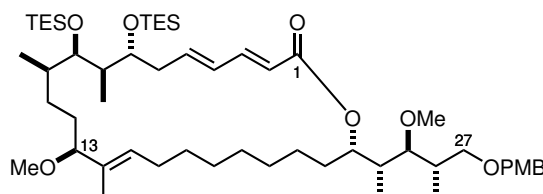


Aldehyde **127** (281 mg, 0.302 mmol) was dissolved in *t*-BuOH (2 mL) and 2-methyl-2-butene (2 mL), and a solution of NaClO₂ (1.02 g, 80% technical grade, 9.02 mmol) and NaH₂PO₄ · 2 H₂O (1.88 g, 12.2 mmol) in H₂O (4 mL) was added. The mixture was stirred at rt for 10 h, after which a yellow colour was observed. A second, equal portion of NaClO₂ (1.02 g), NaH₂PO₄ · 2 H₂O (1.88 g) and 2-methyl-2-butene (2 mL) was added, and stirring continued at 30 °C for 6 h. The reaction mixture was then diluted with EtOAc (10 mL) and brine (10 mL), and the aqueous phase was extracted with EtOAc (3 × 5 mL). The organics were dried over Na₂SO₄ and concentrated *in vacuo* to give crude seco-acid **130** as a pale yellow oil. The yield was determined at the next step.

R_f 0.28 (25:75:1 EtOAc/PE/AcOH); ¹H NMR (500 MHz, CDCl₃) δ_H 7.31 (1H, dd, $J = 15.1$, 9.3 Hz, H₃), 7.25 (2H, d, $J = 8.7$ Hz, ArH), 6.88 (2H, d, $J = 8.7$ Hz, ArH), 6.26–6.14 (2H, m, H₄, H₅), 5.79 (1H, d, $J = 15.3$ Hz, H₂), 5.31 (1H, t, $J = 6.9$ Hz, H₁₅), 4.44 (2H, s, ArCH₂O), 3.94 (1H, dd, $J = 8.4$, 4.8 Hz, H₂₃), 3.80 (3H, s, ArOMe), 3.67–3.61 (1H, m, H₇), 3.55–3.49 (2H, m, H₉, H_{27a}), 3.47 (1H, dd, $J = 8.9$, 3.6 Hz, H_{27b}), 3.45 (3H, s, C₂₅OMe), 3.34 (1H, t, $J = 7.0$ Hz, H₁₃), 3.19 (1H, dd, $J = 8.9$, 2.7 Hz, H₂₅), 3.14 (3H, s, C₁₃OMe), 2.33–2.21 (2H, m, H₆ × 2), 2.12–2.01 (2H, m, H_{16a}, H₂₆), 2.01–1.93 (1H, m, H_{16b}), 1.75–1.66 (2H, m, H₈, H₂₄), 1.61–1.44

(4H, m, H₁₀, H₁₂ × 2, H_{22a}), 1.49 (3H, s, Me₁₄), 1.44–1.19 (12H, m, H_{11a}, H_{17–21}, H_{22b}), 1.04 (3H, d, *J* = 7.1 Hz, Me₂₄), 0.97–0.91 (1H, obs m, H_{11b}), 0.95 (3H, d, *J* = 6.7 Hz, Me₂₆), 0.95 (9H, t, *J* = 7.9 Hz, Si(CH₂CH₃)₃), 0.94 (9H, t, *J* = 7.9 Hz, Si(CH₂CH₃)₃), 0.88 (3H, d, *J* = 6.8 Hz, Me₁₀), 0.85 (3H, d, *J* = 6.8 Hz, Me₈), 0.59 (6H, q, *J* = 8.4 Hz, Si(CH₂CH₃)₃), 0.58 (6H, q, *J* = 8.4 Hz, Si(CH₂CH₃)₃); ¹³C NMR (125 MHz, CDCl₃) δ_C 170.9, 159.1, 146.5, 142.7, 133.6, 130.6, 130.0, 129.8, 129.2, 118.9, 113.7, 89.1, 88.1, 77.2, 74.2, 72.8, 72.0, 70.8, 61.7, 55.5, 55.3, 41.3, 39.1, 37.1, 36.6, 36.3, 34.6, 31.7, 29.7, 29.7, 29.4, 29.3, 28.3, 27.6, 26.1, 15.6, 14.9, 11.5, 10.2, 10.0, 7.1, 7.0, 5.6, 5.2; [α]_D²⁰ –6.0 (*c* 0.99, CHCl₃); IR (thin film) ν_{max} (cm^{–1}) 2948, 2931, 2876, 2853, 1712, 1690, 1643, 1614, 1513, 1459, 1415, 1377, 1302, 1246, 1173, 1084, 1038, 1009, 820, 739, 727; HRMS calc. for C₅₄H₁₀₂O₉Si₂N [M+NH₄]⁺ 964.7088, found 964.7081.

(3*E*,5*E*,8*R*,9*R*,10*R*,11*R*,14*S*,15*E*,24*S*)-14-methoxy-24-((2*R*,3*S*,4*S*)-3-methoxy-5-((4-methoxybenzyl)oxy)-4-methylpentan-2-yl)-9,11,15-trimethyl-8,10-bis((triethylsilyl)oxy)oxacyclotetradeca-3,5,15-trien-2-one (132)



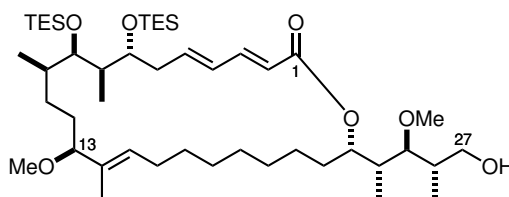
Crude seco-acid **130** (*ca* 285 mg, 0.302 mmol) was dried azeotropically with C₆H₆ and dissolved in THF (10 mL). Et₃N (420 μL, 3.01 mmol) and 2,4,6-trichlorobenzoyl chloride (330 μL, 2.11 mmol) were added at rt. The mixture was stirred for 1.5 h, then diluted with toluene (28 mL) and added *via* syringe pump to a solution of DMAP (369 mg, 3.02 mmol) in toluene (82 mL) over 12 h. The cloudy orange solution was stirred for a further 3 h, then filtered through a plug of silica, rinsed with Et₂O (80 mL), and concentrated *in vacuo*. The resulting oil was purified by flash chromatography (1:15 EtOAc/PE) to give macrocycle **132** as a pale yellow oil (197 mg, 70% over 2 steps).

R_f 0.56 (1:5 EtOAc/PE); ¹H NMR (500 MHz, CDCl₃) δ_H 7.28 (1H, dd, *J* = 15.4, 10.0 Hz, H₃), 7.23 (2H, d, *J* = 8.6 Hz, ArH), 6.86 (2H, d, *J* = 8.7 Hz, ArH), 6.25–6.13 (2H, m, H₄, H₅), 5.83 (1H, d, *J* = 15.3 Hz, H₂), 5.38 (1H, dt, *J* = 10.8, 2.4 Hz, H₂₃), 5.24 (1H, dd, *J* = 8.2, 6.0 Hz, H₁₅), 4.42 (1H, d, *J* = 11.5 Hz, ArCH_aH_bO), 4.39 (1H, d, *J* = 11.7 Hz, ArCH_aH_bO), 3.79 (3H, s, ArOMe), 3.67–3.62 (1H, m, H₇), 3.56–3.49 (2H, m, H₉, H_{27a}), 3.44 (3H, s, C₂₅OMe), 3.32 (1H, dd, *J* = 9.1, 7.8 Hz, H_{27b}), 3.30 (1H, t, *J* = 7.2 Hz, H₁₃), 3.13 (3H, s, C₁₃OMe), 2.90 (1H, dd, *J* = 8.2, 3.6 Hz, H₂₅), 2.35–2.26 (1H, m, H_{6a}), 2.18–2.02 (3H, m, H_{6b}, H_{16a}, H₂₆), 1.89–1.80 (1H,

m, H_{16b}), 1.80–1.73 (1H, m, H₂₄), 1.73–1.64 (2H, m, H₈, H_{22a}), 1.63–1.54 (2H, m, H₁₀, H_{12a}), 1.53–1.45 (1H, m, H_{12b}), 1.47 (3H, s, Me₁₄), 1.44–1.34 (2H, m, H_{21a}, H_{22b}), 1.34–1.15 (10H, m, H_{11a}, H_{17–20}, H_{21b}), 1.06 (3H, d, *J* = 7.0 Hz, Me₂₆), 0.98–0.93 (1H, obs m, H_{11b}), 0.95 (9H, t, *J* = 8.0 Hz, Si(CH₂CH₃)₃), 0.95 (9H, t, *J* = 8.0 Hz, Si(CH₂CH₃)₃), 0.91 (6H, app d, *J* = 7.0 Hz, Me₁₀, Me₂₄), 0.88 (3H, d, *J* = 6.8 Hz, Me₈), 0.59 (6H, q, *J* = 7.8 Hz, Si(CH₂CH₃)₃), 0.58 (6H, q, *J* = 7.9 Hz, Si(CH₂CH₃)₃); ¹³C NMR (125 MHz, CDCl₃) δ_C 167.2 (C₁), 159.0 (Ar C), 144.9 (C₃), 141.5 (C₅), 133.2 (C₁₄), 130.8 (Ar C), 130.1 (C₁₅), 130.0 (C₄), 129.0 (Ar C), 119.8 (C₂), 113.6 (Ar C), 88.0 (C₁₃), 85.7 (C₂₅), 77.2 (C₉), 73.4 (C₇), 73.2 (C₂₃), 72.7 (ArCH₂O), 71.6 (C₂₇), 61.1 (OMe₂₅), 55.4 (OMe₁₃), 55.2 (ArOMe), 41.0 (C₈), 40.8 (C₂₄), 39.5 (C₁₀), 36.4 (C₆), 35.9 (C₂₆), 33.5 (C₂₂), 31.4 (C₁₂), 29.0, 28.6, 28.3, 27.9, 27.8, 27.6 (C₁₁, C₁₆, C₁₇, C₁₈, C₂₀, C₂₁), 24.6 (C₁₉), 16.2 (Me₂₆), 14.5 (Me₁₀), 11.7 (Me₈), 11.2 (Me₂₄), 9.8 (Me₁₄), 7.1, 7.0, 5.4, 5.2 (TES × 4); [α]_D²⁰ +11.4 (*c* 1.04, CHCl₃); IR (thin film) ν_{max} (cm⁻¹) 2952, 2935, 2875, 2857, 1712, 1643, 1614, 1513, 1459, 1364, 1301, 1245, 1211, 1172, 1134, 1092, 1040, 1002, 820, 810, 762, 739, 725; HRMS calc. for C₅₄H₁₀₀O₈Si₂N [M+NH₄]⁺ 946.6982, found 946.6986.

5.5.3 Full carbon skeleton (C₁–C₃₄)

(3*E*,5*E*,8*R*,9*R*,10*R*,11*R*,14*S*,15*E*,24*S*)-24-((2*R*,3*S*,4*S*)-5-hydroxy-3-methoxy-4-methylpentan-2-yl)-14-methoxy-9,11,15-trimethyl-8,10-bis(((triethylsilyl)oxy)oxacyclotetracos-3,5,15-trien-2-one (139)

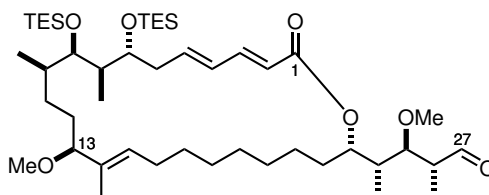


The fully protected macrocycle **132** (81.3 mg, 0.0875 mmol) was dissolved in CH₂Cl₂ (4 mL) and pH 7 buffer (2 mL) and cooled to 0 °C. DDQ (40.0 mg, 0.176 mmol) was added, then the rapidly stirring biphasic solution was warmed to rt. After 2 h, the mixture was quenched with NaHCO₃ (4 mL), extracted with CH₂Cl₂ (3 × 3 mL), dried over MgSO₄ and concentrated *in vacuo*. The crude material was purified by flash chromatography (1:4 EtOAc/PE) to yield alcohol **139** as a colourless oil (63.8 mg, 90%).

R_f 0.19 (1:5 EtOAc/PE); ¹H NMR (500 MHz, CDCl₃) δ_H 7.28 (1H, dd, *J* = 15.3, 10.1 Hz, H₃), 6.25–6.13 (2H, m, H₄, H₅), 5.83 (1H, d, *J* = 15.3 Hz, H₂), 5.37 (1H, dt, *J* = 10.7, 2.6

Hz, H₂₃), 5.24 (1H, dd, $J = 7.9, 5.8$ Hz, H₁₅), 3.79 (1H, dt, $J = 11.0, 3.6$ Hz, H_{27a}), 3.64 (1H, ddd, $J = 7.8, 5.5, 3.0$ Hz, H₇), 3.58–3.48 (2H, m, H₉, H_{27b}), 3.52 (3H, s, C₂₅OMe), 3.30 (1H, dd, $J = 8.2, 5.9$ Hz, H₁₃), 3.13 (3H, s, C₁₃OMe), 2.99 (1H, dd, $J = 8.1, 3.6$ Hz, H₂₅), 2.91 (1H, dd, $J = 6.7, 4.0$ Hz, C₂₇OH), 2.36–2.26 (1H, m, H_{6a}), 2.18–2.06 (2H, m, H_{6b}, H_{16a}), 1.93–1.80 (3H, m, H_{16b}, H₂₄, H₂₆), 1.75–1.65 (2H, m, H₈, H_{22a}), 1.63–1.53 (2H, m, H₁₀, H_{12a}), 1.53–1.42 (2H, m, H_{12b}, H_{22b}), 1.46 (3H, s, Me₁₄), 1.42–1.34 (1H, m, H_{21a}), 1.33–1.16 (10H, m, H_{11a}, H_{17–20}, H_{21b}), 1.12 (3H, d, $J = 7.2$ Hz, Me₂₆), 0.98–0.92 (1H, obs m, H_{11b}), 0.95 (9H, t, $J = 8.0$ Hz, Si(CH₂CH₃)₃), 0.95 (9H, t, $J = 8.0$ Hz, Si(CH₂CH₃)₃), 0.91 (3H, d, $J = 7.1$ Hz, Me₂₄), 0.91 (3H, d, $J = 7.2$ Hz, Me₁₀), 0.88 (3H, d, $J = 6.8$ Hz, Me₈), 0.59 (6H, q, $J = 7.9$ Hz, Si(CH₂CH₃)₃), 0.58 (6H, q, $J = 8.0$ Hz, Si(CH₂CH₃)₃); ¹³C NMR (125 MHz, CDCl₃) δ_C 167.2 (C₁), 145.1 (C₃), 141.8 (C₅), 133.3 (C₁₄), 130.1 (C₁₅), 129.9 (C₄), 119.6 (C₂), 88.6 (C₂₅), 88.0 (C₁₃), 77.2 (C₉), 73.4 (C₇), 73.1 (C₂₃), 65.0 (C₂₇), 61.5 (OMe₂₅), 55.4 (OMe₁₃), 41.2 (C₂₄), 41.1 (C₈), 39.6 (C₁₀), 36.5 (C₆), 36.2 (C₂₆), 33.6 (C₂₂), 31.4 (C₁₂), 29.0, 28.6, 28.3, 27.9, 27.8, 27.7 (C₁₁, C₁₆, C₁₇, C₁₈, C₂₀, C₂₁), 24.5 (C₁₉), 16.3 (Me₂₆), 14.5 (Me₁₀), 11.7 (Me₈), 11.2 (Me₂₄), 9.8 (Me₁₄), 7.1, 7.0, 5.4, 5.2 (TES × 4); [α]_D²⁰ +22.6 (*c* 1.02, CHCl₃); IR (thin film) ν_{max} (cm⁻¹) 3422, 2952, 2933, 2875, 1712, 1642, 1458, 1300, 1261, 1237, 1212, 1174, 1134, 1092, 1056, 1002, 739, 725; HRMS calc. for C₄₆H₉₂O₇NSi₂ [M+NH₄]⁺ 826.6407, found 826.6407.

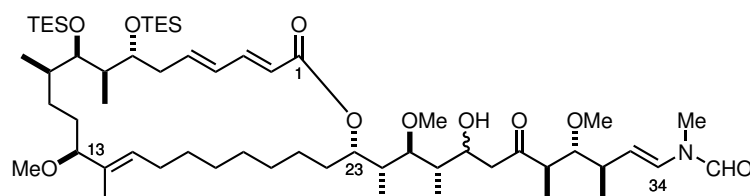
(2*R*,3*R*,4*R*)-3-methoxy-4-((2*S*,10*E*,12*S*,15*R*,16*R*,17*R*,18*R*,20*E*,22*E*)-12-methoxy-11,15,17-trimethyl-24-oxo-16,18-bis((triethylsilyl)oxy)oxacyclotetracos-10,20,22-trien-2-yl)-2-methylpentanal (31)



To oxalyl chloride (13 μL, 0.156 mmol) in CH₂Cl₂ (1.5 mL) at –78 °C was added DMSO (22 μL, 0.311 mmol), followed after 15 min by alcohol **139** (42.0 mg, 0.0519 mmol) in CH₂Cl₂ (1.5 mL), then after a further 15 min Et₃N (65 μL, 0.467 mmol). The reaction was warmed to rt and stirred for 20 min, then quenched with NH₄Cl (3 mL) and diluted with H₂O (15 mL) and Et₂O (15 mL). The biphasic mixture was shaken vigorously and the layers separated. The aqueous phase was extracted with Et₂O (3 × 5 mL), and the combined organics washed with HCl (12 mL, 0.5 M) and H₂O (10 mL), then dried over MgSO₄ and concentrated *in vacuo*. The resulting pale yellow oil containing crude **31** (41.1 mg, 98%) was used directly in the aldol reaction to minimise the risk of epimerisation.

R_f 0.56 (1:5 EtOAc/PE); **¹H NMR** (500 MHz, CDCl₃) δ_{H} 9.72 (1H, s, H₂₇), 7.28 (1H, dd, J = 15.3, 10.0 Hz, H₃), 6.24–6.13 (2H, m, H₄, H₅), 5.82 (1H, d, J = 15.3 Hz, H₂), 5.44 (1H, br d, J = 10.9 Hz, H₂₃), 5.23 (1H, dd, J = 7.9, 6.0 Hz, H₁₅), 3.67–3.60 (1H, m, H₇), 3.55–3.48 (1H, m, H₉), 3.42 (3H, s, C₂₅OMe), 3.32–3.25 (2H, m, H₁₃, H₂₅), 3.12 (3H, s, C₁₃OMe), 2.73–2.64 (1H, m, H₂₆), 2.35–2.24 (1H, m, H_{6a}), 2.17–2.04 (2H, m, H_{6b}, H_{16a}), 1.88–1.75 (2H, m, H_{16b}, H₂₄), 1.75–1.63 (2H, m, H₈, H_{22a}), 1.63–1.52 (2H, m, H₁₀, H_{12a}), 1.52–1.43 (1H, obs m, H_{12b}), 1.45 (3H, s, Me₁₄), 1.43–1.33 (2H, m, H_{21a}, H_{22b}), 1.33–1.17 (10H, m, H_{11a}, H_{17–20}, H_{21b}), 1.15 (3H, d, J = 7.1 Hz, Me₂₆), 0.98–0.91 (1H, obs m, H_{11b}), 0.94 (18H, t, J = 8.2 Hz, Si(CH₂CH₃)₃ × 2), 0.90 (3H, d, J = 6.8 Hz, Me₁₀), 0.87 (3H, d, J = 6.8 Hz, Me₈), 0.81 (3H, d, J = 7.1 Hz, Me₂₄), 0.58 (6H, q, J = 7.8 Hz, Si(CH₂CH₃)₃), 0.57 (6H, q, J = 8.0 Hz, Si(CH₂CH₃)₃); **¹³C NMR** (125 MHz, CDCl₃) δ_{C} 203.9, 167.2, 145.2, 141.9, 133.3, 130.1, 129.9, 119.4, 88.0, 83.4, 77.2, 73.4, 72.6, 59.2, 55.4, 48.1, 40.8, 39.5, 36.4, 33.2, 31.4, 29.7, 29.0, 28.6, 28.3, 27.8, 27.8, 27.6, 24.6, 14.5, 11.6, 10.4, 9.9, 9.8, 7.0, 7.0, 5.4, 5.2; $[\alpha]_{\text{D}}^{20}$ –1.9 (c 1.00, CHCl₃); **IR** (thin film) ν_{max} (cm^{–1}) 2948, 2932, 2876, 1714, 1641, 1615, 1458, 1413, 1361, 1300, 1260, 1236, 1171, 1133, 1096, 1058, 1002, 739, 725; **HRMS** calc. for C₄₆H₉₀O₇Si₂N [M+NH₄]⁺ 824.6250, found 824.6250.

***N*-((3*R*,4*R*,5*R*,9*S*,10*S*,11*R*,*E*)-8-hydroxy-4,10-dimethoxy-11-((2*S*,10*E*,12*S*,15*R*,16*R*,17*R*,18*R*,20*E*,22*E*)-12-methoxy-11,15,17-trimethyl-24-oxo-16,18-bis((triethylsilyl)oxy)oxacyclotetradeca-10,20,22-trien-2-yl)-3,5,9-trimethyl-6-oxododec-1-en-1-yl)-*N*-methylformamide (144)**



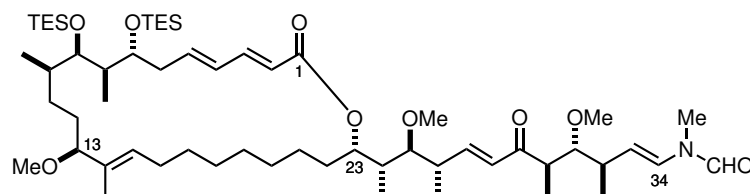
Ketone **32** (48.1 mg, 0.212 mmol) and aldehyde **31** (*ca* 63 mg, 0.0788 mmol) were each dried by forming an azeotrope with C₆H₆ and dried under high vacuum for 16 h. With rigorous exclusion of moisture, the ketone was dissolved in Et₂O (1.8 mL) and cooled to 0 °C. Cy₂BCl (56 μ L, 0.256 mmol) and NEt₃ (35 μ L, 0.251 mmol) were added. The enolising mixture was stirred for 1.5 h, then cooled to –78 °C, and the aldehyde was added dropwise as a solution in Et₂O (1.8 mL). After stirring at low temperature for 1 h, the flask was transferred to a –50 °C bath, and allowed to gradually warm to –20 °C over 1 h. This temperature was maintained for 1 h, whereupon TLC analysis showed that the aldehyde had been consumed. Silica gel (*ca* 400 mg) and Et₂O (2 mL) were added, and the slurry was stirred for 1 h under ambient air while warming

to rt. The mixture was filtered, rinsed with Et₂O (5 mL) and EtOAc (5 mL), and concentrated *in vacuo*. The resulting crude was subjected to flash chromatography (1:2 → 1:1 EtOAc/PE) and all fractions containing the aldol adduct were collected. The resulting oil containing desired product **144** and excess ketone **32** (*ca* 88 mg) was carried through to the next step as a mixture.

R_f 0.38 & 0.33 (1:1 EtOAc/PE); **¹H NMR** (500 MHz, CDCl₃) δ_H 8.29 (0.66H, s, NCHO), [8.07] (0.34H, s, NCHO*), 7.28 (1H, dd, *J* = 15.5, 10.1 Hz, H₃), [7.13] (0.34H, d, *J* = 14.7 Hz, H₃₄*), 6.46 (0.66H, d, *J* = 14.2 Hz, H₃₄), 6.25–6.13 (2H, m, H₄, H₅), 5.83 (1H, d, *J* = 15.3 Hz, H₂), 5.39 (1H, br d, *J* = 10.9 Hz, H₂₃), 5.24 (1H, dd, *J* = 7.6, 5.5 Hz, H₁₅), [5.13] (0.34H, dd, *J* = 14.4, 9.5 Hz, H₃₃*), 5.10 (0.66H, dd, *J* = 14.2, 9.2 Hz, H₃₃), 4.49–4.42 (0.25H, m, H₂₇[†]), 4.25–4.13 (0.75H, m, H₂₇), 3.69–3.62 (1H, m, H₇), 3.58–3.49 (1H, m, H₉), 3.45 (3H, s, C₂₅OMe), 3.41–3.38 (1H, m, C₂₇OH), 3.36 (3H, s, C₃₁OMe), 3.33–3.28 (2H, m, H₁₃, H₃₁), 3.13 (3H, s, C₁₃OMe), [3.08] (1H, s, NMe*), 3.03 (2H, s, NMe), 2.96 (1H, dd, *J* = 8.0, 3.9 Hz, H₂₅), 2.82–2.68 (2H, m, H_{28a}, H₃₀), 2.65–2.56 (1H, m, H_{28b}), 2.48–2.35 (1H, m, H₃₂), 2.35–2.26 (1H, m, H_{6a}), 2.18–2.06 (2H, m, H_{6b}, H_{16a}), 1.97–1.80 (3H, m, H_{16b}, H₂₄, H₂₆), 1.80–1.48 (5H, m, H₈, H₁₀, H₁₂ × 2, H_{22a}), 1.47 (3H, s, Me₁₄), 1.44–1.34 (1H, m, H_{22b}), 1.34–1.18 (11H, m, H_{11a}, H_{17–21}), 1.17 (3H, d, *J* = 6.5 Hz, Me₃₂), 1.00–0.93 (28H, m, H_{11b}, Me₂₄, Me₂₆, Me₃₀, Si(CH₂CH₃)₃ × 2), 0.91 (3H, d, *J* = 7.0 Hz, Me₁₀), 0.88 (3H, d, *J* = 7.4 Hz, Me₈), 0.60 (6H, q, *J* = 7.8 Hz, Si(CH₂CH₃)₃), 0.58 (6H, q, *J* = 7.9 Hz, Si(CH₂CH₃)₃); **¹³C NMR** (125 MHz, CDCl₃) δ_C [215.7] (C₂₉*), 215.6 (C₂₉), 167.2 (C₁), 162.2 (NCHO), [160.9] (NCHO*), 145.0 (C₃), 141.7 (C₅), 133.3 (C₁₄), 130.2 (C₁₅), 130.0 (C₄), 128.9 (C₃₄), [124.9] (C₃₄*), 119.7 (C₂), [113.0] (C₃₃*), 111.2 (C₃₃), 88.0 (C₁₃), [87.6] (C₃₁*), 87.5 (C₃₁), 86.6 (C₂₅), [86.4] (C₂₅*), 77.2 (C₉), 73.4 (C₇), 73.0 (C₂₃), 68.6 (C₂₇), 66.2 (C₂₇[†]), [61.4] (C₃₁OMe*), 61.3 (C₃₁OMe), 60.9 (C₂₅OMe), 55.5 (C₁₃OMe), 49.6 (C₃₀), 48.5 (C₂₈), [48.4] (C₂₈*), 41.6 (C₂₄), [41.5] (C₂₄*), 40.2 (C₂₆), [40.1] (C₂₆*), 39.6 (C₁₀), [37.7] (C₃₂*), 37.5 (C₃₂), 37.2 (C₈), 36.5 (C₆), 33.6 (C₂₂), [33.1] (NMe*), 31.4 (C₁₂), 29.7, 29.0, 28.6, 28.3, 28.0 (C₁₁, C_{17–20}), 27.7 (C₁₆), 27.6 (NMe), 24.6 (C₂₁), 19.4 (Me₃₂), 14.5 (Me₁₀), 14.3 (Me₂₆), [14.1] (Me₂₆*), [13.4] (Me₃₀*), 13.3 (Me₃₀), 11.7 (Me₈), 11.4 (Me₂₄), 9.8 (Me₁₄), 7.1, 7.0, 5.4, 5.2 (TES × 4); [α]_D²⁰ –22.7 (*c* 1.03, CHCl₃); **IR** (thin film) ν_{max} (cm^{–1}) 3209, 2931, 2876, 2853, 1697, 1656, 1457, 1413, 1378, 1260, 1237, 1093, 1069, 1003, 969, 941, 808, 741, 725; **HRMS** calc. for C₅₈H₁₁₁N₂O₁₀Si₂ [M+NH₄]⁺ 1051.7772, found 1051.7774.

Distinguishable resonances of the minor rotamer (*ca* 2:1 ratio) are given in brackets and marked with an asterisk (*). The diastereomeric ratio of the product at C₂₇ is approximately 3:1, and distinguishable resonances of the two diastereomers are noted with a dagger (†).

***N*-((1*E*,3*R*,4*R*,5*R*,7*E*,9*S*,10*S*,11*R*)-4,10-dimethoxy-11-((2*S*,10*E*,12*S*,15*R*,16*R*,17*R*,18*R*,20*E*,22*E*)-12-methoxy-11,15,17-trimethyl-24-oxo-16,18-bis((triethylsilyl)oxy)oxacyclotetracos-10,20,22-trien-2-yl)-3,5,9-trimethyl-6-oxododeca-1,7-dien-1-yl)-*N*-methylformamide (**147**)**



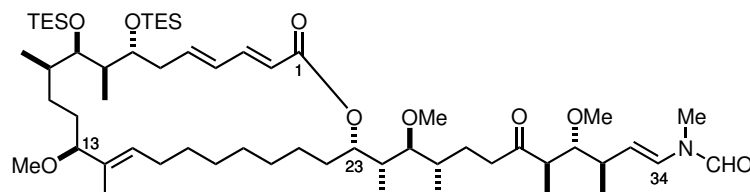
A mixture of aldol adduct **144** and ketone **32** (*ca* 88 mg, ≤ 0.0788 mmol **144**) was dissolved in THF (1.8 mL) and added to Burgess salt (methyl *N*-(triethylammoniumsulfonyl)carbamate, 26 mg, 0.109 mmol). The mixture was warmed to 30 °C and stirred for 16 h. The reaction was quenched with NH₄Cl (1 mL) and stirred for 10 min as a white precipitate formed. The aqueous was extracted with EtOAc (3 \times 1 mL), dried over MgSO₄, and concentrated *in vacuo*. The resulting colourless oil was resubmitted to the same reaction conditions, following which the crude was purified by flash chromatography (1:4 EtOAc/PE). This resulted in isolation of the enone **147** (50.7 mg, 63% over 3 steps) and recovered ketone **32** (28 mg, 93% recovery).

R_f 0.74 & 0.68 (1:1 EtOAc/PE); **¹H NMR** (500 MHz, CDCl₃) δ _H 8.29 (0.66H, s, NCHO), [8.08] (0.34H, s, NCHO^{*}), 7.28 (1H, dd, *J* = 15.4, 10.0 Hz, H₃), [7.14] (0.34H, d, *J* = 15.2 Hz, H₃₄^{*}), 6.90 (0.66H, dd, *J* = 16.0, 8.4 Hz, H₂₇), [6.88] (0.34H, dd, *J* = 15.8, 8.6 Hz, H₂₇^{*}), 6.48 (0.66H, d, *J* = 14.1 Hz, H₃₄), 6.24–6.16 (2H, m, H₄, H₅), 6.15 (0.66H, d, *J* = 15.7 Hz, H₂₈), [6.13] (0.34H, d, *J* = 16.0 Hz, H₂₈^{*}), 5.83 (1H, d, *J* = 15.4 Hz, H₂), 5.39 (1H, br d, *J* = 10.6 Hz, H₂₃), 5.23 (1H, dd, *J* = 7.9, 5.8 Hz, H₁₅), [5.16] (0.34H, dd, *J* = 14.6, 9.5 Hz, H₃₃^{*}), 5.14 (0.66H, dd, *J* = 14.1, 9.3 Hz, H₃₃), 3.67–3.60 (1H, m, H₇), 3.57–3.50 (1H, m, H₉), 3.48 (3H, s, C₂₅OMe), 3.32–3.26 (5H, m, H₁₃, H₃₁, C₃₁OMe), 3.13 (3H, s, C₁₃OMe), [3.09] (1H, s, NMe^{*}), 3.05 (2H, s, NMe), 3.03–2.95 (1H, m, H₃₀), 2.95–2.87 (1H, m, H₂₅), 2.66–2.56 (1H, m, H₂₆), 2.50–2.36 (1H, m, H₃₂), 2.36–2.26 (1H, m, H_{6a}), 2.19–2.04 (2H, m, H_{6b}, H_{16a}), 1.88–1.78 (1H, m, H_{16b}), 1.75–1.65 (2H, m, H₈, H_{22a}), 1.65–1.53 (3H, m, H₁₀, H_{12a}, H₂₄), 1.53–1.45 (1H, m, H_{12b}), 1.46 (3H, s, Me₁₄), 1.42–1.32 (1H, m, H_{22b}), 1.32–1.18 (11H, m, H_{11a}, H_{17–21}), 1.16 (3H, d, *J* = 6.7 Hz, Me₂₆), 1.15 (3H, d, *J* = 6.9 Hz, Me₃₂), 0.98–0.91 (1H, obs m, H_{11b}), 0.95 (9H, t, *J* = 8.0 Hz, Si(CH₂CH₃)₃), 0.95 (9H, t, *J* = 7.9 Hz, Si(CH₂CH₃)₃), 0.94 (3H, obs d, Me₃₀), 0.91 (3H, d, *J* = 6.9 Hz, Me₁₀), 0.88 (3H, d, *J* = 6.9 Hz, Me₈), 0.83 (3H, d, *J* = 7.0 Hz, Me₂₄), 0.59 (6H, q, *J* = 8.0 Hz, Si(CH₂CH₃)₃), 0.58 (6H, q, *J* = 7.9 Hz, Si(CH₂CH₃)₃); **¹³C NMR** (125 MHz, CDCl₃) δ _C [203.5] (C₂₉^{*}), 203.4 (C₂₉), [167.3] (C₁^{*}), 167.3 (C₁), 162.2 (NCHO), [160.9] (NCHO^{*}), 149.3 (C₂₇), [149.2] (C₂₇^{*}), 145.1 (C₃), 141.9 (C₅), 133.3 (C₁₄), [130.6] (C₂₈^{*}), 130.5 (C₂₈), 130.1

(C₁₅), 129.9 (C₄), 128.8 (C₃₄), [124.8] (C₃₄^{*}), 119.6 (C₂), [113.3] (C₃₃^{*}), 111.5 (C₃₃), 88.0 (C₁₃), [87.6] (C₃₁^{*}), 87.5 (C₃₁), [86.0] (C₂₅^{*}), 86.0 (C₂₅), 77.1 (C₉), 73.4 (C₇), [73.0] (C₂₃^{*}), 72.9 (C₂₃), [61.2] (C₃₁OMe^{*}), 61.2 (C₃₁OMe), 61.0 (C₂₅OMe), 55.5 (C₁₃OMe), [46.2] (C₃₀^{*}), 46.1 (C₃₀), 41.5 (C₂₄), 41.2 (C₈), 39.6 (C₂₆), 39.5 (C₁₀), [37.9] (C₃₂^{*}), 37.7 (C₃₂), 36.5 (C₆), 33.5 (C₂₂), [33.0] (NMe^{*}), 31.4 (C₁₂), 29.0, 28.6, 28.3, 27.9, 27.8 (C₁₁, C_{17–20}), 27.7 (C₁₆), 27.5 (NMe), 24.6 (C₂₁), [19.6] (Me₃₂^{*}), 19.5 (Me₃₂), 17.5 (Me₂₆), [17.4] (Me₂₆^{*}), 14.5 (Me₁₀), 13.8 (Me₃₀), [13.7] (Me₃₀^{*}), 11.7 (Me₈), 10.4 (Me₂₄), [10.4] (Me₂₄^{*}), 9.8 (Me₁₄), 7.1, 7.0, 5.4, 5.2 (TES × 4); [α]_D²⁰ –47.6 (c 0.50, CHCl₃); **IR** (thin film) ν_{max} (cm^{–1}) 2931, 2876, 2857, 1694, 1657, 1619, 1458, 1415, 1371, 1359, 1316, 1304, 1260, 1237, 1133, 1095, 1070, 1004, 985, 740, 725; **HRMS** calc. for C₅₈H₁₀₅NO₉Si₂Na [M+Na]⁺ 1038.7220, found 1038.7228.

Distinguishable resonances of the minor rotamer (*ca* 2:1 ratio) are given in brackets and marked with an asterisk.

***N*-((3*R*,4*R*,5*R*,9*S*,10*S*,11*R*,*E*)-4,10-dimethoxy-11-((2*S*,10*E*,12*S*,15*R*,16*R*,17*R*,18*R*,20*E*,22*E*)-12-methoxy-11,15,17-trimethyl-24-oxo-16,18-bis((triethylsilyl)oxy)oxacyclotetracos-10,20,22-trien-2-yl)-3,5,9-trimethyl-6-oxododec-1-en-1-yl)-*N*-methylformamide (148)**



Stryker's reagent (280 μL, 0.025 M in toluene, 7.0 μmol) was added to enone **147** (35.5 mg, 34.9 μmol) in toluene (700 μL). The mixture was stirred for 2 h at rt, then a further aliquot of the reagent solution (280 μL, 7.0 μmol) was added. After a further 2 h, the reaction mixture was loaded directly onto a silica column. Ketone **148** eluted from the column (1:5 → 1:3 EtOAc/PE) and was concentrated to a colourless oil (29.3 mg, 82%).

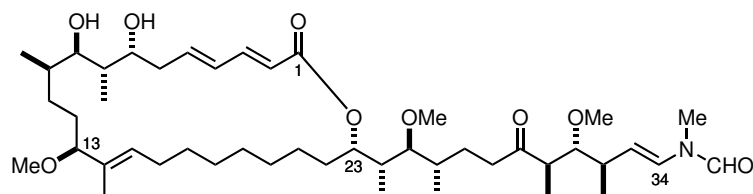
R_f 0.74 & 0.57 (1:1 EtOAc/PE); **¹H NMR** (500 MHz, CDCl₃) δ_H 8.28 (0.66H, s, NCHO), [8.07] (0.34H, s, NCHO^{*}), 7.27 (1H, dd, *J* = 15.4, 9.8 Hz, H₃), [7.12] (0.34H, d, *J* = 14.7 Hz, H₃₄^{*}), 6.45 (0.66H, d, *J* = 14.2 Hz, H₃₄), 6.24–6.13 (2H, m, H₄, H₅), 5.83 (1H, d, *J* = 15.3 Hz, H₂), 5.41 (1H, br d, *J* = 10.8 Hz, H₂₃), 5.24 (1H, dd, *J* = 7.9, 5.9 Hz, H₁₅), [5.12] (0.34H, dd, *J* = 14.3, 10.5 Hz, H₃₃^{*}), 5.10 (0.66H, dd, *J* = 14.1, 9.4 Hz, H₃₃), 3.67–3.59 (1H, m, H₇), 3.56–3.48 (1H, m, H₉), 3.47 (3H, s, C₂₅OMe), 3.33 (3H, s, C₃₁OMe), 3.32–3.27 (2H, m, H₁₃, H₃₁), 3.13 (3H, s, C₁₃OMe), [3.07] (1H, s, NMe^{*}), 3.03 (2H, s, NMe), 2.82–2.72 (1H,

m, H₂₅), 2.71–2.62 (1H, m, H₃₀), 2.62–2.51 (1H, m, H_{28a}), 2.49–2.40 (1H, m, H_{28b}), 2.40–2.34 (1H, m, H₃₂), 2.34–2.26 (1H, m, H_{6a}), 2.18–1.95 (2H, m, H_{6b}, H_{16a}), 1.87–1.79 (1H, m, H_{16b}), 1.79–1.48 (8H, m, H₈, H₁₀, H₁₂ × 2, H_{22a}, H₂₄, H₂₆, H_{27a}), 1.46 (3H, s, Me₁₄), 1.41–1.17 (13H, m, H_{11a}, H_{17–21}, H_{22b}, H_{27b}), 1.15 (3H, d, *J* = 6.9 Hz, Me₃₂), 1.01–0.84 (34H, m, H_{11b}, Me₈, Me₁₀, Me₂₄, Me₂₆, Me₃₀, Si(CH₂CH₃)₃ × 2), 0.59 (6H, q, *J* = 7.4 Hz, Si(CH₂CH₃)₃), 0.58 (6H, q, *J* = 7.4 Hz, Si(CH₂CH₃)₃); ¹³C NMR (125 MHz, CDCl₃) δ_C [214.3] (C₂₉^{*}), 214.2 (C₂₉), 167.3 (C₁), 162.1 (NCHO), [160.8] (NCHO^{*}), 144.9 (C₃), 134.8 (C₅), 133.2 (C₁₄), 130.2 (C₁₅), 129.9 (C₄), 128.7 (C₃₄), [124.7] (C₃₄^{*}), 119.8 (C₂), [113.1] (C₃₃^{*}), 111.3 (C₃₃), 88.0, 87.4, 87.3 (C₁₃, C₂₅, C₃₁), 74.3 (C₉), 73.4 (C₇), 73.2 (C₂₃), 61.4 (C₃₁OMe), 61.3 (C₂₅OMe), 55.5 (C₁₃OMe), [49.2] (C₃₀^{*}), 49.0 (C₃₀), 42.0 (C₂₈), [42.0] (C₂₈^{*}), 41.0 (C₂₄), 40.9 (C₂₆), 39.5 (C₁₀), [37.7] (C₃₂^{*}), 37.5 (C₃₂), 36.4 (C₆), 34.4 (C₈), 33.7 (C₂₂), [33.1] (NMe^{*}), 31.4 (C₁₂), 29.7, 29.0, 28.6, 28.3, 27.9, 27.8 (C₁₁, C_{16–20}), 27.6 (NMe), 24.6 (C₂₁), 23.4 (C₂₇), [19.4] (Me₃₂^{*}), 19.4 (Me₃₂), 17.4 (Me₈), 14.5 (Me₃₀), 13.5 (Me₁₀), 13.5 (Me₂₄), 10.8 (Me₂₆), 9.8 (Me₁₄), 7.1, 7.0, 5.4, 5.2 (TES × 4); [α]_D²⁰ –25.8 (*c* 0.859, CHCl₃); IR (thin film) ν_{max} (cm^{–1}) 2952, 2932, 2876, 2857, 1698, 1657, 1458, 1412, 1371, 1318, 1302, 1258, 1239, 1135, 1094, 1069, 1004, 970, 943, 915, 801, 739, 726; HRMS calc. for C₅₈H₁₁₁N₂O₉Si₂ [M+NH₄]⁺ 1035.7823, found 1035.7840.

Distinguishable resonances of the minor rotamer (*ca* 2:1 ratio) are given in brackets and marked with an asterisk.

5.6 Experimental procedures for Chapter 4

***N*-((3*R*,4*R*,5*R*,9*S*,10*S*,11*R*,*E*)-11-((2*S*,10*E*,12*S*,15*R*,16*R*,17*S*,18*R*,20*E*,22*E*)-16,18-dihydroxy-12-methoxy-11,15,17-trimethyl-24-oxooxacyclotetracos-10,20,22-trien-2-yl)-4,10-dimethoxy-3,5,9-trimethyl-6-oxododec-1-en-1-yl)-*N*-methylformamide (153)**



A stock solution of HF · pyridine was prepared by diluting 70% HF · pyridine (100 μL) into THF (1 mL) and pyridine (200 μL). An aliquot (600 μL) was added to *bis*-TES ether **148** (3.3 mg,

3.2 μmol) at 0 °C. The reaction was warmed to rt and stirred for 16 h, then quenched cautiously with NaHCO_3 at 0 °C and stirred at rt for 30 min. The aqueous was extracted with EtOAc ($3 \times 5 \text{ mL}$), dried over Na_2SO_4 , and concentrated *in vacuo*. Flash chromatography (1:1 EtOAc/ $\text{CH}_2\text{Cl}_2 \rightarrow 5:5:1 \text{ EtOAc}/\text{CH}_2\text{Cl}_2/\text{MeOH}$) to give diol **153** as an oil (2.1 mg, 82%).

R_f 0.54 (5:5:1 EtOAc/ CH_2Cl_2 /MeOH); **¹H NMR** (500 MHz, CDCl_3) δ_{H} 8.28 (0.66H, s, NCHO), [8.07] (0.34H, s, NCHO*), 7.28–7.23 (1H, obs dd, H₃), [7.12] (0.34H, d, $J = 14.7 \text{ Hz}$, H₃₄*), 6.45 (0.66H, d, $J = 14.2 \text{ Hz}$, H₃₄), 6.27 (1H, dd, $J = 15.1, 11.1 \text{ Hz}$, H₄), 6.11 (1H, dt, $J = 15.0, 7.5 \text{ Hz}$, H₅), 5.85 (1H, d, $J = 15.3 \text{ Hz}$, H₂), 5.36 (1H, br d, $J = 10.3 \text{ Hz}$, H₂₃), 5.30 (1H, t, $J = 6.9 \text{ Hz}$, H₁₅), [5.12] (0.34H, dd, $J = 14.8, 10.6 \text{ Hz}$, H₃₃*), 5.11 (0.66H, dd, $J = 14.2, 9.5 \text{ Hz}$, H₃₃), 3.88–3.81 (1H, m, H₇), 3.70–3.64 (1H, m, H₉), 3.45 (3H, s, C₂₅OMe), 3.38–3.32 (1H, obs m, H₁₃), 3.34 (3H, s, C₃₁OMe), 3.31 (1H, br d, $J = 9.5 \text{ Hz}$, H₃₁), 3.15 (3H, s, C₁₃OMe), [3.08] (1H, s, NMe*), 3.04 (2H, s, NMe), 2.85–2.73 (2H, m, C₇OH, H₂₅), 2.72–2.62 (1H, m, H₃₀), 2.62–2.50 (3H, m, H₆ \times 2, H_{28a}), 2.50–2.33 (3H, m, C₉OH, H_{28b}, H₃₂), 2.11–1.93 (2H, m, H₁₆ \times 2), 1.80–1.53 (8H, m, H₈, H₁₀, H₁₂ \times 2, H_{22a}, H₂₄, H₂₆, H_{27a}), 1.53–1.46 (4H, m, H_{11a}, Me₁₄), 1.46–1.38 (2H, m, H_{22b}, H_{27b}), 1.38–1.19 (10H, m, H_{17–21}), 1.16 (3H, d, $J = 6.9 \text{ Hz}$, Me₃₂), 1.05 (3H, d, $J = 7.1 \text{ Hz}$, Me₂₄), 0.99–0.95 (1H, obs m, H_{11b}), 0.97 (3H, d, $J = 6.9 \text{ Hz}$, Me₈), 0.91 (3H, d, $J = 7.1 \text{ Hz}$, Me₃₀), 0.90 (3H, d, $J = 7.0 \text{ Hz}$, Me₂₆), 0.79 (3H, d, $J = 6.8 \text{ Hz}$, Me₁₀); **¹³C NMR** (125 MHz, CDCl_3) δ_{C} [214.3] (C₂₉*), 214.2 (C₂₉), 167.0 (C₁), 162.2 (NCHO), 144.2 (C₃), 138.9 (C₅), 133.7 (C₁₄), 131.0 (C₁₅), 129.9 (C₄), 128.7 (C₃₄), [124.7] (C₃₄*), 120.6 (C₂), [113.2] (C₃₃*), 111.4 (C₃₃), 87.9, 87.5, 87.3 (C₁₃, C₂₅, C₃₁), 75.3 (C₉), 75.2 (C₇), 73.8 (C₂₃), 61.4 (C₂₅OMe), 61.3 (C₃₁OMe), 55.7 (C₁₃OMe), [49.2] (C₃₀*), 49.1 (C₃₀), 42.1 (C₂₈), [42.0] (C₂₈*), 40.7 (C₂₄), 39.0 (C₆), [37.7] (C₃₂*), 37.5 (C₃₂), 37.0 (C₂₆), 37.0 (C₁₀), 34.5 (C₈), 33.7 (C₂₂), [33.1] (NMe*), 30.9 (C₁₂), 29.7, 28.8, 28.7, 28.4, 27.8 (C₁₁, C_{17–20}), 27.6 (NMe), 27.3 (C₁₆), 25.1 (C₂₁), 23.5 (C₂₇), 19.4 (Me₃₂), 17.4 (Me₈), 15.8 (Me₁₀), 13.5 (Me₃₀), 11.6 (Me₂₄), 10.9 (Me₂₆), 10.3 (Me₁₄); $[\alpha]_{\text{D}}^{20} -49.3$ (c 0.035, CHCl_3); **IR** (thin film) ν_{max} (cm^{-1}) 3365, 2924, 2853, 1704, 1655, 1462, 1375, 1276, 1258, 1240, 1137, 1092, 1074, 1002, 969, 808, 800, 737, 723; **HRMS** calc. for $\text{C}_{46}\text{H}_{83}\text{N}_2\text{O}_9$ $[\text{M}+\text{NH}_4]^+$ 807.6093, found 807.6106.

Distinguishable resonances of the minor rotamer (*ca* 2:1 ratio) are given in brackets and marked with an asterisk.

¹³C NMR (125 MHz, CDCl₃) δ_C [214.3], 214.3, 170.2, 167.0, 162.2, [160.9], 143.9, 137.8, 133.8, 131.4, 129.9, 128.7, [124.7], 121.1, [113.2], 111.4, 87.8, 87.4, 87.4, 87.3, 74.0, 73.7, 70.5, 67.4, 61.4, 61.4, [61.3], 59.2, 55.6, [49.2], 49.1, 42.4, 42.1, [40.8], 40.8, [37.7], 37.5, 36.7, 36.4, 36.4, 34.5, 33.8, [33.1], 30.6, 29.7, 29.4, 28.9, 28.4, 28.1, 27.7, 27.6, 27.4, 22.7, [19.4], 19.4, 17.4, 15.5, [13.6], 13.5, 11.8, 10.9, [10.9], 10.1; [α]_D²⁰ −15.7 (*c* 0.032, CHCl₃); **IR** (thin film) ν_{max} (cm^{−1}) 3408, 2956, 2920, 2896, 2853, 1718, 1670, 1657, 1605, 1548, 1508, 1466, 1379, 1363, 1252, 1220, 1084, 1000, 955, 899, 854, 834, 695; **HRMS** calc. for C₅₂H₉₁N₂O₁₁ [M+H]⁺ 919.6617, found 919.6630.

Distinguishable resonances of the minor rotamer (*ca* 2:1 ratio) are given in brackets and marked with an asterisk.

Bibliography

- (1) Masamune, S.; Ali, S. A.; Snitman, D. L.; Garvey, D. S. *Angew. Chemie Int. Ed.* **1980**, *19*, 557–558.
- (2) Yamada, K.; Ojika, M.; Ishigaki, T.; Yoshida, Y.; Ekimoto, H.; Arakawa, M. *J. Am. Chem. Soc.* **1993**, *115*, 11020–11021.
- (3) Martins, A.; Vieira, H.; Gaspar, H.; Santos, S. *Mar. Drugs* **2014**, *12*, 1066–1101.
- (4) Hentschel, U.; Piel, J.; Degnan, S. M.; Taylor, M. W. *Nat. Rev. Microbiol.* **2012**, *10*, 641–654.
- (5) Miller, J. H.; Field, J. J.; Kanakkanthara, A.; Owen, J. G.; Singh, A. J.; Northcote, P. T. *J. Nat. Prod.* **2018**, *81*, 691–702.
- (6) Piel, J. *Nat. Prod. Rep.* **2009**, *26*, 338–362.
- (7) Pita, L.; Rix, L.; Slaby, B. M.; Franke, A.; Hentschel, U. *Microbiome* **2018**, *6*, 46–64.
- (8) Kong, W.; Meldgin, D. R.; Collins, J. J.; Lu, T. *Nat. Chem. Biol.* **2018**, *14*, 821–829.
- (9) Padmaperuma, G.; Kapoore, R. V.; Gilmour, D. J.; Vaidyanathan, S. *Crit. Rev. Biotechnol.* **2018**, *38*, 690–703.
- (10) Brenner, K.; You, L.; Arnold, F. H. *Trends Biotechnol.* **2008**, *26*, 483–489.
- (11) Soldatou, S.; Baker, B. J. *Nat. Prod. Rep.* **2017**, *34*, 585–626.
- (12) World Health Organisation: Cancer. 2018; <http://www.who.int/news-room/fact-sheets/detail/cancer>.
- (13) Newman, D. J.; Cragg, G. M. *Mar. Drugs* **2014**, *12*, 255–278.
- (14) Wender, P. A.; Verma, V. A.; Paxton, T. J.; Pillow, T. H. *Acc. Chem. Res.* **2008**, *41*, 40–49.

- (15) Aicher, T. D.; Buszek, K. R.; Fang, F. G.; Forsyth, C. J.; Jung, S. H.; Kishi, Y.; Matelich, M. C.; Scola, P. M.; Spero, D. M.; Yoon, S. K. *J. Am. Chem. Soc.* **1992**, *114*, 3162–3164.
- (16) Wender, P. A.; Baryza, J. L.; Bennett, C. E.; Bi, F. C.; Brenner, S. E.; Clarke, M. O.; Horan, J. C.; Kan, C.; Lacôte, E.; Lippa, B.; Nell, P. G.; Turner, T. M. *J. Am. Chem. Soc.* **2002**, *124*, 13648–13649.
- (17) Wender, P. A. *Nat. Prod. Rep.* **2014**, *31*, 433–440.
- (18) Allred, T. K.; Manoni, F.; Harran, P. G. *Chem. Rev.* **2017**, *117*, 11994–12051.
- (19) Wender, P. A.; Quiroz, R. V.; Stevens, M. C. *Acc. Chem. Res.* **2015**, *48*, 752–760.
- (20) Wender, P. A.; Donnelly, A. C.; Loy, B. A.; Near, K. E.; Staveness, D. *Natural Products in Medicinal Chemistry*; Wiley-Blackwell, 2014; pp 473–544.
- (21) Wender, P. A.; Hardman, C. T.; Ho, S.; Jeffreys, M. S.; Maclaren, J. K.; Quiroz, R. V.; Ryckbosch, S. M.; Shimizu, A. J.; Sloane, J. L.; Stevens, M. C. *Science* **2017**, *358*, 218–223.
- (22) Ciavatta, M. L.; Lefranc, F.; Carbone, M.; Mollo, E.; Gavagnin, M.; Betancourt, T.; Dasari, R.; Kornienko, A.; Kiss, R. *Med. Res. Rev.* **2017**, *37*, 702–801.
- (23) Gomes, N.; Dasari, R.; Chandra, S.; Kiss, R.; Kornienko, A. *Mar. Drugs* **2016**, *14*, 98–137.
- (24) Mickel, S. J.; Sedelmeier, G. H.; Niederer, D.; Daeffler, R.; Osmani, A.; Schreiner, K.; Seeger-Weibel, M.; Bérod, B.; Schaer, K.; Gamboni, R.; Chen, S.; Chen, W.; Jagoe, C. T.; Kinder, F. R. J.; Loo, M.; Prasad, K.; Repič, O.; Shieh, W.-C.; Wang, R.-M.; Waykole, L.; Xu, D. D.; Xue, S. *Org. Process Res. Dev.* **2004**, *8*, 92–100.
- (25) Mickel, S. J.; Sedelmeier, G. H.; Niederer, D.; Schuerch, F.; Grimler, D.; Koch, G.; Daeffler, R.; Osmani, A.; Hirni, A.; Schaer, K.; Gamboni, R.; Bach, A.; Chaudhary, A.; Chen, S.; Chen, W.; Hu, B.; Jagoe, C. T.; Kim, H.-Y.; Kinder, F. R.; Liu, Y.; Lu, Y.; McKenna, J.; Prashad, M.; Ramsey, T. M.; Repič, O.; Rogers, L.; Shieh, W.-C.; Wang, R.-M.; Waykole, L. *Org. Process Res. Dev.* **2004**, *8*, 101–106.
- (26) Mickel, S. J.; Sedelmeier, G. H.; Niederer, D.; Schuerch, F.; Koch, G.; Kuesters, E.; Daeffler, R.; Osmani, A.; Seeger-Weibel, M.; Schmid, E.; Hirni, A.; Schaer, K.; Gamboni, R.; Bach, A.; Chen, S.; Chen, W.; Geng, P.; Jagoe, C. T.; Kinder, F. R.; Lee, G. T.;

- McKenna, J.; Ramsey, T. M.; Repič, O.; Rogers, L.; Shieh, W.-C.; Wang, R.-M.; Waykole, L. *Org. Process Res. Dev.* **2004**, *8*, 107–112.
- (27) Mickel, S. J.; Sedelmeier, G. H.; Niederer, D.; Schuerch, F.; Seger, M.; Schreiner, K.; Daeffler, R.; Osmani, A.; Bixel, D.; Loiseleur, O.; Cercus, J.; Stettler, H.; Schaer, K.; Gamboni, R.; Bach, A.; Chen, G.-P.; Chen, W.; Geng, P.; Lee, G. T.; Loeser, E.; McKenna, J.; Kinder, F. R.; Konigsberger, K.; Prasad, K.; Ramsey, T. M.; Reel, N.; Repič, O.; Rogers, L.; Shieh, W.-C.; Wang, R.-M.; Waykole, L.; Xue, S.; Florence, G. J.; Paterson, I. *Org. Process Res. Dev.* **2004**, *8*, 113–121.
- (28) Mickel, S. J.; Niederer, D.; Daeffler, R.; Osmani, A.; Kuesters, E.; Schmid, E.; Schaer, K.; Gamboni, R.; Chen, W.; Loeser, E.; Kinder, F. R.; Konigsberger, K.; Prasad, K.; Ramsey, T. M.; Repič, O.; Wang, R.-M.; Florence, G.; Lyothier, I.; Paterson, I. *Org. Process Res. Dev.* **2004**, *8*, 122–130.
- (29) Rohena, C. C.; Mooberry, S. L. *Nat. Prod. Rep.* **2014**, *31*, 335–355.
- (30) Chari, R. V. J.; Miller, M. L.; Widdison, W. C. *Angew. Chemie Int. Ed.* **2014**, *53*, 3796–3827.
- (31) Savage, D. G.; Antman, K. H. *N. Engl. J. Med.* **2002**, *346*, 683–693.
- (32) Jackson, S. E.; Chester, J. D. *Int. J. Cancer* **2015**, *137*, 262–266.
- (33) Palanca-Wessels, M. C.; Press, O. W. *Blood* **2014**, *123*, 2293–2301.
- (34) Casi, G.; Neri, D. *Mol. Pharm.* **2015**, *12*, 1880–1884.
- (35) Beijing Puhua International Hospital: Targeted therapy. 2018; <http://puhuahospital.com/treatments/cancer/targeted>.
- (36) Jain, N.; Smith, S. W.; Ghone, S.; Tomczuk, B. *Pharm. Res.* **2015**, *32*, 3526–3540.
- (37) Wang, Y.-J.; Li, Y.-Y.; Liu, X.-Y.; Lu, X.-L.; Cao, X.; Jiao, B.-H. *Mar. Drugs* **2017**, *15*, 18–45.
- (38) Senter, P. D.; Sievers, E. L. *Nat. Biotechnol.* **2012**, *30*, 631–637.
- (39) Casi, G.; Neri, D. *J. Med. Chem.* **2015**, *58*, 8751–8761.
- (40) Singh, S. K.; Luisi, D. L.; Pak, R. H. *Pharm. Res.* **2015**, *32*, 3541–3571.
- (41) Thomas, A.; Teicher, B. A.; Hassan, R. *Lancet Oncol.* **2016**, *17*, 254–262.

- (42) Agarwal, P.; Bertozzi, C. R. *Bioconjug. Chem.* **2015**, *26*, 176–192.
- (43) Kline, T.; Steiner, A. R.; Penta, K.; Sato, A. K.; Hallam, T. J.; Yin, G. *Pharm. Res.* **2015**, *32*, 3480–3493.
- (44) Axup, J. Y.; Bajjuri, K. M.; Ritland, M.; Hutchins, B. M.; Kim, C. H.; Kazane, S. A.; Halder, R.; Forsyth, J. S.; Santidrian, A. F.; Stafin, K.; Lu, Y.; Tran, H.; Seller, A. J.; Biroc, S. L.; Szydluk, A.; Pinkstaff, J. K.; Tian, F.; Sinha, S. C.; Felding-Habermann, B.; Smider, V. V.; Schultz, P. G. *Proc. Natl. Acad. Sci. U. S. A.* **2012**, *109*, 16101–16106.
- (45) Chudasama, V.; Maruani, A.; Caddick, S. *Nat. Chem.* **2016**, *8*, 114–119.
- (46) Srinivasarao, M.; Galliford, C. V.; Low, P. S. *Nat. Rev. Drug Discov.* **2015**, *14*, 203–219.
- (47) McCombs, J. R.; Owen, S. C. *AAPS J.* **2015**, *17*, 339–351.
- (48) Shah, D. K.; Haddish-Berhane, N.; Betts, A. *J. Pharmacokinet. Pharmacodyn.* **2012**, *39*, 643–659.
- (49) Singh, A. P.; Shin, Y. G.; Shah, D. K. *Pharm. Res.* **2015**, *32*, 3508–3525.
- (50) Villa, A.; Trachsel, E.; Kaspar, M.; Schliemann, C.; Sommariva, R.; Rybak, J.-N.; Rösli, C.; Borsi, L.; Neri, D. *Int. J. Cancer* **2008**, *122*, 2405–2413.
- (51) Linghu, X.; Segraves, N. L.; Abramovich, I.; Wong, N.; Müller, B.; Neubauer, N.; Fantasia, S.; Rieth, S.; Bachmann, S.; Jansen, M.; Sowell, C. G.; Askin, D.; Koenig, S. G.; Gosselin, F. *Chem. Eur. J.* **2018**, *24*, 2837–2840.
- (52) Lehar, S. M.; Pillow, T.; Xu, M.; Staben, L.; Kajihara, K. K.; Vandlen, R.; DePalatis, L.; Raab, H.; Hazenbos, W. L.; Hiroshi Morisaki, J.; Kim, J.; Park, S.; Darwish, M.; Lee, B.-C.; Hernandez, H.; Loyet, K. M.; Lupardus, P.; Fong, R.; Yan, D.; Chalouni, C.; Luis, E.; Khalfin, Y.; Plise, E.; Cheong, J.; Lyssikatos, J. P.; Strandh, M.; Koefoed, K.; Andersen, P. S.; Flygare, J. A.; Wah Tan, M.; Brown, E. J.; Mariathasan, S. *Nature* **2015**, *527*, 323–328.
- (53) Kita, M.; Hirayama, Y.; Yoneda, K.; Yamagishi, K.; Chinen, T.; Usui, T.; Sumiya, E.; Uesugi, M.; Kigoshi, H. *J. Am. Chem. Soc.* **2013**, *135*, 18089–18095.
- (54) Rudman, W. *Aplysia kurodai* (Baba, 1937). 2002; <http://www.seaslugforum.net/factsheet/aplykuro>.

- (55) Yamada, K.; Ojika, M.; Kigoshi, H.; Suenaga, K. In *Drugs from the Sea*; Fusetani, N., Ed.; Karger: Basel, 2000; pp 59–73.
- (56) Ojika, M.; Kigoshi, H.; Suenaga, K.; Imamura, Y.; Yoshikawa, K.; Ishigaki, T.; Sakakura, A.; Mutou, T.; Yamada, K. *Tetrahedron* **2012**, *68*, 982–987.
- (57) Yamada, K.; Ojika, M.; Kigoshi, H.; Suenaga, K. *Nat. Prod. Rep.* **2009**, *26*, 27–43.
- (58) Ojika, M.; Kigoshi, H.; Ishigaki, T.; Yamada, K. *Tetrahedron Lett.* **1993**, *34*, 8501–8504.
- (59) Ojika, M.; Kigoshi, H.; Ishigaki, T.; Nisiwaki, M.; Tsukada, I.; Mizuta, K.; Yamada, K. *Tetrahedron Lett.* **1993**, *34*, 8505–8508.
- (60) Ojika, M.; Kigoshi, H.; Ishigaki, T.; Tsukada, I.; Tsuboi, T.; Ogawa, T.; Yamada, K. *J. Am. Chem. Soc.* **1994**, *116*, 7441–7442.
- (61) Kigoshi, H.; Ojika, M.; Suenaga, K.; Mutou, T.; Hirano, J.; Sakakura, A.; Ogawa, T.; Nisiwaki, M.; Yamada, K. *Tetrahedron Lett.* **1994**, *35*, 1247–1250.
- (62) Kigoshi, H.; Ojika, M.; Ishigaki, T.; Suenaga, K.; Mutou, T.; Sakakura, A.; Ogawa, T.; Yamada, K. *J. Am. Chem. Soc.* **1994**, *116*, 7443–7444.
- (63) Suenaga, K.; Ishigaki, T.; Sakakura, A.; Kigoshi, H.; Yamada, K. *Tetrahedron Lett.* **1995**, *36*, 5053–5056.
- (64) Ojika, M.; Kigoshi, H.; Yoshida, Y.; Ishigaki, T.; Nisiwaki, M.; Tsukada, I.; Arakawa, M.; Ekimoto, H.; Yamada, K. *Tetrahedron* **2007**, *63*, 3138–3167.
- (65) Crews, P.; Gerwick, W.; Schmitz, F.; France, D.; Bair, K.; Wright, A.; Hallock, Y. *Pharm. Biol.* **2003**, *41*, 39–52.
- (66) Saito, S.; Watabe, S.; Ozaki, H.; Kigoshi, H.; Yamada, K.; Fusetani, N.; Karaki, H. *J. Biochem.* **1996**, *120*, 552–555.
- (67) Lodish, H. F. *Molecular cell biology*; W.H. Freeman, 2000; pp 779–815.
- (68) Hirata, K.; Muraoka, S.; Suenaga, K.; Kuroda, T.; Kato, K.; Tanaka, H.; Yamamoto, M.; Takata, M.; Yamada, K.; Kigoshi, H. *J. Mol. Biol.* **2006**, *356*, 945–954.
- (69) Kuroda, T.; Suenaga, K.; Sakakura, A.; Handa, T.; Okamoto, K.; Kigoshi, H. *Bioconjug. Chem.* **2006**, *17*, 524–529.

- (70) Kita, M.; Yoneda, K.; Hirayama, Y.; Yamagishi, K.; Saito, Y.; Sugiyama, Y.; Miwa, Y.; Ohno, O.; Morita, M.; Suenaga, K.; Kigoshi, H. *ChemBioChem* **2012**, *13*, 1754–1758.
- (71) Ohno, O.; Morita, M.; Kitamura, K.; Teruya, T.; Yoneda, K.; Kita, M.; Kigoshi, H.; Suenaga, K. *Bioorg. Med. Chem. Lett.* **2013**, *23*, 1467–1471.
- (72) Yeung, K.-S.; Paterson, I. *Angew. Chemie Int. Ed.* **2002**, *41*, 4632–4653.
- (73) Allingham, J. S.; Klenchin, V. A.; Rayment, I. *Cell. Mol. Life Sci.* **2006**, *63*, 2119–2134.
- (74) Mitchison, T. J.; Cramer, L. P. *Cell* **1996**, *84*, 371–379.
- (75) Tanaka, J.; Yan, Y.; Choi, J.; Bai, J.; Klenchin, V. A.; Rayment, I.; Marriott, G. *Proc. Natl. Acad. Sci. U. S. A.* **2003**, *100*, 13851–13856.
- (76) Kita, M.; Hirayama, Y.; Sugiyama, M.; Kigoshi, H. *Angew. Chemie Int. Ed.* **2011**, *50*, 9871–9874.
- (77) Kigoshi, H.; Suenaga, K.; Mutou, T.; Ishigaki, T.; Atsumi, T.; Ishiwata, H.; Sakakura, A.; Ogawa, T.; Ojika, M.; Yamada, K. *J. Org. Chem.* **1996**, *61*, 5326–5351.
- (78) Suenaga, K.; Kamei, N.; Okugawa, Y.; Takagi, M.; Akao, A.; Kigoshi, H.; Yamada, K. *Bioorg. Med. Chem. Lett.* **1997**, *7*, 269–274.
- (79) Kigoshi, H.; Suenaga, K.; Takagi, M.; Akao, A.; Kanematsu, K.; Kamei, N.; Okugawa, Y.; Yamada, K. *Tetrahedron* **2002**, *58*, 1075–1102.
- (80) Suenaga, K.; Kimura, T.; Kuroda, T.; Matsui, K.; Miya, S.; Kuribayashi, S.; Sakakura, A.; Kigoshi, H. *Tetrahedron* **2006**, *62*, 8278–8290.
- (81) Kitamura, K.; Teruya, T.; Kuroda, T.; Kigoshi, H.; Suenaga, K. *Bioorg. Med. Chem. Lett.* **2009**, *19*, 1896–1898.
- (82) Kobayashi, K.; Fujii, Y.; Hirayama, Y.; Kobayashi, S.; Hayakawa, I.; Kigoshi, H. *Org. Lett.* **2012**, *14*, 1290–1293.
- (83) Kobayashi, K.; Fujii, Y.; Hayakawa, I.; Kigoshi, H. *Org. Lett.* **2011**, *13*, 900–903.
- (84) Suenaga, K.; Miya, S.; Kuroda, T.; Handa, T.; Kanematsu, K.; Sakakura, A.; Kigoshi, H. *Tetrahedron Lett.* **2004**, *45*, 5383–5386.
- (85) Kita, M.; Kigoshi, H. *Nat. Prod. Rep.* **2015**, *32*, 534–542.

- (86) Paterson, I.; Ashton, K.; Britton, R.; Cecere, G.; Chouraqui, G.; Florence, G. J.; Knust, H.; Stafford, J. *Chem. Asian J.* **2008**, *3*, 367–387.
- (87) Saito, S.; Karaki, H. *Clin. Exp. Pharmacol. Physiol.* **1996**, *23*, 743–746.
- (88) Ishibashi, M.; Moore, R. E.; Patterson, G. M. L.; Xu, C.; Clardy, J. *J. Org. Chem.* **1986**, *51*, 5300–5306.
- (89) Spector, I.; Braet, F.; Shochet, N. R.; Bubb, M. R. *Microsc. Res. Tech.* **1999**, *47*, 18–37.
- (90) Tanaka, J.; Craig Blain, J.; Allingham, J. S. *Chem. Biol.* **2008**, *15*, 205–207.
- (91) Paterson, I.; Fink, S. J.; Lee, L. Y. W.; Atkinson, S. J.; Blakey, S. B. *Org. Lett.* **2013**, *15*, 3118–3121.
- (92) Anžiček, N.; Williams, S.; Housden, M. P.; Paterson, I. *Org. Biomol. Chem.* **2018**, *16*, 1343–1350.
- (93) Marshall, J. A.; Grant, C. M. *J. Org. Chem.* **1999**, *64*, 696–697.
- (94) Marshall, J. A.; Johns, B. A. *J. Org. Chem.* **2000**, *65*, 1501–1510.
- (95) Calter, M. A.; Guo, X. *Tetrahedron* **2002**, *58*, 7093–7100.
- (96) Calter, M. A.; Zhou, J. *Tetrahedron Lett.* **2004**, *45*, 4847–4850.
- (97) Calter, M. A. *J. Org. Chem.* **1996**, *61*, 8006–8007.
- (98) Calter, M. A.; Guo, X.; Liao, W. *Org. Lett.* **2001**, *3*, 1499–1501.
- (99) Calter, M. A.; Orr, R. K.; Song, W. *Org. Lett.* **2003**, *5*, 4745–4748.
- (100) Calter, M. A.; Song, W.; Zhou, J. *J. Org. Chem.* **2004**, *69*, 1270–1275.
- (101) El-Awa, A.; Fuchs, P. *Org. Lett.* **2006**, *8*, 2905–2908.
- (102) Hong, W. P.; Noshi, M. N.; El-Awa, A.; Fuchs, P. L. *Org. Lett.* **2011**, *13*, 6342–6345.
- (103) Bobinski, T. P.; Fuchs, P. L. *Tetrahedron Lett.* **2015**, *56*, 4155–4158.
- (104) Torres, E.; Chen, Y.; Kim, I. C.; Fuchs, P. L. *Angew. Chemie Int. Ed.* **2003**, *42*, 3124–3131.
- (105) Noshi, M. N.; El-awa, A.; Torres, E.; Fuchs, P. L. *J. Am. Chem. Soc.* **2007**, *129*, 11242–11247.

- (106) Noshi, M. N.; El-Awa, A.; Fuchs, P. L. *J. Org. Chem.* **2008**, *73*, 3274–3277.
- (107) Hayakawa, I.; Saito, K.; Matsumoto, S.; Kobayashi, S.; Taniguchi, A.; Kobayashi, K.; Fujii, Y.; Kaneko, T.; Kigoshi, H. *Org. Biomol. Chem.* **2017**, *15*, 124–131.
- (108) Williams, S. PhD thesis: Total synthesis of the marine natural products leiodermatolide and the aplyronines. Dissertation, University of Cambridge, 2015.
- (109) Paterson, I.; Blakey, S. B.; Cowden, C. J. *Tetrahedron Lett.* **2002**, *43*, 6005–6008.
- (110) Paterson, I.; Tillyer, R. D. *Tetrahedron Lett.* **1992**, *33*, 4233–4236.
- (111) Fink, S. J. PhD thesis: A total synthesis of aplyronine C and related analogues. Dissertation, University of Cambridge, 2012.
- (112) Anžiček, N. PhD thesis: Studies towards a second-generation synthesis of the aplyronines. Dissertation, University of Cambridge, 2017.
- (113) Paterson, I.; Cowden, C. J.; Woodrow, M. D. *Tetrahedron Lett.* **1998**, *39*, 6037–6040.
- (114) Paterson, I.; Woodrow, M. D.; Cowden, C. J. *Tetrahedron Lett.* **1998**, *39*, 6041–6044.
- (115) Jaschinski, T.; Hiersemann, M. *Org. Lett.* **2012**, *14*, 4114–4117.
- (116) Omura, K.; Swern, D. *Tetrahedron* **1978**, *34*, 1651–1660.
- (117) Zimmerman, H. E.; Traxler, M. D. *J. Am. Chem. Soc.* **1957**, *79*, 1920–1923.
- (118) Lee, L. Y. W. PhD thesis: Studies towards a total synthesis of the aplyronines as promising anticancer agents. Dissertation, University of Cambridge, 2010.
- (119) Paterson, I.; Lister, M. A. *Tetrahedron Lett.* **1988**, *29*, 585–588.
- (120) Solsona, J. G.; Nebot, J.; Romea, P.; Urpí, F. *J. Org. Chem.* **2005**, *70*, 6533–6536.
- (121) Dale, J. A.; Dull, D. L.; Mosher, H. S. *J. Org. Chem.* **1969**, *34*, 2543–2549.
- (122) Dale, J. A.; Mosher, H. S. *J. Am. Chem. Soc.* **1973**, *95*, 512–519.
- (123) Ohtani, I.; Kusumi, T.; Ishitsuka, M. O.; Kakisawa, H. *Tetrahedron Lett.* **1989**, *30*, 3147–3150.
- (124) Ohtani, I.; Kusumi, T.; Kashman, Y.; Kakisawa, H. *J. Am. Chem. Soc.* **1991**, *113*, 4092–4096.

- (125) Ohtani, I.; Kusumi, T.; Kashman, Y.; Kakisawa, H. *J. Org. Chem.* **1991**, *56*, 1296–1298.
- (126) Hoye, T. R.; Jeffrey, C. S.; Shao, F. *Nat. Protoc.* **2007**, *2*, 2451–2458.
- (127) Neises, B.; Steglich, W. *Angew. Chemie Int. Ed.* **1978**, *17*, 522–524.
- (128) Evans, D. A.; Hoveyda, A. H. *J. Am. Chem. Soc.* **1990**, *112*, 6447–6449.
- (129) Porter, R. J. CPGS: Synthetic analogues of the aplyronines as cytotoxic payloads for antibody–drug conjugates. Dissertation, University of Cambridge, 2016.
- (130) Howard, K. T.; Chisholm, J. D. *Org. Prep. Proced. Int.* **2016**, *48*, 1–36.
- (131) Porter, R. J. PhD thesis: manuscript in preparation. Dissertation, University of Cambridge, 2019.
- (132) Liu, C.; Richards, M. R.; Lowary, T. L. *Org. Biomol. Chem.* **2011**, *9*, 165–176.
- (133) Lam, N. Y. S. PhD thesis: manuscript in preparation. Dissertation, University of Cambridge, 2019.
- (134) Anketell, M. CPGS: Studies towards the total synthesis of the actinoallolides. Dissertation, University of Cambridge, 2017.
- (135) Garegg, P. J.; Samuelsson, B. *J. Chem. Soc. Chem. Commun.* **1979**, 978–980.
- (136) Horita, K.; Yoshioka, T.; Tanaka, T.; Oikawa, Y.; Yonemitsu, O. *Tetrahedron* **1986**, *42*, 3021–3028.
- (137) Paterson, I.; Cowden, C. J.; Rahn, V. S.; Woodrow, M. D. *Synlett* **1998**, 915–917.
- (138) Grieco, P. A.; Pogonowski, C. S. *J. Am. Chem. Soc.* **1973**, *95*, 3071–3072.
- (139) Goodman, J. M.; Paton, R. S. *Chem. Commun.* **2007**, 2124–2126.
- (140) Paton, R. S.; Goodman, J. M. *J. Org. Chem.* **2008**, *73*, 1253–1263.
- (141) Paton, R. S. Computational studies on boron-mediated C-C bond formation. Ph.D. thesis, University of Cambridge, 2008.
- (142) Rychnovsky, S. D.; Kim, J. *J. Org. Chem.* **1994**, *59*, 2659–2660.
- (143) Woodrow, M. D. PhD thesis: Studies towards a total synthesis of the aplyronines. Dissertation, University of Cambridge, 1998.

- (144) Housden, M. P. unpublished work. Ph.D. thesis, University of Cambridge, 2015.
- (145) Wadsworth, W. S.; Emmons, W. D. *J. Am. Chem. Soc.* **1961**, *83*, 1733–1738.
- (146) Paterson, I.; Yeung, K.-S.; Smaill, J. B. *Synlett* **1993**, *10*, 774–776.
- (147) Alvarez-Ibarra, C.; Arias, S.; Bañón, G.; Fernández, M. J.; Rodríguez, M.; Sinisterra, V. *J. Chem. Soc., Chem. Commun.* **1987**, 1509–1511.
- (148) Nicolaou, K. C.; Heretsch, P.; Nakamura, T.; Rudo, A.; Murata, M.; Konoki, K. *J. Am. Chem. Soc.* **2014**, *136*, 16444–16451.
- (149) Crimmins, M. T.; Shamszad, M.; Mattson, A. E. *Org. Lett.* **2010**, *12*, 2614–2617.
- (150) Winbush, S. M.; Mergott, D. J.; Roush, W. R. *J. Org. Chem.* **2008**, *73*, 1818–1829.
- (151) Hirao, A.; Itsuno, S.; Nakahama, S.; Yamazaki, N. *J. Chem. Soc. Chem. Commun.* **1981**, 315–317.
- (152) Corey, E. J.; Bakshi, R. K.; Shibata, S. *J. Am. Chem. Soc.* **1987**, *109*, 5551–5553.
- (153) Corey, E. J.; Bakshi, R. K.; Shibata, S.; Chen, C. P.; Singh, V. K. *J. Am. Chem. Soc.* **1987**, *109*, 7925–7926.
- (154) Corey, E. J.; Helal, C. J. *Angew. Chemie Int. Ed.* **1998**, *37*, 1986–2012.
- (155) Lindgren, B. O.; Nilsson, T. *Acta Chem. Scand.* **1973**, *27*, 888–890.
- (156) Bal, B. S.; Childers, W. E.; Pinnick, H. W. *Tetrahedron* **1981**, *37*, 2091–2096.
- (157) Kraus, G. A.; Roth, B. *J. Org. Chem.* **1980**, *45*, 4825–4830.
- (158) Kraus, G. A.; Taschner, M. J. *J. Org. Chem.* **1980**, *45*, 1175–1176.
- (159) Inanaga, J.; Hirata, K.; Saeki, H.; Katsuki, T.; Yamaguchi, M. *Bull. Chem. Soc. Jpn.* **1979**, *52*, 1989–1993.
- (160) Hikota, M.; Sakurai, Y.; Horita, K.; Yonemitsu, O. *Tetrahedron Lett.* **1990**, *31*, 6367–6370.
- (161) Dhimitruka, I.; SantaLucia, J. J. *Org. Lett.* **2006**, *8*, 47–50.
- (162) Tsakos, M.; Schaffert, E. S.; Clement, L. L.; Villadsen, N. L.; Poulsen, T. B. *Nat. Prod. Rep.* **2015**, *32*, 605–632.

- (163) Cergol, K. M.; Coster, M. J. *Nat. Protoc.* **2007**, 2, 2568–2573.
- (164) Dalby, S. M.; Goodwin-Tindall, J.; Paterson, I. *Angew. Chemie Int. Ed.* **2013**, 52, 6517–21.
- (165) Paterson, I.; Chen, D. Y.-K.; Coster, M. J.; Aceña, J. L.; Bach, J.; Wallace, D. J. *Org. Biomol. Chem.* **2005**, 3, 2431–2440.
- (166) Burgess, E. M.; Penton, H. R.; Taylor, E. A. *J. Org. Chem.* **1973**, 38, 26–31.
- (167) Atkins, G. M.; Burgess, E. M. *J. Am. Chem. Soc.* **1968**, 90, 4744–4745.
- (168) Mahoney, W. S.; Brestensky, D. M.; Stryker, J. M. *J. Am. Chem. Soc.* **1988**, 110, 291–293.
- (169) Bezman, S. A.; Churchill, M. R.; Osborn, J. A.; Wormald, J. *J. Am. Chem. Soc.* **1971**, 93, 2063–2065.
- (170) Churchill, M. R.; Bezman, S. A.; Osborn, J. A.; Wormald, J. *Inorg. Chem.* **1972**, 11, 1818–1825.
- (171) Rendler, S.; Oestreich, M. *Angew. Chemie Int. Ed.* **2007**, 46, 498–504.
- (172) Chiu, P.; Li, Z.; Fung, K. C. *Tetrahedron Lett.* **2003**, 44, 455–457.
- (173) Lipshutz, B. H.; Keith, J.; Papa, P.; Vivian, R. *Tetrahedron Lett.* **1998**, 39, 4627–4630.
- (174) Lee, D.; Yun, J. *Tetrahedron Lett.* **2004**, 45, 5415–5417.
- (175) Baker, B. A.; Bošković, Ž. V.; Lipshutz, B. H. *Org. Lett.* **2008**, 10, 289–292.
- (176) Lee, D.; Yun, J. *Tetrahedron Lett.* **2005**, 46, 2037–2039.
- (177) Boden, E. P.; Keck, G. E. *J. Org. Chem.* **1985**, 50, 2394–2395.
- (178) Oishi, T.; Nakata, T. *Acc. Chem. Res.* **1984**, 17, 338–344.
- (179) Mitsunobu, O.; Yamada, M.; Mukaiyama, T. *Bull. Chem. Soc. Jpn.* **1967**, 40, 935–939.
- (180) Mitsunobu, O.; Yamada, M. *Bull. Chem. Soc. Jpn.* **1967**, 40, 2380–2382.
- (181) Pereira, J. H.; Petchprayoon, C.; Hoepker, A. C.; Moriarty, N. W.; Fink, S. J.; Cecere, G.; Paterson, I.; Adams, P. D.; Marriott, G. *ChemMedChem* **2014**, 9, 2286–2293.
- (182) Kita, M. Personal communication at Gordon Research Conference on Marine Natural Products, Ventura, CA. 2018.

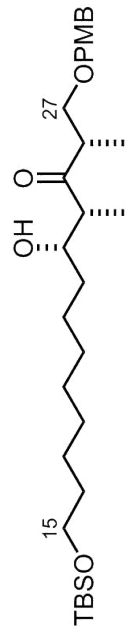
- (183) Ohyoshi, T.; Takano, A.; Namiki, M.; Ogura, T.; Miyazaki, Y.; Ebihara, Y.; Takeno, K.; Hayakawa, I.; Kigoshi, H. *Chem. Commun.* **2018**, Advance Online (doi: 10.1039/C8CC04613A).
- (184) Ducry, L.; Stump, B. *Bioconjug. Chem.* **2010**, *21*, 5–13.
- (185) Nani, R. R.; Gorka, A. P.; Nagaya, T.; Kobayashi, H.; Schnermann, M. J. *Angew. Chemie Int. Ed.* **2015**, *54*, 13635–13638.
- (186) Ho, S.; Sackett, D. L.; Leighton, J. L. *J. Am. Chem. Soc.* **2015**, *137*, 14047–14050.
- (187) Pillow, T. H.; Tien, J.; Parsons-Reponete, K. L.; Bhakta, S.; Li, H.; Staben, L. R.; Li, G.; Chuh, J.; Fourie-O'Donohue, A.; Darwish, M.; Yip, V.; Liu, L.; Leipold, D. D.; Su, D.; Wu, E.; Spencer, S. D.; Shen, B.-Q.; Xu, K.; Kozak, K. R.; Raab, H.; Vandlen, R.; Lewis Phillips, G. D.; Scheller, R. H.; Polakis, P.; Sliwkowski, M. X.; Flygare, J. A.; Junutula, J. R. *J. Med. Chem.* **2014**, *57*, 7890–7899.
- (188) Staben, L. R.; Koenig, S. G.; Lehar, S. M.; Vandlen, R.; Zhang, D.; Chuh, J.; Yu, S.-F.; Ng, C.; Guo, J.; Liu, Y.; Fourie-O'Donohue, A.; Go, M.; Linghu, X.; Segraves, N. L.; Wang, T.; Chen, J.; Wei, B.; Lewis Phillips, G. D.; Xu, K.; Kozak, K. R.; Mariathasan, S.; Flygare, J. A.; Pillow, T. H. *Nat. Chem.* **2016**, *8*, 1112–1119.
- (189) Rodrigues, T.; Bernardes, G. J. L. *Nat. Chem.* **2016**, *8*, 1088–1090.
- (190) Burke, P. J.; Hamilton, J. Z.; Pires, T. A.; Setter, J. R.; Hunter, J. H.; Cochran, J. H.; Waight, A. B.; Gordon, K. A.; Toki, B. E.; Emmerton, K. K.; Zeng, W.; Stone, I. J.; Senter, P. D.; Lyon, R. P.; Jeffrey, S. C. *Mol. Cancer Ther.* **2016**, *15*, 938–945.
- (191) Gnaim, S.; Shabat, D. *Acc. Chem. Res.* **2014**, *47*, 2970–2984.
- (192) Erez, R.; Shabat, D. *Org. Biomol. Chem.* **2008**, *6*, 2669.
- (193) Baell, J. B.; Holloway, G. A. *J. Med. Chem.* **2010**, *53*, 2719–2740.
- (194) Baell, J. B. *J. Nat. Prod.* **2016**, *79*, 616–628.
- (195) Bisson, J.; McAlpine, J. B.; Friesen, J. B.; Chen, S.-N.; Graham, J.; Pauli, G. F. *J. Med. Chem.* **2016**, *59*, 1671–1690.
- (196) Staben, L. R.; Yu, S.-F.; Chen, J.; Yan, G.; Xu, Z.; Del Rosario, G.; Lau, J. T.; Liu, L.; Guo, J.; Zheng, B.; dela Cruz-Chuh, J.; Lee, B.-C.; Ohri, R.; Cai, W.; Zhou, H.

- Kozak, K. R.; Xu, K.; Lewis Phillips, G. D.; Lu, J.; Wai, J.; Polson, A. G.; Pillow, T. H. *ACS Med. Chem. Lett.* **2017**, *8*, 1037–1041.
- (197) Kita, M.; Hirayama, Y.; Yamagishi, K.; Yoneda, K.; Fujisawa, R.; Kigoshi, H. *J. Am. Chem. Soc.* **2012**, *134*, 20314–20317.
- (198) Lyon, R. P.; Bovee, T. D.; Doronina, S. O.; Burke, P. J.; Hunter, J. H.; Neff-LaFord, H. D.; Jonas, M.; Anderson, M. E.; Setter, J. R.; Senter, P. D. *Nat. Biotechnol.* **2015**, *33*, 733–735.
- (199) Christie, R. J.; Fleming, R.; Bezabeh, B.; Woods, R.; Mao, S.; Harper, J.; Joseph, A.; Wang, Q.; Xu, Z.-Q.; Wu, H.; Gao, C.; Dimasi, N. *J. Control. Release* **2015**, *220*, 660–670.
- (200) Lyon, R. P.; Setter, J. R.; Bovee, T. D.; Doronina, S. O.; Hunter, J. H.; Anderson, M. E.; Balasubramanian, C. L.; Duniho, S. M.; Leiske, C. I.; Li, F.; Senter, P. D. *Nat. Biotechnol.* **2014**, *32*, 1059–1062.
- (201) Fontaine, S. D.; Reid, R.; Robinson, L.; Ashley, G. W.; Santi, D. V. *Bioconjug. Chem.* **2015**, *26*, 145–152.
- (202) Hallam, T. J.; Wold, E.; Wahl, A.; Smider, V. V. *Mol. Pharm.* **2015**, *12*, 1848–1862.
- (203) Anami, Y.; Xiong, W.; Gui, X.; Deng, M.; Zhang, C. C.; Zhang, N.; An, Z.; Tsuchikama, K. *Org. Biomol. Chem.* **2017**, *15*, 5635–5642.
- (204) Walsh, S. CPGS: Design and synthesis of novel linkers for antibody-drug conjugates (ADCs). Dissertation, University of Cambridge, 2016.
- (205) Dannheim, F. CPGS: Design and synthesis of cysteine-bridging linkers for antibody-drug conjugates (ADCs). Dissertation, University of Cambridge, 2018.
- (206) Kwan, T. T.-L.; Boutureira, O.; Frye, E. C.; Walsh, S. J.; Gupta, M. K.; Wallace, S.; Wu, Y.; Zhang, F.; Sore, H. F.; Galloway, W. R. J. D.; Chin, J. W.; Welch, M.; Bernardes, G. J. L.; Spring, D. R. *Chem. Sci.* **2017**, *8*, 3871–3878.
- (207) Gaynord, J. CPGS: Design and synthesis of novel sequence-dependent bioconjugation linkers for antibody-drug conjugates (ADCs). Dissertation, University of Cambridge, 2017.
- (208) Bargh, J. CPGS: Design and synthesis of novel enzyme-cleavable linkers for antibody-drug conjugates (ADCs). Dissertation, University of Cambridge, 2017.

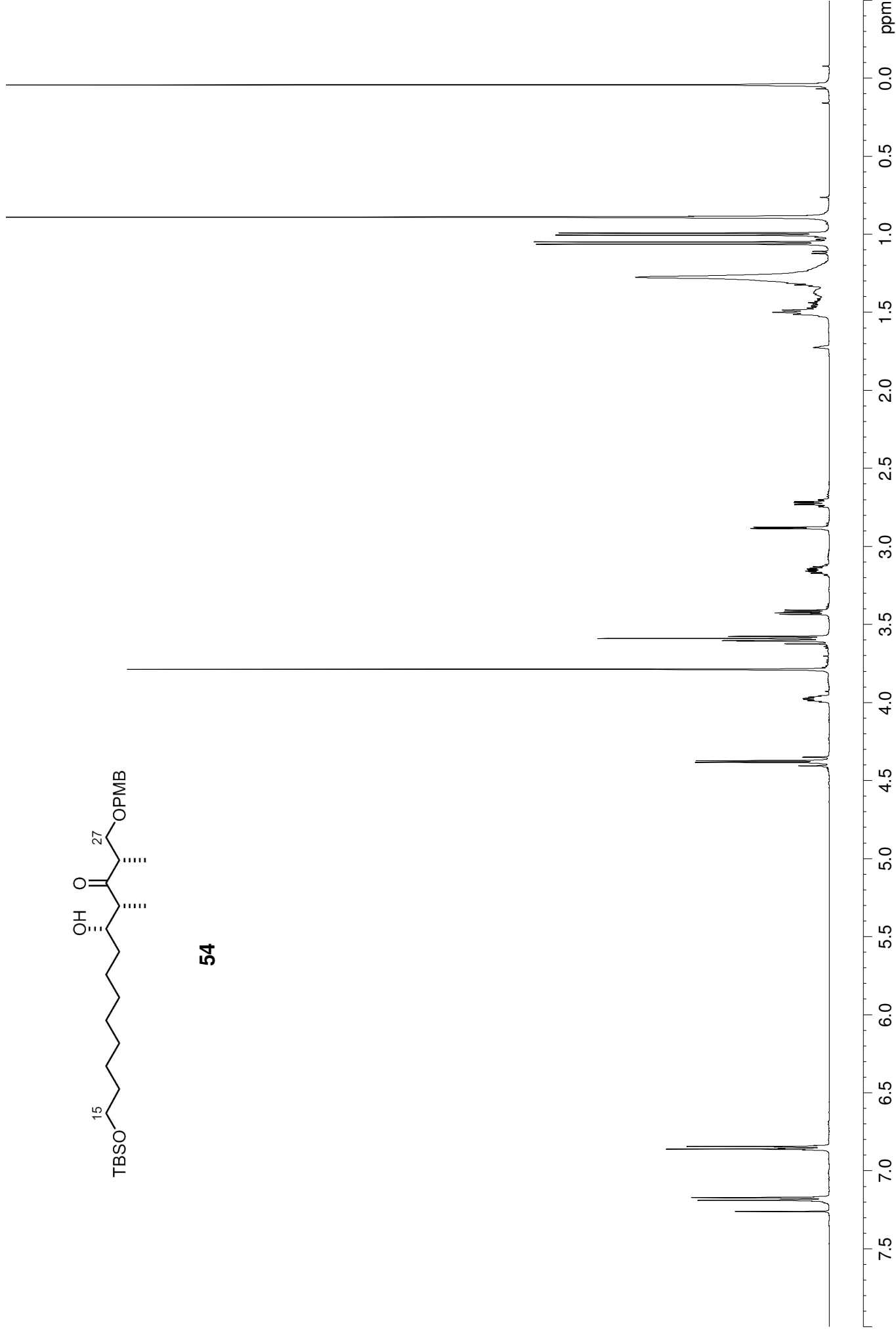
- (209) Altschuler, S. J.; Wu, L. F. *Cell* **2010**, *141*, 559–563.
- (210) Perrin, D. A.; Armarego, W. L. F. *Purification of Laboratory Reagents*; Pergamon Press: Oxford, 1988.
- (211) Wessel, H.-P.; Iversen, T.; Bundle, D. R. *J. Chem. Soc. Perkin Trans. 1* **1985**, 2247–2250.
- (212) Hong, R.; Chen, Y.; Deng, L. *Angew. Chemie Int. Ed.* **2005**, *44*, 3478–3481.
- (213) Böhme, H.; Raude, E. *Chem. Ber.* **1981**, *114*, 3421–3429.
- (214) Couture, A.; Deniau, E.; Grandclaude, P.; Woisel, P. *Tetrahedron* **1996**, *52*, 4433–4448.
- (215) Paterson, I.; Cowden, C. J.; Watson, C. *Synlett* **1996**, 209–211.
- (216) Li, L.; Huang, W.; Chen, L.; Dong, J.; Ma, X.; Peng, Y. *Angew. Chemie Int. Ed.* **2017**, *56*, 10539–10544.
- (217) Girard, P.; Namy, J. L.; Kagan, H. B. *J. Am. Chem. Soc.* **1980**, 2693–2698.
- (218) Imamoto, T.; Ono, M. *Chem. Lett.* **1987**, 501–502.
- (219) Gregg, C.; Perkins, M. V. *Tetrahedron* **2013**, *69*, 387–394.
- (220) Handa, M.; Scheidt, K. A.; Bossart, M.; Zheng, N.; Roush, W. R. *J. Org. Chem.* **2008**, *73*, 1031–1035.
- (221) Arai, N.; Chikaraishi, N.; Ikawa, M.; Åñmura, S.; Kuwajima, I. *Tetrahedron: Asymmetry* **2004**, *15*, 733–741.
- (222) Paterson, I.; Temal-Laïb, T. *Org. Lett.* **2002**, *4*, 2473–2476.
- (223) Diab, L.; Šmejkal, T.; Geier, J.; Breit, B. *Angew. Chemie Int. Ed.* **2009**, *48*, 8022–8026.
- (224) Cryle, M. J.; Hayes, P. Y.; De Voss, J. J. *Chem. Eur. J.* **2012**, *18*, 15994–15999.
- (225) Paterson, I.; Norcross, R. D.; Ward, R. A.; Romea, P.; Lister, M. A. *J. Am. Chem. Soc.* **1994**, *116*, 11287–11314.
- (226) Blakey, S. B. PhD thesis: Synthesis of an advanced macrocyclic intermediate for the aplyronines. Dissertation, University of Cambridge, 2002.

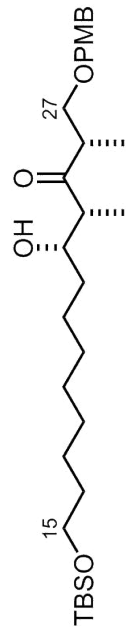
Appendix

Selected ^1H and ^{13}C NMR spectra

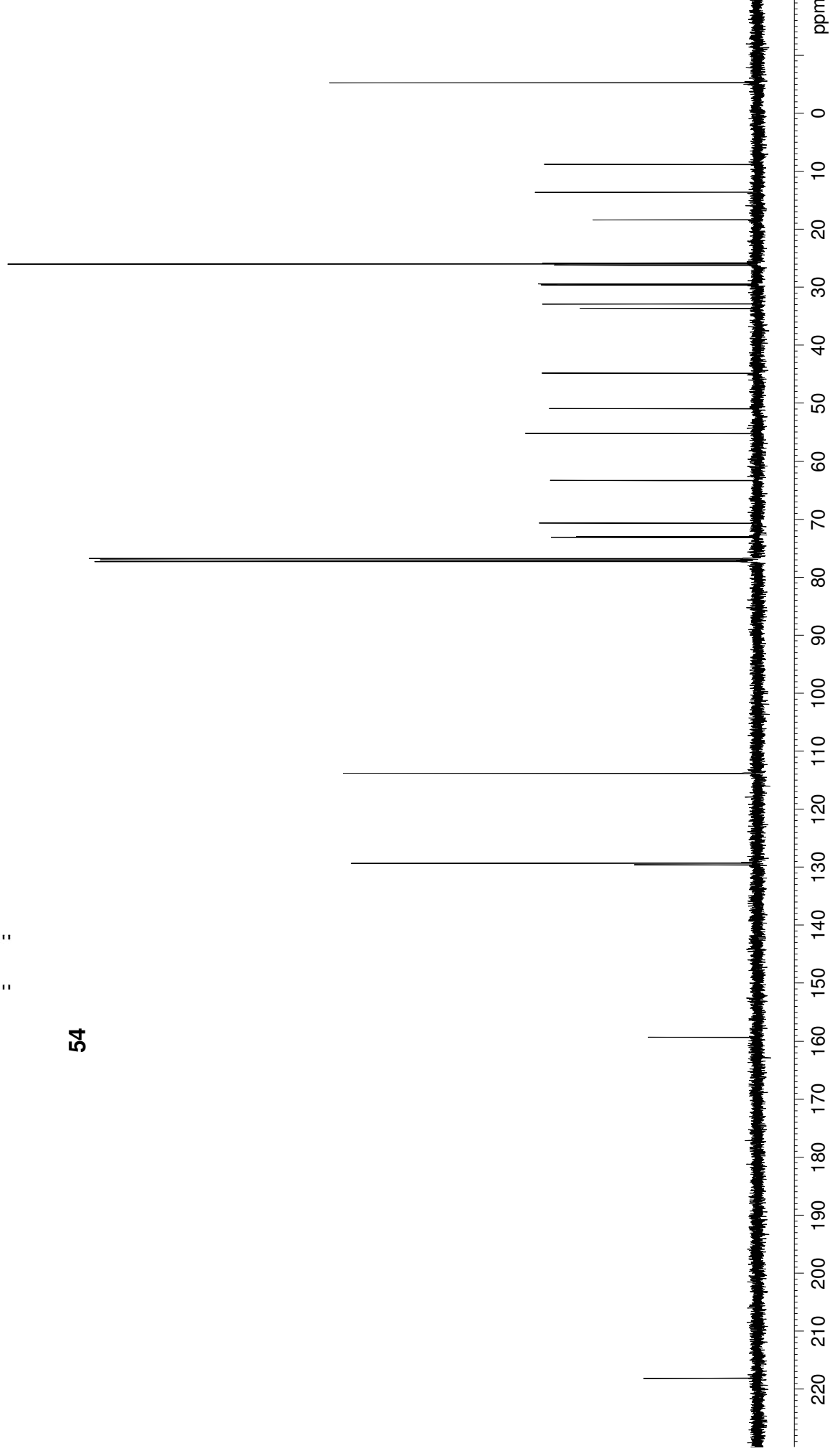


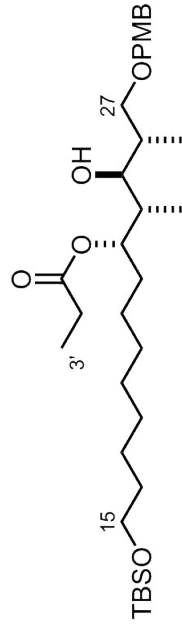
54



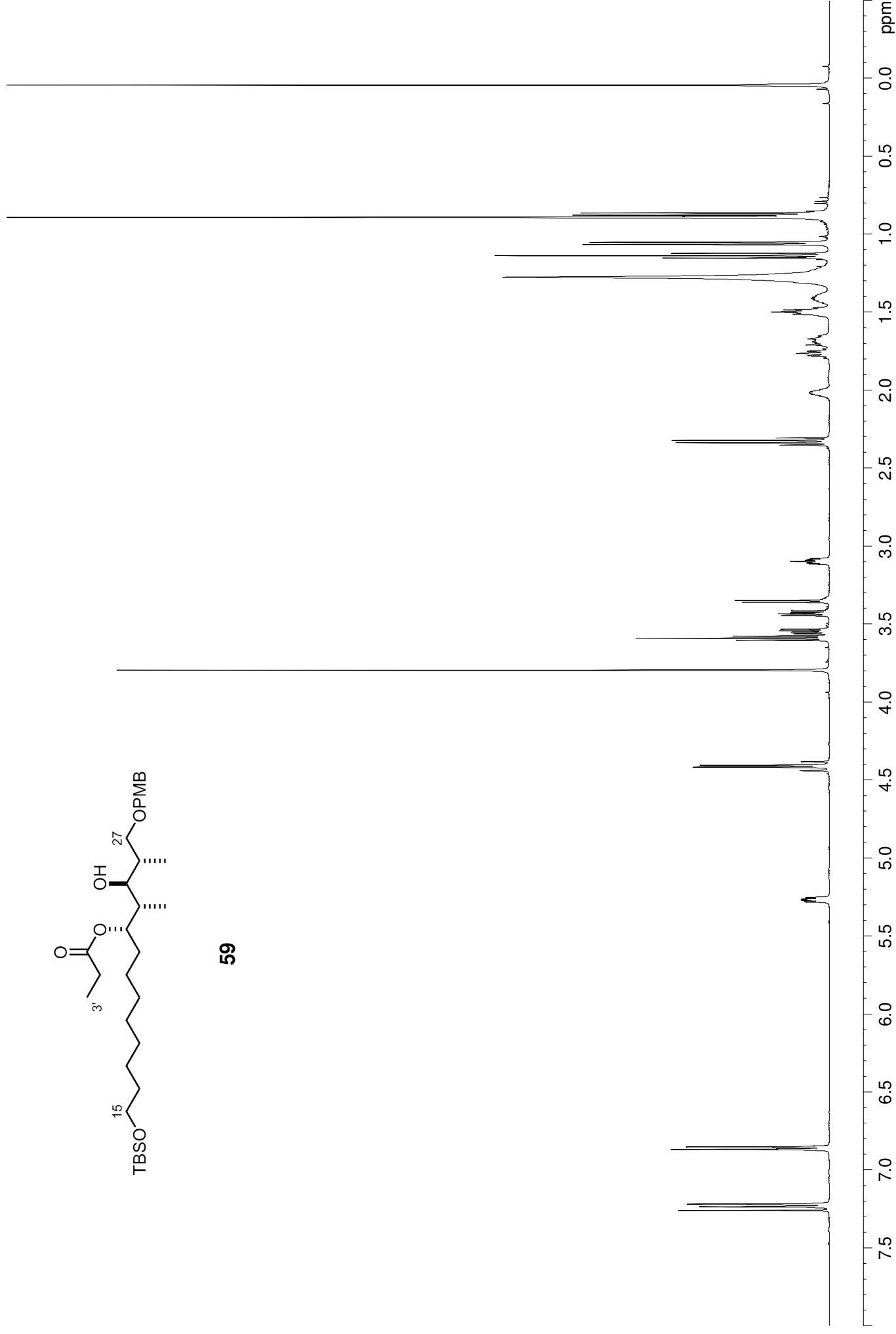


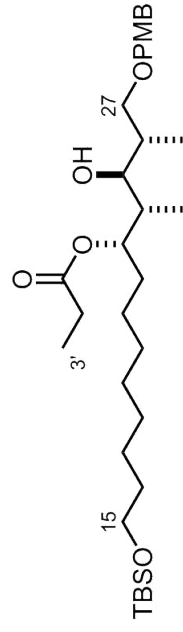
54



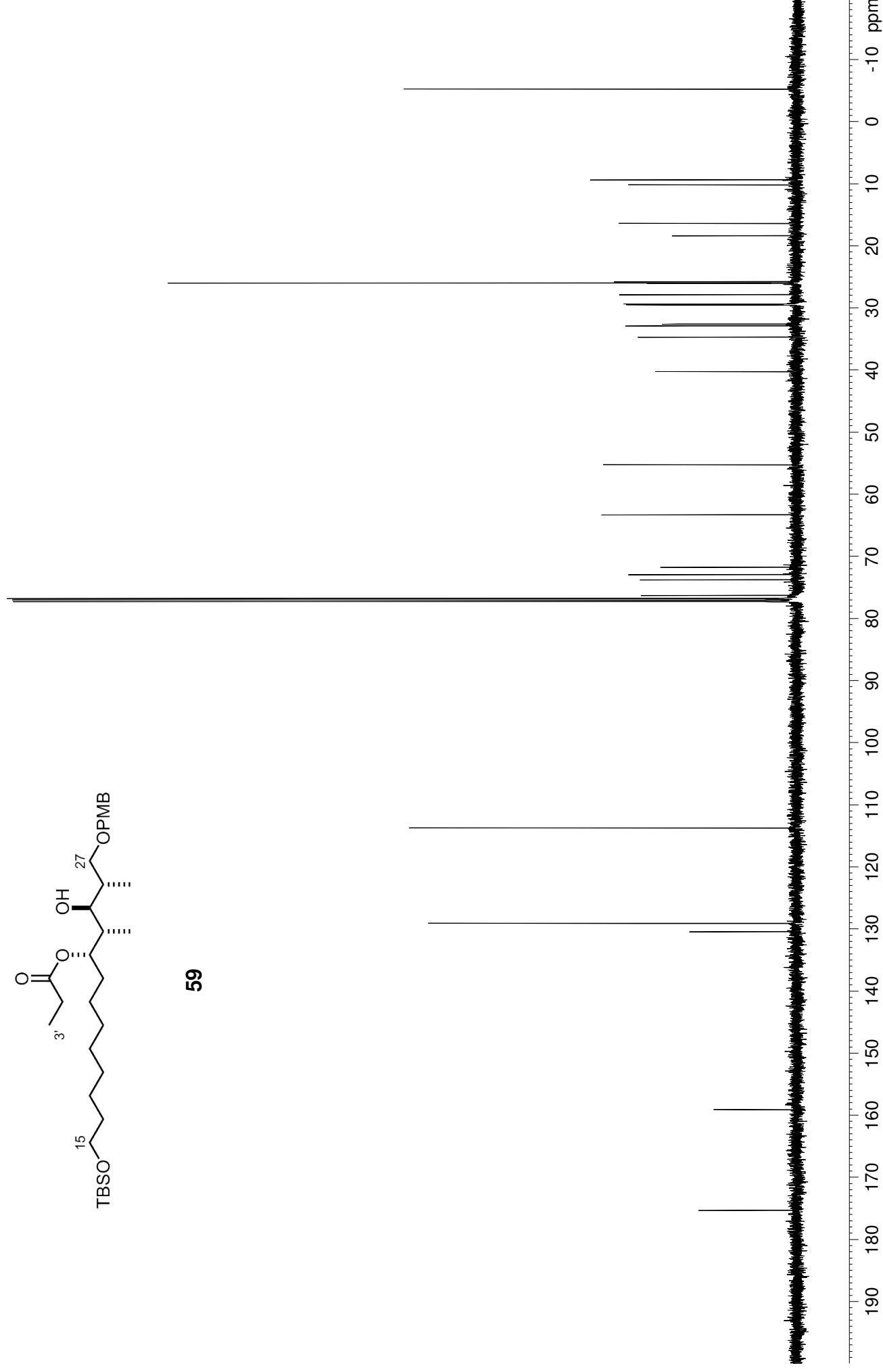


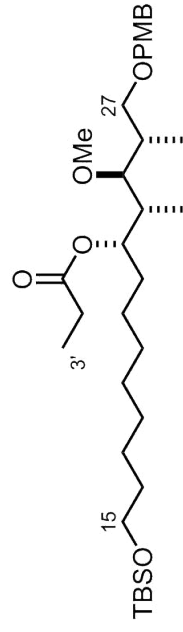
59



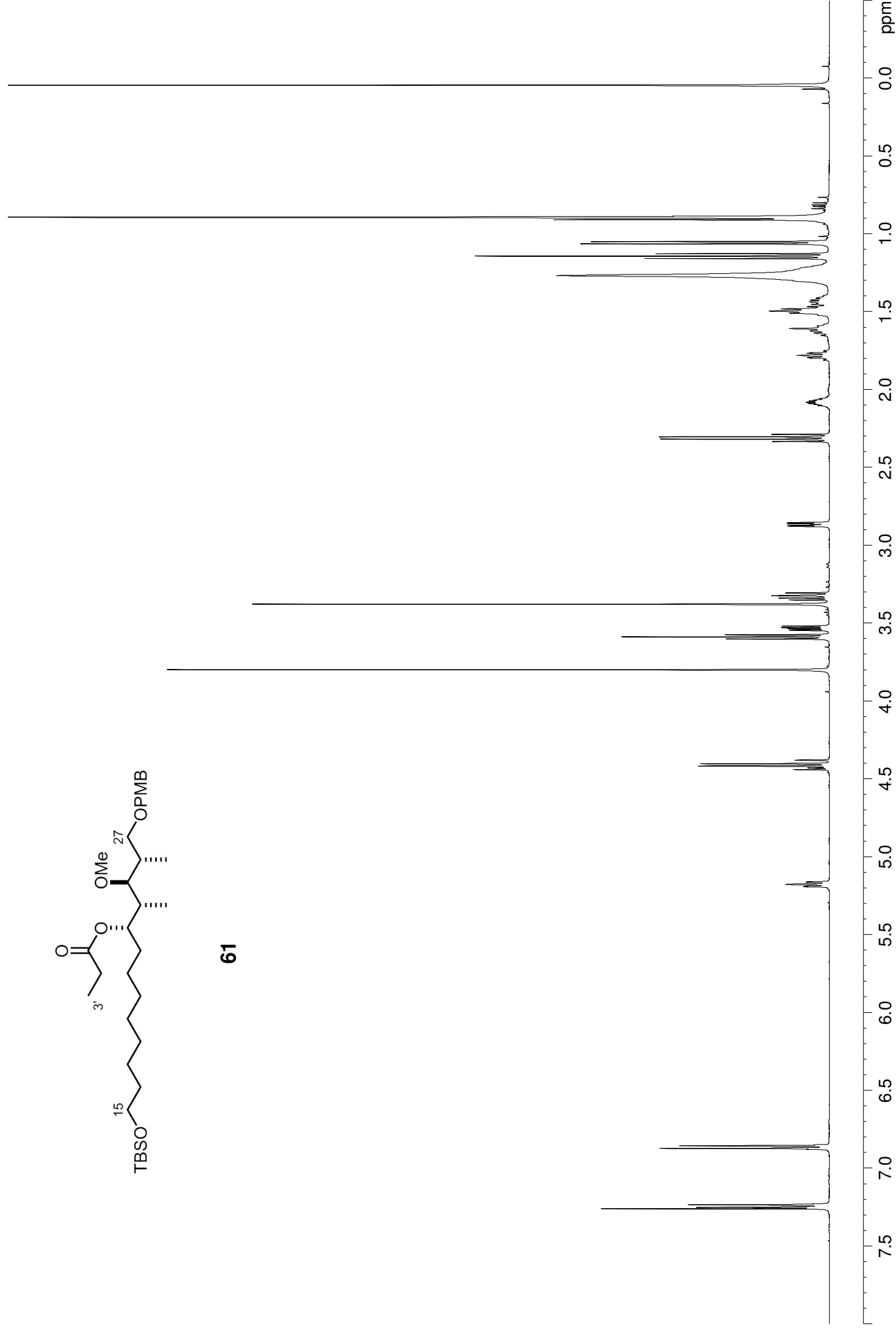


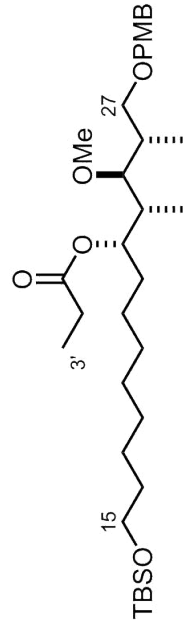
59



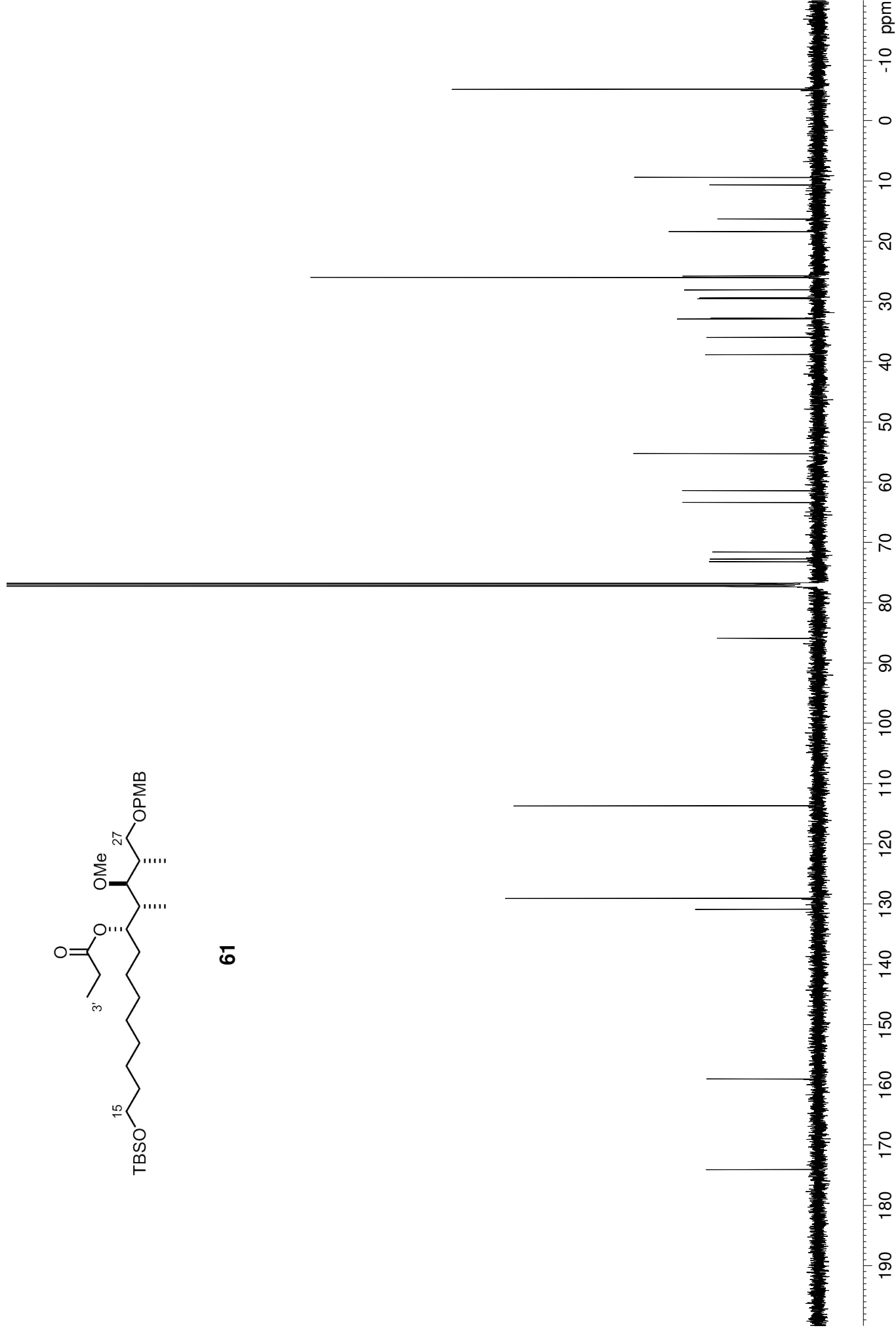


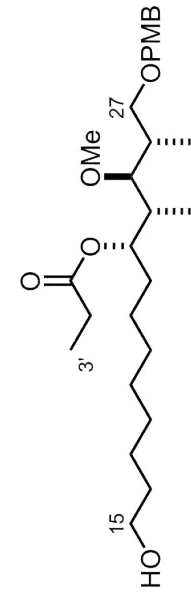
61



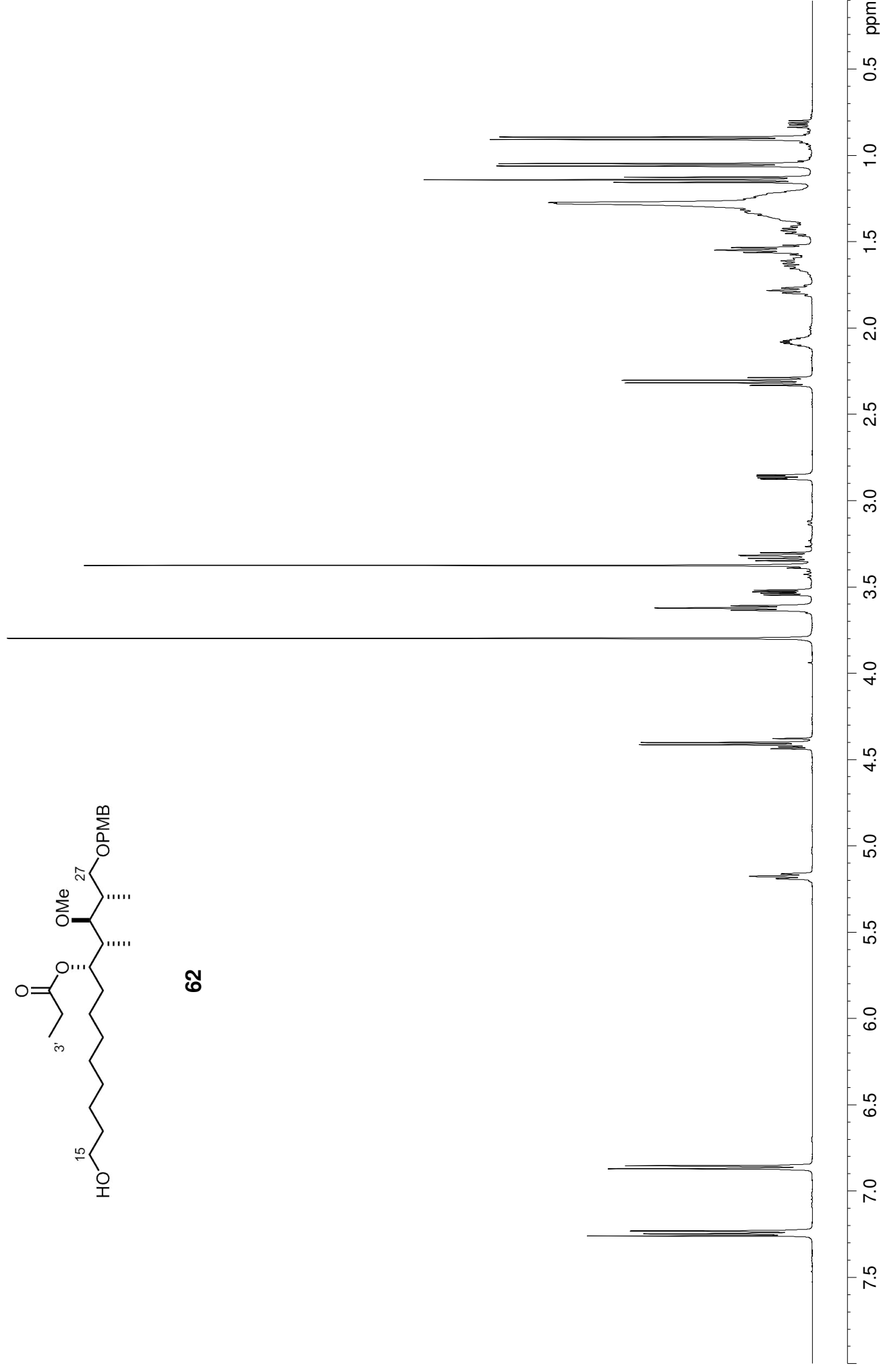


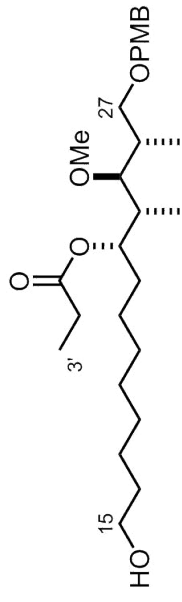
61



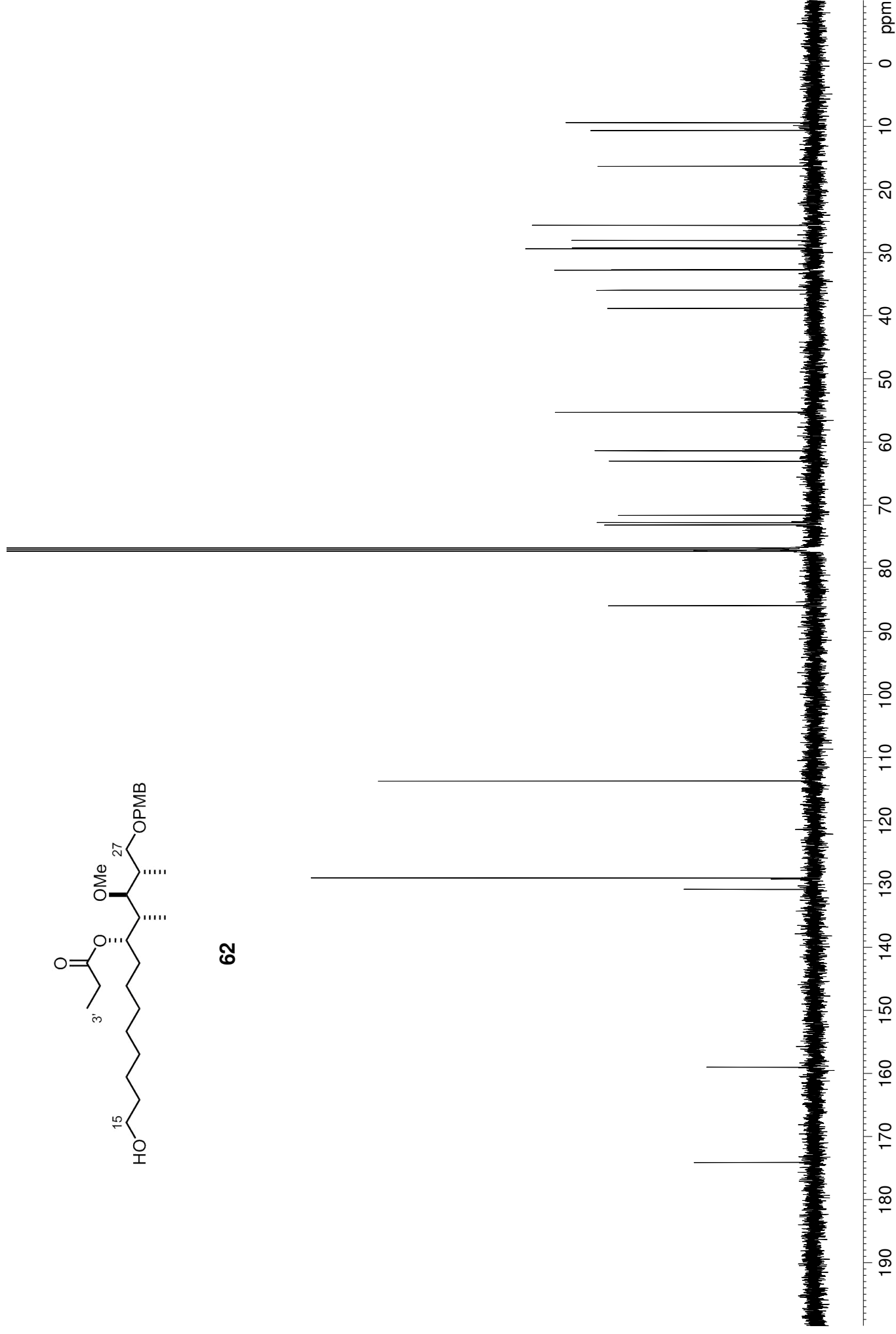


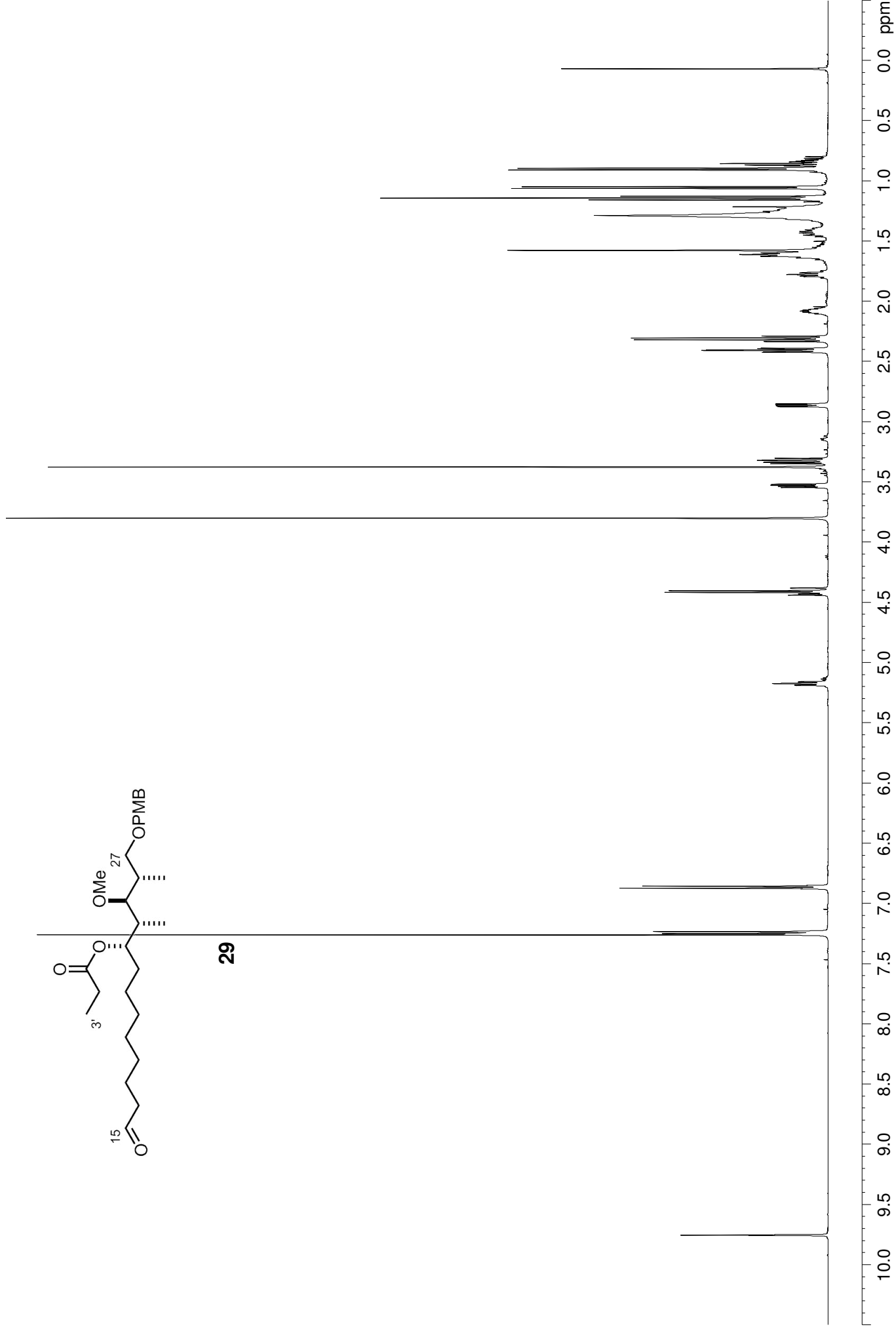
62

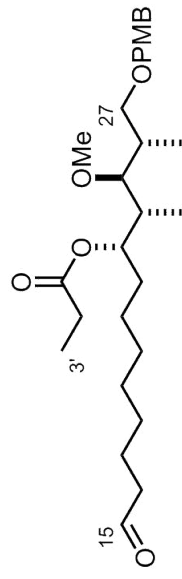




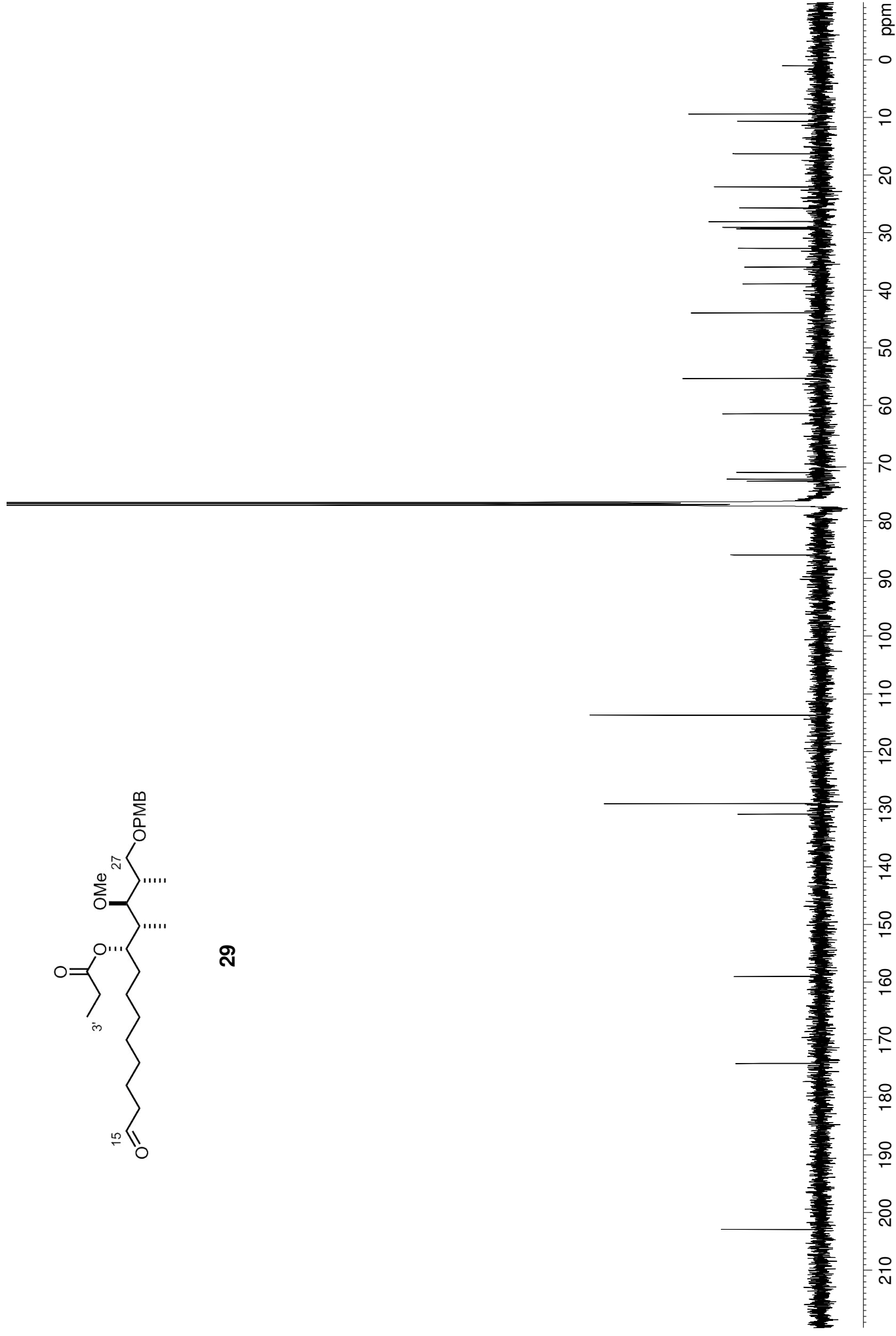
62

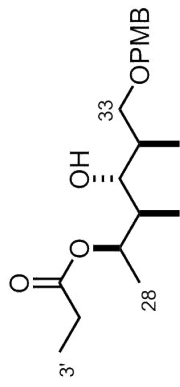




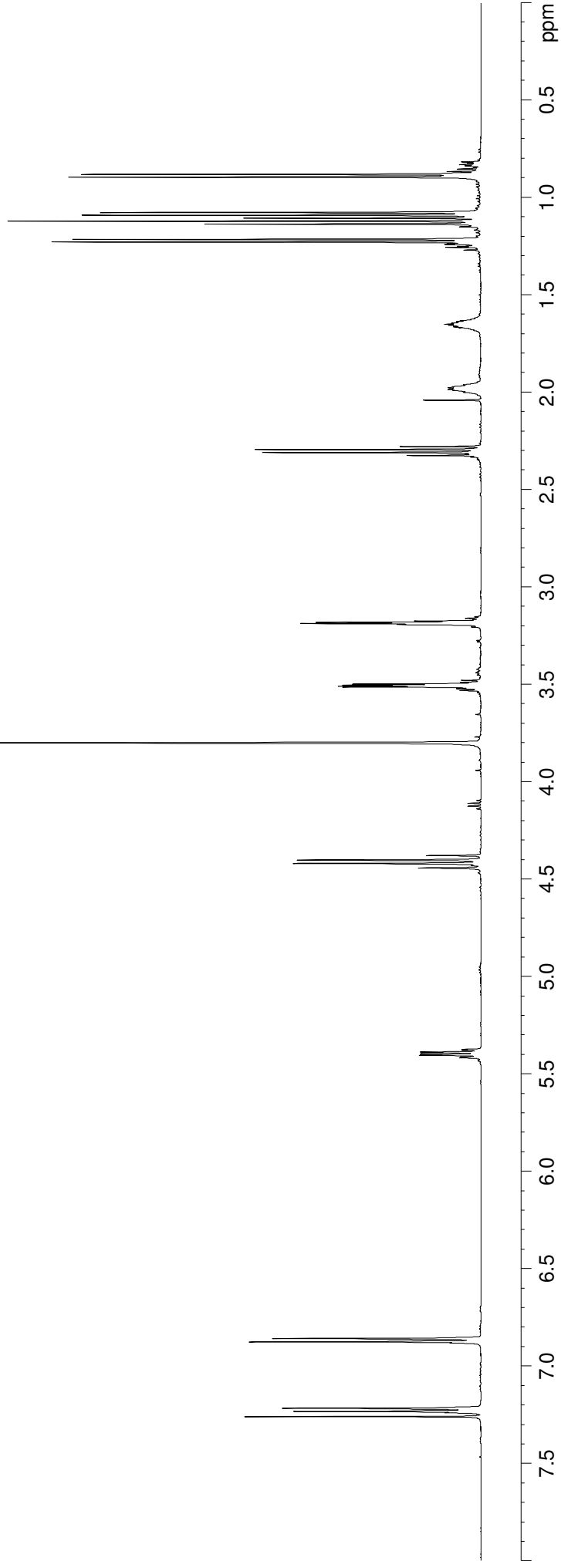


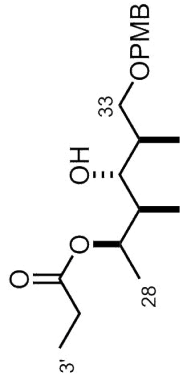
29



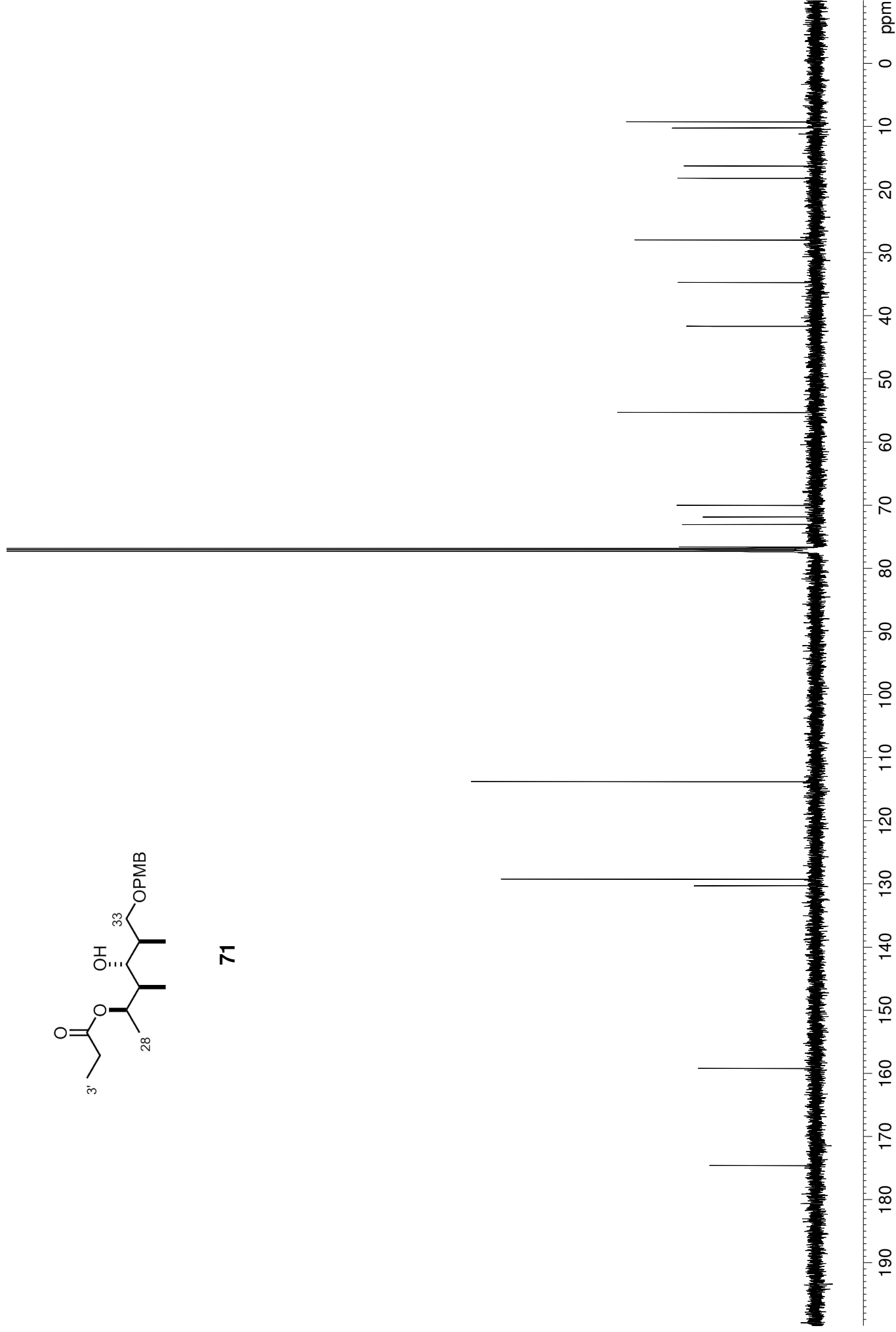


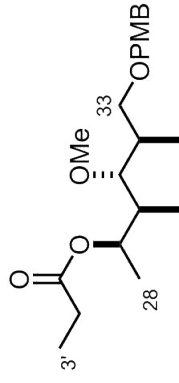
71



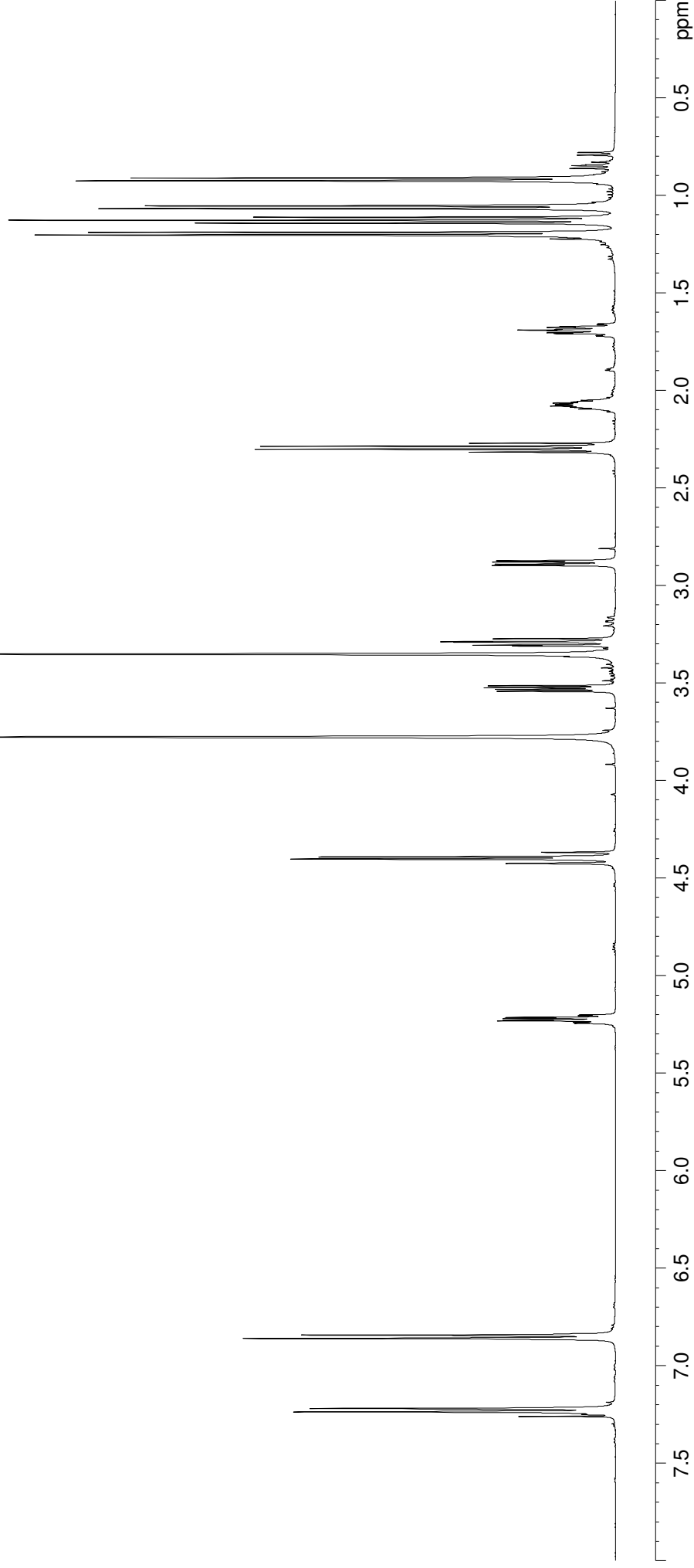


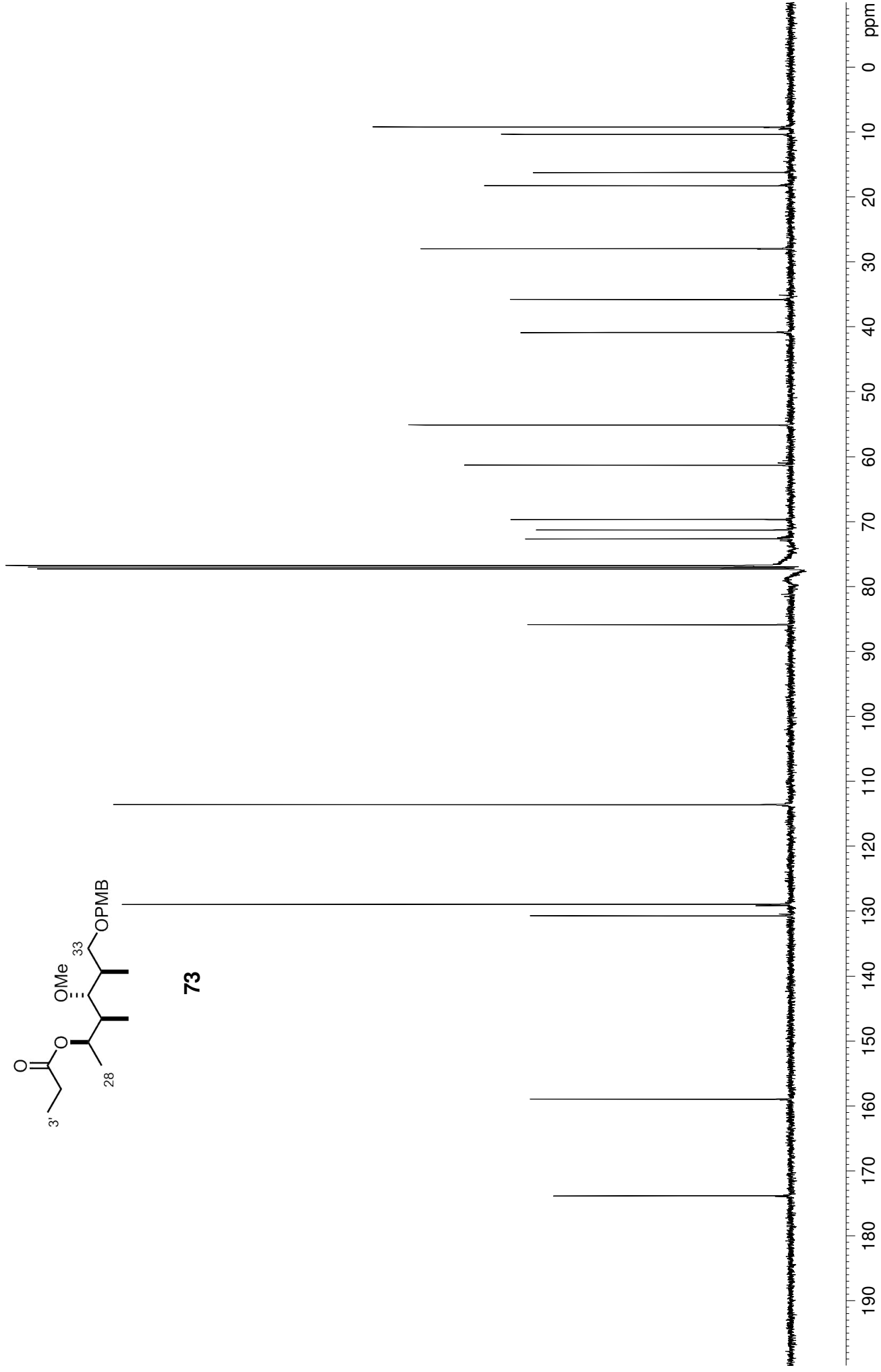
71

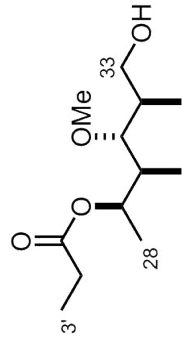




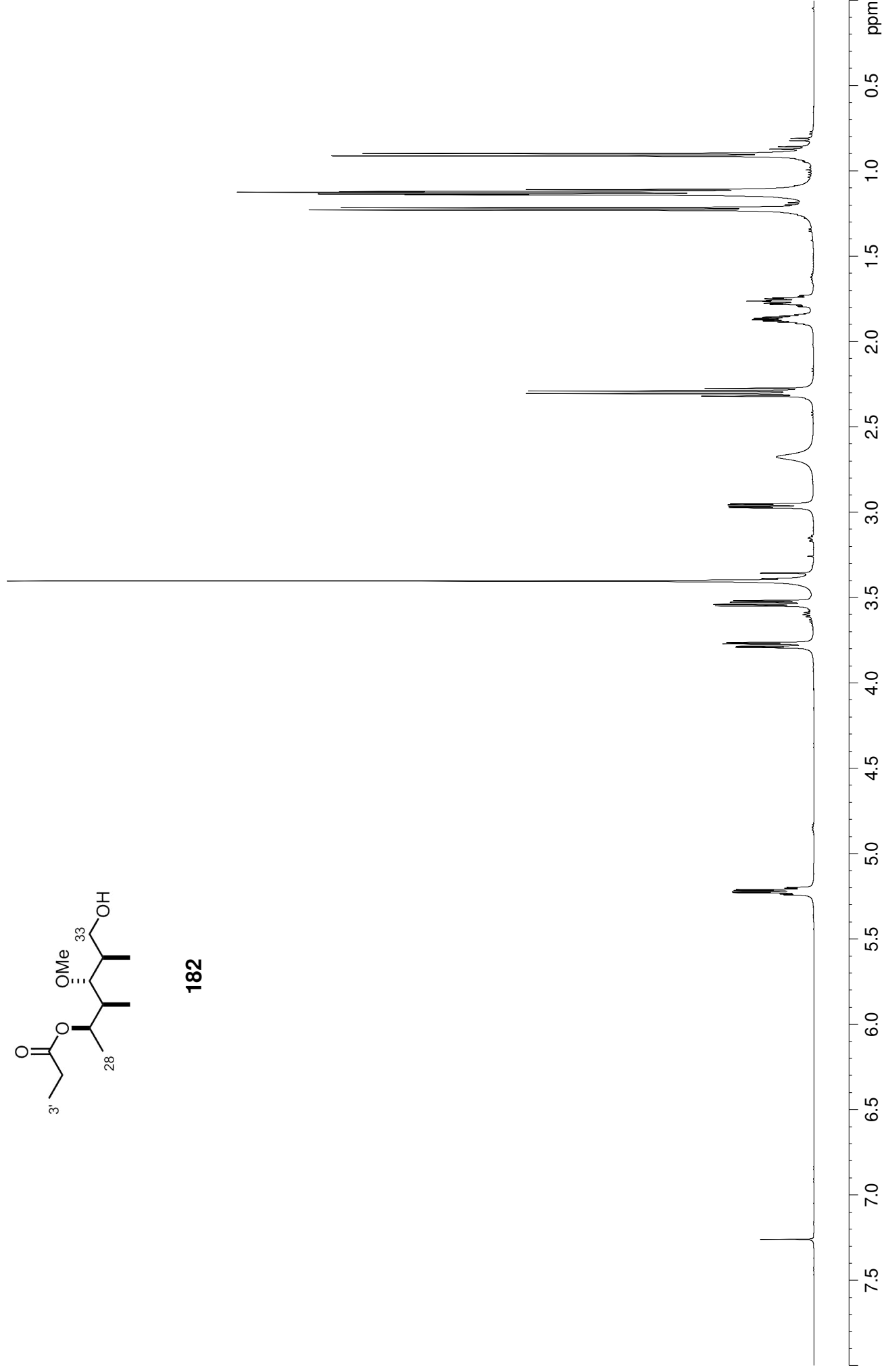
73

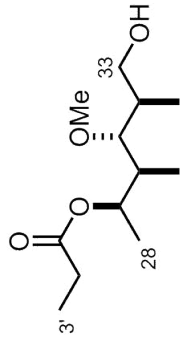




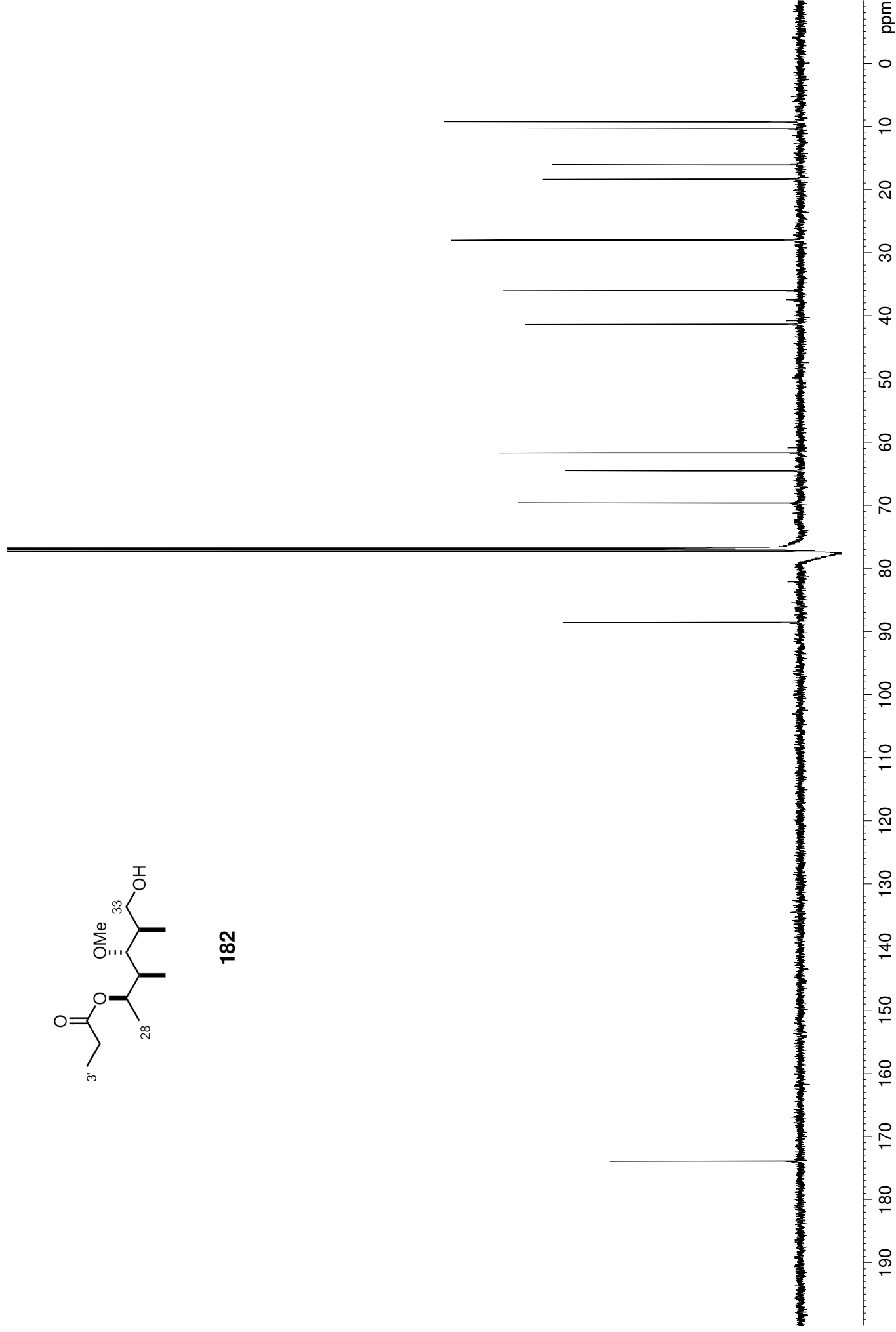


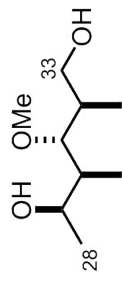
182



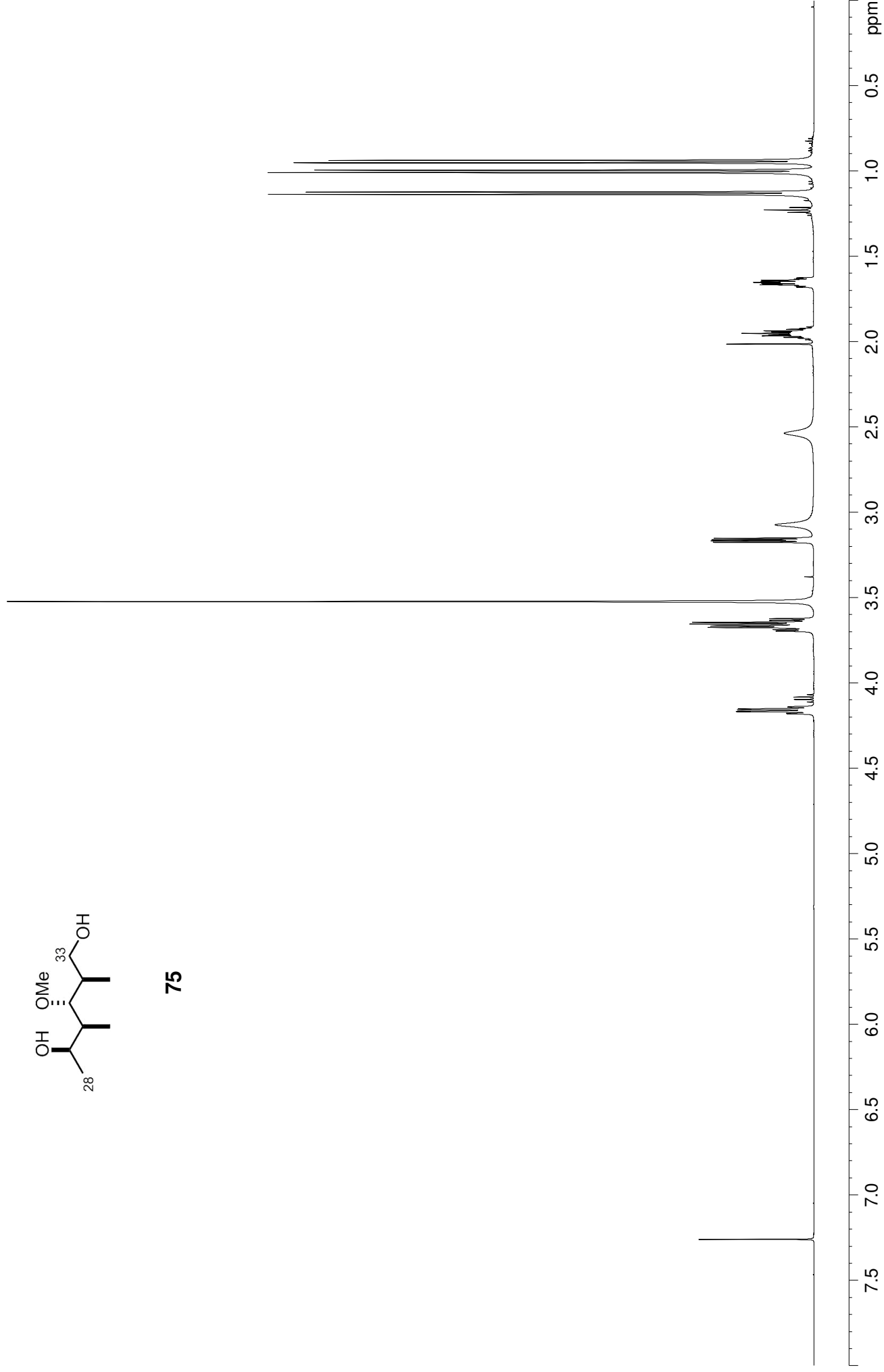


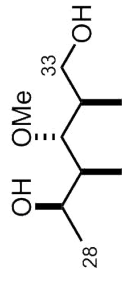
182



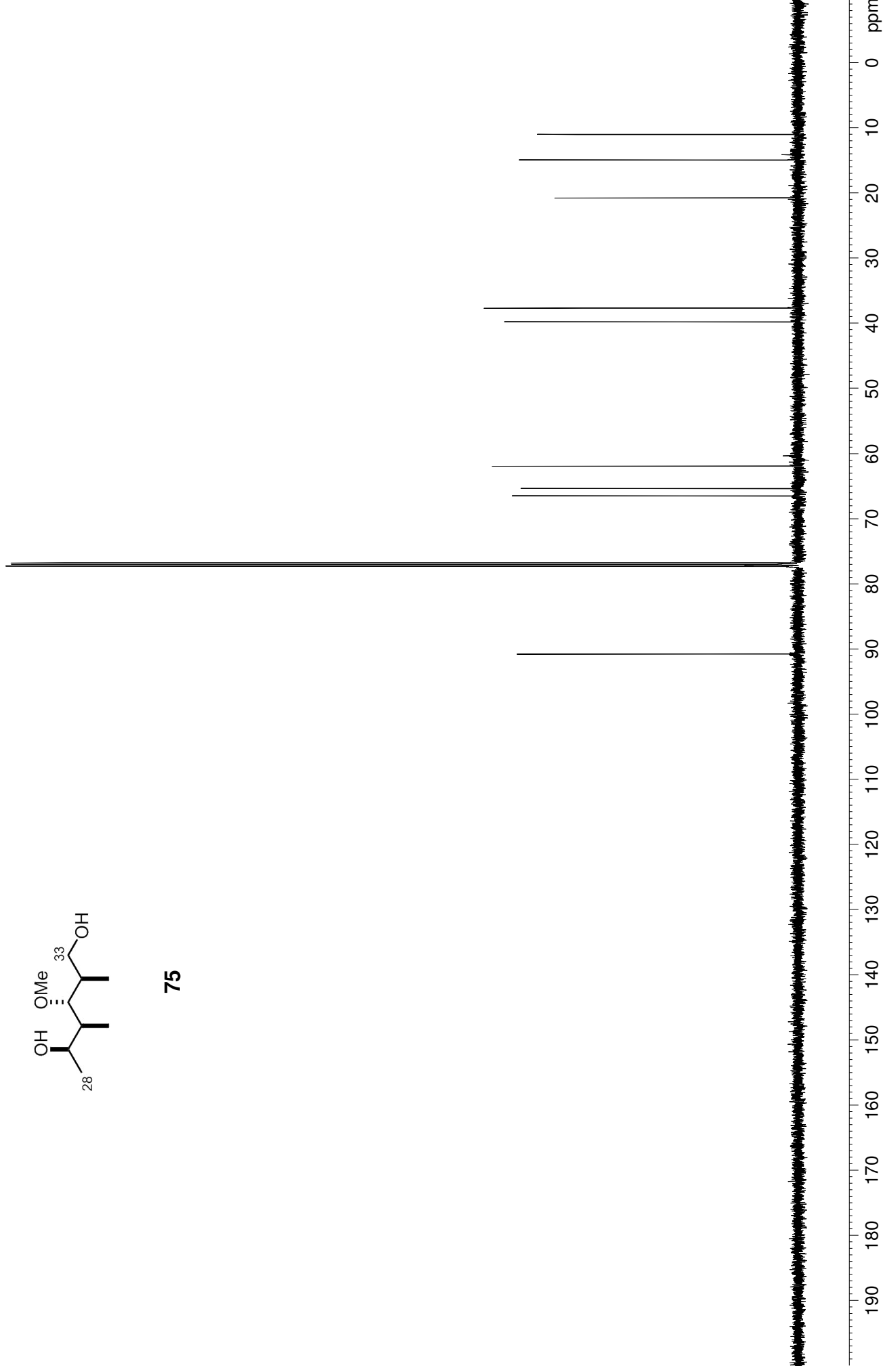


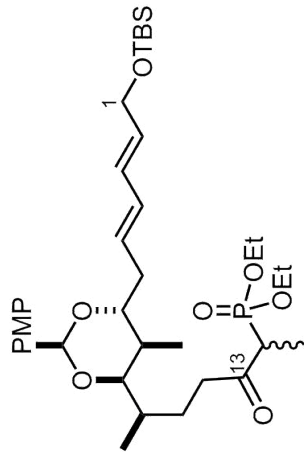
75



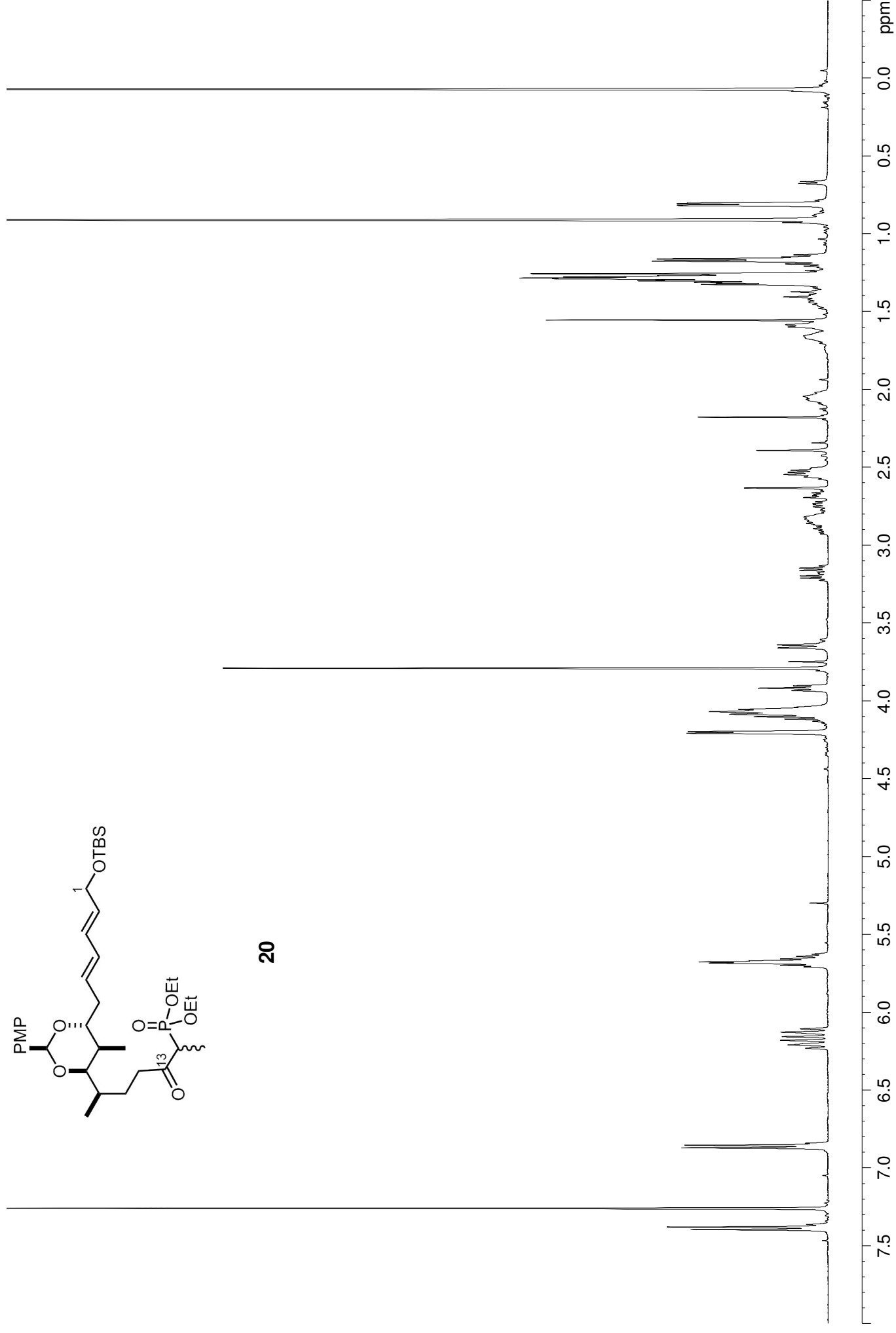


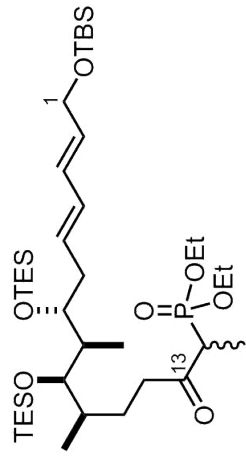
75



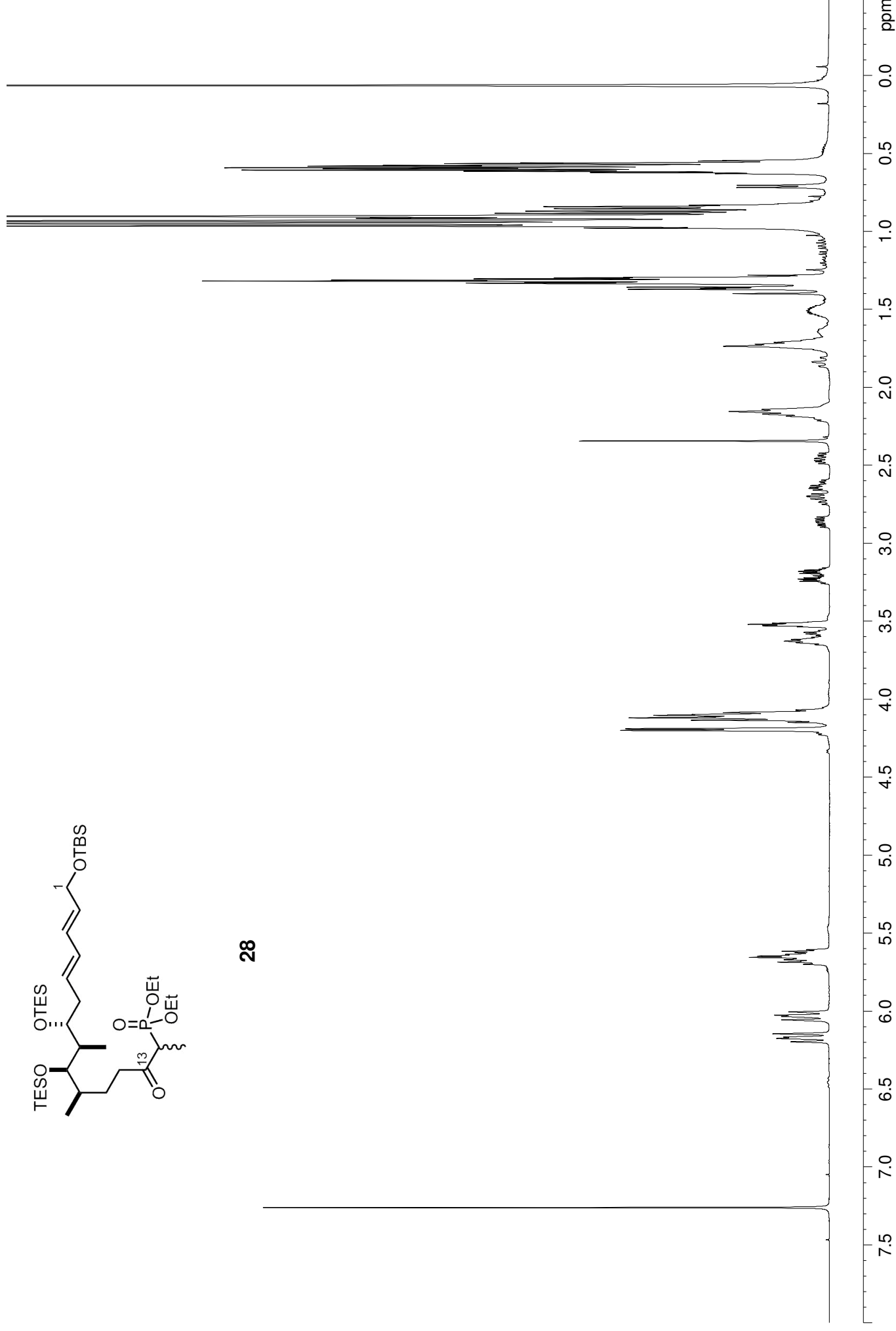


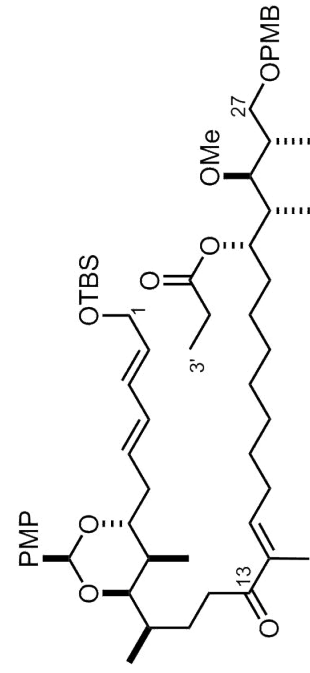
20



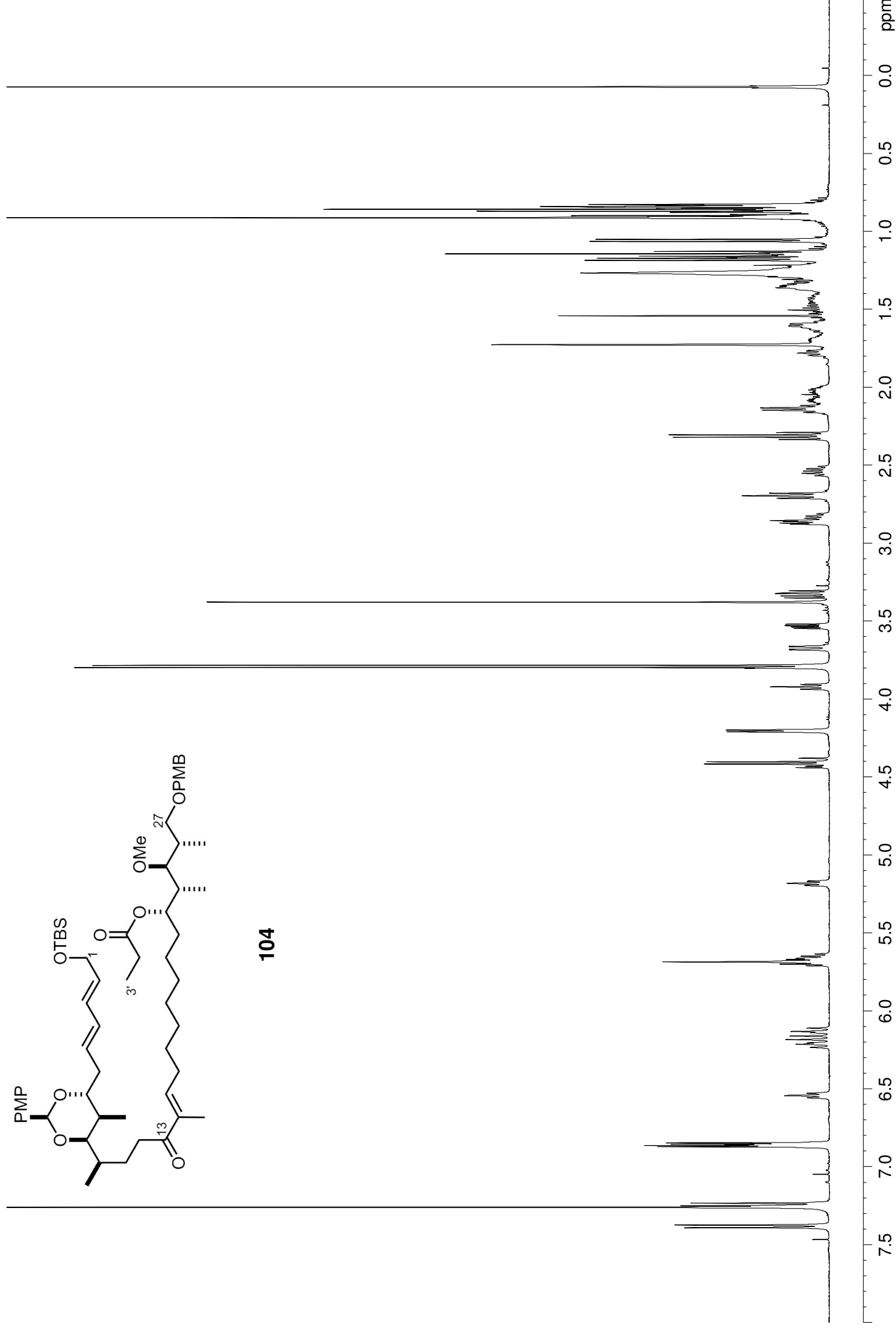


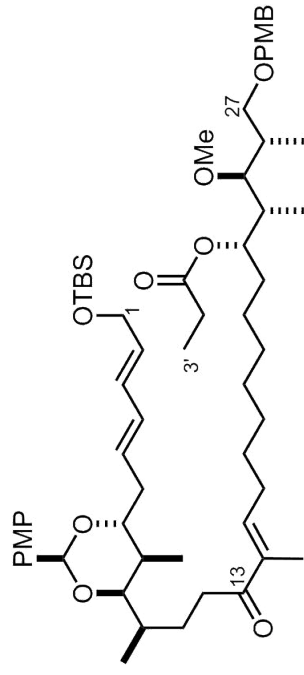
28



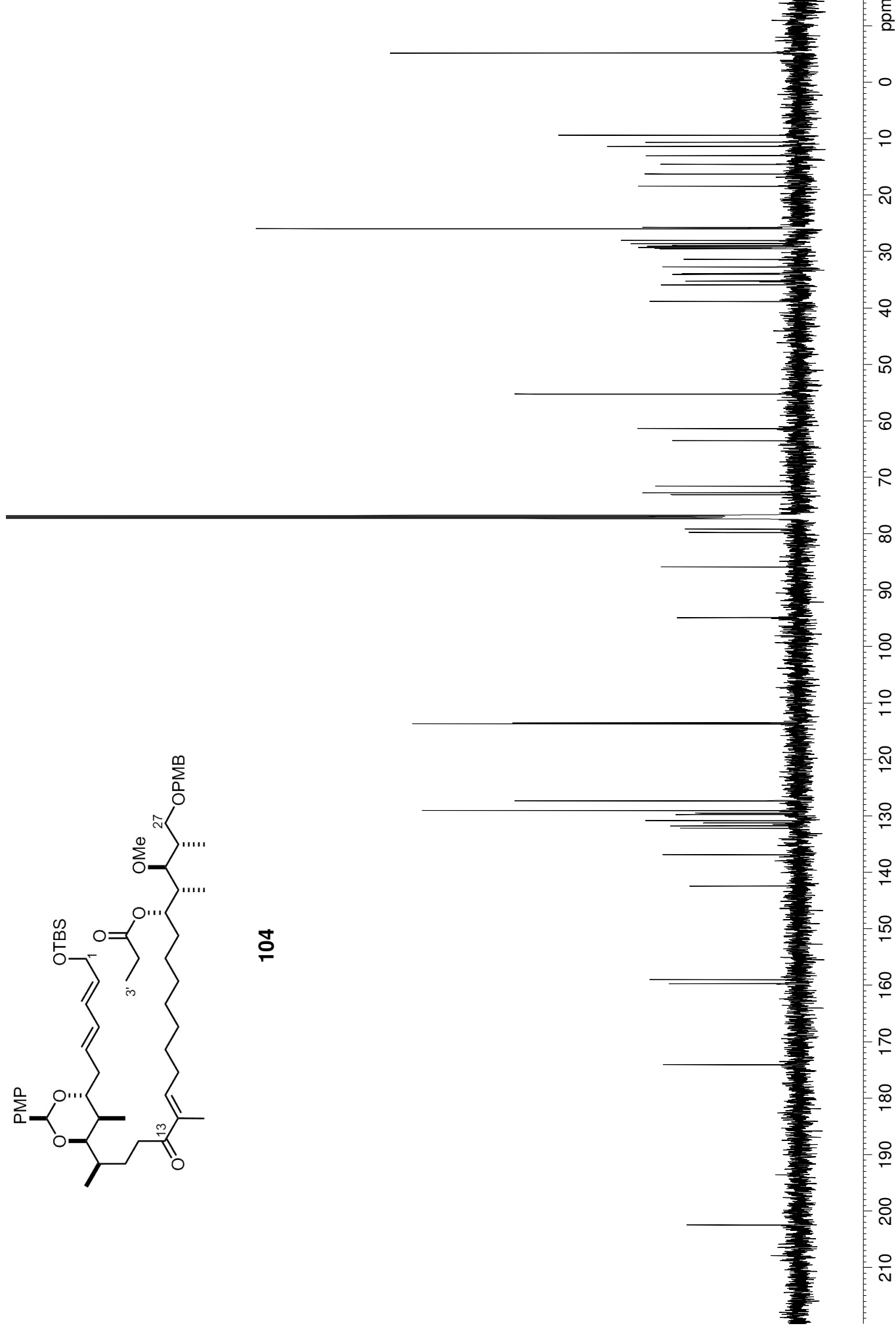


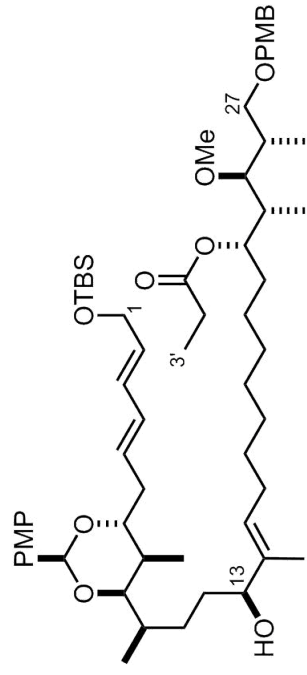
104



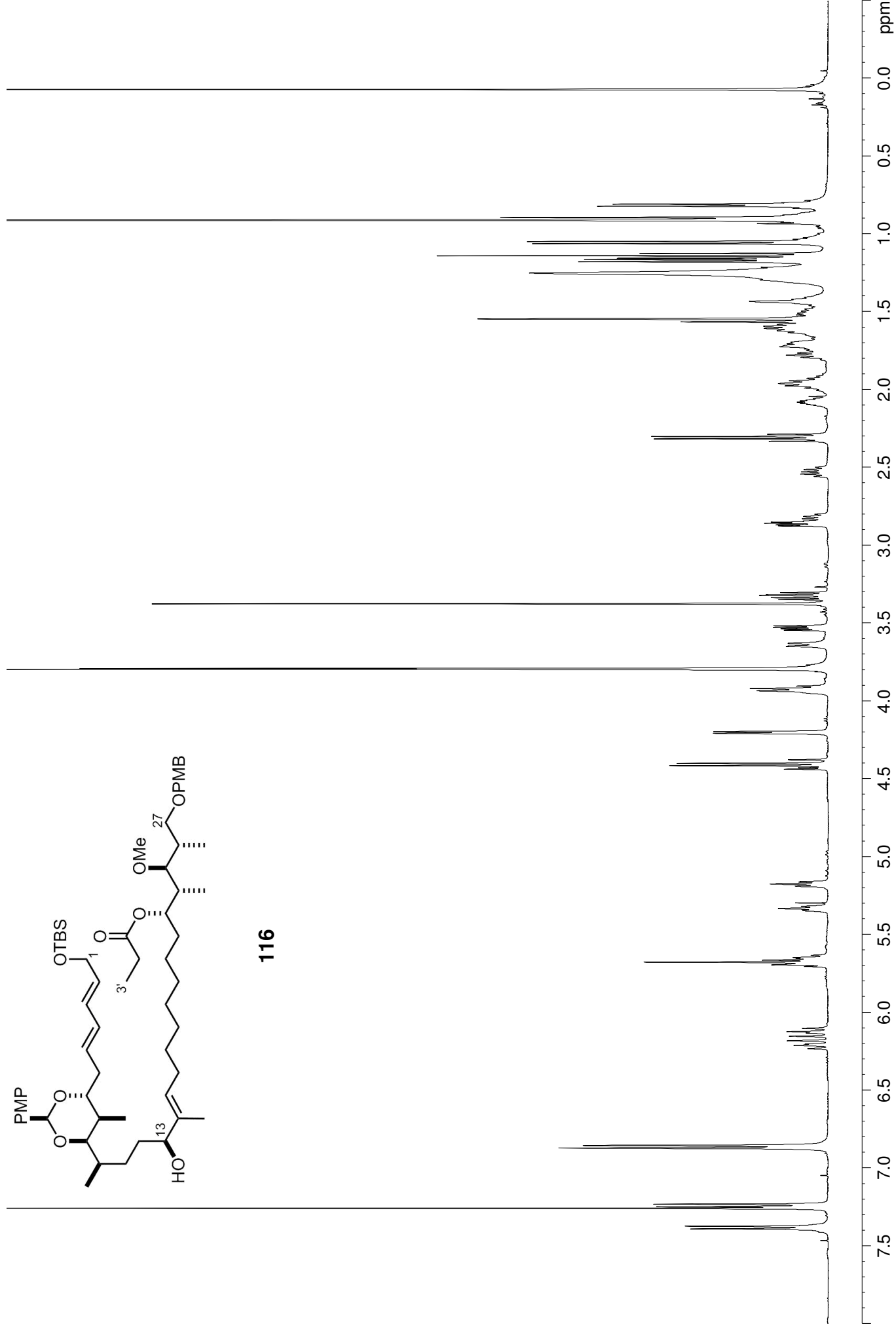


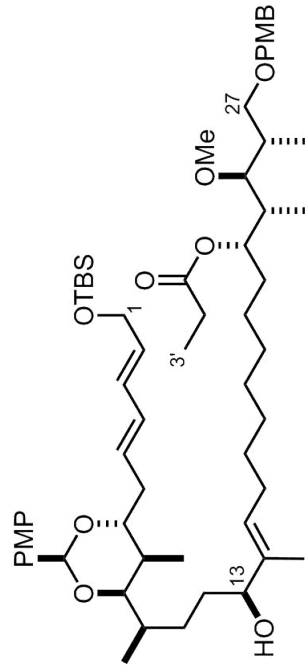
104



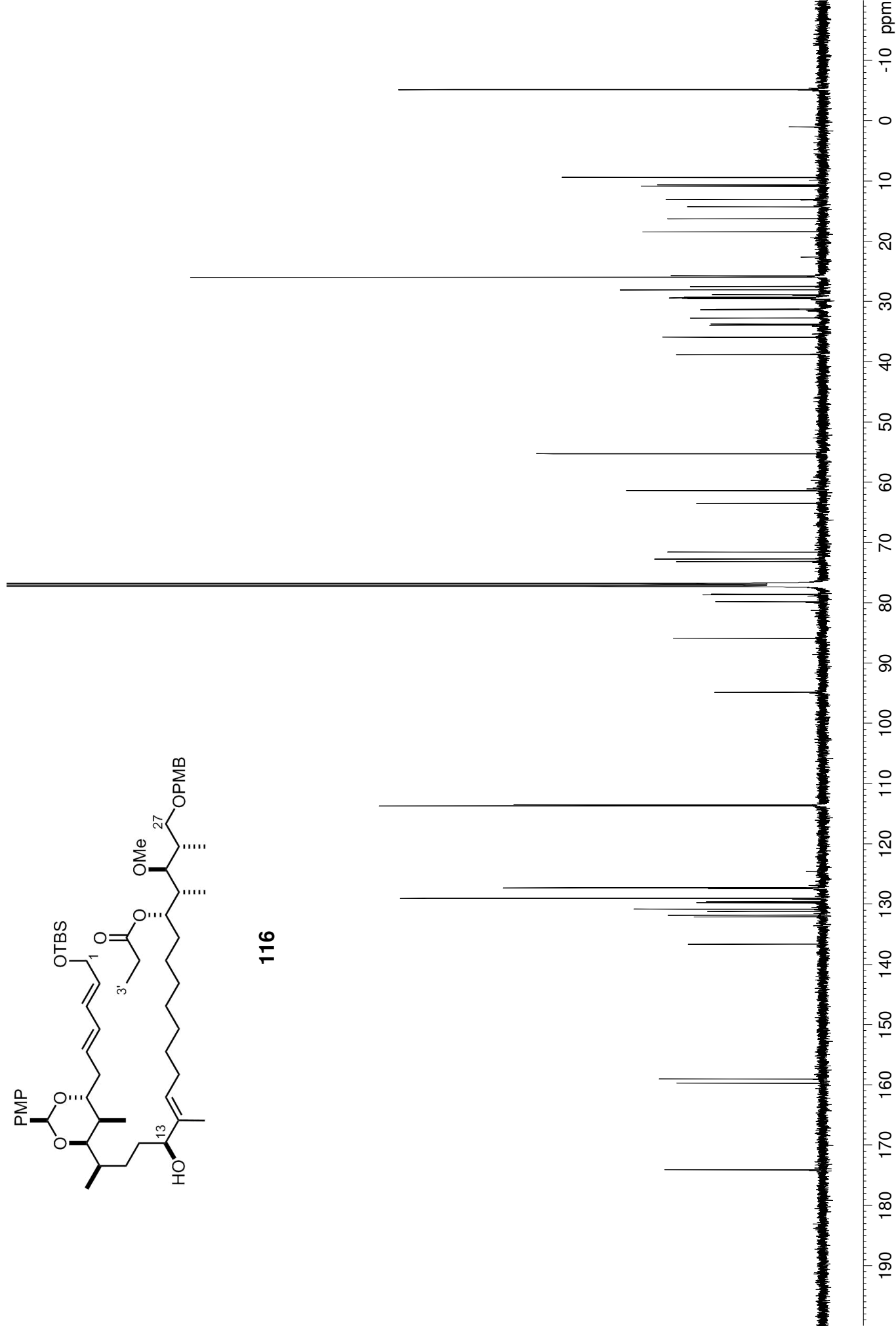


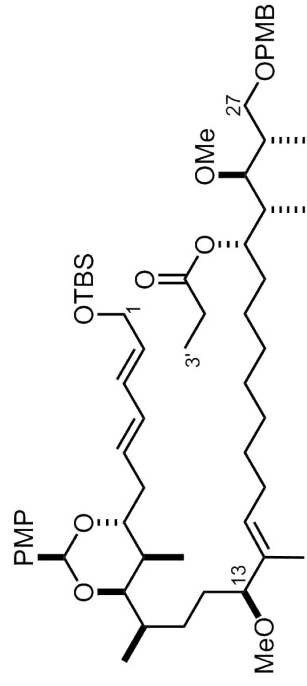
116



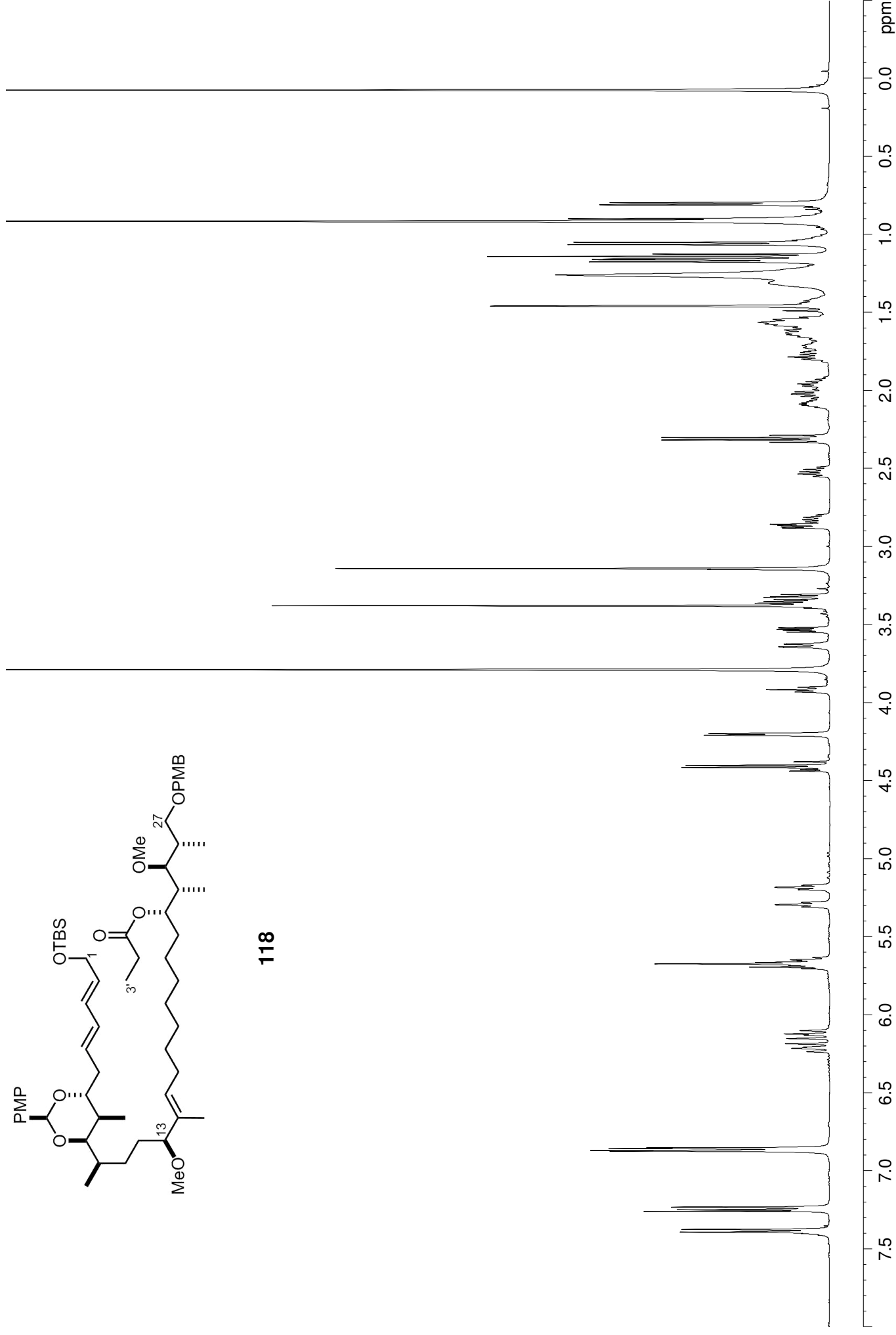


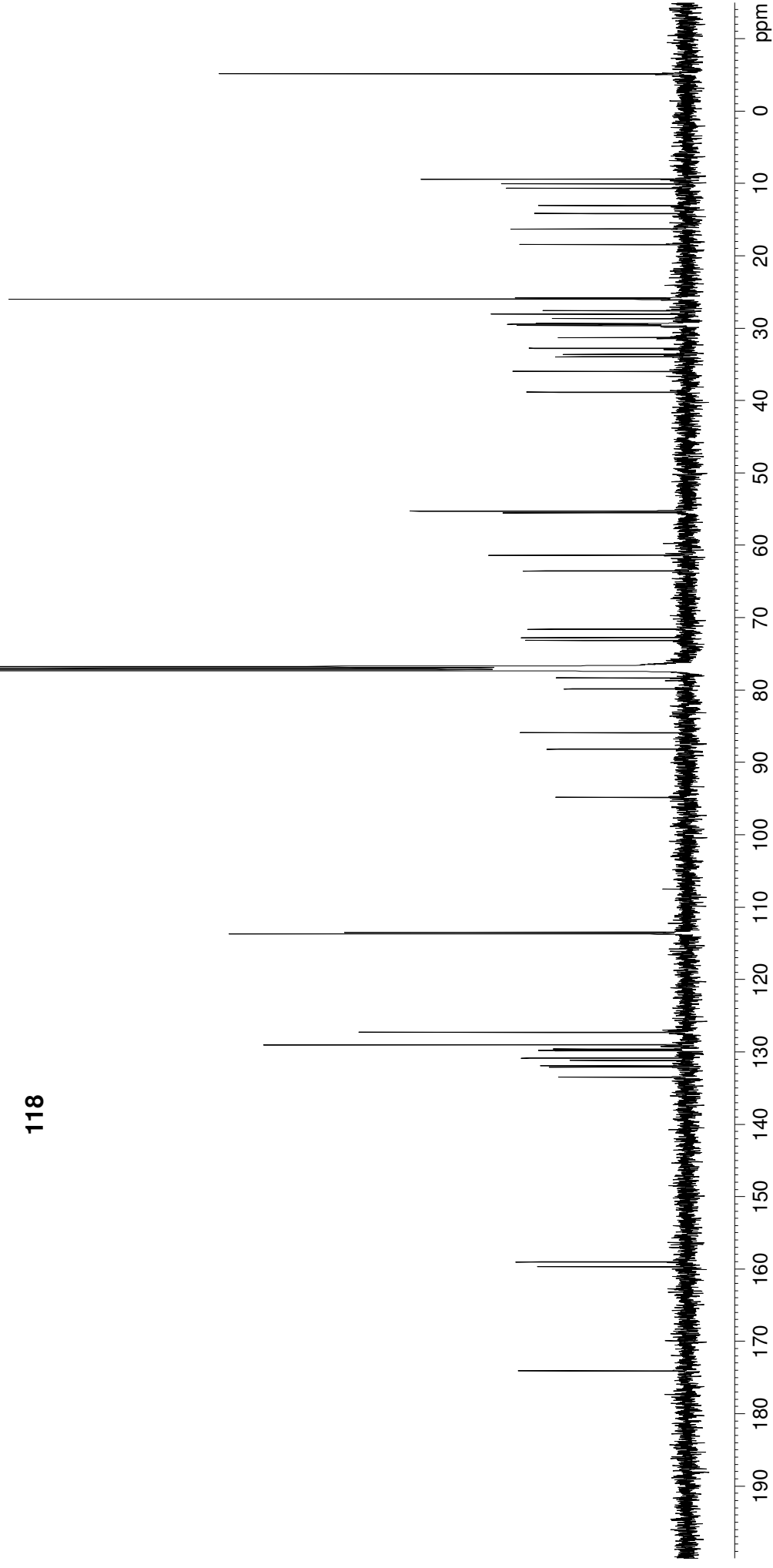
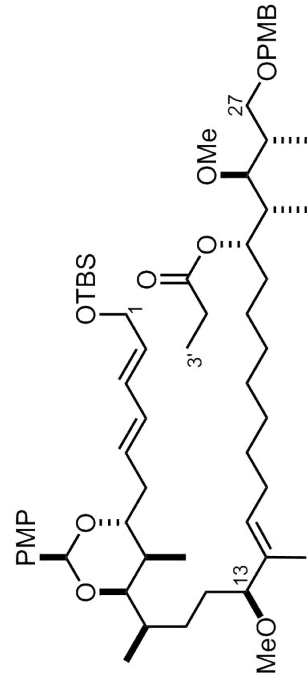
116

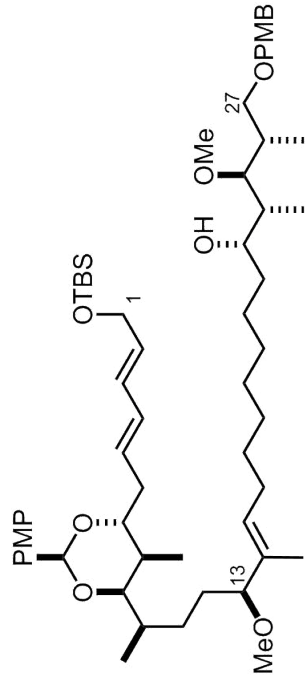




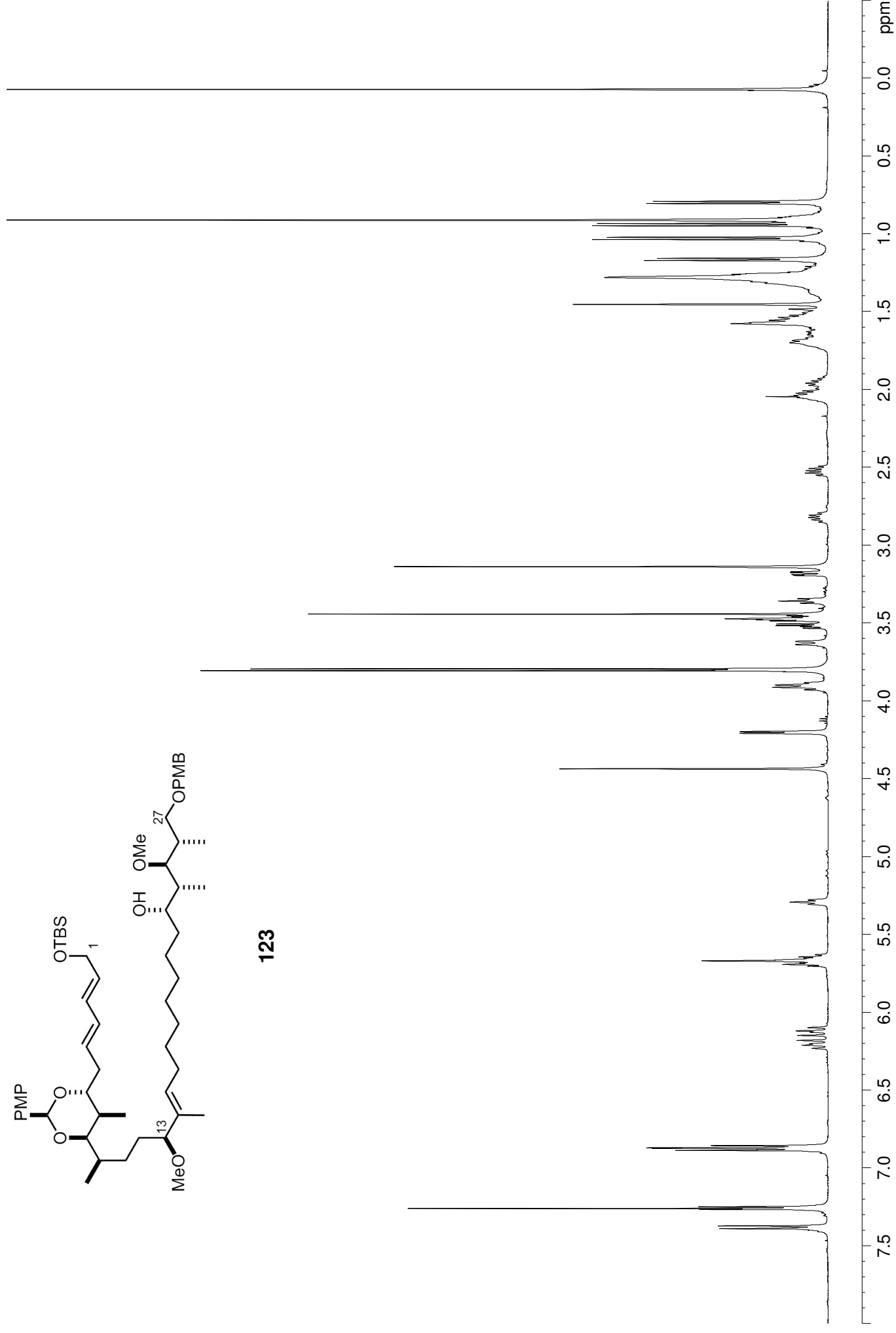
118

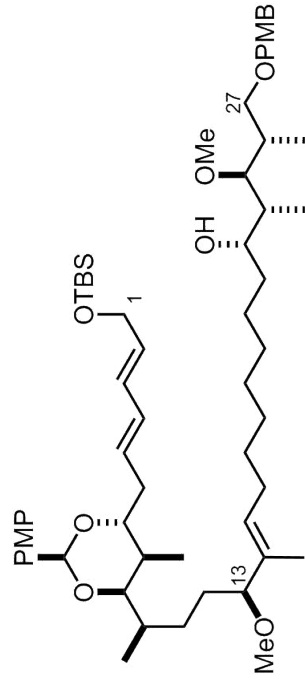




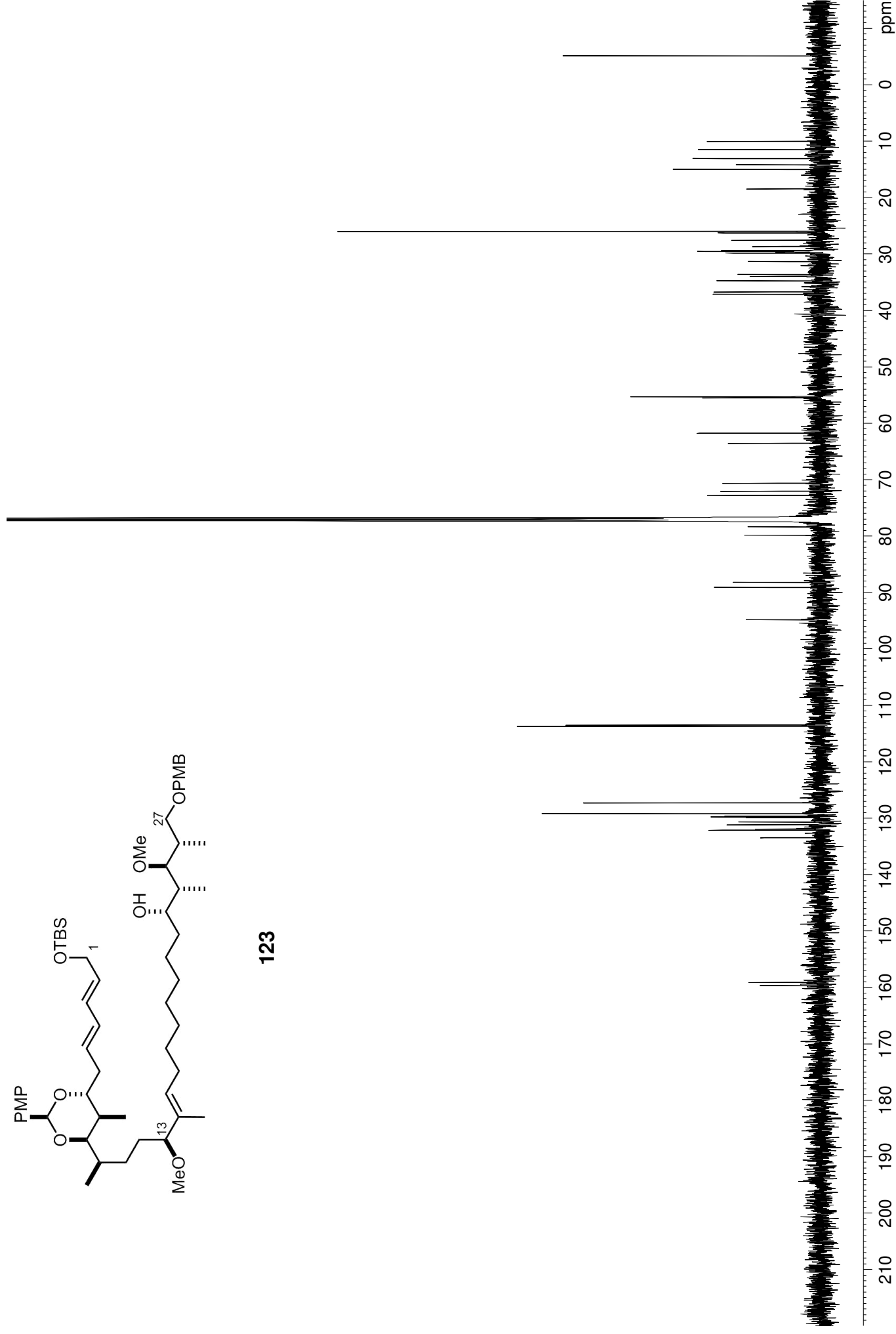


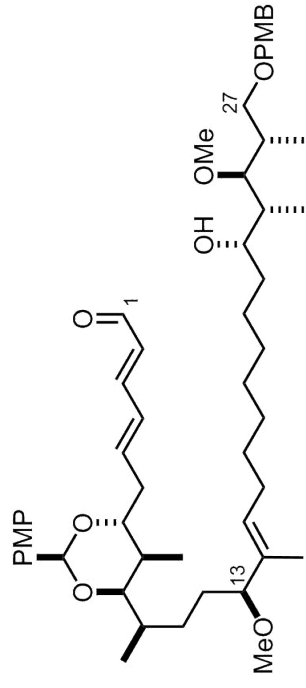
123



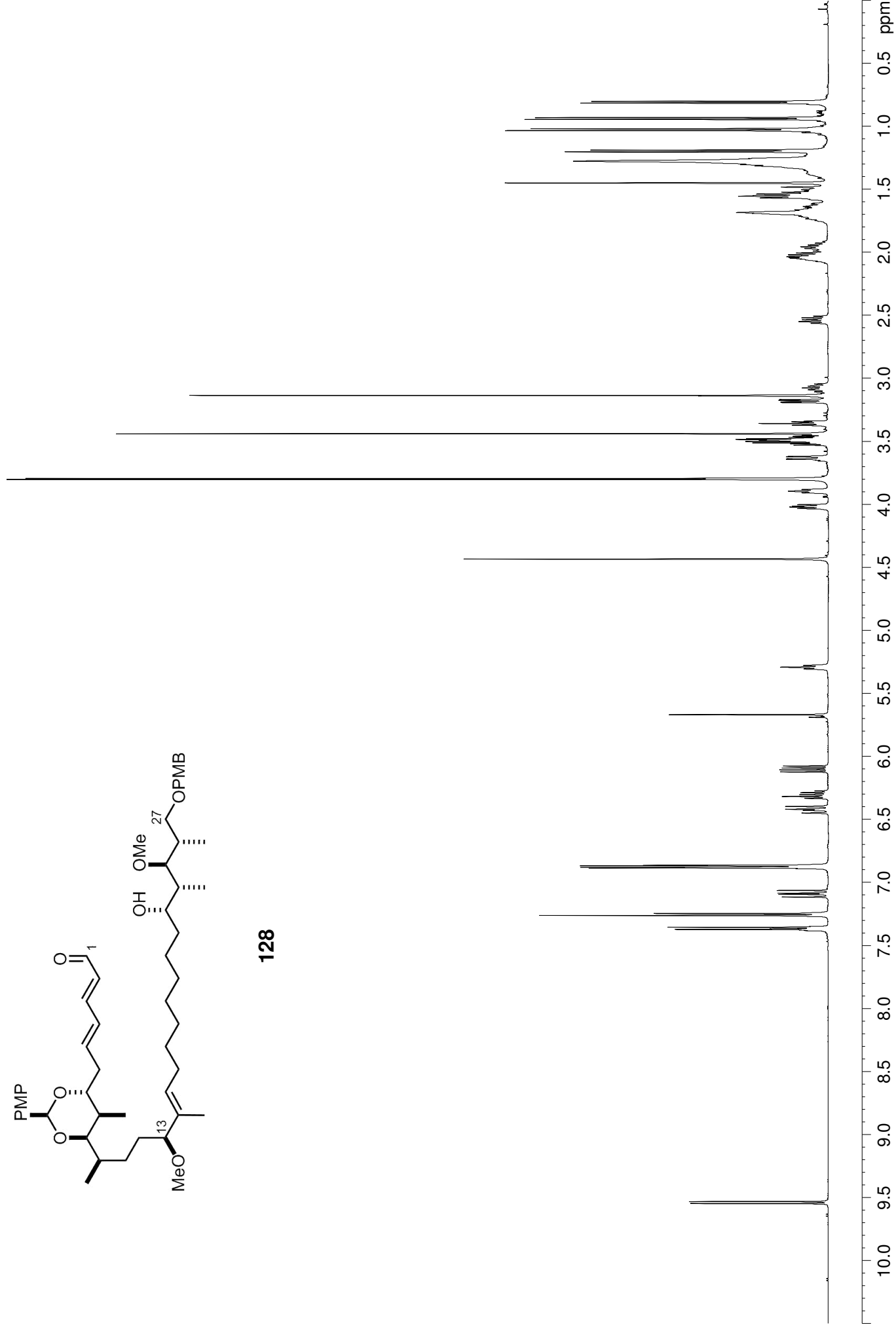


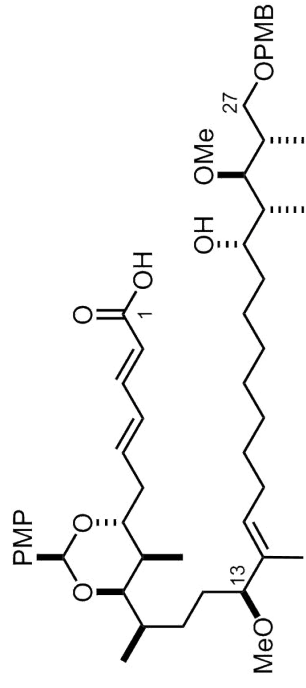
123



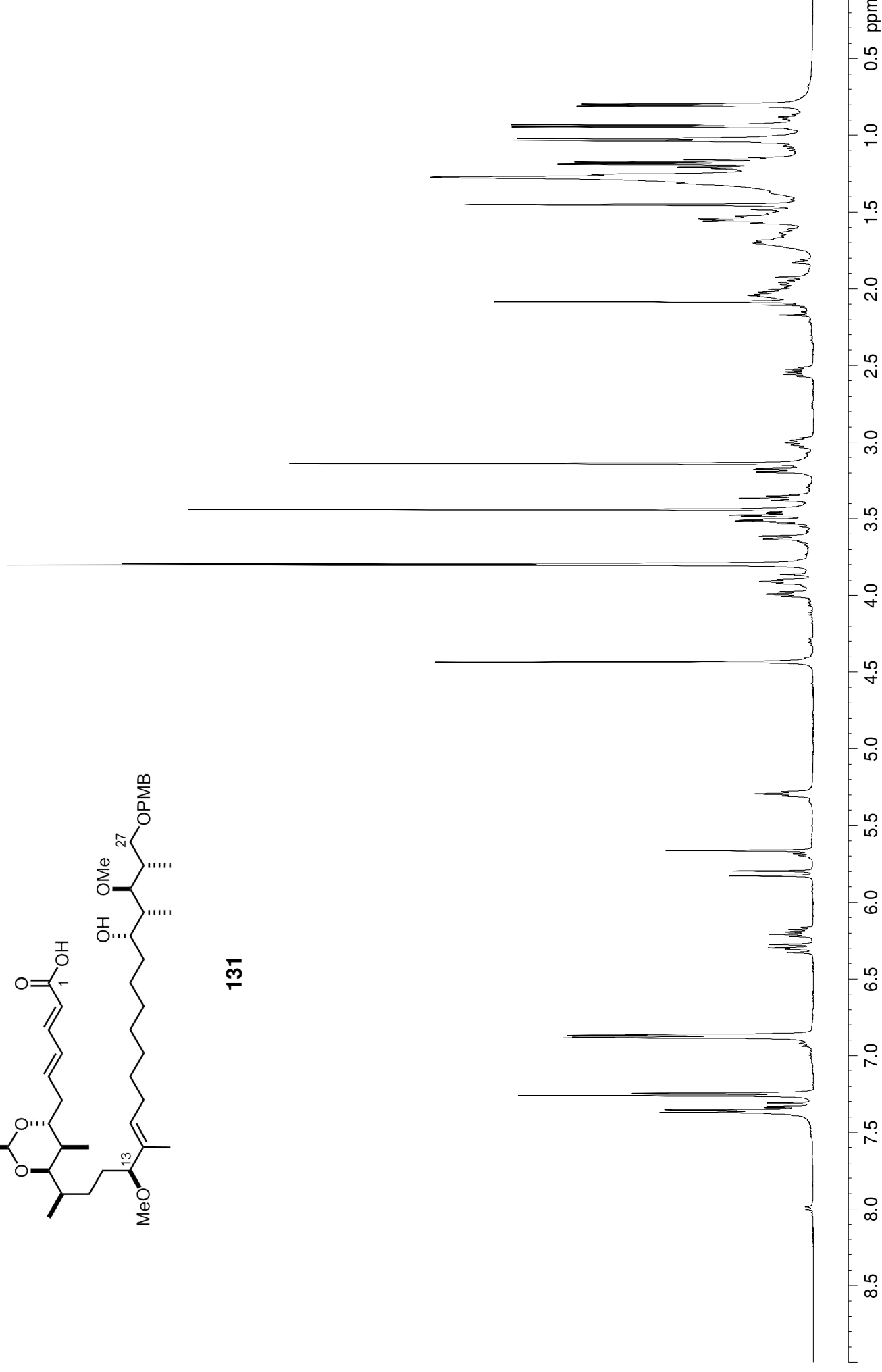


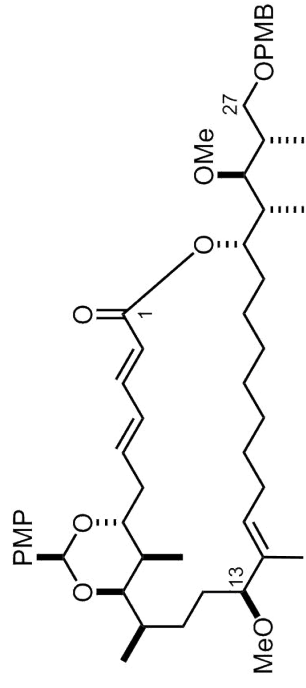
128



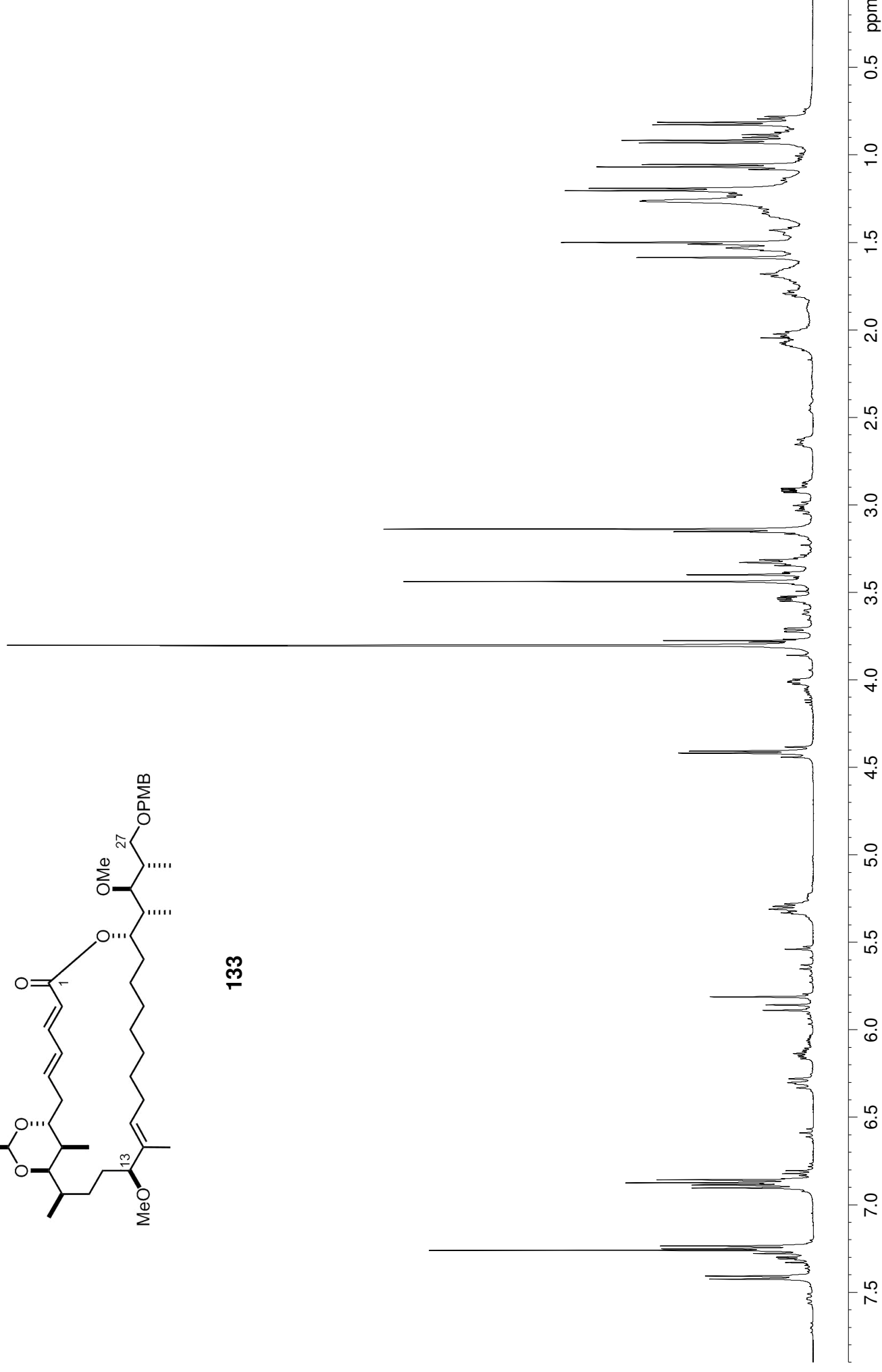


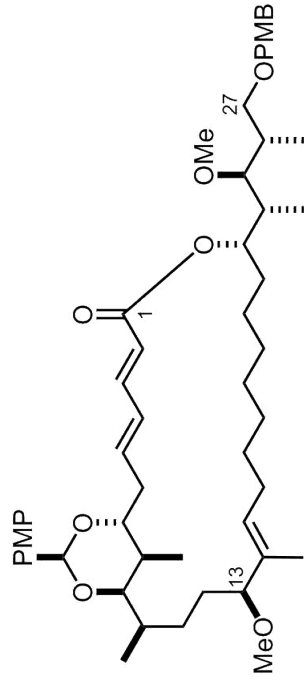
131



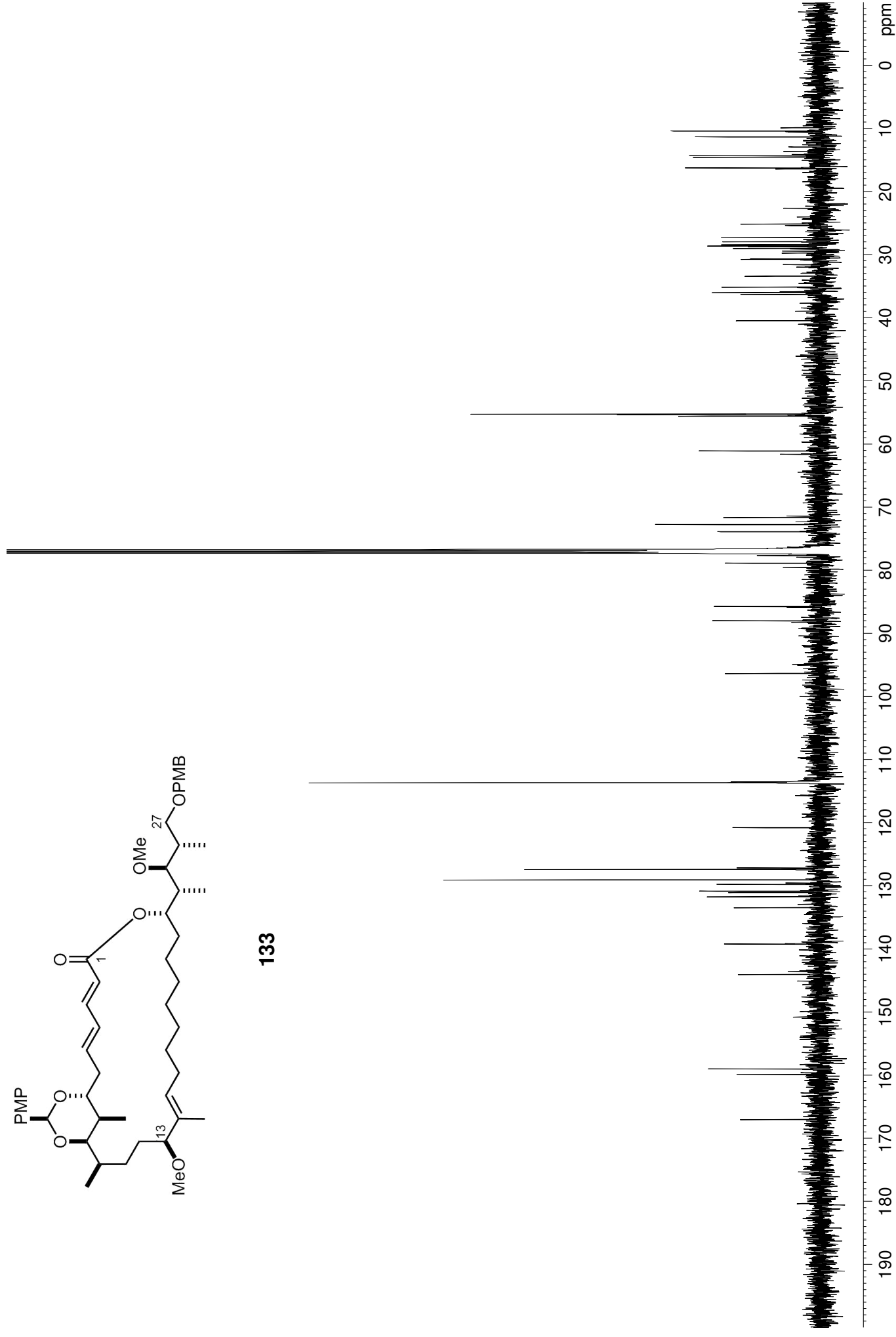


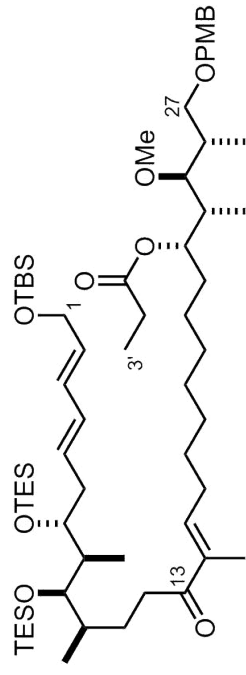
133



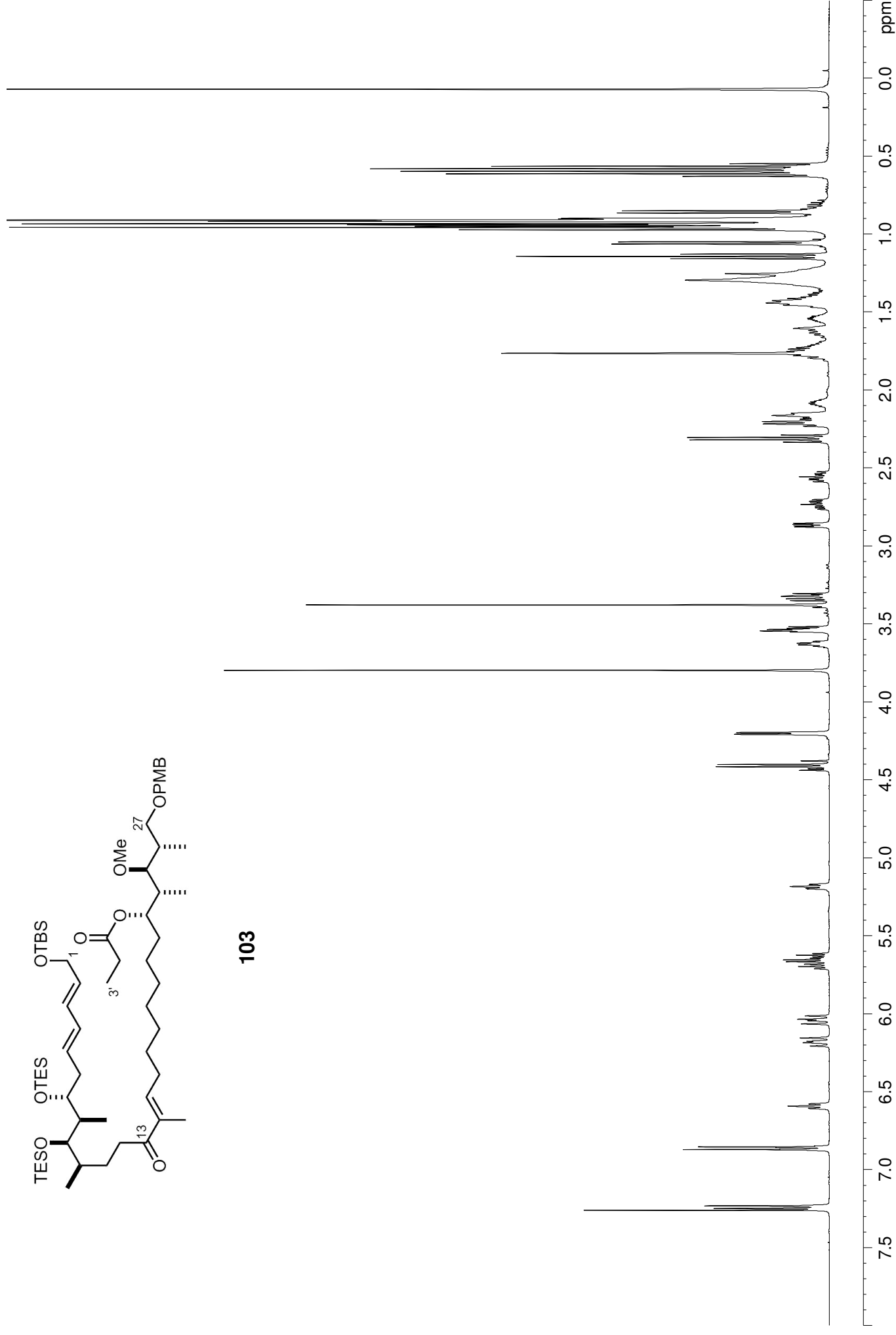


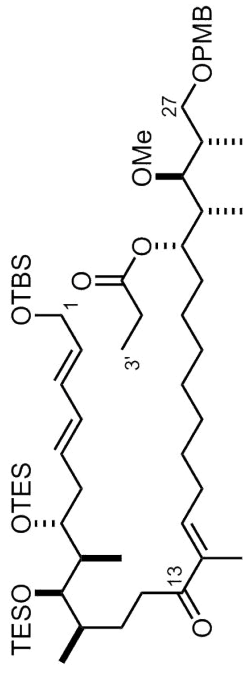
133



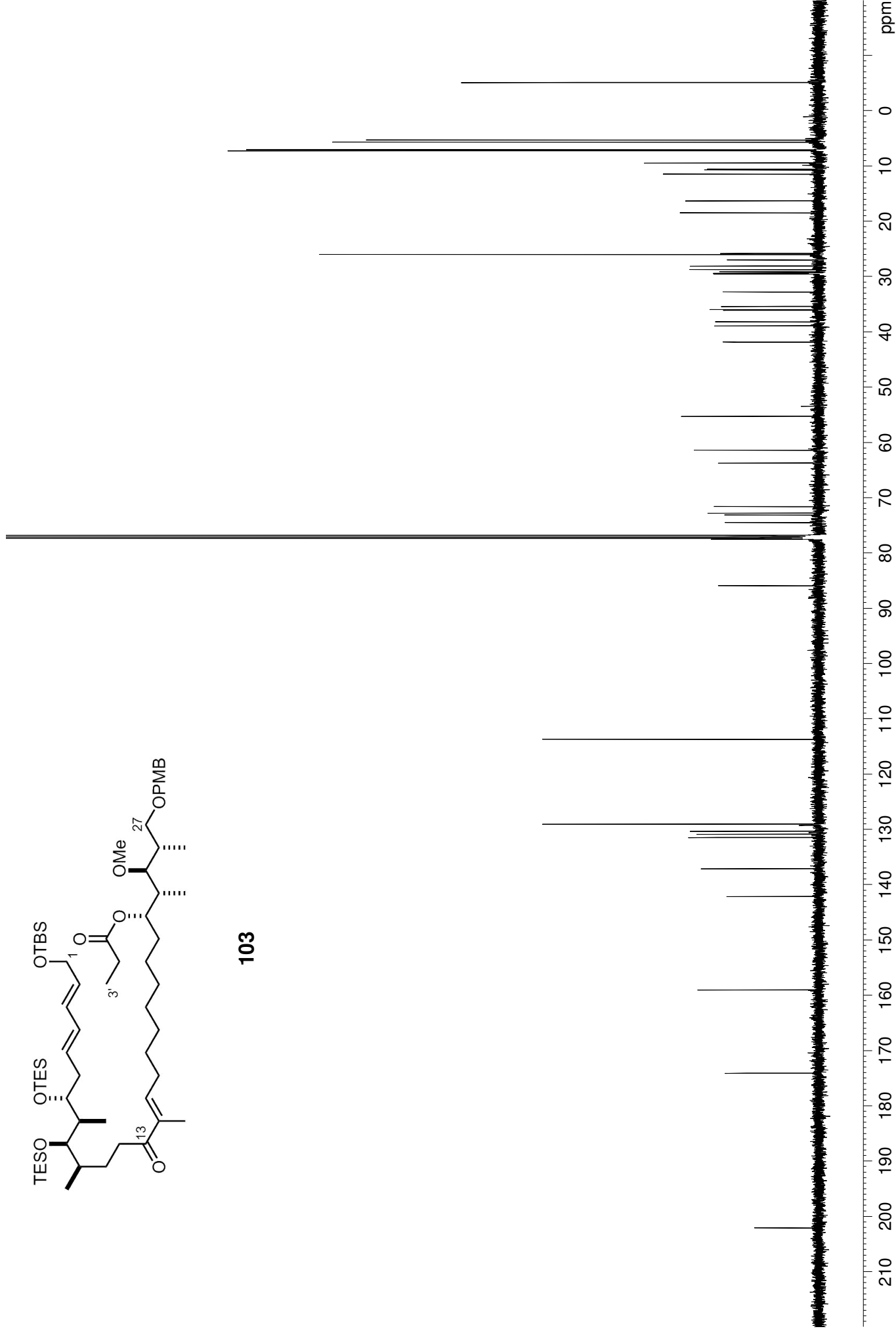


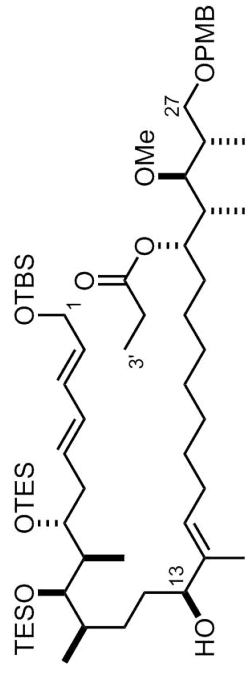
103



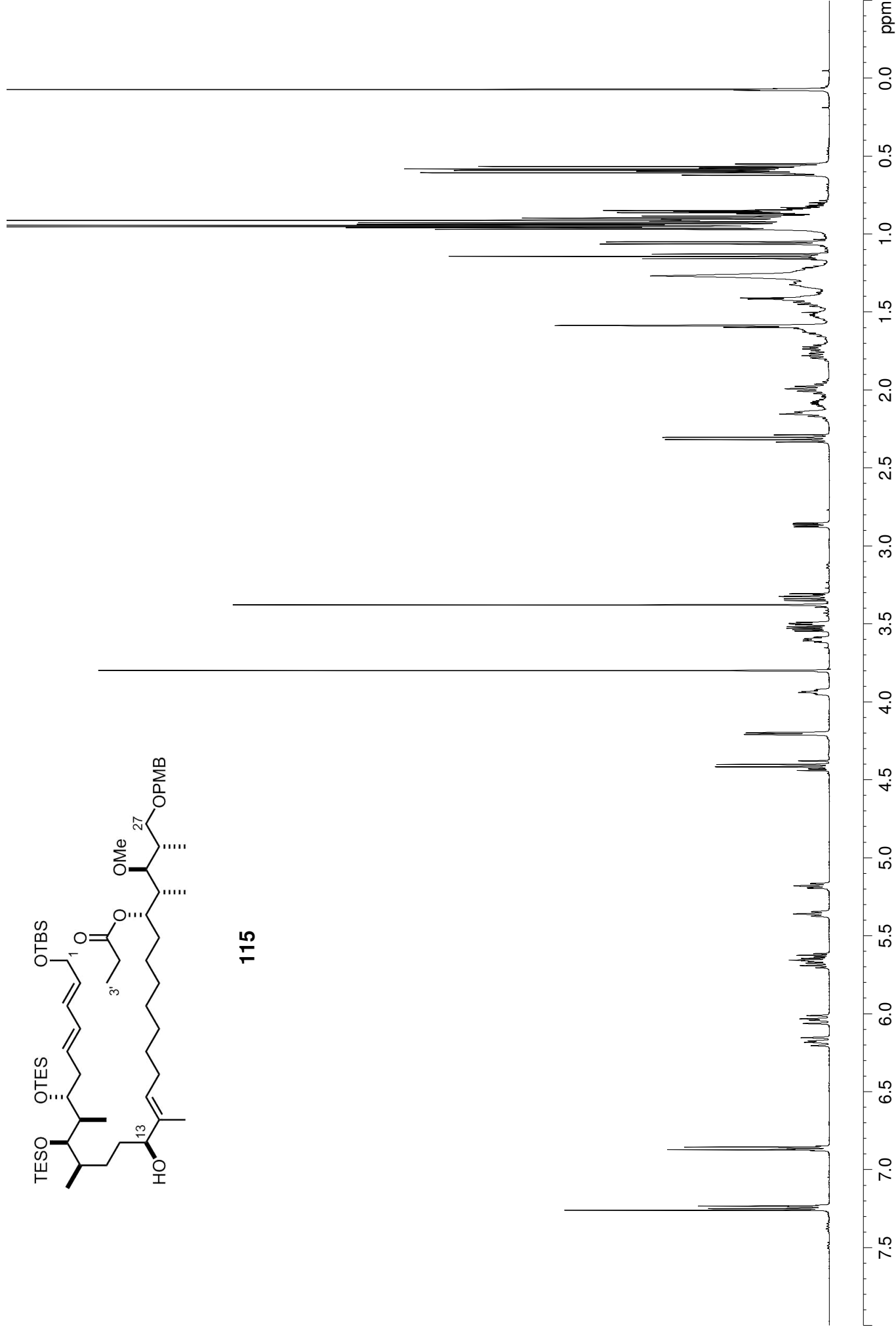


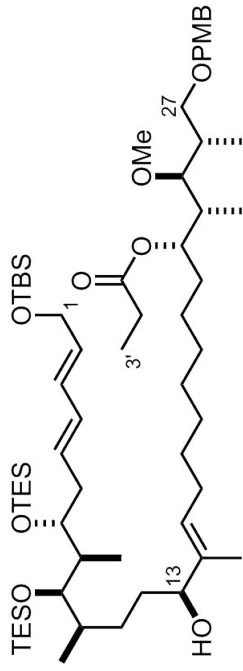
103



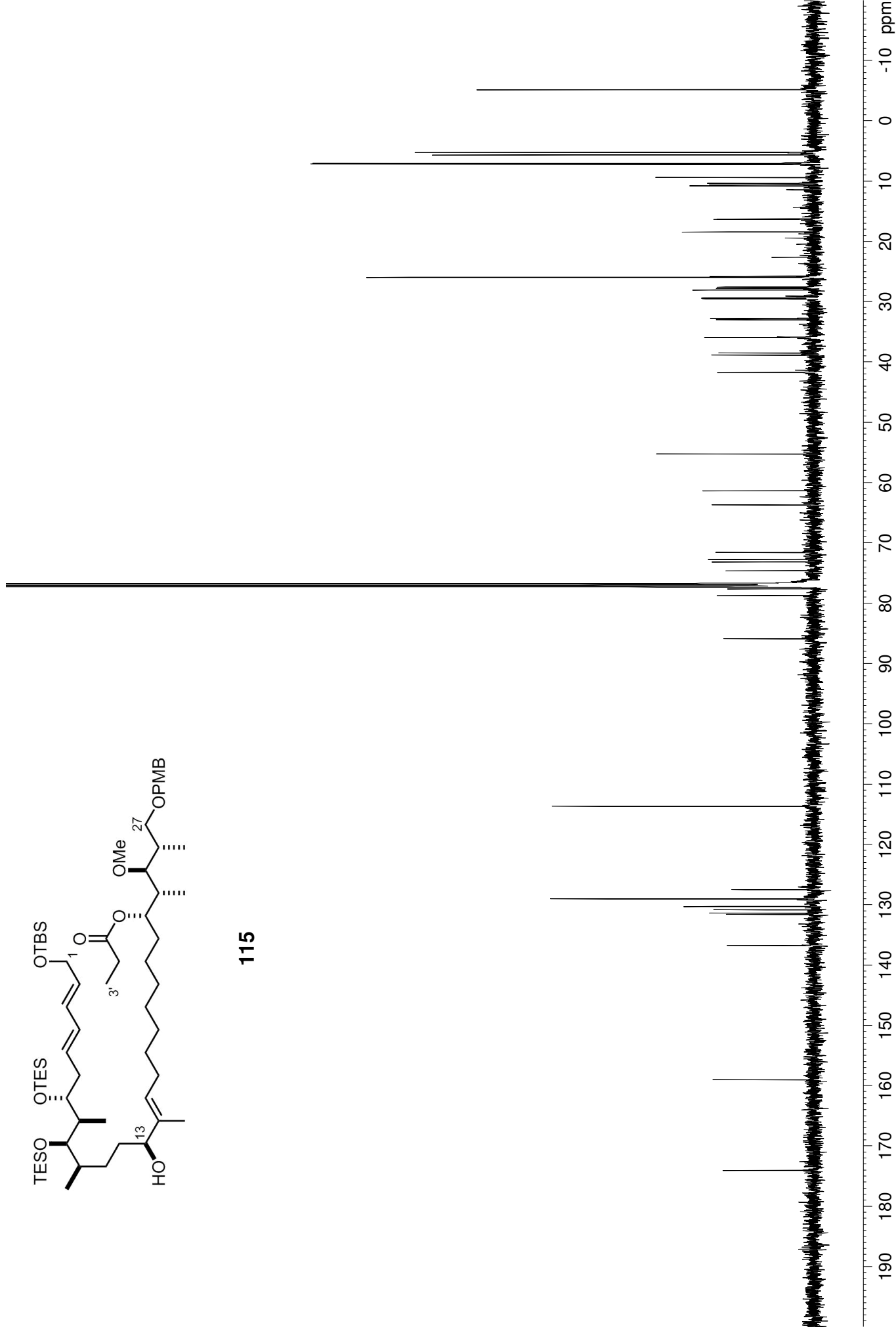


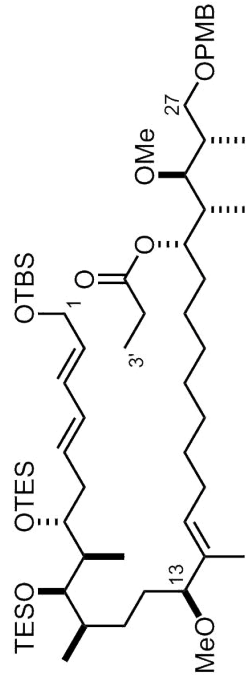
115



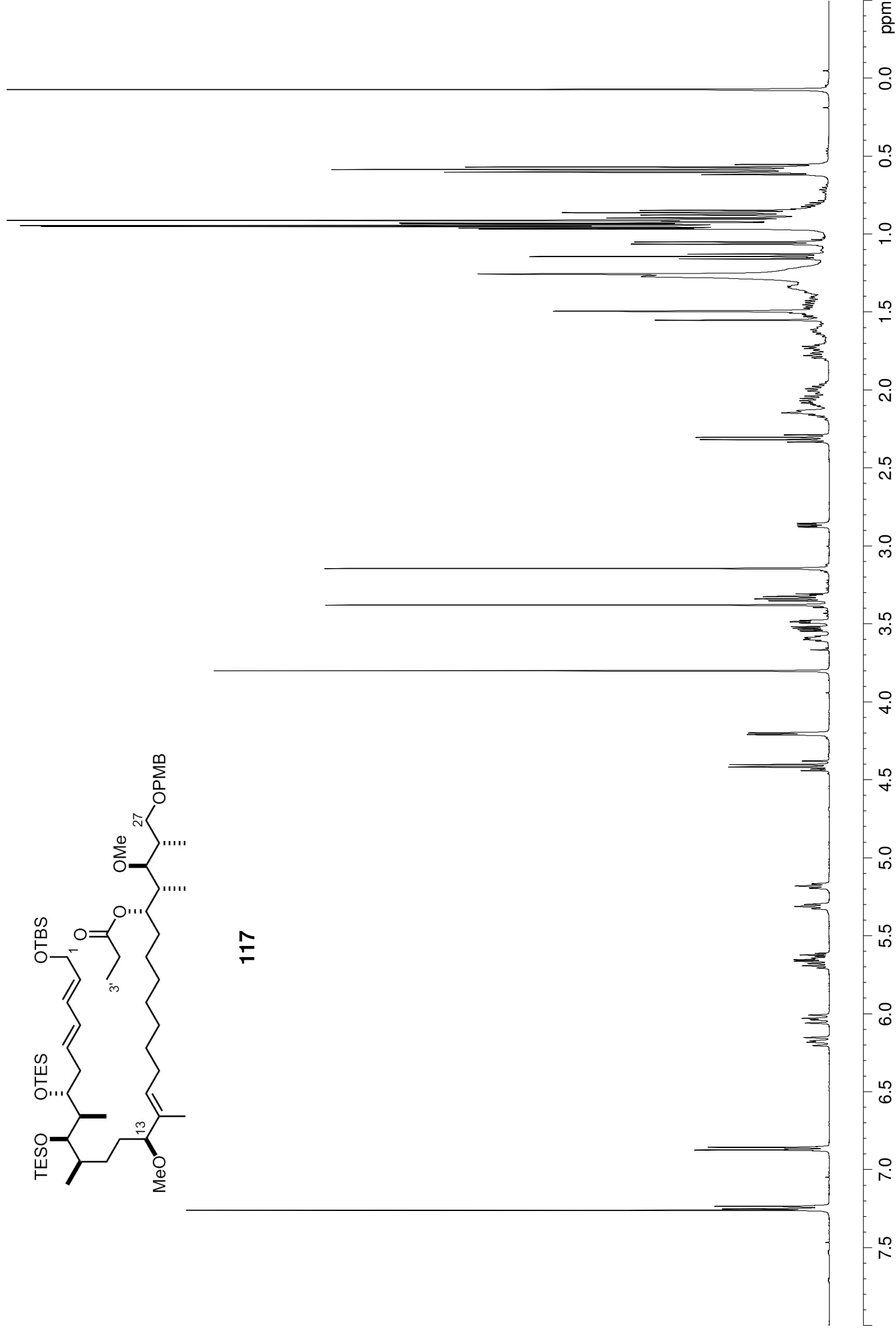


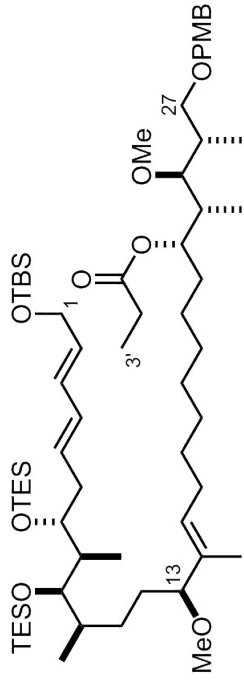
115



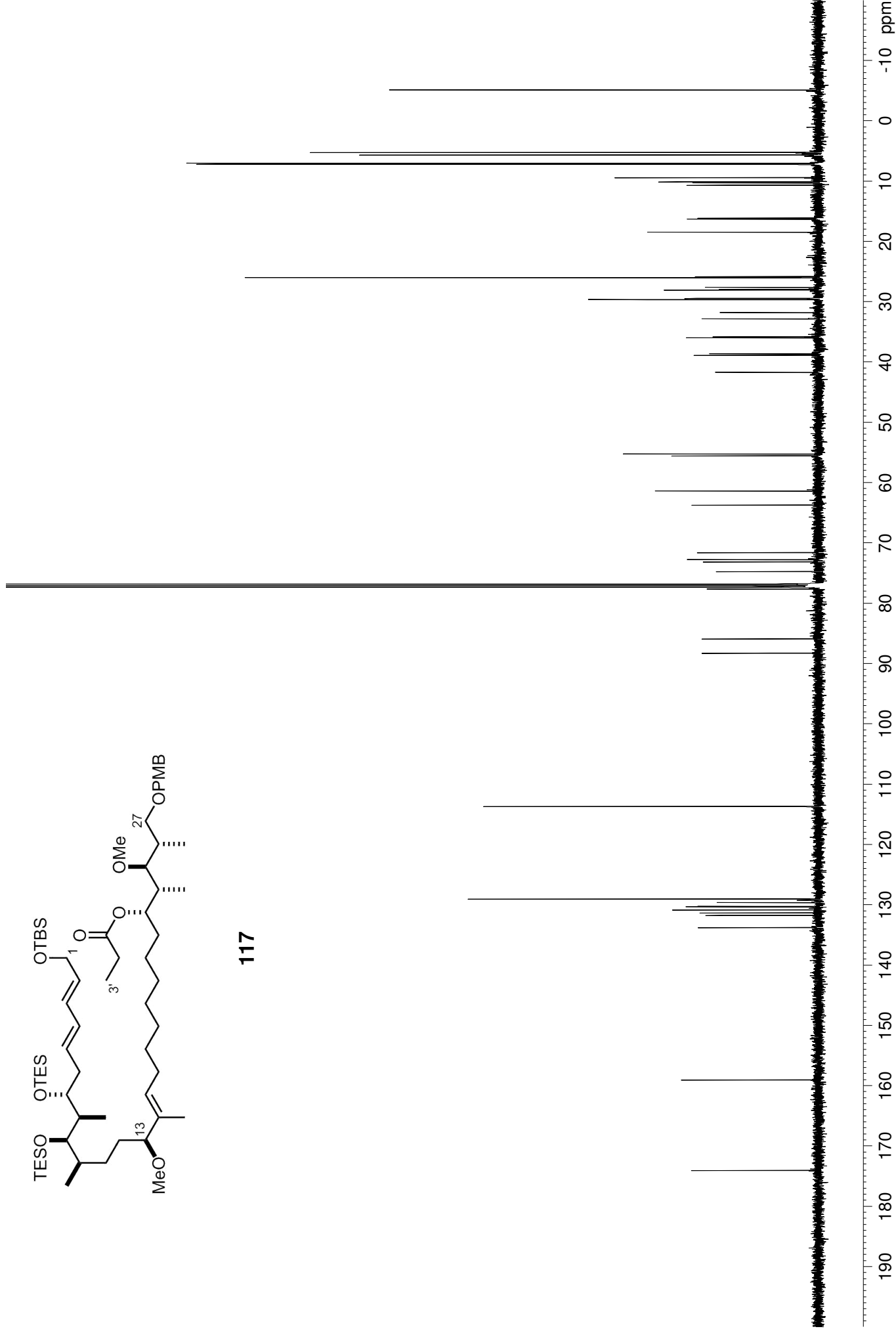


117

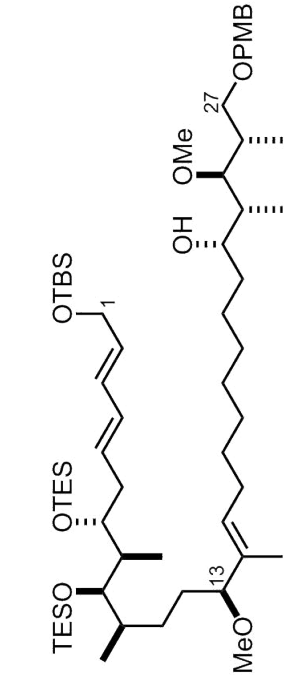




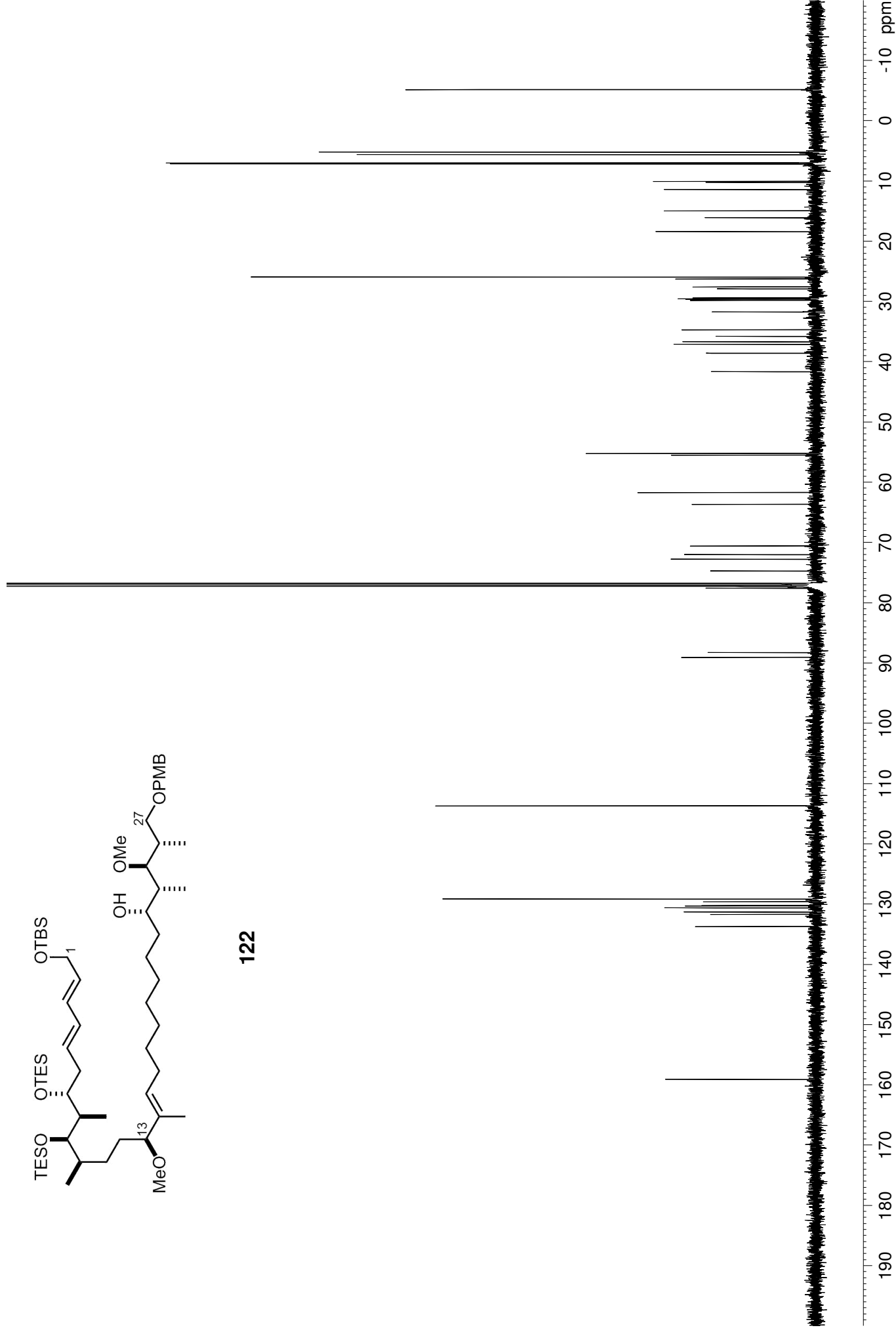
117

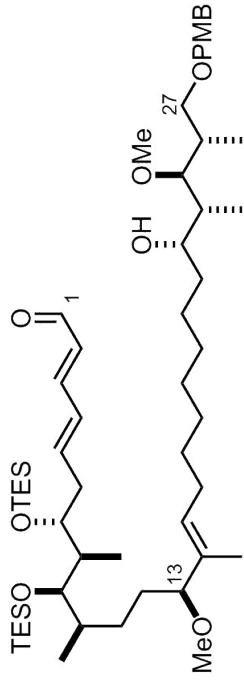




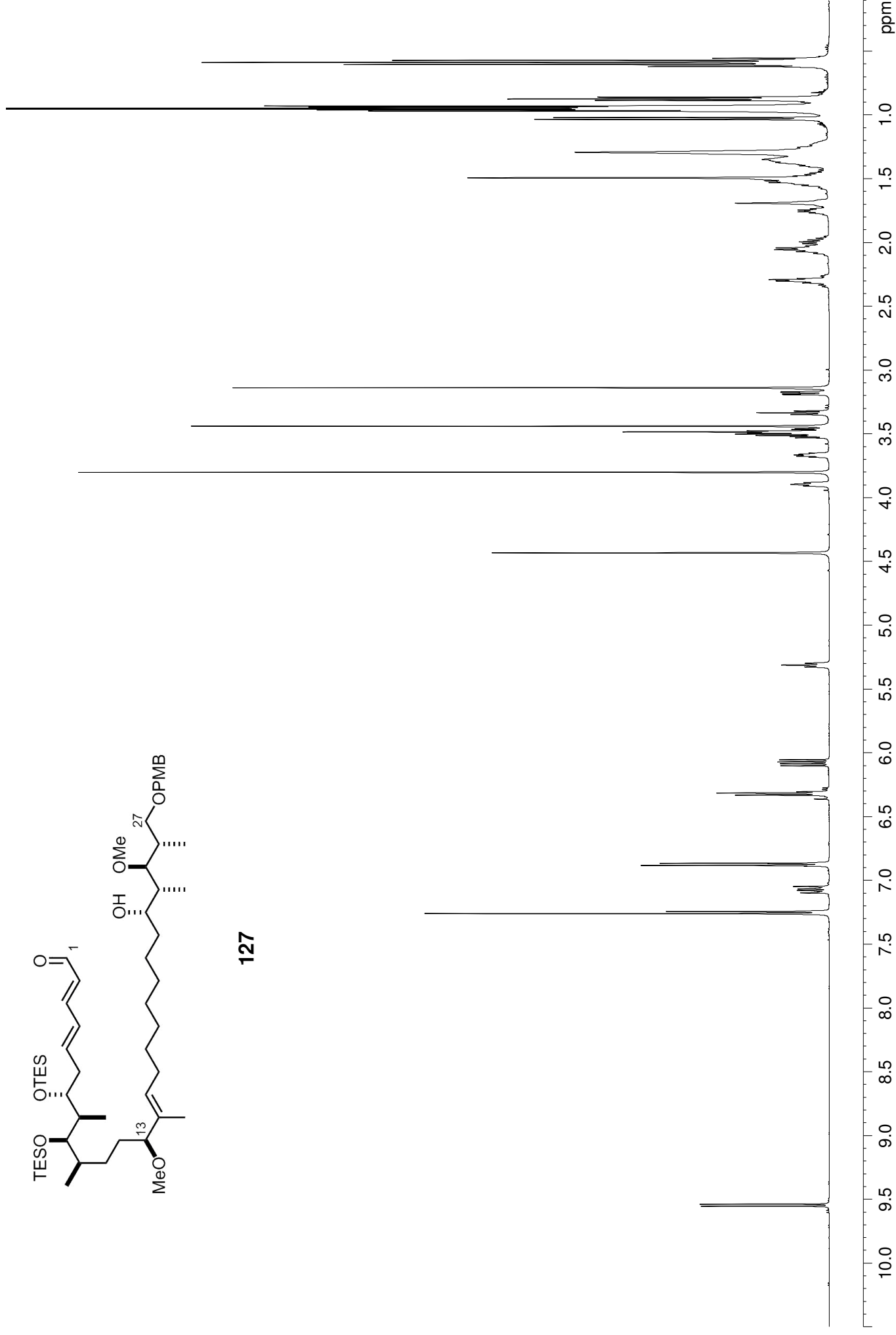


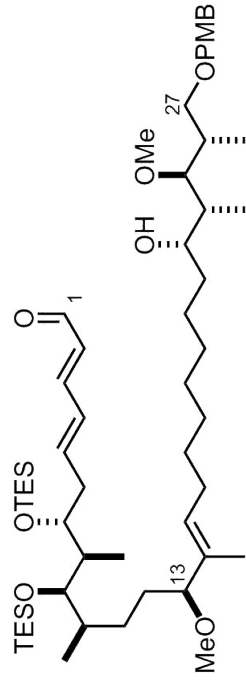
122



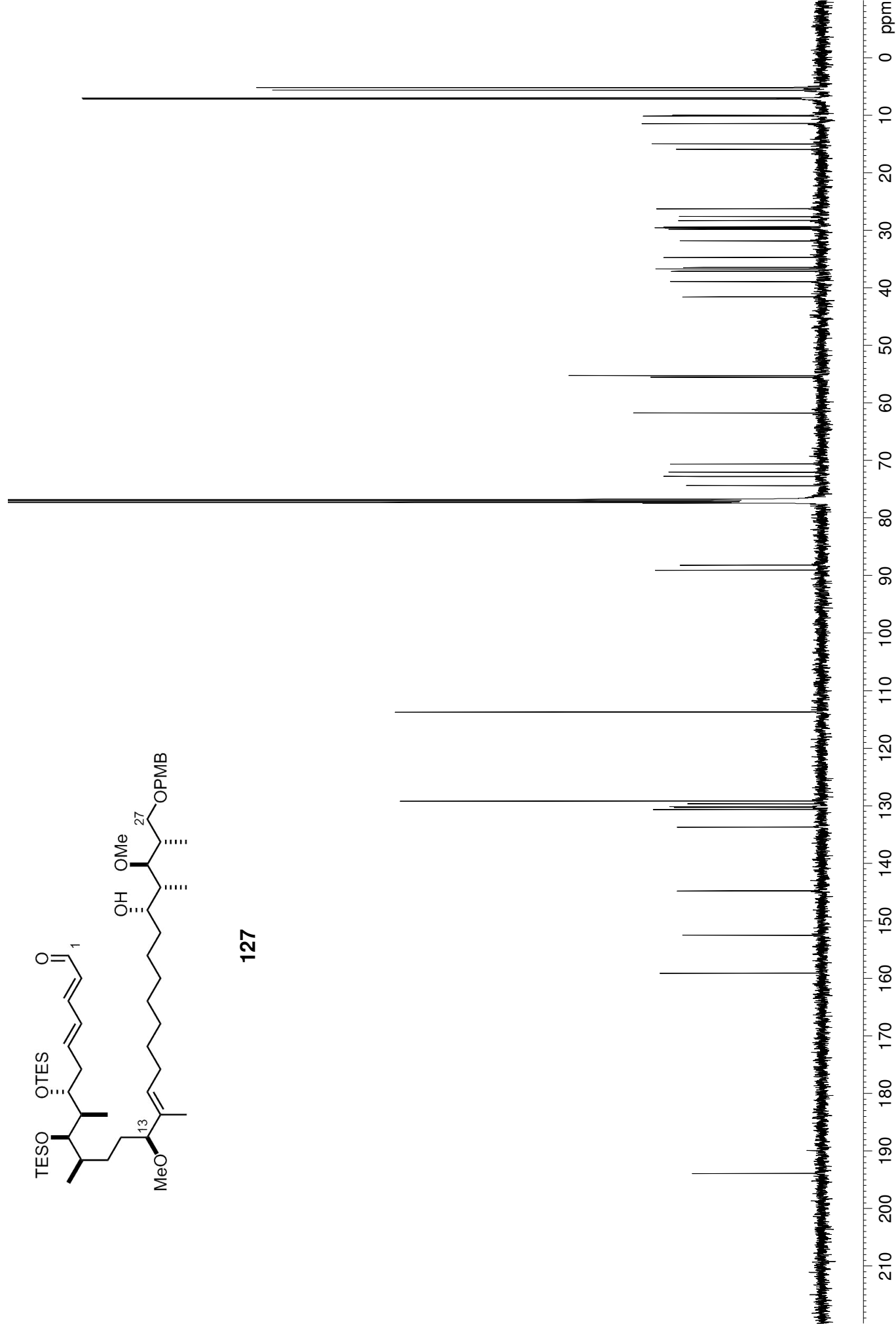


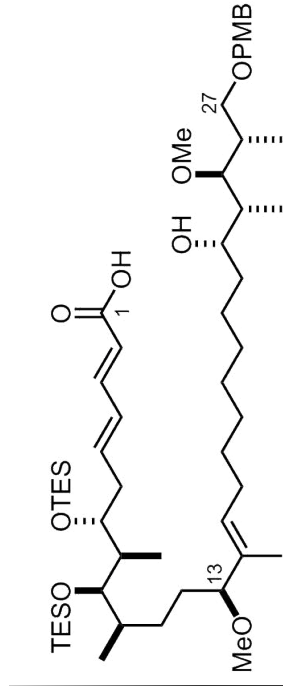
127



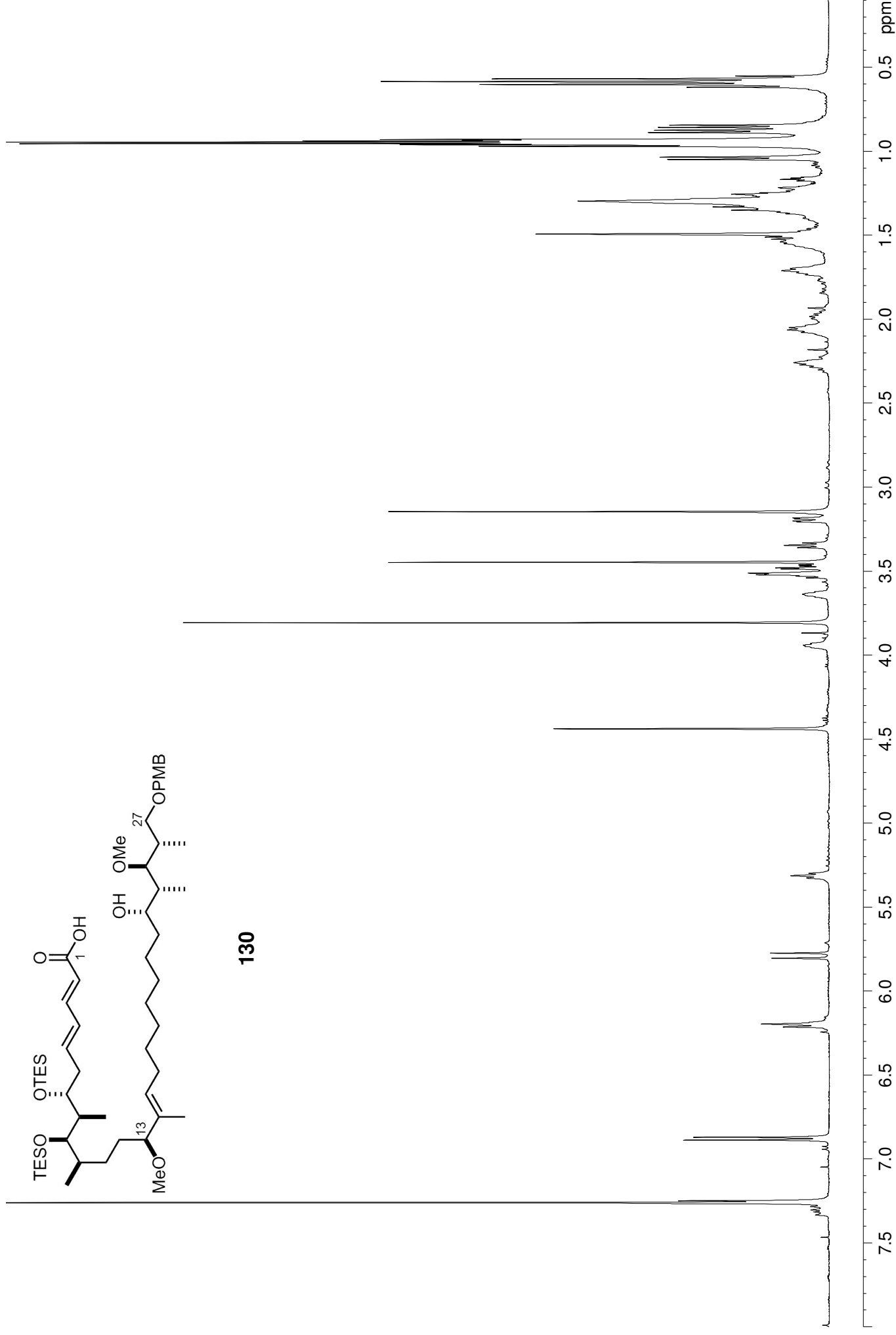


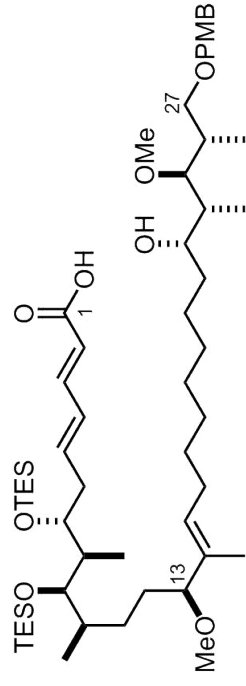
127



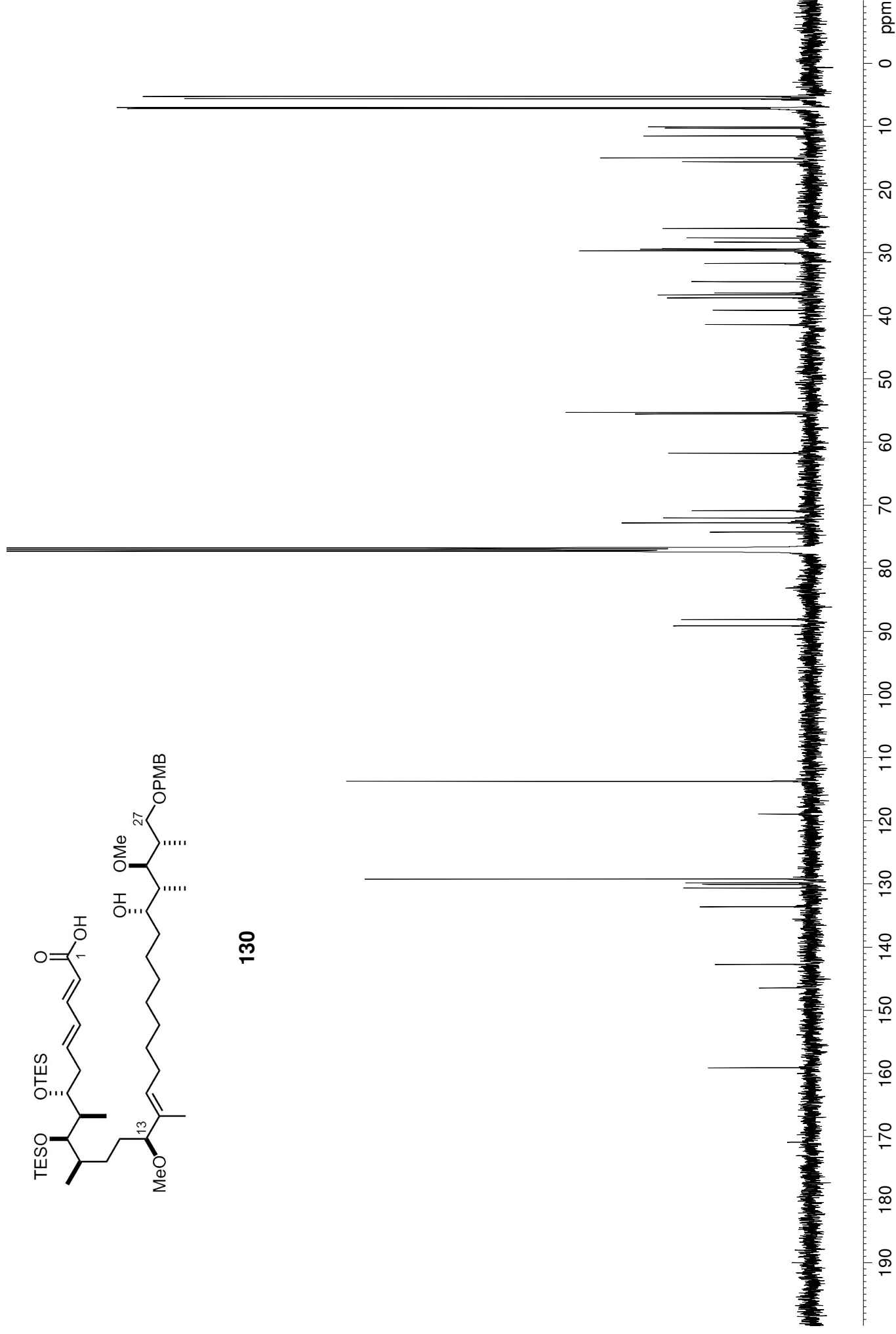


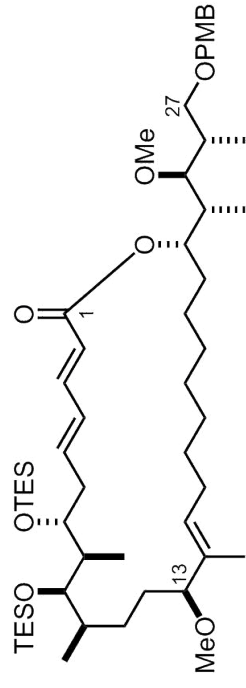
130



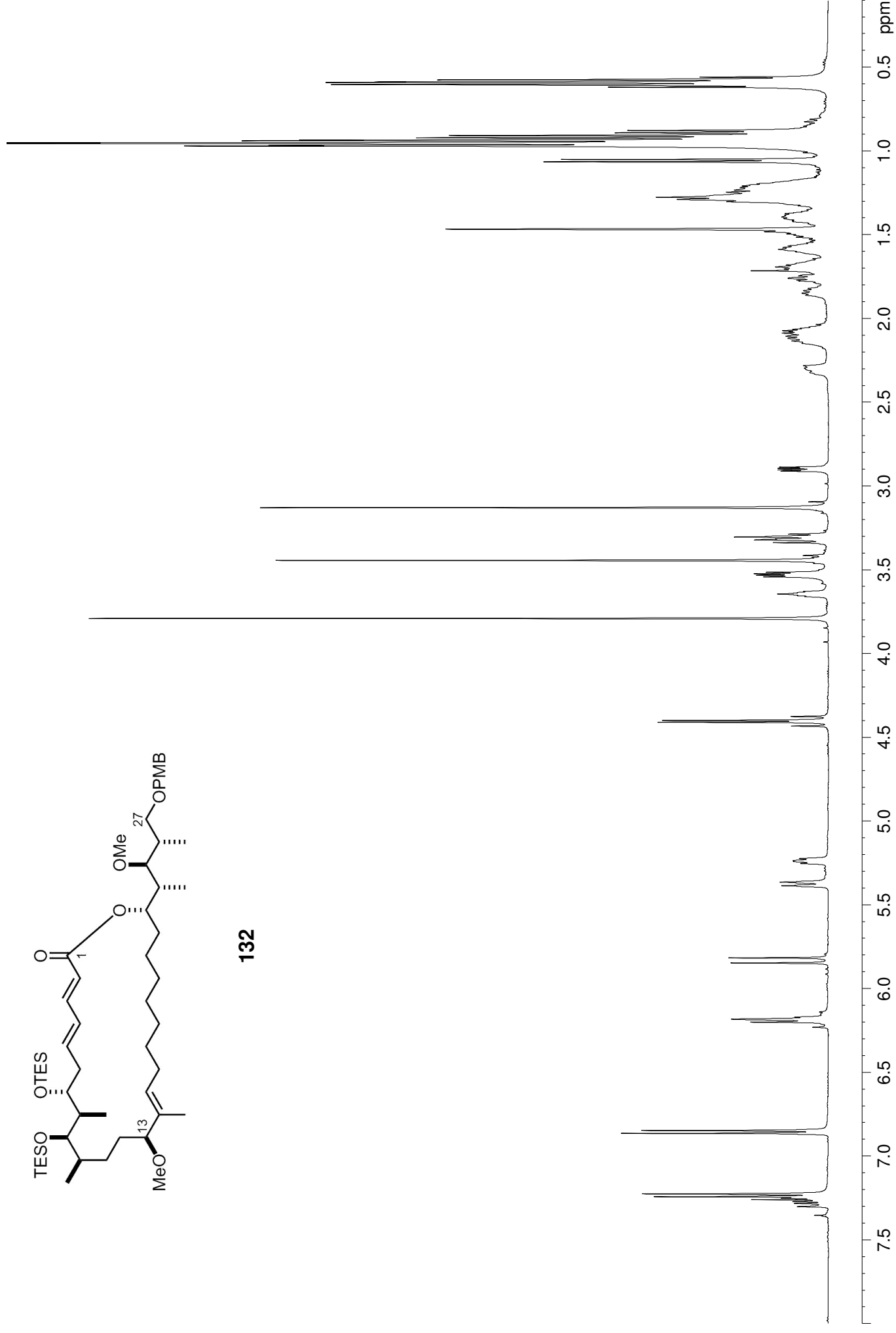


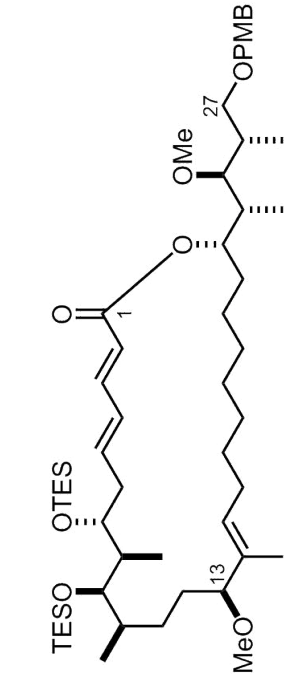
130



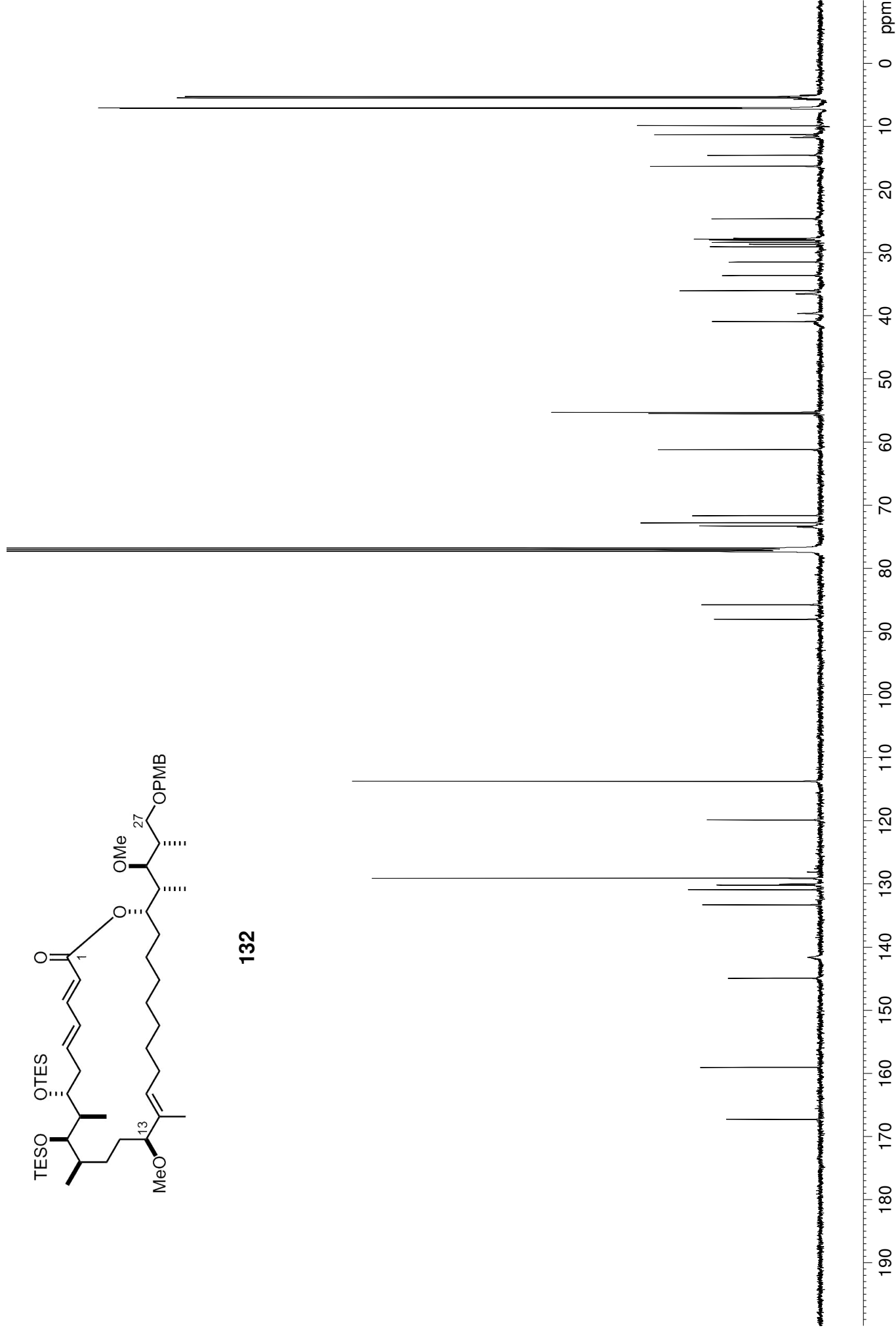


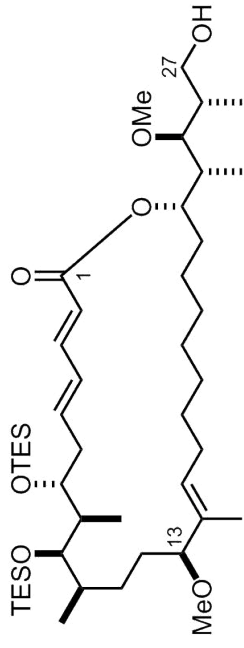
132



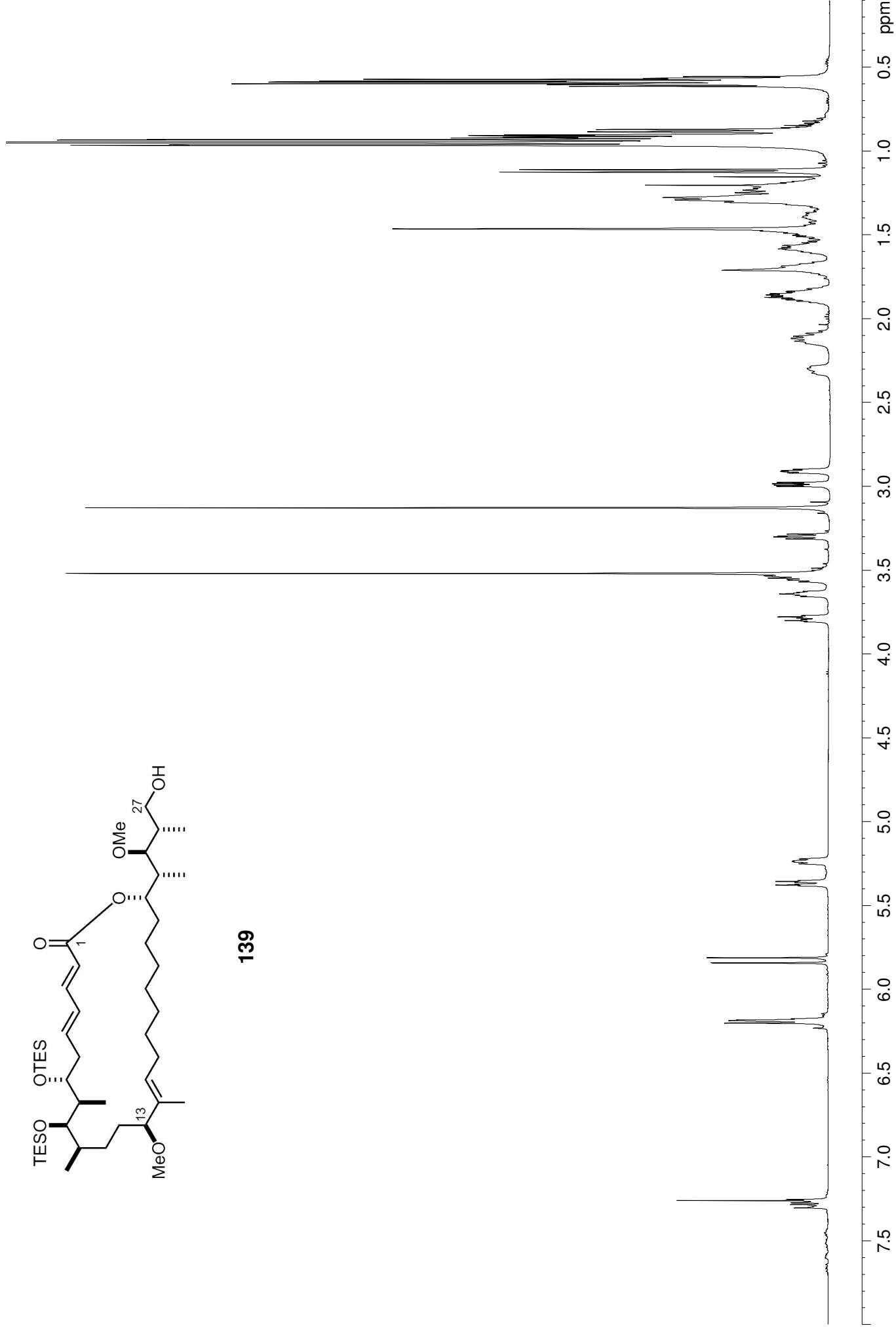


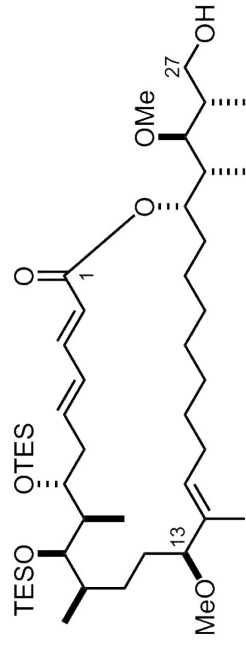
132



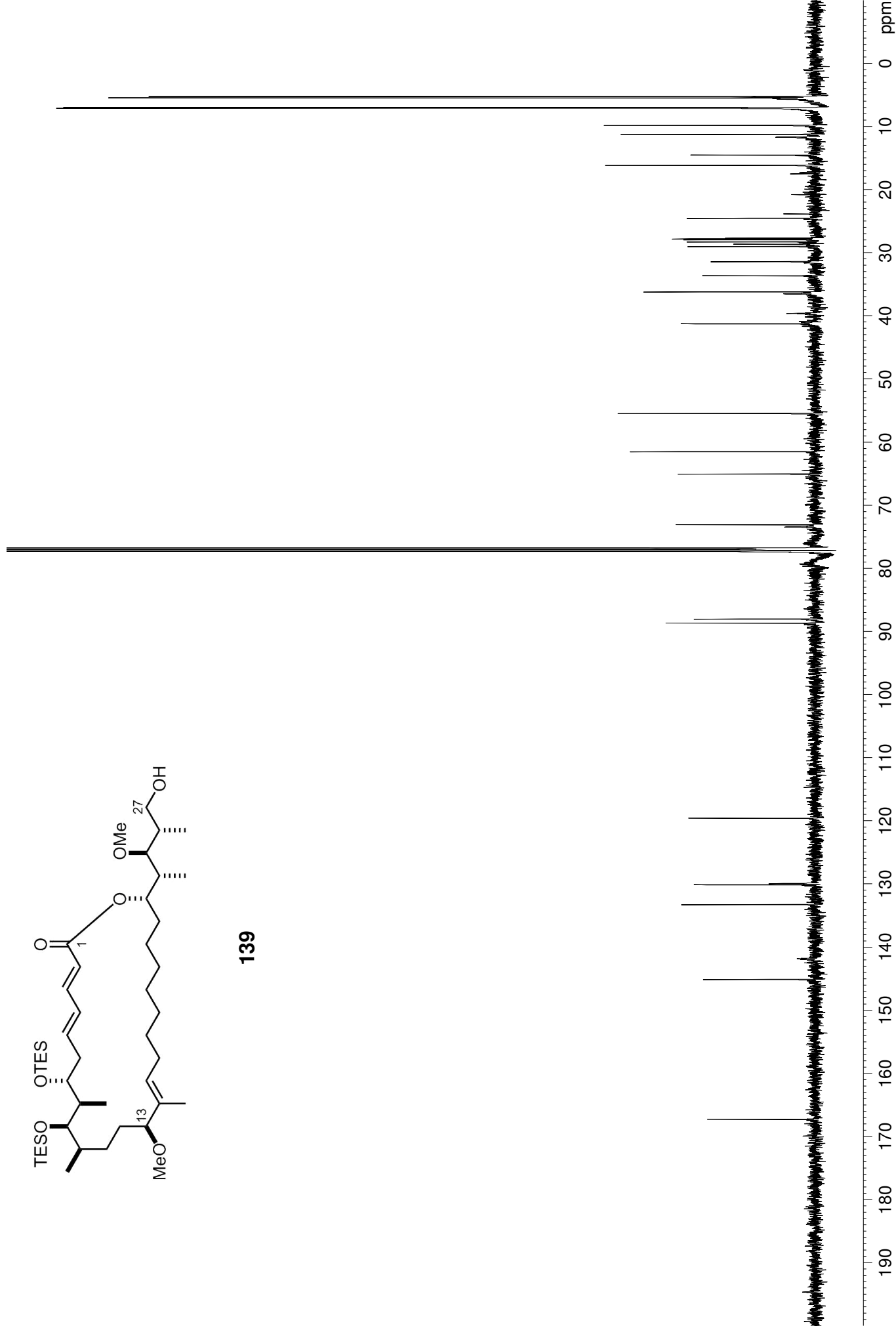


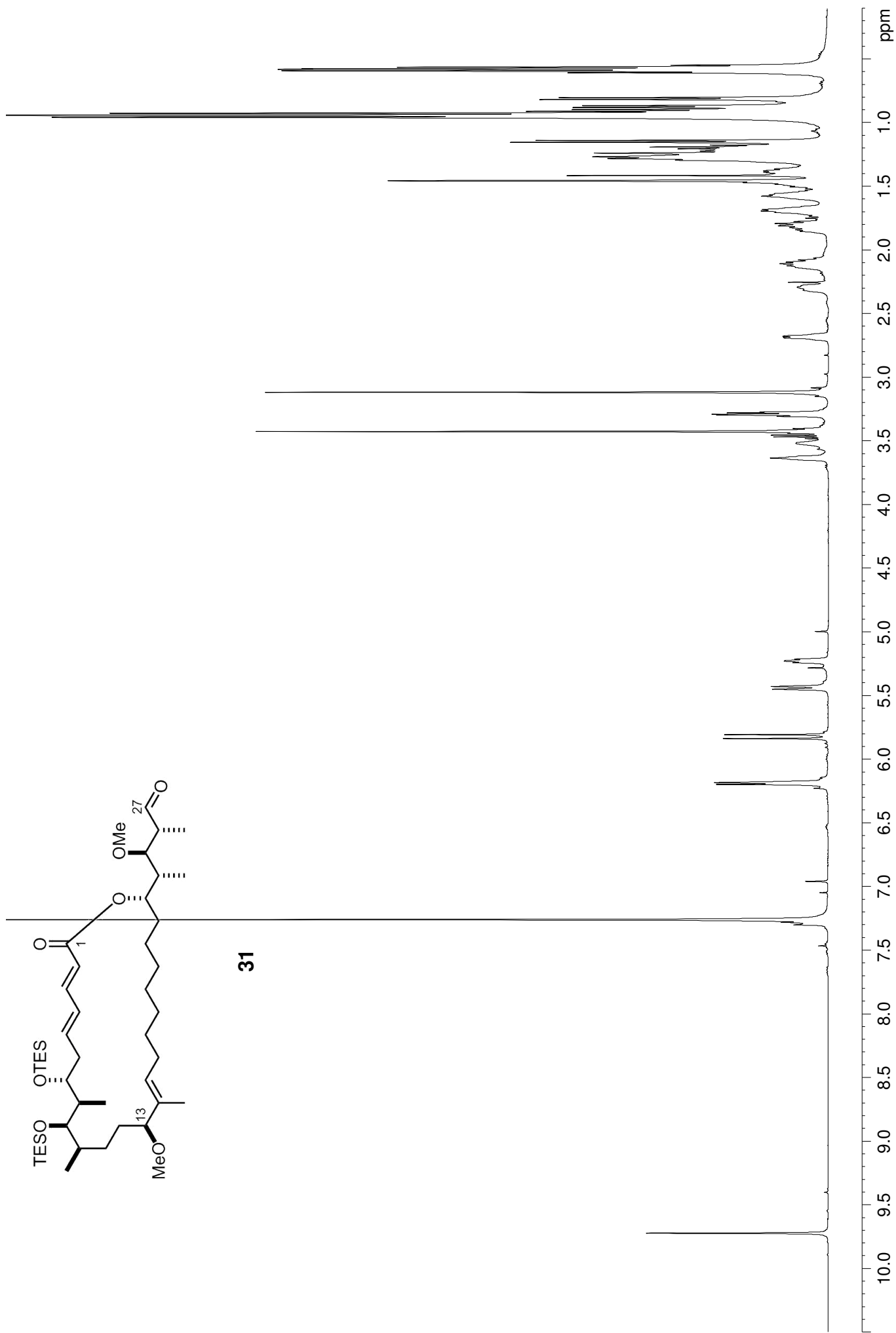
139





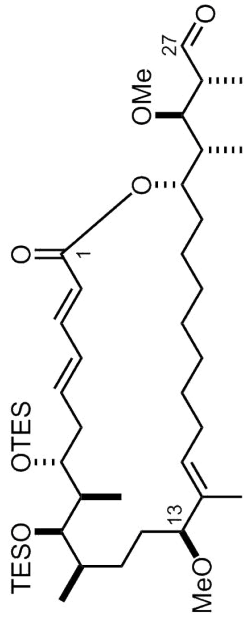
139



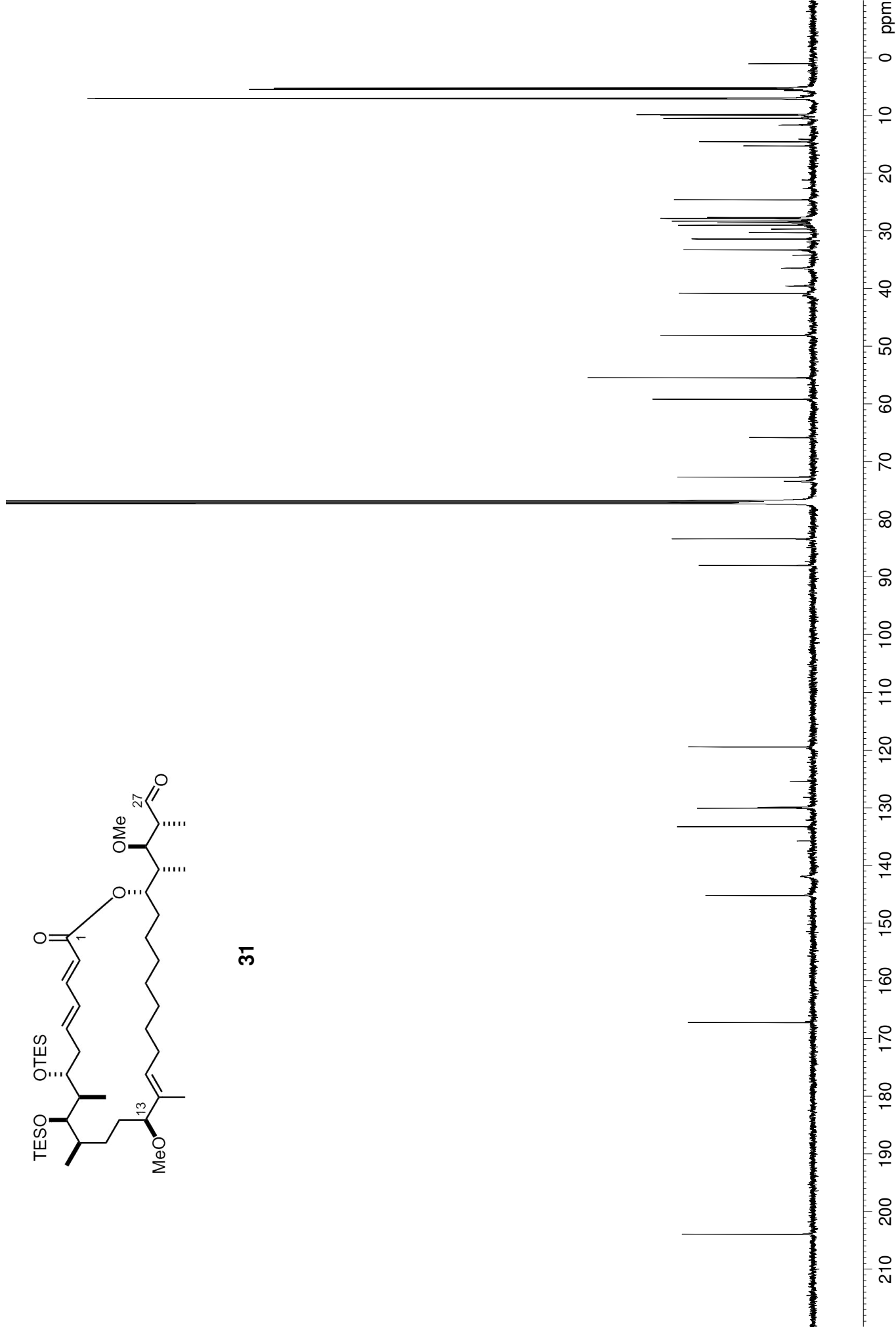


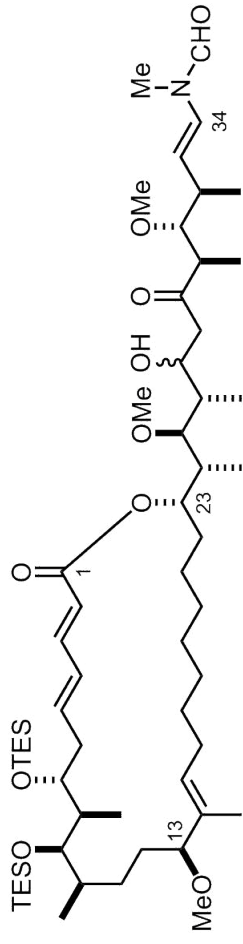
31

10.0 9.5 9.0 8.5 8.0 7.5 7.0 6.5 6.0 5.5 5.0 4.5 4.0 3.5 3.0 2.5 2.0 1.5 1.0 ppm

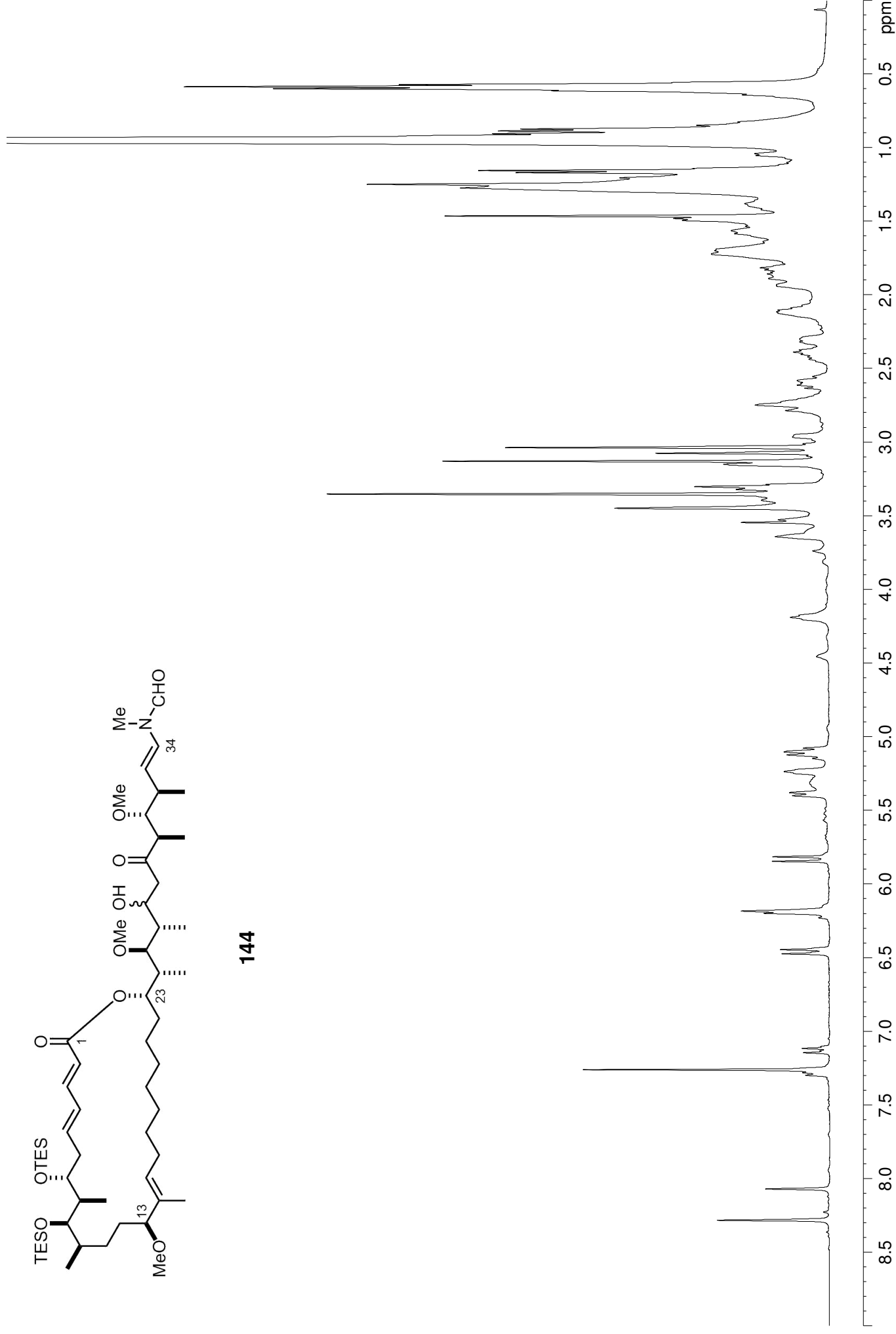


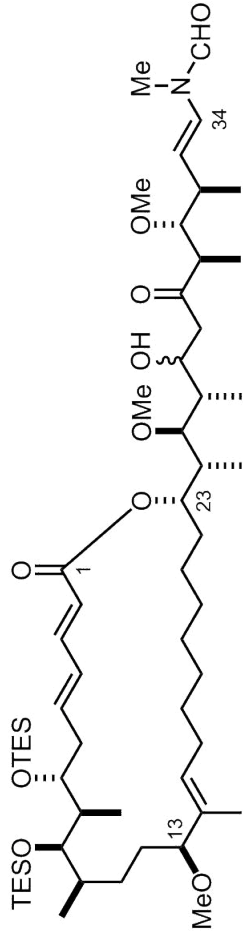
31



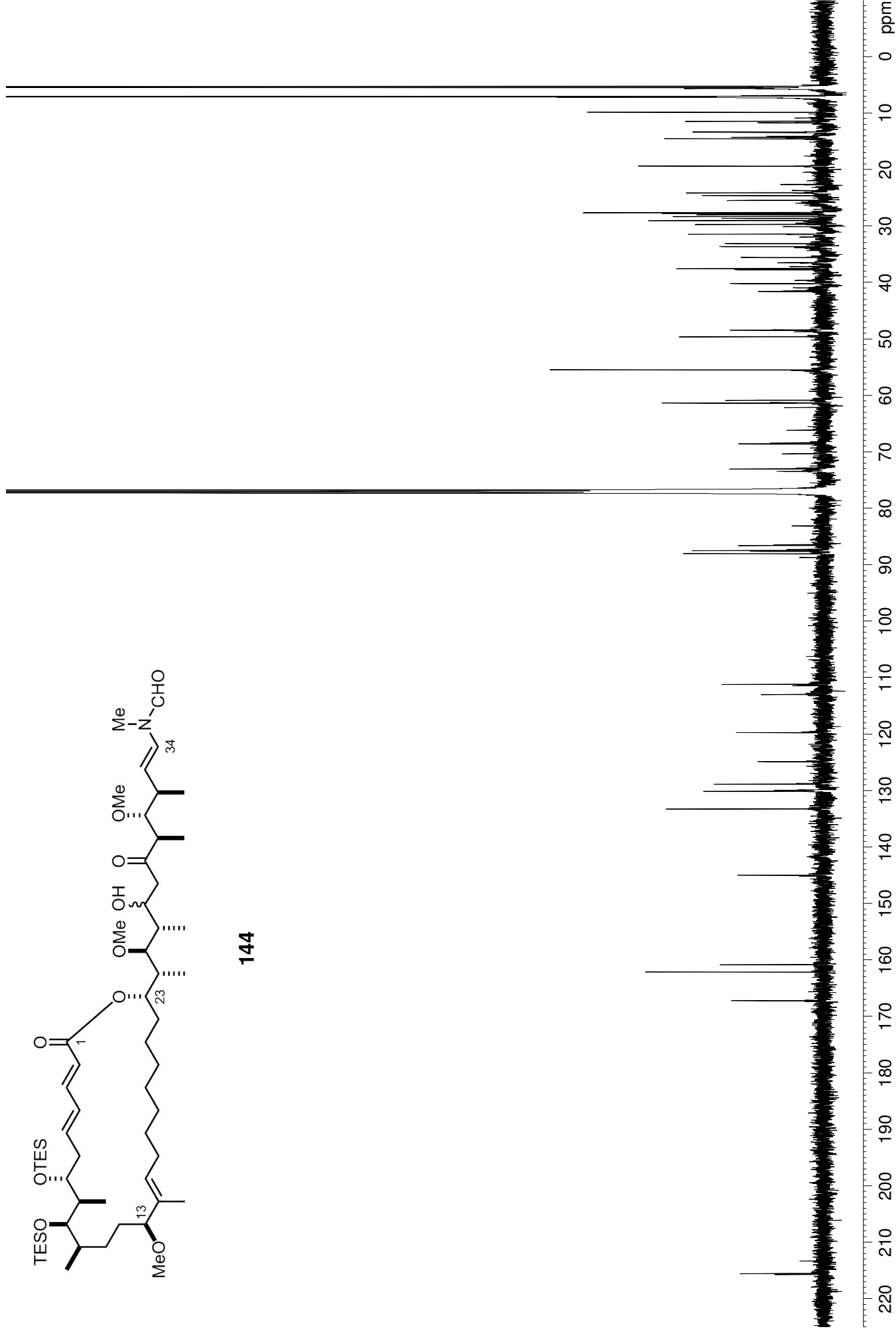


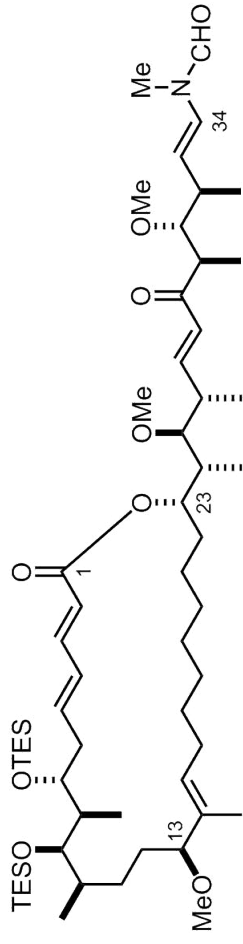
144



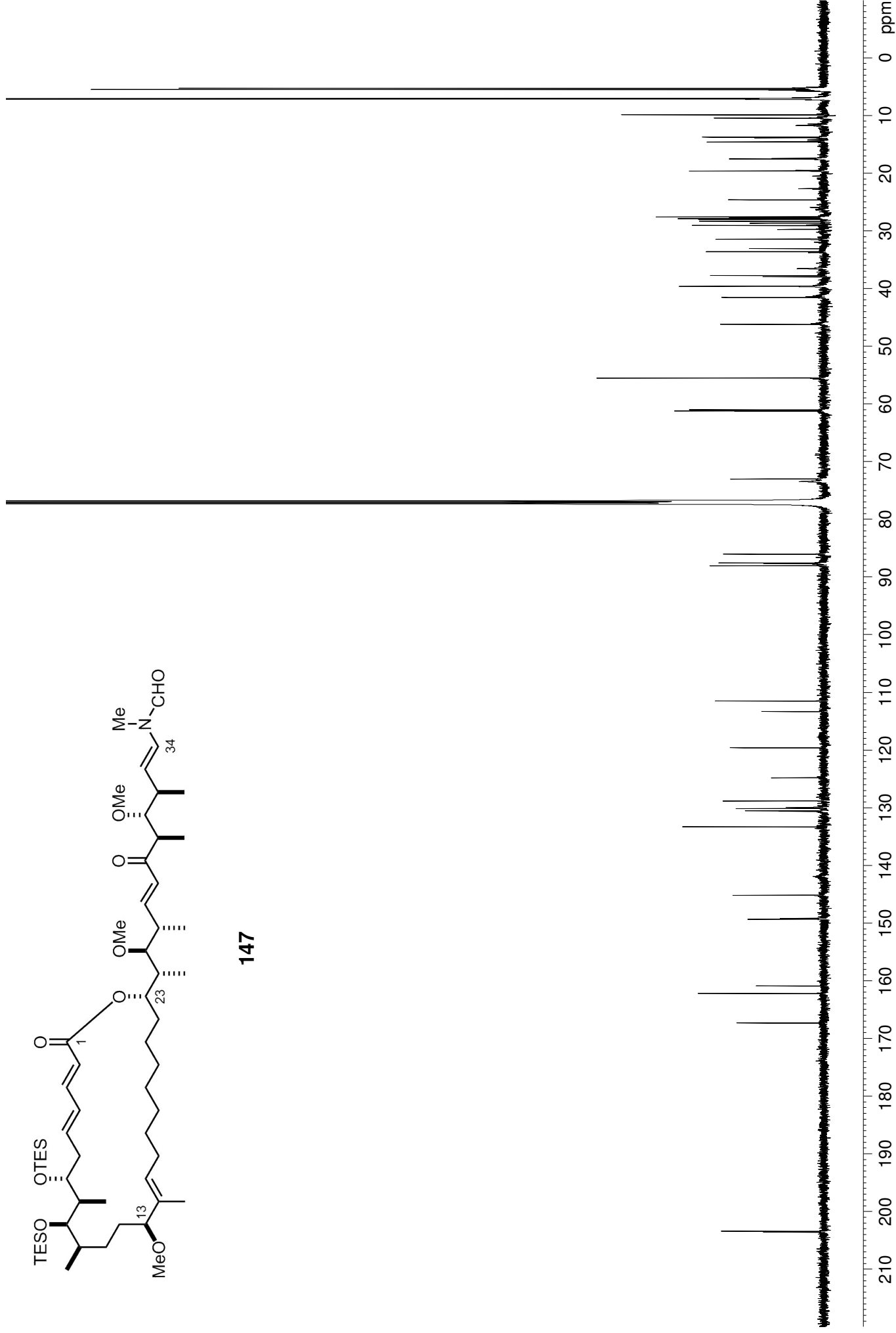


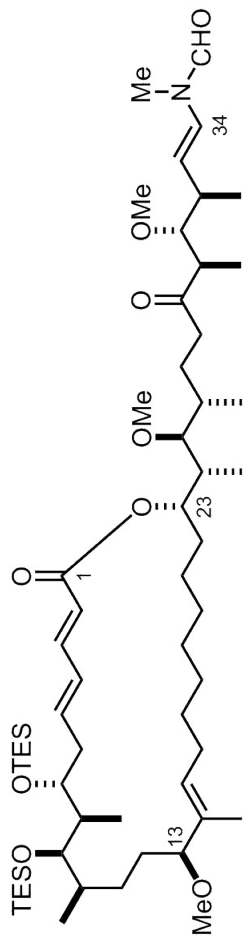
144



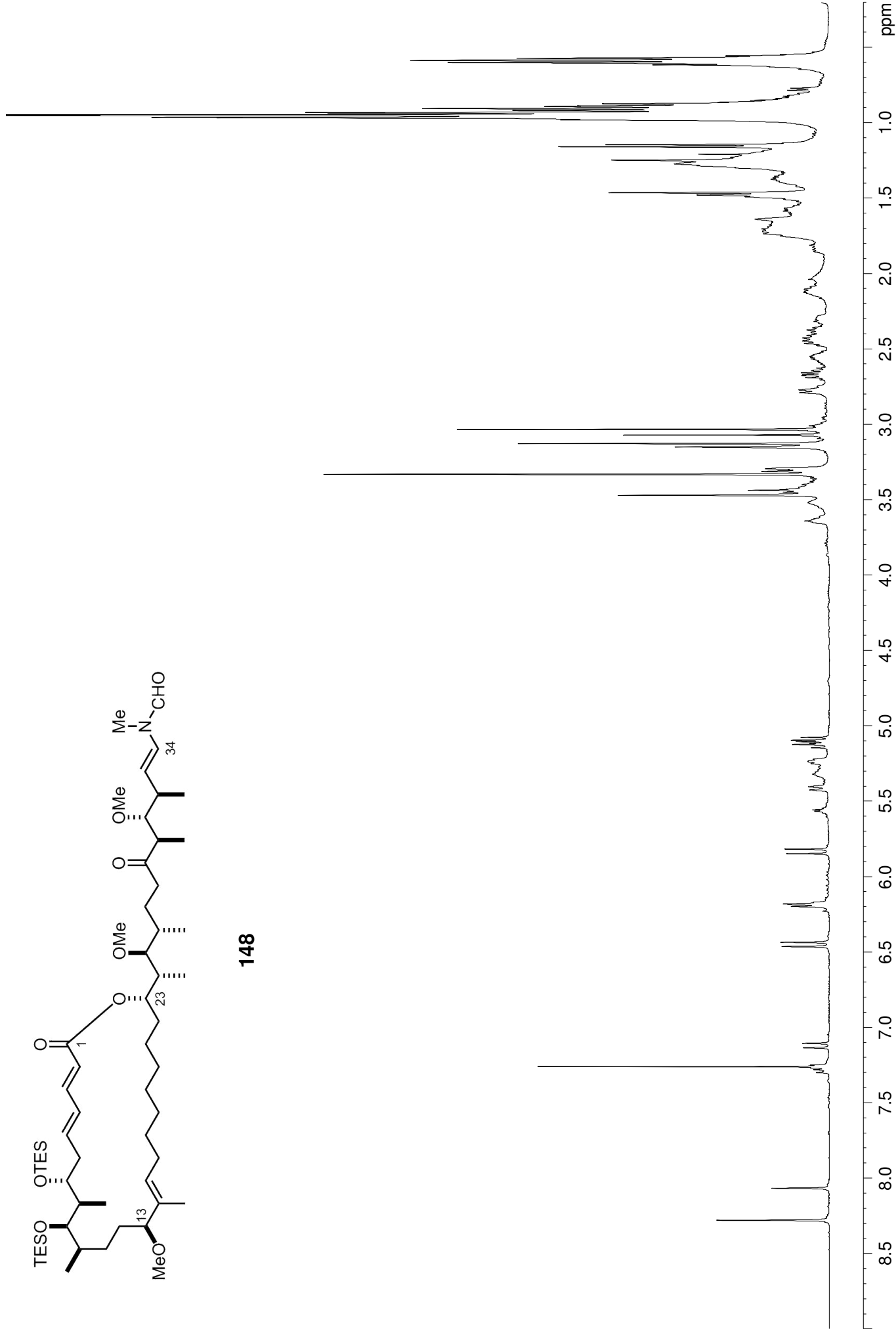


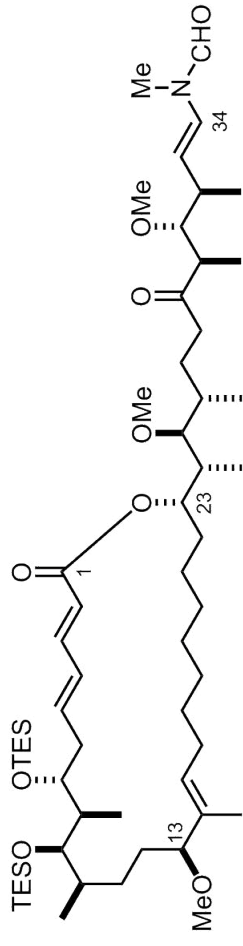
147



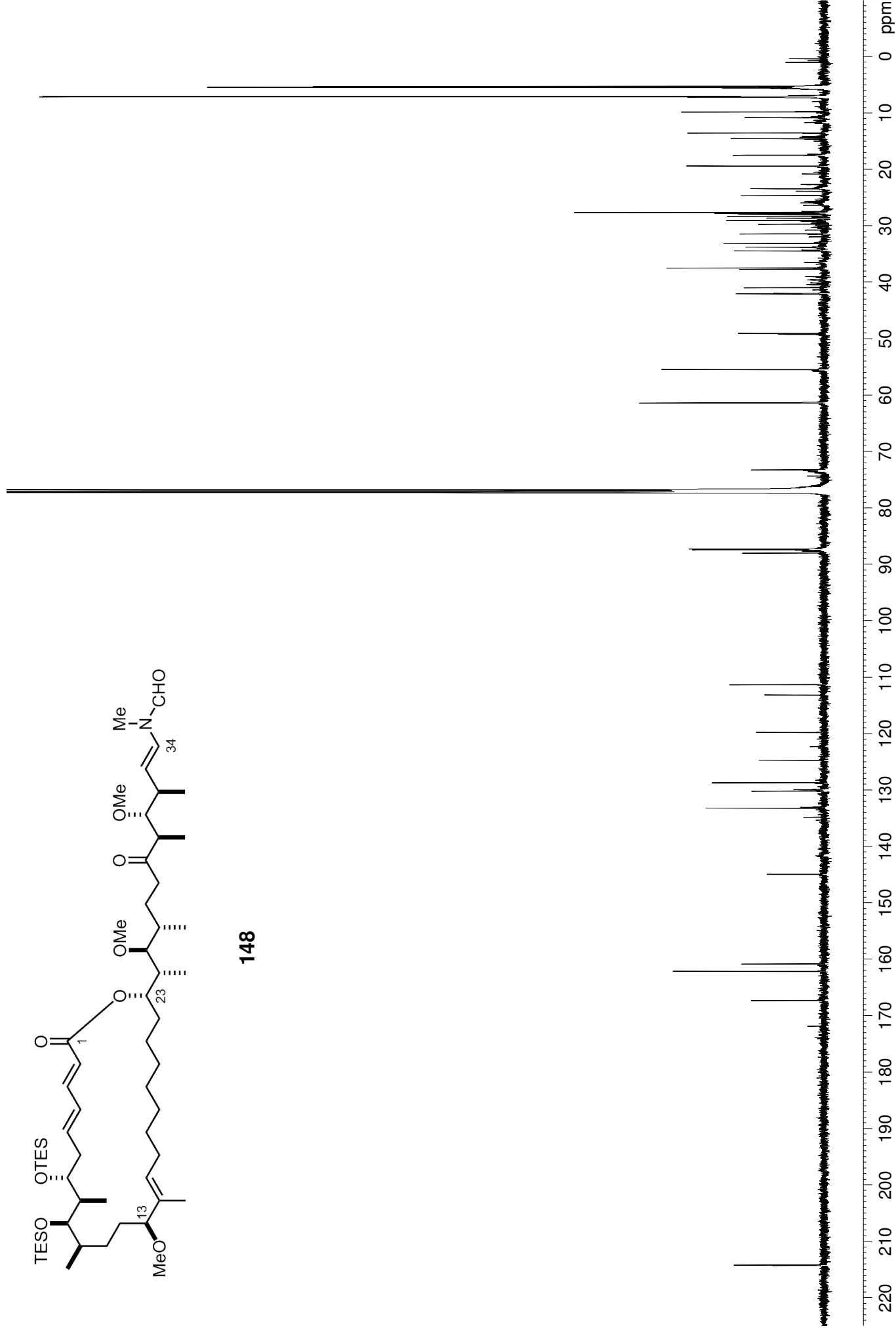


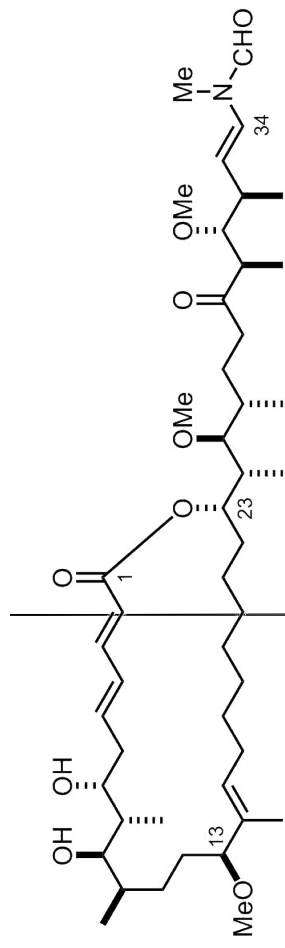
148



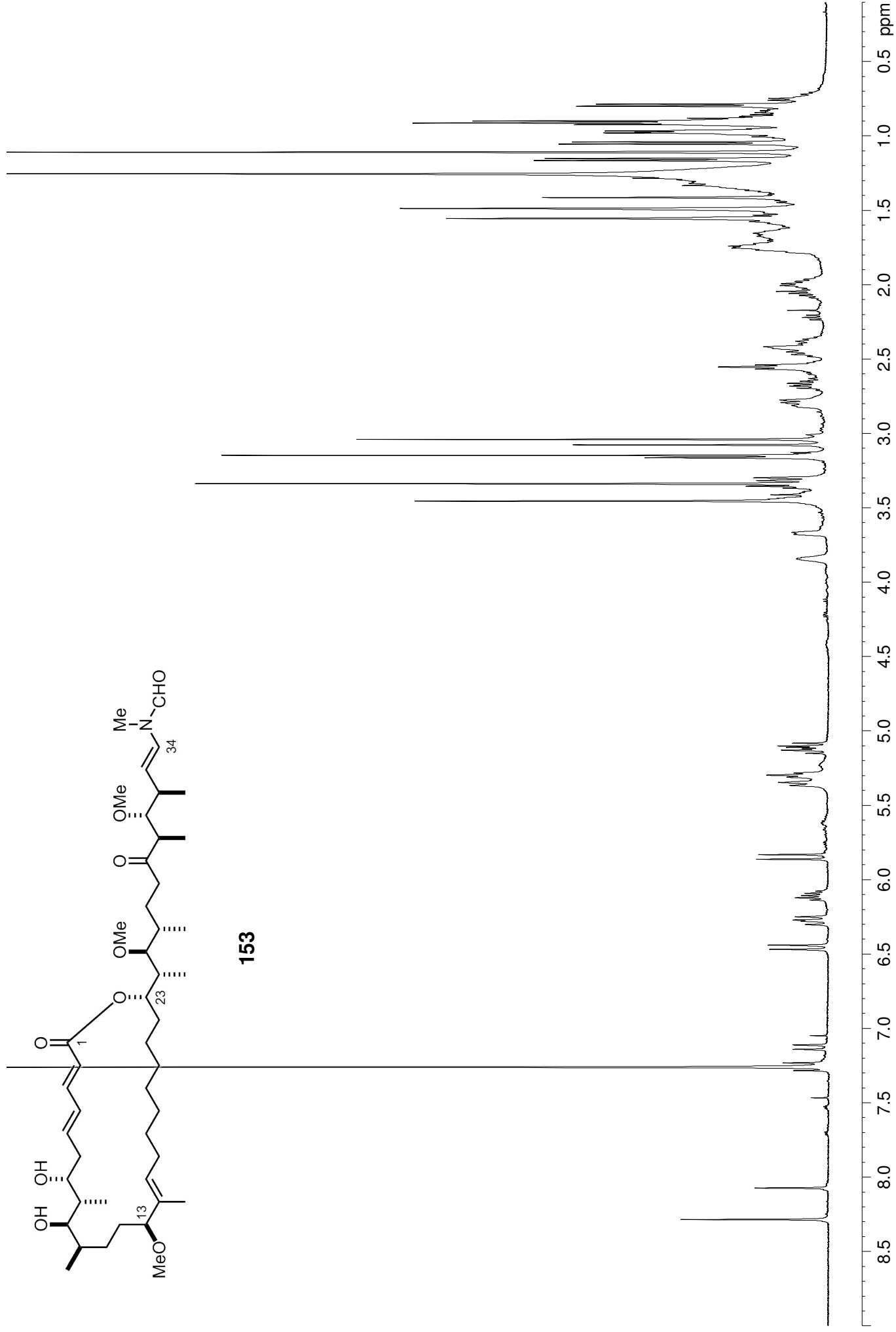


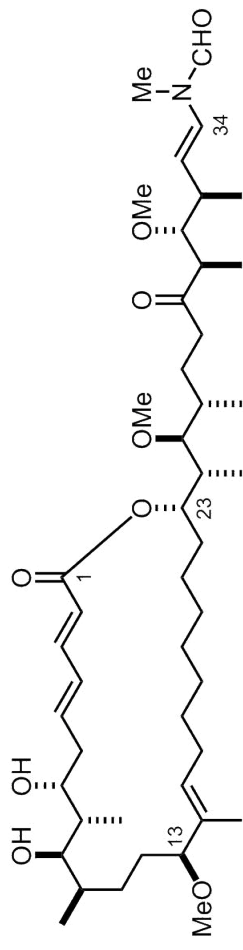
148



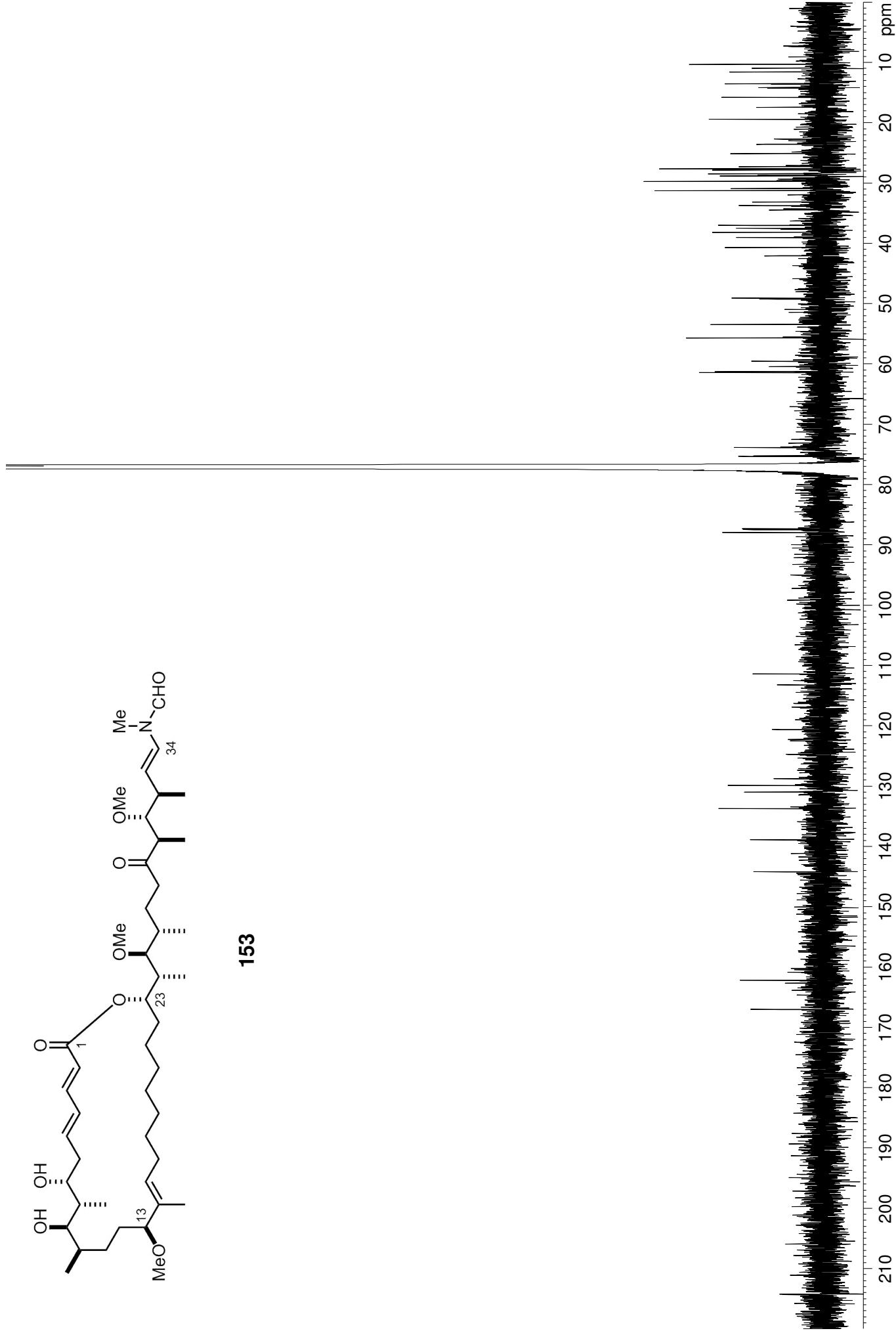


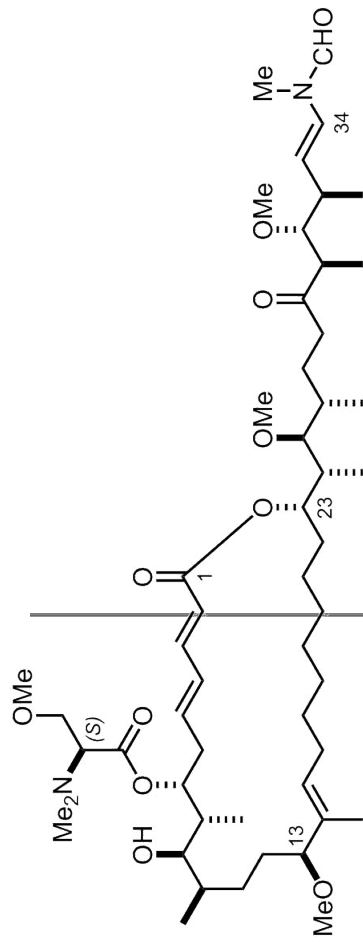
153



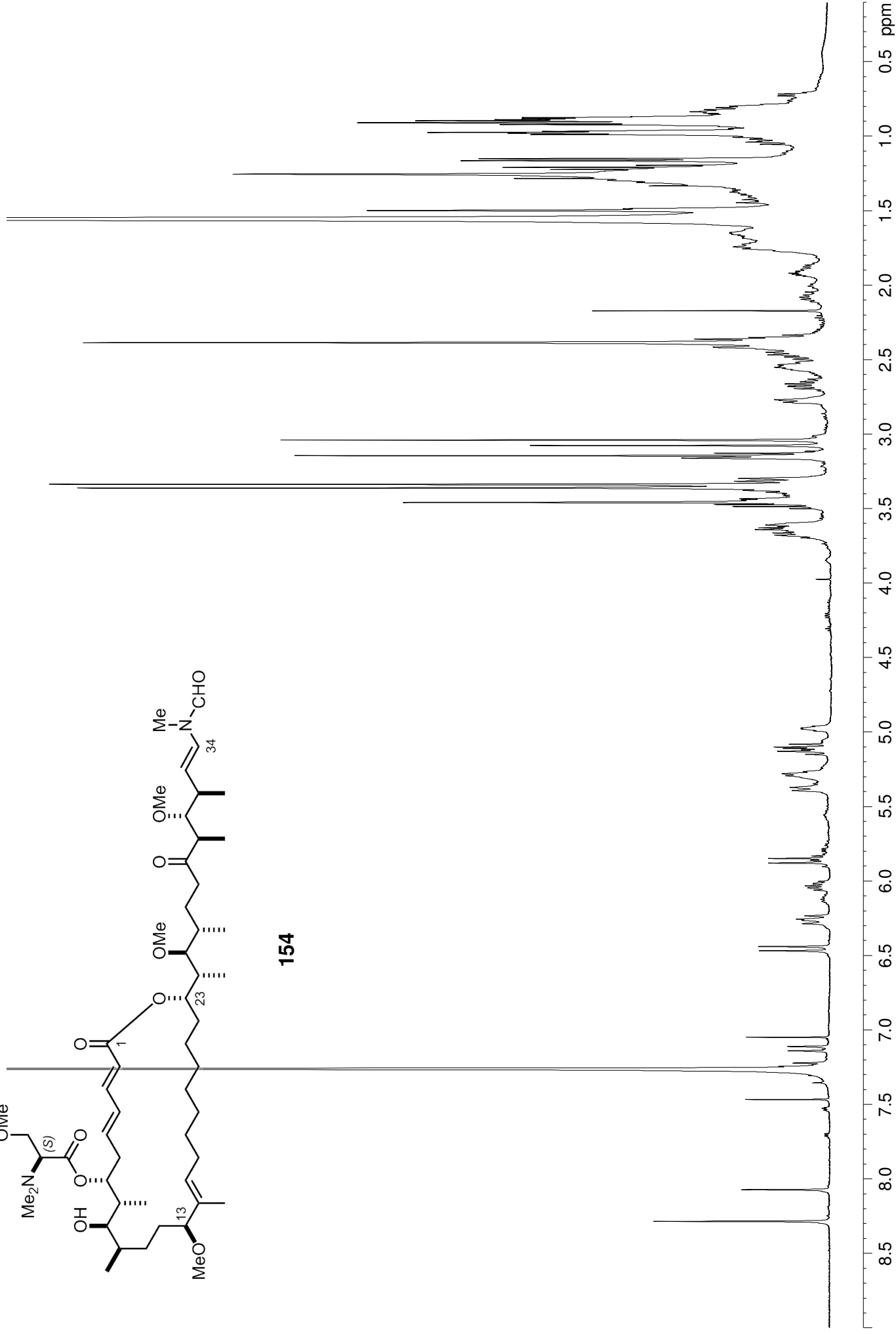


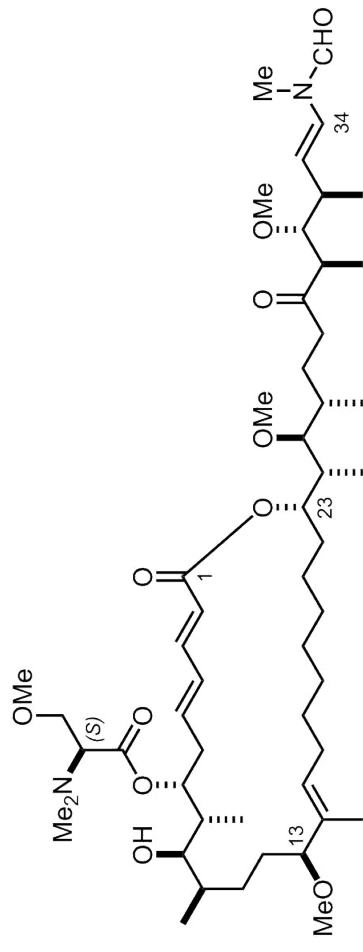
153





154





154

